

**Sedimentary Diatom Assemblages of Prydz Bay and Mac.Robertson Shelf, East
Antarctica, and their use as Palaeoecological Indicators.**

Fiona Taylor
B.Sc. (Hons.)
University of Tasmania

Submitted in fulfillment of the requirements for the degree of

Doctor of Philosophy

University of Tasmania

(January 1999).

Declaration

This thesis contains no material which has been accepted for a degree or diploma by the University or any other institution, except by way of background information and duly acknowledged in the Thesis, and to the best of the candidate's knowledge and belief no material previously published or written by another person except where due acknowledgement is made in the text of the Thesis.

Signed:

Date:16/8/99.....

Authority of Access

This thesis may be made available for loan. Copying of any part of this thesis is prohibited for two years from the date this statement was signed; after that time limited copying is permitted in accordance with the Copyright Act 1968.

Signed: ..

Date:16/8/99.....

Abstract

The use of diatoms as palaeoecological indicators is well established, particularly in polar marine and lake environments where the frustules are well preserved in, and often dominate, the sedimentary record. Until recently, marine studies have been concentrated primarily in West Antarctica, namely the Ross Sea, Weddell Sea and Antarctic Peninsula. In comparison, relatively little research has been conducted in East Antarctica, which is the focus of this study. Here, diatom assemblages preserved in over 100 surface sediment samples, collected from Prydz Bay and Mac.Robertson Shelf, have been analysed for diatom distribution and abundance. They are compared to the assemblages preserved in six sedimentary cores from the same area, as a means of reconstructing the natural variability of Holocene palaeoclimates on the East Antarctic continental shelf.

The distribution and composition of four diatom assemblages are identified in the surface sediments of Prydz Bay and Mac.Robertson Shelf using multivariate statistical analyses. Multiple regression is used to identify the relationship between these assemblages and known environmental variables. The "coastal" assemblage, characterised by sea-ice species, is present in near-shore and shallow regions where seasonal sea ice breakout does not regularly occur. In the centre of the bay, and extending west along Mac.Robertson Shelf, the "shelf" diatom assemblage is characterised by sea-ice and ice-edge diatoms. Offshore of the continental shelf break zone, the "oceanic" assemblage is characterised by open water species. This assemblage also extends along the eastern margin of Prydz Bay, and it is suggested that they have been transported onshore by the slowly circulating, cyclonic Prydz Bay gyre. The fourth diatom assemblage contains both sea-ice and open water species. All are characteristically large and heavily silicified, and the assemblage is interpreted to represent one from which the smaller and more fragile diatom frustules have been removed by current winnowing.

The diatom assemblages in cores from Prydz Bay and Mac.Robertson Shelf are analysed and compared to the surface assemblages using the same multivariate methods. Down core assemblages that are analogous to those in the surface sediment indicate periods during which the depositional regime and palaeoecological conditions on the continental shelf were similar to that of those today. These assemblages dominate the cores, providing a useful indicator of sea ice concentration and extent since the Late Pleistocene.

It is also suggested that they indicate changes in both the geographic position of the Prydz Bay gyre and strength in water currents exiting the bay.

The presence of down core assemblages that have no modern analogue indicate periods of deposition that were significantly different from today. This is most evident in the depositional basins of Iceberg Alley and Nielsen Basin, on Mac.Robertson Shelf, where laminated core intervals are characterised by *Chaetoceros* resting spores or *Corethron criophilum*. Compared to similar assemblages observed in West Antarctica, the intervals suggest that, during the Holocene, parts of the East Antarctic continental shelf experienced periods of decreased sea ice concentration and increased primary production. *Chaetoceros* resting spores may also be a useful proxy to record changes in the position of maximum summer ice retreat.

Acknowledgements

Thanks go to my supervisors, *Andrew McMinn* (IASOS) and *Peter Harris* (Antarctic CRC), for continued support and guidance during my presence (and absence) of this thesis. Not to mention their providing my first opportunity to experience Antarctica, as it should be, first-hand.

Thanks to the following people, whose generosity contributed to the findings of this thesis:

- *Bob Connell* and *Lisette Robertson* (Antarctic CRC) for technical support and laboratory assistance;
- *Andrew Forbes* (CSIRO), for making available unpublished FISHOG 92 oceanographic data;
- *Dennis Franklin* (IASOS), for making available sediment samples collected during the ANARE 1992/1993 field season, and providing unpublished grain size data;
- *Graham Hosie* (Australian Antarctic Division), for advice with statistical analyses;
- *German Leitchenkov* (VNIIOkeangeolgia, Russia), *Pat Quilty* (Australian Antarctic Division) and *Tony Rathburn* (ANU), for providing sediment samples collected during various Soviet/Russian and Australian geoscience expeditions.

The old friends and colleagues of IASOS and the University of Tasmania. For many memorable days of morning tea, afternoon tea, long lunches, late dinners, and good friends to have it with.

To *Jason Whitehead*. All my thanks for your constant encouragement, support, assistance, advice, and more, throughout the rocky thesis road. From start, to finish, and beyond.

Table of Contents

| | |
|---------------------|------|
| Declaration | i |
| Authority of Access | ii |
| Abstract | iii |
| Acknowledgements | v |
| Table of Contents | vi |
| List of Figures | xiii |
| List of Tables | xvi |

Part A – Distribution of Diatoms in Surface Sediments of Prydz Bay and Mac.Robertson Shelf

| | |
|--|----|
| 1 Introduction | 1 |
| 2 Biology of Diatoms | 3 |
| 3 Sedimentation and Dissolution of Diatoms | 7 |
| 3.1 Sedimentation | 7 |
| 3.2 Dissolution | 9 |
| 3.3 Diatomaceous Oozes in Antarctica | 11 |
| 4 Diatom Assemblage Studies in Antarctica | 14 |
| 4.1 Assemblage Studies in the 19 th Century | 14 |
| 4.2 Modern Assemblage Studies | 14 |
| 4.3 Assemblage Studies in Prydz Bay | 19 |
| 4.4 Aims of the Current Research | 22 |
| 5 Prydz Bay and Mac.Robertson Shelf | 23 |
| 5.1 Physical Setting | 23 |
| 5.1.1 Prydz Bay | 23 |

| | |
|---|----|
| 5.1.2 Mac.Robertson Shelf | 27 |
| 5.2 Sea Ice Distribution | 28 |
| 5.3 Oceanography | 29 |
| 5.3.1 Horizontal Circulation | 29 |
| 5.3.2 Water Masses and Vertical Structure | 34 |
| 5.3.3 Summary | 40 |
| | |
| 6 Material and Methods | 42 |
| 6.1 Sediment Preparation | 42 |
| 6.2 Slide Preparation | 42 |
| 6.3 Diatom Counts | 42 |
| 6.4 Grain Size Analysis | 43 |
| | |
| 7 Statistical Analysis | 49 |
| 7.1 Data Transformation | 49 |
| 7.2 Cluster Analysis | 49 |
| 7.3 Indicator Species (SNK and ANOVA) | 50 |
| 7.4 Ordination (NMDS) | 51 |
| 7.5 Multiple Regression | 52 |
| | |
| 8 Environmental Variables | 55 |
| 8.1 Latitude, Longitude and Water Depth | 55 |
| 8.2 Water Temperature, Salinity and Density | 55 |
| 8.3 Sea Ice | 56 |
| 8.4 Horizontal Water Circulation | 56 |
| | |
| 9 Results | 62 |
| 9.1 Cluster Analysis | 62 |
| 9.2 SNK and ANOVA | 63 |
| 9.3 NMDS | 64 |

| | |
|---|-----|
| 9.4 Multiple Regression | 65 |
| 9.5 Grain Size Analysis | 66 |
| 10 Discussion | 76 |
| 10.1 Coastal Assemblage | 76 |
| 10.2 Shelf Assemblage | 79 |
| 10.3 Oceanic Assemblage | 81 |
| 10.4 Cape Assemblage | 84 |
| 11 Conclusion | 89 |
| Part B – Late Pleistocene / Holocene Diatom Assemblages of Prydz Bay and Mac.Robertson Shelf | |
| 12 Introduction to Down Core Analysis | 90 |
| 13 Methods for Down Core Analysis | 91 |
| 13.1 Gravity Cores | 91 |
| 13.2 Sample Preparation and Statistical Analysis | 92 |
| 13.3 Radiocarbon Analysis | 92 |
| 14 KROCK GC1 | 95 |
| 14.1 Site Description | 95 |
| 14.2 Core Description | 95 |
| 14.3 Fossil Assemblages | 96 |
| 14.4 Results | 98 |
| 14.4.1 Radiocarbon Dates | 98 |
| 14.4.2 Diatom Assemblages | 100 |
| 14.4.3 Statistical Analyses | 100 |
| 14.5 Diatom Assemblages in GC1 | 108 |

| | | |
|--------|---|-----|
| 14.5.1 | <i>Chaetoceros</i> Assemblage | 108 |
| 14.5.2 | Basin Assemblage | 111 |
| 14.5.3 | <i>Corethron</i> Assemblage | 113 |
| 14.6 | Holocene Palaeoecology of Iceberg Alley | 120 |
| 14.6.1 | Upper Pleistocene (>10.0 Ka) | 120 |
| 14.6.2 | Late Holocene to Present (<10.0 Ka) | 121 |
| 14.7 | 250-Year High-Productivity Events? | 123 |
| 14.8 | Conclusion | 125 |
| 15 | KROCK GC2 | 128 |
| 15.1 | Site Description | 128 |
| 15.2 | Core Description | 128 |
| 15.3 | Fossil Assemblages | 128 |
| 15.4 | Results | 131 |
| 15.4.1 | Radiocarbon Dates | 131 |
| 15.4.2 | Diatom Assemblages | 131 |
| 15.4.3 | Statistical Analyses | 133 |
| 15.5 | Diatom Assemblages in GC2 | 141 |
| 15.5.1 | Reworked/Dissolution Assemblage | 141 |
| 15.5.2 | Shelf Assemblage | 141 |
| 15.5.3 | Coastal Assemblage | 142 |
| 15.6 | Holocene Palaeoecology of Nielsen Basin | 144 |
| 15.6.1 | Mid Holocene (>5.7 Ka) | 144 |
| 15.6.2 | Mid Holocene (5.7 to 5.5 Ka) | 145 |
| 15.6.3 | Mid Holocene to Present (<5.5 Ka) | 146 |
| 15.7 | Conclusion | 148 |
| 16 | KROCK GC29 | 150 |
| 16.1 | Site Description | 150 |
| 16.2 | Core Description | 150 |

| | |
|--|-----|
| 16.3 Fossil Assemblages | 150 |
| 16.4 Results | 153 |
| 16.4.1 Radiocarbon Dates | 153 |
| 16.4.2 Diatom Assemblages | 154 |
| 16.4.3 Statistical Analyses | 155 |
| 16.5 Diatom Assemblages in GC29 | 162 |
| 16.5.1 Shelf Assemblage | 162 |
| 16.5.2 Open Shelf Assemblage | 162 |
| 16.6 Holocene Palaeoecology of Inner Prydz Bay | 166 |
| 16.6.1 Upper Pleistocene (>12.4 Ka) | 166 |
| 16.6.2 Early to late Holocene (12.4 to 3.2 Ka) | 167 |
| 16.6.3 Late Holocene (<3.2 Ka) | 169 |
| 16.7 Conclusion | 171 |
| | |
| 17 AA149 | 173 |
| 17.1 Site Description | 173 |
| 17.2 Core Description | 173 |
| 17.3 Fossil Assemblages | 173 |
| 17.4 Results | 176 |
| 17.4.1 Radiocarbon Dates | 176 |
| 17.4.2 Diatom Assemblages | 178 |
| 17.4.3 Statistical Analyses | 178 |
| 17.5 Diatom Assemblages in AA149 | 188 |
| 17.5.1 Oceanic Assemblage “A” | 188 |
| 17.5.2 Oceanic Assemblage “B” | 189 |
| 17.5.3 Reworked Assemblage | 190 |
| 17.6 Upper Pleistocene / Holocene Palaeoecology of Outer Prydz Bay | 191 |
| 17.6.1 Upper Pleistocene (>30.0 Ka?) | 192 |
| 17.6.2 Upper Pleistocene (~30.0 Ka to ~22.5 Ka) | 193 |
| 17.6.3 Upper Pleistocene (~22.5 Ka to ~16.5 Ka) | 194 |

| | | |
|--------|---|-----|
| 17.6.4 | Upper Pleistocene to Late Holocene (~16.5 Ka to ~2.5 Ka) | 196 |
| 17.6.5 | Late Holocene to Present (<~2.5 Ka) | 196 |
| 17.7 | Conclusion | 198 |
| 18 | AA186 | 201 |
| 18.1 | Site Description | 201 |
| 18.2 | Core Description | 201 |
| 18.3 | Fossil Assemblages | 201 |
| 18.4 | Results | 204 |
| 18.4.1 | Radiocarbon Dates | 204 |
| 18.4.2 | Diatom Assemblages | 205 |
| 18.4.3 | Statistical Analyses | 205 |
| 18.5 | Diatom Assemblages in AA186 | 213 |
| 18.5.1 | Oceanic Assemblage "A" | 213 |
| 18.5.2 | Oceanic Assemblage "B" | 213 |
| 18.5.3 | Shelf Assemblage | 216 |
| 18.6 | Upper Pleistocene / Holocene Palaeoecology of Prydz Bay (Four Ladies Bank) | 216 |
| 18.6.1 | Upper Pleistocene to Early Holocene (~17.0 Ka to ~7.7 Ka) | 216 |
| 18.6.2 | Mid to late Holocene (~7.7 Ka to ~2.7 Ka) | 218 |
| 18.6.3 | Late Holocene (2.7 Ka to 0.5 Ka) | 219 |
| 18.6.4 | Late Holocene to Present (<0.5 Ka) | 220 |
| 18.7 | Conclusion | 221 |
| 19 | KROCK GC33 | 224 |
| 19.1 | Site Description | 224 |
| 19.2 | Core Description | 224 |
| 19.3 | Fossil Assemblages | 224 |
| 19.4 | Results | 226 |

| | |
|---|-----|
| 19.4.1 Radiocarbon Dates | 226 |
| 19.4.2 Diatom Assemblages | 228 |
| 19.4.3 Statistical Analyses | 228 |
| 19.5 Diatom Assemblages in GC33 | 236 |
| 19.5.1 Cape Assemblage | 236 |
| 19.5.2 Shelf Assemblage | 236 |
| 19.5.3 <i>Chaetoceros</i> Assemblage | 237 |
| 19.5.4 Oceanic Assemblage | 238 |
| 19.6 Holocene Palaeoecology of Mac.Robertson Shelf (Fram Bank) | 239 |
| 19.6.1 Mid Holocene (3.8 Ka to 3.1 Ka) | 239 |
| 19.6.2 Mid Holocene (3.1 Ka to 3.0 Ka) | 240 |
| 19.6.3 Late Holocene (3.0 Ka to 2.7 Ka) | 241 |
| 19.6.4 Late Holocene to Present (<2.7 Ka) | 242 |
| 19.7 Conclusion | 244 |
| | |
| 20 General Discussion | 247 |
| 20.1 Upper Pleistocene (>30.0 Ka to 12.4 Ka) | 248 |
| 20.2 Early to Mid Holocene (<10.0 Ka to 5.0 Ka) | 251 |
| 20.3 Mid Holocene to Present (<5.0 Ka) | 253 |
| | |
| 21 Summary and Future Recommendations | 258 |
| 21.1 Summary | 258 |
| 21.2 Future Recommendations | 259 |
| | |
| 22 References | 260 |
| | |
| Appendix 1 – Abundance (%) and distribution of species in surface samples | |
| Appendix 2 – Preliminary cluster analysis of surface sediment samples | |
| Appendix 3 – Abundance (%) and distribution of species in GC1 | |
| Appendix 4 – Preliminary cluster analysis of GC1 | |

| | |
|---|--|
| Appendix 5 – Abundance (%) and distribution of species in GC2 | |
| Appendix 6 – Preliminary cluster analysis of GC2 | |
| Appendix 7 – Abundance (%) and distribution of species in GC29 | |
| Appendix 8 – Abundance (%) and distribution of species in AA149 | |
| Appendix 9 – Abundance (%) and distribution of species in AA186 | |
| Appendix 10 – Preliminary cluster analysis of AA186 | |
| Appendix 11 – Abundance (%) and distribution of species in GC33 | |
| Appendix 12 – Taxonomy and species plates | |

List of Figures

| | | |
|-----|--|----|
| 2.1 | Orders of diatoms (Centrales and Pennales) | 5 |
| 2.2 | Habitats in sea ice occupied by diatoms | 6 |
| 3.1 | Settling rates for unaggregated silica particles | 7 |
| 3.2 | Effect of temperature on the dissolution of silica frustules | 10 |
| 3.3 | Distribution of sediment types around Antarctica | 12 |
| 3.4 | Distribution of biogenic silica in Prydz Bay. | 13 |
| 4.1 | Distribution of the three dominant diatom assemblages, defined by Pichon <i>et al.</i> (1992). | 18 |
| 4.2 | Distribution and abundance of diatom species in Prydz Bay net hauls | 20 |
| 4.3 | Distribution of diatom assemblages in Prydz Bay surface sediments | 21 |
| 5.1 | Location of Prydz Bay and Mac.Robertson Shelf, East Antarctica | 24 |
| 5.2 | Surface sediment lithofacies identified in Prydz Bay | 26 |
| 5.3 | Geomorphic zones on Mac.Robertson Shelf | 28 |
| 5.4 | Horizontal water circulation patterns | 30 |
| 5.5 | Schematic distribution of potential water temperature and salinity determination for Prydz Bay | 35 |
| 5.6 | Schematic distribution of water masses and core layers in Antarctic waters | 35 |
| 6.1 | Surface sediment locations | 48 |

| | | |
|------|--|-----|
| 7.1 | Summary of steps in statistical analysis of data | 54 |
| 8.1 | Average sea ice distribution around Antarctic for the months Oct – Feb between the years 1978-1991 | 61 |
| 9.1 | Dendrogram of cluster analysis comparing surface sediment samples, based on diatom distribution | 67 |
| 9.2 | Geographic distribution of diatom assemblages identified by cluster analysis | 68 |
| 9.3 | Graphical method of Kruskal and Wish (1978) for selecting the appropriate level of NMDS ordination | 70 |
| 9.4 | Ordination plot of sample sites | 72 |
| 9.5 | Dendrogram of cluster analysis comparing sample sites, based on grain size distribution | 73 |
| 9.6 | Geographic distribution of grain size cluster groups | 75 |
| 10.1 | Light micrographs of typical diatom assemblages in surface sediment | 87 |
| 10.2 | Distribution of sediment fractions in diatom assemblages | 88 |
| 13.1 | Gravity core localities | 94 |
| 14.1 | GC1 core log | 97 |
| 14.2 | Linear regression (radiocarbon ages v depth) from GC1 | 99 |
| 14.3 | Dendrogram of cluster analysis comparing GC1 samples | 104 |
| 14.4 | Dendrogram of cluster analysis comparing GC1 and surface sediment samples | 106 |
| 14.5 | Distribution of <i>Chaetoceros</i> resting spores in GC1 | 108 |
| 14.6 | Light micrograph of <i>Corethron</i> and <i>Chaetoceros</i> assemblages in GC1 | 109 |
| 14.7 | Photograph illustrating “fluffy” <i>Corethron</i> -rich layers in GC1 | 115 |
| 14.8 | Distribution of <i>C. criophilum</i> in GC1 | 116 |
| 15.1 | GC2 core log | 130 |
| 15.2 | Linear regression (age v depth) from GC2 | 132 |
| 15.3 | Dendrogram of cluster analysis comparing GC2 samples | 137 |
| 15.4 | Dendrogram of cluster analysis comparing GC2 and surface sediment samples | 139 |

| | |
|---|-----|
| 16.1 GC29 core log | 152 |
| 16.2 Linear regression (age v depth) from GC29 | 154 |
| 16.3 Dendrogram of cluster analysis comparing GC29 samples | 158 |
| 16.4 Dendrogram of cluster analysis comparing GC29 and surface sediment samples | 160 |
| 16.5 Distribution of <i>F. curta</i> , <i>F. kerguelensis</i> and <i>T. antarctica</i> resting spores in GC29 | 168 |
| 17.1 AA149 core log | 175 |
| 17.2 Dendrogram of cluster analysis comparing AA149 samples | 182 |
| 17.3 Dendrogram of cluster analysis comparing AA149 and surface sediment samples | 184 |
| 17.4 Dendrogram of cluster analysis comparing AA149 and oceanic diatom assemblage sediment samples | 186 |
| 17.5 Distribution of <i>F. curta</i> and <i>F. kerguelensis</i> in AA149 | 190 |
| 17.6 Distribution of extinct diatom taxa in AA149 | 191 |
| 18.1 AA186 core log | 203 |
| 18.2 Dendrogram of cluster analysis comparing AA186 | 209 |
| 18.3 Dendrogram of cluster analysis comparing AA186 and surface sediment samples | 211 |
| 18.4 Distribution of <i>F. curta</i> and <i>F. kerguelensis</i> in AA186 | 215 |
| 18.5 Distribution of extinct taxa in AA186 | 215 |
| 19.1 GC33 core log | 225 |
| 19.2 Linear regression (age v depth) from GC33 | 227 |
| 19.3 Dendrogram of cluster analysis comparing GC33 | 232 |
| 19.4 Dendrogram of cluster analysis comparing GC33 and surface sediment samples | 234 |
| 19.5 Distribution of <i>Chaetoceros</i> resting spores in GC33 | 238 |
| 20.1 ¹⁸ O v depth in the Vostok ice core. | 250 |
| 20.2 Interpreted ice-flow paths for periods of maximum ice extent in Prydz Bay | 250 |

List of Tables

| | | |
|------|---|-----|
| 4.1 | Diatom publications from early Antarctic expeditions | 15 |
| 5.1 | ANARE marine science oceanographic surveys conducted between 1981-1987 | 31 |
| 6.1 | Expeditions to Prydz Bay – Mac.Robertson Shelf from which sediment sample were obtained | 43 |
| 6.2 | Latitude, longitude and water depth from which samples were recovered | 44 |
| 7.1 | Interpretation of stress values | 52 |
| 8.1 | Environmental data data used in regression analysis | 57 |
| 8.2 | Rank values used to estimate water temperature, salinity and density at each sample site | 60 |
| 9.1 | Arithmetic mean abundance, analysis of variance, and SNK tests of diatom species in cluster groups | 69 |
| 9.2 | Multiple regression analysis between environmental variables and NMDS scores for two-axis ordination | 71 |
| 9.3 | Cosine and acosine values | 71 |
| 9.4 | Arithmetic mean abundance, analysis of variance, and SNK tests of sediment types in cluster groups | 74 |
| 10.1 | Arithmetic mean abundance and preferred ecological habitat of species characteristic of coastal diatom assemblage | 77 |
| 10.2 | Arithmetic mean abundance and preferred ecological habitat of species characteristic of shelf diatom assemblage | 80 |
| 10.3 | Arithmetic mean abundance and preferred ecological habitat of species characteristic of oceanic diatom assemblage | 82 |
| 10.4 | Arithmetic mean abundance and preferred ecological habitat of species characteristic of cape diatom assemblage | 85 |
| 13.1 | Gravity cores analysed for diatom assemblages | 91 |
| 14.1 | AMS radiocarbon dates obtained from GC1 | 99 |
| 14.2 | Arithmetic mean abundance, analysis of variance, and SNK tests of species in cluster groups in GC1 | 105 |

| | | |
|------|---|-----|
| 14.3 | Arithmetic mean abundance, analysis of variance, and SNK tests of species in cluster groups in GC1 and surface sediment samples | 107 |
| 14.4 | Summary of Holocene palaeoclimate on Mac.Robertson Shelf (Iceberg Alley), as inferred from GC1 | 127 |
| 15.1 | AMS radiocarbon dates obtained from GC2 | 132 |
| 15.2 | Arithmetic mean abundance, analysis of variance, and SNK tests of species in cluster groups in GC2 | 138 |
| 15.3 | Arithmetic mean abundance, analysis of variance, and SNK tests of species in cluster groups in GC2 and surface sediment samples | 140 |
| 15.4 | Summary of Holocene palaeoclimate on Mac.Robertson Shelf (Nielsen Basin), as inferred from GC2 | 149 |
| 16.1 | AMS radiocarbon dates obtained from GC29 | 153 |
| 16.2 | Arithmetic mean abundance, analysis of variance, and SNK tests of species in cluster groups in GC29 | 159 |
| 16.3 | Arithmetic mean abundance, analysis of variance, and SNK tests of species in cluster groups in GC29 and surface sediment samples | 161 |
| 16.4 | Relative abundance of indicator species in shelf, open shelf and oceanic diatom assemblages from GC29 | 163 |
| 16.5 | Summary of Holocene palaeoclimate on Mac.Robertson Shelf (Nielsen Basin), as inferred from GC29 | 172 |
| 17.1 | AMS radiocarbon dates obtained from AA149 | 176 |
| 17.2 | Arithmetic mean abundance, analysis of variance, and SNK tests of species in cluster groups in AA149 | 183 |
| 17.3 | Arithmetic mean abundance, analysis of variance, and SNK tests of species in cluster groups in AA149 and surface sediment samples | 185 |
| 17.4 | Arithmetic mean abundance, analysis of variance, and SNK tests of species in cluster groups in AA149 and “oceanic” diatom assemblage sediment samples | 187 |
| 17.5 | Summary of Holocene palaeoclimate on outer Prydz Bay, as inferred from AA149 | 200 |

| | | |
|------|---|-----|
| 18.1 | AMS radiocarbon dates obtained from AA186 | 204 |
| 18.2 | Arithmetic mean abundance, analysis of variance, and SNK tests of species in cluster groups in AA186 | 210 |
| 18.3 | Arithmetic mean abundance, analysis of variance, and SNK tests of species in cluster groups in AA186 and surface sediment samples | 212 |
| 18.4 | Extinct diatom taxa identified in AA186 | 214 |
| 18.5 | Summary of Holocene palaeoclimate on inner Prydz Bay (Four Ladies Bank), as inferred from AA186 | 223 |
| 19.1 | AMS radiocarbon dates obtained from GC33 | 226 |
| 19.2 | Arithmetic mean abundance, analysis of variance, and SNK tests of species in cluster groups in GC33 | 233 |
| 19.3 | Arithmetic mean abundance, analysis of variance, and SNK tests of species in cluster groups in GC33 and surface sediment samples | 235 |
| 19.4 | Summary of Holocene palaeoclimate on inner Prydz Bay (Fram Bank), as inferred from GC33 | 246 |
| 20.1 | Pleistocene / Holocene palaeoenvironments in Prydz Bay and Mac.Robertson Shelf | 255 |

- Part A -

*Distribution of Diatoms in Surface Sediments of
Prydz Bay and Mac.Robertson Shelf.*

– Chapter 1 –

Introduction

Knowledge of palaeoclimates is particularly important in Antarctic areas to study ice-cap advance and retreat (Pickard, 1982). Climate change data from the Southern Hemisphere is limited, however, particularly that concerning the response of the high latitude Southern Ocean during the Holocene (<10.0 Ka) (Leventer *et al.*, 1993). Interpretation of Antarctica's glacial and climate history is largely based on evidence from marine sedimentary records from the Southern Ocean, due to the inaccessibility of most terrestrial sediments (Ciesielski and Weaver, 1974). These estimates have come principally from oxygen isotopic composition of ocean waters, the distribution of ice-rafted debris, occurrence of subglacial volcanism, terrestrial floral assemblages, and marine biostratigraphic work (chiefly diatom occurrence and abundance) (Mercer, 1978).

Diatoms make an excellent indicator of the palaeoenvironment and relative palaeotemperatures in Antarctica (Barron, 1993). Differences in temperature, nutrients, salinity, and other physical and chemical parameters influence the distribution of living species. They can also be used to estimate palaeosalinity, to recognise glacial or interglacial stages in the Quaternary, and to trace Antarctic Bottom Water characterised by the presence of endemic Antarctic diatoms in the south Atlantic and Indian Oceans. Diatoms also offer many advantages for biostratigraphy over other microfossils (Barron, 1993). These include their:

1. Abundance and diversity (calcareous microfossils are generally sparse or low in diversity at high latitude).
2. Good preservation in sediment (unlike calcareous microfossils).
3. Ease to process (due to small size and large number).

Surface sediment assemblages represent modern, planktonic diatom assemblages in the water column. When correlated to known oceanographic and sea ice conditions, they

can then be used as the basis for a model to interpret down core changes in the diatom assemblage, as a response to the palaeoclimate. Upon this basis, the aim of the following project is two-fold:

1. To identify the composition and distribution of diatom assemblages in surface sediments from Prydz Bay and Mac.Robertson Shelf, East Antarctica.
2. To identify the fossil (down core) changes in diatom assemblages, and interpret these changes in response to the palaeoenvironment.

– Chapter 2 –

Biology of Diatoms

Diatoms (Division: Bacillariophyceae) are unicellular, golden brown algae that inhabit the euphotic zone (generally <100 m) of almost all aquatic environments. They are characterised by an external, box-like skeleton (frustule), and range in size from 1 μm – 1000 μm (Barron, 1985). The frustule is comprised of hydrated, amorphous silica that is deposited in a regular pattern to create a highly ornamented cell surface with, for example, extensions, pores and striae. Taxonomy is based upon the frustule structure and its ornamentation and, from this, two diatom orders are recognised (Fig. 2.1): Centrales (radial symmetry) and Pennales (bilateral symmetry).

Diatoms occur as photosynthetic autotrophs, colourless heterotrophs or photosynthetic symbiotes (Schmaljohann and Rottger, 1978) and adopt various modes of lifestyle. Benthic colonies form commonly within the euphotic zone by excreting a mucilaginous substance with which they adhere to rocks and macroalgae. In polar regions, sea ice also forms a suitable substrate. Ice assemblages may occur within the ice (interstitial), in pools on the ice surface, or consist of large strands floating directly beneath, or attached to, the underside of the ice (Horner, 1990) (Fig. 2.2). In Antarctica, the dominant ice-associated species are usually from the genera *Amphiprora*, *Pleurosigma*, *Nitzschia* (*Fragilariopsis*), *Navicula* and *Pinnularia* (Leventer and Harwood, 1993). Planktonic diatoms are dispersed passively by ocean currents in the surface layers of the ocean, but may possess various adaptations to promote flotation. These include frustule shape and extensions, colony formation and fat or oil storage within the cell (Barron, 1993).

The requirement for phosphorus, nitrate, and silica for incorporation into the frustule limits diatoms. In the open marine environment, these nutrients are typically concentrated below the euphotic zone, but become available in areas where deep water upwelling transports them to the surface (Barron, 1985). In boreal, equatorial and Antarctic latitudes, free exchange of surface waters with deeper waters, due to a weak

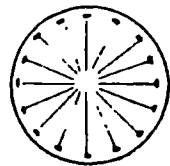
thermocline, constantly replenishes the euphotic zone with nutrients (Jousé *et al.*, 1971; Barron, 1985).

In the Antarctic marine environment, diatoms occur in high abundance and are the main primary producers, forming up to 90% of the suspended silica in surface water (Barron, 1985). Their distribution and abundance in the water column is influenced by a variety of environmental variables, which, along with macro- and micro-nutrients, include light, temperature, salinity, silica, sea ice, and water column stability (Leventer and Harwood, 1993). An understanding of how these variables control the distribution of specific species and species assemblages is a valuable tool, from which the study of fossil diatoms can be used to reconstruct past oceanographic and climatic conditions (Leventer and Harwood, 1993). Only a small proportion of the living diatom assemblage (biocoenose) becomes a part of the fossil assemblage (thanatocoenose), however. This is due to the effects of recycling, during sedimentation, and silica dissolution, prior to burial at the sediment-water interface.

CENTRALES

Shape of cell, \pm ring of processes, polarity, elevations

Coscinodiscineae :



ring of processes



Rhizosoleniineae :



pervalvar axis



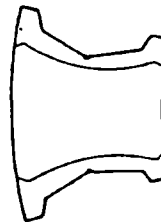
Biddulphiineae :



bipolar

elevations

pseudocellus / ocellus



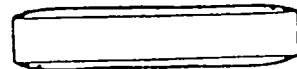
PENNALES

Apical pore field, labiate process, \pm raphe, shape of raphe

Araphidineae :



no raphe



Raphidineae :

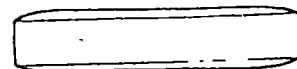
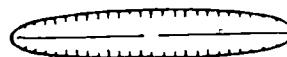


Fig. 2.1. Orders of diatoms (Centrales and Pennales), upon which taxonomy is based. (From Medlin and Priddle, 1990).

SEA ICE BIOTA

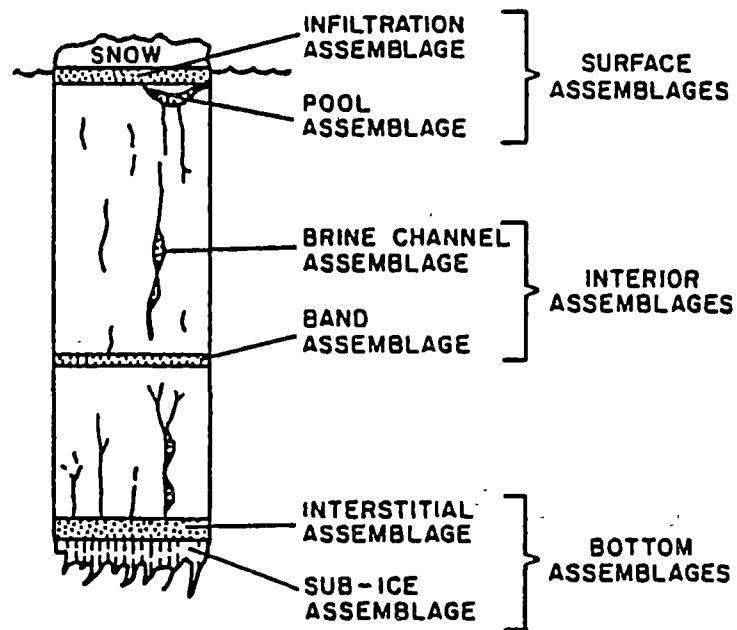


Fig. 2.2. Habitats in sea ice occupied by diatoms. (From Leventer and Harwood, 1993).

– Chapter 3 –

*Sedimentation and Dissolution of Diatoms***3.1 Sedimentation**

Most siliceous material in suspension settles at a rate equivalent to that of $1\ \mu\text{m} - 5\ \mu\text{m}$ quartz spheres (Lisitzin, 1971) (Fig. 3.1). It takes the heaviest and coarsest diatom frustules from 30 to 100 days to descend 5000 m through the water column; the finest frustules may take tens of years. During this time, some lateral transport of the frustules by water currents may occur, but a relatively accurate record of the overlying biocoenose can still be recorded in the underlying sediment (Kozlova, 1966; Kozlova and Mukhina, 1967; Leventer and Dunbar, 1986, 1987a, 1988).

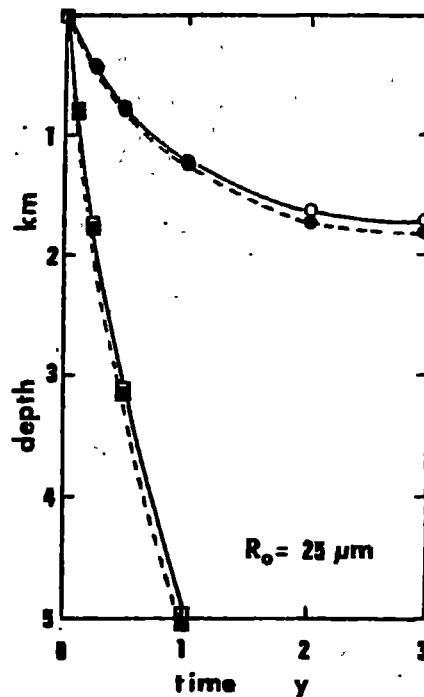


Fig. 3.1 Settling rates for unaggregated silica particles, with a radius of $25\ \mu\text{m}$, through waters of the Antarctic Divergence. Circles: ideal conditions; squares: non-ideal conditions. Continuous line: upwelling rate (rate = $0.00016\ \text{cm s}^{-1}$). Dashed line: no upwelling (rate = $0\ \text{cm s}^{-1}$). (From Kamatani and Riley, 1979).

Some frustules may survive the sinking process as individuals, as noted by Gersonde and Wefer (1987) who observed the presence of intact *Corethron criophilum* and chains of *Nitzschia* species in sediment traps deployed in the Drake Passage, Bransfield Strait and Powell Basin (west of the South Orkney Islands). Broken, individual frustules may also be filled with diatomaceous debris, which includes the intact, smaller frustules of other species. Only a small proportion of diatom frustules descend freely to the ocean floor, however. At least two other mechanisms act to aggregate the frustules and increase their sinking rate: incorporation into faecal pellets, and frustule aggregation.

The grazing of diatoms by zooplankton incorporates the frustules into faecal pellets, acting to increase both the rate of settling and to inhibit dissolution by enclosing them in a protective membrane (Schrader, 1971). Water exchange across the faecal pellet is limited as long as the membrane remains intact to protect the frustules from further dissolution. Although the pellets disintegrate mostly by 500 m water depth, due to bacterial decomposition and secondary grazing, they do act to rapidly transport silica from the active zone of dissolution, in the water's surface layer, to a relatively more passive zone (Hurd, 1972).

Grazing by zooplankton does not have an entirely beneficial effect on frustule preservation. During grazing, the frustules undergo mechanical breakage by mastication, which increases the surface area, and chemical breakdown by digestion. Both factors increase the rate of frustule dissolution (Hurd, 1972). Mechanical breakdown by zooplankton has been demonstrated to most strongly affect large diatoms, including *C. criophilum* (Gersonde and Wefer, 1987). Such species, which may be an important component of the biocoenose, may therefore be under-represented in the thanatocoenose. Similarly, weakly silicified frustules may also be under-represented.

Intact diatoms may also sink as a frustule aggregation, either incorporated in, or attached to, "large amorphous aggregates" or "marine snow" (Honjo *et al.*, 1982). Aggregates are formed during increased mucous secretion by diatoms, leading to entanglement and

aggregate formation (Smetacek, 1985). Sinking rates for such aggregates range from 43 m – 95 m day⁻¹ and is an important role in marine transport from the euphotic to aphotic zone (Shanks and Trent, 1980).

3.2 Dissolution

The world's oceans are undersaturated in respect to the opaline silica from which diatom frustules are constructed (Heath, 1974). As a consequence, frustules undergo differential dissolution during the sedimentation process, which continues at the sediment – water interface prior to their burial. Dissolution alters the planktonic diatom assemblage in several ways: up to 99% of the biocoenose can be removed (Shemesh *et al.*, 1989), and there is preferential dissolution of the smaller and more fragile frustules, leading to a decline in both species diversity and abundance (Dunbar *et al.*, 1989; Mikkelsen, 1990).

Dissolution in the Water Column

Dissolution is temperature dependent (Hurd, 1972; Kamatani and Riley, 1979) (Fig. 3.2). The surface-water temperature controls the rate at which silica dissolves in the ocean (Tréguer *et al.*, 1989), and is most rapid in surface waters, where temperatures are relatively higher and silicate concentrations low because of its utilisation by both phytoplankton (diatoms and silicoflagellates) and zooplankton (Kamatani and Riley, 1979). In Antarctica, dissolution of biogenic silica within the water column is exceptionally slow due to the low temperatures that prevail throughout the whole water column (Tréguer *et al.*, 1989), and the effect of dissolution may not alter the palaeological expression of diatoms in all sediments (Shemesh *et al.*, 1989). A comparison of the diatom biocoenose with Holocene sediment assemblages in Prydz Bay by Stockwell *et al.* (1991), for example, demonstrated that, although selective dissolution of diatom frustules is apparent, it does not appear to greatly affect diatom diversity within the sediment. They observed that two out of the three species dominant in the plankton (*Fragilariopsis curta* and *F. cylindrus*) survive sedimentation and the selective dissolution process to dominate the sediments. Numerous studies have also demonstrated successfully that fossil diatoms in Antarctic marine sediments can be used

demonstrated successfully that fossil diatoms in Antarctic marine sediments can be used as proxies for past oceanographic and climatic conditions. These include sea surface temperature, water mass distribution and sea ice distribution (e.g. Jousé *et al.*, 1963; Burckle, 1972, 1984; Kellogg and Truesdale, 1979; Defelice and Wise, 1981; Pichon *et al.*, 1987; Leventer and Dunbar, 1988; Leventer, 1992; Leventer *et al.*, 1993, 1996; Cunningham *et al.*, in press).

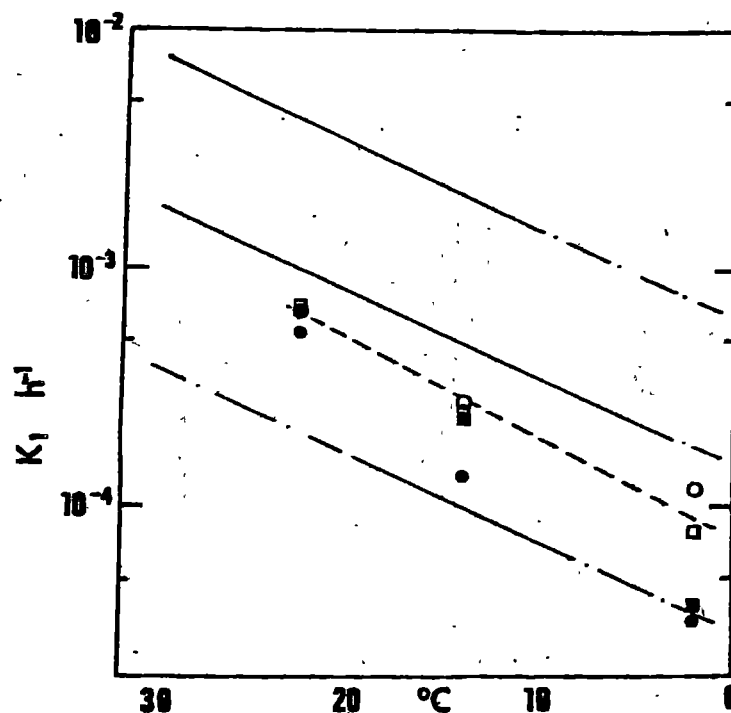


Fig. 3.2. Effect of temperature on the dissolution of silica frustules. Rate (K_1) versus temperature ($^{\circ}C$). Continuous line: delimits the domain of variations of the rate constant, for different species. Monospecific assemblages of *Chaetoceros deflandrei* (hollow circles: pH 7.5; filled circles: pH 8.5) and *Fragilariopsis cylindrus* (hollow squares: pH 7.5; filled squares: pH 8.5). Dashed line indicates the regression at pH 7.5. (From Kamatani and Riley, 1979).

Dissolution at the Sediment – Water Interface

Dissolution of diatom frustules continues at the sediment – water interface, prior to burial. This is enhanced by the burrowing and foraging of benthic animals, which macerate and resuspend the frustules, before they finally settle. Dissolution may then continue in the upper few centimetres of the sedimentary sequence (Schrader, 1971; Lisitzin, 1985).

It is estimated that only 1% – 10% of biogenic silica fixed in the euphotic zone actually reaches the bottom sediments (Kozlova and Mukhina, 1967; Calvert, 1968; Lisitzin, 1971, 1985; Heath, 1974). Of this, only ~ 2% avoids post-depositional dissolution (Heath, 1974). In the Atlantic Sector of the Southern Ocean, Gersonde and Wefer (1987) noted that it is prior to burial that the majority of weakly silicified diatom frustules are dissolved. The remaining moderately to strongly-silicified frustules, which still represent a significant proportion of the biocoenose, are incorporated into the sediment and become part of the geologic record.

3.3 Diatomaceous Oozes in Antarctica

Below the most productive of the world's oceans, diatom frustules form the dominant biogenic component in sediment. Three such areas are recognised (Lisitzin, 1971; Baldauf and Barron, 1990):

1. Southern Belt (Antarctica) – encompassing the Southern Hemisphere in an almost continuous belt.
2. Northern Belt (Boreal) – in the Pacific Ocean, Sea of Okhotsk, Japan Sea, and Bering Sea.
3. Equatorial Belt – in the Pacific and Indian Oceans.

The diatomaceous oozes of Antarctica (Fig. 3.3) appear to be the richest in the world (Jousé *et al.*, 1971), with biogenic silica contributing up to 75% of the total sediment (Kozlova, 1966; DeMaster, 1981; Gersonde and Wefer, 1987). More than 75% of all oceanic silica accumulates here, as a 900 km – 2000 km broad, circum-Antarctic

siliceous sediment belt (the Southern Belt) of the Southern Ocean (Lisitzin, 1971). The belt is bounded to the south by the Antarctic Divergence (65°S) and silty, diatomaceous clay. The northern boundary coincides roughly with the Antarctic Convergence ($58^{\circ} - 63^{\circ}\text{S}$) (Gordon, 1971) and sediment rich in biogenic carbonate (Burckle and Cirilli, 1987).

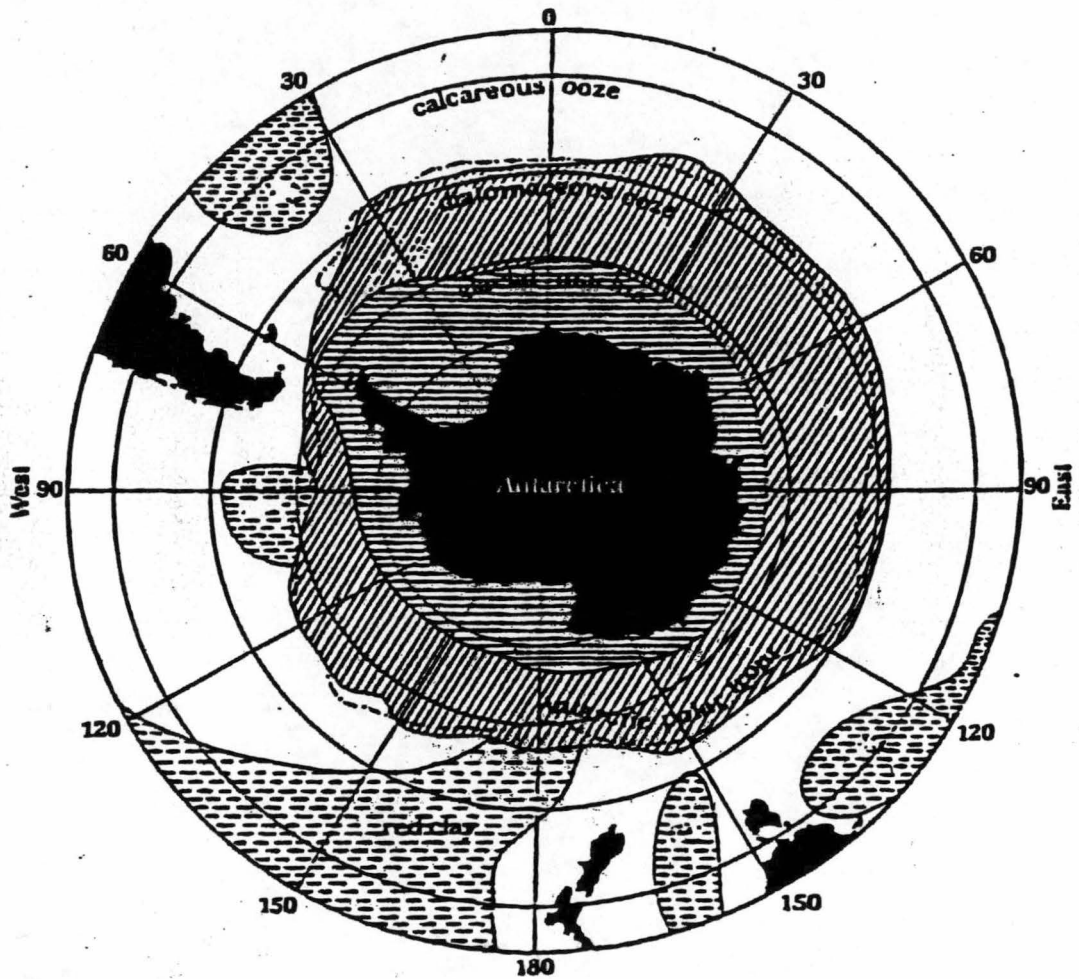


Fig. 3.3. Distribution of sediment types around Antarctica. Angled lines illustrate circumpolar belt of diatomaceous ooze extending north to the Antarctic Polar Front, where it gives way to calcareous ooze (dashed lines), and south to the Antarctic Divergence, where it gives way to diatomaceous silt (horizontal lines). (From Leventer and Harwood, 1993).

The rate at which diatomaceous oozes are deposited around Antarctica locally exceed 2.2 cm / 1000 years. The highest rates of accumulation in the Southern Ocean have been attributed to high rates of primary production. Direct measurements indicate typically low to moderate rates of production (Holm-Hansen *et al.*, 1977; El Sayed *et al.*, 1983), however, suggesting that the efficiency of preservation plays an important role in the processes contributing to silica accumulation (DeMaster *et al.*, 1992). Silica concentrations are not evenly distributed in the Southern Belt, being absent on steep scarps and where there are underwater elevations (Lisitzin, 1971). On the Antarctic Shelf, where the biogenic silica content of sediment ranges from <1% to 46%, by weight (Dunbar *et al.*, 1984), the impact of siliceous sedimentation may be also masked by terrigenous deposition (Heath, 1974). Prydz Bay is characterised by clayey deposits enriched in diatom frustules, whose remnants constitute 30% – 60% of the sedimentary matter (Stockwell *et al.*, 1991). Sediments with the highest concentration of biogenic silica (opal) are distributed predominantly in the deeper depressions and basins (Harris *et al.*, in press) (Fig. 3.4).

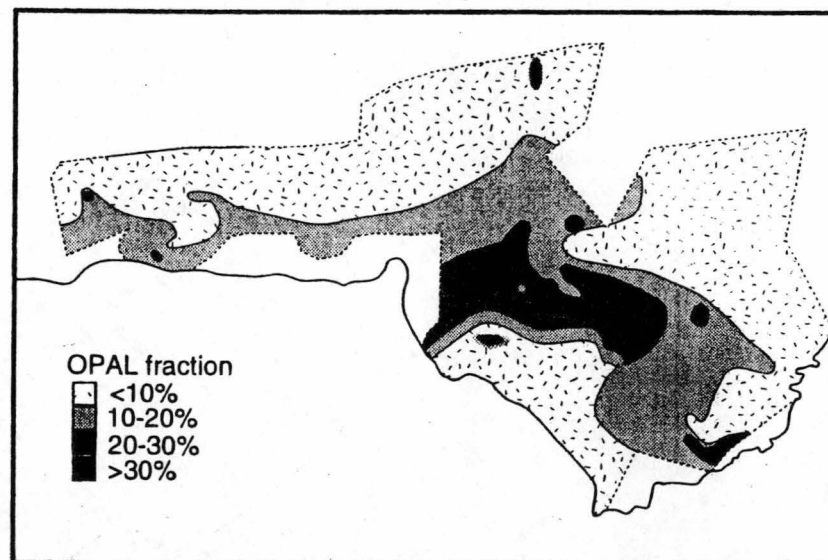


Fig. 3.4. Distribution of biogenic silica in Prydz Bay. (From Harris *et al.*, in press).

– Chapter 4 –

Diatom Assemblage Studies in Antarctica

4.1 Assemblage Studies in the 19th Century

Antarctic diatoms have been studied since the 19th Century, commencing with Hooker's observations made during the *Erebus* and *Terror* Expeditions (1839 – 1843). Hooker reported of diatoms during the Antarctic summer that occurred "... in such countless myriads, as to stain the Berg and Pack-Ice,...., they imparted to the Brash and Pancake-Ice a pale ochreous colour" (Hooker, 1847, cited in Hasle, 1969). Samples collected between Cape Horn and the Ross Sea during these expeditions were returned to the German diatomist Ehrenberg, and resulted in the first published account of diatoms from Antarctica. Following expeditions to Antarctica were concerned primarily with geographic exploration, but some planktonic diatom samples were collected and systematic descriptions published (Table 4.1).

4.2 Modern Assemblage Studies

It was not until the work of Jousé *et al.* (1963) that diatoms in Antarctic marine sediments were investigated extensively, and their value as indicators of climate change in the Southern Ocean recognised. Investigating diatoms from both the water column and sediment – water interface, Jousé *et al.* (1963) defined two diatom floral zones (cited in Burckle, 1972): the Antarctic and sub-Antarctic zones. The Antarctic zone is characterised by species such as *Eucampia antarctica*, *Actinocyclus actinochilus*, *Fragilariopsis curta*, *F. rhombica* (= *F. angulata*) and *Thalassiosira gracilis*. Most are benthic primarily on the underside of sea-ice and therefore have a restricted distribution close to the Antarctic continent. The sub-Antarctic zone is characterised by *T. lentiginosa* and *F. kerguelensis*; species with a broad latitudinal distribution in the Southern Ocean. Similar diatoms zones were described by Kozlova (1966) from surface sediments in the Indian and Pacific sectors of the Southern Ocean.

Table 4.1. *Diatom publications resulting from early Antarctic expeditions.*

| Expedition | Duration | Diatom Publication |
|--|-------------|------------------------|
| <i>Erebus and Terror Expeditions</i> | 1839 - 1843 | Ehrenberg, 1844 |
| <i>H.M.S. Challenger</i> | 1873 - 1876 | Castracane, 1886 |
| <i>Belgica Expedition</i> | 1897 - 1899 | Van Heurck, 1909 |
| German Deep Sea Expedition | 1898 - 1899 | Karsten, 1905 - 1907 |
| German South Pole Expedition | 1901 - 1903 | Heiden and Kolbe, 1928 |
| Scottish National Antarctic Expedition | 1902 - 1904 | Manguin, 1922 |
| 2nd French Antarctic Expedition | 1908 - 1910 | Manguin, 1915 |
| <i>Discovery Expedition</i> | 1929 - 1931 | Hart, 1934 |

The use of diatoms as palaeoclimatic indicators has since become well established. This is particularly so in the Southern Ocean, where diatoms form a major component of both the plankton (Fenner *et al.*, 1976) and sediment (Kozlova, 1966). Numerous studies have used the environmental tolerance-ranges of extant species as models for the past (DeFelice and Wise, 1981). The work of Burckle (1972), Truesdale and Kellogg (1979), DeFelice and Wise (1981), Kellogg and Kellogg (1987), Pichon *et al.* (1987), Leventer and Dunbar (1988), Leventer *et al.* (1993; 1996) and Cunningham *et al.* (in press), for example, have all successfully used Antarctic marine diatom assemblages as a proxy to interpret climate change down-core.

Many diatom studies have used statistical techniques to reconstruct Quaternary glacial history, such as the transfer function (factor analysis) developed by Imbrie and Kipp (1971). Factor analysis is based on knowing the environmental preferences of extant species and, using this knowledge, analysing changes in species abundance and diversity in fossil (down-core) assemblages. The changes can be interpreted as a response to environmental change, based on the assumption that the ecological response of a given species to physical and chemical parameters of the ocean is unchanged over time (Imbrie and Kipp, 1971).

Using factor analysis, three major diatom zones have been defined in surface sediments from the Scotia and Weddell Seas (Burckle, 1972). The shelf zone (dominated by *F. curta*) and meroplanktonic zone (dominated by *E. antarctica*) are essentially identical to the Antarctic zones of Jousé *et al.* (1963) and Kozlova (1966). All are dominated by species that occur principally as benthic colonies on the underside of sea-ice. The holoplanktonic zone (dominated by *T. lentiginosa* and *F. kerguelensis*) corresponds with the sub-Antarctic zone of Jousé *et al.* (1963). Burckle (1972) further identified the Pleistocene / Holocene boundary in deep-sea cores from the South Atlantic, based on the upward change from predominantly shelf and meroplanktonic diatoms to holoplanktonic forms.

Investigating marine diatoms from surface sediments of the Ross Sea, Truesdale and Kellogg (1979) used factor analysis to define four significant diatom assemblages. Assemblage 1, consisting of epontic species dominated by *F. curta*, formed the most important assemblage (explaining 52.5% of the assemblage variance), with high factor loadings on the continental shelf in locations where sediments are undisturbed. Assemblage 2 (explaining 25.0%), dominated by *E. antarctica*, is considered to indicate winnowed sediments from which the fine material and fragile, lightly silicified species have been removed selectively by bottom currents. *Eucampia* is found normally only in small numbers in the plankton, but is more important in sediments as its highly-silicified, robust frustules resist dissolution during sedimentation and burial (Kozlova, 1966; Fenner *et al.*, 1976). Assemblage 3 (10.35%) contained a number of diatoms from widely differing stratigraphic ranges and is interpreted as being reworked. The assemblage is distributed mainly on the continental slope, where diatoms have probably been reworked from the continental shelf, and near the southern ice-shelf margin of the Ross Sea where relict sediments are exposed (Truesdale and Kellogg, 1979). Assemblage 4 (5.3%), dominated by *F. kerguelensis*, is an oceanic assemblage characteristic of Antarctic waters north of the Antarctic Divergence.

Using the same method, Pichon *et al.* (1987) demonstrated that the geographic distribution of Antarctic diatoms (and two silicoflagellates) in surface sediments can be correlated with modern sea surface parameters, such as summer sea surface temperature, phosphate concentration and sea ice distribution. Their study identified three significant assemblages: two associated with Antarctic waters and one with sub-Antarctic waters. To further this study, Pichon *et al.* (1992) developed a model to estimate past sea surface temperatures from the Antarctic fossil diatom record. Factor analysis again identified three assemblages (two Antarctic and one sub-Antarctic), correlated with water mass distribution (Fig.4.1), and a fourth assemblage characterised as a “dissolution assemblage”.

Most recently, principal component analysis has been used to identify three, geographically distinct diatom assemblages in surface sediments of the Ross Sea (Cunningham, 1997). Assemblages in the west-central Ross Sea are characterised by taxa associated with a wind-mixed, open water column; in the western Ross Sea they are dominated by sea ice taxa. A south-central assemblage, characterised by extinct and / or heavily silicified taxa, is interpreted to have been current reworked, similar to that described by Truesdale and Kellogg (1979). Using these data, Cunningham (1997) analysed down-core diatom assemblages as a proxy to infer a Late Pleistocene to Holocene glacial / interglacial transition in the Ross Sea, followed by a mid-Holocene climatic optimum and Late Holocene cooling.

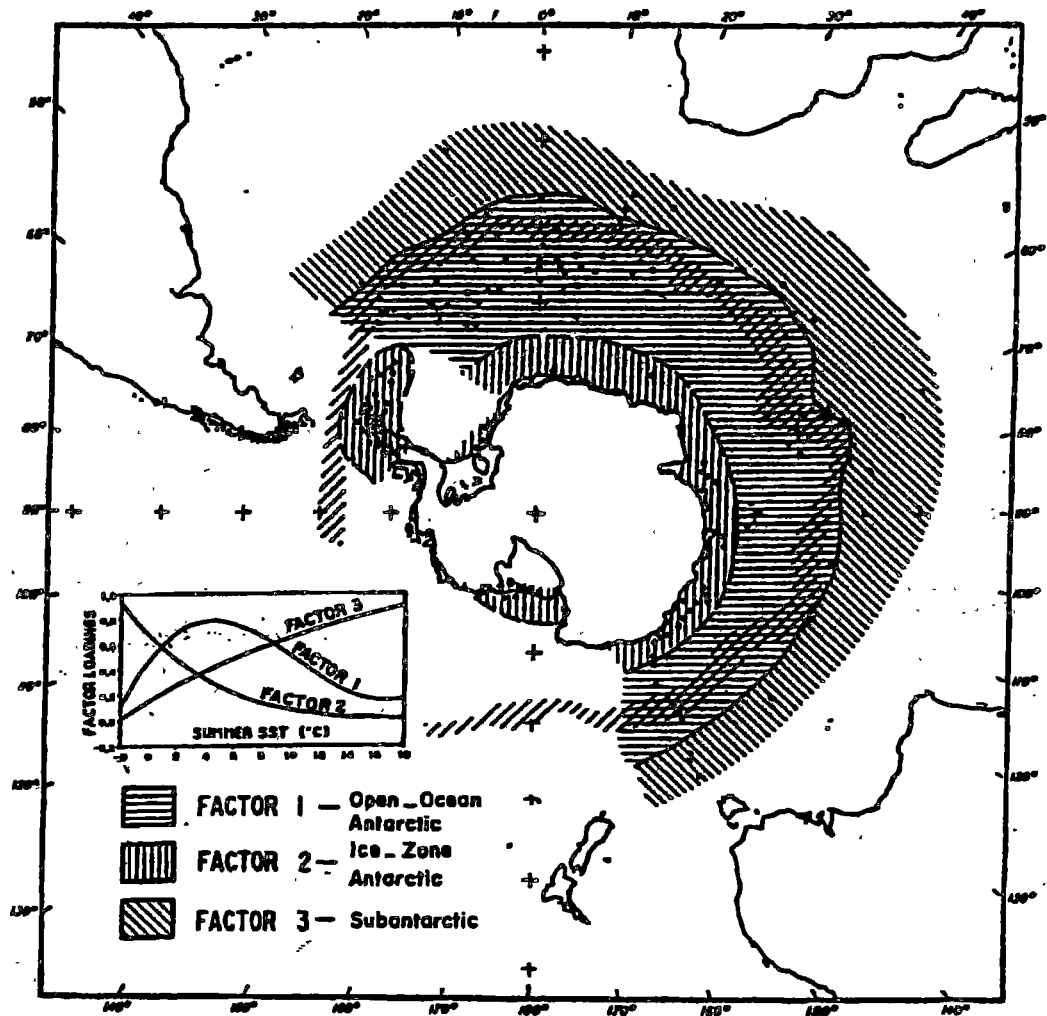


Fig. 4.1. Distribution of the three dominant diatom assemblages defined by Pichon et al. (1992) in sub-Antarctic and Antarctic waters.

4.3 Assemblage Studies in Prydz Bay

Many Antarctic studies investigating the distribution of diatoms in modern marine sediments, and their relation to fossil assemblages, have been concentrated in West Antarctica, chiefly the Ross and Weddell Seas. In comparison, systemic studies of diatoms in surface sediments from East Antarctica, including Prydz Bay, have been limited and, with the exception of lake studies in the Vestfold Hills (e.g. Roberts and McMinn, 1996, 1998), a statistical comparison of these assemblages virtually non-existent.

A qualitative and quantitative comparison of phytoplankton samples from 34 stations in Prydz Bay, collected during February 1969, by Ligowski (1983) enabled the abundance and distribution of the most common species to be identified (Fig. 4:2). In the littoral and central zones of the bay, the most abundant species observed were *Chaetoceros dicheata*, *Nitzschia curta* (= *F. curta*) and *Thalassiothrix antarctica*. To the north, *C. criophilum*, *Rhizosolenia alata* and *T. antarctica* dominated. A study by Stockwell *et al.* (1991), compared planktonic diatom assemblages, from 14 stations, to surface sediment assemblages from five stations. The water column biomass was dominated primarily by three ice-related, pennate taxa, which formed up to 96% of the assemblage: *N. cloisterium*, *N. cylindrus* (= *F. cylindrus*) and *N. curta* (= *F. curta*). In the surface sediment, *N. cylindrus* and *N. curta* formed up to 78% of the assemblage, and *Chaetoceros* resting spores subdominated. An important observation by Stockwell *et al.*'s (1991) study was that, whilst selective preservation of the diatom frustules in the sediment was apparent, dissolution did not seem to greatly affect diatom diversity within the sediments and Prydz Bay appeared to be an ideal site for further diatom studies.

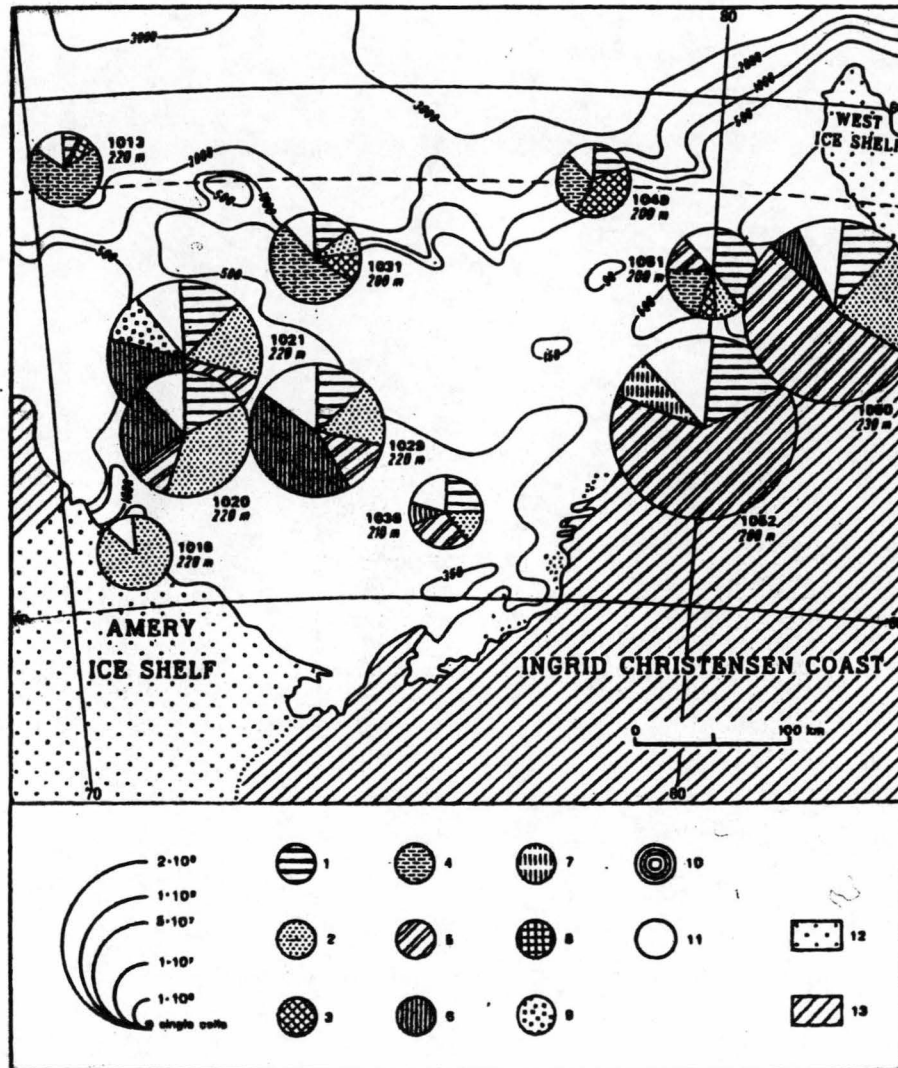


Fig. 4.2. Distribution and abundance of diatom species in Prydz Bay net hauls. 1: *Thalassiothrix antarctica*. 2: *Fragilariopsis curta*. 3: *Chaetoceros criophilum*. 4: *Rhizosolenia alata*. 5: *C. dichæta*. 6: *Nitzschia barkleyi*. 7: *F. sublineata*. 8: *Rhizosolenia hebetata* var. *styliformis*. 9: *F. cylindrus*. 10: *C. atlanticus*. 11: other species. 12: ice shelf. (From Ligowski, 1983).

The analysis of 33 surficial bottom sediments from Prydz Bay by Franklin (1993) identified three sedimentary facies, and four foraminiferal and two diatom assemblages (Fig.4.3). Diatom assemblages were dominated by *N. curta* in all but one site (site T11), near the seaward end of Prydz Channel; here, *N. kerguelensis* (= *F. kerguelensis*) dominated. The abundance of *N. kerguelensis* at site T11 was interpreted to represent the strong, oceanic influence that the incoming, southward current associated with the Prydz Bay gyre (discussed in Chapter 5) as it crosses the continental shelf into the bay (Franklin, 1993). A more comprehensive analysis of surface sediments from both Prydz Bay and Mac.Robertson Shelf has been carried out most recently by Harris *et al.* (in press). Using 206 samples, and incorporating cluster analysis, Harris *et al.* (in press) identified five lithofacies on the continental shelf. The abundance and distribution of two, key indicator diatom species, *F. curta* and *F. kerguelensis*, among other parameters defined the lithofacies. The distribution and significance of the lithofacies is discussed in Chapter 5.

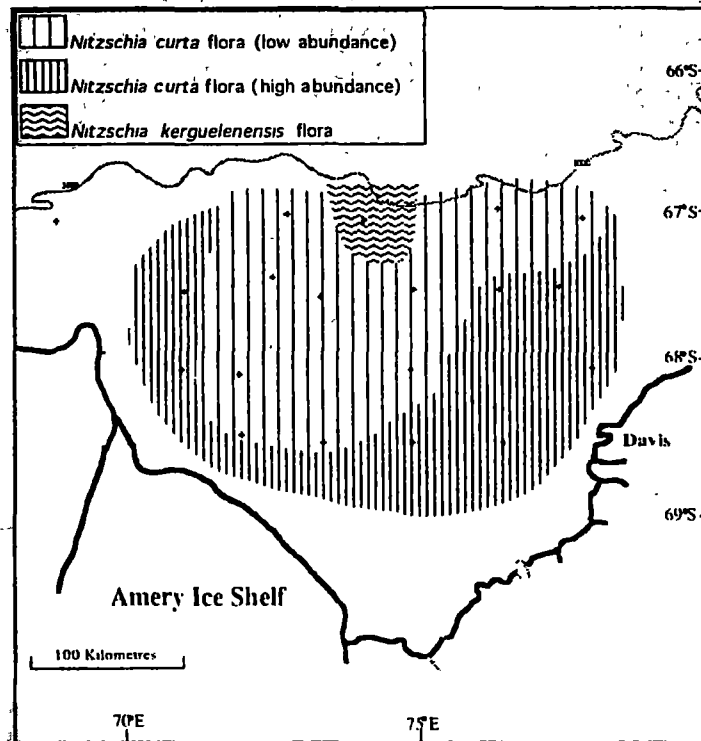


Fig. 4.3. Distribution of diatom assemblages in Prydz Bay surface sediments. (From Franklin, 1993).

Detailed, qualitative and quantitative analyses of down-core, sedimentary diatom assemblages in Prydz Bay are even more limited than water column or surface sediment assemblage studies. Pushina *et al.* (1997) used diatom data from eight cores, collected during several Soviet Antarctic Expeditions, to interpret the Holocene, palaeoecological environment of Prydz Bay. Rathburn *et al.* (1997) incorporated the diatom and foraminiferal data of two gravity cores, collected from Fram Bank, to indicate changes in sea-ice patterns and oceanographic conditions over the past 8000 years. Both studies used a multi-disciplinary approach (micropalaeontological, lithological and geochemical) data as part of the analysis, but neither used quantitative, statistical procedures to compare fossil diatom assemblages with those being deposited today.

4.4 Aims of the Current Research

In order to determine the response of ice-caps to climate change, knowledge of palaeoclimates in polar regions is of major concern. Compared to Northern Hemisphere, data from the Southern Hemisphere has been relatively limited, however, particularly that concerning the response of the high latitude Southern Ocean during the Late Quaternary (Leventer *et al.*, 1993). Given that the success of palaeoecological studies on the West Antarctic continental shelf, such as those discussed above, have yielded valuable results, the need for similar studies in East Antarctica is obvious. This is particularly so if we are to address the response of the Antarctic Ice Sheet, as a whole, to past and future global climate change.

The aims of the current research project are two-fold. The first involves an extensive survey of over 100 surface sediments recovered from Prydz Bay and Mac.Robertson Shelf, East Antarctica, to determine the abundance and distribution of modern, planktonic diatom assemblages. Using multivariate statistical techniques, the relationship between these assemblages and known oceanographic parameters will be determined. From this knowledge, the second aim compares the surface diatom assemblages to those down-core, as a means of reconstructing the natural variability of Holocene palaeoclimates on the East Antarctic continental shelf. Six gravity cores, with ages spanning from the Late Pleistocene to Holocene, are examined.

– Chapter 5 –

Prydz Bay and Mac.Robertson Shelf

5.1 Physical Setting

5.1.1 Prydz Bay

Prydz Bay is a triangular-shaped embayment lying in the Indian Ocean sector of the Southern Ocean, East Antarctica (Fig. 5.1). Mac.Robertson Land (69°E) to the west, and by Princess Elizabeth Land and the West Ice Shelf (80°E) to the east border it. The south-western apex of the bay has direct contact with the Amery Ice Shelf (70°S), which forms almost 200 km of the bay's coastline (Wong, 1994). The ice shelf is 300 m thick at the ice-front (Budd *et al.*, 1982). The northern limit of the bay extends offshore into the Princess Elizabeth Trough (Wong, 1994); however, Prydz Bay proper is normally considered that area south of the imaginary line between the West Ice Shelf and Cape Darnley. The dimensions of this area are approximately 400 km east-west and 300 km north-south (Franklin, 1993), and cover a total area of ~80 000 km² (Stagg, 1985).

Morphologically, the continental shelf of Prydz Bay is typical of other Antarctic continental shelves (O'Brien, 1994). The broad, deep Amery Depression occupies the inner region of the bay and descends to a depth of 800 m. Deep trenches extend northwards from the depression to form the Prydz Channel, along which cold shelf water has a direct contact with warmer, deep ocean water (Smith and Tréguer, 1994; Nunes Vaz and Lennon, 1996). The narrower and deeper Svenner Channel also connects shelf waters from the West Ice Shelf, east of the bay, with the inner part (Nunes Vaz and Lennon, 1996). Unlike Prydz Channel, the Svenner Channel is a morphologically complex structure and has several shallower saddles along its axis (O'Brien and Harris, 1996). Landward of the continental shelf break, the Amery Depression is bordered by two shallow banks. Four Ladies Bank, to the north-east, and Fram Bank, to the north-west, rise to a minimum depth of 200 m and form a partial barrier to water exchange with the deep ocean (Smith and Tréguer, 1994).

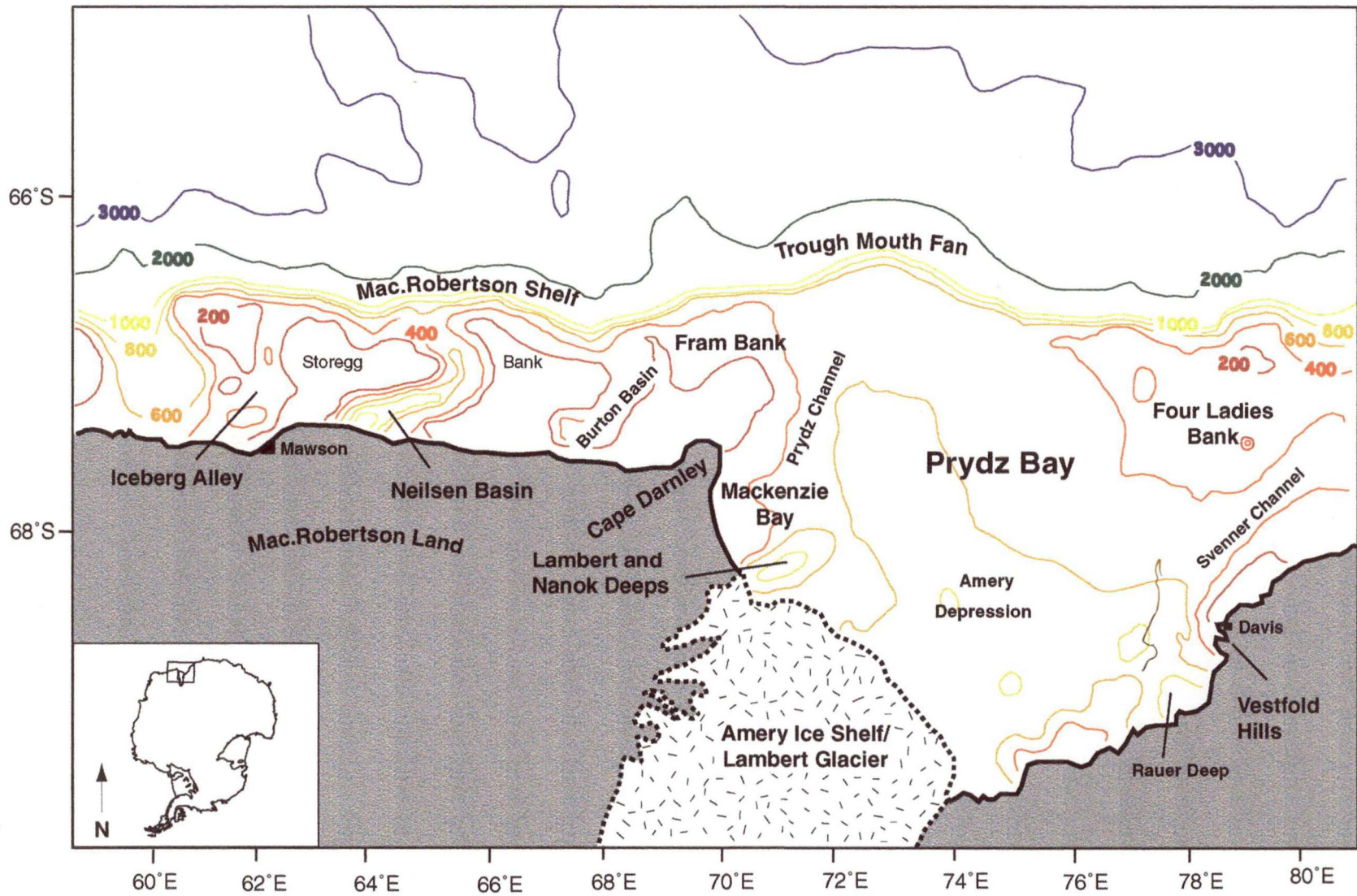


Fig. 5.1. Location of Prydz Bay and Mac.Robertson Shelf, East Antarctica.

The maximum depth of Prydz Bay occurs adjacent to the Amery Ice Shelf, where the Lambert and Nanok Deeps exceed 1000 m (Franklin, 1993). The smaller, and deeper, Lambert Deep is a narrow trough, trending north-east and south-west. Surrounding the Nanok Deep is an irregular, crescent-shaped rim – the Nella Rim – that delineates water from the Nanok Deep and Amery Depression (Quilty, 1985). Southwest of Davis Station lies another small depression, the Rauer Deep, thought to exceed 1100 m water depth (Quilty, 1985; Stagg, 1985).

Sediment-laden ice is deposited in Prydz Bay from the Lambert Glacier / Amery Ice Shelf system (Harris *et al.*, in press). Where sediments have been deposited along the axis of the glacier, they have prograded offshore to form the Prydz Bay Trough Mouth Fan. The fan is a major area of deposition for the bay and extends at least 90 km offshore and is up to 140 km in width (O'Brien and Harris, 1995). On the outer shelf banks, sediments are thickset, and thin to absent over much of the inner shelf (Stagg, 1985). Iceberg plough marks are common on the outer shelf, in particular on Fram Bank and Four Ladies Bank (Harris *et al.*, in press). On parts of Four Ladies Bank, however, the seafloor is so shallow that icebergs ground before crossing them. After breaking up by calving and spalling, the icebergs drift across the rest of the bank unhindered and here undisturbed sediments have been deposited (O'Brien, 1994).

Five surface sediment lithofacies have been identified in Prydz Bay, based on biogenic silica, calcium carbonate, grain size analysis, and the relative abundance of the diatom taxa *Fragilariopsis curta* and *F. kerguelensis* (Harris *et al.*, in press) (Fig. 5.2):

1. Slightly gravelly, sandy mud (g)sM.
2. Siliceous mud and diatom ooze (SMO).
3. *F. kerguelensis* pelagic ooze.
4. *F. curta* gravelly, sandy mud (mgS).
5. Calcareous gravel.

The (g)sM lithofacies is distributed on the shallower areas of the shelf, including Four Ladies Bank and western Prydz Bay, and Mac.Robertson Shelf. It contains coarse,

poorly-sorted sediment that has been reworked by iceberg ploughing. The SMO is the most extensively distributed lithofacies in Prydz Bay. It occurs in the deepest areas of the continental shelf, such as the Amery Depression, Burton Basin, Nielsen Basin, and Iceberg Alley, where it is protected from iceberg and current reworking, and forms thicknesses >5 m. *Fragilariopsis kerguelensis* pelagic ooze is similar to the (g)sM lithofacies, but is characterised by the abundance of *F. kerguelensis* frustules in the sediment and is distributed offshore of the continental shelf break zone. *Fragilariopsis curta* mgS forms a transitional belt between the (g)sM and SMO and is also correlated to the iceberg ploughed zone on Four Ladies Bank. Calcareous gravel is the rarest lithofacies and has been described from only two locations: on the shallowest portion of Storegg Bank, and a small area adjacent to the shelf break at the apex of the Prydz Bay Trough Mouth Fan.

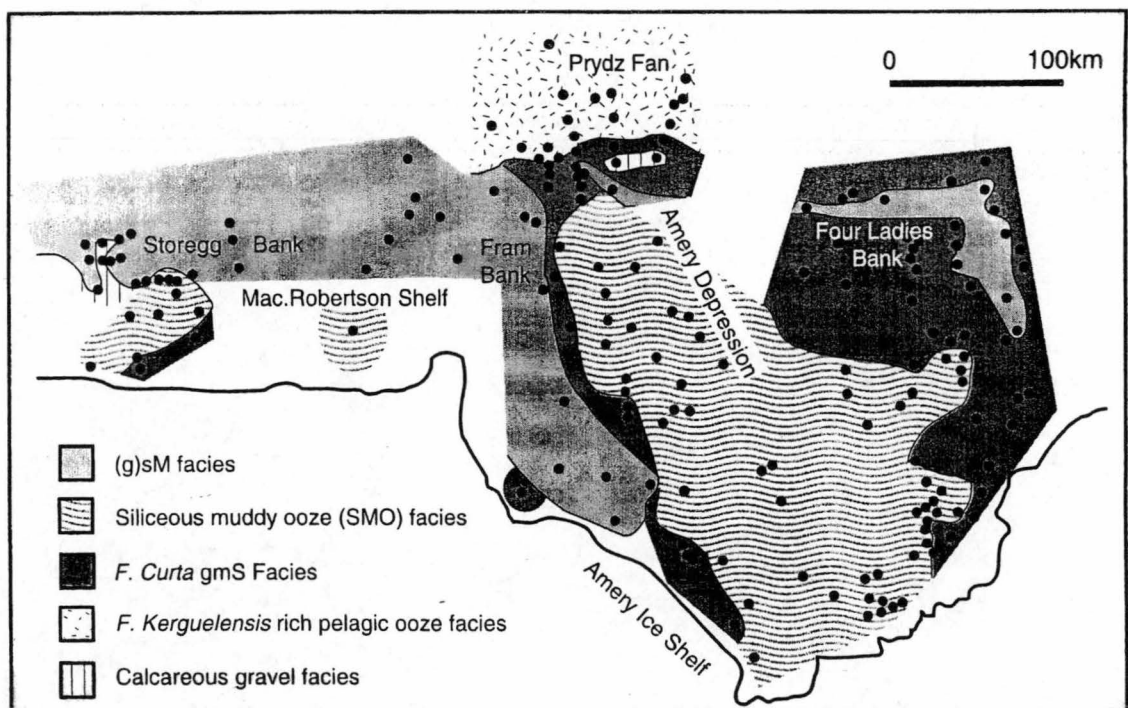


Fig. 5.2. Surface sediment lithofacies identified in Prydz Bay. (From Harris et al., in press).

5.1.2 Mac.Robertson Shelf

The Mac.Robertson Shelf lies adjacent to Mac.Robertson Land. It extends west of Prydz Bay for 400 km, from 69° to ~60°E, and is bounded by ice cliffs and small glaciers to the south (O'Brien *et al.*, 1994). Compared to Prydz Bay, it is much narrower and more rugged, with an average shelf width of 90 km (Harris *et al.*, 1996). It is otherwise similar to most other Antarctic continental shelves, with inshore deeps separated from the shelf edge by flat-topped, shallow banks (Stagg, 1985).

The average shelf depth on Mac.Robertson Shelf is 350 m (Harris and O'Brien, 1996). This rises to a minimum depth of 110 m to 150 m on East and West Storegg Banks, and Fram Bank (O'Brien *et al.*, 1994). The banks separate three, steep-sided valleys that are joined to the shelf break by arcuate shelf valleys (Harris and O'Brien, 1996). All are typically fjordal, being steep-sided (up to 70°), flat-floored and U-shaped (O'Brien, 1994; Harris and O'Brien, 1996). The deepest, Nielsen Basin, has a maximum depth of ~1400 m and is characterised by several closed depressions that are separated by shallower sills (Harris *et al.*, 1996). The depths of both Burton Basin and Iceberg Alley also locally exceed 1200 m.

Mac.Robertson Shelf is largely an erosional environment, compared to Prydz Bay (Stagg, 1985; O'Brien, 1994). This is due to a strong, westward flowing shelf current associated with the East Wind Drift, which resuspends sediment as it is settling. As a result the outer shelf and upper slope of Mac.Robertson Shelf are characterised by a high sand and gravel content, in comparison to the ice-rafted, fine sand and diatoms that accumulate within the deep shelf basins (Harris *et al.*, 1997a).

Four geomorphological zones are described on Mac.Robertson Shelf (Harris and O'Brien, 1996), based on a compilation of geophysical, sedimentological and bathymetric data (Fig. 5.3). These are:

1. High-relief, ridge and valley topography.
2. Smooth sea-floors associated with depositional environments.
3. Low-relief, planated bank-tops.

4. Sea-ward bank margins exhibiting iceberg gouges and dunes.

The high-relief, ridge and valley topography of geomorphic zone one was formed probably by subglacial incision and erosion during Pleistocene and older glacial maxima; zone two was formed by deposition of subglacial and glacial-marine sediment (Harris and O'Brien, 1996). Zones three and four are a product of iceberg grounding and erosion by strong bottom currents (Harris and O'Brien, 1996).

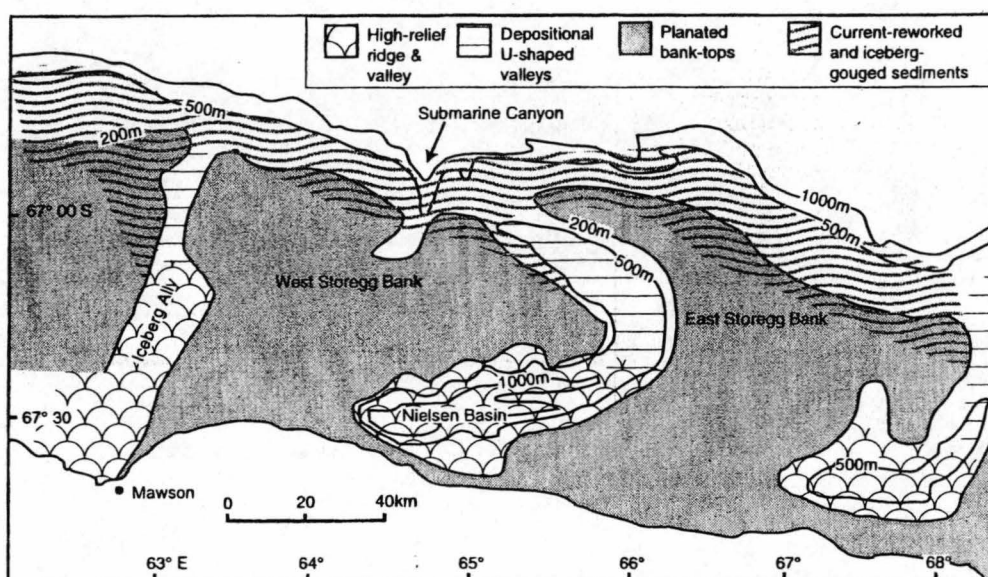


Fig. 5.3. Geomorphic zones of Mac.Robertson Shelf. (From Harris and O'Brien, 1996).

5.2 Sea Ice Distribution

Sea ice covers Prydz Bay throughout autumn, winter and spring (Smith *et al.*, 1984; Smith and Tréguer, 1994) and extends northwards to 58°–60°S (Jacka, 1983). Polynyas are commonly found to the north-west (MacKenzie Bay), and to the south-east (off Davis Station) (Smith *et al.*, 1984). Smith and Tréguer (1994) associate these with the presence of anomalously warm waters found towards the centre of the bay. Ice breakout occurs in early summer, so that open water is predominate by January, and is often associated with seasonal phytoplankton blooms.

5.3 Oceanography

There is relatively little known about the oceanography of Prydz Bay and Mac.Robertson Shelf. This contrasts with the vast amount of physical and chemical data collected from the two largest Antarctic embayments – the Ross Sea (Pacific Sector) and Weddell Sea (Atlantic Sector). Prior to 1970, a number of exploratory voyages were carried out by Soviet research expeditions (summarised in Nunes Vaz and Lennon, 1996). These were followed by large-scale, U.S. operations from the Antarctic Shelf (62°E) to the Crozet and Kerguelen Plateaux and South Africa (Jacobs and Georgi, 1977) and in the southwest Indian Ocean (Gordon and Molinelli, 1982). Following Australia's involvement with BIOMASS¹ during the early 1980's, a number of ANARE voyages aboard the MV *Nella Dan* were carried out in Prydz Bay (Table 5.1). Although these were concerned primarily with biological data collection, some hydrographic data was obtained with the collection of physical and chemical oceanographic data. More recently, a systematic oceanographic survey of Prydz Bay was carried out aboard the RSV *Aurora Australis* during the FISHOG92², from which Wong (1994) analysed the structure and dynamics of water masses and circulation. The discussion below reviews the current knowledge of oceanography in Prydz Bay, Mac.Robertson Shelf and the surrounding waters.

5.3.1 Horizontal Water Circulation

Horizontal water circulation in Prydz Bay is characterised by four principal features (Fig. 5.4), based on geostrophic (density) measurements from water salinity and temperature. These are the:

1. Eastward zonal flow.
2. Westward flowing slope current.
3. Westward flowing coastal current.
4. Cyclonic gyre system.

¹ BIOMASS – Biological Investigation of Marine Antarctic Systems and Stocks

² FISHOG92 – 1992 Fisheries and Oceanography Voyage

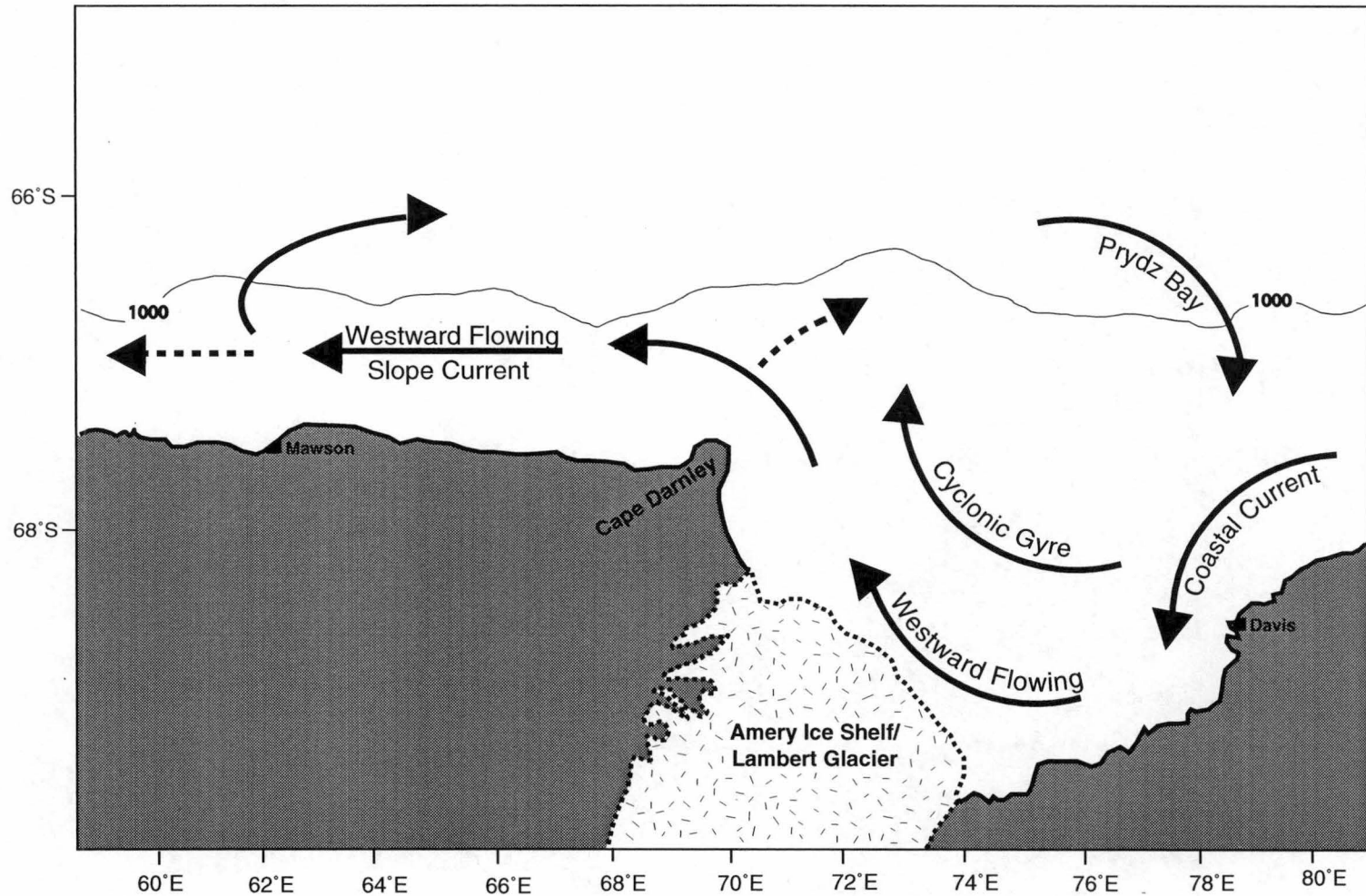


Fig. 5.4. Distribution of major horizontal water currents in Prydz Bay. Eastward Zonal Flow (65°S) not illustrated. (After Smith et al., 1984; Wong, 1994; and Nunes Vaz and Lennon, 1996).

The four features are analysed and described in detail by Wong (1994) and confirm the findings of previous surveys carried out over the last two decades – chiefly that of Smith *et al.* (1984), Middleton and Humphries (1989), Smith and Tréguer (1994), and Nunes Vaz and Lennon (1996).

Table 5.1. ANARE marine science oceanographic surveys conducted between 1981 – 1987.

| Voyage | Year | Publication |
|----------------------|----------------|-------------------------------|
| FIBEX-1 ³ | Jan - Mar 1981 | Kerry <i>et al.</i> , 1987a |
| GEOSCIENCE | Jan - Mar 1981 | Woehler <i>et al.</i> , 1987 |
| ADBEX-1 ⁴ | Nov - Dec 1982 | Kerry and Woehler, 1987 |
| ADBEX-2 | Jan - Feb 1984 | |
| SIBEX-2 ⁵ | Jan 1985 | Kerry <i>et al.</i> , 1987b |
| ADBEX-3 | Sep - Dec 1985 | |
| AAMBER ⁶ | Feb - Mar 1987 | Woehler and Williams, 1988 |

Eastward Zonal Flow

The eastward zonal flow is characterised by waters from the broad, deep Antarctic Circumpolar Current (ACC), which is driven by prevailing westerly winds that transport surface water eastwards. As coastal, easterly winds create a westward flow, divergence and deep water upwelling occurs at ~65°S. Here the Antarctic Divergence (AD) allows deep water contact with the atmosphere (Gordon, 1971). Data compiled by Nunes Vaz and Lennon (1996) from ADBEX-1, AAMBER and FIBEX-1 indicate that the primary source of water inflow to Prydz Bay at lower levels (200 m – 500 m) is warm water diverted across the continental shelf break from the offshore ACC. The upwelling processes associated with tides and continental shelf waves, generated by strong coastal

³ FIBEX-1 – First International BIOMASS Experiment

⁴ ADBEX – Antarctic Division BIOMASS Experiment

⁵ SIBEX-2 – Second International BIOMASS Experiment

⁶ AAMBER – Australian Antarctic Marine Biological Ecosystem Research

winds in the bay, aid this inflow (Middleton and Humphries, 1989; Smith and Tréguer, 1994).

Westward Flowing Slope Current

The westward flowing slope current is defined as a narrow current centered on 66° – 67°S that is associated with the East Wind Drift, which dominates south of the AD (Wong, 1994). Smith *et al.* (1984) suggest that the westward slope current is not a distinct current, but instead is a broken band of flow that occurs between the AD and the Prydz Bay continental shelf rise.

Westward Flowing Coastal Current

The westward flowing coastal current is a strong current (8.0 sec^{-1} ; Wong, 1994) that is also suggested to be associated with the East Wind Drift (Wong, 1994). It is the principal source of inflow to Prydz Bay at upper water levels (<200 m), and provides a source of cold water that has originated from the east, in the vicinity of the West Ice shelf, and penetrated into the southeast of the bay (Smith *et al.*, 1984).

Summer AAMBER data have demonstrate that the westward flowing coastal current is very well defined and continuous around the bay (Nunes Vaz and Lennon, 1996). Iceberg sightings and ice conditions in the bay are also consistent with a westward coastal flow regime. Icebergs off Princess Elizabeth Land, for example, have been observed to move in a south-west direction, whilst those calving off the Amery Ice Shelf follow the western periphery of the bay, towards Cape Darnley (Smith *et al.*, 1984). Spring ADBEX-1 data, however, indicate that the southeast region of Prydz Bay might be a zone of confluence for inflowing water, prior to its turning westward along the coast. Nunes Vaz and Lennon (1996) suggest that this represents a seasonal difference or an inter-annual cycle, rather than a separate coastal flow regime.

Within the Prydz Bay, water flow is at least partially controlled by bathymetry (Smith and Tréguer, 1994) and contours of “effective” geopotential anomaly, which allow the westward coastal current to flow beneath the Amery Ice Shelf (Hellmer and Jacobs,

1992; Wong, 1994). As a consequence of this flow, high salinity shelf water (HSSW) is introduced to the base of the Amery Ice Shelf, by a process other than normal thermohaline convection and slope of the continental shelf towards the grounding line. From beneath the western end of the ice shelf, HSSW, which entered from the east, emerges as a considerable volume of very cold ice shelf water (ISW). The ISW is characterised by a temperature $< -1.89^{\circ}\text{C}$, which it has obtained by heat loss to, and melting below, the Amery Ice Shelf. As it rises in the water column ice crystals form to compensate for the super-cooling that would otherwise occur (Hellmer and Jacobs, 1992).

Water emerging from beneath the Amery Ice Shelf continues its westward flow and exits Prydz Bay as a concentrated flow west along Mac.Robertson Shelf. Here it joins with the westward flowing slope current (Wong, 1994) and both are ultimately diverted offshore at $\sim 62^{\circ}\text{E}$. An unknown proportion continues along the shelf towards Enderby Land (Nunes Vaz and Lennon, 1996). This flow has been confirmed by the direction of icebergs tracked leaving Prydz Bay (Hosie, 1994). Some have been observed to continue moving west along the shelf, past Mawson Station ($\sim 62^{\circ}\text{E}$), and beyond Enderby Land.

An increase in water salinity and decrease in potential temperatures have also been noted around the coastal perimeter of Prydz Bay, from east to west. Similar observations have been made in the Weddell and Ross Seas. In Prydz Bay, the phenomenon is attributed to the progressive salinity enhancement by brine rejection that occurs during westward coastal flow around the bay (Nunes Vaz and Lennon, 1996).

Cyclonic Gyre System

A major feature of the horizontal circulation in Prydz Bay is a large, cyclonic gyre that is fed by a broad inflow of water from the north-east (Smith and Tréguer, 1994). The gyre is centered in the bay at $\sim 73^{\circ}\text{E}$ (Wong, 1994), and appears on the western side of the bay where it is bordered by Cape Darnley and Fram Bank (Smith *et al.*, 1984). Its formation is the combined result of cold, fresh water at the western end of Prydz Bay

(HSSW, contributed by the Amery Ice shelf), which produces a dynamic high, and a pool of salty water in the middle of the bay, which forms a dynamic low due to brine rejection during winter sea ice formation (Wong, 1994). Water flow within the gyre involves partial re-circulation, so that some of the outflow, exiting near Cape Darnley, is re-circulated offshore and fed back into the bay. The re-circulated proportion is significantly less than that entering from the east (as westward flowing coastal water; Nunes Vaz and Lennon, 1996). The proportion that is not re-circulated continues west along Mac.Robertson Shelf as part of the westward flowing coastal current. The presence of the cyclonic gyre is consistent with all data reviewed by Nunes Vaz and Lennon (1996) (ADBEX-1, AAMBER, FIBEX-1, SIBEX-2) and Wong (1994).

5.3.2 Water Masses and Vertical Structure

Seven principal vertical water masses can be identified in the vicinity of Prydz Bay, based on temperature and salinity profiles (Fig. 5.5):

1. Summer surface water.
2. Circumpolar deep water.
3. Winter water.
4. High salinity shelf water.
5. Ice shelf water.
6. Warm deep water.
7. Antarctic bottom water and Prydz Bay bottom water.

The water masses geographical distribution is illustrated in Fig. 5.6.

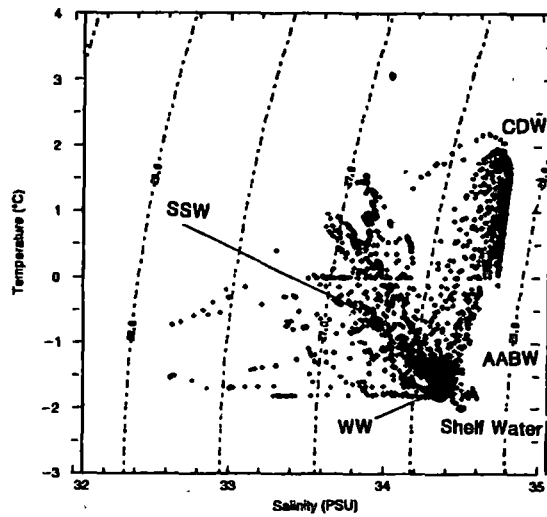


Fig. 5.5. Schematic distribution of potential temperature and salinity determination for Prydz Bay. (From Smith et al., 1984).

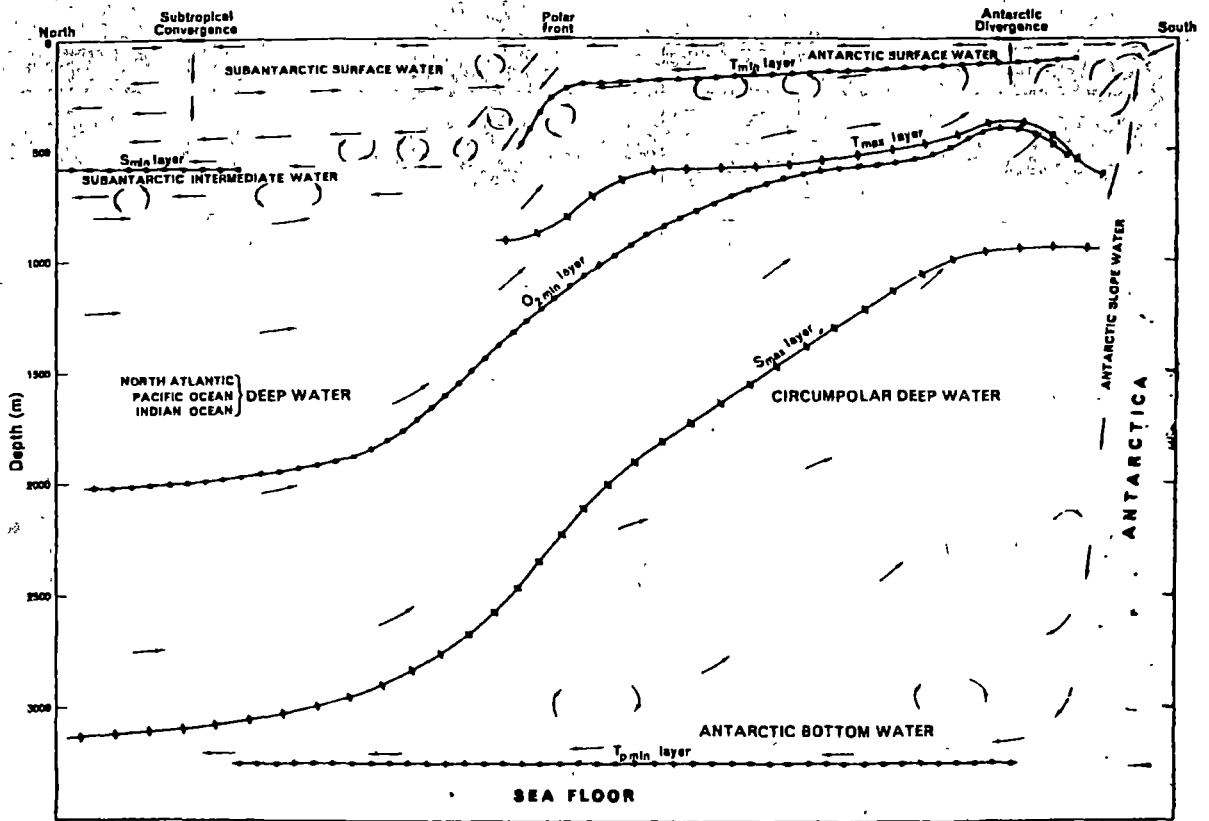


Fig. 5.6. Schematic distribution of water masses and core layers in Antarctic waters. (From Gordon, 1971).

Summer Surface Water

Summer surface water (SSW) is a distinct, but highly variable, Antarctic water mass. It is generally characterised as a relatively fresh water layer (salinity ~33.5‰ to ~34.0‰) with a temperature $> 0^{\circ}\text{C}$. These characters are dependent on the distribution and thickness of sea ice (Wong, 1994). Within the shelf zone, SSW typically forms to a depth from 10 m to 60 m, depending on the prevailing ice conditions. North of Prydz Bay, where sea ice is less thick, depth can exceed 100 m (Smith and Tréguer, 1994) as lesser amounts of solar radiation are required to melt the ice and it instead acts to raise the surface water temperature (Grigor'yev, 1970).

Due to the heating and the melting of sea ice during summer, SSW forms a pronounced, seasonal halocline on both the continental shelf and adjacent offshore zone (Smith *et al.*, 1984; Hosie, 1994). It has also been noted that within Prydz Bay, relatively warmer SSW temperatures have been recorded in the southwest, just north of the Amery Ice Shelf. These anomalously warm temperatures are attributed to the earlier breakout of sea ice in this region, compared to elsewhere within the bay (Wong, 1994). Smith *et al.* (1984) also note that SSW depth tends to be greatest here. The coldest SSW, which forms near the West Ice shelf, is correlated with ice conditions.

Circumpolar Deep Water

Circumpolar deep water (CDW) is the most abundant water mass in the Antarctic oceanic domain. It is characterised as a modified, warm ($0.0^{\circ} - 2.0^{\circ}\text{C}$), salty subantarctic water (Hosie, 1994a), which originates from the North Atlantic, Pacific and Indian Oceans (Gordon, 1971). To the south it is bordered by the AD. Circumpolar deep water occupies the water column between depths of 300 m - 2000 m north of the AD, rising to ~600 m at its southern-most extent in association with upwelling (Wong, 1994). Like SSW, it produces a pronounced, seasonal thermocline.

Circumpolar deep water is comprised of two components (Smith and Tréguer, 1994): a deep layer, identified by a salinity maximum (34.70‰ - 34.75‰) and formed by a water mass related to North Atlantic deep water; and an upper layer with a characteristic

oxygen minimum and influenced by the Pacific and Indian Oceans. South of the AD, the two layers become modified so that along the continental shelf slope only a single core layer of warm CDW is evident. This layer is suggested to be the product of mixing between CDW and continental shelf water, and is referred to as Prydz Bay bottom water (Middleton and Humphries, 1989), discussed below.

Winter Water

Below the SSW and above the CDW lies a temperature minimum water mass, considered to be the remnant of a winter mixed layer, which forms from spring to autumn. Unlike SSW, this winter water (WW) possesses distinct properties, with temperature $< -1.5^{\circ}\text{C}$ and salinity $34.2\text{‰} - 34.56\text{‰}$ (Smith *et al.*, 1984; Smith and Tréguer, 1994).

Winter water forms a layer up to 300 m thick over the continental shelf, which decreases north of Prydz Bay to a minimum of ~ 30 m (Wong, 1994). A sharp transition zone, present near the continental rise, distinguishes shelf zone WW from oceanic WW. Winter water over the continental shelf is not so clearly defined from CDW, due to the greater penetration of winter mixing (Smith *et al.*, 1984), and in Prydz Bay such water has been referred to as low salinity shelf water (LSSW) (Smith *et al.*, 1984).

High Salinity Shelf Water

A relatively salty and dense layer of high salinity shelf water (HSSW) is present over the continental shelf. It is a subclass of continental shelf water (CSW) (Smith *et al.*, 1984; Wong, 1994). High salinity shelf water lies below WW in places where seafloor depressions act to trap the saline, dense water that is formed by brine rejection during the formation of winter sea ice (Middleton and Humphries, 1989; Wong, 1994). Like WW, HSSW has a temperature $< -1.5^{\circ}\text{C}$, but is characterised by a salinity $> 34.50\text{‰}$ (Smith *et al.*, 1984).

High salinity shelf water is mostly confined to Prydz Bay and Mac.Robertson Shelf, but some may be forced off the shelf. As it flows down the continental slope, the HSSW

mixes with CDW, forming modified Prydz Bay Bottom Water (PBBW) (Middleton and Humphries, 1989). Although PBBW is able to flow to intermediate depths, it is not dense enough to reach abyssal depths and form true Antarctic bottom water (AABW) (Middleton and Humphries, 1989; Smith and Tréguer, 1994).

Ice Shelf Water

Ice shelf water (ISW) is a saline, super-cooled water mass, produced near WW, with a temperature $< -2.0^{\circ}\text{C}$. It is formed by heat loss and salt rejection beneath the Amery Ice Shelf (Smith *et al.*, 1984). Jacobs *et al.* (1992) suggest that HSSW draining into ice shelf cavities below the Amery Ice Shelf, which have formed where the continental shelf deepens towards the grounding line (Wong, 1994), may evolve into the cold ISW by providing latent heat for basal melting of the ice shelf. Refreezing on the underside of the shelf would then lead to the accumulation of super-cooled, salty ISW (Smith *et al.*, 1984) that is circulated out into the bay at intermediate depths by thermohaline convection (Wong, 1994). Together, the majority of cold, Prydz Bay water $< -1.6^{\circ}\text{C}$ (i.e. ISW, WW, and HSSW) leave the bay either directly offshore or initially westward. Eventually most of this water joins the eastward ACC as a lens of relatively cold water centered at a depth of 100 m (Nunes Vaz and Lennon, 1996).

Warm Deep Water

Warm deep water (WDW) is often referred to as CDW. Wong (1994) distinguishes it as water that occurs in the oceanic domain and with salinity similar to CDW ($\sim 34.70\text{‰}$), but a cooler temperature ($0.0^{\circ} - 1.0^{\circ}\text{C}$) and with a slightly higher dissolved O_2 content compared to CDW. In the Weddell Sea, the mixing of WDW and WW intrudes over the continental shelf break and mixes with HSSW. The resulting water mass descends the continental slope to form AABW. In Prydz Bay, WDW has been noted only in the oceanic domain, where it occupies a depth of ~ 300 m, and not over the continental shelf (Wong, 1994) below CDW. It rises to a depth of 650 m south of CDW, at the continental slope.

Antarctic Bottom Water and Prydz Bay Bottom Water

Antarctic bottom water (AABW) is the deepest water close to the Antarctic continent and is generally characterised by temperatures $< 0^{\circ}\text{C}$ and salinity $34.6\text{‰} - 34.7\text{‰}$ (Smith *et al.*, 1984; Wong, 1994). Its precise method of production is unknown, although it is generally accepted that cold, dense HSSW water mixes with saline CDW near the continental shelf to form modified AABW. The resulting, denser water mass flows down the continental slope and is dispersed into the abyssal layers of the major oceanic basins (Gordon, 1971; Smith *et al.*, 1984; Wong, 1994).

Antarctic bottom water is found in almost all sections of the deep ocean off Prydz Bay; however, it is uncertain if deep mixing in the bay and the adjacent continental shelf contribute to this water mass. As discussed above, a modified form of AABW (PBBW) can be found to intermediate depths, at least, when HSSW and CDW mix and flow down the continental slope. A water mass suggested to be AABW, and with sufficient characteristics to penetrate to the ocean floor, has been identified laying against the continental slope of Prydz Bay, between 2500 m - 5000 m and with a temperature $< -0.3^{\circ}\text{C}$ and salinity $< 34.66\text{‰}$ (Jacobs and Georgi, 1977; Mantyla and Reid, 1983). The high dissolved oxygen values ($> 5.57 \text{ ml l}^{-1}$) and low silicate values ($< 120 \mu\text{m l}^{-1}$) indicate that the water was formed locally (Nunes Vaz and Lennon, 1996), possibly arisen from a continual process of mixing between Enderby Land / Prydz Bay coastal waters and dense, deep water (Smith and Tréguer, 1994). A similar penetration of cold water over the continental slope at 62°E has been observed by Smith *et al.* (1984).

For the production of ABBW in Prydz Bay to be confirmed, water of sufficient potential density must be produced within the bay and be observed descending towards the foot of the continental slope west of the bay (Nunes Vaz and Lennon, 1996). The SSW and ISW present in Prydz Bay are not dense enough to promote bottom water formation during summer, but their salinity is thought to increase significantly during active winter sea ice formation (Nunes Vaz and Lennon, 1996). During this time, dense water plumes would have the potential to descend the continental slope, and perhaps reach its base. Such plumes have been observed at 62°E (Smith *et al.*, 1984), but were sufficiently

dense to form AABW. Similarly, a plume of HSSW mixed with CDW has been observed flowing down the continental slope from Prydz Bay, forming PBBW (Middleton and Humphries, 1989). This plume, however, did not reach the ocean floor. Such evidence has led to the conclusion that Prydz Bay is a source of dense water that descends the continental slope to intermediate depths, but not necessarily to the ocean floor to form true AABW (Nunes Vaz and Lennon, 1996).

Wong (1994) has identified two types of PBBW: a low salinity type and high salinity type. Low salinity PBBW has similar salinity values to AABW west of the Kerguelen Plateau. East of this, AABW, originating from the Adelie Coast and Ross Sea and with higher salinity values, is present. The high salinity PBBW observed by Wong (1994) is higher still in salinity than that observed east of the Kerguelen Plateau, and is interpreted as having originated from a more local source. It is therefore hypothesised that winter shelf water is more saline than summer shelf water, due to sea ice formation and brine rejection (Wong, 1994; Nunes Vaz and Lennon, 1996). The salty, shelf water is then thought to sink in a northeast direction, down the continental slope, to mix with CDW and form high salinity PBBW in winter (Wong, 1994).

5.3.3 Summary

The four main features of horizontal water circulation in Prydz Bay are consistently supported by the data collected by oceanographic surveys to the region. At lower water depths, warm water originating from the ACC is diverted into the bay across the continental shelf break from the west. A westerly flowing slope current also supports a smaller inflow. The major source of inflow to Prydz Bay, however, comes from a westward flowing coastal current, fed by the East Wind Drift from the West Ice Shelf. The current flows continuously around the perimeter of the bay and exits as a concentrated flow that continues west along Mac.Robertson Shelf. A portion of the westerly outflow may be re-circulated around Prydz Bay by a cyclonic gyre system. The gyre is a major feature of Prydz Bay's horizontal circulation, and is fed primarily by waters from a broad inflow to the northeast.

Distinct vertical water masses are evident in Prydz Bay (i.e. SSW, WW, CDW, HSSW, ISW, and WDW), but there is no direct evidence to indicate that the bay is a local source of AABW. High salinity shelf water is thought to mix with CDW and descend the continental shelf to intermediate depths as modified warm PBBW. For conclusive evidence of bottom water formation, however, a sufficiently dense water mass, produced within the bay, must be observed descending towards the base of the continental slope in winter.

– Chapter 6 –

Materials and Methods

6.1 Sediment Preparation

Sediment samples collected from Prydz Bay and Mac.Robertson Shelf, from five separate research expeditions (Table 6.1, Fig. 6.1), were analysed to determine diatom abundance and distribution. Samples were collected using a Van Veen grab, Ekman grab, pipe dredge, or gravity core. In the case of core samples, only core-tops were analysed. Individual sample locations are listed in Table 5.2. Approximately 0.5 g of sediment was sub-sampled from each, and left to soak for three days in 10 ml of 15% H₂O₂, to remove organic matter. They were then centrifuged three times at 2500 revs⁻¹ for 5 minutes; between each, samples were washed in distilled water to remove residue.

6.2 Slide Preparation

Washed samples were diluted (about 1 - 3 drops per 10 ml distilled water), pipetted onto a glass cover slip and allowed to dry on a warm hotplate (50°C). Permanent slides were then made by mounting in Norland Optical Adhesive 61 (refractive index 1.56) and cured under an UV light for at least 5 minutes.

6.3 Diatom Counts

Diatoms were identified and counted using a phase contrast Zeiss Standard 20 microscope at 1000x magnification, with an oil immersion objective lens. Each slide was traversed horizontally, until at least 600 valves had been counted. Such large counts are necessary where the fluctuations of ecologically important species are masked by the mass occurrence of more important species (Battarbee, 1986). Only cells in which more than half of the valve was intact were counted, to avoid counting the same specimen twice. For elongate species, such as *Trichotoxin*, *Thalassiothrix*, and *Pseudonitzschia*, only end pieces were counted as these cells are rarely preserved intact.

The abundance of the silicoflagellate *Distephanus speculum* and the Chrysophyte *Pentalamina corona* was included in diatom counts.

6.4 Grain Size Analysis

Grain size analysis was carried out on 41 sediment samples (Table 6.2). An aliquot of wet sediment was weighed in a pre-weighed jar, then dried in an oven (50°C) for 24 h. Each sample was then wet sieved with distilled water to extract the following grain size fractions: mud (<63 µm), fine sand (>63 µm) and course sand (>125 µm). Fractions were again dried in an oven for 24 h, and the course sand sieved to extract gravel (>2 mm). Grain size fractions were expressed as a percentage of the total sediment.

Table 6.1. Expeditions to Prydz Bay – Mac.Robertson Shelf from which sediment samples were obtained.

| Expedition | Year | Acronym |
|--|-------------|----------------|
| ANARE Geoscience Survey | 1982 | Geo |
| ANARE Krill and Rock Survey | 1993 | KROCK† |
| ANARE Field Season 1993/94 (Davis Station) | 1993 – 1994 | DCF |
| 2 nd ANARE / Antarctic CRC / AGSO Geoscience Program | 1995 | BANG†† |
| Soviet Antarctic Expeditions | Various | SAE††† |

† KROCK core and grab samples have the prefix “KRGC” (core) and “KRGR” (grab) herein. †† The 2nd ANARE / Antarctic CRC / AGSO Geoscience Program is designated “AGSO Survey 149” (AA149) in AGSO records, and “BANGSS” (Big Antarctic Geological and Seismic Survey) in Antarctic Division records. ††† SAE core and grab samples have the prefix “RC” (core) and “RG” (grab) herein.

Table 6.2. Latitude, longitude and water depth from which samples were recovered.

† Grain size analysis carried out on these samples.

| Expedition | Station | Latitude | Longitude | Water Depth |
|------------|----------|----------|-----------|-------------|
| | | °S | °W | m |
| KROCK | 6/GR1† | 66 43.45 | 77 31.18 | 803 |
| KROCK | 6/GR2A† | 68 25.87 | 77 48.38 | 179 |
| KROCK | 12/GR4† | 68 42.20 | 77 30.70 | 707 |
| KROCK | 13/GR5† | 68 40.34 | 77 16.31 | 538 |
| KROCK | 14/GR6† | 68 49.00 | 77 10.00 | 760 |
| KROCK | 15/GR7† | 68 54.72 | 76 53.61 | 700 |
| KROCK | 17/GR8† | 68 46.92 | 76 48.25 | 798 |
| KROCK | 18/GR9† | 68 42.61 | 76 44.66 | 820 |
| KROCK | 19/GR10† | 68 39.32 | 76 43.00 | 775 |
| KROCK | 21/GR11† | 68 00.74 | 76 32.83 | 460 |
| KROCK | 23/GR12† | 67 21.27 | 76 35.28 | 318 |
| KROCK | 24/GR13† | 66 58.16 | 76 18.63 | 330 |
| KROCK | 37/GR14† | 68 58.00 | 75 11.10 | 740 |
| KROCK | 38/GR15† | 68 36.87 | 74 31.29 | 667 |
| KROCK | 39/GR16† | 68 27.10 | 74 12.52 | 665 |
| KROCK | 41/GR17† | 68 56.66 | 73 34.43 | 792 |
| KROCK | 42/GR18† | 68 11.08 | 75 53.53 | 695 |
| KROCK | 43/GR19† | 69 13.68 | 76 05.95 | 548 |
| KROCK | 60/GR23† | 68 06.16 | 72 15.03 | 788 |
| KROCK | 62/GR24† | 68 30.58 | 70 29.96 | 1060 |
| KROCK | 63/GR25† | 66 52.79 | 72 16.12 | 532 |
| KROCK | 73/GR26† | 66 36.85 | 69 23.80 | 1435 |
| KROCK | 74/GR27† | 66 49.42 | 69 17.77 | 907 |
| KROCK | 75/GR28† | 66 54.89 | 9 13.23 | 512 |
| KROCK | 76/GR29† | 67 02.79 | 68 50.82 | 200 |
| KROCK | 77/GR30† | 67 30.91 | 68 11.74 | 460 |

Table 6.2. (Cont.)

| Expedition | Station | Latitude °S | Longitude °W | Water Depth m |
|------------|-----------|----------------|-----------------|------------------|
| KROCK | 93/GR31† | 67 16.17 | 65 25.38 | 110 |
| KROCK | 93/GR32 | 67 25.18 | 65 06.14 | 1057 |
| KROCK | 105/GR34† | 66 33.58 | 62 44.40 | 1882 |
| KROCK | 106/GR35† | 66 52.03 | 63 09.60 | 434 |
| KROCK | 125/GC1† | 66 53.95 | 63 09.26 | 478 |
| KROCK | 128/GC2† | 67 28.46 | 64 58.36 | 1091 |
| KROCK | 136/GC8† | 66 56.38 | 69 40.94 | 433 |
| KROCK | 139/GC9 | 66 20.16 | 71 58.59 | 1879 |
| KROCK | 143/GC14† | 66 50.13 | 70 29.04 | 430 |
| KROCK | 144/GC15† | 67 00.50 | 71 00.24 | 480 |
| KROCK | 146/GC16† | 67 00.23 | 71 00.03 | 480 |
| KROCK | 150/GC20 | 67 14.15 | 76 33.31 | 318 |
| KROCK | 153/GC24† | 68 05.63 | 73 11.36 | 705 |
| KROCK | 158/GC28 | 68 54.92 | 76 35.36 | 710 |
| KROCK | 162/GC32† | 67 10.28 | 69 50.87 | 279 |
| KROCK | 163/GC33† | 67 10.88 | 68 32.30 | 376 |
| Geo | 2 | 66 51 | 77 06 | 1050 |
| Geo | 5 | 67 56 | 72 17 | 730 |
| Geo | 15 | 66 36 | 71 19 | 1506 |
| Geo | 16 | 66 39.50 | 71 20 | 1128 |
| Geo | 19 | 68 23 | 71 11 | 784 |
| Geo | 22 | 67 20 | 71 21 | 553 |
| Geo | 25 | 66 43 | 71 18 | 855-916 |
| SAE | 3116 | 67 38.20 | 72 23.90 | 624 |
| SAE | 3305 | 69 00.77 | 75 58.71 | 805 |
| SAE | 3606 | 66 59.86 | 75 00.03 | 396 |
| SAE | 3607 | 67 21.46 | 74 55.37 | 433 |

Table 6.2. (Cont.)

| Expedition | Station | Latitude °S | Longitude °W | Water Depth m |
|------------|---------|----------------|-----------------|------------------|
| SAE | 3616 | 68 37.11 | 72 30.49 | 440 |
| SAE | 3109 | 67 58.60 | 72 15.50 | 696 |
| SAE | 3111 | 67 37.30 | 71 32.70 | 560 |
| SAE | 3117 | 67 48.80 | 72 44.20 | 634 |
| SAE | 3119 | 67 51.90 | 73 44.00 | 534 |
| SAE | 3121 | 67 33.90 | 73 00.50 | 595 |
| SAE | 3203 | 69 30.30 | 74 01.50 | 664 |
| SAE | 3207 | 69 20.02 | 75 30.91 | 218 |
| SAE | 3218 | 66 56.67 | 75 28.48 | 357 |
| SAE | 3219 | 67 24.94 | 75 31.28 | 409 |
| SAE | 3222 | 66 57.94 | 76 13.42 | 336.5 |
| SAE | 3314 | 67 43.09 | 77 56.19 | 240 |
| SAE | 3315 | 67 42.10 | 78 00.90 | 220 |
| SAE | 3318 | 67 12.87 | 78 03.73 | 267 |
| SAE | 3321 | 66 54.00 | 77 37.73 | 235 |
| SAE | 3324 | 67 06.08 | 77 08.13 | 292 |
| SAE | 3328 | 67 24.96 | 77 21.70 | 322 |
| SAE | 3329 | 67 33.26 | 77 17.63 | 310 |
| SAE | 3331 | 67 42.10 | 77 18.18 | 340 |
| SAE | 3333 | 67 50.20 | 77 16.75 | 395 |
| SAE | 3335 | 67 57.01 | 77 17.00 | 430 |
| SAE | 3346 | 69 11.00 | 76 24.72 | 417 |
| BANGS | 7 | 66 55.9 | 64 56.3 | 376 |
| BANGS | 8 | 67 05.1 | 65 13.6 | 130 |
| BANGS | 10 | 67 05.1 | 65 27.9 | 627 |
| BANGS | 11 | 67 05.2 | 65 38.9 | 587 |
| BANGS | 12 | 67 06.7 | 65 46.7 | 626 |

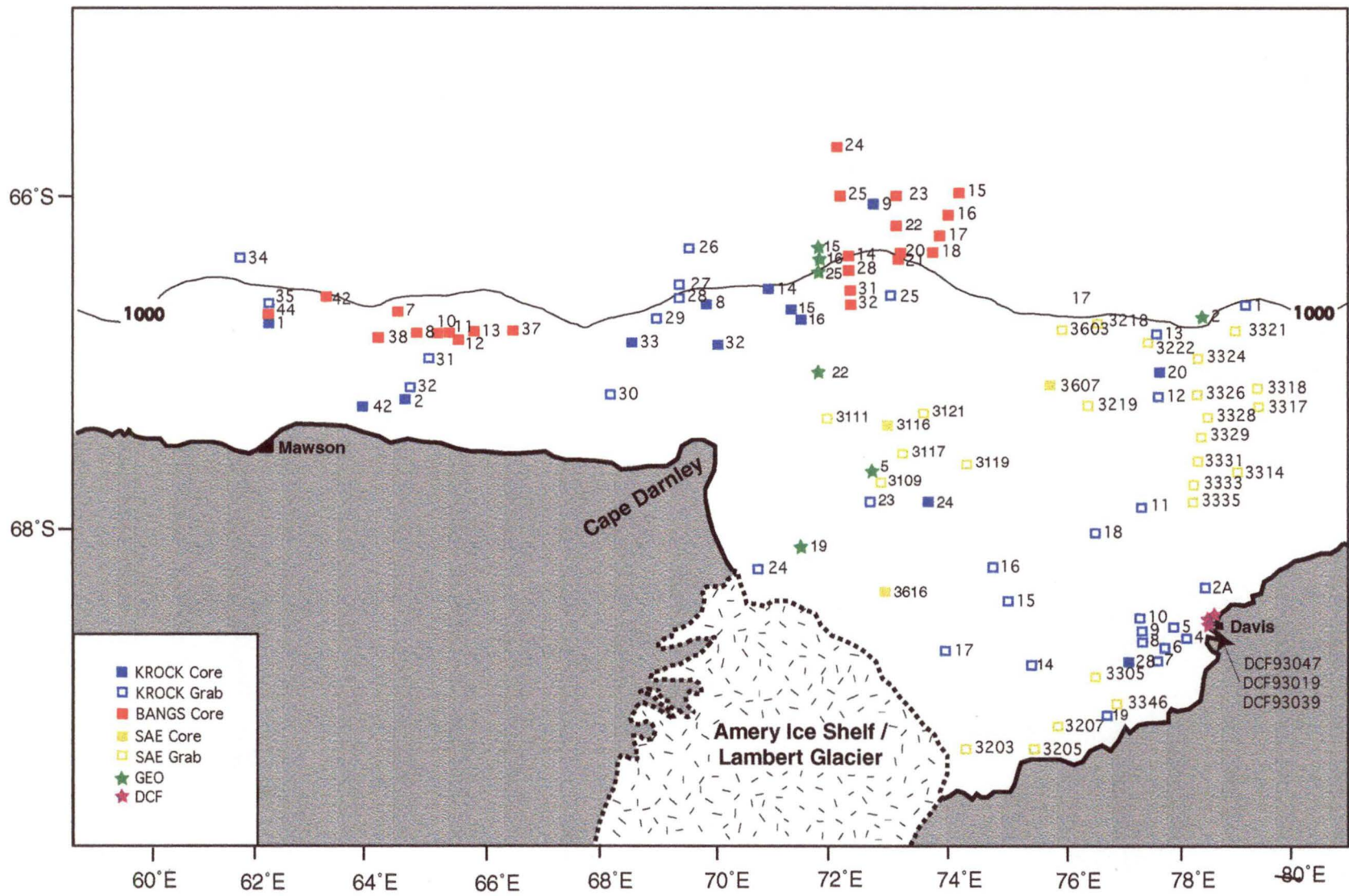


Fig. 6.1. Location of surface sediment samples analysed for diatom abundance and grain size analysis.

– Chapter 7–
Statistical Analyses

A diagram illustrating a summary of the statistical procedures used is illustrated in Fig. 7.1.

7.1 Data Transformation

Diatoms were expressed as a percentage of the total number of cells counted per sample, and arranged in a species by sample matrix. Rare species (classified as those with a maximum abundance <2% in any given sample) were removed from the data matrix prior to further analysis. These species are not present in large enough quantities to be adequately sampled statistically (Webb and Bryson, 1973). In diatom studies, the deletion of rare species is the most popular method of data reduction and causes little distortion to the data (Kato, 1993).

The remaining data was logarithmically transformed using the equation:

$$Y_{ij} = \log(X_{ij} + 1)$$

where X_{ij} = raw data score of the i th species in the j th sample; Y_{ij} = corresponding transformed score. The effect of log transformation is to reduce the score (and hence bias) of very abundant species so that they do not mask the effect of less common species (Field *et al.*, 1982). Data transformation does not alter zero values.

7.2 Cluster Analysis

Using the transformed data, a species by sample (Q-mode) matrix was analysed using the cluster analysis option of BioStat II (Pimental and Smith, 1985). Cluster analysis is a multivariate statistical technique aimed at summarising large data sets by forcing samples into discrete groups of clusters, illustrated as a two-dimensional dendrogram, even if the data points are randomly distributed (Shi, 1995). The method does not require multi-normal distribution, or for variation to be linearly correlated with

environmental gradients (Shi, 1995). In this study, clusters are interpreted as representing diatom assemblages, but the relationship between the assemblages and environmental variables cannot be determined (Shi, 1993).

Cluster analysis was carried out using the Bray-Curtis dissimilarity index in association with unweighted pair group average linkage (UPGMA). The advantage of using the Bray-Curtis dissimilarity index is its ability to effectively analyse matrices with a high zero component (i.e. joint absences) (Field *et al.*, 1982). UPGMA joins two samples together at the average level of similarity between all members of one group and all members of the other (Field *et al.*, 1982).

Samples that appeared as outliers in the cluster analysis were re-sampled and counted using the methods described in Chapter 6. This removed the chance of sample contamination or mis-labelling. Cluster analysis was then repeated, and outliers still remaining deleted from further analysis. Outlying samples usually contain unusual species compositions and have low similarities with other sites. Their deletion from analysis is recommended as they may otherwise act to bias or dominate the analysis and compress the distribution of remaining sites (Gauch, 1982; Shi, 1993).

7.3 Indicator Species (SNK and ANOVA)

Sample groups identified by cluster analysis were further analysed to determine the indicator species characteristic of each group. The student Newman-Keuls multiple range test (SNK), in association with a single factor Analysis of Variance (ANOVA), enables the species that occur in significantly higher abundance between the cluster groups to be determined. SNK and ANOVA were carried out using the multi-dimensional analysis (MDA) option of BioStat II (Pimental and Smith, 1985).

SNK calculates a q (“studentised range”) using the equation:

$$q = (X_B - X_A) / SE$$

where the q value, which is based on the pairwise differences between ranked means of increasing magnitude, is divided by the standard error (Zar, 1984). If q is equal to or greater than the critical value, α, ν, k , (where α = significance level, ν = error DF for the analysis of variance, k = total number of means being tested) then the paired means are significantly different and the indicator species is identified (Zar, 1984).

7.4 Ordination (NMDS)

Following cluster analysis, the data were analysed by indirect ordination. This is a two-step process, the first of which is similar to classification (cluster analysis) as many variables are reduced into relatively few categories, enhancing the major patterns of variation (Beals, 1984). Unlike classification, however, the variation can be interpreted in relation to known environmental gradients.

Ordination rearranges the original data set into a multi-dimensional space and extracts the major directions for variation along principal axes. A product of ordination is a scatter plot, usually based on two or three dimensions, in which the samples are located relative to one another according to their variation on these axes. Groups of samples that occur naturally in the original data are highlighted, lying as points close together in the scatter plot. The axes represent major directions of data variations and may be interpreted as representing environmental variations, which in turn control the variations in the sample data (Shi, 1993).

Nonmetric multi-dimensional scaling (NMDS) was chosen as the appropriate method for ordination and carried out using the principal co-ordinates analysis (PCA) option. The method attempts to match the rankings of distances between sample pairs, from the original data, with the rankings of the respective distances in the ordination (Beals, 1984). NMDS is one of the most robust ordination techniques, especially when dealing with a large number of zero counts (Field *et al.*, 1982).

A product of NMDS is stress values for each ordination axis. Stress, based on the distortion of compressing or stretching distances, is an indication of how well each axis

matches the original data. Values range between 0.0 and 1.0; the lower the stress value the closer the configuration to the ranked order of the dissimilarity (Table 7.1), and the better the NMDS ordination (Shi, 1993).

Table 7.1. Interpretation of stress values (from Hosie, 1994).

| Stress | Goodness-of-fit |
|---------------|------------------------|
| 0.40 | Poor |
| 0.20 | Fair |
| 0.10 | Good |
| 0.05 | Excellent |
| 0.00 | Perfect |

The transformed data in a species by sample matrix were analysed using BioStat II (Pimental and Smith, 1985). Four ordination axes were used in the preliminary analysis; this number was then reduced using the graphical method of Kruskal and Wish (1978). The graphical method involves plotting the stress values against the respective number of ordination axes, and selecting the appropriate ordination axis at the point where the plot shows the maximum change in direction.

7.5 Multiple Regression

Regression analysis was used to determine the relationship between species assemblages and environmental variables, a procedure that cannot be resolved by cluster analysis or ordination. Using multiple regression, it is possible to express the response variable (i.e. species abundance) as a function of two or more known environmental variables (Jongman *et al.*, 1987). Tests of statistical significance can then be used to assess which environmental variable(s) contribute most to the species response.

Multiple regression was carried out using StatView (Feldman *et al.*, 1988), treating the ordination scores obtained by NMDS as the independent variable, and environmental parameters (discussed in Chapter 8) as the dependent variable. The fraction of variance accounted for by the environmental variable is termed the “adjusted coefficient of

determination” (R^2_{adj}) (Jongman *et al.*, 1987), defined by the equation:

$$R^2_{adj} = 1 - (\text{residual variance} / \text{total variance})$$

where R^2_{adj} is a measure of the strength of the straight-line relationship; $R^2_{adj} = 1.00$ demonstrates a perfect relationship and $R^2_{adj} = 0.00$ demonstrates no relationship.

R^2_{adj} is suggested by Shroeder *et al.* (1986) and Jongman *et al.* (1987) to provide a more accurate relationship than unadjusted coefficient of determination values (R^2) (Schroeder *et al.*, 1986; Jongman *et al.*, 1987). The simple R^2 value does not take into account how many environmental parameters are fitted as compared to the number of observations. When a large number of parameters are fitted, R^2 may result in a value close to 1.0, even when the expected response is not dependent on the environmental variable.

The direction of maximum correlation of the regression line is determined by the multiple correlation coefficient. The direction cosine (regression weight), c_r , of that angle is derived from Kruskal and Wish's (1978) formula:

$$c_r = b_r / \sqrt{b^2_1 + b^2_2 + \dots b^2_m}$$

where b^2_1 , b^2_2 etc are the regression coefficients from the multiple regression $a + b_1X_1 + b_2X_2 + \dots b_mX_m$, where m is the number of independent variables x_i (Hosie, 1994).

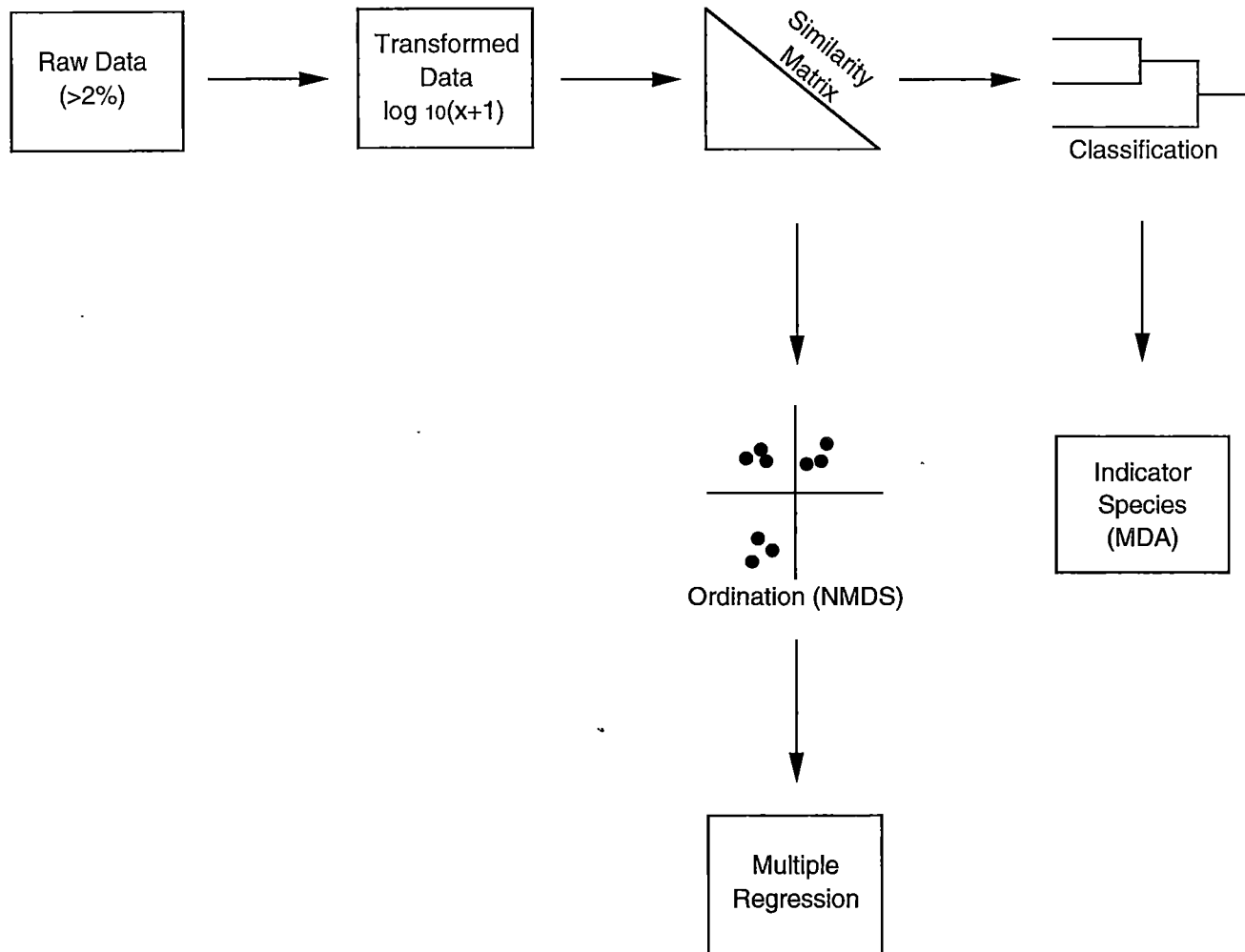


Fig. 7.1 Summary of steps in statistical analysis of data (adapted from Field et al., 1982).

– Chapter 8 –

Environmental Variables

Seven environmental variables (Table 8.1) were used in the regression analysis to determine the relationship between diatom assemblages and their environment. The variables are discussed below.

8.1 Latitude, Longitude and Water Depth

The latitude (°S), longitude (°E) and water depth (m) at each sample location were recorded at the time of sample collection.

8.2 Water Temperature, Salinity and Density

Water temperature (°C), salinity (‰) and density (kg⁻³) were determined from data collected by ANARE oceanographic expeditions to the Prydz Bay region (Kerry *et al.*, 1987a, 1987b; Forbes, unpubl. data). Water profile locations do not coincide exactly with sediment sample locations, and the coverage of any one oceanographic cruise was insufficient to estimate the value of these variables at each sample site. It was therefore necessary to plot and contour the oceanographic data from numerous cruises, from which water temperature, salinity and density could be estimated at each sediment sample location. The average of each variable between 0 m - 100 m water depth was calculated as this is within the euphotic zone, the depth to which 1% of the incident photosynthetic radiation penetrates and planktonic diatoms are most abundant. Over much of the Southern Ocean, the euphotic depth varies between 20 m – 100 m (Priddle *et al.*, 1986). The length of time that diatoms spend in this zone depends on the extent of vertical mixing, which is usually less than 100 m in depth (Lewis *et al.*, 1984).

Temperature, salinity and density value ranges were very narrow (see Table 8.2), making it impossible to extrapolate contoured data precisely to each sediment sample site. It was therefore necessary to subjectively rank the oceanographic data, based on a scale of 1 to 4 (Table 8.2), for use in the statistical analysis.

8.3 Sea Ice

Average sea ice cover was determined for the months October – February, when sea ice is at its maximum and minimum extent, respectively (Gloersen *et al.*, 1992) (Fig. 8.1), between the years 1978 and 1991. This information was obtained from SMMR and SSM/I passive microwave records with a pixel size 25 x 25 km (US National Climatic Data Centre).

8.4 Horizontal Water Circulation

It was not possible to quantify horizontal water circulation for comparison using multiple regression analysis, due to a lack of current strength data. Instead, this variable was visually compared with the diatom assemblages identified by cluster analysis. The water circulation patterns in Prydz Bay are well documented (e.g. Smith *et al.*, 1984; Wong, 1994; Nunez Vas and Lennon, 1996) and a summary of these illustrated in Fig. 5.4 (Chapter 5).

Table 8.1. Environmental data used in regression analysis. † Data not available Value based on next closest location (i.e. pixel, not sediment sample). Rank scale values for water properties tabulated in Table 8.2

| Station | Lat. (°S) | Long. (°E) | Water | % Ice Cover (1978-1991) | | | | | | | |
|---------|-----------|------------|-------|-------------------------|-------|----------|---------|---------|----------|----------|---------|
| | | | | Depth (m) | Temp. | Salinity | Density | October | November | December | January |
| KRGR1 | 66 43.45 | 77 31 18 | 803 | 4 | 3 | 2 | 75 | 57 | 40 | 19 | 14 |
| KRGR2A | 68 25.87 | 77 48 38 | 179 | 4 | 1 | 1 | 68 | 54 | 42 | 42 | 39 |
| KRGR4 | 68 42.20 | 77 30.70 | 707 | 4 | 1 | 1 | 69 | 53 | 37 | 33 | 30 |
| KRGR5 | 68 40.34 | 77 16.31 | 538 | 4 | 1 | 1 | 69 | 53 | 37 | 32 | 30 |
| KRGR6 | 68 49 00 | 77 10 00 | 760 | 4 | 1 | 1 | 72 | 59 | 45 | 38 | 36 |
| KRGR7 | 68 54 72 | 76 53 61 | 700 | 3 | 1 | 2 | 75 | 66 | 55 | 47 | 45 |
| KRGR8 | 68 46 92 | 76 48 25 | 798 | 3 | 1 | 2 | 74 | 57 | 34 | 23 | 22 |
| KRGR9 | 68 42.61 | 76 44 66 | 820 | 3 | 1 | 2 | 74 | 57 | 34 | 23 | 22 |
| KRGR10 | 68 39 32 | 76 43.00 | 775 | 4 | 1 | 2 | 71 | 49 | 21 | 14 | 16 |
| KRGR11 | 68 00.74 | 76 32.83 | 460 | 4 | 3 | 2 | 70 | 37 | 5 | 3 | 6 |
| KRGR12 | 67 21.27 | 76 35 28 | 318 | 4 | 3 | 2 | 72 | 43 | 22 | 11 | 6 |
| KRGR13 | 66 58.16 | 76 18.63 | 330 | 4 | 3 | 3 | 75 | 53 | 34 | 15 | 8 |
| KRGR14 | 68 58 00 | 75 11 10 | 740 | 3 | 3 | 2 | 81 | 66 | 31 | 14 | 7 |
| KRGR15 | 68 36.87 | 74 31.29 | 667 | 3 | 3 | 2 | 81 | 64 | 19 | 4 | 2 |
| KRGR16 | 68 27.10 | 74 12.52 | 665 | 3 | 3 | 2 | 82 | 61 | 12 | 1 | 1 |
| KRGR17 | 68 56.66 | 73 34.43 | 792 | 2 | 1 | 3 | 78† | 74† | 49† | 21† | 4† |
| KRGR18 | 68 11.08 | 75 53.53 | 695 | 4 | 3 | 3 | 76 | 44 | 5 | 1 | 4 |
| KRGR19 | 69 13.68 | 76 05.95 | 548 | 3 | 1 | 1 | 79 | 72 | 58 | 49 | 12 |
| KRGR23 | 68 06.16 | 72 15.03 | 788 | 3 | 3 | 3 | 76 | 75 | 45 | 13 | 1 |
| KRGR24 | 68 30.58 | 70 29.96 | 1060 | 1 | 1 | 1 | 64† | 67† | 64† | 48† | 27† |
| KRGR25 | 66 52 79 | 72 16 12 | 532 | 3 | 3 | 3 | 84 | 82 | 43 | 8 | 0 |
| KRGR26 | 66 36.85 | 69 23 80 | 1435 | 3 | 4 | 4 | 72 | 67 | 43 | 10 | 1 |
| KRGR27 | 66 49.42 | 69 17.77 | 907 | 3 | 4 | 4 | 64 | 58 | 41 | 14 | 2 |
| KRGR28 | 66 54.89 | 9 13.23 | 512 | 3 | 4 | 4 | 58 | 49 | 35 | 15 | 4 |
| KRGR29 | 67 02.79 | 68 50 82 | 200 | 3 | 4 | 3 | 57 | 78 | 26 | 11 | 3 |
| KRGR30 | 67 30.91 | 68 11.74 | 460 | 3 | 4 | 2 | 60 | 46 | 32 | 25 | 21 |
| KRGR32 | 67 25.18 | 65 06.14 | 1057 | 3 | 4 | 2 | 75 | 68 | 60 | 43 | 30 |
| KRGR34 | 66 33.58 | 62 44.40 | 1882 | 3 | 4 | 3 | 84 | 71 | 37 | 7 | 24 |
| KRGR35 | 66 52 03 | 63 09.60 | 434 | 3 | 4 | 3 | 85 | 77 | 59 | 2 | 4 |
| KRGC1 | 66 53.95 | 63 09.26 | 478 | 3 | 4 | 3 | 85 | 77 | 59 | 24 | 4 |
| KRGC2 | 67 28.46 | 64 58.36 | 1091 | 3 | 4 | 1 | 75 | 68 | 60 | 43 | 30 |
| KRGC8 | 66 56.38 | 69 40.94 | 433 | 3 | 4 | 3 | 58 | 49 | 35 | 15 | 4 |
| KRGC9 | 66 20.16 | 71 58 59 | 1879 | 3 | 4 | 3 | 85 | 83 | 42 | 4 | 0 |

Table 8.1. Cont.

| Station | Lat. (°S) | Long. (°E) | Water | % Ice Cover (1978-1991) | | | | | | | |
|---------|-----------|------------|---------|-------------------------|-------|----------|---------|---------|----------|----------|---------|
| | | | | Depth (m) | Temp. | Salinity | Density | October | November | December | January |
| KRGC14 | 66 50.13 | 70 29.04 | 430 | 3 | 4 | 4 | 72 | 70 | 52 | 22 | 3 |
| KRGC15 | 67 00.50 | 71 00.24 | 480 | 3 | 4 | 4 | 78 | 78 | 54 | 23 | 2 |
| KRGC16 | 67 00 23 | 71 00.03 | 480 | 3 | 4 | 3 | 78 | 69 | 54 | 23 | 2 |
| KRGC20 | 67 14.15 | 76 33.31 | 318 | 4 | 3 | 2 | 73 | 48 | 28 | 13 | 7 |
| KRGC24 | 68 05.63 | 73 11.36 | 705 | 4 | 3 | 4 | 81 | 71 | 25 | 3 | 0 |
| KRGC28 | 68 54.92 | 76 35.36 | 710 | 3 | 1 | 2 | 74 | 57 | 34 | 23 | 22 |
| KRGC32 | 67 10.28 | 69 50.87 | 279 | 3 | 3 | 2 | 62 | 55 | 42 | 21 | 5 |
| KRGC33 | 67 10.88 | 68 32.30 | 376 | 3 | 4 | 3 | 57 | 40 | 26 | 11 | 3 |
| GEO2 | 66 51 | 77 06 | 1050 | 4 | 3 | 2 | 75 | 57 | 70 | 19 | 14 |
| GEO5 | 67 56 | 72 17 | 730 | 3 | 4 | 3 | 80 | 78 | 42 | 13 | 0 |
| GEO15 | 66 36 | 71 19 | 1506 | 3 | 4 | 4 | 83 | 82 | 46 | 9 | 0 |
| GEO16 | 66 39.50 | 71 20 | 1128 | 3 | 4 | 4 | 83 | 82 | 46 | 9 | 0 |
| GEO19 | 68 23 | 71 11 | 784 | 2 | 1 | 2 | 62 | 64 | 58 | 38 | 19 |
| GEO22 | 67 20 | 71 21 | 553 | 4 | 3 | 3 | 80 | 81 | 57 | 25 | 2 |
| GEO25 | 66 43 | 71 18 | 855-916 | 4 | 4 | 4 | 81 | 79 | 63 | 16 | 1 |
| RC3116 | 67 38.20 | 72 23.90 | 624 | 4 | 4 | 3 | 83 | 79 | 40 | 12 | 1 |
| RC3305 | 69 00.77 | 75 58.71 | 805 | 3 | 1 | 2 | 79 | 65 | 37 | 23 | 18 |
| RC3606 | 66 59.86 | 75 00.03 | 396 | 4 | 3 | 3 | 85 | 79 | 35 | 5 | 0 |
| RC3607 | 67 21.46 | 74 55.37 | 433 | 4 | 3 | 2 | 81 | 55 | 20 | 5 | 2 |
| RC3616 | 68 37.11 | 72 30.49 | 440 | 2 | 3 | 2 | 77† | 70† | 33† | 10† | 2† |
| RG3109 | 67 58.60 | 72 15.50 | 696 | 3 | 3 | 3 | 76 | 75 | 45 | 13 | 1 |
| RG3111 | 67 37.30 | 71 32.70 | 560 | 4 | 3 | 3 | 79 | 80 | 45 | 13 | 3 |
| RG3117 | 67 48.80 | 72 44.20 | 634 | 4 | 4 | 4 | 82 | 75 | 31 | 7 | 0 |
| RG3119 | 67 51.90 | 73 44.00 | 534 | 4 | 4 | 4 | 83 | 70 | 21 | 7 | 0 |
| RG3121 | 67 33.90 | 73 00.50 | 595 | 4 | 4 | 3 | 84 | 74 | 29 | 6 | 1 |
| RG3203 | 69 30.30 | 74 01.50 | 664 | 1 | 1 | 1 | 77† | 78† | 85† | 92† | 73† |
| RG3207 | 69 20.02 | 75 30.91 | 218 | 2 | 1 | 1 | 80† | 76† | 64† | 41† | 30† |
| RG3218 | 66 56.67 | 75 28.48 | 357 | 4 | 3 | 3 | 82 | 61 | 28 | 7 | 2 |
| RG3219 | 67 24.94 | 75 31.28 | 409 | 4 | 3 | 2 | 78 | 48 | 18 | 7 | 3 |
| RG3222 | 66 57.94 | 76 13.42 | 336.5 | 4 | 3 | 3 | 79 | 59 | 32 | 12 | 4 |
| RG3314 | 67 43.09 | 77 56.19 | 240 | 4 | 3 | 2 | 62 | 37 | 17 | 15 | 16 |
| RG3315 | 67 42.10 | 78 00.90 | 220 | 4 | 3 | 2 | 63 | 39 | 20 | 17 | 17 |
| RG3318 | 67 12.87 | 78 03.73 | 267 | 4 | 3 | 2 | 66 | 44 | 29 | 22 | 20 |

Table 8.1 Cont

| Station | Lat. (°S) | Long. (°E) | Water | % Ice Cover (1978-1991) | | | | | | | |
|----------|-----------|------------|---------|-------------------------|-------|----------|---------|---------|----------|----------|---------|
| | | | | Depth (m) | Temp. | Salinity | Density | October | November | December | January |
| RG3321 | 66 54.00 | 77 37 73 | 235 | 4 | 3 | 2 | 74 | 56 | 43 | 25 | 19 |
| RG3324 | 67 06 08 | 77 08.13 | 292 | 4 | 3 | 2 | 68 | 41 | 27 | 15 | 11 |
| RG3328 | 67 24 96 | 77 21 70 | 322 | 4 | 3 | 2 | 63 | 34 | 27 | 14 | 14 |
| RG3329 | 67 33.26 | 77 17 63 | 310 | 4 | 3 | 2 | 63 | 34 | 18 | 14 | 14 |
| RG3331 | 67 42 10 | 77 18 18 | 340 | 4 | 3 | 2 | 63 | 32 | 11 | 10 | 11 |
| RG3333 | 67 50.20 | 77 16.75 | 395 | 4 | 3 | 2 | 64 | 33 | 9 | 8 | 10 |
| RG3335 | 67 57 01 | 77 17 00 | 430 | 4 | 3 | 2 | 63 | 38 | 19 | 17 | 19 |
| RG3346 | 69 11 00 | 76 24 72 | 417 | 3 | 1 | 1 | 79 | 72 | 58 | 49 | 49 |
| BANG7 | 66 55.9 | 64 56 3 | 376 | 3 | 4 | 3 | 77 | 62 | 43 | 14 | 4 |
| BANG8 | 67 05.1 | 65 13 6 | 130 | 3 | 4 | 3 | 77 | 62 | 43 | 14 | 4 |
| BANG10 | 67 05 1 | 65 27 9 | 627 | 3 | 4 | 3 | 73 | 57 | 37 | 11 | 4 |
| BANG11 | 67 05.2 | 65 38.9 | 587 | 3 | 4 | 3 | 73 | 57 | 37 | 11 | 4 |
| BANG12 | 67 06.7 | 65 46 7 | 626 | 3 | 4 | 3 | 73 | 57 | 37 | 11 | 4 |
| BANG13 | 67 05 3 | 65 59 0 | 413 | 3 | 4 | 3 | 71 | 53 | 33 | 11 | 6 |
| BANG14 | 66 38.4 | 71 44.0 | 849 | 3 | 4 | 4 | 83 | 82 | 46 | 9 | 0 |
| BANG15 | 66 15 2 | 73 20.4 | 2250 | 3 | 4 | 3 | 87 | 80 | 33 | 1 | 0 |
| BANG16 | 66 23.1 | 73 11.1 | 1960 | 3 | 4 | 3 | 87 | 82 | 35 | 1 | 0 |
| BANG17 | 66 30.2 | 73 05.5 | 1540 | 3 | 3 | 3 | 86 | 82 | 37 | 2 | 0 |
| BANG18 | 66 36.0 | 73 00.5 | 1174 | 3 | 3 | 2 | 86 | 82 | 37 | 2 | 0 |
| BANG20 | 66 37.1 | 72 18.3 | 697 | 3 | 3 | 2 | 84 | 83 | 44 | 7 | 0 |
| BANG21 | 66 37.1 | 72 17.6 | 1060 | 3 | 3 | 2 | 86 | 83 | 40 | 3 | 0 |
| BANG22 | 66 27.4 | 72 17.8 | 1450 | 3 | 3 | 3 | 86 | 83 | 40 | 3 | 0 |
| BANG23 | 66 19.2 | 72 17.6 | 1884 | 3 | 4 | 3 | 87 | 83 | 37 | 1 | 0 |
| BANG31 | 66 50.3 | 71 49.0 | 512 | 3 | 4 | 3 | 83 | 83 | 48 | 13 | 1 |
| BANG32 | 66 55.6 | 71 50.8 | 502 | 3 | 4 | 3 | 83 | 83 | 48 | 13 | 1 |
| BANG37 | 67 04.8 | 66 42.1 | 168 | 3 | 4 | 3 | 69 | 48 | 27 | 7 | 4 |
| BANG38 | 67 09.4 | 65 45 1 | 722-620 | 3 | 4 | 3 | 73 | 57 | 37 | 11 | 4 |
| BANG42 | 67 04.8 | 64 35.7 | 345 | 3 | 4 | 3 | 81 | 72 | 59 | 27 | 8 |
| DCF93019 | 68 04 | 78 05 | 122 | 4 | 1 | 1 | 68 | 54 | 42 | 42 | 39 |
| DCF93032 | 68 07 | 78 04 | 124 | 4 | 1 | 1 | 68 | 54 | 42 | 42 | 39 |
| DCF93047 | 68 07 | 78 15 | 104 | 4 | 1 | 1 | 68 | 54 | 42 | 42 | 39 |

Table 8.2. Rank values used to estimate water temperature, salinity and density at each sediment sample site. Rank values were determined by hand-contouring know data onto a bathymetric map.

| Variable | Value | Rank Value |
|-----------------------------|----------------|-------------------|
| Temperature (°C) | >0.0 | 1 |
| | -0.1to -0.5 | 2 |
| | -0.6 to -1.0 | 3 |
| | <-1.1 | 4 |
| Salinity (‰) | <33.59 | 1 |
| | 33.60 to 33.79 | 2 |
| | 33.80 to 33.99 | 3 |
| | >34.00 | 4 |
| Density (kg ⁻³) | <27.02 | 1 |
| | 27.21 to 27.30 | 2 |
| | 27.31 to 27.40 | 3 |
| | >27.41 | 4 |

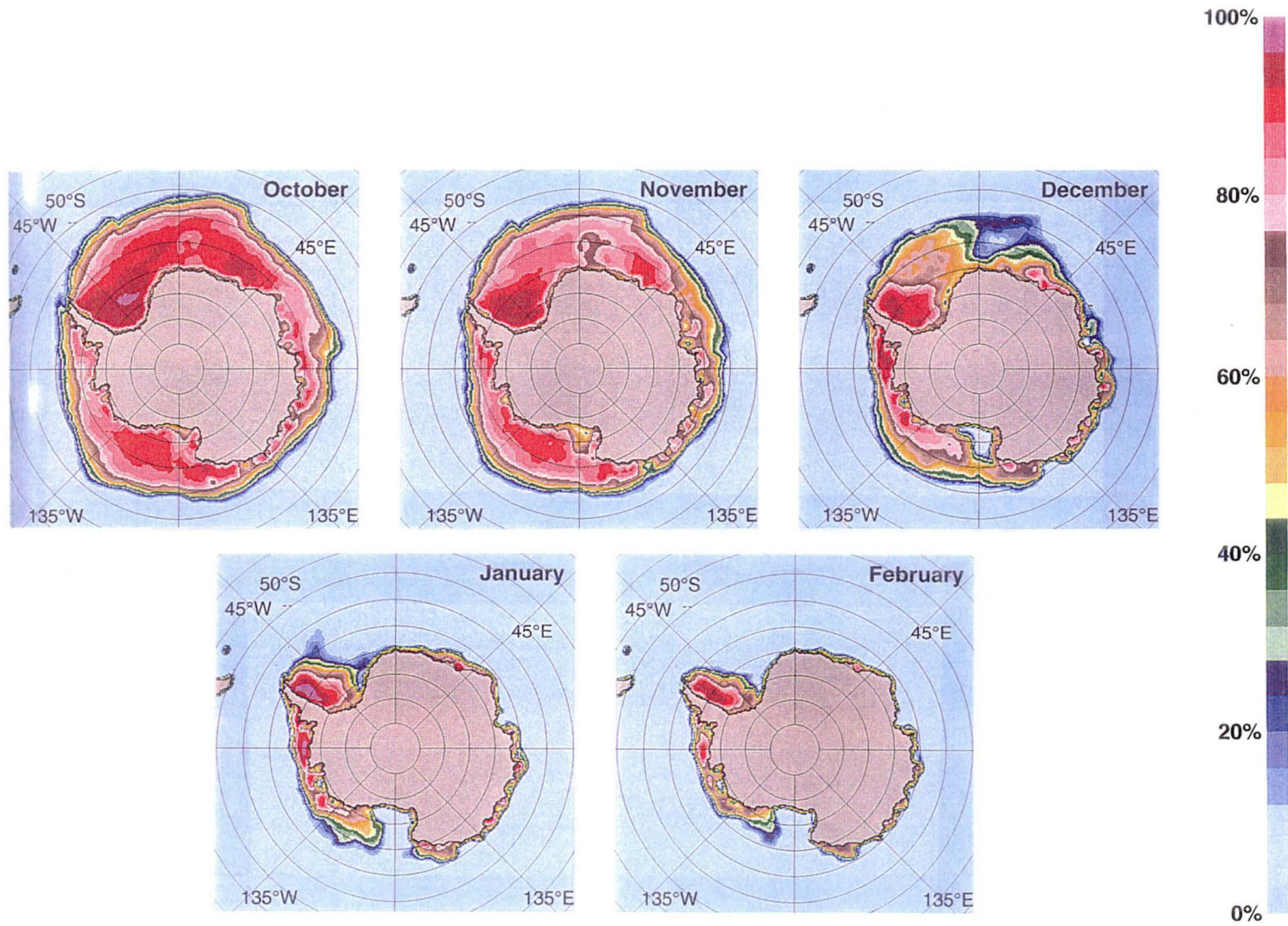


Fig. 8.1. Mean Antarctic sea ice concentration for the months Oct – Feb, averaged over the SMMR lifetime (1978-1987). From Gloersen et al., 1992).

– Chapter 9 –

Results¹

9.1 Cluster Analysis

Twenty-four diatom species with an abundance >2% were observed in the 104 surface sediment samples from Prydz Bay and Mac.Robertson Shelf (Appendix 1). The initial cluster analyses identified three outliers (samples BANG25, RC3116 and KRGR32; Appendix 2), which were removed from further analysis, as recommended by Gauch (1982) and Shi (1993). Four cluster groups were identified in the subsequent analysis, at 38.9% dissimilarity and with a cophenetic correlation of 0.58 (0.00 indicating no match with the original data; 1.00 indicating a perfect match). A dendrogram illustrating cluster groups is illustrated in Fig. 9.1, and the geographic distribution of the groups, as diatom assemblages, illustrated in Fig. 9.2.

Cluster group 1 (hereafter referred to as the coastal diatom assemblage) contains 12 samples that are located on the continental shelf. Seven samples are concentrated in the southeast corner of Prydz Bay, and three sites located on Mac.Robertson Shelf, in Iceberg Alley, Nielsen Basin and east Storegg Bank. No samples from closer to the Mawson Coast were available for analysis and, from the spatial coverage of the coastal assemblage on Mac.Robertson Shelf, it cannot be determined whether the assemblage extends east of this area towards Cape Darnley. Two samples are located towards the centre of the bay, but results from NMDS (discussed below) indicate that at least one of these (RG3317) should probably be included within cluster group 2.

Cluster group 2 (the shelf diatom assemblage) is the largest group identified. It contains 45 samples that cover a broad geographic area of Prydz Bay, and extend west from Cape Darnley along Mac.Robertson Shelf to 63°E. The northern boundary of the shelf assemblage coincides with the continental shelf break; no samples extend beyond this zone.

¹ Published as Taylor *et al.*, 1997.

Cluster group 3 (the cape assemblage) is the smallest group, containing only six samples. The cluster group has a distinct geographic distribution, centred in an area north of Cape Darnley and Fram Bank. No samples extend offshore of the continental shelf break.

Cluster group 4 (the oceanic assemblage) contains 38 samples. The group extends east from 62°E, mostly along the offshore side (>1000 m water depth) of the continental shelf break. East of ~75°E, the cluster group is distributed within Prydz Bay, crossing the shelf break zone and extending south as a distinctive diatom assemblage over Four Ladies Bank (Fig. 9.2).

9.2 SNK and ANOVA

Results from the SNK test and ANOVA are summarised in Table 9.1.

The coastal and shelf assemblages are characterised by a significant abundance of the pennate diatoms *Fragilariopsis curta* (Van Heurck) Hasle, *F. cylindrus* (Grunow?) Hasle and *F. angulata* Hustedt. *Fragilariopsis curta* is the dominant member of both assemblages, forming up to 70.5%. The coastal assemblage can be differentiated by the abundance of the elongate *Pseudonitzschia turgiduloides* (Hasle) Hasle. Although this species does not form a dominant component of the assemblage (maximum abundance 1.49%²), the abundance of *P. turgiduloides* is significantly greater compared to that in either the shelf, oceanic or cape assemblages. No species uniquely characterise the shelf assemblage, but it can be distinguished from the coastal assemblage by a significantly greater abundance of *Porosira glacialis* (Grunow) Jørgensen, *Thalassiosira antarctica* (Comber) resting spores and the Chrysophyte (Parnales) *Pentalamina corona* Marchant.

The oceanic assemblage is characterised by four indicator species: *F. kerguelensis* (O'Meara) Hasle, the centric species *T. gracilis* var. *expecta* (Van Landingham) Fryxell

² The highest abundance of *P. turgiduloides* (4.0%) occurred in KRGR32. This sample was identified as an outlier in the initial cluster analysis (Appendix 1), and removed from further analyses.

and Hasle and *T. lentiginosa* (Janisch) Fryxell, and the elongate *Trichotoxin reinboldii* (Van Heurck) Reid & Round. All are indicative of open water primary production. *Fragilariopsis kerguelensis* is the dominant indicator species, forming up to 43.3%. Several species shared with the cape and shelf assemblages are also significantly abundant in the oceanic assemblage (see Table 9.1).

There are no indicator species that uniquely characterise the cape assemblage. The assemblage contains a significant abundance of shelf and coastal assemblages taxa (*F. curta* and *F. angulata*) and oceanic assemblage taxa (*Actinocyclus actinochilus* (Ehrenberg) Simonsen, *Eucampia antarctica* (Castracane) Manguin, *F. separanda* (Hustedt) Hasle, *Stellarima microtrias* (Ehrenberg) Hasle and Sims, *T. antarctica* resting spores, and *T. gracilis* Karsten (Hustedt)). *Fragilariopsis curta* is the dominant species in the cape assemblage, forming up to 72%. It is considered notable that the lowest abundance of small and lightly silicified frustules, such as *F. cylindrus*, *Chaetoceros* resting spores and *P. corona*, occur in the cape assemblage. The implications of this are discussed in Chapter 10.

9.3 NMDS

NMDS was carried out using the same similarity matrix as for cluster analysis, based on $\log_{10}(x+1)$ species abundance. Four axes were chosen for the initial analysis, cycling down to one axis. Using Kruskal and Wish's (1978) graphical method, two axes were selected as adequately summarising the data set (Fig. 9.3) Stress for a two dimensional plot converged after 20 iterations, with a value of 0.15 indicating a good-to-fair match of the ordination axes with the original data.

Results of the two dimensional ordination are illustrated in Fig. 9.4. By superimposing the assemblages identified by cluster analysis over this, it is observed that essentially the same results as that obtained by cluster analysis is reproduced by NMDS. Four cluster groups can be recognised, three of which form a tight-knit group corresponding with the coastal, shelf and oceanic assemblages. The similarity between these assemblages can be observed in the gradational transition from coastal, to shelf to oceanic assemblage.

As noted by the SNK test, the diatom composition of these assemblage is extremely similar and only the presence of statistical indicator species can be used to identify each one. Sample RG3317, which formed part of the coastal assemblage in the cluster analysis, is more closely associated with the shelf assemblage in NMDS. Based on the geographical location of this sample, and its diatom composition, the NMDS result may be more accurate. The cape assemblage forms a distinct group in NMDS. This confirms the results obtained by cluster analysis and the SNK test, which indicated that the assemblage contains a distinct species composition compared to the coastal, shelf and oceanic assemblages.

9.4 Multiple Regression

Using the ordination scores obtained by the two-dimensional NMDS, multiple regression analysis was carried out to compare the data with 11 environmental variables (detailed in Chapter 8). Six variables are identified to be significantly correlated with the diatom data (Table 9.2), and the direction of maximum correlation for each (Table 9.3) illustrated in Fig. 9.4.

The latitudinal distribution of the diatom assemblages is evident, with latitude accounting for 56.0% of the variation. The environmental variables that co-vary with latitude also correlate significantly with the data. Water salinity, water depth and water density account for 29.6%, 25.3% and 15.3% of the variation, respectively. All were observed to decrease in increasing latitude.

Sea ice cover is highly variable in Prydz Bay, reaching its maximum extent in September / October and minimum extent in February. Only ice cover in January and February correlates significantly with the data, contributing 27.1% and 21.8%, respectively. During these months, ice remains concentrated in southeast Prydz Bay and in shallow coastal areas along Mac.Robertson Shelf. The rest of the area is essentially ice free (<10% cover).

9.5 Grain Size Analysis

Grain size analysis was carried out on samples (see Table 6.2) that represented three of the four diatom assemblages identified by cluster analysis (no samples from the oceanic assemblage were available). This was used as a method to identify the presence of current winnowed sediment. Only samples from KROCK and DCF could be analysed, due to the amount of sediment available in these collections. A dendrogram illustrating sample affinities, based on grain size analysis, is illustrated in Fig. 9.5. Two cluster groups can be identified at 57.7% dissimilarity, with a cophenetic correlation of 0.79. Cluster group 1 is characterised by a significantly greater abundance of sand ($>63\ \mu\text{m}$) and gravel ($>2\ \text{mm}$) (Table 9.4). These fractions form up to 84% and 29%, respectively, of the total sediment. The cluster group is concentrated in the vicinity of Cape Darnley, Four Ladies Bank and south-east Prydz Bay (Fig. 9.6).

Cluster group 2 is divided at 24.8% dissimilarity into two subgroups. Subgroup 2A is characterised by a significantly greater abundance of mud ($<63\ \mu\text{m}$), which forms up to 100% of the sediment, compared to subgroup 2B. The abundance of sand is significantly greater in subgroup 2B compared to subgroup 2A. Cluster group 2 is distributed throughout the centre of Prydz Bay and in Nielsen Basin. The sediments corresponding to this group have been previously shown to be dominated by diatomaceous, skeletal remains (Franklin, 1993), which form siliceous, muddy ooze. They are indicative of little or no reworking (Franklin, 1993).

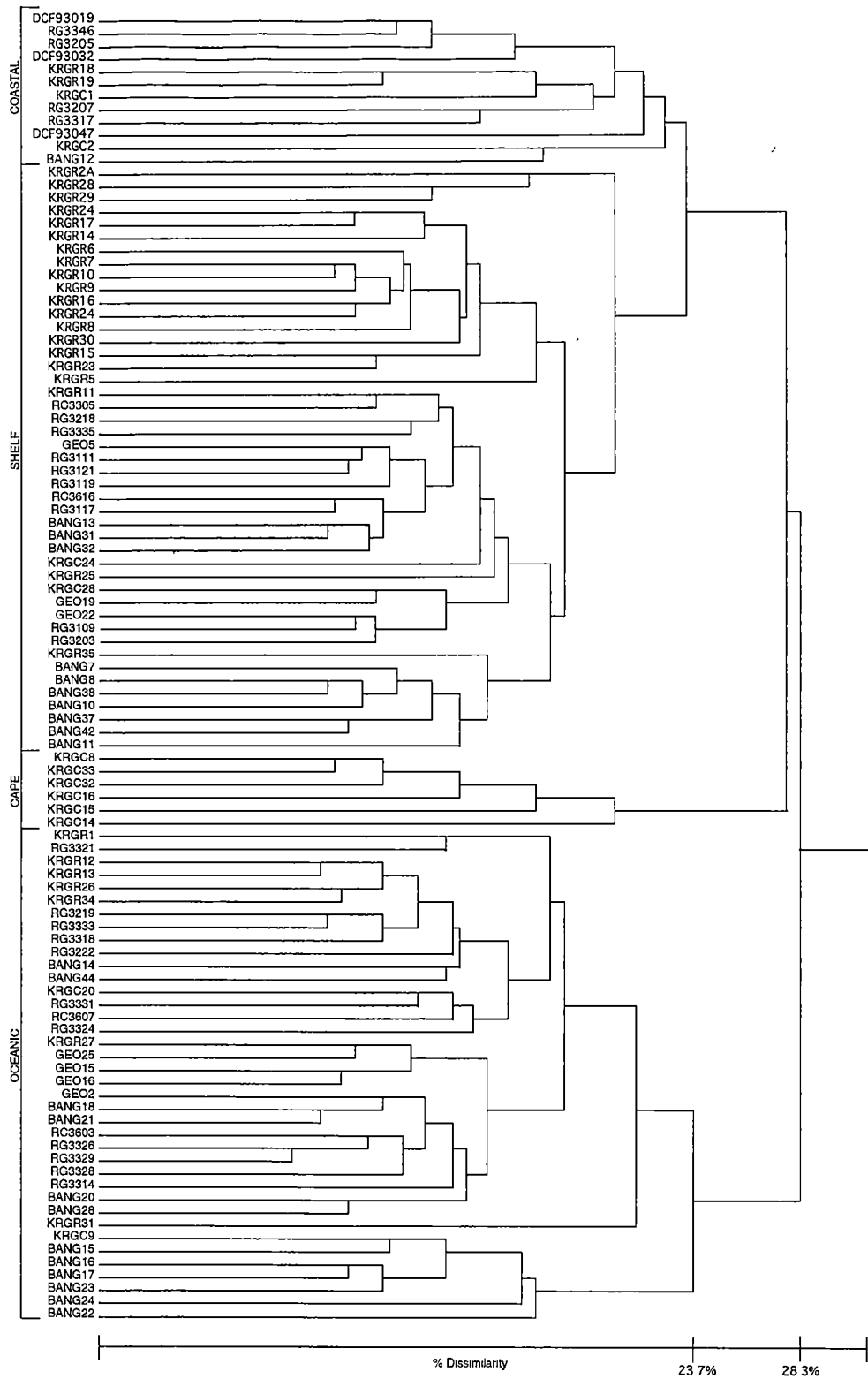


Fig. 9.1. Dendrogram of cluster analysis comparing surface sediment samples. Analysis based on species abundance (>2% log10).

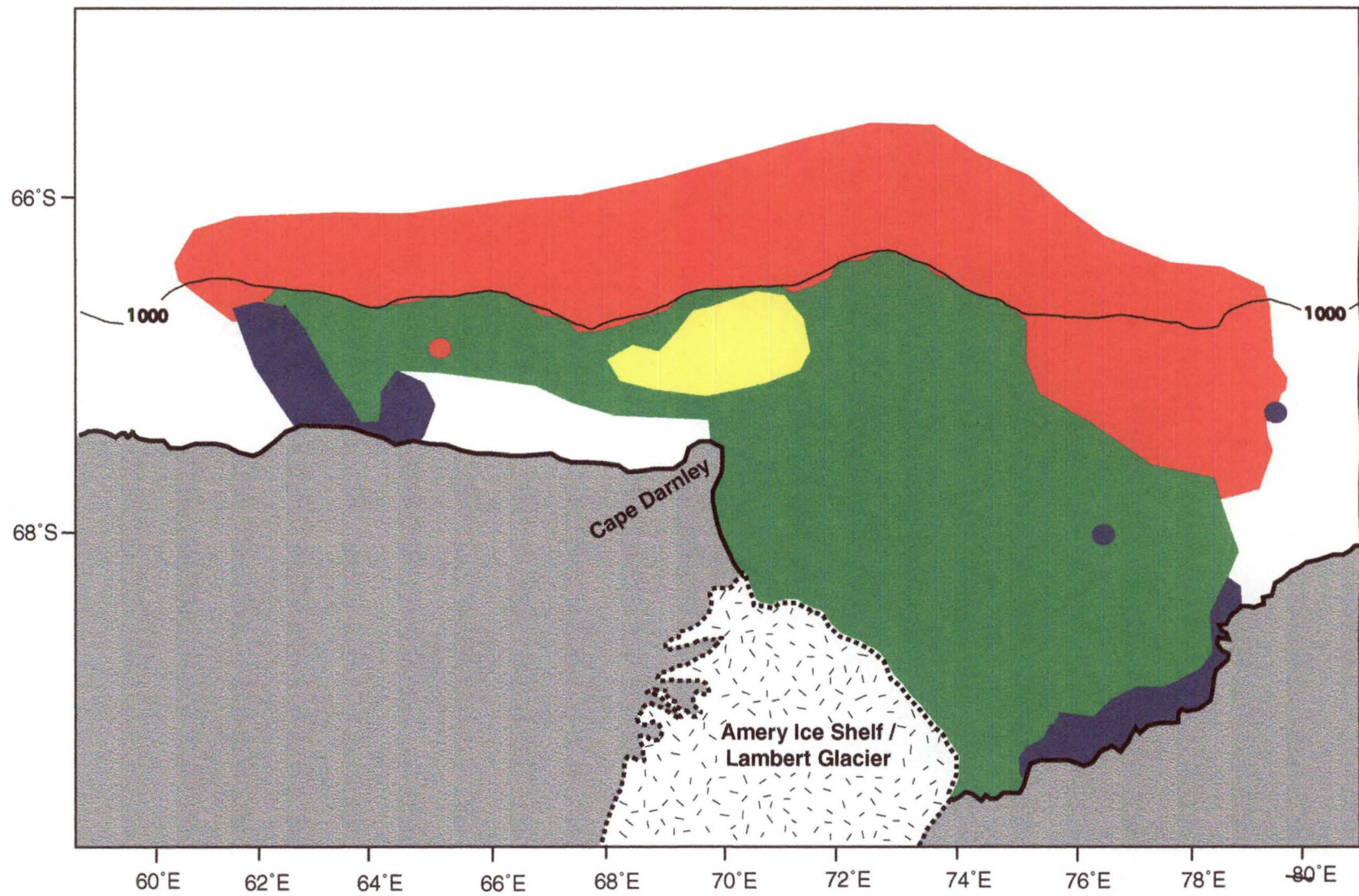


Fig. 9.2. Geographic distribution of diatom assemblages in Prydz Bay and Mac.Robertson Shelf, identified by cluster analysis. Blue: coastal. Green: shelf. Red: oceanic. Yellow: cape.

Table 9.1 Mean arithmetic abundance (%) analysis of variance (F) and SNK multiple range tests of dominant (>2%) species in cluster groups.

| Species | Cluster Group | | | | F | P |
|--|---------------|-------------|-------------|-------------|-------|------|
| | Coastal | Shelf | Cape | Oceanic | | |
| <i>A. actinophilus</i> | 0.1 | 0.2 | <u>0.5</u> | <u>0.7</u> | 22.06 | *** |
| <i>Chaetoceros</i> spp. | 0.4 | 0.2 | 0.0 | 0.1 | 3.72 | * |
| <i>Chaetoceros</i> (spores) | <u>5.3</u> | <u>7.9</u> | 1.1 | <u>12.6</u> | 32.63 | *** |
| <i>D. antarcticus</i> | 0.2 | 0.5 | <u>0.9</u> | <u>0.8</u> | 8.46 | *** |
| <i>D. speculum</i> | 0.3 | 0.5 | 0.6 | <u>0.8</u> | 3.86 | * |
| <i>E. antarctica</i> | 0.1 | 0.4 | <u>2.3</u> | <u>1.2</u> | 17.03 | *** |
| <i>F. angulata</i> | <u>4.2</u> | <u>3.9</u> | <u>5.6</u> | 2.1 | 22.32 | *** |
| <i>F. curta</i> | <u>54.7</u> | <u>48.5</u> | <u>62.8</u> | 28.6 | 37.47 | *** |
| <i>F. cylindrus</i> | <u>22.3</u> | <u>15.6</u> | 2.6 | <u>13.1</u> | 16.06 | *** |
| <i>F. kerguelensis</i> | 0.5 | 1.0 | 2.0 | <u>13.7</u> | 77.88 | *** |
| <i>F. lineata</i> | 0.7 | 0.9 | 1.1 | 1.1 | 1.79 | N.S. |
| <i>F. obliquecostata</i> | 1.8 | 2.5 | 2.7 | 1.8 | 4.73 | ** |
| <i>F. separanda</i> | 0.2 | <u>0.8</u> | <u>1.7</u> | <u>1.7</u> | 28.78 | *** |
| <i>F. sublineata</i> | 0.4 | 0.7 | 0.6 | 0.4 | 2.79 | * |
| <i>P. corona</i> | <u>1.6</u> | <u>3.8</u> | 1.1 | <u>3.1</u> | 14.94 | *** |
| <i>P. glacialis</i> | 0.2 | <u>0.9</u> | <u>0.6</u> | 0.2 | 24.25 | *** |
| <i>P. turgiduloides</i> | <u>0.4</u> | 0.1 | 0.1 | 0.0 | 8.49 | *** |
| <i>S. microtrias</i> | 0.2 | 0.3 | <u>0.9</u> | <u>0.6</u> | 7.97 | *** |
| <i>T. antarctica</i> (spores) | 1.3 | <u>6.7</u> | <u>8.5</u> | <u>6.1</u> | 17.81 | *** |
| <i>T. antarctica</i> (vegetative) | 0.2 | 0.0 | 0.0 | 0.0 | 2.36 | N.S. |
| <i>T. gracilis</i> | 0.8 | <u>1.3</u> | <u>2.1</u> | <u>3.8</u> | 42.26 | *** |
| <i>T. gracilis</i> var. <i>expecta</i> | 0.2 | 0.2 | 0.0 | <u>0.7</u> | 11.87 | *** |
| <i>T. lentiginosa</i> | 0.2 | 0.4 | <u>0.8</u> | <u>2.2</u> | 51.02 | *** |
| <i>T. reinboldii</i> | 0.1 | 0.3 | 0.2 | <u>0.9</u> | 16.95 | *** |

Analyses were carried out on log₁₀(x+1) transformed abundance. Degrees of freedom = 3, 97. ANOVA P values: * <0.05, ** <0.005, *** <0.0005, N.S. not significant. Bold: species with significant differences in mean abundance. Underlined: species with significantly higher abundance in a cluster group.

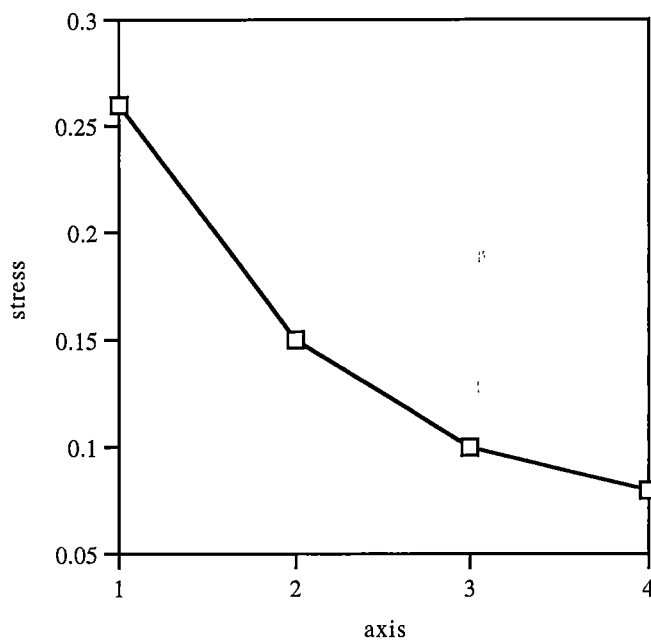


Fig. 9.3. Graphical method of Kruskal and Wish (1978) for selecting the appropriate level of NMDS ordination. Two axes were selected, based on the point of maximum change in direction of the curve.

Table 9.2. Multiple regression analysis between environmental variables and NMDS scores for two-axis ordination of comparison samples.

| Variable | Direction Cosine | | R^2_{adj} | F | P |
|-------------|------------------|---------|-------------|--------|------|
| | x | y | | | |
| Latitude | 0.723 | 0.312 | 0.56 | 64.754 | *** |
| Longitude | 0.213 | 0.447 | -0.016 | 0.221 | N.S. |
| Depth | -273.678 | -91.906 | 0.253 | 17.931 | *** |
| Temperature | -0.097 | -0.164 | 0.009 | 1.470 | * |
| Salinity | -0.716 | -0.181 | 0.296 | 22.015 | *** |
| Density | -0.409 | 0.082 | 0.153 | 10.052 | *** |
| Ice (Oct) | -2.413 | -3.136 | 0.083 | 5.507 | * |
| Ice (Nov) | -3.300 | 0.560 | 0.018 | 1.929 | N.S. |
| Ice (Dec) | 2.855 | 2.528 | 0.015 | 1.748 | N.S. |
| Ice (Jan) | 9.328 | 4.389 | 0.271 | 19.580 | *** |
| Ice (Feb) | 8.647 | 1.159 | 0.218 | 14.936 | *** |

Degrees of freedom: 2, 98. ANOVA P values: *** <0.0005, ** <0.005, * <0.05, N.S. not significant.

R^2_{adj} = adjusted coefficient of determination, which gives the fraction of variance accounted for by the explanatory variable (Jongman et al., 1987).

Table 9.3 Cosine and acosine values (using NMDS axis 1 and axis 2 coefficient values) used to determine direction of arrows in Fig 8.4 for each environmental variable.

| Variable | Coeff 1 | Coeff 2 | C1 Cos | C2 Cos | C1 Acos | C2 Acos |
|-------------|----------|---------|--------|--------|---------|---------|
| Latitude | 0.723 | 0.312 | 0.92 | 0.40 | 23.34 | 66.66 |
| Longitude | 0.213 | 0.447 | 0.43 | 0.90 | 64.52 | 25.48 |
| Depth | -273.678 | -91.906 | -0.95 | -0.32 | 161.44 | 108.56 |
| Temperature | -0.097 | -0.164 | -0.51 | -0.86 | 120.60 | 149.40 |
| Salinity | -0.716 | -0.181 | -0.97 | -0.25 | 165.81 | 104.19 |
| Density | -0.406 | 0.082 | -0.98 | 0.20 | 168.66 | 78.66 |
| Ice (Oct) | -2.413 | -3.136 | -0.61 | -0.79 | 127.58 | 142.42 |
| Ice (Nov) | -3.300 | 0.560 | -0.99 | 0.17 | 170.37 | 80.37 |
| Ice (Dec) | 2.855 | 2.528 | 0.75 | 0.66 | 41.52 | 48.48 |
| Ice (Jan) | 9.328 | 4.389 | 0.90 | 0.43 | 25.20 | 64.80 |
| Ice (Feb) | 8.647 | 1.159 | 0.99 | 0.13 | 7.63 | 82.37 |

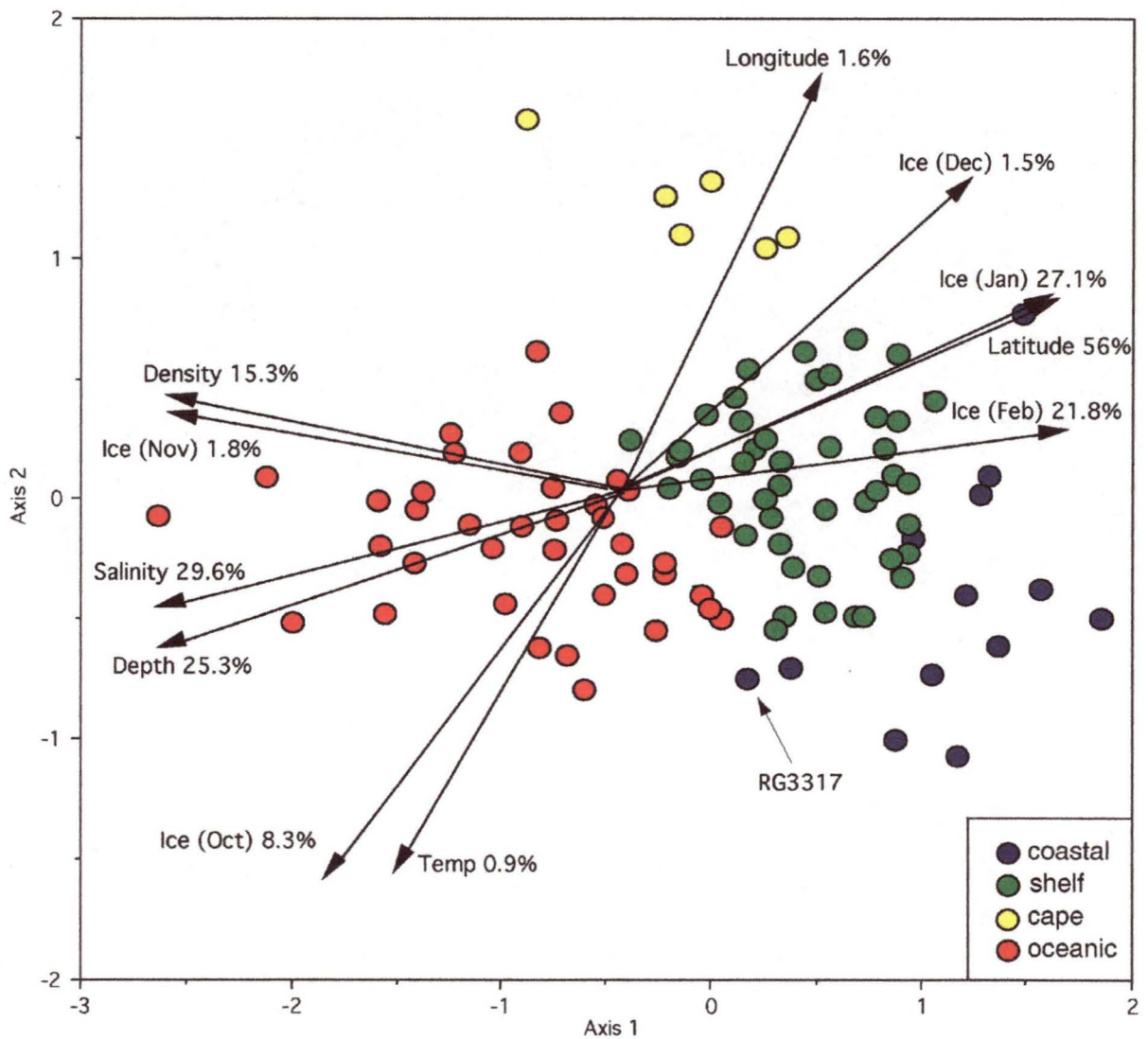


Fig. 9.4. Ordination plot of sample sites, based on species abundance (>2% log₁₀). Cluster groups identified in Fig. 9.1 are superimposed. Arrows indicate direction of maximum correlation for significant multiple regressions between ordination scores and environmental variables.

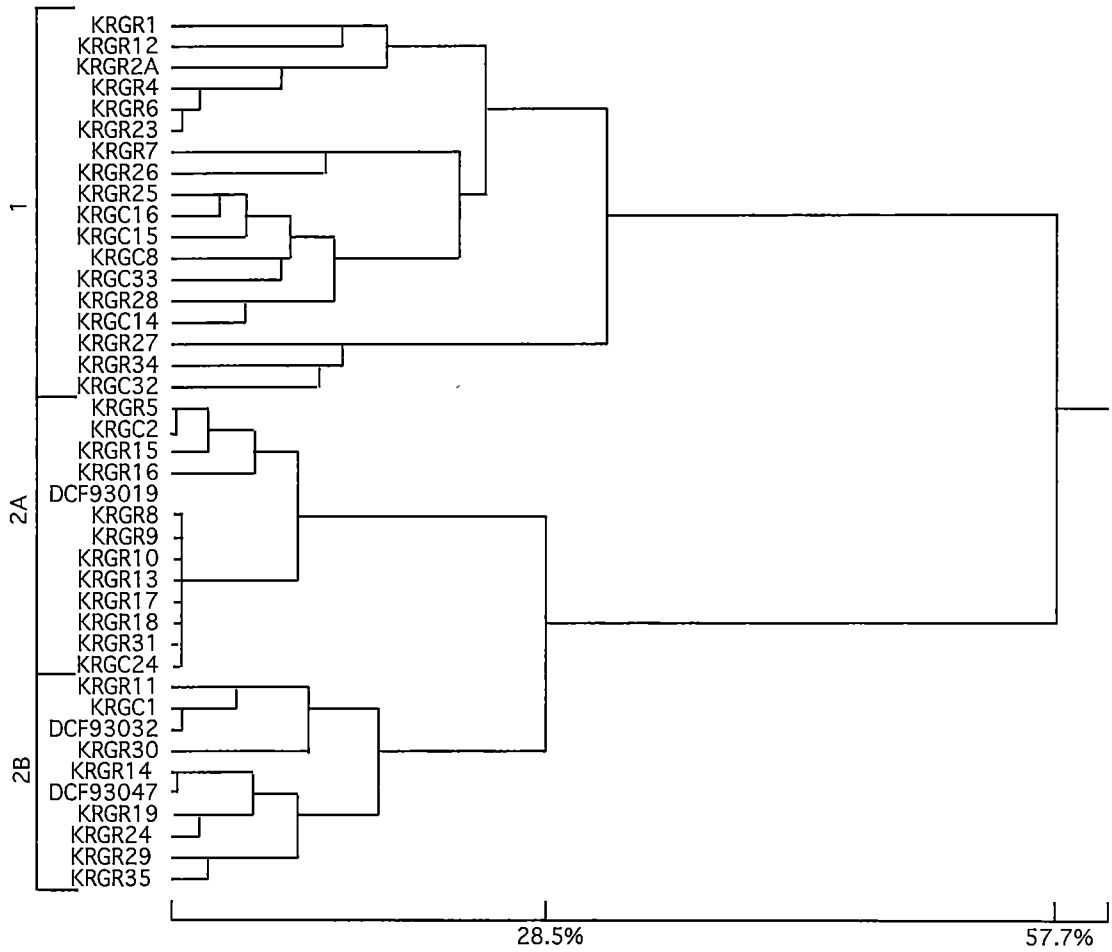


Fig. 9.5. Dendrogram of cluster analysis comparing sample sites, based on grain size distribution.

Table 9.4. Mean abundance (%), analysis of variance (F) and SNK multiple range tests of dominant sediment types in cluster groups.

| Sediment Type | Cluster Group | | | F | P |
|---------------|---------------|--------------|--------------|--------|-----|
| | 1 | 2A | 2B | | |
| Gravel | <u>7.87</u> | 0.04 | 1.68 | 8.95 | *** |
| Sand | <u>63.70</u> | <u>3.39</u> | <u>26.49</u> | 137.31 | *** |
| Mud | <u>28.43</u> | <u>96.63</u> | <u>71.83</u> | 188.49 | *** |

Analyses were carried out on % abundance. $DF = 2, 38$. ANOVA P values: *** < 0.0005 . **Bold text:** sediment type with significant differences in mean abundance. **Underlined text:** sediment type with significantly higher abundance in a cluster group.

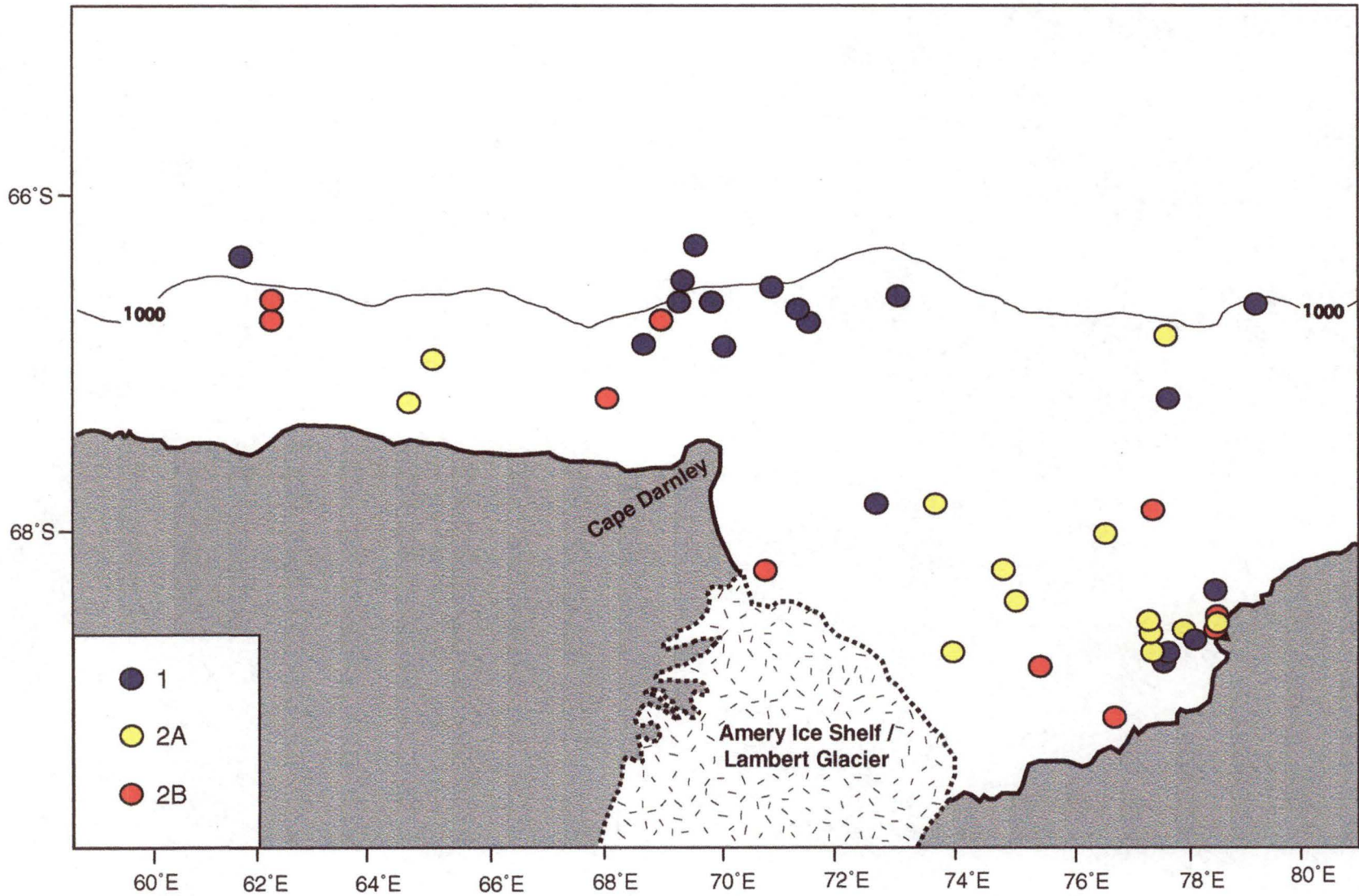


Fig. 9.6. Geographic distribution of grain size cluster groups in Prydz Bay and Mac.Robertson Shelf. Cluster group characteristics: 1 (gravelly sand), 2A (mud), 2B (sandy mud).

– Chapter 10 –

Discussion

Four diatom assemblages are identified in Prydz Bay and Mac.Robertson Shelf using classification (cluster analysis) and ordination (NMDS) (Fig. 10.1). No species of diatom is unique to any one assemblage; however, there are significant differences in species abundance between each. Results suggest that deposition of the coastal, shelf and oceanic assemblages is a function of latitude, and environmental variables that covary with latitude, in association with horizontal water circulation patterns. The cape assemblage is described as an “artificial” diatom assemblage, from which small and delicate frustules have been removed by winnowing from strong bottom currents.

10.1 Coastal Assemblage

The coastal assemblage is characterised by the indicator species *F. curta*, *F. cylindrus*, *F. angulata*, and *P. turgiduloides* (Table 10.1). *Fragilariopsis curta* is the dominant species, forming up to 70.5% of the assemblage. High abundance of this pennate diatom have previously been observed in coastal Antarctic regions, where it occurs in both the water column and within the sea ice (e.g. Kozlova, 1966; Gersonde, 1984; Garrison and Buck, 1985; Leventer and Dunbar, 1988; Scott *et al.* 1994). It is also abundant in surface sediments (e.g. Kozlova, 1967; Truesdale and Kellogg, 1979; Leventer and Dunbar, 1988; Stockwell *et al.*, 1991).

The coastal assemblage coincides with areas of Prydz Bay and Mac.Robertson Shelf where sea ice cover persists well into summer, water depth is relatively shallow and surface water salinity is low. Sea ice in the Indian sector of the Southern Ocean varies widely, from $\sim 6.3 \times 10^6 \text{ km}^2$ (September – October) to $\sim 1 \times 10^6 \text{ km}^2$ (February) (Jacka, 1983; Glöersen *et al.*, 1992). The sea ice within this zone consists primarily of first-year ice (Jacka *et al.*, 1987; Allison *et al.*, 1993), but it does not form a continuous sheet. Rather it is a highly mobile mix of different ice thickness and open water, in the form of leads and polynyas (Allison *et al.*, 1993).

Table 10.1. Mean abundance and preferred ecological habitat of species characteristic of the coastal diatom assemblage.

| Species | Mean Abundance (%) | Habitat |
|-------------------------|--------------------|-------------------------|
| <i>F. angulata</i> | 4.2 | Sea ice and open water? |
| <i>F. curta</i> | 54.7 | Sea ice and open water |
| <i>F. cylindrus</i> | 22.3 | Sea ice and open water |
| <i>P. turgiduloides</i> | 0.4 | Sea ice |

Eighty percent of the winter sea ice does not survive the summer (Parkinson *et al.*, 1987). That which does survive undergoes no significant surface melt (Andreas and Ackley, 1982). In Prydz Bay, the areas where sea ice persists throughout summer are concentrated in the south-east, where ice concentration can remain up to ~ 80% (personal observation, based on 1978 – 1991 SMMR and SSM/I passive microwave records). Summer ice also occurs at shallow sites along Mac.Robertson Shelf, where it regularly persists in the vicinity of Four Ladies Bank, Fram Bank, Storegg Bank and an area north of Scullins Monolith (Streten and Pike, 1984). In those areas, grounded icebergs act to constrain the sea ice, preventing its seasonal melt and breakout, so that it is able to survive more than one summer.

Although the salinity range of surface waters in Prydz Bay – Mac.Robertson Shelf is small (in the order of 33.0‰ to 34.0‰), there is a general decrease in salinity from north to south, such that areas of low salinity coincide with areas of summer sea ice. Smith *et al.* (1984), Nunez Vas and Lennon (1996) and Wong (1994) have also reported a general north to south decrease in water salinity, and corresponding association with sea ice. The lower salinity, southern-most water is attributed to both melt of the sea ice that is present, and fresh-water runoff from the Antarctic ice sheet to the coast. The effect of seasonal sea ice melt on water structure has been observed at a site of annual ice cover near Mawson (Allison *et al.*, 1982; Allison, 1989). Here, a slight decrease in water column salinity occurs prior to December, due wholly to melting on the underside of the seasonal sea ice. From December onwards, there is a significant input of freshwater melt from the nearby ice plateau. The input reaches its maximum in early January and

forms a shallow surface layer (~100-m) that is only mixed to the full depth of the halocline after the ice breaks out.

Although water salinity and density are correlatable ($R^2 = 5.15$), it is unlikely that either of these variables have a major influence on the distribution of diatoms in surface waters of Prydz Bay or Mac.Robertson Shelf. The range over which both vary is small (see Table 8.2) and probably insufficient to affect diatom distribution, as most species have a far-wider tolerance. Salinity-tolerance experiments conducted on *F. curta* and *F. cylindrus*, for example, indicate that both have maximum growth rates in water where salinity ranges from 29.0‰ to 31.5‰ (Vargo *et al.*, 1986). As salinity and density co-vary with latitude and ice cover, it is more likely that the latter variables have a greater effect on diatom distribution.

The coastal diatom assemblage in Prydz Bay is interpreted to represent the sea ice assemblage identified by Stockwell *et al.* (1991) and Scott *et al.* (1994). They observed that pack-ice diatom communities in Prydz Bay are characterised by the dominance of *F. curta*, in association with *F. cylindrus* and *P. turgiduloides*. These species have been noted also amongst the dominant diatoms in pack ice from the Weddell Sea and Antarctic Peninsula (Garrison and Buck, 1989). In fast ice from Lützow-Holm Bay, chain-forming pennate diatoms, such as *Amphiprora* and *Berkeleyea* are dominant, but *Fragilariopsis* and *Pseudonitzschia* species are abundant (Watanabe, 1988; Tanimura *et al.*, 1990). Kang and Fryxell (1988) identify *F. cylindrus* as the most abundant species in ice edge zones from Prydz Bay; Leventer and Dunbar (1996) identify *F. curta* as dominant in the Ross Sea. A similar assemblage to the coastal assemblage has been identified in surface sediments of the Ross Sea (Truesdale and Kellogg, 1979), which is considered to indicate undisturbed, continental shelf sediments. The Ross Sea assemblage is similar to the Antarctic neritic assemblage described by Kozlova (1966) and Jousé *et al.* (1971), which they found to be characteristic of sediments of the coastal regions of Antarctica. Results from the present study suggest that their neritic assemblages could be further subdivided into the coastal and shelf assemblages identified here.

Three of the diatom species – *F. curta*, *F. cylindrus* and *P. turgiduloides* – identified as dominant in pack and fast ice communities of Antarctica (Stockwell *et al.*, 1991; Scott *et al.*, 1994) are characteristic of the coastal diatom sediment assemblage. Many of the species also noted by those authors as abundant in sea ice algal assemblages (e.g. *Chaetoceros* spp., *Entomeneis kjellmanii* (Cleve) Poulin, *Nitzschia cloisterium* Van Heurck, *N. stellata* Manguin, and *N. subcurvata* Hasle) are not preserved in abundance in sediments, however. The lightly silicified and fragile frustules of such species are likely to have been lost to the sediment by mechanical breakage and selective dissolution. Coupled with bioturbation and selective predation, these processes alter the original diatom assemblage, leading to a decline in species diversity and abundance (Mikkelsen, 1990; Dunbar *et al.*, 1989). Although *F. cylindrus* is a small and lightly silicified, its high abundance in the water column and in ice communities is preserved in the sediment. This species is also common in faecal pellets of zooplankton; some of which have been observed to contain *F. cylindrus* exclusively (Fryxell *et al.*, 1988; Buck *et al.*, 1990). The grazing of diatoms by zooplankton incorporates the frustules into faecal pellets, acting to both increase the rate of settling and inhibit dissolution by enclosing them in a protective membrane (Schrader, 1971).

10.2 Shelf Assemblage

The shelf assemblage is characterised by a significant abundance of ice-associated species that are indicative of the coastal assemblage (i.e. *F. curta*, *F. cylindrus* and *F. angulata*). This assemblage is further characterised, however, by the abundance of the centric diatoms *Porosira glacialis* and *Thalassiosira antarctica* (resting spores), and the silicified Chrysophyte *Pentalamina corona* (Table 10.2).

Thalassiosira antarctica reaches maximum abundance in Antarctic inshore and ice-edge waters (Hasle and Heimdal, 1968; Fryxell, 1977; Johansen and Fryxell, 1985; Medlin and Priddle, 1990) where temperatures and salinity are low (Fryxell *et al.*, 1981). It does not occur within sea ice assemblages, and, in contrast to many *Fragilariopsis* species, is unable to survive the low light intensities under the ice or in brine channels within the ice (Fryxell *et al.*, 1987). Similarly, *P. glacialis* is considered indicative of ice

conditions (Krebs *et al.*, 1987), but has not been observed as a member of ice-communities (e.g. Watanabe, 1988; Garrison and Buck, 1989; Scott *et al.*, 1994). Results from this study would suggest *P. glacialis* is associated with ice-edge conditions. *Fragilariopsis cylindrus* has also been reported to form ice-edge blooms in Prydz Bay (Kang and Fryxell, 1992).

Table 10.2. Mean abundance and preferred ecological habitat of species characteristic of the shelf diatom assemblage.

| Species | Mean Abundance (%) | Habitat |
|-------------------------------------|--------------------|-------------------------|
| <i>F. angulata</i> | 3.9 | Sea ice and open water? |
| <i>F. curta</i> | 48.5 | Sea ice and open water |
| <i>F. cylindrus</i> | 15.6 | Sea ice and open water |
| <i>P. corona</i> | 3.8 | Open water |
| <i>P. glacialis</i> | 0.9 | Ice edge / open water |
| <i>T. antarctica</i> resting spores | 6.7 | Neritic / open water |

Although Parmales, a group of Chrysophyte with siliceous wall plates, is abundant in the waters of Prydz Bay (Marchant, 1993), only two species have been identified in sediment from here (Franklin and Marchant, 1995; Taylor *et al.*, in prep.): *Triparma laevis* and *Pentalamina corona*. Both have also been observed in surface sediment from the Weddell Sea (Zielinski, 1997). Franklin and Marchant (1995) suggest that these species preserve in sediment due to their smooth and heavily silicified wall plates that are less susceptible to dissolution. Only *P. corona* was observed in the sediments of the present study. The reason for this is most likely attributable to the extremely small size of the cells (<5 µm), making them difficult to see and identify under the light microscope. This species occurred in significant abundance in both the shelf and oceanic assemblages, suggesting it is indicative of cold water, ice-edge conditions, but does not occur within sea ice. This distribution supports the findings of Marchant (1993), who suggests that they may be a useful biostratigraphic marker of cold-water deposition.

The shelf assemblage is suggested to represent a near-shore / ice-edge Antarctic community. Even though species indicative of sea ice communities are significantly abundant, such pennate diatoms may also be abundant in the water column (e.g. *F. curta* and *F. cylindrus*). Kang and Fryxell (1992) observed *F. curta*, *F. cloisterium* and *F. cylindrus* to dominate the water column in Prydz Bay during ODP Leg 119, with cell maxima being located above the thermocline (20 m – 50 m). Here the vertical stratification created by summer heating and ice melt has a major influence on the vertical distribution of diatom cells (Kang and Fryxell, 1992). The high degree of similarity between the shelf and coastal assemblages may also be attributed to either the close proximity of recently receded ice edges, which release cells from ice, and / or advection from a previously ice-covered area (Garrison *et al.*, 1987). The abundance of *P. glacialis* and *T. antarctica* resting spores is typical, for example, of ice edge communities.

10.3 Oceanic Assemblage

The oceanic assemblage indicator species (Table 10.3) are characteristic of open-water primary production. *Fragilariopsis kerguelensis*, which forms up to 52.7% of the assemblage, increases with distance from the Antarctic continent in both the plankton (Kozlova, 1966) and sediment (Leventer, 1992). The northern distribution of *F. kerguelensis* is limited by the Antarctic Convergence (Kozlova, 1966; Hasle, 1969). Laboratory-based salinity experiments have demonstrated that it has a maximum growth rate at 34.0‰, which corresponds with its preferred oceanic habitat where there is little fresh-water influx compared to coastal areas. The abundance of *F. kerguelensis* is also negatively correlated with sea-ice concentration (Burckle *et al.*, 1987). It is considered to be an open-water species, dominating summer surface waters between 52°S and 63°S (Burckle and Cirilli, 1987; Burckle *et al.*, 1987; Zielinski and Gersonde, 1997) where temperatures are >0°C (Burckle *et al.*, 1987; Krebs *et al.*, 1987).

The oceanic assemblage is similar to assemblages that have been described in the subantarctic, Southern Ocean water column (Kozlova, 1966) and sediment (Jousé *et al.*, 1962, 1971). All assemblages are characterised by abundant *F. kerguelensis* and

T. lentiginosa. Similarly, a diatom assemblage dominant by *F. kerguelensis* has been identified in sediments on the continental slope and abyssal plain of the Ross Sea (Truesdale and Kellogg, 1979), and the George V Coast (Leventer, 1992).

Table 10.3. Mean abundance and preferred ecological habitat of species characteristics of the oceanic diatom assemblage.

| Species | Mean Abundance (%) | Habitat |
|--|--------------------|----------------------|
| <i>A. actinochilus</i> | 0.7 | Neritic |
| <i>Chaetoceros</i> resting spores | 12.6 | Open water |
| <i>D. antarcticus</i> | 0.8 | Open water |
| <i>Distephanus</i> | 0.8 | Open water |
| <i>E. antarctica</i> | 1.2 | Sea ice |
| <i>F. cylindrus</i> | 13.3 | Sea ice / Open water |
| <i>F. kerguelensis</i> | 13.8 | Open water |
| <i>F. separanda</i> | 1.7 | Open water |
| <i>P. corona</i> | 3.1 | Open water |
| <i>S. microtrias</i> | 0.6 | Sea ice / Open water |
| <i>T. antarctica</i> resting spores | 6.1 | Neritic / Open water |
| <i>T. gracilis</i> | 3.7 | Open water |
| <i>T. gracilis</i> var. <i>expecta</i> | 0.7 | Open water |
| <i>T. lentiginosa</i> | 2.2 | Open water |
| <i>T. reinboldii</i> | 0.9 | Open water |

Actinocyclus actinochilus and *E. antarctica* are significantly more abundant in the oceanic assemblage but, numerically, they form only a minor component (a maximum of 2.7% and 6.7%, respectively). Both species are considered widespread, but rare, in Antarctic waters, being most abundant in near-shore and neritic environments (e.g. Jousé *et al.*, 1962; Kozlova, 1966; Burckle, 1984). Jousé *et al.* (1962) observed that the abundance of *E. antarctica* in sediments from the Indian sector of the Antarctic ranged from 1% - 5% north of the Polar Front (Antarctic Convergence), to 2% - 50% south of the Polar Front, reaching a maximum of 80% in sediments from the Antarctic coast.

Similarly, Kozlova (1966) noted that the abundance of *E. antarctica* is greatest in sediments on the Antarctic continental shelf, ranging from 0.9% to 4%; in the open ocean, it ranges from 0.1% to 0.9%. The northern limit of this species coincides with the Antarctic Convergence (Kozlova, 1966). Having reviewed the literature extensively, Burckle (1984) concluded that *E. antarctica* is neritic. Although widely distributed throughout the Southern Ocean, it forms only a minor part of the oceanic plankton. In the vicinity of sea ice, icebergs and the Antarctic coastline, however, *E. antarctica* becomes a more abundant, but not dominant, component of the plankton.

The significant abundance of *A. actinochilus* and *E. antarctica* in the open water, oceanic assemblage of the present study is attributed to dissolution. Truesdale and Kellogg (1979) have suggested that surface sediments enriched in *E. antarctica* may be due to selective dissolution of the less robust species and / or winnowing by strong bottom currents. Both species are strongly silicified and robust, making them less susceptible to both of these processes (Fenner *et al.*, 1976; Truesdale and Kellogg, 1979). Current reworking is a less likely cause of the oceanic assemblage, as smaller diatom frustules are present in significant abundance (e.g. *F. cylindrus*), similar to that on the continental shelf.

Chaetoceros resting spores are most abundant in the oceanic assemblage, forming up to they 25.1% of the frustules observed. Abundant *Chaetoceros* resting spores have also been noted in sediments from George V Coast, where their highest concentrations are associated with the maximum summer retreat of the annual ice edge (Leventer, 1992). High concentrations of *Chaetoceros* resting spores are generally interpreted as indicative of high primary production (Donegan and Schrader, 1982). Leventer (1992) suggests that their abundance in sediment may also be due to dissolution and / or environmental stress, such as that which may occur with decreased water salinity in association with ice melt.

Although considered indicative of open-water, subantarctic conditions, the oceanic diatom assemblage intrudes across the continental shelf, between 75°E and 78°E, and

extends south into Prydz Bay to ~ 68°S. It is suggested that the shelf distribution reflects the horizontal water circulation of Prydz Bay. A large, slow-moving, cyclonic gyre is centred in the mid- to western part of the bay, extending offshore to ~ 65°S (Smith *et al.*, 1984; Wong, 1994). The circulation of the gyre introduces waters from the Antarctic Circumpolar Current across the continental shelf and into the bay. This may also be acting as a transport mechanism to bring the oceanic diatom assemblage onto the continental shelf, where it eventually merges with the shelf and / or coastal assemblages and loses its identity. The high abundance of *F. kerguelensis* and the oceanic foraminifera *Neogloboquadrina pachyderma* in sediment at the seaward end of the Prydz Channel also prompted Franklin (1993) to suggest that a strong, oceanic influence is present in Prydz Bay, due to the circulation of the gyre.

10.4 Cape Assemblage

The most striking characteristic of the cape assemblage is its composition of both open-water species and ice-associated species (Table 10.4). The abundant species all possess heavily silicified, large frustules, such as *Eucampia antarctica* and *F. kerguelensis*. Fragile and lightly silicified frustules that are abundant in the surrounding oceanic and shelf assemblages (e.g. *F. cylindrus*, *P. corona* and *Chaetoceros* resting spores) are significantly lower in abundance.

A similar assemblage, dominated by *Eucampia antarctica* (= *E. balaustium*), has been observed in the sediments of the Ross Sea (Truesdale and Kellogg, 1979), and in the southeast Atlantic Ocean (Defelice and Wise, 1981). These assemblages are considered indicative of lag deposits, from which the lighter, more fragile diatoms have been selectively winnowed by bottom currents. Although *E. antarctica* does not dominate the cape assemblage identified in Prydz Bay, it does reach its maximum abundance here, forming up to 5.5% of the assemblage. It is therefore suggested that the cape assemblage does not reflect the surrounding ecological environment, but is rather a product of some other oceanographic process. A similar situation has been noted by Quilty (1985) with the distribution of foraminifera in Prydz Bay. The cape diatom assemblage coincides with a sharp foraminiferid-associated boundary. Surface sediment

samples from Prydz Bay contain foraminifera in low abundance, low diversity and low planktonic number (Quilty, 1985). Where foraminifera are present, they occur mainly as benthic, agglutinated species (Quilty, 1985). Sediment from Cape Darnley and Mac.Robertson Shelf, however, contain very abundant benthic and planktonic foraminifera, in association with a very diverse, dominantly calcareous, macrofauna. It has been suggested that the clear demarcation of the two associations at 71°E may be controlled by an oceanographic boundary (Quilty, 1985).

Table 10.4. Mean abundance and preferred ecological habitat of species characteristic of the cape diatom assemblage.

| Species | Mean Abundance (%) | Habitat |
|-------------------------------------|---------------------------|-----------------------|
| <i>A. actinochilus</i> | 0.5 | Neritic |
| <i>D. antarcticus</i> | 0.9 | Open water |
| <i>Distephanus</i> | 0.6 | Open water |
| <i>E. antarctica</i> | 2.3 | Sea ice |
| <i>F. angulata</i> | 5.6 | Sea ice |
| <i>F. curta</i> | 62.8 | Sea ice |
| <i>F. separanda</i> | 1.7 | Open water |
| <i>P. glacialis</i> | 0.6 | Ice Edge / Open water |
| <i>S. microtrias</i> | 0.9 | Sea ice / Open water |
| <i>T. antarctica</i> resting spores | 8.5 | Neritic / Open water |
| <i>T. gracilis</i> | 2.1 | Open water |

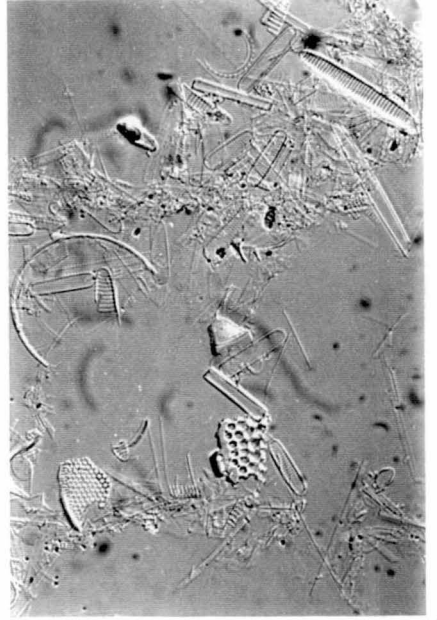
Grain size analysis, coupled with a lack of small and fragile diatom frustules, supports the hypothesis that the cape assemblage is a product of current reworking (Fig. 10.2). Sediment from this assemblage is dominated by sand and has a significantly greater proportion of gravel, compared to the coastal, shelf and oceanic assemblage sediment. Similar sediment ratios to that observed near Cape Darnley are present on Four Ladies Bank and at coastal sites near the Vestfold Hills. These are likely to reflect terrigenous

input from icebergs and iceberg grounding, whilst around Cape Darnley it is probably due to strong currents.

The strong, westward flowing Antarctic Coastal Current exits the bay around Cape Darnley. At this point water converges with a narrow, westward flowing slope current (Wong, 1994), and some is recirculated into the bay as part of the slow-moving, cyclonic gyre. In comparison to the gyre, the westward shelf current is strong enough to decouple primary production in the surface waters from the underlying sediments, transporting material falling through the water column some distance before it settles (O'Brien *et al.*, 1995a). Fine-grained particles may be further lost at the sediment – water interface due to the processes of bottom currents and bioturbation (Singer and Anderson, 1984), and at the shelf edge where deep-water currents can impinge on the shelf (Anderson and Smith, 1989, cited in Anderson, 1989).

Fig. 10.1. Light micrographs of typical diatom assemblages in the surface sediment of Prydz Bay and Mac.Robertson Shelf.

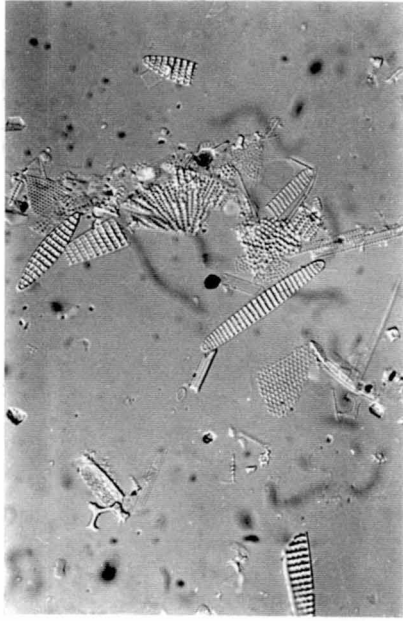
- 1. Coastal assemblage*
- 2. Shelf assemblage*
- 3. Oceanic assemblage*
- 4. Cape (reworked) assemblage*



1



2



3



4

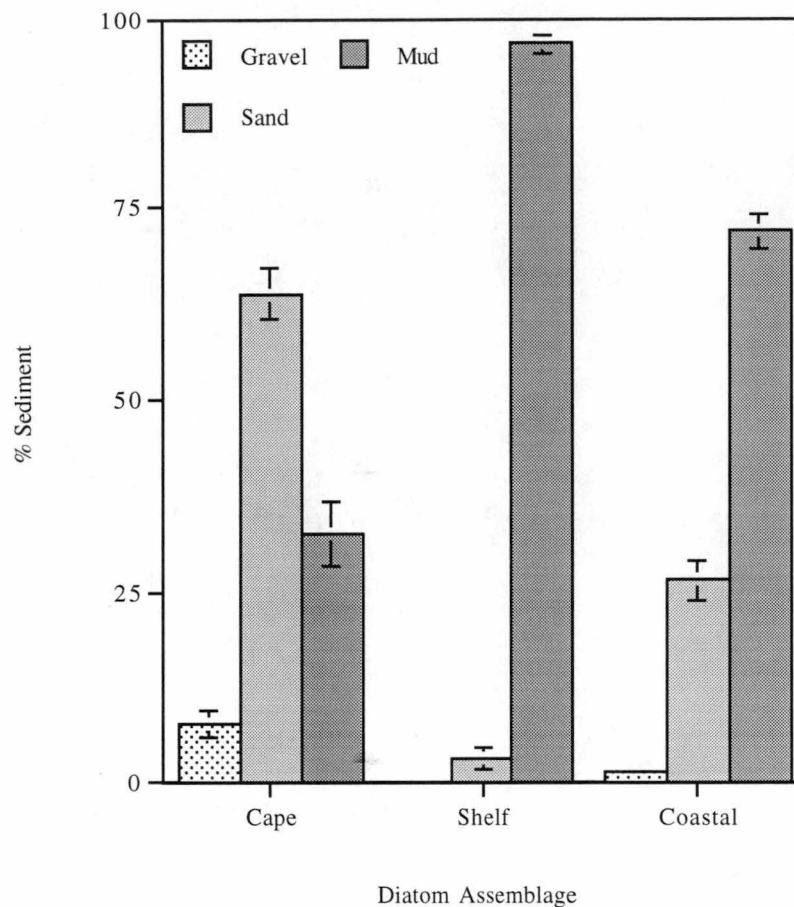


Fig. 10.2. Distribution of sediment fractions in diatom assemblages identified in Prydz Bay. The cape assemblage contains a significantly greater abundance of sand ($>63\ \mu\text{m}$) and gravel ($>2\text{mm}$), and significantly less mud ($<63\ \mu\text{m}$) sized particles, compared to the coastal assemblage. No samples from the oceanic assemblage were available for comparison.

– *Chapter 11* –
Conclusion

Using classification (cluster analysis) and ordination (NMDS) techniques, four diatom assemblages can be recognised in the surface sediments of Prydz Bay and Mac.Robertson Shelf:

1. Coastal– characterised by sea ice species.
2. Shelf– characterised by sea ice and ice-edge species.
3. Oceanic – characterised by open water species.
4. Cape – characterised by heavily-silicified, robust sea ice and open water species.

Using multiple regression analysis, evidence strongly suggests that primarily latitude, and the environmental variables that co-vary with latitude, control the assemblages. Most importantly, the summer (January – February) distribution of sea ice, and the influence this has on water salinity, appears to be major variable affecting diatom distribution. Horizontal water circulation may also play an important role, most noticeably the Prdyz Bay gyre that acts as a transport mechanism to introduce the open water, oceanic diatom assemblage across the continental shelf and into Prydz Bay ~75°E.

The cape assemblage is suggested to represent an “artificial” diatom assemblage, reflecting strong bottom currents. In the vicinity of Cape Darnley a coastal current exits Prydz Bay, with some water diverging to the west, along Mac.Robertson Shelf, as a westward flowing shelf current, and the rest being redirected into the bay as part of the cyclonic gyre. Grain size analysis indicates that sediments from the cape assemblage have undergone extensive winnowing, possibly by intensification of the coastal current as it exits Prydz Bay and / or intermittent impinging of ocean currents. This process removes fragile and small diatom frustules, leaving a lag deposit of robust, heavily silicified species indicative of both open water and ice-algal assemblages.

– *Part B* –

*Late Pleistocene / Holocene Diatom Assemblages of
Prydz Bay and Mac.Robertson Shelf*

– Chapter 12 –

Introduction to Down Core Analyses

Four diatom assemblages are identified in the surface sediments of Prydz Bay and Mac.Robertson Shelf, using statistical methods: coastal, shelf, oceanic, and cape. The assemblages are correlated with four environmental (oceanographic) variables: latitude, percentage sea ice cover (January and February) and water salinity. The cape assemblage is interpreted to be an “artificial” assemblage, from which current winnowing has removed the smaller species.

Using the surface diatom assemblages as a model, six gravity cores are analysed to identify changes in down core assemblages. The cores extend in age from the Upper Pleistocene to Holocene, and cover a broad geographic area – inner and out Prydz Bay, shelf banks, and inner shelf deeps on Mac.Robertson Shelf – which includes all surface assemblage zones. Interpretation of the down core assemblages will provide information on the Upper Pleistocene / Holocene palaeoecology of the Prydz Bay and Mac.Robertson Shelf (East Antarctica), and a useful comparison to similar palaeoecological studies from West Antarctica.

– Chapter 13 –

*Methods for Down Core Analysis***13.1 Gravity cores**

Six gravity cores from Prydz Bay and Mac.Robertson Shelf (Table 13.1; Fig. 13.1) were sub-sampled at 5.0 cm intervals to compare diatom assemblages with those in the surface sediment.

The cores were collected between 1992 and 1997, during ANARE marine science expeditions aboard the RSV *Aurora Australis*. The corer was deployed from the stern of the vessel, using a 1 tonne bomb connected to 3 m or 6 m length by 10 cm diameter core barrel, lined with 9 cm diameter PVC. A one-way flap, fitted to the top of the corer, allowed water to escape during its descent, and prevent through-flow during its ascent. A custom-built cradle designed to minimise corer disturbance during deployment and recovery was used. The cradle also maintains the core at a tilt of at least 15° when returned to the deck, to prevent disturbance of the sediment-water interface (Harris *et al.*, 1997b). The cores were split on board using an electric saw, logged and sampled. They were then wrapped in plastic film, sealed in polyethylene bags and stored horizontally in refrigerators.

Table 13.1 Gravity cores analysed for diatom assemblages.

| Core Station No. | Name | Latitude °S | Longitude °E | Water Depth (m) | Core length (cm) |
|------------------|------------|----------------|-----------------|--------------------|---------------------|
| KROCK/125/GC1 | KROCK GC1 | 66 53.95 | 63 09.26 | 478 | 375 |
| KROCK/128/GC2 | KROCK GC2 | 67 28.46 | 64 58.26 | 1091 | 200 |
| KROCK/159/GC29 | KROCK GC29 | 68 39.78 | 76 41.73 | 789 | 300 |
| KROCK/163/GC33 | KROCK GC33 | 67 10.88 | 68 32.30 | 376 | 240 |
| AA149/28/GC28 | AA149 | 66 43.69 | 71 46.47 | 527 | 152 |
| AA186//28/GC28 | AA186 | 67 16.05 | 76 23.92 | 338 | 186 |

13.2 Sample Preparation and Statistical Analyses

Sample preparation followed the same method outlined in Chapter 6. Statistical analyses (cluster analysis and SNK) were carried out on $\log_{10}(x+1)$ transformed data, following the same methods as outlined in Chapter 7.

13.3 Radiocarbon Analysis

Radiocarbon dates from core samples were determined by accelerator mass spectrometry (AMS) of bulk organic carbon at the New Zealand Institute of Geological and Nuclear Sciences Rafter Radiocarbon Laboratory, Lower Hutt (NZA). Only samples from cores AA186 GC28 and KROCK GC29 (135-135 cm) were submitted by F. Taylor; all other dates are based on samples submitted by the Antarctic CRC, or published records.

Radiocarbon dates from Antarctica must be interpreted with caution. Antarctic marine waters are deficient in ^{14}C (Stuiver *et al.*, 1981; Omoto, 1983), due to a lag in the carbon dioxide exchange between the oceans and atmospheric carbon reservoirs. The lag effect leads to anomalously old radiocarbon dates being obtained from marine material, compared to terrestrial material, which must be corrected for by converting the conventional radiocarbon age to a reservoir-corrected age for marine carbon. The reservoir age describes the difference in ^{14}C activity between atmospheric CO_2 and surface-dissolved inorganic carbon (DIC) in marine systems resulting from the mixing of older waters from depth into the surface layers of the ocean (Eglinton *et al.*, 1997).

In Antarctica, the reservoir effect is particularly marked due to other processes acting in combination with the effects on the CO_2 reservoir from upwelling. Anomalously old Antarctic marine radiocarbon ages may also reflect the depletion of ^{14}C in surface waters. This is due to CO_2 sources derived from glacial melting (Omoto, 1983), and the input of older, eroded sediment that has been re-deposited by lateral transport, current winnowing, and possible mass wasting processes (Harden *et al.*, 1992). Anomalies appear greatest in samples recovered from close to the continental ice margin (Omoto, 1983).

A unanimous, reservoir correction date for Antarctic material has not been determined and the correction factor is variable. Stuiver *et al.* (1981) suggest that the greatest possible correction for an Antarctic radiocarbon dates between 1 200 radiocarbon years before present (yBP) and 1 400 yBP. Omoto (1983) suggests that correction ranges from 800 yBP to 3 000 yBP, and that it should be determined by radiocarbon dates obtained from living organisms similar to the fossil material to be dated. In eastern Prydz Bay, a reservoir correction age of 1 750 yBP obtained by Domack *et al.* (1991A), from unconsolidated sediments at ODP Hole 740A, compares reasonably to a date of 1 300 yBP obtained by Adamson and Pickard (1986) from modern marine sediments collected adjacent to the Vestfold Hills.

In the present study, reservoir corrected ^{14}C dates have been used, unless otherwise indicated. A correction date of 1 733 yBP has been used for KROCK GC1 and KROCK GC2, based on the measured age of a surface-sediment grab sample recovered near the location of KROCK GC2 (Sedwick *et al.*, in press). The age attempts to correct for the non-zero radiocarbon age of the sediment-water interface. The non-zero age includes(Sedwick *et al.*, in press):

1. Reservoir correction.
2. The reservoir age of organic matter in the photic zone.
3. Bioturbation.
4. The addition of resuspended older organic matter from other areas on Mac.Robertson Shelf.

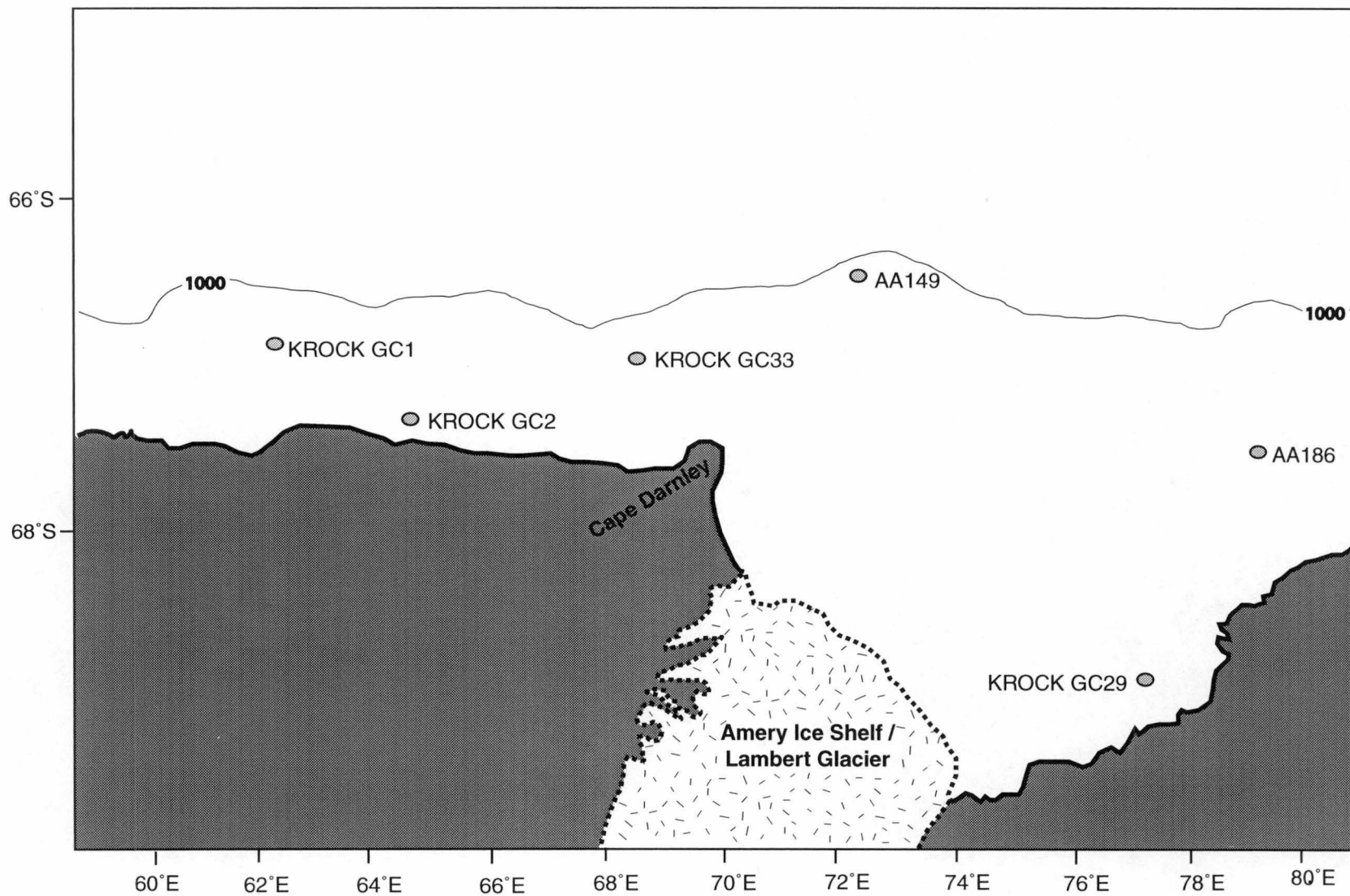


Fig. 13.1. Location of gravity cores used for diatom analysis.

– Chapter 14 –

KROCK GC1

14.1 Site Description

Core KROCK/125/GC1 (GC1, hereafter) was recovered from Iceberg Alley (66° 58.95' S, 63° 09.26' E), Mac.Robertson Shelf (Fig.13.1), in a water depth of 478 m. Iceberg Alley is a deep, fjord valley trending north from Mawson Station to the continental shelf break. Icebergs ground on shallow banks to either side of the valley, creating a stretch of unobstructed, open water that forms an easily navigable shipping channel. From this feature, Iceberg Alley gains its name.

The sample site is approximately 80 km from the Mawson Coast and 25 km from the continental shelf break. Sea ice covers the region throughout autumn, winter and spring. Ice breakout occurs in early summer and open water usually dominates the general area by January.

14.2 Core Description

GC1 is 363.0 cm long and consists predominantly of olive-green (5Y 5/3) to olive-grey (5Y 3/2), biosiliceous ooze (Fig. 14.1). The ooze contains from 10% to 20% very well sorted, fine to very fine, angular, quartzose sand. This facies is typical of the glacial-marine sediments being deposited on the continental shelf of Antarctica today (Anderson *et al.*, 1980). The core is described as one lithological unit.

Numerous alternating layers, devoid of sand and ~1-5 cm thick, are present at intervals throughout the core. The layers are visibly lighter in colour (5Y 8/3) and have a “fluffy” appearance. They are most prevalent between 140 cm and 200 cm, either as distinct bands or grading in colour and texture between the predominant olive-green biosiliceous ooze. A sand lens of very fine to medium angular quartz is present at ~335 cm and contains a 3 mm dark lamina of, possibly, organic material.

14.3 Fossil Assemblages

Large, glass sponge spicules form visible layers at 40-42 cm, 60-62 cm, and 79-80 cm. The biosiliceous ooze otherwise consists predominantly of diatom frustules. Members of the genus *Fragilariopsis* dominate the diatom assemblage, most notably *F. curta* and *F. cylindrus*. Below 335 cm, the assemblage is dominated in near-monospecific abundance by *Chaetoceros* resting spores. The lighter, “fluffy” layers, described above, contain a higher abundance of *Corethron criophilum* Castracane than the surrounding ooze. Foraminifera are absent, as indicated by no visible reaction when HCl is applied to the sediment.

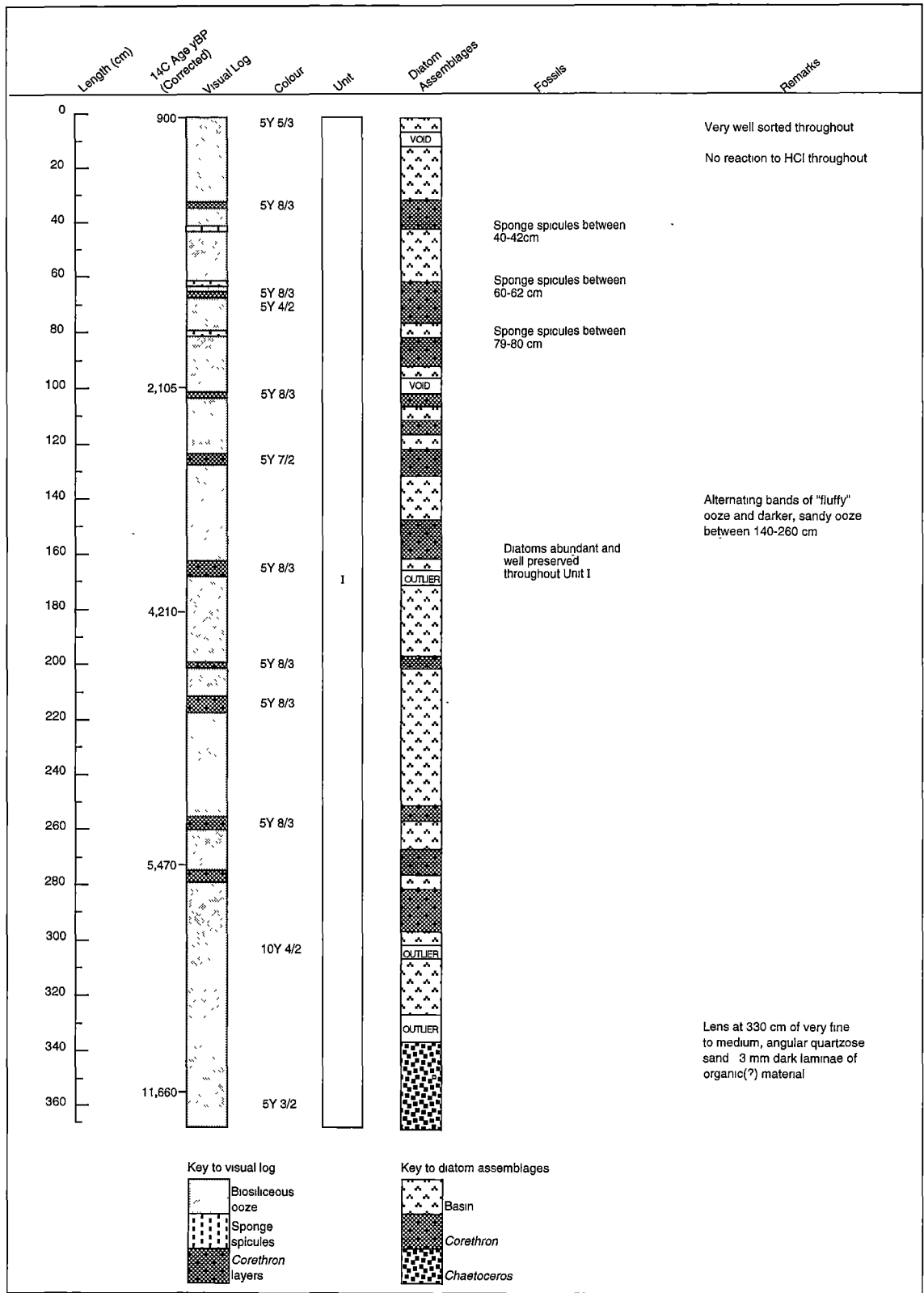


Fig. 14.1. GC1 core log, radiocarbon dates and diatom assemblages when compared to surface sediment.

14.4 GC1 – Results

14.4.1 Radiocarbon Dates

Five AMS radiocarbon dates were obtained from bulk organic carbon samples (Table 14.1). Sedwick *et al.* (in press) suggest that an ocean reservoir correction factor of 1 733 radiocarbon years be subtracted from the ^{14}C age. This estimate is based on the measured age of a surface sample recovered from Nielsen Basin, less than 90 km away. Using this, GC1 has a corrected, core top AMS age of 900 yBP. The absence of unsupported ^{210}Pb indicates that at least 200 years of the uppermost sediment have been lost (Sedwick *et al.*, in press). This most likely occurred during the recovery by impact from the gravity core barrel. The base of GC1 extends into the Early Holocene, with a corrected AMS age of 11 660 yBP obtained at 356.5-357.5 cm.

Simple linear regression indicates a good age versus depth in the upper 273 cm of the core ($R^2 = 0.98$; Fig14.2). Below 273 cm, the sedimentation rate decreases. There is no evidence to suggest the presence of unconformities or sediment reworking. As a result, GC1 provides a continuous, Holocene, sedimentary depositional history for northern Iceberg Alley.

Table 14.1. AMS radiocarbon dates obtained from GCI.

| Interval (cm) | ¹⁴ C Date (y BP) | | Deposition Rate†† (cm yr ⁻¹) |
|---------------|-----------------------------|-----------|---|
| | Uncorrected | Corrected | |
| 0 - 1 | 2 630 | 895 | |
| 100† | 3 838 +/-84 | 2 105 | 0.083 |
| 181 - 182 | 5 940 | 4 207 | 0.039 |
| 272 - 273 | 7 200 | 5 467 | 0.073 |
| 356.5 - 357.5 | 13 390 +/-150 | 11 657 | 0.014 |

† The top section of GCI was originally 100 cm, and appears to have shrunk, from the bottom up, to a total length of 86.5 cm, probably due to water loss. The sample was taken at 85.5 - 86.5 cm, but due to the shrinking is more likely from 100 cm

†† Deposition rates determined between 0-100 cm, 100-181 cm, 181-272 cm, 272-356.5 cm.

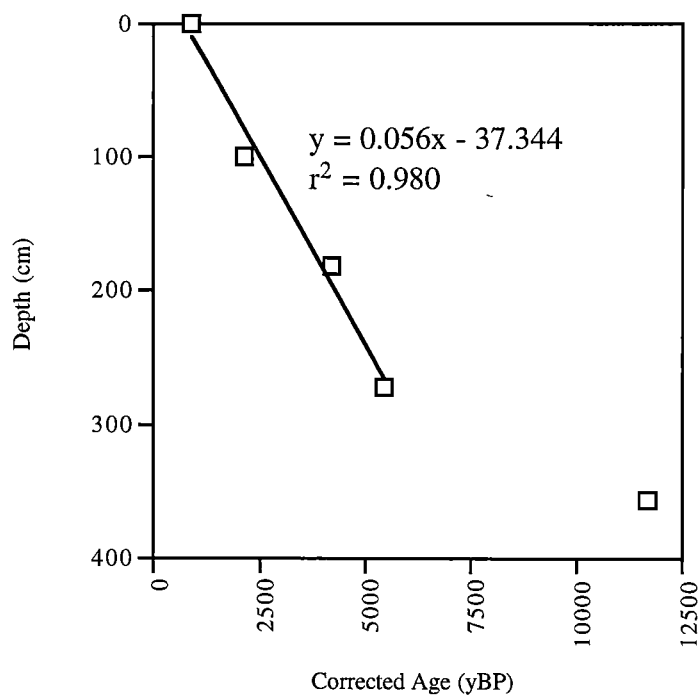


Fig. 14.2. Linear regression of corrected radiocarbon ages versus depth for the upper 273 cm of GCI.

14.4.2 Diatom Assemblages

Members of the pennate genus *Fragilariopsis* dominate the biosiliceous ooze between 0 cm and 335 cm. *Fragilariopsis curta* and *F. cylindrus* are the most common species and abundance ranges from 12.5% to 55.9% and 10.0% to 67.0%, respectively. The subdominant taxa are *Chaetoceros* resting spores, *Corethron criophilum*, and *F. angulata*; none form >25% of the assemblage.

Chaetoceros resting spores dominate below 335 cm. The resting spores are almost monospecific in abundance, forming up to 93.8% of the assemblage. Here, *F. curta* and *F. cylindrus* do not form >10%. No other diatom species occur at >2%.

14.4.3 Statistical Analyses

GC1

A dendrogram illustrating core sample affinities, based on cluster analysis, is illustrated in Fig. 14.3. Twenty-two species with an abundance >2% are observed in the 68 core samples (Appendix 3). Four outliers were identified in the preliminary cluster analysis (165 cm, 305 cm, 325 cm, and 330 cm; Appendix 4), and removed from further analysis. Subsequent cluster analysis identified four cluster groups at 50.3% dissimilarity, with a cophenetic correlation of 0.85. Significantly abundant species in each cluster group are listed in Table 14.2. Analyses were carried out on log₁₀ data. Values in the following discussion are based on arithmetic mean abundance.

Cluster group 1 is the largest group in GC1. It dominates the upper-most sections of the core, from 0-55 cm, 70-125cm, 140-150 cm, 195 cm, 205-220 cm, 250 cm, 260-265 cm, and 280 cm. *Fragilariopsis cylindrus* (36.4%) and *F. curta* (31.7%) dominate the assemblage. *Chaetoceros* resting spores (6.5%) are subdominant. *Fragilariopsis angulata*, *C. criophilum*, and *F. obliquecostata* Heiden are common (>2%). There are no unique abundance indicator species within the cluster group; however, it can be differentiated from cluster group 2 by a statistically greater abundance of *C. criophilum*, *F. cylindrus*, *F. pseudonana* Hasle, and Unidentified Genus A.

Cluster group 2 dominates the lower half of the core, from 130-135 cm, 160-185 cm, 200 cm, 225-240 cm, 255 cm, 275 cm, and 295-320 cm. The diatom assemblage is most similar to that in cluster group 1, being dominated by *F. curta* (35.1%) and *F. cylindrus* (23.7%), and subdominated by *Chaetoceros* resting spores (10.8%). *Fragilariopsis angulata*, *F. obliquecostata* and *Thalassiosira gracilis* are present at >2%. Four indicator species are present: *Distephanus speculum*, *Eucampia antarctica*, *F. separanda*, and *T. lentiginosa*. These species are numerically rare, but statistically more abundant in cluster group 2 compared cluster groups 1, 3 and 4. The diatom assemblage can be further distinguished from that of cluster group 1 by a statistically greater abundance of *T. gracilis*, *F. kerguelensis* and *Dactyliosolen antarcticus* Castracane.

Cluster group 3 is the smallest group identified in GC1, occurring at only 60-65 cm, 270 cm, and 285-290 cm. The diatom assemblage is characterised by the dominance of *F. cylindrus* (53.9%). *Fragilariopsis curta* (25.85%) subdominates. *Chaetoceros* resting spores and *C. criophilum* are the only other common species in the assemblage, with an average abundance of 4.6% and 4.7%, respectively. *Corethron criophilum* and Unidentified Genus A are statistically more abundant in cluster group 3 compared to all other groups.

Cluster group 4 occurs below 335 cm. The diatom assemblage is dominated by *Chaetoceros* resting spores (84.6%). The resting spores occur in near-monospecific abundance, ranging from 76.7% to 93.83%, and are a unique indicator of the assemblage. *Fragilariopsis cylindrus* (5.6%) and *F. curta* (5.0%) are subdominant. No other taxa have an average abundance >1%. *Thalassiosira antarctica* resting spores are relatively common, with a maximum abundance of 2%.

KROCK GC1 and Surface Samples

A dendrogram illustrating the affinity between GC1 and surface sediment samples is illustrated in Fig. 14.4. Twenty-nine species with an abundance >2% are observed in 164 samples. Seven cluster groups are identified at 52.9% dissimilarity, with a cophenetic correlation of 0.75. Significantly abundant species in each cluster group are listed in Table 14.3.

Cluster group 1 consists of most of the core intervals that form cluster groups 1 and 2, above, and surface samples BANG12, BANG37, BANG42, KRGR35, KRGC2, and KRGC1 (= 0 cm). With the exception of two samples (BANG37 and BANG42), all form part of the coastal diatom assemblage discussed in Chapters 9 and 10. In the surface analysis, BANG37 and BANG42 were nested in the shelf diatom assemblage. Based on the geographic distribution of the surface samples that occur in the current analysis, it is observed that they are members of the coastal diatom assemblage that occur in, or near, the sedimentary basins on Mac.Robertson Shelf. The group is therefore, hereafter, referred to as the “basin assemblage”.

The basin assemblage is dominated by *F. curta* (35.6%) and *F. cylindrus* (28.4%). *Chaetoceros* resting spores are subdominant (9.6%). *Fragilariopsis obliquecostata* and the Chrysophyte *Pentalamina corona* Marchant are common, but do not form >3%. There are no indicator species present. This differs from the analysis of the surface samples alone, where the coastal diatom assemblage was characterised by *Pseudonitzschia turgiduloides*.

Cluster groups 2, 3, 4, and 5 correspond to the surface diatom assemblages identified as the shelf, coastal, cape, or oceanic, respectively. There are no intervals from GC1 that are analogous to these assemblages and they will not be discussed further here. A minor difference to note, however, is that sample KRGC24 has been included as a member of the cape assemblage in the present analysis (previously, it formed a member of the shelf assemblage). The cape assemblage is unique in its species composition and distinctive

geographical location. It is interpreted to represent an assemblage that has been current winnowed. The inclusion of KRGC24 in the cape assemblage when compared to GC1 should be regarded with caution. It is not located in close geographical proximity to the cape assemblage, nor is it subject to the oceanographic processes to which the formation of the cape assemblage is attributed.

Cluster groups 6 and 7 contain diatom assemblages from GC1 that have no analogue in the Prydz Bay or Mac.Robertson Shelf surface sediment. Cluster group 6 occurs at alternating intervals in the core, between 30 cm and 290 cm. It is dominated by *F. cylindrus* (41.4%); *F. curta* (28.5%) subdominates. Less common, but present at >2%, are *Chaetoceros* resting spores, *C. criophilum*, *F. angulata*, *F. obliquecostata*, and *F. pseudonana*. *Rhizosolenia hebetata* fo. *semispina* (Hensen) Gran is an indicator species, but numerically rare (maximum abundance 2.2%). Cluster group 6 can be further characterised by several species that, although not indicators, are statistically more abundant here compared to the other cluster groups. These are *Chaetoceros* spp., *C. criophilum*, *F. cylindrus*, *F. pseudonana*, *P. turgiduloides*, and Unidentified Genus A. *Corethron criophilum* reaches maximum abundance (10.0%) in cluster group 6 and is a valuable “visual” indicator of the assemblage. Its presence is attributed to the formation of the lighter, “fluffy” layers in the core described in the core log. When viewed under the light microscope, the abundance of *Corethron* is obvious, but as most of the frustules are broken into small fragments it is difficult to quantify its abundance. This feature is considered an important, subjective, indicator of cluster group 6, however, and it is hereafter referred to as the “*Corethron* assemblage”.

Cluster group 7 corresponds with the *Chaetoceros* assemblage identified above (GC1, cluster group 4). The spores create an almost monospecific assemblage (mean abundance 84.6%) and are an indicator of the cluster group. *Fragilariopsis cylindrus* (5.6%) and *F. curta* (5.0%) are subdominant. No other species are present with an abundance >1.0%.

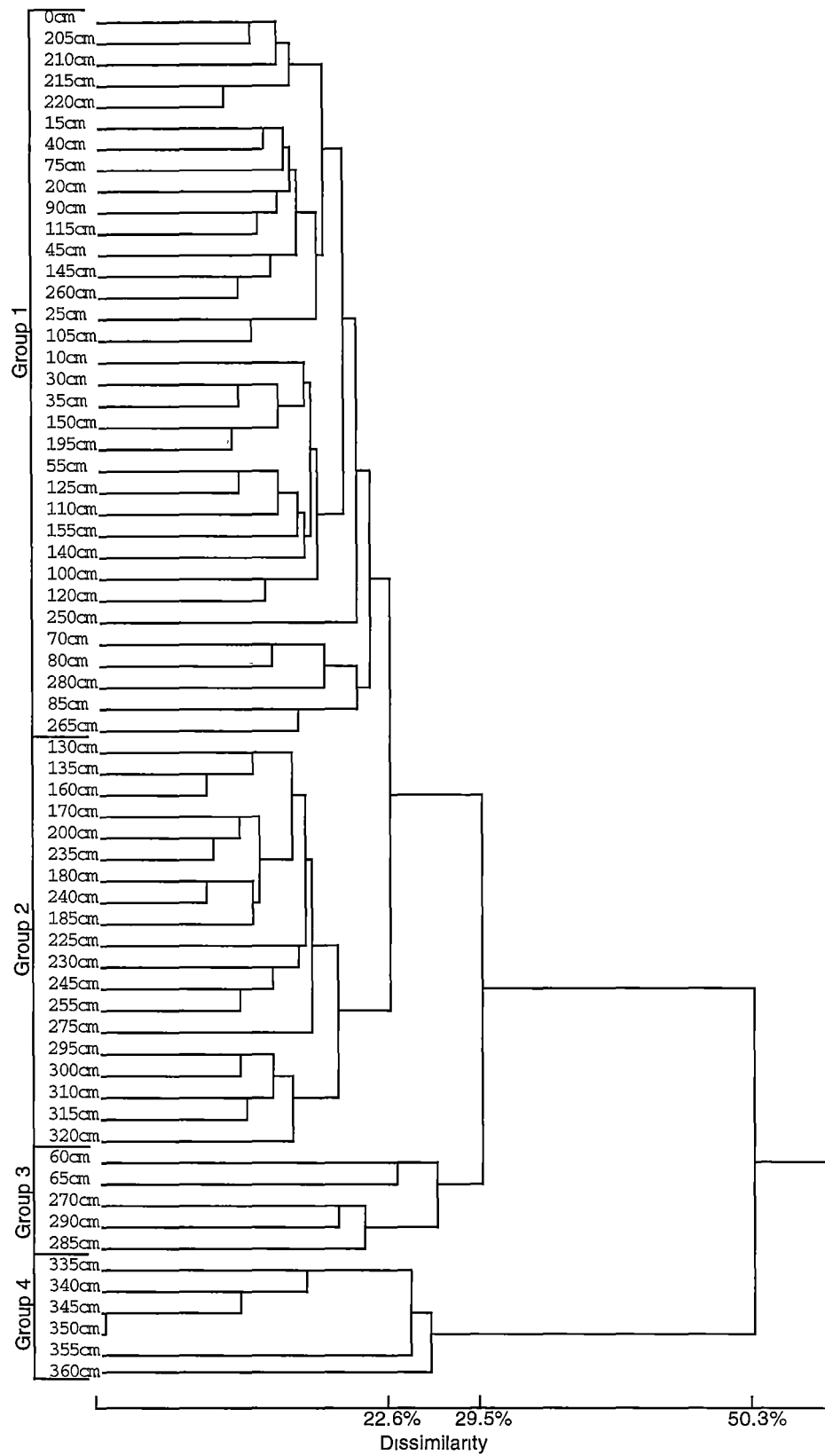


Fig. 14.3. Dendrogram of cluster analysis comparing GCI samples. Analysis based on species abundance (>2% log₁₀).

Table 14 .2. Arithmetic mean abundance (%), analysis of variance (F) and SNK multiple range test of species in cluster groups of GC1.

| Species | Cluster Group | | | | F | P |
|--|---------------|-------------|-------------|-------------|-------|-----|
| | 1 | 2 | 3 | 4 | | |
| <i>Chaetoceros</i> spp. | 1.4 | 0.6 | 0.8 | 0.2 | 4.64 | * |
| <i>Chaetoceros</i> spores | 6.5 | <u>10.8</u> | 4.6 | <u>84.6</u> | 54.86 | *** |
| <i>C. criophilum</i> | 2.6 | 0.7 | <u>4.7</u> | 0.2 | 12.65 | *** |
| <i>D. antarcticus</i> | 0.7 | <u>1.6</u> | 0.1 | 0.03 | 28.98 | *** |
| <i>D. speculum</i> | 0.6 | <u>1.0</u> | 0.1 | 0.3 | 5.99 | ** |
| <i>E. antarctica</i> | 0.4 | <u>0.9</u> | 0.1 | 0.1 | 10.14 | *** |
| <i>F. angulata</i> | <u>4.6</u> | <u>5.5</u> | <u>1.8</u> | 0.2 | 28.17 | *** |
| <i>F. curta</i> | <u>31.7</u> | <u>35.1</u> | <u>25.3</u> | 5.0 | 72.71 | *** |
| <i>F. cylindrus</i> | <u>36.4</u> | <u>23.7</u> | <u>53.9</u> | 5.6 | 73.76 | *** |
| <i>F. kerguelensis</i> | <u>0.6</u> | <u>1.8</u> | 0.2 | <u>0.8</u> | 28.82 | *** |
| <i>F. obliquecostata</i> | <u>2.3</u> | <u>4.2</u> | 1.2 | 0.6 | 23.42 | *** |
| <i>F. pseudonana</i> | <u>1.8</u> | 0.4 | <u>1.7</u> | 0.1 | 18.87 | *** |
| <i>F. ritscheri</i> | 0.4 | 0.3 | 0.4 | 0.0 | 1.61 | – |
| <i>F. separanda</i> | <u>0.4</u> | <u>0.9</u> | 0.1 | 0.0 | 13.42 | *** |
| <i>P. corona</i> | <u>1.6</u> | <u>1.8</u> | 0.6 | 0.1 | 9.95 | *** |
| <i>P. turgiduloides</i> | 0.8 | 0.5 | 0.4 | 0.3 | 1.97 | – |
| <i>R. hebetata</i> | 0.1 | 0.0 | 0.2 | 0.0 | 1.30 | – |
| <i>T. antarctica</i> spores | 0.6 | <u>1.1</u> | 0.2 | 0.7 | 6.21 | ** |
| <i>T. gracilis</i> | <u>1.0</u> | <u>2.5</u> | 0.4 | 0.0 | 32.83 | *** |
| <i>T. gracilis</i> var. <i>expecta</i> | 0.4 | <u>0.7</u> | 0.3 | 0.1 | 4.38 | ** |
| <i>T. lentiginosa</i> | <u>0.3</u> | <u>0.6</u> | 0.1 | 0.0 | 6.96 | *** |
| Unknown sp. A† | <u>0.6</u> | 0.1 | <u>1.0</u> | 0.0 | 10.35 | *** |

Analyses were carried out on $\log_{10}(x+1)$ transformed abundance. Degrees of freedom 3, 60. ANOVA P values: *

<0.05, ** <0.005, *** <0.0005, – not significant. Bold type: species with significant differences in mean abundance.

Underlined type: species with significantly higher abundance in a cluster group.

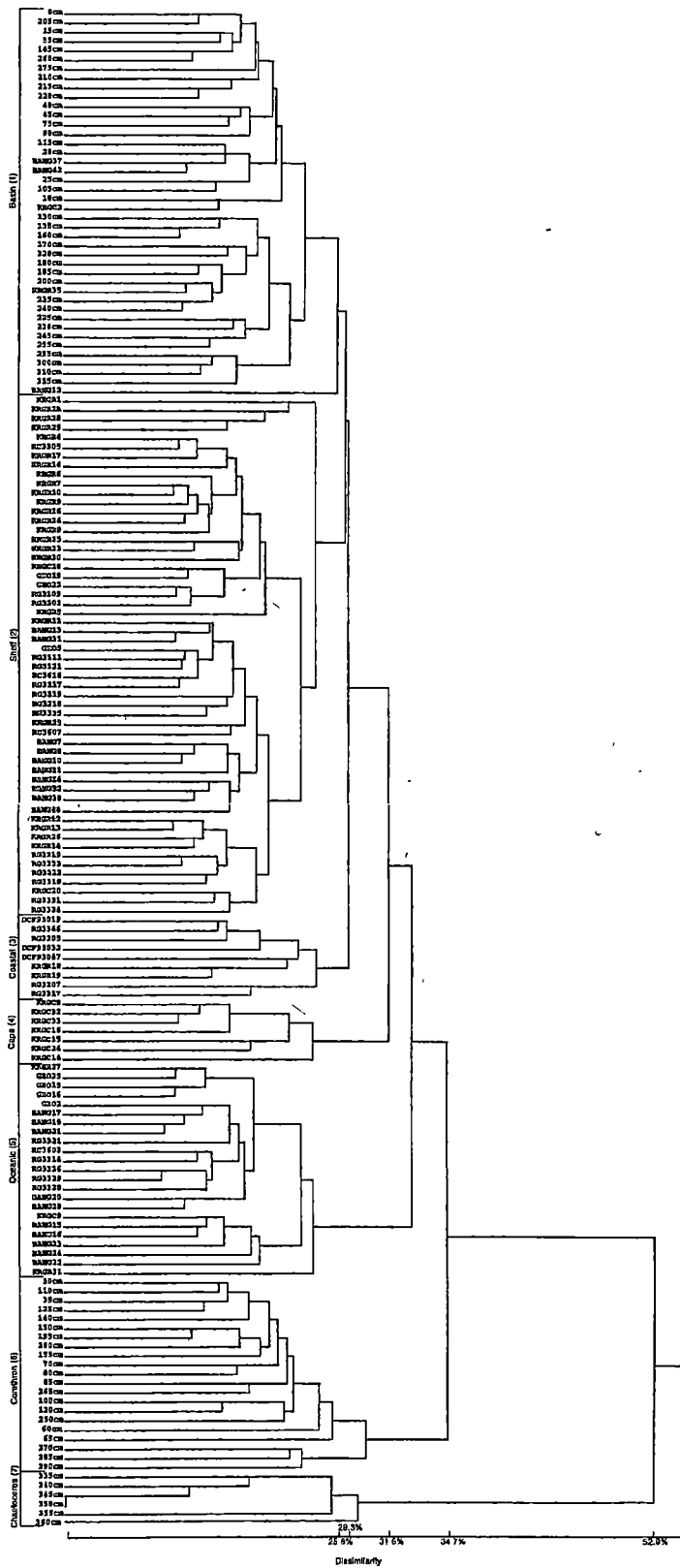


Fig. 14.4. Dendrogram of cluster analysis comparing GCI and surface samples. Analysis based on species abundance (>2% log10)

Table 14.3 Arithmetic mean abundance (%), analysis of variance (F), and SNK multiple range test of species in cluster groups of GC1 and surface sediment samples

| Species | Cluster Group | | | | | | | F | P |
|--|---------------|-------------|-------------|-------------|-------------|-------------|-------------|--------|-----|
| | 1 | 2 | 3 | 4 | 5 | 6 | 7 | | |
| <i>A. actinochilus</i> | 0.1 | <u>0.3</u> | 0.1 | <u>0.5</u> | <u>0.8</u> | 0.1 | 0.0 | 21.96 | *** |
| <i>Chaetoceros</i> spp. | <u>0.8</u> | 0.2 | 0.2 | 0.0 | 0.0 | <u>1.5</u> | 0.2 | 21.58 | *** |
| <i>Chaetoceros</i> spores | <u>9.6</u> | <u>8.9</u> | <u>3.8</u> | 1.5 | <u>13.1</u> | <u>4.8</u> | <u>84.6</u> | 45.95 | *** |
| <i>C. criophilum</i> | <u>0.8</u> | 0.1 | 0.0 | 0.0 | 0.0 | <u>4.5</u> | 0.2 | 111.16 | *** |
| <i>D. antarcticus</i> | <u>1.1</u> | 0.5 | 0.1 | <u>0.9</u> | <u>1.0</u> | 0.5 | 0.0 | 13.01 | *** |
| <i>D. speculum</i> | 0.7 | 0.6 | 0.4 | 0.7 | 0.8 | 0.6 | 0.3 | 1.35 | – |
| <i>E. antarctica</i> | 0.5 | 0.4 | 0.1 | <u>2.2</u> | <u>1.6</u> | 0.4 | 0.1 | 14.07 | *** |
| <i>F. angulata</i> | <u>4.9</u> | <u>3.4</u> | <u>4.1</u> | <u>5.4</u> | <u>2.0</u> | <u>3.7</u> | 0.2 | 19.87 | *** |
| <i>F. curta</i> | <u>35.6</u> | <u>45.0</u> | <u>57.3</u> | <u>61.3</u> | <u>24.3</u> | <u>28.5</u> | 5.0 | 69.52 | *** |
| <i>F. cylindrus</i> | <u>28.4</u> | <u>16.9</u> | <u>22.0</u> | 4.0 | <u>8.0</u> | <u>41.4</u> | 5.6 | 51.69 | *** |
| <i>F. kerguelensis</i> | <u>1.2</u> | <u>2.2</u> | 0.5 | <u>1.8</u> | <u>19.3</u> | 0.4 | 0.8 | 60.30 | *** |
| <i>F. lineata</i> | <u>0.6</u> | <u>1.0</u> | <u>0.8</u> | <u>1.2</u> | <u>1.1</u> | 0.4 | 0.1 | 9.42 | *** |
| <i>F. obliquecostata</i> | <u>3.2</u> | <u>2.3</u> | <u>1.6</u> | <u>2.9</u> | <u>1.4</u> | <u>2.2</u> | 0.6 | 11.47 | *** |
| <i>F. pseudonana</i> | <u>0.7</u> | 0.2 | 0.1 | 0.0 | 0.1 | <u>2.4</u> | 0.1 | 37.67 | *** |
| <i>F. ritscheri</i> | 0.3 | 0.2 | 0.3 | 0.4 | 0.1 | 0.4 | 0.0 | 2.40 | * |
| <i>F. separanda</i> | <u>0.7</u> | <u>0.9</u> | 0.2 | <u>1.5</u> | <u>2.1</u> | 0.3 | 0.0 | 30.20 | *** |
| <i>F. sublineata</i> | <u>0.7</u> | <u>0.7</u> | <u>0.5</u> | <u>0.6</u> | <u>0.3</u> | <u>0.7</u> | 0.0 | 5.87 | *** |
| <i>Pe. corona</i> | <u>2.0</u> | <u>3.9</u> | <u>1.7</u> | <u>1.2</u> | <u>2.6</u> | <u>1.0</u> | 0.1 | 27.15 | *** |
| <i>P. glacialis</i> | 0.2 | <u>0.8</u> | 0.1 | <u>0.8</u> | 0.2 | 0.1 | 0.0 | 15.88 | *** |
| <i>P. turgiduloides</i> | <u>0.5</u> | 0.1 | 0.2 | 0.1 | 0.0 | <u>0.9</u> | 0.3 | 25.32 | *** |
| <i>R. hebetata</i> | 0.0 | 0.0 | 0.0 | 0.0 | 0.0 | <u>0.2</u> | 0.0 | 6.33 | *** |
| <i>S. microtrias</i> | 0.1 | <u>0.4</u> | 0.7 | <u>0.9</u> | <u>0.7</u> | 0.0 | 0.0 | 18.56 | *** |
| <i>T. antarctica</i> (veg) | 0.1 | 0.0 | 0.0 | 0.0 | 0.0 | 0.0 | 0.0 | 0.40 | – |
| <i>T. antarctica</i> (spores) | <u>1.0</u> | <u>6.4</u> | <u>1.4</u> | <u>8.4</u> | <u>7.2</u> | 0.4 | 0.7 | 72.57 | *** |
| <i>T. gracilis</i> | <u>1.7</u> | <u>1.7</u> | <u>0.9</u> | <u>1.9</u> | <u>4.5</u> | <u>0.8</u> | 0.0 | 27.88 | *** |
| <i>T. gracilis</i> var. <i>expecta</i> | <u>0.5</u> | 0.3 | 0.2 | 0.0 | <u>0.7</u> | 0.3 | 0.1 | 5.06 | *** |
| <i>T. lentiginosa</i> | <u>0.5</u> | <u>0.5</u> | 0.2 | <u>0.7</u> | <u>3.0</u> | 0.3 | 0.0 | 47.61 | *** |
| <i>Tr. reinboldii</i> | 0.2 | <u>0.4</u> | 0.1 | 0.1 | <u>1.1</u> | 0.1 | 0.0 | 24.32 | *** |
| Unknown sp. A | 0.2 | 0.1 | 0.1 | 0.0 | 0.0 | <u>0.9</u> | 0.0 | 26.57 | *** |

Analyses were carried out on $\log_{10}(x+1)$ transformed abundance. Degrees of freedom 1, 157. ANOVA P values: * <0.05, ** <0.005, *** <0.0005, – not significant.

Bold type: species with significant differences in mean abundance. Underlined type: species with significant higher abundance in a cluster group. Cluster group (diatom assemblage) names: 1 = Basin, 2 = Shelf, 3 = Coastal, 4 = Cape; 5 = Oceanic, 6 = Corethron; 7 = Chaetoceros.

14.5 Diatom Assemblages in GC1

14.5.1 *Chaetoceros* Assemblage

The diatom assemblage in GC1, between 363 cm and 335 cm, is characterised by *Chaetoceros* resting spores (Figs. 14.5 and 14.6). There is no modern analogue for this assemblage in the surface sediments of Prydz Bay and Mac.Robertson Shelf.

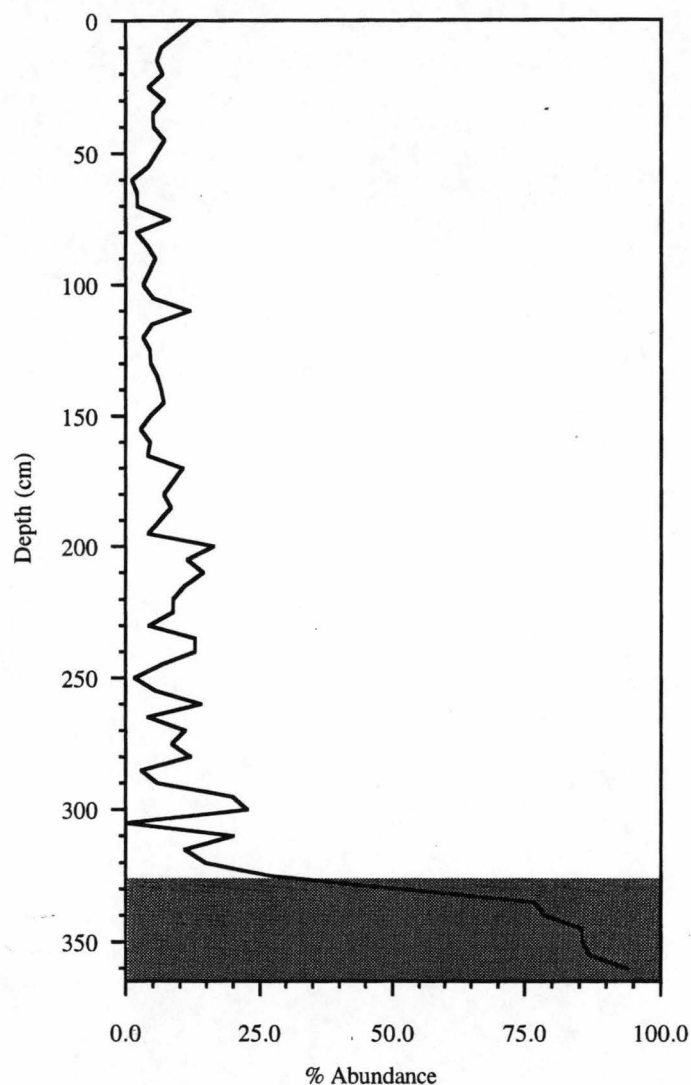
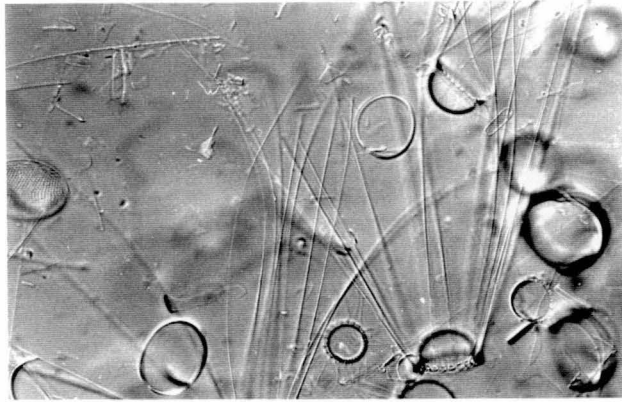


Fig. 14.5. Distribution of *Chaetoceros* resting spores in GC1. Cluster analysis identified the samples below 325 cm (shaded) as forming a distinct diatom assemblage.

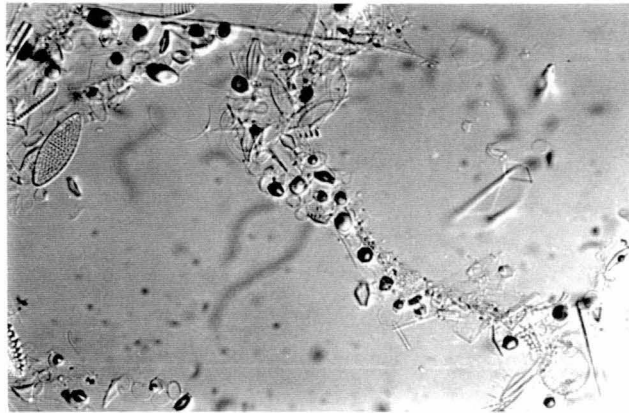
Fig. 14.6. Light micrograph of Corethron and Chaetoceros assemblages in GC1.

1. Corethron assemblage (sampled from 65 cm). Magnification x400.

2. Chaetoceros assemblage (sampled from 345 cm). Magnification x400.



1



2

Spore formation is an evolutionary survival strategy, designed to remove the vegetative cells from the euphotic zone during times of environmental stress. In response, vegetative cells, such as those of *Chaetoceros*, shed their overlying theca and produce a heavily silicified, planktonic resting spore (Fryxell, 1994), which sinks through the water column and may remain at the sediment / water interface until favourable conditions induce germination. The physical attributes of *Chaetoceros* resting spores also aid their preservation in sediment. The resting spores form aggregates that rapidly descend through the water column, decreasing the chance for dissolution and grazing to take effect. On the sea floor, the aggregates quickly build-up and bury the spores, forming fine laminations that are less susceptible to bioturbation. In coastal Antarctica, spore formation is most often a result of storm-induced mixing and decreased light during the polar winter (Fryxell, 1994), or nutrient depletion in surface waters (Davis *et al.*, 1980).

High concentrations of *Chaetoceros* resting spores, in Antarctica, are generally considered indicative of high primary productivity in the water column (Donegan and Schrader, 1982; Leventer 1992; Leventer *et al.*, 1993, 1996). During the spring, receding pack ice creates a temporarily stratified water column, in which a marginal ice-edge zone diatom bloom annually develops (Smith and Nelson, 1985, 1986; Nelson *et al.*, 1987). At this time, water, which is normally high in nutrients, can become sufficiently depleted so as to limit diatom growth (Nelson and Smith, 1986; McMinn *et al.*, 1995). Substantial depletion by algal blooms has been observed in the ice edge zone of Prydz Bay (Fukai *et al.*, 1986) and the Ross Sea (Nelson and Tréguer, 1992). To demonstrate nutrient depletion in the Antarctic Circumpolar Current, Mitchell *et al.* (1991) use a model to show that the phytoplankton blooms are dependent upon increased stratification of the upper water column and the presence of a shallow mixed layer. A *Chaetoceros* bloom documented by Mitchell and Holm-Hansen (1991; Leventer *et al.*, 1993) in Gerlache Strait was probably due to the presence of a relatively warm, low salinity lens of surface water, and protection from intense Antarctic storm activity. Both would have functioned to stabilise the water column (Leventer *et al.*, 1993).

Sediment dominated by *Chaetoceros* resting spores may also be indicative of increased seasonal sea ice (in the form of pack ice or an ice shelf). In this instance, vegetative cells being advected under the ice during summer months, and / or conditions associated with an adjacent stationary summer ice edge, could induce resting spore formation. This has been observed by Leventer (1992), who notes that the highest relative abundance of *Chaetoceros* resting spores in surface sediments off the George V Coast corresponds with a line that marks the maximum summer retreat of the ice edge. Leventer (1992) suggests that the decreased water salinity associated with the stationary ice edge could stimulate spore production, but several factors may contribute. Even when melting stops at a stationary ice edge, the elevated phytoplankton biomass in this zone can persist (Nelson *et al.*, 1987). When this occurs, it is possible for phytoplankton standing stocks in ice-edge blooms to become self-limiting as a result of reduced light penetration (Nelson and Smith, 1991). Platelet ice, which underlies sea ice, may also restrict seawater influx and limit nutrient supply (Lizotte and Sullivan, 1991). These factors, coupled with significant nutrient depletion, could contribute to enhanced *Chaetoceros* resting spore production.

14.5.2 Basin Assemblage

The basin assemblage is the most common diatom assemblage in GC1, above 320 cm. It is described as a subgroup of the modern coastal assemblage, which forms in near-shore and / or shallow areas of the continental shelf where sea ice frequently persists year round. An abundance of sea ice taxa characterise the coastal assemblage, especially those from the genus *Fragilariopsis*, and they are interpreted to represent the preserved proportion of sea ice assemblages identified in the Prydz Bay biocoenose by Stockwell *et al.* (1991) and Scott *et al.* (1994). The same taxa have been similarly noted amongst the dominant and abundant diatoms in pack ice from the Weddell Sea (Garrison and Buck, 1989) and in fast ice from Lützow-Holm Bay (Watanabe, 1988; Tanimura *et al.*, 1990). Many of the species found in abundance in these assemblages are not preserved

in abundance in sediments, however. Such species include *Chaetoceros* spp., *C. criophilum* and *P. turgiduloides*.

The basin assemblage is described as a subgroup of the coastal assemblage because, when GC1 and the surface samples are compared statistically, it includes the samples recovered from the inner-shelf basins on Mac.Robertson Shelf. It is similar to the surface coastal assemblage in its abundance of *F. curta* and *F. cylindrus* (that form $\geq 50\%$). Several rare, but statistically significant, species are present, however, and these include *Chaetoceros* spp., *C. criophilum*, *F. pseudonana*, and *P. turgiduloides* (the latter being an indicator species of the coastal assemblage). All have typically fragile or lightly silicified frustules, and their abundance in the phytoplankton is not normally preserved in sediment.

It has been demonstrated that smaller, more fragile diatom frustules are preferentially preserved in anoxic marine basins in the Vestfold Hills, Prydz Bay, compared to preservation in oxic basins (McMinn, 1995). This is attributed to the absence of burrowing and foraging benthic fauna, which decrease bioturbation and mechanical breakage of the diatom frustules, and decreased corrosion due to a lower pH. Elevated pH levels are known to increase the rate of silica dissolution (Barker *et al.*, 1994). Although Mac.Robertson Shelf is dominated by erosional processes, Late Pleistocene and Holocene sediments occur in the inner shelf deeps, such as Neilsen Basin and Iceberg Alley, which act as sediment traps for fine-grained, biosiliceous mud and ooze (Harris and O'Brien, 1996). The accumulating ooze is relatively thick (>5 m), protected from iceberg and current reworking (Harris *et al.*, in press), highly anoxic and contains few of the organisms that would normally contribute to mechanical breakage and dissolution of diatom frustules at the sediment-water interface. Under these conditions, it is suggested that the sea ice biocoenose may be sufficiently altered during preservation for two assemblages to become recognisable in the sediment. One is preserved on shallower coastal areas of the continental shelf, and from which the smaller and more fragile species have been lost (= coastal assemblage). The other is preserved in the deep,

anoxic shelf basins (= basin assemblage) and contains a significantly greater proportion of the fragile and lightly silicified species.

Thalassiosira gracilis and *T. gracilis* var. *expecta* are also present in greater abundance in the basin assemblage compared to the surface's coastal assemblage. Although common in ice edge waters (Kozlova, 1966), and fjords of the Vestfold Hills (McMinn, *pers. comm.*), *T. gracilis* is also abundant in the subantarctic and has even been recorded from subtropical waters (Fryxell and Hasle, 1979a). Cunningham and Leventer (1998) consider it to be an open water indicator (Cunningham and Leventer, 1998). It is possible that part of the offshore, oceanic diatom assemblage is being transported into Nielsen Basin and Iceberg Alley via the open connection that they have to the edge of the continental shelf. Upwelling along the continental shelf, or water associated with the Antarctic Circumpolar Current, may be transporting a small open water or ice-edge element onshore. A similar observation has been made by Harris and O'Brien (in press), who note that a two-layer water flow exists along Mac.Robertson Shelf. Flow onshore occurs in the upper water column, whilst offshore flow occurs at deeper depths.

14.5.3 *Corethron* Assemblage

Interbedded between the darker diatom ooze of GC1, which is characteristic of the basin assemblage, are less dense, more lightly coloured sediment layers with a "fluffy" structure (Figs. 14.6 and 14.7). The layers are present between 290 cm and 30 cm, and the visible abundance of *C. criophilum* is characteristic (Fig 14.8).

It is important to understand the morphology and ecology of *C. criophilum* before its unusual abundance in the sedimentary record can be interpreted. *Corethron* is a lightly silicified, large, centric genus, with separate, articulating spines on the valve (Crawford and Round, 1989). *Corethron criophilum* has a cosmopolitan distribution. It occurs in low abundance in tropical waters (Medlin and Priddle, 1990), is common in the South Atlantic and many parts of the Southern Ocean (Fryxell and Hasle, 1971), and reaches highest concentration in Antarctic inshore waters (Kozlova, 1966; Hasle, 1969). Up to

98% of the phytoplankton collected by net hauls from the Antarctic Peninsula have been found to contain *C. criophilum* (e.g. Hart, 1934; Hendeby, 1937; Hasle, 1969). Fryxell and Hasle (1971) note a similar abundance in a net haul collected from one station during the 1968 Weddell Sea Oceanographic Expedition, although it accounted for only 2.5% of diatoms counted in other samples at the time. A large diatom bloom, overwhelmingly dominated by *C. criophilum*, was observed between water depths from 0 m to 300 m in the South Atlantic between 47°S and 48°S (Crawford, 1995). Monospecific blooms have been reported from the subarctic Pacific (Clemons and Miller, 1984). The largest populations of *C. criophilum* are often found in waters that are poor in other phytoplankton species (Fryxell and Hasle, 1971).

Corethron criophilum is essentially a planktonic, oceanic species. Fryxell and Hasle (1971) report a “slight indication” that it is more abundant in open waters with less sea ice cover, although it is abundant in neritic areas and also found living in pack ice (Hart, 1942). Marra and Boardman (1984) suggest that *C. criophilum* may be an important component of the ice-edge phytoplankton in the Weddell Sea in late winter. This has been supported by Garrison and Close (1993), who observe it amongst the most abundant, but not dominant, diatom species in the winter sea ice biota of the Weddell and Scotia Seas pack ice.

The abundance of *C. criophilum* in the water column is rarely reflected in the underlying sediment. Frustules are usually partially preserved and spineless, having undergone dissolution, by chemical processes, and mechanical breakdown, by grazing zooplankton in the upper water column (Gersonde and Wefer, 1987). Rapid transport through the water column, to avoid these problems, is critical for their preservation in sediment. The presence of sedimentary layers with abundant *C. criophilum* suggests that environmental conditions must have favoured rapid transport, immediately prior to deposition at the sea floor (Leventer et al., 1996).

Fig. 14.7. Photograph illustrating the “fluffy”, lighter-coloured appearance of Corethron-rich sediment layers, interbedded between the darker diatom ooze in GC1, between 100 cm – 120 cm.

← KROCK 125. GC01 ←



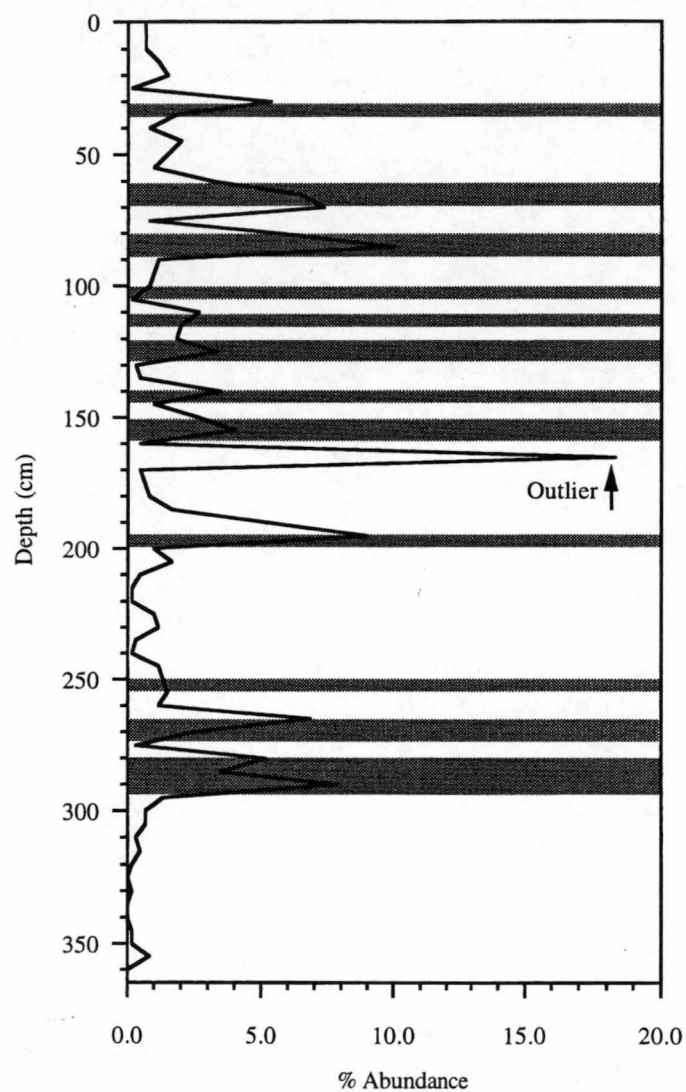


Fig. 14.8. Distribution of C. criophilum in GC1. Shaded areas illustrate samples identified as forming a distinct Corethron assemblage.

Unusually high abundance of *C. criophilum* has been observed in numerous sediment cores recovered from the Antarctic continental shelf, e.g. the Weddell Sea (Pudsey, 1990; Jordan *et al.*, 1991), Ross Sea (Leventer *et al.*, 1993), and Antarctic Peninsula (Leventer *et al.*, 1996). In two cores from the northern Weddell Sea, Jordan *et al.* (1991) observe distinct sediment bands, up to 3 cm thick, that contain well preserved diatom frustules and abundant *C. criophilum*. Similarly, Leventer *et al.* (1993, 1996) observe nearly monospecific assemblages of *C. criophilum* as a white “cottony” layer in sediment cores from Granite Harbour (Ross Sea), and the Palmer Deep (Antarctic Peninsula). The *Corethron* layers from the latter also contain a higher than normal abundance of *Rhizosolenia* spp. (similar to that observed in GC1). *Rhizosolenia* has been reported in large quantities from Antarctic waters and can form blooms (Alldredge and Silver, 1982). But like *Corethron*, it is large and fragile, and rarely preserves well in sediment unless rapidly transported through the water column (Sancetta *et al.*, 1991).

Several hypotheses explaining the formation of *Corethron*-rich sediment layers, following mass sedimentation of a diatom bloom and rapid burial, have been suggested. Pudsey (1990) interprets their presence in Weddell Sea cores as being consistent with the occurrence of high primary production, associated with a semi-permanent polynya over many years, and reduced circulation with less oxygenated bottom water to explain the lack of scavenging benthos. Jordan *et al.* (1991) expand this idea to formulate two hypotheses. Hypothesis 1 is dependent on a consistent change in sedimentation and preservation over time, resulting in the enhanced survival of diatom frustules in the sediment. Such a long-term change should be widespread, yet they have not observed *Corethron*-rich layers in nearby cores and it seems unlikely that the layers could have accumulated over decades or centuries. Hypothesis 2 suggests that horizontal concentration, in the euphotic zone or from transport across the seabed, and subsequent deposition in a “quiet” area, such as a depression, is responsible for the *Corethron*-rich layers. This, coupled with a physical feature of the water column, such as an eddy or “chimney”, could have entrained phytoplankton biomass from a wide area of the surface

mixed layer and caused it to settle in a smaller area of the sea floor. Leventer *et al.* (1993) suggest that the *Corethron*-rich layers in Granite Harbour cores record an unusual episode of early seasonal warmth and primary production, which has taken place under conditions of extreme water column stratification. Most evidence indeed suggests that *C. criophilum* blooms occur during spring (Karsten, 1905 [in Crawford, 1995]; Hart, 1934; Gersonde and Wefer, 1985; Crawford, 1995) and enhanced, early season ice-free conditions, which would normally occur during the late summer / early autumn, might explain why some blooms are recorded in sediment.

Corethron criophilum blooms simultaneously undergoing a mass phase of sexual reproduction may also provide a mechanism for rapid accumulation and preservation in the sediment (Crawford, 1995). Diatoms commonly reproduce by vegetative (asexual) reproduction, resulting in a steady decrease in the physical size of the valves. When a critical minimum size is reached, sexual reproduction is triggered and gametangia are produced. The resulting auxospore grows to the maximum cell size, forms silicified valves, and vegetative reproduction is resumed. Sexual reproduction by *C. criophilum* has been observed in Prydz Bay, where up to 60% of the cells were either forming gametes or were present as auxospores (Stockwell *et al.*, 1991). Crawford (1995) encountered a large bloom undergoing a mass sexual stage in the upper 100 m of the water column at the Polar Front Zone of the Weddell Sea. The rapid downward transport of empty cells that coincides with this event, due to large losses in the population following, for example, failure of the male gametes to achieve fertilisation, is considered by Crawford (1995) as sufficient to create monospecific layers of *C. criophilum* in Southern Ocean sediments. Leventer *et al.* (1996) further suggest that the presence of a shallow mixed layer in the water column during such an event could only serve to enhance this process.

The question thus arises: if *C. criophilum* blooms are a seasonal event, why are they not preserved more regularly in sediment? Based on the results obtained in the present study, and above hypotheses, it is suggested herein that the formation of *Corethron*-rich

layers observed in Iceberg Alley, and elsewhere on the Antarctic continental shelf, is due to a combination of factors:

1. An unusual episode of warmth, resulting in intense stratification in the upper water layer and an enhanced spring *Corethron* bloom.
2. The unusual conditions and enhanced bloom may trigger a period of mass sexual reproduction, during which an even greater number than of frustules than normal rapidly sink through the water column. Crawford (1995) notes that a large number of empty cell wall components are released in the water column during sexual reproduction, which subsequently appear in the sediment record as a recognisable “signature”. This signature could be used to determine what phase the cells were undergoing at the time they were deposited in Iceberg Alley layers.
3. The presence of some unknown, but localised, event in Iceberg Alley, such as an eddy or chimney in the water column. If this “event” is a seasonal feature, its appearance must coincide with a *Corethron* bloom as a method to further concentrate the number of well preserved cells reaching the sediment. If it does not coincide with a bloom, the frustules will not be concentrated sufficiently to preserve in the sediment.

Several factors suggest that the presence of a localised event in Iceberg Alley is important for the formation of *Corethron* layers. A preliminary analysis of gravity cores recovered from the same vicinity (ANARE cruise AA186, 1997) has revealed the presence of *Corethron*-rich layers in at least two other cores (Harris *et al.*, 1997a). A more detailed analysis of these cores is required (e.g. to determine the extent, age and sediment accumulation rate) to determine whether these intervals correlate with the *Corethron* layers in GC1. Similar deposition events have not been reported in other cores recovered from Nielsen Basin (O’Brien *et al.*, 1995a; Harris *et al.*, 1997a). Nielsen Basin is less than 100 km in distance from Iceberg Alley, is subject to similar oceanographic conditions as Iceberg Alley (both are low energy, deep valleys that accumulate fine-grained sediment dominated by biosiliceous ooze) and the cores

recovered are arguably better preserved than those deposited during the Holocene in Iceberg Alley.

Circumstantial evidence suggests that a plume or “chimney” is at least periodically present in the vicinity of Iceberg Alley. The summer surface water and ice shelf water present in Prydz Bay are not dense enough to promote bottom water formation during summer, but their salinity is thought to increase significantly during active winter sea ice formation (Nunes Vaz and Lennon, 1996). During this time, dense water plumes would have the potential to descend the continental slope. Dense water plumes have been observed at 62°E during late spring / early summer (Smith *et al.*, 1984). Coupled with an unusually warm spring and early ice break-out, could this have contributed to the mass and rapid sedimentation of *C. criophilum*?

14.6 Holocene Palaeoecology of Iceberg Alley

14.6.1 Upper Pleistocene (>10.0 Ka)

Based on reservoir-corrected radiocarbon dates, the *Chaetoceros* assemblage in GC1 was deposited from at least 11.6 thousand years (11.6 Ka) until 10.0 Ka, or the end of the Last Glacial Maximum (LGM). The spores are not found in comparable abundance in the surface sediments of Prydz Bay and Mac.Robertson Shelf today, but their ecology and distribution elsewhere in Antarctica are sufficiently well documented for their presence in GC1 to be speculated upon. They are interpreted to indicate the presence of a stabilised water column associated with a stationary ice edge. In GC1, their presence could therefore be indicative of the maximum summer ice edge retreat in Iceberg Alley during the LGM.

Little research has been carried out on Mac.Robertson Shelf sediments, but diatom analyses from Prydz Bay show the beginning of open-marine conditions in the Early Holocene (Pushina *et al.*, 1997; Domack *et al.*, 1991a). Domack *et al.* (1991a) hypothesise that open marine conditions and siliceous ooze deposits commenced

~10.7 Ka in Prydz Bay, based on reservoir-corrected ages for unconsolidated sediment samples recovered from ODP Site 740. Longer cores from Iceberg Alley are required to determine the size and duration of the *Chaetoceros* layer, and could yield further information on ice extent on Mac.Robertson Shelf during and prior the Early Holocene.

14.6.2 Late Holocene to Present (<10.0 Ka)

Approximately 10.0 Ka, the type of diatom assemblage being preserved in Iceberg Alley changed. Deposition of the *Chaetoceros* assemblage ceased, and deposition of an assemblage analogous to that forming in the inner shelf basins today commenced. In GC1, this transition is interpreted to represent the onset of Holocene warming, following the LGM, during which the permanent summer ice edge became less extensive.

Deposition of the basin assemblage has dominated in GC1 from 10.0 Ka to the present.

Interbedded between the basin assemblage are layers of *C. criophilum*-rich diatom ooze. Based on reservoir-corrected radiocarbon dates, the *Corethron* layers were deposited between 6.9 Ka and 1.3 Ka. Within this period, two episodes of maximum *Corethron* abundance are identified: one in the lower core (at 270 cm and from 285 cm to 290 cm), and another in the upper core (60 cm). When the core was statistically analysed alone, the intervals form a distinct cluster group, in which *Corethron* is the indicator species.

A reservoir-corrected radiocarbon date of 6.9-6.5 Ka is applied to the *Corethron* layer deposited at 285-290 cm, and 5.6 Ka to the layer at 270 cm. These layers may represent the mid Holocene climatic optimum. The mid Holocene is generally characterised as a period during which Antarctica underwent a period of climatic warming (Burckle, 1972; Truesdale and Kellogg, 1979; Domack *et al.*, 1991b; Cunningham *et al.*, in press). Burckle (1972) suggests that warming was significant in the South Atlantic from 7.0 Ka to 5.5 Ka, which is similar to the time during which the *Corethron* layers were deposited in the lower section of GC1. This is further supported by Pushina *et al.* (1997) who identify a relative warming in climatic conditions in Prydz Bay during the mid Holocene, based on diatom analyses.

The abundance of *Corethron* in the upper layers of the core is greatest at 65 cm to 60 cm. Based on the corrected radiocarbon ages, and assuming a constant deposition rate from 0 cm to 273.5 cm, this assemblage was deposited from 1.9 Ka to 1.8 Ka. As a high abundance of *Corethron* in the sedimentary record is associated with periods of unusual warmth and early ice break out, it could be suggested that the layer in GC1 is correlated with the “Little Climatic Optimum” (LCO), or Mediaeval Warm Period?

The LCO occurred between from 900 AD and 1300 AD, based on studies in the Northern Hemisphere (e.g. Lamb, 1965; Grove, 1988). Data from the Southern Hemisphere are limited, but a period of significant warmth seems to be indicated by a decrease in microparticle deposition between 1200 AD and 1540 AD in an ice core recovered from the South Pole (Mosley-Thompson and Thompson, 1982). Isotopic measurements from a New Zealand speleotherm also suggest warming between 1100 AD and 1300 AD; and tree ring data from Patagonia and Tasmania indicate warm, dry periods, between 1080 AD and 1250 AD, and 950 AD and 1000 AD, respectively (Villalba, 1990; Cook *et al.*, 1992). More recently, deposition of the *Corethron*-rich sediment layers documented from the Antarctic Peninsula have been dated by Leventer *et al.* (1993) at approximately 1000 yBP.

The *Corethron* layers in GC1, between 65 cm and 60 cm are interpreted to have been deposited several hundred years prior the LCO. But, based on the available data, it cannot be determined with certainty whether they were actually deposited during the LCO, or if they record a previous, undocumented, warming event in East Antarctica. If the *Corethron* layers were deposited during the LCO, the discrepancy in timing could be attributed to at least two mechanisms. There could be a time lag between other LCO records and those herein, similar to that observed at the onset of the Neoglacial between Antarctic marine sediments and Greenland ice (Domack and Mayewski, in press). Alternatively, the precision of the radiocarbon ages obtained from GC1 and the reservoir-correction factor applied may not be accurate. Until a better-resolved Antarctic radiocarbon chronology has been calculated, there will always be

inconsistencies, errors and subsequent misinterpretations on Antarctic ^{14}C dated material (Björk *et al.*, 1991).

14.7 250-Year High-Productivity Events?

Enhanced cycles of palaeoproductivity every ~270 years were first observed in glacial marine records from the Antarctic Peninsula by Mashiotta (1992) and Domack *et al.* (1993). This observation was later expanded by Leventer *et al.* (1996) and Brachfeld (1997), who note that the downcore variability of a multitude of physical parameters, including diatom and benthic foramiferal assemblages, in a high-resolution, Holocene core from the Antarctic Peninsula demonstrates recurring 200-year cycles. Leventer *et al.* (1996) propose solar forcing, based on the “Maunder minimum” in sunspot activity, as the mechanism behind these cycles. More recently, Domack and Mayewski (in press) also identify a continuous, ^{14}C -dated palaeoenvironmental proxy, from the Antarctic Peninsula glacial marine record, which demonstrates a pronounced, recurring ~200-year cycle of elevated productivity in response to sea surface conditions. This record has been correlated with cycles of multi-century, and millennial, frequency from the Greenland Ice Sheet Project 2 (GISP2) ice core record (Domack and Mayewski, in press), which reflects atmospheric conditions.

A similar, recurring event is recognisable in GC1, based on the abundance of *C. criophilum*. Between 4.3 Ka and the present, the abundance of *Corethron* reaches a maximum every ~250 years. Five, well-defined peaks in *Corethron* abundance can be observed (Fig. 14.8), which correspond with 4.1 Ka, 3.6 Ka, 2.2 Ka, 1.9 Ka, and 1.2 Ka. (Using cluster analysis, only the event at 1.8 Ka to 1.9 Ka was identified in this section of the core). Prior 4.3 Ka, the frequency of the cycles become less intense, with the exception of that observed between 6.9 Ka and 5.6 Ka.

Does the ~250 year, cyclic increase and decrease in *C. criophilum* in GC1 correlate with high production events recorded from the Antarctic Peninsula? The observations made herein are speculative, but indicate that high-resolution cores from East Antarctica have

the potential for correlation with those from the Antarctic Peninsula, and possibly elsewhere. As demonstrated by Leventer *et al.* (1996) and Domack and Mayewski (in press), such correlations will be important for the understanding of bipolar and global palaeoclimate variation during the Holocene, and possibly the future.

The ~250 year, cyclic increase and decrease in *Corethron* abundance is not recorded in GC2 (see Chapter 15), a core of similar age to GC1 and also formed in a quiet, depositional environment (Nielsen Basin), ~90 km from Iceberg Alley. *Corethron* layers are not present in GC2, and it is speculated here that their absence is due to the absence of the oceanographic feature (such as an eddy) suggested as necessary to concentrate the cells in sufficient density for preservation in the sediment.

14.8 Conclusion

The diatom assemblages in GC1 provide a continuous record of the depositional environment on the outer-shelf on Mac.Robertson Shelf throughout the Holocene. A summary of these is listed in Table 14.4. Deposition before ~10.0 Ka is characterised by a near-monospecific assemblage of *Chaetoceros* resting spores. Their presence is interpreted to indicate a stabilised water column associated with a stationary ice edge, and delineates the maximum summer ice retreat during the Early Holocene.

Chaetoceros resting spore layers are not present in the surficial sediments of the study area today.

The appearance of a diatom assemblage analogous to that being deposited in the coastal areas of Prydz Bay and Mac.Robertson Shelf today first appeared ~10.0 Ka. The assemblage is known to be associated with areas where seasonal summer ice breakout may be restricted due to the presence of icebergs grounded in shallow areas. In GC1, appearance of the assemblage suggests warming during throughout the Early- to mid-Holocene to climatic conditions that are contemporary with that observed in East Antarctica today. Unlike the coastal diatom assemblage preserved in Prydz Bay, however, the coastal assemblage found in Iceberg Alley sediments contains more abundant fragile and lightly silicified species. Whilst these species are abundant members of sea ice algal assemblages, they rarely preserve well in sediment unless favourable conditions such as that found in an anoxic basin are present.

The mid-Holocene is also characterised by episodes of enhanced *C. criophilum* preservation. As with the *Chaetoceros*-dominated sediment layers, the *Corethron* assemblage has no modern analogue, but is interpreted to represent unusually warm periods during which early spring ice melt has produced an enhanced *Corethron* bloom. This event may be associated with an oceanographic feature, such as an eddy or plume, and / or a mass sexual reproduction phase that have further enhanced the preservation of *C. criophilum* in the fossil record. *Corethron criophilum* in the sediment reaches maximum abundance 6.5 Ka to 6.9 Ka and 1.8 Ka to 1.9 Ka. These events are

correlatable to significant warming observed in the South Atlantic between 5.5 Ka and 7.0 Ka (Burckle, 1972) and a late Holocene climatic event analogous to the Northern Hemisphere's "Little Climatic Optimum".

Table. 14.4. Summary of Holocene palaeoclimate on Mac.Robertson Shelf (Iceberg Alley), as inferred from GCI.

| Corrected radiocarbon years (Ka) | Lithology | Diatom Assemblage | Major Species | Climate Interpretation |
|----------------------------------|-------------------------|--------------------|---|--|
| 0.0 – 10.0* (*see below) | Biosiliceous ooze | Basin | <i>F. curta</i> <i>F. cylindrus</i> | Early to mid Holocene warming; seasonal sea ice persists in some areas; preferential preservation of fragile diatoms in sedimentary basins |
| *1.8 – 1.9 and 6.5 – 6.9 | <i>Corethron</i> layers | <i>Corethron</i> | <i>F. curta</i> <i>F. cylindrus</i> <i>C. criophilum</i> <i>Chaetoceros</i> spores | Climatic optimum? |
| ≥ 10.0 | Biosiliceous ooze | <i>Chaetoceros</i> | <i>Chaetoceros</i> spores | End of LGM; warming with increased meltwater and water stratification; OR indicative of maximum summer ice retreat |

– Chapter 15 –
KROCK GC2

15.1 Site Description

Core KROCK/128/GC2 (GC2, hereafter) was recovered from Nielsen Basin, Mac.Robertson Shelf (67° 28.46' S, 64° 58.38' E; Fig. 13.1), in a water depth of 1 091 m. Nielsen Basin is a U-shaped, glacially-cut valley, trending east-west and connected to the continental slope by an arcuate trough (O'Brien *et al.*, 1994). It is the deepest of three fjord valleys on the shelf, with a maximum depth of 1 400 m. The basin acts as a sediment trap for surrounding portions of Mac.Robertson Shelf, accumulating fine-grained, siliceous muddy ooze (Harris and O'Brien, 1996).

The core site is approximately 20 km from Mawson Coast and 70 km from the continental shelf break. Sea ice covers the region throughout autumn, winter and spring. Ice breakout occurs in early summer and open water usually dominates the general area by January. Grounded icebergs on Storegg Bank, to either side of Nielsen Basin, frequently trap the sea ice and may prevent its seasonal breakout.

15.2 Core Description

GC2 is 300.0 cm long (Fig.15.1) and described as one lithological unit. The sedimentary facies is relatively uniform with massive, moderate olive brown (5Y 4/4) to greyish olive (10Y 4/2), biosiliceous ooze between 0 cm and 293 cm. Approximately 1% fine, quartzose sand is present. Sedimentary structures are absent, although some lighter greenish grey (5GY 9/2) mottling occurs between 80 cm and 121 cm. The lower ~10 cm of the core contain light, olive-grey (5Y 3/2), fine, sandy clay.

15.3 Fossil Assemblages

Diatom frustules comprise the bulk of the biosiliceous ooze. Members of the genus *Fragilariopsis* are most common, dominated by the sea ice species *F. curta*. Between

290 cm and 300 cm, *F. curta* is less abundant (although still dominant), and *Chaetoceros* resting spores are subdominant.

No visible reaction to HCl was observed, indicating that foraminifera are absent.

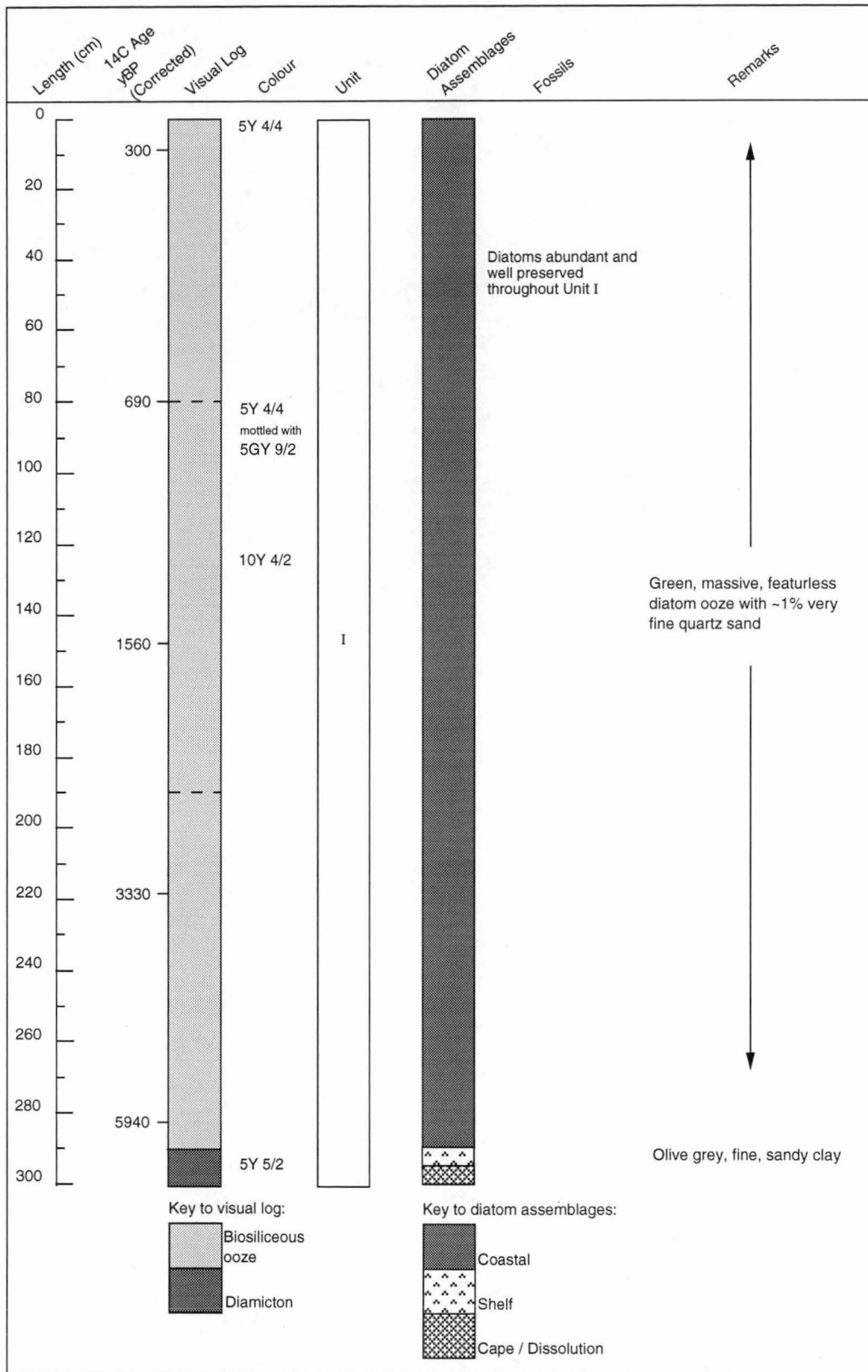


Fig. 15.1. GC2 core log, radiocarbon dates and diatom assemblages when compared to surface sediment.

15.4 GC2 – Results

15.4.1 Radiocarbon Dates

Five AMS radiocarbon dates were obtained from bulk organic samples (Table 15.1). An ocean reservoir correction factor of 1 733 radiocarbon years has been subtracted from the ^{14}C ages, as recommended by Sedwick *et al.* (in press), based on the measured age of a nearby surface sediment grab. Using this, GC2 has a corrected age of 300 yBP at 7-8 cm, and 5 940 years at 274-275 cm (near the biosiliceous ooze – glacial diamict boundary). The absence of unsupported ^{210}Pb in the upper 10 cm of the core indicates that at least 200 years of sediment has been lost (Sedwick *et al.*, in press). This most likely occurred at the time of collection from impact by the gravity corer.

There is no evidence to suggest the presence of unconformities or sediment reworking in GC2. Harris *et al.* (1996) consider the radiocarbon ages as reliable, with no evidence for contamination (e.g. such as the Jurassic pollen and dark, woody material present in some cores from Mac.Robertson Shelf). There is a good correlation between age and core depth, as indicated by simple linear regression ($R^2 = 0.93$; Fig. 15.2), implying a near-uniform sedimentation rate. Deposition rates interpolated between the radiocarbon dates, however, indicate that the sedimentation rate at the base of GC2 (0.025 cm yr^{-1}) is seven times lower than at the top (0.179 cm yr^{-1}). To account for this, the varying sedimentation rate will be used to discuss the core's Holocene chronology in Section 15.6.

15.4.2 Diatom Assemblages

Fragilariopsis dominate the core. The sea ice species *F. curta* is most abundant, forming $\geq 74.8\%$. *Fragilariopsis cylindrus* subdominates, forming between 12.6% and 27.5%. Between 290 cm and 300 cm, *F. cylindrus* and *Chaetoceros* resting spores are subdominant.

Table 15.1. AMS radiocarbon dates obtained from bulk organic carbon for GC2.

| Depth (cm) | Normalised Depth* (cm) | ¹⁴ C Date (y BP) | | Deposition Rate† (cm yr ⁻¹) |
|------------|---------------------------|--------------------------------|-----------|---|
| | | Uncorrected | Corrected | |
| 7 - 8 | 7 - 8 | 2030 ± 310 | 297 | |
| 78 - 80 | 98 - 100 | 2420 ± 80 | 687 | 0.179 |
| 147 - 147 | 108 - 110 | 3330 ± 100 | 1597 | 0.076 |
| 218 - 219 | 193 - 195 | 5060 ± 180 | 3327 | 0.401 |
| 274 - 275 | 281 - 283 | 7673 ± 84 | 5940 | 0.025 |

* Depths have been normalised with respect to water content to correct for sediment compaction (after Harris et al., 1996). † Deposition rates determined between 8-80 cm, 80-147 cm, 147-219 cm, and 21-275 cm.

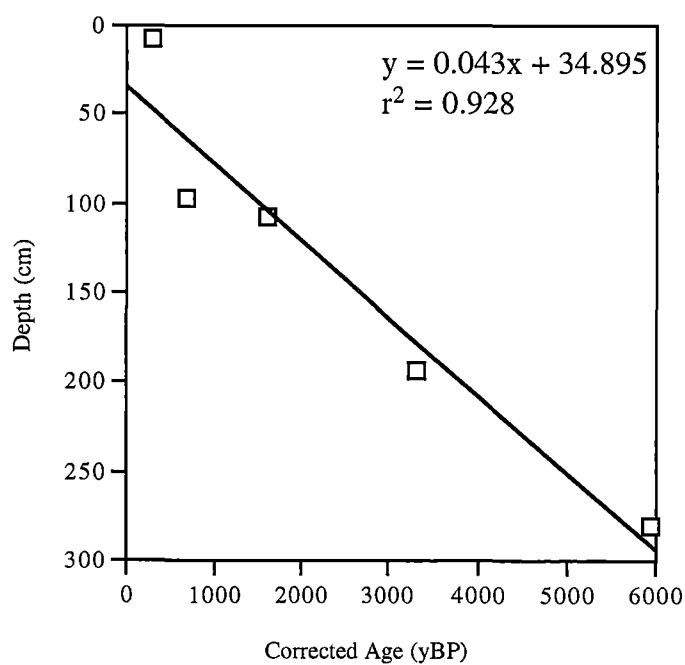


Fig. 15.2. Linear regression of corrected radiocarbon ages versus depth.

15.4.3 Statistical Analyses

GC2

A dendrogram illustrating core sample affinities is illustrated in Fig. 15.3. Eighteen species have an abundance >2% in the 60 samples analysed (Appendix 5). Two samples were identified as outliers in the first cluster analysis (55 cm and 235 cm, Appendix 6) and removed from further analysis. Three cluster groups are subsequently identified at 25.3% dissimilarity, with a cophenetic correlation of 0.61. Indicator species for each cluster group are listed in Table 15.2. All analyses were carried out using \log_{10} values; values in the following discussion are based on arithmetic mean percent.

Cluster group 1 dominates the upper 100 cm of GC2, from 7-15 cm, 25 cm, 35-65 cm, 80-85 cm, and 95 cm. Two samples from 120 cm and 275 cm are also present. The diatom assemblage is dominated by *F. curta* (59.6%), which forms up to 72.3%. The subdominant species are *F. cylindrus* (11.5%) and *Chaetoceros* resting spores (7.6%). Also common (>2%) are *F. obliquecostata* and *F. angulata*. Members of the genus *Thalassiosira* do not form a significant component of cluster group 1. Two taxa are identified as unique indicators of the cluster group: *Chaetoceros* spp. and *P. turgiduloides*. Both are numerically rare (maximum abundance $\leq 3.6\%$). Based on \log_{10} values, however, they are significantly more abundant in cluster group 1 compared cluster groups 2, 3 and 4.

Cluster group 2 is the largest group in GC2. It is interbedded between cluster group 1, at 20 cm and 30 cm, and becomes increasingly dominant down-core, at 70-80 cm, 90 cm, and 100-115 cm. The cluster group is continuous between 125-285 cm, (except where cluster group 1 occurs at 275 cm). The diatom assemblage is similar to that in cluster group 1, dominated by the genus *Fragilariopsis*. *Fragilariopsis curta* is the most abundant species (56.6%); *F. cylindrus* (13.9%) is subdominant. Neither are significantly different in abundance compared to cluster group 1. Common (>2%) are *F. angulata*, *F. obliquecostata*, and *Chaetoceros* resting spores. There are no unique indicator species in the cluster group; however, it can be differentiated from cluster group 1 by a significantly greater abundance of *F. angulata*. This species has a

maximum abundance of 13.3% in cluster group 2, compared to 9.3% in cluster group 1. Also significantly more abundant in cluster group 2, but numerically rare, are the centric species *Dactyliosolen antarcticus* and *T. gracilis*.

Cluster group 3 is the smallest group in GC2 and occurs between 290 cm and 300 cm. *Fragilariopsis curta* (31.9%) remains the dominant member of the diatom assemblage and, although it occurs in smaller abundance compared to cluster groups 1 and 2, its abundance is not significantly different. *Chaetoceros* resting spores (12.5%), *F. cylindrus* (9.6%) and *F. obliquecostata* (7.3%) are subdominant. The cluster group is also characterised by a greater diversity of less abundant (2-5%) species. These are *T. antarctica* resting spores, *T. gracilis*, *F. kerguelensis*, *F. separanda*, and *D. antarcticus*. All, except *D. antarcticus*, are unique indicators of the assemblage.

GC2 and Surface Samples

To objectively compare the diatom assemblages identified in GC2 with those from the surface sediment, a combined cluster analysis using both data sets was carried out (Fig. 15.4). This analysis uses 26 diatom species with an abundance >2%, from 156 samples. Surface sample DCF93047 forms an outlier and was removed from further analysis; outliers identified above and in Chapter 9 were not included. Four cluster groups are present at 30.8% dissimilarity, with a cophenetic correlation of 0.64. Significantly abundant species in each cluster group are listed in Table 15.3. Analyses are based on \log_{10} values; the following discussion is based on arithmetic mean percentage.

Cluster group 1 is the largest group identified, containing 66 surface and core sediment samples. The group includes all surface samples that form the coastal diatom assemblage, and GC2 intervals 7-285 cm. The assemblage is dominated by *Fragilariopsis curta* (56.9%), which forms up to 74.8%. This species is dominant in all cluster groups, but significantly more abundant compared only to cluster group 4. *Fragilariopsis cylindrus* (14.7%) subdominates. Less abundant, but common with an average abundance >2% are *Chaetoceros* resting spores, *F. angulata* and *F. obliquecostata*. Two taxa are unique indicators of the cluster group: *Chaetoceros*

spp. and *P. turgiduloides*. Both are numerically rare (maximum abundance $\leq 4.0\%$), but are significantly more abundant in cluster group 1 compared to all other groups, based on \log_{10} values. *Pseudonitzschia turgiduloides* is an indicator species of the surface sediment coastal assemblage.

Cluster group 2 contains 45 samples. It consists of all surface sediment samples identified as the shelf diatom assemblage, surface sample KRGR25, and 290 cm. The diatom assemblage is dominated by *F. curta* (47.6%) and subdominated by *F. cylindrus* (15.9%). The abundance of both species is not significantly different compared to that in cluster group 1. Taxa that are less abundant, but present at $>2\%$, are *Chaetoceros* resting spores, *T. antarctica* resting spores, *F. angulata*, *F. obliquecostata*, and the Chrysophyte *Pentalamina corona*. There are no unique indicator species in the assemblage; however, it can be differentiated from cluster group 1 by a significantly greater abundance of several species (see Table 15.3).

Cluster group 3 is the smallest group identified, and contains only 9 samples. It includes all surface samples that form the cape assemblage, surface sample KRGC24 (previously included in the shelf surface assemblage), and core intervals 295-300 cm.

Fragilariopsis curta (55.2%) dominates in similar abundance to that observed in the cluster groups 1 and 2. There is no obvious subdominant species in the cluster group, although *T. antarctica* resting spores are the second most abundant (7.7%).

Fragilariopsis cylindrus (4.9%) is significantly less abundant in cluster group 3, compared to all other cluster groups where it forms a subdominant species. The diversity of less abundant (2-5%), but common, taxa is greater in cluster group 3 compared to all others. These include *F. angulata*, *F. kerguelensis*, *Chaetoceros* resting spores, *Eucampia antarctica*, and *T. gracilis*. Many of these are significantly more abundant in cluster group 3 (see Table 15.3), but there are no unique indicator species in the assemblage.

Cluster group 4 contains all surface sediment samples identified as the oceanic assemblage. There are no intervals from GC2 that are analogous to this assemblage and it will not be discussed further here.

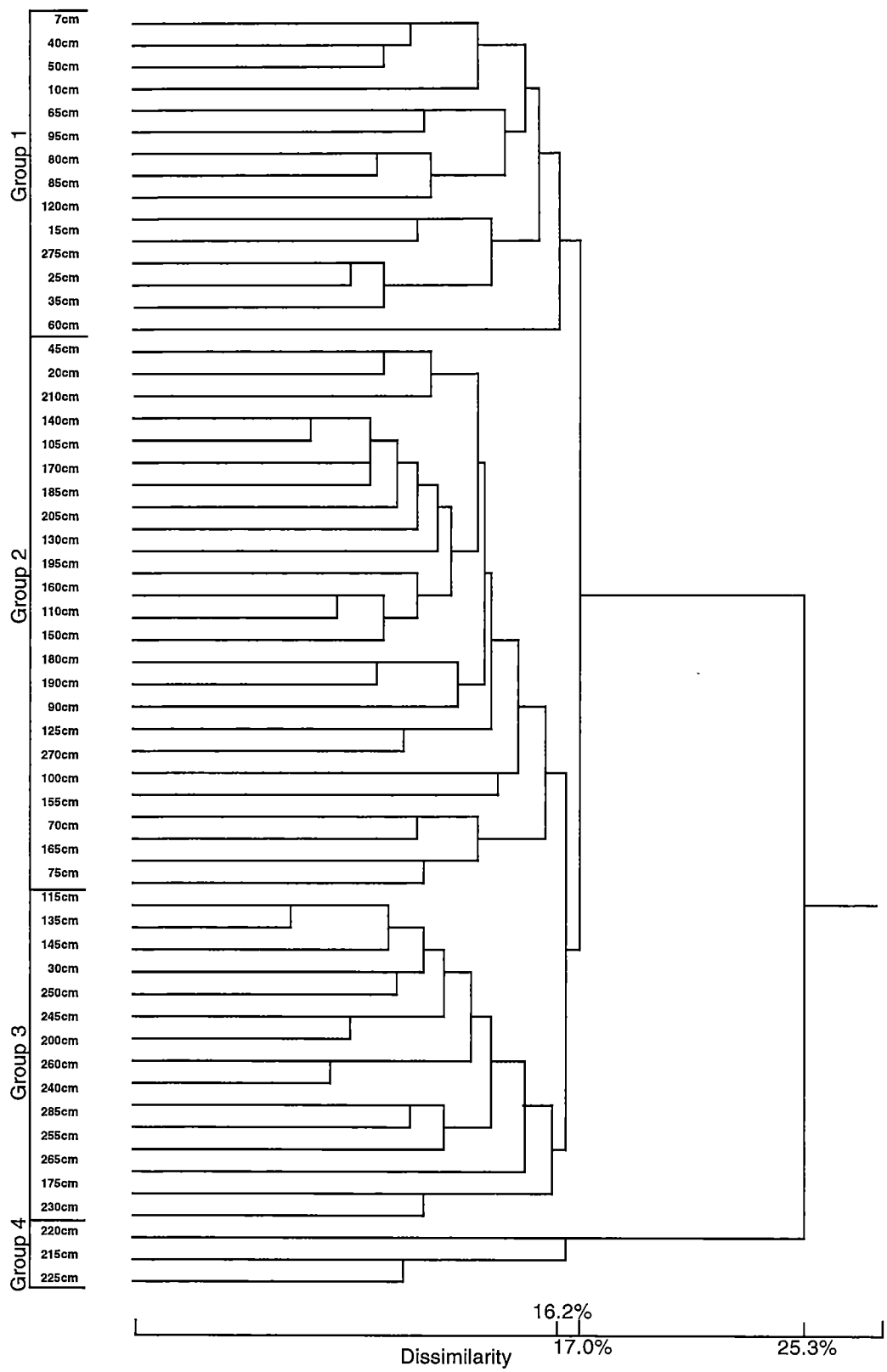


Fig. 15.3. Dendrogram of cluster analysis, comparing GC2 samples. Analysis based on species abundance (>2% log10).

Table 15.2. Arithmetic mean abundance (%), analysis of variance (F) and SNK multiple range test of species in cluster groups of GC2.

| Species | Cluster Group | | | F | P |
|------------------------------------|---------------|-------------|------------|-------|-----|
| | 1 | 2 | 2 | | |
| <i>Chaetoceros</i> spp. | <u>1.7</u> | 0.7 | 0.5 | 8.16 | *** |
| <i>Chaetoceros</i> spores | 7.6 | 5.2 | 12.5 | 1.96 | – |
| <i>C. criophilum</i> | 0.7 | 0.4 | 0.1 | 4.05 | * |
| <i>D. antarcticus</i> | <u>0.6</u> | <u>0.9</u> | <u>2.3</u> | 8.84 | *** |
| <i>Di. speculum</i> | 0.7 | 0.8 | 1.1 | 0.63 | – |
| <i>E. antarctica</i> | 0.8 | 0.8 | 2.1 | 3.03 | * |
| <i>F. angulata</i> | <u>3.6</u> | <u>5.6</u> | <u>9.7</u> | 13.29 | *** |
| <i>F. curta</i> | 59.6 | 56.6 | 31.9 | 2.19 | * |
| <i>F. cylindrus</i> | 11.5 | <u>13.9</u> | 9.6 | 3.24 | * |
| <i>F. kerguelensis</i> | 0.2 | 0.5 | <u>3.5</u> | 31.77 | *** |
| <i>F. obliquecostata</i> | 4.2 | 5.1 | 7.3 | 0.97 | – |
| <i>F. separanda</i> | 0.2 | 0.4 | <u>2.3</u> | 6.34 | *** |
| <i>P. corona</i> | 0.9 | <u>1.6</u> | 1.3 | 7.22 | *** |
| <i>P. glacialis</i> | 0.2 | 0.5 | 0.3 | 1.30 | – |
| <i>Ps. turgiduloides</i> | <u>1.7</u> | <u>0.9</u> | <u>0.1</u> | 15.79 | *** |
| <i>T. antarctica</i> spores | 1.8 | 1.6 | <u>4.7</u> | 8.65 | *** |
| <i>T. gracilis</i> | <u>0.6</u> | <u>0.9</u> | <u>3.6</u> | 26.98 | *** |
| <i>T. lentiginosa</i> | 0.2 | 0.2 | <u>1.4</u> | 17.52 | *** |

Analyses were carried out on $\log_{10}(x+1)$ transformed abundances. Degrees of freedom 2, 55. ANOVA P values: * <0.05, ** <0.005, *** <0.0005, – not significant. Bold type: species with significant differences in mean abundance. Underlined type: species with significant higher abundances in a cluster group.

Table 15.3. Arithmetic mean abundance (%), analysis of variance (F) and SNK multiple range test of species in cluster groups of GC2.

| Species | Cluster Group | | | | F | P |
|--|---------------|-------------|-------------|-------------|--------|-----|
| | 1 | 2 | 3 | 4 | | |
| <i>A. actinochilus</i> | <u>0.1</u> | <u>0.2</u> | <u>0.4</u> | <u>0.8</u> | 50.24 | *** |
| <i>Chaetoceros</i> spp. | <u>0.9</u> | 0.2 | 0.2 | 0.1 | 26.77 | *** |
| <i>Chaetoceros</i> spores | <u>5.8</u> | <u>8.6</u> | <u>2.3</u> | <u>12.6</u> | 31.21 | *** |
| <i>C. criophilum</i> | <u>0.4</u> | 0.1 | 0.1 | 0.1 | 20.78 | *** |
| <i>D. antarcticus</i> | <u>0.7</u> | 0.5 | <u>1.2</u> | <u>0.8</u> | 5.89 | ** |
| <i>D. speculum</i> | 0.7 | 0.5 | 0.9 | 0.8 | 4.38 | * |
| <i>E. antarctica</i> | <u>0.7</u> | <u>0.4</u> | <u>2.3</u> | <u>1.2</u> | 17.99 | *** |
| <i>F. angulata</i> | <u>4.9</u> | <u>3.9</u> | <u>6.9</u> | <u>2.1</u> | 34.26 | *** |
| <i>F. curta</i> | <u>56.93</u> | <u>47.6</u> | <u>55.2</u> | 28.8 | 71.81 | *** |
| <i>F. cylindrus</i> | <u>14.7</u> | <u>15.9</u> | 4.9 | <u>13.6</u> | 14.10 | *** |
| <i>F. kerguelensis</i> | <u>0.4</u> | <u>1.0</u> | <u>2.4</u> | <u>12.9</u> | 158.91 | *** |
| <i>F. lineata</i> | 0.7 | 0.9 | 1.1 | 1.1 | 6.46 | *** |
| <i>F. obliquecostata</i> | <u>4.4</u> | 2.5 | <u>4.0</u> | 1.8 | 28.60 | *** |
| <i>F. separanda</i> | 0.3 | <u>0.8</u> | <u>1.8</u> | <u>1.7</u> | 60.32 | *** |
| <i>F. sublineata</i> | 0.2 | <u>0.7</u> | 0.5 | 0.4 | 15.60 | *** |
| <i>Pentalamina</i> | 1.5 | <u>3.9</u> | 1.2 | <u>3.1</u> | 42.52 | *** |
| <i>P. glacialis</i> | 0.4 | <u>0.9</u> | <u>0.7</u> | 0.2 | 20.71 | *** |
| <i>P. turgiduloides</i> | <u>1.0</u> | 0.1 | 0.1 | 0.1 | 66.28 | *** |
| <i>S. microtrias</i> | 0.1 | 0.3 | <u>0.8</u> | <u>0.6</u> | 31.93 | *** |
| <i>T. antarctica</i> spores | 1.6 | <u>6.7</u> | <u>7.7</u> | <u>6.3</u> | 65.60 | *** |
| <i>T. antarctica</i> (veg) | 0.1 | 0.0 | 0.0 | 0.0 | 0.59 | - |
| <i>T. gracilis</i> | <u>0.8</u> | <u>1.4</u> | <u>2.22</u> | <u>3.8</u> | 70.89 | *** |
| <i>T. gracilis</i> var. <i>expecta</i> | 0.2 | 0.2 | 0.1 | <u>0.7</u> | 20.44 | *** |
| <i>T. gravida</i> | 0.1 | 0.1 | 0.0 | 0.1 | 1.82 | - |
| <i>T. lentiginosa</i> | <u>0.2</u> | <u>0.4</u> | <u>0.9</u> | <u>2.2</u> | 88.01 | *** |
| <i>Trichotoxin reinboldii</i> | 0.1 | 0.3 | 0.2 | <u>0.9</u> | 47.22 | *** |

Analyses were carried out on $\log_{10}(x+1)$ transformed abundance. Degrees of freedom 3, 156. ANOVA P values: * <0.05, ** <0.005, *** <0.0005, – not significant. Bold type: species with significant differences in mean abundance. Underlined type: species with significantly higher abundance in a cluster group.

15.5 Diatom Assemblages in GC2

15.5.1 Reworked / Dissolution Assemblage

The lower 10 cm of GC2 contains a diatom assemblage that is analogous to the cape assemblage identified in the surface sediments of Prydz Bay and Mac.Robertson Shelf. *Fragilariopsis curta* is dominant, forming >50% of the frustules observed. The assemblage is also characterised by a significantly greater abundance of heavily silicified, robust taxa, indicative of oceanographic conditions that range from open water (e.g. *Actinocyclus actinochilus* and *F. kerguelensis*) to sea ice (e.g. *Eucampia antarctica* and *F. angulata*). Smaller, more fragile taxa are less common in the cape assemblage, including *F. cylindrus*, which is otherwise subdominant in diatom assemblages on both the continental shelf and immediately offshore of the shelf-break zone.

In the surface sediments, the cape assemblage is interpreted to be indicative of current reworking. The assemblage's formation is discussed in detail in Chapter 10. In summary, it consists of a lag deposit characterised robust taxa. Smaller, more fragile, and lightly-silicified frustules have been winnowed. Grain size analysis of surface sediments supports this hypothesis. The diatom assemblage is also observed to coincide with a sharp foraminiferid-association that Quilty (1985) suggests is controlled by an oceanographic boundary. Similar diatom assemblages have been observed in surface sediments of the Ross Sea (Truesdale and Kellogg, 1979) and in the southeastern Atlantic (Defelice and Wise, 1981). These are also considered to be lag deposits from which the lighter, more fragile diatoms have been winnowed selectively by bottom currents.

15.5.2 Shelf Assemblage

At 290 cm, one analogous to the shelf assemblage in the surface sediment replaces the reworked diatom assemblage. As with the cape assemblage, it is dominated by *F. curta*, but subdominated by *F. cylindrus*. Many of the large, robust taxa that characterise the underlying, reworked assemblage are less abundant. The shelf assemblage is also

characterised by the centric taxa *T. antarctica* resting spores, *Porosira glacialis* and the Chrysophyte *P. corona*.

In surface sediments, the shelf assemblage is interpreted to represent Antarctic inshore and ice-edge waters. *Thalassiosira antarctica* has been reported to occur in maximum abundance in these environments (Hasle and Heimdal, 1968; Fryxell, 1977; Johansen and Fryxell, 1985; Medlin and Priddle, 1990), but does not occur within sea ice communities. Fryxell *et al.* (1987) suggest that, unlike many *Fragilariopsis* species, *T. antarctica* is unable to survive the low light intensities that occur under the ice, or in brine channels within the ice. Similarly, *P. glacialis* is indicative of sea ice (Krebs *et al.*, 1987), but has not been recorded as a member of within-ice communities (Watanabe, 1988; Garrison and Buck, 1989; Scott *et al.*, 1994).

Our knowledge of the ecology of the siliceous marine Chrysophyte Parmales is limited compared to that of diatoms. A single “siliceous cyst” noted in the Middle America Trench was presumed to prefer cool water and to have been transported to its Quaternary strata by cold-water currents at greater depth (Stradner and Allram, 1982). The siliceous wall plates and nearly-intact cell walls of two Parmales species have also been described in surface and down-core sediments from Prydz Bay (Franklin and Marchant, 1995). The distribution and abundance of the same two species in surface sediment from the Weddell Sea has prompted Zielinski (1997) to suggest that they occur in neritic areas that are influenced by sea ice and / or ice-edge conditions. The findings herein support these accounts. *Pentalamina corona* is significantly abundant in the shelf and oceanic surface sediment assemblages, suggesting that it is indicative of ice edge primary production. Its absence from the coastal assemblage suggests that it does not occur within sea ice algal communities.

15.5.3 Coastal Assemblage

Above 285 cm, the diatom assemblage is analogous to the coastal assemblage in the surface sediment. It is dominated by the genus *Fragilariopsis*. *Fragilariopsis curta* is

the most abundant, forming >50% of the total frustules observed, and *F. cylindrus* is subdominant. Two, numerically rare, taxa are unique indicators of the assemblage: *Chaetoceros* spp. and *P. turgiduloides*.

In the surface sediments of Prydz Bay and Mac.Robertson Shelf, the coastal assemblage represents the preserved portion of the sea ice biocoenose identified by Stockwell *et al.* (1991) and Scott *et al.* (1994). The same species have been similarly noted amongst the dominant and abundant diatoms in the coastal southern waters of Prydz Bay (Kopczynska *et al.*, 1995) and in pack ice from the Weddell Sea (Garrison and Buck, 1989) and fast ice from Lützow-Holm Bay (Watanabe, 1988; Tanimura *et al.*, 1990). Many of the fragile diatoms, found in abundance in these sea-ice algal assemblages, are not preserved in abundance in sediments. Such species include *Chaetoceros* spp., *C. criophilum* and *P. turgiduloides*. Although not preserved in large abundance ($\leq 3.6\%$), *P. turgiduloides* and *C. criophilum* are significantly more abundant in the coastal assemblage compared to their distribution elsewhere in the surface sediments. *Pseudonitzschia turgiduloides* is the unique abundance indicator species of the coastal assemblage, when only the surface sediments are analysed; inclusion of GC2 samples also identifies *C. criophilum* as an indicator species of the assemblage.

The relative abundance of the *C. criophilum* in GC2 has probably been caused by preferential preservation. The effect of anoxia on frustule preservation is discussed in Chapter 14. In the anoxic conditions of Nielsen Basin, *C. criophilum* may be preferentially preserved compared to the frustules of this species in Prydz Bay. The relatively high abundance of *C. criophilum* in sediment from Iceberg Alley is also attributed to the same mechanism.

15.6 Holocene Palaeoecology of Nielsen Basin

15.6.1 Mid Holocene (>5.7 Ka)

The diatom assemblage in the lower 10 cm of GC2 is interpreted to have been deposited prior to ~5.7 Ka, based on reservoir-corrected radiocarbon dates. In the surface sediment, evidence suggests that strong bottom currents have formed this assemblage, which is analogous to the reworked cape assemblage. In GC2, dissolution is suggested as an alternative mechanism that has produced a similar assemblage.

The sedimentation rate at the base of GC2 is seven times lower than that at the top of the core (Table 15.2), at only 0.025 cm yr⁻¹ (between 5.9 Ka and 3.3 Ka), compared to 0.179 cm yr⁻¹ (between 0.7 Ka and 0.3 Ka). The slow deposition rate, and characteristic sandy facies at the base of the core, suggests that in GC2 the cape assemblage was deposited in close proximity to, or beneath, a floating ice shelf. Deposition rates beneath an ice shelf (or ice tongue) are much slower than rates seaward of the calving zone (Kellogg and Kellogg, 1988). This would allow for increased chemical and physical dissolution of diatom frustules in both the water column and at the sediment-water interface. During this time many of the smaller and more fragile diatom species can be removed. An ice shelf over Nielsen Basin prior to 5.7 Ka may have formed locally, and / or represent the advance of a small glacier tongue from the adjacent Strahan Glacier. Harris and O'Brien (1996) use this hypothesis to explain the formation of their geomorphic Zone 1 (high-relief, ridge and valley topography) on Mac.Robertson Shelf. It probably formed under the influence of subglacial incision and erosion during Pleistocene and older glacial maxima when the East Antarctic Ice Sheet expanded to the shelf-break (Harris and O'Brien, 1996).

Does the presence of an ice shelf over Nielsen Basin prior ~5.7 Ka correspond with the advance in East Antarctic outlet glaciers 7.3-3.8 Ka, as noted by Domack *et al.* (1991b), and attributed to the hypsithermal? The hypsithermal is generally regarded as a period of warmest conditions in the Northern Hemisphere, 7.0-4.0 Ka (Pielou, 1991). Glacial expansion along the Antarctic coast during such an event would be possible as warming

gives rise to increased precipitation (in the form of snowfall), rather than ablation, in polar climates. A temperature increase $>5^{\circ}\text{C}$ would be required to induce negative or neutral mass balance for ice retreat to eventually occur in Antarctica (Huybrechts and Oerlemans, 1990). Imbrie and Imbrie (1986) have demonstrated that the hypsithermal in other parts of the world was, on average, only 2°C warmer than present, and would have favoured an expansion of the Antarctic ice sheet. If katabatic winds off the East Antarctic Ice Sheet were also reduced, as might be expected with a reduced surface-temperature gradient, then accumulation would also have been greater during this time (Domack *et al.*, 1991b).

Documentation of an Antarctic hypsithermal is limited, but there are two schools of thought for the timing of this event. Average temperature curves calculated from six ice cores recovered from coastal and inland Antarctica suggest that the Early Holocene (11.0-9.0 Ka) was warmer than the present by $\sim 1\text{-}2^{\circ}\text{C}$ (Ciais *et al.*, 1992, 1994). In comparison, the sedimentological record from ODP Site 740A in Prydz Bay suggests that the Antarctic hypsithermal occurred in East Antarctica 4.3-3.8 Ka (Domack *et al.*, 1991b). And independent evidence (e.g. Burckle, 1972; Truesdale and Kellogg, 1979; Domack *et al.*, 1991a, 1991b; Shevenell *et al.*, 1996; Pushina *et al.*, 1997; Kirby *et al.*, 1998; Cunningham *et al.*, in press) also implies that, in Antarctica, the mid-Holocene was a period of climatic warming. These records closely link to the diatom evidence from GC2.

15.6.2 Mid Holocene (5.7 Ka to 5.5 Ka)

The shelf diatom assemblage is interpreted to have been deposited in GC2 between 5.7 Ka and 5.5 Ka. Its appearance suggests that open marine conditions had become established, and that seasonal sea ice was present. Deposition of the shelf assemblage also coincides with a transition in the core's stratigraphy, from the fine, sandy clay associated with the underlying dissolution assemblage, to massive, biosiliceous ooze. The transition is probably indicative of a relative increase in the rate of biogenic sediment supply. Alternatively, it may indicate a decreased input (and decreased

accumulation rate) of terrigenous sediment, such as would occur if a permanent ice shelf retreated (Domack *et al.*, 1989; 1991a).

An increase in the sediment accumulation rate is synchronous with a change in the diatom assemblage and sedimentary facies at ~290 cm (5.6 Ka). Two hypotheses to account for this increase are suggested by Sedwick *et al.* (in press). It may have been caused by changes in sediment transport processes or sediment focusing, such that sediments were being transported into Nielsen Basin from a progressively increasing “catchment” area, due to ice sheet retreat or changes in shelf-water circulation. Alternatively, the increase may reflect real increases in pelagic sedimentation in overlying waters, perhaps as a result of a progressive decrease in ice cover over this site during the Holocene.

The combined evidence (change in diatom assemblage, change in sediment facies, and increased sediment accumulation rate) suggest that during the mid Holocene (5.7-5.5 Ka) glacial retreat occurred near Nielsen Basin. This is considerably earlier than glacial recession recorded elsewhere along the East Antarctic coast. For example, Domack *et al.* (1991b) suggest that the transition from glacial- to open-marine sedimentation in Mertz-Ninnis Trough, Dumont D’Urville Trough and the Amery Depression commenced between 4.3 Ka and 3.8 Ka, based on the presence of glacial marine diamictos and sands that overly biosiliceous ooze. If an expanded ice shelf near Nielsen Basin was comparatively smaller, it may have responded to climate change more rapidly (Harris, *pers. comm.*). This could account for this apparent time difference of ~1 000 years. Alternatively, a more precise radiocarbon chronology between all four sites may need to be established.

15.6.3 Mid Holocene to Present (<5.5 Ka)

Based on reservoir corrected radiocarbon dates, the coastal diatom assemblage in GC2 has been deposited, without interruption, in Nielsen Basin since 5.5 Ka. For the coastal diatom assemblage to form in preference to the shelf assemblage, multi-year sea ice

must be present. Today, this occurs in areas of Prydz Bay and Mac.Robertson Shelf where grounded icebergs prevent sea ice from its annual summer breakout, normally in shallower coastal areas or on shelf banks.

The uninterrupted deposition of a coastal assemblage in GC2 suggests that the depositional environment of Nielsen Basin has not been significantly altered by oceanographic or climatic conditions during this time. Geochemical records from this core also suggest that accumulation of biogenic and terrigenous material has been relatively constant since the mid to late Holocene (Sedwick *et al.*, in press). Climatic cooling following the Antarctic hypsithermal probably allowed the establishment of open marine conditions, with summer sea ice building up on shallow shelf breaks. On Mac.Robertson Shelf, the grounded icebergs on East and West Storegg Banks, which flank Nielsen Basin, are able to trap seasonal sea ice and restrict its breakout each summer. In this environment, the ice-associated coastal diatom assemblage forms and is being preserved in Nielsen Basin.

15.7 Conclusion

A good, continuous record of the Holocene depositional environment on the inner-shelf of Mac.Robertson Shelf is provided by the diatom assemblages preserved in GC2. The assemblages and their palaeoecological interpretation are summarised in Table 15.4. Prior to ~5.7 Ka, the diatom assemblage, in association with a sandy sediment facies, indicates that Nielsen Basin was in close proximity to, or beneath, a floating ice shelf. Expansion of glacial ice across Mac.Robertson Shelf at this time was probably in response to mid Holocene warming. Slower sediment accumulation rates also during this time would have caused increased chemical and physical dissolution of the diatom frustules, producing an assemblage characterised by robust and heavily silicified taxa. In GC2, this assemblage is analogous to the modern cape assemblage present on Mac.Robertson Shelf, formed by current reworking. It is important to note that the two different oceanographic regimes can produce a similar sedimentary diatom assemblage. This has implications for future palaeoecological interpretations of similar assemblages and care must be taken in interpreting their origin.

After 5.7 Ka, glacial retreat across Nielsen Basin saw the temporary deposition of a shelf diatom assemblage. The shelf assemblage indicates the onset of open marine conditions, with seasonal sea ice. This was replaced by a coastal assemblage, which has been deposited continuously in Nielsen Basin since 5.5 Ka. In the modern environment, the coastal assemblage is indicative of areas where summer sea ice does not seasonally break out and multi-year ice builds up. Climatic cooling that has remained relatively constant, following the mid Holocene climatic optimum, or hypsithermal, has probably lead to the development of this assemblage in GC2.

Table 15.4. Summary of Holocene palaeoclimate of Nielsen Basin, inferred from GC2.

| Corrected ^{14}C Age (Ka) | Core Lithology | Diatom Assemblage | Major Species | Climate Interoperation |
|------------------------------------|-------------------|-------------------|---|---|
| <5.5 | Biosiliceous ooze | Coastal | <i>F. curta</i> <i>F. cylindrus</i> | Mid to Late Holocene cooling, following Mid Holocene climatic optimum |
| 5.5 – 5.7 | Biosiliceous ooze | Shelf | <i>F. curta</i> <i>F. cylindrus</i> <i>Chaetoceros</i> spores | Open marine deposition |
| >5.7 Ka | Fine, sandy clay | Cape | <i>F. cylindrus</i> <i>F. curta</i> <i>F. kerguelensis</i> | Floating ice shelf |

– *Chapter 16* –
KROCK GC29

16.1 Site Description

Core KROCK/15/GC29 (GC29, hereafter) was recovered from southeast Prydz Bay (68° 39.78'S, 76° 41.73'E; Fig. 13.1), in a water depth of 789 m. The site is ~50 km from the Vestfold Hills – a rocky, coastal, ice-free outcrop that extends north east from the Amery Ice Shelf towards the West Ice Shelf, and covers an area of ~410 km² (Adamson and Pickard, 1989). During the late Pleistocene, the Vestfold Hills were covered by ~1000 m of ice. The ice sheet retreated to its present position during the Holocene to expose the hills (Adamson and Pickard, 1989). In Prydz Bay, sea ice is present throughout autumn, winter and spring, with ice breakout occurring in early spring and open water generally predominating the area by January.

16.2 Core Description

GC29 is 352 cm long (Fig. 16.1). It shows no sign of internal structure, erosional surfaces, laminations, or bioturbation, and appears to represent an uninterrupted sedimentary record (Franklin, 1997). Three lithological units can be recognised. Unit 1 (0 cm to 130 cm) consists of massive, diatomaceous ooze, which is typical of the compound glacial-marine sediments being deposited on the continental shelf of Antarctica today (Anderson *et al.*, 1980; Domack, 1988). The ooze is moderate, olive brown (5Y 4/4) in colour at the top, grading to moderate, olive grey (5Y 4/2) at the base. Below unit 1, the ooze grades into diamicton (Unit 2; 130 cm to 305 cm). Unit 2 contains gneiss dropstones with a diameter 1-2 cm, supported by current reworked, massive sand and silt deposits, typical of iceberg-rafted debris (Kellogg and Kellogg, 1988). It is medium, greenish grey (5GY 5/1). Unit 3 is characterised by a gradual increase in compaction and colour change to dark, greenish grey (5GY 4/1). Sediment compaction may be indicative of compacted tillite, such as that deposited below the grounding line of an ice sheet. There is no distinct structural boundary between units 2 and 3.

16.3 Fossil Assemblages

Diatoms are abundant and well preserved between 0 cm and 135 cm. They are present between 135 cm and 145 cm, but are poorly preserved and not quantifiable. Diatoms are rare to absent below 145 cm. *Fragilariopsis curta* is the most abundant species in the

upper 25 cm, forming >50% of the frustules observed. Below this, *F. curta* and *T. antarctica* resting spores co-dominate, until 105 cm. *Thalassiosira antarctica* resting spores are dominant below 105 cm. There is no visible reaction to HCl throughout GC29, indicating that calcareous shells, such as foraminifera, are absent. No other fossils or fossilised structures were observed.

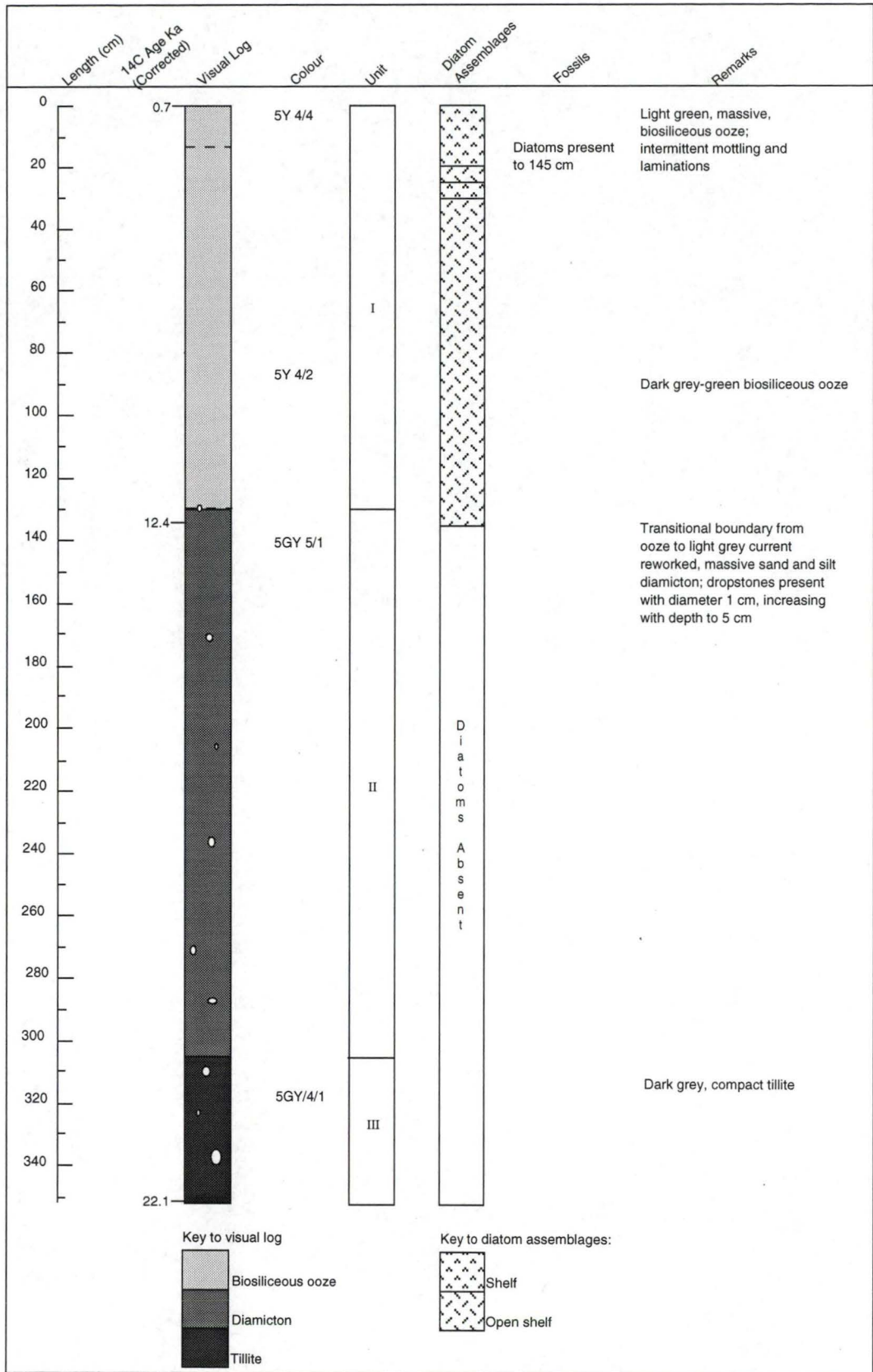


Fig. 16.1. GC29 core log, radiocarbon dates and diatom assemblages when compared to surface sediments.

16.4 GC29 – Results

16.4.1. Radiocarbon Dates

Three AMS radiocarbon dates were obtained from bulk organic carbon samples (Table 16.1). An ocean reservoir correction factor of 1 750 radiocarbon years has been subtracted from the ^{14}C ages, based on the work of Domack *et al.* (1991a) from nearby ODP Site 740A. This gives GC29 a corrected core top age of 740 yBP, which is similar to the corrected ages obtained from the surface of cores GC1 and GC2 on Mac.Robertson Shelf. A corrected age of 12 400 yBP was obtained from 134-135 cm. This coincides with the transitional boundary from biosiliceous ooze to diamicton, implying a change from open marine to beneath-ice deposition around this time. Based on ODP Site 740A, the initiation of open-marine conditions in Prydz Bay is estimated to have commenced about 10 700 yBP (Domack *et al.*, 1991a). The bottom of GC29 extends into the late Pleistocene, with a corrected age of 22 060 yBP obtained between 350 cm and 352 cm.

Table 16.1. Uncorrected AMS radiocarbon dates obtained from bulk organic carbon for GC29.

| Interval (cm) | ^{14}C Date (yBP) | | Deposition Rate (cm yr ⁻¹)† |
|---------------|----------------------------|-----------|--|
| | Uncorrected | Corrected | |
| 0 - 2 | 2493 ± 67 | 743 | |
| 134 - 135 | 14 140 ± 120 | 12 390 | 0.012 |
| 350 - 352 | 23 810 ± 230 | 22 060 | 0.022 |

† Deposition rates determined between 2-135 cm and 135-352 cm.

Simple linear regression indicates a good age v depth correlation ($R^2 = 0.965$; Fig. 16.2). Sediment accumulation rates in the core are relatively constant throughout, from 0.012 cm yr⁻¹ (between 0 cm and 135cm) to 0.022 cm yr⁻¹ (between 135 cm and 352 cm). Average sediment accumulation rate over the entire core is 0.017 cm yr⁻¹. This rate is

similar to that determined by Harris (*pers. comm.*), who calculates an average Holocene sedimentation rate in Prydz Bay of 0.02 cm yr^{-1} . Domack *et al.* (1991a), however, have estimated sedimentation rates to range from 0.187 cm yr^{-1} to 0.144 cm yr^{-1} , from ODP Site 740. There is no evidence to suggest that unconformities are present in the core and the work herein agrees with Franklin (1997), whose findings indicate that GC29 records sedimentation without erosional processes in Prydz Bay since the late Pleistocene.

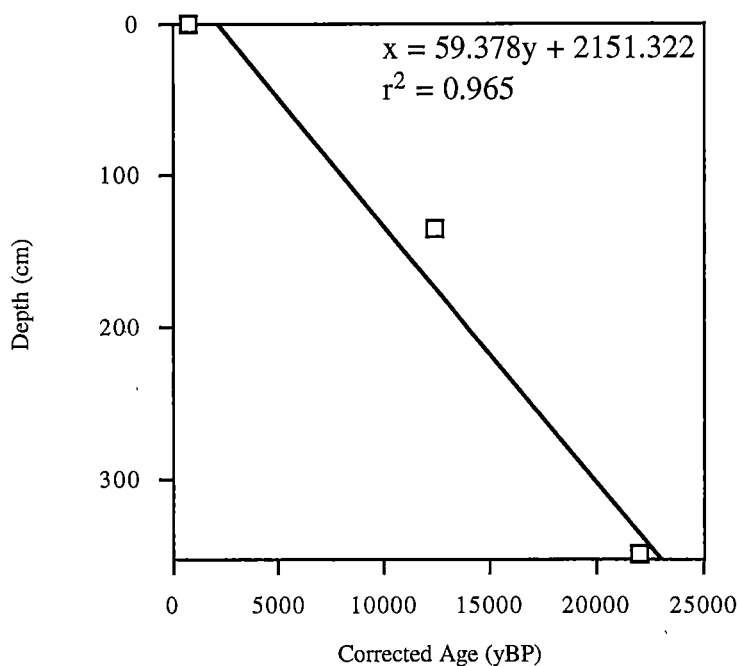


Fig. 16.2. Linear regression of corrected radiocarbon ages versus depth.

16.4.2. Diatom Assemblages

Diatoms are present in quantifiable abundance to 135 cm. This corresponds with the massive biosiliceous ooze of lithological unit 1, below which the sediment grades into the diamicton of unit 2. Downward throughout unit 1, there is a synchronous decrease in abundance of *F. curta* and increase in *T. antarctica* resting spores. Members of the genus *Fragilariopsis* dominate between 0 cm and 25 cm. *Fragilariopsis curta* is the most abundant species, forming up to 65.2% of the assemblage. Below 30 cm, *F. curta* and *T. antarctica* resting spores co-dominate the assemblage. Both species are present at

~35%, and *Chaetoceros* resting spores subordinate. The lower-most intervals of GC29 are dominated by *T. antarctica* resting spores and subdominated by *F. curta*.

16.4.3. Statistical analyses

GC29

Fifteen diatom species with an abundance >2% are observed in 28 samples from GC29, between 0 cm and 135 cm (Appendix 7). A dendrogram illustrating the sample affinities is illustrated in Fig. 16.3. Three cluster groups are identified, with a dissimilarity of 18.8% and a cophenetic correlation of 0.55. Significantly abundant species in each cluster group are listed in Table 16.2. Analyses are based on \log_{10} values; all values in the following discussion are based on arithmetic mean percent values.

Cluster group 1 occurs in the upper 25 cm of GC29. The diatom assemblage is dominated by *F. curta* (49.8%), and subdominated by *T. antarctica* resting spores (15.7%). Less abundant but common (>2%), are *Chaetoceros* resting spores, *F. angulata*, *F. cylindrus*, *F. obliquecostata*, and the Chrysophyte *P. corona*. Based on \log_{10} values, *F. curta* is a unique abundance indicator species of the cluster group. The group is also characterised by a significantly higher abundance *Porosira glacialis* (1.9%).

Cluster group 2 is the largest cluster group, occurring uninterrupted between 30 cm and 100 cm, and at 110 cm. *Thalassiosira antarctica* resting spores (29.5%) and *F. curta* (27.0%) are co-dominant, and *Chaetoceros* resting spores are subordinate (11.9%). Less common are *F. angulata*, *F. cylindrus*, *F. kerguelensis*, and *P. corona*. There are no unique indicators of the diatom assemblage; however, it can be differentiated from that of cluster group 1 by the significantly greater abundance of *Chaetoceros* resting spores, *Dactyliosolen antarcticus*, *F. cylindrus*, *F. kerguelensis*, *F. obliquecostata*, and *T. antarctica* resting spores. The abundance of *P. glacialis* is significantly greater compared to cluster group 3, but less abundant compared to cluster group 1.

Cluster group 3 contains a small number of samples from the base of the biosiliceous ooze (unit 1). The cluster group is present at 105 cm, and also occurs from 115 cm to 135 cm. *Thalassiosira antarctica* resting spores (36.5%) are dominant, and *F. curta* (28.8%) subdominant. Neither are significantly different in abundance compared to that of cluster group 2. Present at >2% are *Chaetoceros* resting spores, *F. cylindrus*, *F. kerguelensis*, and *F. obliquecostata*. There are no indicator species in the assemblage, but it can be identified by a significantly higher abundance of *F. kerguelensis*, compared to its abundance in both cluster groups 1 and 2.

GC29 and Surface Samples

Core and surface sediment sample affinities, based on cluster analysis, are illustrated as a dendrogram in Fig. 16.4. Using 23 species with an abundance >2%, from 126 samples, five cluster groups are identified at 28.30% dissimilarity and with a cophenetic correlation of 0.54. The significantly abundant species in each cluster group are listed in Table 16.3. Values in the following discussion are based on arithmetic mean percent values, unless otherwise indicated.

Cluster group 1 contains all surface samples identified as the coastal diatom assemblage. There are no samples from GC29. The coastal diatom assemblage is described in detail in Chapters 9 and 10, and will not be further discussed here.

Cluster group 2 contains all surface sediment samples identified as the shelf assemblage, and GC29 samples 0-15 cm and 25 cm. The diatom assemblage is most similar to the coastal assemblage, and is dominated by *F. curta* (48.4%). Based on \log_{10} values the abundance is not significantly different from that observed in the coastal assemblage. Similarly, *F. cylindrus* (15.1%) is subdominant in the shelf assemblage; however, its abundance is significantly lower compared to the coastal assemblage. Less abundant, but common (>2%), are *Chaetoceros* resting spores, *F. angulata*, *F. kerguelensis*, *T. antarctica* resting spores, and the Chrysophyte *P. corona*. There are no unique indicator species, but it can be identified by the significantly greater abundance of

several species compared to the other cluster groups (see Table 16.3). The most notable of these is *P. corona*, which reaches its maximum, and most significant, abundance in cluster group 2.

Cluster group 3 contains GC29 intervals 20 cm and 30-135 cm. There are no surface sediments in Prydz Bay or Mac.Robertson Shelf with diatom assemblages that are analogous. It is characterised by the co-dominance of *T. antarctica* resting spores (31.0%), and *F. curta* (28.1%). The abundance of *T. antarctica* spores is significantly greater in cluster group 3 compared to all other clusters groups. *Fragilariopsis curta* is significantly less abundant compared to cluster groups 1, 2 and 5. The assemblage is subdominated by *Chaetoceros* resting spores (11.0%); common (>2%) are *F. angulata*, *F. cylindrus*, *F. kerguelensis*, *F. obliquecostata*, and *P. corona*. Two indicator species characterise the assemblage: *F. obliquecostata* and the silicoflagellate *Distephanus speculum* (Ehrenberg) Manguin. Several species can also be noted as significantly more abundant in cluster group 3 compared to other cluster groups, but are not indicator species (Table 16.3). Cluster group 3 is hereafter referred to as the “open shelf” diatom assemblage.

Cluster groups 4 and 5 contain all surface samples identified as the oceanic and cape diatom assemblages, respectively. There are no analogous samples from GC29. Both assemblages are described in detail in Chapters 9 and 10 and, will not be further discussed here.

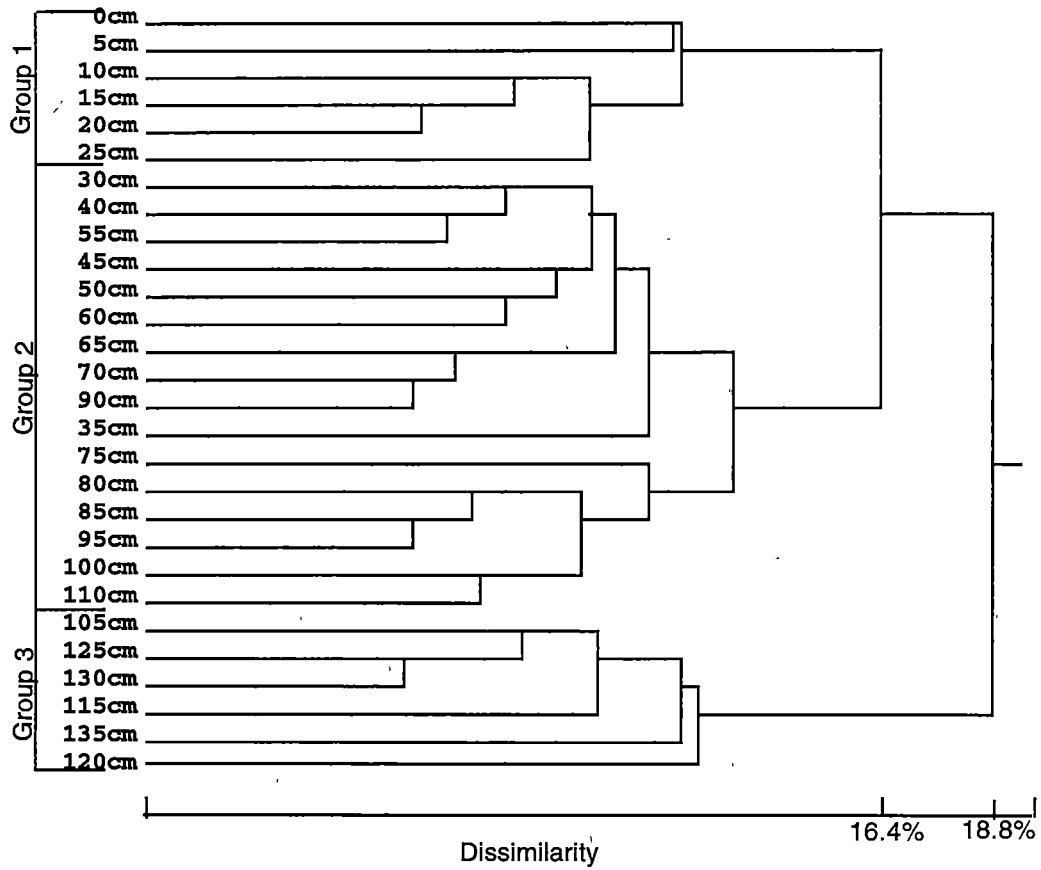


Fig. 16.3. Dendrogram of cluster analysis comparing GC29 samples. Analysis based on species abundance (>2% log₁₀).

Table 16.2. Arithmetic mean abundance (%), analysis of variance (F) and SNK multiple range tests of dominant species in cluster groups of GC29.

| Species | Cluster Group | | | F | P |
|------------------------------------|---------------|-------------|-------------|-------|-----|
| | 1 | 2 | 3 | | |
| <i>Chaetoceros</i> spores | 4.7 | <u>11.9</u> | <u>9.5</u> | 10.79 | *** |
| <i>D. antarcticus</i> | 0.2 | <u>0.8</u> | <u>0.8</u> | 11.44 | *** |
| <i>D. speculum</i> | 1.3 | 1.8 | 1.4 | 0.92 | – |
| <i>E. antarctica</i> | 0.4 | 0.8 | 0.8 | 4.05 | * |
| <i>F. angulata</i> | <u>3.7</u> | 2.6 | 1.2 | 4.95 | * |
| <i>F. curta</i> | <u>49.8</u> | 27.0 | 28.8 | 30.51 | *** |
| <i>F. cylindrus</i> | <u>7.4</u> | <u>8.3</u> | 2.5 | 18.52 | *** |
| <i>F. kerguelensis</i> | <u>1.0</u> | <u>2.1</u> | <u>6.2</u> | 36.92 | *** |
| <i>F. obliquecostata</i> | 3.7 | 4.4 | 4.6 | 0.75 | – |
| <i>F. separanda</i> | 0.6 | 0.7 | 0.6 | 0.00 | – |
| <i>P. corona</i> | <u>4.6</u> | <u>3.6</u> | 0.7 | 18.32 | *** |
| <i>P. glacialis</i> | <u>1.9</u> | <u>0.9</u> | <u>0.6</u> | 18.31 | *** |
| <i>T. antarctica</i> spores | 15.7 | <u>29.5</u> | <u>36.5</u> | 24.14 | *** |
| <i>T. gracilis</i> | 0.8 | 1.2 | 0.8 | 4.50 | * |
| <i>T. lentiginosa</i> | 0.5 | 0.6 | 0.4 | 0.40 | – |

Analysis was carried out on $\log_{10}(x+1)$ transformed abundance. Degrees of freedom 2, 25. ANOVA P values: * <0.05, ** <0.005, *** <0.0005, – not significant. Bold: species with significant differences in mean abundance. Underlined: species with significantly higher abundance in a cluster group.

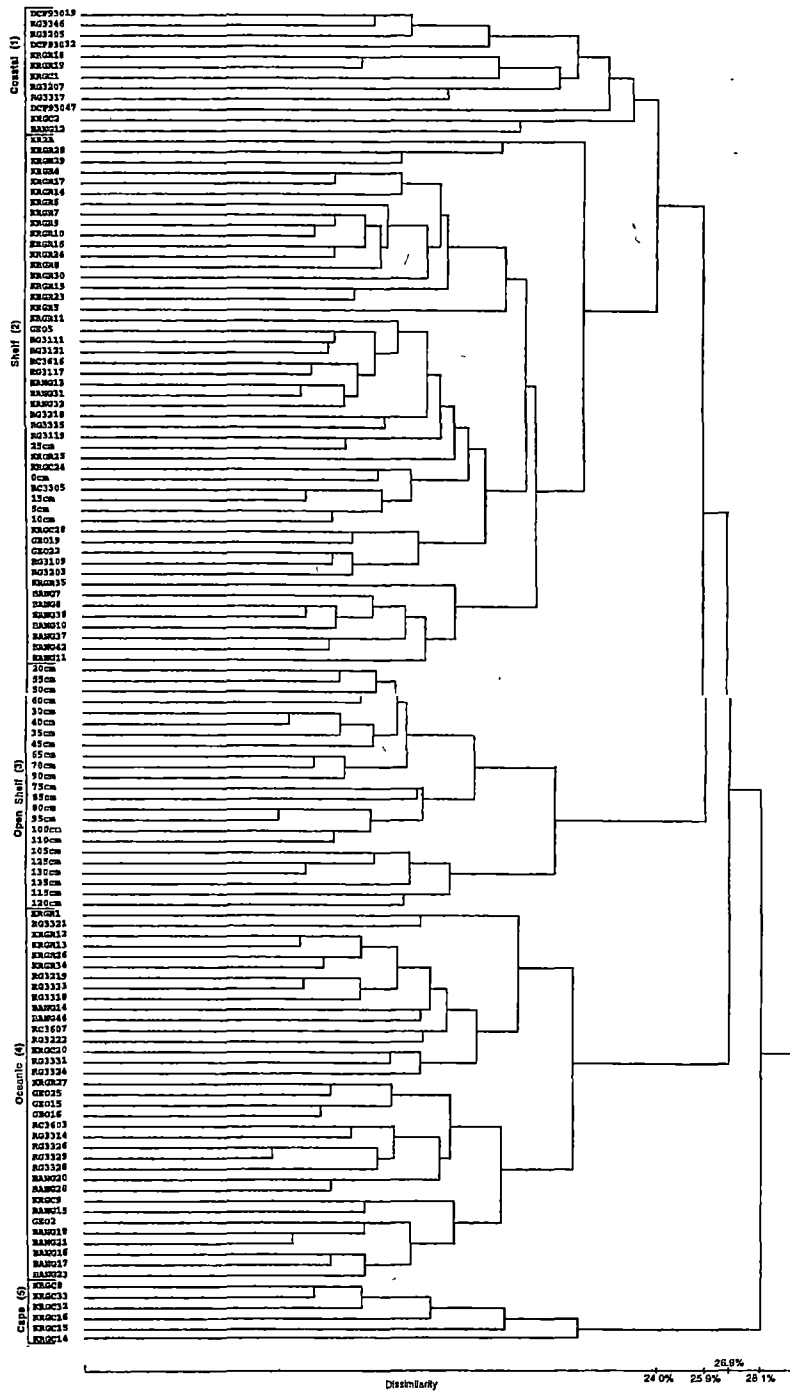


Fig 16.4. Dendrogram of cluster analysis comparing GC29 and surface samples. Analysis based on species abundance (>2% log10).

Table 16.3. Arithmetic mean abundance (%), analysis of variance (F) and SNK multiple range tests of dominant species in cluster groups of GC29 and surface sediment samples.

| Species | Cluster Group | | | | | F | P |
|--|---------------|-------------|-------------|-------------|-------------|-------|-----|
| | 1 | 2 | 3 | 4 | 5 | | |
| <i>A. actinochilus</i> | 0.1 | 0.2 | 0.2 | <u>0.8</u> | <u>0.5</u> | 20.97 | *** |
| <i>Chaetoceros</i> spp. | 0.1 | 0.1 | 0.3 | 0.1 | 0.0 | 3.34 | * |
| <i>Chaetoceros</i> spores | <u>5.3</u> | <u>7.8</u> | <u>11.0</u> | <u>12.6</u> | <u>1.1</u> | 23.51 | *** |
| <i>D. antarcticus</i> | 0.2 | 0.4 | <u>0.8</u> | <u>0.8</u> | <u>0.9</u> | 8.57 | *** |
| <i>D. speculum</i> | 0.4 | 0.6 | <u>1.7</u> | 0.8 | 0.6 | 15.21 | *** |
| <i>E. antarctica</i> | 0.1 | 0.4 | <u>0.8</u> | <u>1.2</u> | <u>2.3</u> | 13.74 | *** |
| <i>F. angulata</i> | <u>4.2</u> | <u>3.9</u> | 2.2 | 2.1 | <u>5.6</u> | 17.75 | *** |
| <i>F. curta</i> | <u>54.7</u> | <u>48.4</u> | 28.1 | 28.8 | <u>62.8</u> | 50.05 | *** |
| <i>F. cylindrus</i> | <u>22.3</u> | <u>15.1</u> | <u>6.7</u> | <u>13.6</u> | <u>2.6</u> | 17.14 | *** |
| <i>F. kerguelensis</i> | 0.5 | 1.0 | <u>3.1</u> | <u>12.9</u> | 2.0 | 69.72 | *** |
| <i>F. lineata</i> | 0.70 | 0.9 | 0.6 | <u>1.1</u> | 1.1 | 3.92 | ** |
| <i>F. obliquocostata</i> | 1.8 | 2.6 | <u>4.5</u> | 1.8 | 2.7 | 19.69 | *** |
| <i>F. separanda</i> | <u>0.2</u> | <u>0.7</u> | <u>0.7</u> | <u>1.7</u> | <u>1.7</u> | 23.44 | *** |
| <i>F. sublineata</i> | 0.4 | 0.7 | 0.4 | 0.4 | 0.6 | 2.21 | * |
| <i>P. corona</i> | 1.6 | <u>4.0</u> | <u>2.9</u> | <u>3.1</u> | 1.1 | 9.44 | *** |
| <i>P. glacialis</i> | 0.2 | <u>1.1</u> | <u>0.7</u> | 0.2 | 0.6 | 19.13 | *** |
| <i>P. turgiduloides</i> | <u>0.4</u> | 0.1 | 0.1 | 1.8 | 0.1 | 6.04 | *** |
| <i>S. microtrias</i> | 0.2 | 0.3 | 0.3 | <u>0.6</u> | <u>0.9</u> | 8.29 | *** |
| <i>T. antarctica</i> | 0.1 | 0.0 | 0.0 | 0.0 | 0.0 | 2.3 | – |
| <i>T. antarctica</i> spores | <u>1.3</u> | <u>7.5</u> | <u>31.0</u> | <u>6.3</u> | <u>8.5</u> | 74.30 | *** |
| <i>T. gracilis</i> | 0.8 | 1.2 | 1.1 | <u>3.8</u> | <u>2.1</u> | 40.53 | *** |
| <i>T. gracilis</i> var. <i>expecta</i> | 0.2 | 0.2 | 0.2 | <u>0.7</u> | 0.0 | 9.90 | *** |
| <i>T. lentiginosa</i> | 0.2 | 0.4 | 0.5 | <u>2.2</u> | 0.8 | 44.60 | *** |
| <i>T. reinboldii</i> | 0.1 | 0.3 | 0.2 | <u>0.9</u> | 0.2 | 18.93 | *** |

Analysis was carried out on $\log_{10}(x+1)$ transformed abundance. Degrees of freedom 4, 121. ANOVA P values: * <0.05, ** <0.005, *** <0.0005, – not significant. Bold: species with significant differences in mean abundance. Underlined: species with significantly different abundance in a cluster group. Cluster group (diatom assemblage) names. 1 = Coastal, 2 = shelf; 3 = Open shelf; 4 = Oceanic; 5 = Cape.

16.5 Diatom Assemblages in GC29

16.5.1 Shelf Assemblage

A diatom assemblage analogous to the modern shelf assemblage in Prydz Bay and Mac.Robertson Shelf occurs at the top of GC29. *Fragilariopsis curta* is the dominant species, and *F. cylindrus* is subdominant. In surface sediments, the shelf assemblage represents continental shelf and ice edge waters where summer sea ice has recently retreated, but a stationary ice edge may persist nearby.

The shelf assemblage differs from the coastal diatom assemblage, which is indicative of shallow and coastal areas where sea ice does not seasonally break out, by a significantly greater abundance of the centric diatoms *T. antarctica* resting spores and *P. glacialis*, and the Chrysophyte *P. corona*. *Thalassiosira antarctica* has been reported to occur in maximum abundance in Antarctic inshore and ice-edge waters (Hasle and Heimdal, 1968; Fryxell, 1977; Johansen and Fryxell, 1985; Medlin and Priddle, 1990). This is in contrast to many *Fragilariopsis* species that occur under the ice, or in brine channels within the ice, probably because they are able to survive the low light intensities here (Fryxell *et al.*, 1987). Similarly, *P. glacialis* is ice associated (Krebs *et al.*, 1987), but does not occur within ice algal communities (Watanabe, 1988; Garrison and Buck, 1989; Scott *et al.*, 1994). The known ecology of the Chrysophyte order Parmales, and their distribution in sediment, is limited. They are discussed in preceding chapter. The findings of the present study generally support the hypothesis that Parmales do not occur within sea ice algal communities, but are indicative of the ice edge zone.

16.5.2 Open Shelf Assemblage

There is no modern analogue for the open shelf assemblage in GC29. The assemblage is co-dominated by *T. antarctica* resting spores and *F. curta*. *Chaetoceros* resting spores subdominate. Cluster analysis indicates that it is intermediate between the modern shelf and oceanic assemblages in both species composition and abundance (Table 16.4).

Table 16.4. Relative abundance of indicator species in shelf, open shelf, and oceanic diatom assemblages (GC29).

| Species | Relative Abundance | | | Primary Environment |
|--------------------------|--------------------|------------|---------|---------------------|
| | Shelf | Open Shelf | Oceanic | |
| <i>F. curta</i> | High | Low | Low | Ice |
| <i>F. kerguelensis</i> | Intermediate | Low | High | Open water |
| <i>F. obliquocostata</i> | Intermediate | High | Low | Open water |
| <i>T. antarctica</i> | Low | High | Low | Open water |

The shelf assemblage characterises regions on the continental shelf where open water dominates in summer, but seasonal sea ice may have only recently retreated to expose the area and a permanent, nearby ice edge may persist. The diatom assemblage contains species that are typically associated with ice edge zones. The oceanic assemblage has been found, in this study, to be distributed mainly in the surface sediments offshore of the continental shelf break, and extending as a “tongue” into Prydz Bay between 75°E and 78°E. This is probably via transportation in deep, warm Antarctic Circumpolar Current waters that cross the continental shelf via the Prydz Bay cyclonic gyre. The oceanic assemblage contains species indicative of open water, such as *F. kerguelensis*, which dominates at subantarctic latitudes (Burckle and Cirilli, 1987; Burckle *et al.*, 1987).

Abundant *T. antarctica* resting spores, comparable to that in the open shelf assemblage, does not occur in the surface sediments of Prydz Bay or Mac.Robertson Shelf. But before the palaeoenvironmental implications of the spores can be discussed, it is important to consider the ecology of the genus. *Thalassiosira* is widespread in Antarctic waters, but generally considered indicative of open water (Fryxell and Kendrick, 1988). It is uncommon in sea ice (Leventer and Dunbar, 1988, 1996; Garrison and Buck, 1985; Fryxell and Kendrick, 1988; Zielinski and Gersonde, 1997), with maximum abundance up to only 0.5% having been reported in sea ice samples from McMurdo Sound

(Leventer and Dunbar, 1987b). Fryxell *et al.* (1987) suggest that the absence of *Thalassiosira* in sea ice may be explained by its inability to survive the low light intensities that occur under the ice, and in the brine channels within the ice. This appears true for most members of the genus, with the exception of *T. australis* that has been observed amongst the dominant species beneath snow-free fast ice (McMinn, 1996; McMinn, in press; McMinn *et al.*, in press a & b).

The specific ecology of the *T. antarctica* is less well known. It, too, is considered to be an open water species, but has been observed in association with ice edge regions (Hasle and Heimdal, 1968; Fryxell, 1977; Villareal and Fryxell, 1983a; Pichon *et al.*, 1992). These observations are supported by the findings herein, where *T. antarctica* resting spores are indicators of the shelf diatom assemblage. *Thalassiosira antarctica* has also been reported to be a member of sea ice samples (Horner, 1985; Krebs *et al.*, 1987), and in the platelet ice that gathers under coastal pack and fast ice (Villareal and Fryxell, 1983a; Horner, 1985; Krebs *et al.*, 1987; Smetacek *et al.*, 1992; Leventer and Dunbar, 1996). Krebs *et al.* (1987) considered the resting spores to be truly cryophilic, based on their study of sea-ice microflora collected from a variety of sea ice types from the Antarctic Peninsula. Their interpretation should be regarded with caution, however, given that the spores occurred in only four out of 21 sea ice samples analysed, and were not observed to form >1.3% of the total number of cells counted.

Recently, Cunningham and Leventer (1998) speculate that an unusually high abundance of *T. antarctica* resting spores in Ross Sea surface sediment may be due to the increased significance of an autumn bloom, initiated by the scavenging of *T. antarctica* by loose ice crystals. *Thalassiosira antarctica* resting spores have not been observed in comparable abundance in the water column, which they suggest is due to the majority of phytoplankton studies having been carried out in spring and summer months. If *T. antarctica* does bloom in autumn, this, they suggest, would also explain an increase in the percent of *T. antarctica* resting spores from May to January in sediment trap studies observed by Leventer and Dunbar (1988) in the Ross Sea.

Based on this hypothesis, Cunningham *et al.* (in press) speculate that an increase in *T. antarctica* resting spores, and decrease in *F. curta*, between 6.0 Ka and 3.0 Ka in gravity cores from the Ross Sea indicates:

1. a decrease in the significance of spring and summer ice edge blooms; and
2. an increase in the temporal occurrence or amount of loose pack ice during autumn.

This may be due to the seasonally late development of solid ice cover, due to increased wind stress, and / or increasing contributions of platelet ice, due to increased melting at the base of a receding Ross Ice Shelf (Cunningham *et al.*, in press). Either alternative implies a separate climate regime, however, which needs to be resolved. Windier conditions tend to be associated with a cooler climate, such as that experienced in East Antarctica during the Little Ice Age between ~1500 AD and ~1800 AD (Mosley-Thompson, 1992). Increased melting and recession of an ice shelf may be indicative of warmer atmospheric temperatures. Leventer *et al.* (1993) also note that seasonal changes in sea ice extent around Antarctica clearly demonstrates the role that temperature plays in the distribution of sea ice.

Rather than being associated with platelet ice during part of its life cycle, it is suggested herein that the formation of *T. antarctica* resting spores could be triggered by the low light intensities that occur beneath developing pack and platelet ice. Diatom communities that are associated with platelet ice have been demonstrated to possess photosynthetic properties for extreme shade adaptation (Arrigo *et al.* 1993; Robinson *et al.*, 1995). Sea ice studies from Prydz Bay (Scott *et al.*, 1994) and Lützow-Holm Bay (Tanimura *et al.*, 1990) have not recorded *T. antarctica* (resting spores or vegetative cells) to be present in sufficient abundance for them to be considered a significant member of the ice assemblage, however. This would imply that *T. antarctica*, like most other members of the genus, is not photosynthetically adapted to low light.

Nutrient depletion may also contribute to spore formation in *T. antarctica*. Antarctic waters are generally high in nutrients and only in certain circumstances, such as during algal blooms, may they become sufficiently depleted so as to be limiting to phytoplankton growth (Fukai *et al.*, 1986; Nelson and Smith, 1986; Nelson and Tréguer, 1992; McMinn *et al.*, 1995). Lizotte and Sullivan (1991) have noted that although water beneath sea ice is usually high in nutrients, the platelet ice that accumulates here may restrict seawater flux and restrict nutrient resupply. Whether spore formation occurs in autumn, however, as suggested by Cunningham and Leventer (1998), is still to be determined.

16.6 Holocene Palaeoecology of Inner Prydz Bay

16.6.1 Upper Pleistocene (> 12.4 Ka)

Diatoms are not in quantifiable abundance from the base of GC29 to 135 cm. The rare frustules that are present occur mainly as fragments, indicating extensive mechanical breakage that has probably taken place during deposition and burial. The low abundance of diatoms corresponds with lithological units 2 and 3 (Fig.16.1). Unit 3 extends from the base of the core and consists of dark grey, compact tillite. It is separated from unit 2, at 305 cm, by a transitional boundary. Unit 2 grades into massively bedded, sand and silt diamicton. It was last deposited at ~130 cm

Based on reservoir corrected radiocarbon dates, and assuming a relatively constant sedimentation rate, the base of the core has an age of ~23.0 Ka. At 135 cm, a corrected radiocarbon age of 12.4 Ka was obtained. O'Brien (1992) and Franklin (1997) suggest that a significant inlet of marine water was present along the Ingrid Christensen Coast during this time. Franklin (1997) also notes that GC29 shows no signs of internal structure, erosional surfaces, lamination, or bioturbation, and appears to represent a period of uninterrupted deposition. High levels of biogenic silica suggest that the area was subject to open marine conditions for most of this time (Franklin, 1997). The lithology of the core and low abundance of diatoms observed herein, however, implies

that ice was grounded over the site from at least ~23.0 Ka, until 12.4 Ka. This can be correlated with the Last Glacial Maximum (LGM), which, in Antarctica, is placed between 10.0 Ka and 25.0 Ka (Adamson and Pickard, 1986).

A study of seismic profiles and gravity cores from Prydz Bay by Domack *et al.* (1998), does imply that the LGM was associated with the grounding of an ice sheet, or ice shelf, at least along the western periphery of Prydz Channel. Ice shelf conditions probably existed across the channel during this interval (Domack *et al.*, 1998). Recession across the channel led to the deposition of fossiliferous diamicton, and eventually siliceous, muddy ooze, indicating seasonally open marine conditions. The age for the transition from a grounded ice sheet to an open marine environment in the east Prydz Channel is ~11.0 Ka (O'Brien and Harris, 1996), based on a core collected from the Amery Depression. Similarly, Domack *et al.* (1991a) suggest that the transition from glaciomarine clays to diatom ooze at ODP Site 740A commenced 10.7 Ka and marks the onset of open marine conditions in eastern Prydz Bay.

16.6.2 Early to Late Holocene (12.4 Ka to 3.2 Ka)

Diamicton is replaced by massive siliceous ooze (unit 1) at about 130 cm. Diatoms are present in quantifiable abundance above 135 cm, when deposition of the open shelf assemblage commenced 12.4 Ka. Deposition of this assemblage continued throughout the Holocene, until 3.2 Ka.

In GC29, the open shelf assemblage is interpreted to represent increased open water relative to that on the continental shelf today. Loose sea ice may have also been present, but it probably broke out earlier, and reformed later, in the season. Pack ice is inferred to be the primary ice type due to the high abundance of *T. antarctica* resting spores, and the relatively low abundance of *F. curta* (Fig. 16.5). A negative correlation ($R^2 = 0.658$) is also observed between *T. antarctica* resting spores and *F. curta*. The ecology of *T. antarctica*, discussed in detail above, is not certain, but it is generally considered an open water species with some minor ice association. In contrast, *F. curta* is commonly found in both fast and pack ice, as well as in the meltwater-stratified surface layer

associated with a retreating ice edge (review in Cunningham and Leventer, 1998), where it has been released into the water column by melting ice (McMinn, *pers. comm.*). Based on this, Cunningham and Leventer (1998) use it as a proxy for meltwater stratification that results from fast and pack ice melt-out. Similarly, the abundance of *F. curta* in the surface sediment coastal and shelf assemblages is used as a proxy for summer ice distribution.

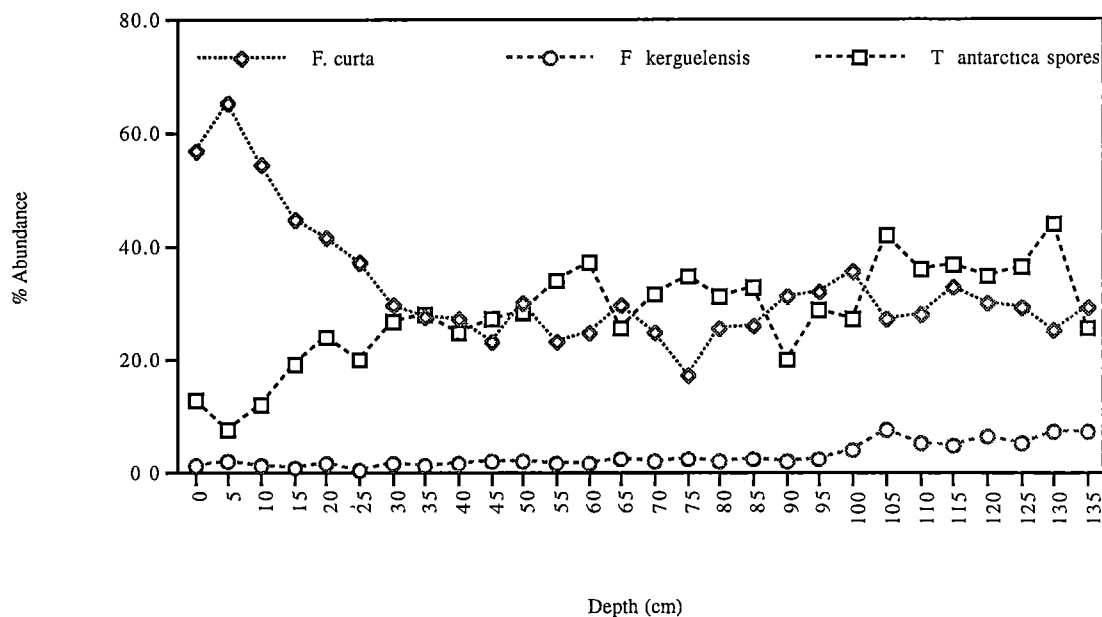


Fig. 16.5. Distribution of *F. curta*, *F. kerguelensis* and *T. antarctica* resting spores in GC29. Open water and loose pack ice are interpreted to dominate below 30 cm (i.e. prior 3.2 Ka). Above 30 cm, the increase in *F. curta* is inferred to represent and increase in sea ice.

Evidence for seasonally open water with some pack ice between the Early to mid Holocene is also implied by the abundance of the oceanic indicator species, *F. kerguelensis*. Compared to the surface shelf assemblage, *F. kerguelensis* is significantly more abundant in the open shelf assemblage, but it does not reach a comparable abundance to that observed in the modern oceanic assemblage.

Fragilariopsis kerguelensis is not an active member of sea ice assemblages (Krebs *et al.*,

1987) and it has been negatively correlated to sea ice concentration (Burckle *et al.*, 1987). The abundance of *F. kerguelensis* is greatest between 135 cm and 105 cm. These intervals formed a distinct cluster group when the core was analysed alone (Fig. 16.2), and may indicate that between 12.4 Ka and 11.0 Ka the Early Holocene experienced even less ice coverage than after this period.

Increased open water in Antarctica may be formed due to either seasonally warmer conditions, or increased wind stress (Leventer *et al.*, 1993; Cunningham and Leventer, 1998). It is not possible to say with certainty which of these scenarios the open shelf assemblage of GC29 is indicative of, but it is tentatively suggested that seasonally warmer conditions were responsible. Glacial marine records from Antarctica indicate that the mid Holocene was generally a period of increased warming (e.g. Burckle, 1972; Truesdale and Kellogg, 1979; Domack *et al.*, 1991b; Shevenell *et al.*, 1996; Kirby *et al.*, 1998; Cunningham *et al.*, in press). The diatom evidence from GC29 also implies that if the period 12.4-3.2 Ka was warmer, it underwent little fluctuation and remained relatively stable.

16.6.3 Late Holocene (<3.2 Ka)

There is a rapid fluctuation from deposition of the open shelf assemblage to the shelf assemblage, and back again, between 3.2 Ka and 2.8 Ka. Deposition of the shelf assemblage recommenced at 2.0 Ka, and has been deposited in GC29 without interruption.

The appearance of the shelf assemblage 2.8 Ka is probably a response to the onset of climatic cooling and an increase in temporal sea ice coverage. Evidence for cooling during the Late Holocene has also been recognised in other Antarctic marine sediments (Burckle 1972; Domack *et al.*, 1994; Shevenell *et al.*, 1996; Cunningham *et al.*, in press) and ice cores (Ciais *et al.*, 1994). A return to the open shelf assemblage 2.3 Ka suggests that the climate and oceanographic conditions during the transition from a warm mid Holocene to cool Late Holocene on the East Antarctic continental shelf were unstable. Alternatively, it could document a previously unrecognised, brief, warm event in East

Antarctica, similar to that suggested to be indicated by a *Corethron*-layer in GC1 from 1.9 Ka to 1.8 Ka.

Deposition of the shelf assemblage recommenced 2.0 Ka, and has been since deposited without interruption. It implies that the break up of annual sea ice commences later in the season, and that the ice edge may have remained in close proximity to the site of GC29. This is observed today, where sea ice close to the Prydz Bay coast does not regularly break out. It is speculated that there was also a possible shift in the dominant type of sea ice being formed, with both pack ice and fast ice becoming more common. Increased sea ice would account for the increase in ice-associated diatom species, relative to their abundance in the open shelf assemblage. These include *F. curta*, *P. glacialis* and *P. corona*. There has been a corresponding decrease in the abundance of *T. antarctica* resting spores.

16.7 Conclusion

A summary of the diatom assemblages and their palaeoecological interpretation is illustrated in Table 16.5. Diatom frustules are rare to absent from the base of the core to 135 cm. Here, core lithology is of compact tillite and diamicton that, combined with the lack of diatoms, is used to suggest that an ice sheet was grounded over the site. Based on reservoir corrected radiocarbon dates, ice was grounded since ~23.0 Ka, until 12.4 Ka.

At the onset of siliceous, muddy ooze deposition and open marine conditions, a diatom assemblage with no modern analogue in the surface sediment of Prydz Bay was deposited, from 12.4 Ka until 3.2 Ka. *Thalassiosira antarctica* resting spores and *F. curta* dominates the assemblage. It is interpreted to indicate that during the Late to Early Holocene, south east Prydz Bay experienced more seasonally open water and loose sea ice than today. A permanent ice edge was probably not present during summer.

Climatic and oceanographic conditions underwent rapid fluctuation between 3.2 Ka and 2.8 Ka. The open shelf assemblage was replaced by the shelf assemblage, and back again. Following 2.0 Ka, deposition of the shelf assemblage recommenced and has been deposited continuously since. The shelf assemblage today is associated with seasonally open water, and a permanent ice edge in close proximity. Deposition of this assemblage suggests that cooling commenced in East Antarctica in the Late Holocene and has been associated with an increase in both the amount of sea ice on the continental shelf and its temporal distribution.

Table 16.5 Summary of Holocene palaeoclimate in inner Prydz Bay, inferred from GC29.

| Corrected ¹⁴ C Age (Ka) | Core Lithology | Diatom Assemblage | Major Species | Climate Interpretation |
|------------------------------------|-----------------------|-------------------|---|--|
| <2.0 | Siliceous, muddy ooze | Shelf | <i>F. curta</i> <i>F. cylindrus</i> | Cool; open water in summer; permanent ice edge nearby |
| 2.0 – 2.8 | Siliceous, muddy ooze | Open Shelf | As for above | As for above |
| 2.8 – 3.2 | Siliceous, muddy ooze | Shelf | As for above | As for above |
| 3.2 – 12.4 | Siliceous, muddy ooze | Open Shelf | <i>T. antarctica</i> spores <i>F. curta</i> <i>Chaetoceros</i> spores | Warm and stable; open water in summer with loose sea ice |
| >12.4 | Diamicton and tillite | Diatoms absent | | Ice sheet grounded until end of LGM |

– Chapter 17 –

AA149

17.1 Site Description

Core AA149/28/GC28 (AA149, hereafter) was recovered from the entrance of Prydz Channel, on the Prydz Bay trough mouth fan (66° 43.69'S, 71° 46.47'E; Fig. 13.1). The site is ~16 km from the continental shelf break (delineated by the 1000 m bathymetric contour), in a water depth of 527 m. Prydz Channel is bounded by shallow banks to either side, and characterised by a large sediment fan sloping seaward from the continental shelf break. The fan, which is 148 km wide and extends 93 km off the continental shelf break, is thought to have been formed by the Lambert Glacier when it crossed the shelf, delivering subglacial debris to the shelf edge (Boulton, 1990).

The core was collected during AGSO Cruise 149 aboard the RSV *Aurora Australis*, 1995. The cruise is also known by the acronym BANGSS (Big Antarctic Geological and Seismic Survey) in Australian Antarctic Division records.

17.2 Core Description

The core is 152 cm long and can be split into five lithological units (Fig. 17.1). The sediments are derived mostly from floating ice in a low energy, marine environment, and contain a significant current-derived silt component (Anderson *et al.*, 1980). Poorly sorted, biosiliceous ooze is present in the upper 5 cm of the core, below that it grades into medium, silty sand with some pebbles. Between 61 cm and 94 cm poorly sorted, fine sand is present. There is a distinct boundary at 94 cm where very compact, clayey, medium sand replaces the silty sand. Pebbles are more common in this unit (unit 4). Below 125 cm, silty sand dominates and pebbles are absent.

17.3 Fossil Assemblages

Diatom frustules are abundant and well preserved throughout most of AA149. At 70 cm and 85 cm, and from 95 cm to 125 cm, frustules are less abundant and less well preserved. Mechanical breakage and dissolution are evident, with many frustules appearing as fragments. Synchronous with the poorly preserved assemblage is sediment consisting of compact, clayey sand. Several extinct diatoms taxa were observed in the assemblage (see Fig. 17.6), reaching maximum abundance in the compact sand layer.

Foraminifera and sponge spicules were noted throughout the core, and a small wood fragment was observed at 25 m.

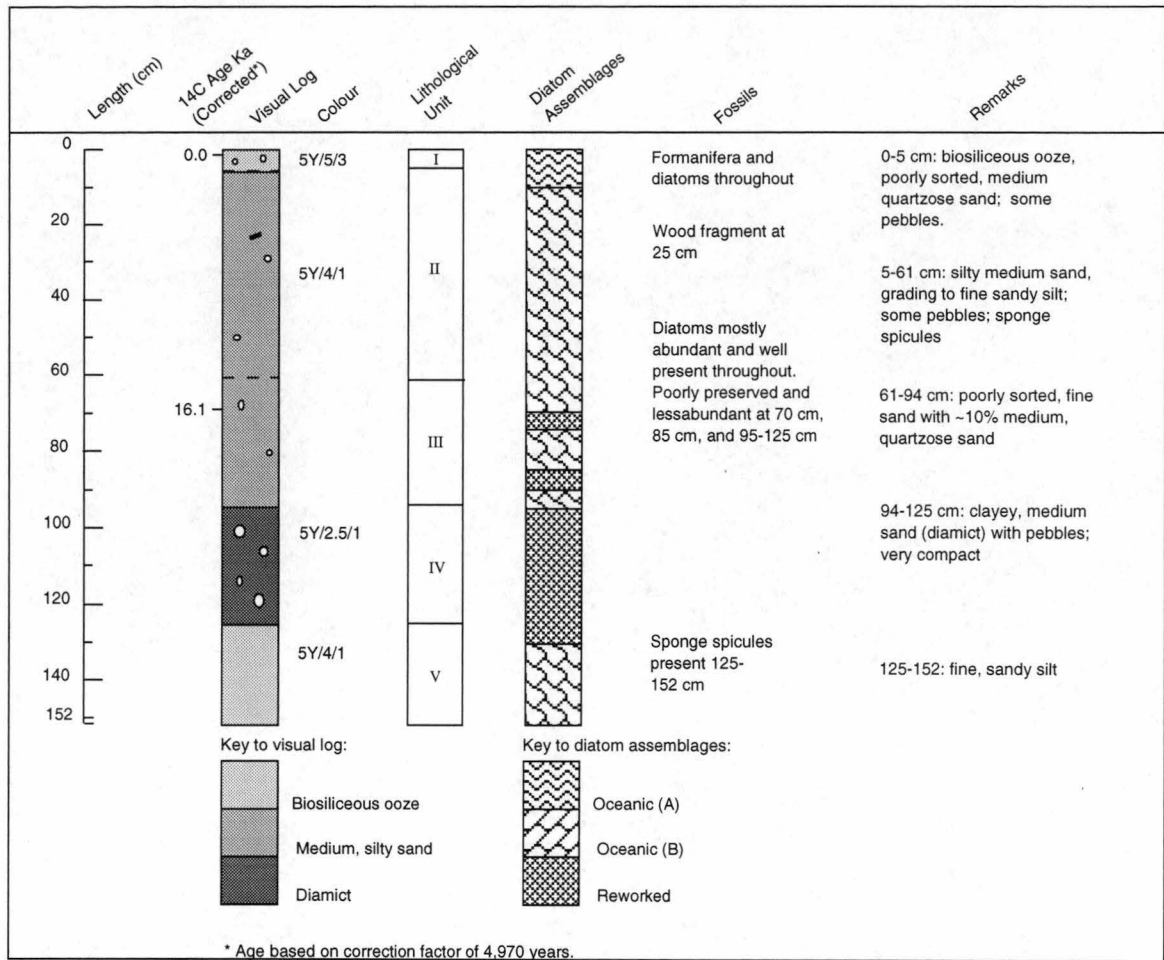


Fig. 17.1. AA149 core log, radiocarbon dates and diatom assemblages compared to surface sediment.

17.4 AA149 – Results

17.4.1 Radiocarbon Dates

Two bulk organic samples from AA149 were analysed for AMS radiocarbon dating (Table 17.1). The core has an uncorrected surface age of 4 970 (± 89) yBP, and extends into the Pleistocene with an age of 19 300 yBP, obtained from 68-69 cm. Even after applying a correction factor of 1 750 years (Domack *et al.*, 1991a), to obtain a corrected surface ^{14}C date of 3 220 yBP, the age is considerably older than the top of cores GC1 and GC2 (Mac.Robertson Shelf) and GC29 (inner Prydz Bay). It has already been demonstrated that at least 200 years of the upper sediment is missing from GC1 and GC2 (Sedwick *et al.*, in press). It is reasonable to expect that some of the surface sediment may have been also lost from AA149 during core recovery. Based on a deposition rate of 0.006 cm yr⁻¹, this would account for up to 19.2 cm missing from the core top. The “old” surface date from the core is therefore likely a combination of sediment loss, reworking, and / or input of reservoir organic material.

Table 17.1. Uncorrected and corrected AMS radiocarbon dates obtained from bulk organic carbon for core AA149. A correction factor of 1 750 radiocarbon years was applied (after Domack *et al.*, 1989).

| Interval (cm) | ^{14}C Date (yBP) | | Deposition rate (cm yr ⁻¹) † |
|------------------|-------------------------------|-----------|---|
| | Uncorrected | Corrected | |
| 0 - 2 | 4970 (± 89) | 3200 | |
| 68 - 69 | 21130 (± 230) | 19380 | 0.006 |

† Deposition rate determined between 2 - 69 cm.

Strong bottom currents and / or iceberg gouging can rework sediment and contaminate the surface with older carbon from lower intervals. In Prydz Bay, the maximum depth of iceberg gouging is 690 m (O'Brien, 1994). This is well within the range from which AA149 was recovered (572 m). Plough marks caused by this are present on the banks adjacent to the site, and in the shallower parts of Prydz Channel (O'Brien, 1994; Harris *et al.*, 1997a). Icebergs also ground on the banks, where they resuspend sediment before breaking up and drifting across the area without touching the seafloor. Iceberg gouging may have contributed to the anomalously old surface age of AA149, although this effect should have been kept to a minimum. Most icebergs ground on the shallowest parts of

the bank, then break up and drift across the deeper areas without touching the seafloor. Here gouging is limited and sediments are preserved mostly undisturbed (O'Brien, 1994).

Extinct diatom species, mostly Pliocene in age, were recorded from lower intervals in the core. Although they were not observed in the upper intervals of AA149 they may be present in rare abundance and have been overlooked during routine diatom counts. These, along with the wood fragment noted at 25 cm, could provide a source of older carbon reworked into the surface of AA149 by currents, iceberg ploughing and / or bioturbation.

A further possible explanation for the old surface age of AA149 comes from the work of Domack *et al.* (1989). They note that although reworked, organic material is present in the siliceous ooze of some cores from the East Antarctic continental shelf, its contribution to the total carbon is minimal. Instead, anomalously old surface ages can be caused by the effect that sea ice marginal zones can have on phytoplankton primary production. During winter, the production and advection of basal meltwater from beneath ice shelves should result in the retention of old CO₂ in the surface waters, as mixing distributes the meltwater beneath the ice. If an upward component to circulation is present, sea ice can effectively limit the mixing and dilution of the old CO₂ with modern (atmospheric) CO₂ within the surface layer. Thus, carbon dioxide sources for phytoplankton during the spring bloom, as sea ice recedes, could include a significant proportion of old CO₂ originating from beneath an ice shelf (Domack *et al.*, 1989).

In Prydz Bay, the release of basal meltwater from beneath the Amery Ice Shelf should certainly be considered a possible source of old carbon in the of AA149. The majority of cold (<1.6°C), saline water that emerges from beneath the ice shelf leaves Prydz Bay either directly offshore, or initially westward (Nunes Vaz and Lennon, 1996). Further sources of older carbon could be from limited mixing, and retention of old carbon upwelled from deeper water depths along the continental shelf edge.

To compensate for the anomalously old surface date obtained in AA149, it has been assumed that the old carbon has been mixed evenly through the core. A correction factor of 4970 years can therefore be subtracted to make the surface of the core equal 0 yBP. Based on this, an estimated radiocarbon age of 16 160 years can be calculated at 67-68 cm.

17.4.2 Summary of Diatom Assemblages

Diatoms are present throughout AA149. They are mostly well preserved and abundant, but at 70 cm, 85 cm and 95-125 cm the frustules are poorly preserved, have undergone more extensive mechanical breakage, and are less abundant. It was only possible to count 300 frustules from these intervals, due to their low abundance.

Members of the genus *Fragilariopsis* are dominant. *Fragilariopsis curta* is most abundant in the upper 5 cm, and is codominant with *F. kerguelensis* at most other intervals. *Fragilariopsis kerguelensis* is dominant in the samples from which only 300 frustules were counted. The high abundance of this species may indicate that mechanical breakage and preferential dissolution of less robust species, including *F. curta*, has occurred.

Several extinct taxa are noted in AA149. The species range principally in age from the Pliocene to early Pleistocene, and indicate that reworking has occurred in the core. Extinct taxa are most abundant in the samples from which only 300 frustules were counted. *Thalassiosira torokina* Brady is the most abundant species, forming up to 5.0% of the total cells counted at 120 cm. No other extinct taxa were observed at >2% abundance.

17.4.3 Statistical Analyses

AA149

A dendrogram illustrating core interval affinities is illustrated in Fig. 17.2. There are 16 species with abundance >2% are in the 31 samples (Appendix 8). Three cluster groups are identified at 23.10% dissimilarity, with a cophenetic correlation of 0.71. The SNK test could not be carried out in this instance as the analysis requires a minimum of three samples per cluster group (cluster group 1 contains only two samples). A one-way ANOVA was therefore substituted to determine the significantly abundant and indicator species for each cluster group (Table 17.2). Analyses were carried out on \log_{10} species abundance values. Values in the following discussion are based on arithmetic mean percent, unless otherwise indicated.

Cluster group 1 contains two samples: 0 cm and 5 cm. The diatom assemblage is dominated by *F. curta* (34.3%), forming up to 43.0% of the total frustules observed. *Thalassiosira antarctica* resting spores are subdominant (16.3%). Less abundant taxa, but common at >2%, are *Chaetoceros* resting spores, *F. angulata*, *F. cylindrus*, *F. kerguelensis*, *T. gracilis*, *T. lentiginosa*, and the Chrysophyte *Pentalamina corona*. Three species are identified by the one-way ANOVA as unique indicators of the

assemblage: *F. angulata*, *F. cylindrus* and *P. corona*. The assemblage can be further characterised from cluster group 2 by a significantly greater abundance of *T. gracilis*.

Cluster group 2 is the largest group in the core, occurring from 10-65 cm, 75-80 cm, 90 cm, and 130-150 cm. The diatom assemblage is codominated by the open water species *F. kerguelensis* (29.7%) and the sea ice species *F. curta* (24.5%). *Chaetoceros* resting spores are subdominant (15.1%). All have a maximum abundance 34% - 39%. Less abundant are *F. angulata* and *T. lentiginosa*. There are no unique abundance indicators characteristic of cluster group 2, although *Chaetoceros* resting spores, *F. kerguelensis* and *F. obliquecostata* are significantly greater than that observed in cluster group 1. The abundance of *F. curta* is not significantly different to group 1, but the abundance in both cluster groups is significantly greater compared to cluster group 3.

Cluster group 3 is interbedded between cluster group 2 at 70 cm and 85 cm, and between 95-125 cm. The cluster group corresponds with the sediment samples from which diatom frustules are less abundant and poorly preserved. Only 300 frustules were counted from each, but this should not have affected the analysis because counts were standardised as a percentage. It must also be assumed that as all samples were prepared in the laboratory at the same time the method should not have produced significantly different results. *Fragilariopsis kerguelensis* is the most abundant species (32.2%), forming up to 47.8%. *Chaetoceros* resting spores are subdominant (23.0%). *Fragilariopsis curta* is relatively abundant, with an average abundance of 12.0%. Less abundant are *Eucampia antarctica*, *F. separanda*, *T. antarctica* resting spores, *T. gracilis*, *T. lentiginosa*, and *T. torokina*. The one-way ANOVA identifies *E. antarctica*, *F. separanda* and *T. torokina* as indicator species. *Thalassiosira torokina* is an extinct species that has a last appearance datum in Antarctica of 1.8 Ma (Harwood and Maruyama, 1992). Although significantly abundant only in cluster group 3, *T. torokina* was also recorded in cluster group 2, where it has a maximum abundance of 0.3%.

AA149 and Surface Samples

A dendrogram illustrating core AA149 sample and surface sediment sample affinities is illustrated in Fig. 17.3. There are 26 species with an abundance > 2% from the 129 samples. Four cluster groups are identified at 33.3% dissimilarity, with a cophenetic correlation of 0.61. The SNK test was carried out to determine indicator species for each cluster group (Table 17.3).

Cluster groups 1, 2 and 3 contain all surface sediment samples identified as the coastal, shelf and cape diatom assemblages, respectively. There are no analogous samples from AA149. All are described in detail in Chapter 9, and will not be discussed further here.

Cluster group 4 contains all surface sediment samples identified as the oceanic diatom, and all samples from AA149. *Fragilariopsis curta* (25.0%) and *F. kerguelensis* (20.8%) are codominant, and *Chaetoceros* resting spores (14.7%) are subdominant. Less abundant species, but common (>2%), are *F. cylindrus*, *T. antarctica* resting spores, *T. gracilis*, and *T. lentiginosa*. The oceanic assemblage is characterised by 4 indicator species: *F. kerguelensis*, *T. lentiginosa*, *Thalassiothrix antarctica* Fryxell, and *Trichotoxin reinboldii*. The abundance of *T. antarcticus* is unique to the core as this species is not present at >2% in the surface samples. Several taxa are also significantly more abundant in the oceanic assemblage compared to at least one other cluster group. These are listed in Table 17.3. The low abundance of *F. curta* is also a notable feature of the oceanic assemblage. This species is significantly less abundant compared to all other cluster groups where it forms, on average, at least 50% of the total cells counted.

AA149 and Oceanic Assemblage

Within the oceanic and core cluster group (group 4, above), three subgroups can be recognised (Fig. 17.4). To further aid interpretation of these intervals with the surface samples, a second cluster analysis and SNK test was carried out, using only this cluster group. The three subgroups are identified at 28.0% dissimilarity, with a cophenetic correlation of 0.66. Indicator species are listed in Table 17.4.

Cluster group 1 (oceanic assemblage A, hereafter) contains the core top and 5 cm samples, and all but two surface samples identified as the oceanic diatom assemblage. The diatom assemblage is dominated by *F. curta* (29.0%), and co-subdominated by three taxa: *F. cylindrus* (13.7%), *F. kerguelensis* (12.3%) and *Chaetoceros* resting spores (12.0%). Less abundant are *F. angulata*, *T. antarctica* resting spores, *T. gracilis*, *T. lentiginosa*, and the Chrysophyte *P. corona*. Six indicator species characterise the assemblage: *F. cylindrus*, *F. lineata* (Castracane) Hasle, *P. corona*, *T. gracilis*, *T. gracilis* var. *expecta*, and *T. reinboldii*. The oceanic assemblage in the surface sediments of Prydz Bay is characterised by its abundance of open-water indicator species; however, when this assemblage is compared to the AA149 it is characterised more by ice-associated and ice-marginal species.

Cluster group 2 (oceanic assemblage *B*, hereafter) contains surface samples BANG22 and BANG24 and core samples 10-65 cm, 75-80 cm, 90 cm, and 130-150 cm. The two surface samples are amongst the most northerly samples recovered adjacent to Prydz Bay and contain the highest abundance of open water species. These samples could be conveniently described as the “most oceanic” of the “oceanic assemblage” in the surface sediment. Cluster group 2, in the present analysis, is dominated by *F. kerguelensis* (32.2%), which is significantly more abundant compared to cluster group 1. *Fragilariopsis curta* (23.8%) is subdominant. The less abundant taxa, but common at >2%, are *Chaetoceros* resting spores, *T. antarctica* resting spores, *T. gracilis*, *T. lentiginosa*, and *T. torokina*. *Thalassiosira antarctica* resting spores are indicators of the assemblage.

Cluster group 3 contains core samples 70 cm, 85 cm, 95-110 cm, and 120-125 cm. The assemblage corresponds with those from which diatoms were poorly preserved, less abundant, and having the highest abundance of extinct species. *Fragilariopsis kerguelensis* dominates (32.2%), but is not significantly different in abundance compared to cluster group 2. The assemblage is subdominated by *Chaetoceros* resting spores (23.0%). *Eucampia antarctica*, *F. curta*, *F. separanda*, *T. gracilis*, *T. lentiginosa*, and *T. torokina* are common (>2%). Three abundance indicator species identify the assemblage: *E. antarctica*, *T. torokina* and *Thalassiothrix antarctica*.

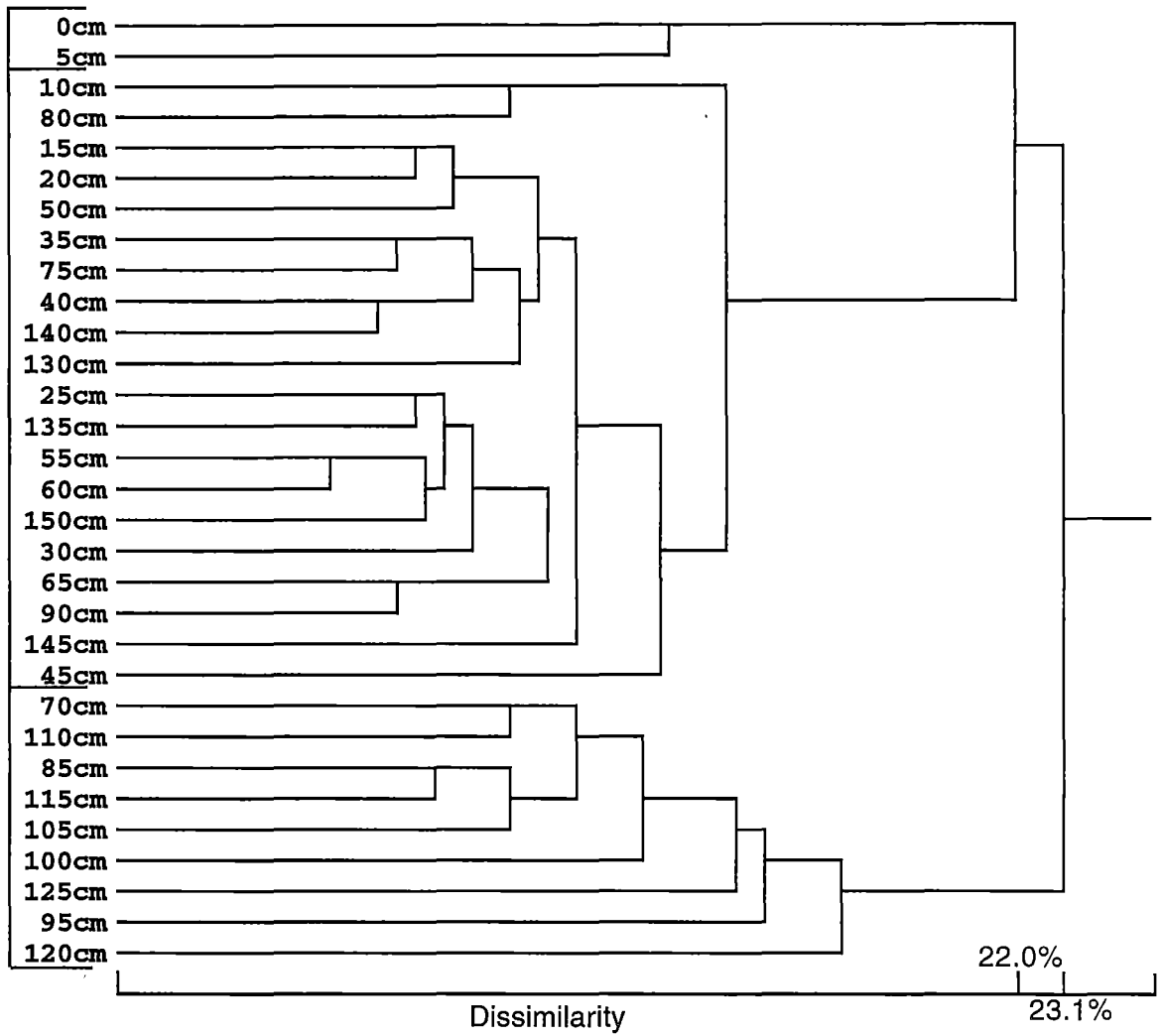


Fig. 17.2. Dendrogram of cluster analysis comparing AA149 samples. Analysis based on species abundance (>2% log₁₀).

Table 17.2. Arithmetic mean abundance (%), analysis of variance (F) and one way ANOVA of species in cluster groups from core AA149.

| Species | Cluster Group | | | F | P |
|-----------------------------|---------------|-------------|-------------|--------|-----|
| | 1 | 2 | 3 | | |
| <i>Chaetoceros</i> spores | 5.8 | <u>15.1</u> | <u>23.0</u> | 8.154 | ** |
| <i>D. antarcticus</i> | 1.3 | 1.9 | 1.4 | 1.400 | – |
| <i>E. antarctica</i> | 1.3 | 1.2 | <u>5.5</u> | 40.803 | *** |
| <i>F. angulata</i> | <u>3.6</u> | 1.6 | 1.5 | 4.417 | * |
| <i>F. curta</i> | <u>34.3</u> | <u>24.5</u> | 12.1 | 26.655 | *** |
| <i>F. cylindrus</i> | <u>9.0</u> | <u>2.1</u> | 1.5 | 9.430 | ** |
| <i>F. kerguelensis</i> | 6.9 | <u>29.7</u> | <u>32.2</u> | 49.794 | *** |
| <i>F. obliquecostata</i> | <u>1.8</u> | <u>2.0</u> | 0.2 | 35.248 | *** |
| <i>F. separanda</i> | 1.8 | 1.4 | <u>5.0</u> | 29.137 | *** |
| <i>P. corona</i> | <u>3.8</u> | 0.2 | 0.2 | 50.431 | *** |
| <i>S. microtrias</i> | 0.7 | 0.2 | <u>0.9</u> | 6.327 | ** |
| <i>T. antarctica</i> spores | <u>16.3</u> | <u>8.9</u> | 4.1 | 15.792 | *** |
| <i>T. gracilis</i> | <u>3.8</u> | 1.9 | 2.0 | 3.871 | * |
| <i>T. lentiginosa</i> | 2.3 | 2.0 | 2.4 | 0.836 | – |
| <i>T. torokina</i> | 0.0 | 0.3 | <u>2.4</u> | 36.338 | *** |
| <i>Thalassiothrix</i> | 0.5 | 0.46 | <u>1.1</u> | 5.911 | * |

Analyses were carried out on $\log_{10}(x+1)$ transformed abundance. Degrees of freedom 2, 28. ANOVA P values: * <0.05, ** <0.005, *** <0.0005, – not significant. Bold type: species with significant differences in mean abundance. Underlined type: species with significantly higher abundance in a cluster group.

Table 17.3. Arithmetic mean abundance (%), analysis of variance (F) and SNK multiple range test of species in cluster groups from AA149 and surface samples..

| Species | Cluster Group | | | | F | P |
|--|---------------|-------------|-------------|-------------|--------|-----|
| | 1 | 2 | 3 | 4 | | |
| <i>A. actinochilus</i> | 0.1 | 0.2 | <u>0.5</u> | <u>0.6</u> | 19.80 | *** |
| <i>Chaetoceros</i> spp. | <u>0.4</u> | 0.2 | 0.0 | 0.1 | 5.89 | ** |
| <i>Chaetoceros</i> spores | <u>5.3</u> | <u>8.3</u> | <u>1.5</u> | <u>14.6</u> | 41.44 | *** |
| <i>D. antarcticus</i> | 0.2 | 0.5 | <u>0.9</u> | <u>1.2</u> | 17.24 | *** |
| <i>D. speculum</i> | 0.3 | 0.5 | 0.7 | 0.7 | 3.35 | * |
| <i>E. antarctica</i> | 0.1 | 0.4 | <u>2.2</u> | <u>1.8</u> | 22.96 | *** |
| <i>F. angulata</i> | <u>4.2</u> | <u>3.8</u> | <u>5.4</u> | 1.9 | 36.54 | *** |
| <i>F. curta</i> | <u>54.7</u> | <u>47.7</u> | <u>61.3</u> | 25.0 | 57.73 | *** |
| <i>F. cylindrus</i> | <u>22.3</u> | <u>15.9</u> | 4.0 | 8.2 | 21.59 | *** |
| <i>F. kerguelensis</i> | 0.5 | 1.1 | 1.8 | <u>21.1</u> | 137.41 | *** |
| <i>F. lineata</i> | 0.7 | 0.9 | 1.2 | 0.8 | 1.61 | – |
| <i>F. obliquecostata</i> | 1.8 | <u>2.4</u> | <u>2.9</u> | 1.6 | 8.11 | *** |
| <i>F. separanda</i> | 0.2 | <u>0.8</u> | <u>1.5</u> | <u>2.1</u> | 27.46 | *** |
| <i>F. sublineata</i> | 0.4 | <u>0.8</u> | <u>0.6</u> | 0.4 | 4.25 | * |
| <i>P. corona</i> | 1.6 | <u>3.9</u> | 1.2 | 1.8 | 19.52 | *** |
| <i>P. glacilis</i> | 0.2 | <u>0.9</u> | <u>0.8</u> | 0.2 | 28.82 | *** |
| <i>P. turgiduloides</i> | <u>0.4</u> | 0.1 | 0.1 | 0.1 | 10.66 | *** |
| <i>S. microtrias</i> | 0.2 | 0.4 | <u>0.9</u> | <u>0.5</u> | 5.28 | ** |
| <i>T. antarctica</i> (spores) | 1.3 | <u>6.7</u> | <u>8.4</u> | <u>6.9</u> | 18.01 | *** |
| <i>T. antarctica</i> (veg) | 0.2 | 0.0 | 0.0 | 0.0 | 3.25 | * |
| <i>T. gracilis</i> | 0.8 | <u>1.3</u> | <u>1.9</u> | <u>3.0</u> | 27.88 | *** |
| <i>T. gracilis</i> var. <i>expecta</i> | 0.2 | <u>0.3</u> | 0.0 | <u>0.5</u> | 4.80 | ** |
| <i>T. lentiginosa</i> | 0.2 | 0.4 | 0.7 | <u>2.2</u> | 78.18 | *** |
| <i>T. torokina</i> | 0.0 | 0.0 | 0.0 | 0.4 | 3.19 | * |
| <i>Thalassiothrix</i> | 0.0 | 0.1 | 0.0 | <u>0.6</u> | 34.22 | *** |
| <i>T. reinboldii</i> | 0.1 | 0.3 | 0.1 | <u>0.6</u> | 7.73 | *** |

Analyses were carried out on $\log_{10}(x+1)$ transformed abundance. Degrees of freedom 3, 127. ANOVA P values:

* <0.05, ** <0.005, *** <0.0005, – not significant. Bold type: species with significant differences in mean abundance.

Underlined type: species with significantly higher abundance in a cluster group

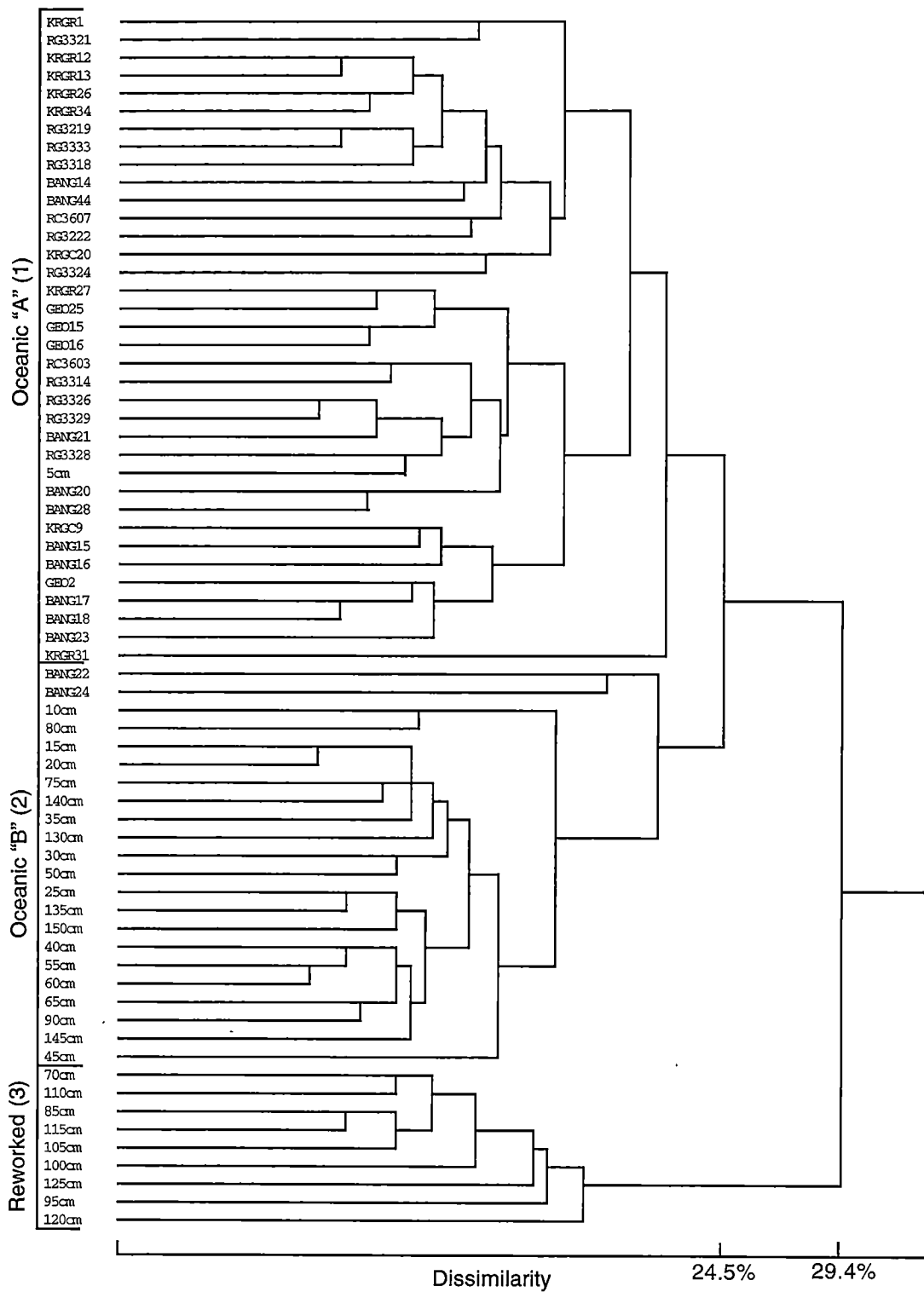


Fig. 17.4. Dendrogram of cluster analysis comparing AA149 with oceanic diatom assemblage.

Table 17.4. Arithmetic mean abundance (%), analysis of variance (F) and one way ANOVA† of species in cluster groups from AA149 and surface “oceanic” assemblage.

| Species | Cluster Group | | | F | P |
|--|---------------|-------------|-------------|-------|-----|
| | 1 | 2 | 3 | | |
| <i>A. actinochilus</i> | 0.7 | 0.5 | 0.8 | 2.77 | – |
| <i>Chaetoceros</i> spp. | 0.1 | 0.1 | 0.3 | 0.46 | – |
| <i>Chaetoceros</i> spores | 12.0 | 15.4 | <u>46.0</u> | 8.44 | ** |
| <i>D. antarcticus</i> | 0.8 | 1.9 | <u>2.7</u> | 14.48 | *** |
| <i>D. speculum</i> | <u>0.7</u> | <u>1.0</u> | <u>0.3</u> | 18.74 | *** |
| <i>E. antarctica</i> | <u>1.2</u> | 1.3 | <u>7.0</u> | 32.18 | *** |
| <i>F. angulata</i> | <u>2.2</u> | 1.5 | 2.7 | 4.82 | *** |
| <i>F. curta</i> | <u>29.4</u> | <u>23.1</u> | <u>20.2</u> | 23.63 | *** |
| <i>F. cylindrus</i> | <u>13.6</u> | 2.1 | 2.5 | 64.23 | *** |
| <i>F. kerguelensis</i> | 12.1 | <u>31.2</u> | <u>47.8</u> | 35.46 | *** |
| <i>F. lineata</i> | <u>1.1</u> | 0.5 | 1.0 | 18.67 | *** |
| <i>P. turgiduloides</i> | 0.0 | 0.1 | 0.0 | 2.14 | – |
| <i>F. obliquecostata</i> | <u>1.8</u> | <u>1.8</u> | 0.7 | 27.62 | *** |
| <i>F. separanda</i> | <u>1.7</u> | 1.4 | <u>6.0</u> | 31.57 | *** |
| <i>F. sublineata</i> | <u>0.5</u> | 0.5 | 0.3 | 3.35 | * |
| <i>P. corona</i> | <u>3.2</u> | 0.2 | <u>1.0</u> | 90.73 | *** |
| <i>P. glacialis</i> | 0.2 | 0.2 | 1.0 | 0.25 | – |
| <i>S. microtrias</i> | <u>0.6</u> | 0.2 | <u>2.0</u> | 10.06 | *** |
| <i>T. antarctica</i> (spores) | 6.7 | <u>8.4</u> | 7.3 | 6.06 | ** |
| <i>T. antarctica</i> (veg) | 0.0 | 0.0 | 0.0 | – | – |
| <i>T. gracilis</i> | <u>3.8</u> | 2.1 | <u>4.0</u> | 15.24 | *** |
| <i>T. gracilis</i> var. <i>expecta</i> | <u>0.7</u> | 0.3 | 0.3 | 12.29 | *** |
| <i>T. lentiginosa</i> | 2.2 | 2.2 | 3.7 | 0.49 | – |
| <i>T. torokina</i> | 0.0 | 0.0 | <u>5.0</u> | 88.63 | *** |
| <i>Thalassiothrix</i> | <u>0.5</u> | 0.5 | <u>2.0</u> | 6.17 | ** |
| <i>T. reinboldii</i> | <u>0.9</u> | 0.2 | 0.7 | 16.89 | *** |

Analyses were carried out on $\log_{10}(x+1)$ transformed abundance. Degrees of freedom 2, 64. ANOVA P values: * <0.05, ** <0.005, *** <0.0005, – not significant. Bold type: species with significant differences in mean abundance. Underlined type: species with significantly higher abundance in a cluster group.

17.5 Diatom Assemblages in AA149

17.5.1 Oceanic Assemblage “A”

The upper 5.0 cm of AA149 contains a diatom assemblage analogous to the oceanic assemblage in the surface sediments of Prydz Bay and Mac.Robertson Shelf. The assemblage is dominated by *F. curta* and co-subdominated by three taxa: *F. cylindrus*, *F. kerguelensis* and *Chaetoceros* resting spores. This assemblage forms a subgroup of the oceanic assemblage, as originally described when the surface sediments alone were analysed. To avoid confusion with the surface assemblage, the subgroup is referred to as the oceanic assemblage “A” .

In the surface sediment, the oceanic assemblage is distributed offshore of the continental shelf break, and in the eastern part of the bay where offshore waters are transported into Prydz Bay via a cyclonic gyre. The gyre is a major oceanographic feature of Prydz Bay and described in detail in Chapter 5. Although dominated by the sea ice species *F. curta*, the assemblage is characterised by taxa indicative of open water primary production, such as *F. kerguelensis*, *T. gracilis* var. *expecta* and *T. reinboldii*. *Fragilariopsis kerguelensis*, which forms up to 45.0% of the assemblage, is negatively correlated with sea ice concentration (Burckle *et al.*, 1987), and its abundance increases with distance from the Antarctic continental shelf in both sedimentary and planktonic diatom assemblages (Kozlova, 1966; Leventer, 1992). It is considered to be an indicator of open water, dominating summer surface waters between 52°S and 63°S where temperatures are greater than 0°C (Burckle and Cirilli, 1987; Burckle *et al.*, 1987; Krebs *et al.*, 1987). Blooms of this species have also been reported from the Derwent River, Tasmania, at 42°S (McMinn, *pers. comm.*). *Fragilariopsis cylindrus* is associated with both sub-sea ice and ice edge environments (Burckle *et al.*, 1987; Kang and Fryxell, 1992) and open water (Leventer *et al.*, 1993). *Chaetoceros* resting spores do not occur in sea ice communities, but are high in abundance at the sea ice edge (Garrison *et al.*, 1987). Leventer (1992) and Leventer *et al.* (1996) suggest that they may be associated

with stratified, low salinity and poorly mixed water columns that occur along a stationary ice edge following its maximum summer retreat.

17.5.2 Oceanic Assemblage “B”

Deposited below oceanic assemblage “A”, is an assemblage that forms as large, uninterrupted unit in the core, from 10-65 cm. It is also present at 75-80 cm and 90 cm, dispersed between an apparently extensively reworked assemblage, and as another large unit at the base of the core, below 130 cm. The assemblage is most similar to the modern oceanic assemblage samples BANG22 and BANG24. For convenience, this sub-group of the oceanic assemblage will be referred to as oceanic “B” assemblage.

Oceanic assemblage “B” is characterised by a significantly greater abundance of *F. kerguelensis*, and a significantly lower abundance of *F. curta* (Fig. 17.5). The core samples also contain a significantly greater abundance of *T. antarctica* resting spores and *F. obliquecostata*. Coupled with the abundance of open water indicator species in oceanic assemblage “B”, is the unique geographic location of the two surface samples that form part of the assemblage. Both are amongst a group of samples recovered furthest offshore from the continental shelf. BANG24, for example, is the most northerly surface sample recovered, from 66°S. This implies that the assemblage is probably less influenced by coastal oceanographic processes and more by warmer surface water, perhaps associated with the Antarctic Circumpolar Current (ACC). Summer surface water typically forms to a depth of about 30 m on the continental shelf, but can exceed 100 m north of Prydz Bay (Smith and Tréguer, 1994). Here lesser amounts of solar radiation are required to melt the sea ice, as it is not as thick as that within the shelf zone, and the temperature of the surface water layers are raised (Wong, 1994).

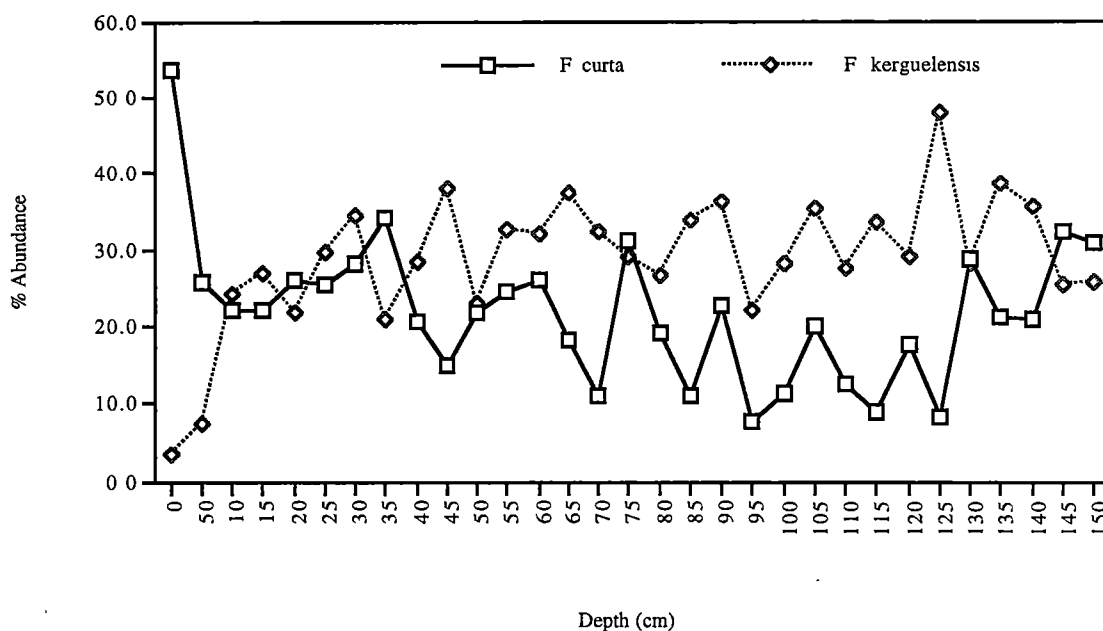


Fig. 17.5. Distribution of *F. curta* and *F. kerguelensis* in AA149. Note the change in abundance for both below 5 cm, which coincides with the transition from oceanic assemblage "A" to oceanic assemblage "B".

17.5.3 Reworked Assemblage

A large, poorly preserved and, apparently, reworked, diatom assemblage has been deposited in AA149 as small intervals dispersed between oceanic assemblage "B", at 70 cm and 85 cm. It also forms a continuous unit from 90 cm to 122 cm. *Fragilariopsis kerguelensis* and *Chaetoceros* resting spores are the dominant taxa. Also significantly abundant are heavily silicified, robust species such as *E. antarctica*, *Stellarima microtrias*, *T. gracilis*, and the extinct *T. torokina*. All have undergone extensive mechanical and chemical dissolution, and frustules are more poorly concentrated than elsewhere in the core. In this assemblage it was possible to only count 300 frustules per sample.

Evidence for reworking comes from the abundance of extinct taxa present in the assemblage (Fig. 17.6). These taxa also occur in oceanic assemblage "B", but form a minor component. None were observed to form >2% of the total cells counted. In the reworked assemblage, *T. torokina* is present with a maximum abundance of 5.0%.

Extinct taxa not included in the statistical analysis due to insignificant abundance (<2%), but notable due to their presence are: *Actinocyclus ingens*, *Nitzschia reinholdii*, *Rouxia* spp., and an unidentified *Denticula* species (*Denticula* sp. A). Also present are *Paralia* spp. Whilst this genus is not extinct today, it is not commonly found in the Antarctica marine environment. Biostratigraphic markers, based on Harwood and Maruyama (1992), indicate that the bed from which this assemblage has been reworked was deposited ~5.8 Ma to ~1.5 Ma.

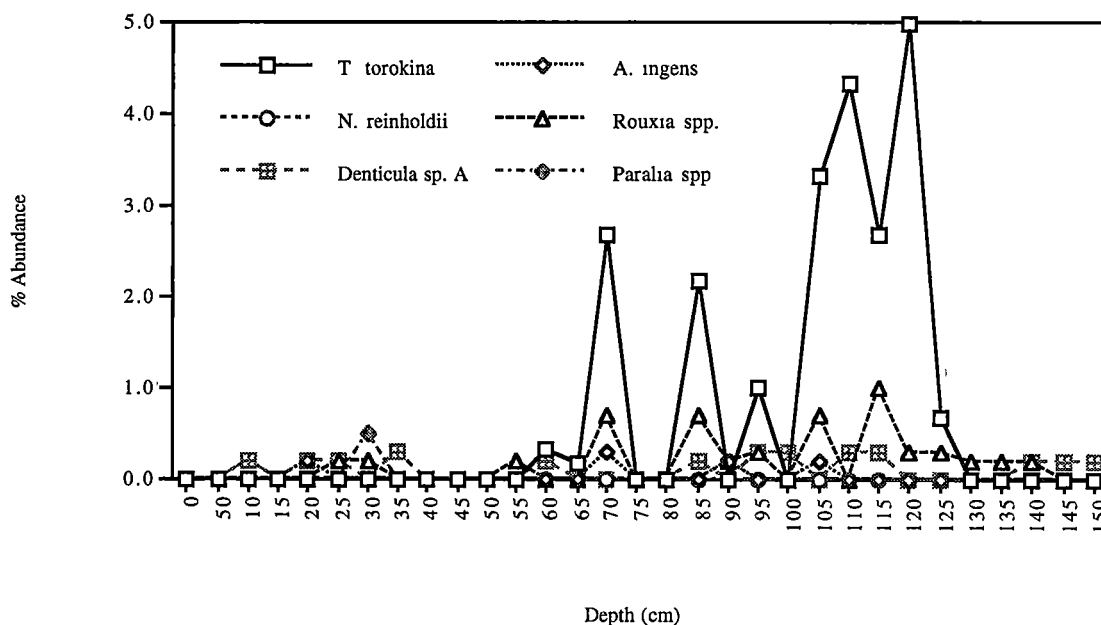


Fig. 17.6. Distribution of extinct diatom taxa in AA149. Note the abundance of *T. torokina* and *Rouxia* spp. between 70 cm and 120 cm.

17.6 Upper Pleistocene / Holocene Palaeoecology of Outer Prydz Bay

It was not possible to obtain accurate radiocarbon dates from AA149 due to contamination by old carbon contamination. To correct for the old carbon source, it will be assumed that contamination is evenly mixed throughout the core. This allows a core top age of zero to be calculated, using 4 970 years (the AMS date obtained from the core top sample) as the correction factor. At 67-69 cm the core is estimated to be ~16.0 Ka. With only two radiocarbon dates it is impossible to derive an accurate sediment

accumulation rate. A regression between the two dates at least gives some indication for the timing of events downcore. For this a constant deposition rate must be assumed. This is unlikely, however, as the diamict in unit 4 (94 cm to 122.5 cm), at least, is interpreted to have been deposited beneath a floating ice shelf and sediment transport processes and accumulation rates would differ from that in an open water setting.

17.6.1 Upper Pleistocene (>30.0 Ka?)

Using the data available, it is estimated that lithologic unit 5 (152 cm to 122.5 cm) was deposited in the Upper Pleistocene, before ~30.0 Ka. Based on the diatom assemblage, dominated by *F. kerguelensis* and being most comparable to the surface samples located furthest offshore from the shelf zone, it is assumed that more open water conditions prevailed on the edge of the continental shelf than those that exist here today.

The estimated radiocarbon dates suggest that the assemblage was deposited during a glacial interstadial that pre-dated the LGM. $\delta^{18}\text{O}$ data values from a Vostok (East Antarctic plateau) ice core also support evidence for a interstadial event to have taken place at this time, with an $\sim 2^\circ\text{C}$ rise in air temperature calculated between 58-30 Ka (Lorius *et al.*, 1985). If this is correlatable to AA149, seasonal sea ice must have been present, as indicated by the presence, but significantly lower abundance, of sea ice diatoms in AA149. The ice was probably thinner than that which exists on the shelf today, and probably broke out earlier in the season so that open water prevailed early summer. Today the region is generally free of sea ice (<10%) by January. Warmer, oceanic water associated with the different water masses and horizontal circulation, such as the Antarctic Circumpolar Current (ACC), may also have penetrated further onto the continental shelf than today.

Today the broad, deep ACC is driven by westerly winds that transport surface water eastwards, creating an eastward zonal flow. Coastal, easterly winds also create a westward flow, resulting in divergence and deep water upwelling at $\sim 65^\circ\text{S}$, where deep water comes in contact with atmosphere. In summer, this phenomenon shifts

southwards and occurs closer to Prydz Bay (Gordon, 1971). A water mass, perhaps similar to that described as Warm Deep Water (WDW) (Wong, 1994), may also have intruded further onto the continental shelf during the Upper Pleistocene. This water is often referred to as Circumpolar Deep Water (CDW) due to a similar salinities (~34.70‰), but is characterised by a cooler temperature of 0.0°C to 1.0°C and slightly higher dissolved O₂ content. In Prydz Bay, WDW has only been observed in the oceanic domain, where it occupies a depth of ~300 m, below CDW, and does not occur over the continental shelf (Wong, 1994). Intrusion of this water over the shelf break, however, could have transported the more open water, oceanic assemblage “B” onshore.

17.6.2 Upper Pleistocene (~30.0 Ka to ~22.5 Ka)

The large, reworked diatom assemblage deposited between 122.5 cm and 95 cm is estimated to have been deposited between ~30.0 Ka and ~22.5 Ka. The onset of its deposition coincides with an upward transition in the core’s lithology, from fine, sandy silt (Unit 5) to compact, clayey diamict with ice rafted debris (Unit 4). The lithology, in association with the poorly preserved diatom assemblage and abundance of reworked taxa, indicate that prior to the LGM, which commenced ~22.5 Ka, a floating ice shelf extended to the edge of the continental shelf, over what is now the Prydz Bay trough mouth fan. The low concentration of diatom frustules in the sediment also implies that primary production was reduced, probably due to reduced light levels below the ice shelf. Alternatively, if ice thickness and snow cover were insufficient for primary production to occur in the underlying water column, diatoms could have been transported and deposited under the ice shelf by water currents. At the same time, water levels may have been lower, allowing icebergs to ground, rework and resuspend sediment. Today the site of AA149 is in 527 m water depth. O’Brien *et al.* (1997) note that although most areas of Prydz Bay shallower than 690 m are covered with iceberg plough marks, some shallow areas are undisturbed. These areas are surrounded by shallower areas where icebergs ground before crossing them.

A bed of reworked diatom ooze (SMO-2), similar to that described in AA149 and containing the extinct taxa *A. ingens*, *Rouxia* spp. and *T. torokina* has also been observed in two gravity cores retrieved from the Prydz Channel. These overlie an older, similar unit (SMO-3) that is interpreted to have been deposited in an earlier period of ice sheet grounding along the periphery of Prydz Channel >33.6 Ka. SMO-2 can be traced across more than 15 000 km² of the Prydz Channel (Domack *et al.*, 1998). Radiocarbon analysis from a single piece of organic matter in one of the cores has provided an uncorrected age of 22.2 Ka, putting it within the time-frame that the reworked assemblage in AA149 is estimated to have been deposited. Domack *et al.* (1998) hypothesise that the deposition of this bed most likely occurred beneath an ice shelf that extended along the Prydz Channel, and is related to the interstadial retreat of a grounded ice, east to west across the channel, prior to the LGM. Subsequent ice readvance during the LGM removed this unit in areas landward of the grounding line. Deposition beneath an ice shelf is inferred based on the lower C/Si_{bio} ratio in the SMO-2 unit and differing diatom flora compared to the modern (SMO-1) biosiliceous ooze that is deposited today.

The reworked diatom assemblage identified in AA149, and that identified in the Prydz Channel (Domack *et al.*, 1998), are undoubtedly correlatable and originate from the same source, which Domack *et al.* (1998) suggest to be the outer reaches of Prydz Channel. The hypothesis herein, that the reworked assemblage was deposited during a glacial maximum, contrasts to that of Domack *et al.* (1998), however, who suggest that it was deposited during a glacial interstadial when grounded ice further inshore had retreated.

17.6.3 Upper Pleistocene (~22.5 Ka to ~16.5 Ka)

A relatively rapid, alternating transition between the oceanic “B” and reworked assemblages occurred between ~22.5 Ka and ~16.5 Ka. Deposition of the oceanic “B” assemblage recommenced for a period of 1000-2000 years at ~20.0 Ka and ~16.5 Ka, and could have occurred during interstadials or brief warm intervals that occurred just prior to, and during, the LGM, respectively. This interpretation is tentative until a better

radiocarbon chronology can be established. Ice sheets have been observed to suddenly recede or advance, though, during what is otherwise a glacial maximum or interglacial, as noted by Larter and Vanneste (1995). They attribute the formation of sub-glacial deltas on the Antarctic Peninsula to a late-stage readvance of grounding lines during the waning of the last ice sheet that covered the region, perhaps during the Younger Dryas (12.9-11.6 Ka).

There is a general lack of data concerning the LGM in coastal East Antarctica (Stuiver *et al.*, 1981) or West Antarctica (Hughes *et al.*, 1981). Colhoun (1991) summarises much of what is available in a review of geological evidence for changes in the East Antarctic ice sheet during the last glaciation. For the ice sheets to have expanded to the edge of the continental shelf, it is assumed that sea levels were reduced by up to 150 m (Hollin, 1962). At the same time, an increase in mass balance would be required to allow ice sheets to develop to maximum size (Colhoun, 1991). In coastal East Antarctica, reduced precipitation and an air temperature at least 5° to 6°C cooler than the present would permit sea ice extent and thickness to increase (Colhoun, 1991).

The last glacial advance in West Antarctica (Ross Sea / McMurdo Sound) is believed to have occurred after 24.0 Ka, reaching its maximum extent 21.0-17.0 Ka and retreating after 12.5 Ka (Stuiver *et al.*, 1981; Denton *et al.*, 1989). In East Antarctica, evidence for an LGM ice advance comes from striae and erratics on the volcanic cone of Gaussberg (Tingey, 1982), and shell material from the Vestfold Hills (Zhang and Peterson, 1984; Adamson and Pickard, 1986). Ice sheets on the continental shelf were estimated to have been 100-500 m thick (Hollin, 1962; Hughes *et al.*, 1981), but this was probably not the case everywhere. Where the shelf is wide, ice probably terminated against shallow banks on the outer edge; whilst large outlet glaciers (such as the Lambert Glacier) could have filled shelf depressions and conveyed ice to the edge of the shelf (Colhoun, 1991). Sedimentological evidence from Domack *et al.* (1998) suggests that during the LGM, ice advanced in Prydz Bay via drainage of the Lambert Glacier / Amery Ice Shelf, rather than by a widespread advance of the East Antarctic Ice Sheet. Ice grounded along the periphery of the Prydz Channel, but did not ground on the edge of the continental shelf.

In coastal East Antarctica, deposition of oceanic “B” assemblage deposition may have recommenced with atmospheric warming after the LGM maximum, ~16.0 Ka. This has been observed in Vostok ice core records where $\delta^{18}\text{O}$ values indicate that warming commenced ~18.0 Ka, with a gradual increase in surface temperature by ~8°C until the Holocene interglacial (Lorius *et al.*, 1985).

Based on the available data, the alternating sequences of reworked / oceanic assemblages between ~22.5 Ka and 16.0 Ka in AA149 suggest that the LGM did not create stable conditions on the edge of the continental shelf of Prydz Bay. Diatom data suggest that ice reached its maximum extent between ~22.5 Ka and 21.4 Ka and deposited a reworked diatom assemblage below a floating ice shelf. Ice retreated between ~20.0 Ka and 18.0 Ka, and then readvanced until ~16.5 Ka. Oceanic “B” assemblage was thereafter deposited without interruption on the continental shelf edge until the Late Holocene

17.6.4 Upper Pleistocene to Late Holocene (~16.5 Ka to ~2.5 Ka)

Deposition of the oceanic “B” assemblage occurred from ~16.5 Ka to ~2.5 Ka. It is interpreted to indicate that, following the advance and retreat of ice across the continental shelf during the early to mid LGM, ice retreated and did not re-advance across the bay to the shelf edge. Pebbles observed in lithologic unit 2 suggest that ice rafted debris were being deposited, most likely from icebergs calving from the terminus a nearby ice shelf. There is no evidence in the diatom record indicating the end of the LGM, which is placed at ~10.0 Ka .

17.6.5 Late Holocene to Present (< ~2.5 Ka)

Deposition of the oceanic “A” assemblage commenced ~2.5 Ka and has continued to the present. During this periods there has been a synchronous decrease in the abundance of the open water indicator *F. kerguelensis* and an increase in the sea ice indicator *F. curta*. The transition from the oceanic “B” assemblage to “A” is consistent with

having been deposited in conjunction with Late Holocene cooling. This correlates with the general cooling trend observed elsewhere in the Antarctic marine record between the mid- to Late Holocene (e.g. Burckle, 1972; Domack *et al.*, 1991a; Leventer *et al.*, 1993; Shevenell *et al.*, 1996; Cunningham *et al.*, in press), and with the GISP 2 (Greenland) ice core (O'Brien *et al.*, 1995b). Diatom evidence from cores GC1, GC2 and GC29 also indicate that a marked cooling event has taken place on the East Antarctic margin during the Late Holocene.

17.7 Conclusion

Contamination by old carbon and sediment reworking do not allow an accurate radiocarbon chronology to be determined from AA149. A correction factor of ~5 000 years (based on the AMS date obtained from a sample from 0-2 cm) has been applied to the core, however, assuming that contamination is evenly mixed throughout.

A summary of the palaeoecological interpretation of AA149 is listed in Table 17.5. The base of the core is estimated to be >30.0 Ka. It is characterised by a diatom assemblage most similar to that in the surface samples analysed and deposited furthest offshore of the continental shelf today. Here, open water oceanographic processes are more likely to affect the planktonic diatom assemblage, rather than coastal processes in the shelf zone. These include warmer ocean currents and thinner sea ice that fully breaks out earlier in the summer.

A reworked assemblage with no modern analogue has been deposited in the core ~30.0-~25.0 Ka. Diatom frustules have undergone extensive mechanical and chemical dissolution and are more poorly concentrated than in the over- and under-lying sediment. Combined with the lithology of the core, the assemblage is interpreted to have been deposited during a glacial maximum that preceded the LGM. A floating ice shelf probably expanded over the trough mouth fan, as an extension of the Lambert Glacier, to the edge of the continental shelf. Similar assemblages occur ~21.0 Ka, interpreted to record the onset of the LGM, and ~16.5 Ka.

The reworked assemblage is interrupted by deposition of oceanic “B” assemblage as short-lived (1000 years to 2000 years) events 25.0 Ka and ~18.0 Ka. The open water conditions that occurred during its deposition are most likely interstadials that occurred prior to, and during the LGM. Oceanic “B” assemblage is thereafter deposited without interruption in AA149 until ~2.5 Ka. There is no further evidence in this core for the

Early to mid-Holocene climatic events that have been recorded in other cores analysed herein.

Assuming the estimated radiocarbon dates are correct, deposition analogous to that on the Prydz Bay trough mouth fan today commenced ~2.5 Ka. The assemblage probably reflects the mid- to Late Holocene cooling that has been recorded elsewhere from Antarctic marine sediments. In the modern environment, the oceanic assemblage is characterised by open water indicator species and characterises areas of Prydz Bay where open water is present during the summer months.

Table 17.5. Summary of Holocene palaeoclimate on outer Prydz Bay, as inferred from AA149.

| Corrected radiocarbon years (Ka) | Lithology | Diatom Assemblage | Major Species | Climate Interpretation |
|----------------------------------|---|--|--|---|
| <2.5 | Biosiliceous ooze | Oceanic "A" | <i>F. curta</i> <i>F. cylindrus</i> <i>Chaetoceros</i> spores <i>F. kerguelensis</i> | Modern conditions |
| 2.5 – 16.5 | Medium, silty sand | Oceanic "B" | <i>F. kerguelensis</i> <i>F. curta</i> <i>Chaetoceros</i> spores | Late Holocene cooling; decrease in <i>F. kerguelensis</i> |
| 16.5 – 22.5 | Alternating between clayey diamict and sandy silt | Alternating between Oceanic "B" and Reworked | As for above | Retreat of ice shelf prior to LGM, followed by advance during the LGM, and subsequent retreat. Ice maxima 22.5-21.4 Ka and 18.0-16.5 Ka |
| 22.5 – 30.0 | Clayey diamict with IRD | Reworked | As for above | Ice shelf grounded and / or current reworking |
| >30.0 | Fine, sandy silt | Oceanic "B" | <i>F. kerguelensis</i> <i>F. curta</i> <i>Chaetoceros</i> spores <i>T. antarctica</i> | Interstadial; warmer (>2° C?) |

– Chapter 18 –

AA186

18.1 Site Description

Core AA186/28/GC28 (AA186, hereafter) was recovered from Four Ladies Bank, Prydz Bay (67° 16.05' S, 76° 23.92' E; Fig. 13.1), during AGSO Cruise 186 aboard the RSV *Aurora Australis*, 1997. Four Ladies Bank borders to the north east of the Amery Depression, and is a shallow bank rising to a minimum depth of ~200 m. Parts of the bank are so shallow that icebergs ground before crossing, then break up and calve to drift across the deeper depressions without touching the seafloor. In areas where iceberg gouging is limited, relatively undisturbed bank sediments have been deposited since ice retreated from the shelf edge (O'Brien *et al.*, 1997). AA186 was recovered from a water depth of 338 m, which bathymetric surveys indicate to be a depression on Four Ladies Bank. The site was chosen as an area on the bank where the likelihood of iceberg grounding and sediment reworking would be minimal.

18.2 Core Description

The core is 186 cm long (Fig. 18.1) and can be divided into two stratigraphic units. Unit 1 (0-80 cm) consists of homogenised, siliceous, muddy diamicton. The upper 2 cm is moderate, olive brown (5Y 4/4) in colour, grading to dark, greenish grey (5GY 4/1). One small, greyish olive (10Y 4/2) dropstone is present at 30 cm. A transitional boundary is present at 80 cm, over which the diamicton becomes sandier. The boundary is characterised by distinct sediment clasts of darker, greyish olive (10Y 4/2), diamicton matrix. At 100 cm a distinct boundary is present, and the muddy diamicton is replaced by compact, sandy diamicton (unit 2). The colour is a homogenous to dark, greenish grey (5GY 4/1).

18.3 Fossil Assemblages

Diatom frustules are present in quantifiable abundance from 0 cm to 175 cm. The assemblage is dominated by taxa indicative of Holocene deposition, with members of the genus *Fragilariopsis* most abundant. Several extinct taxa were also noted throughout all core intervals (see Table 18.4 and Fig. 18.5).

Foraminifera fragments and broken bryozoans are present between 0 cm and 80 cm. At 86 cm, a narrow, but distinct, layer of foraminifera fragments is present. Below 100 cm, the fragments and sponge spicules are abundant in the sandy diamicton.

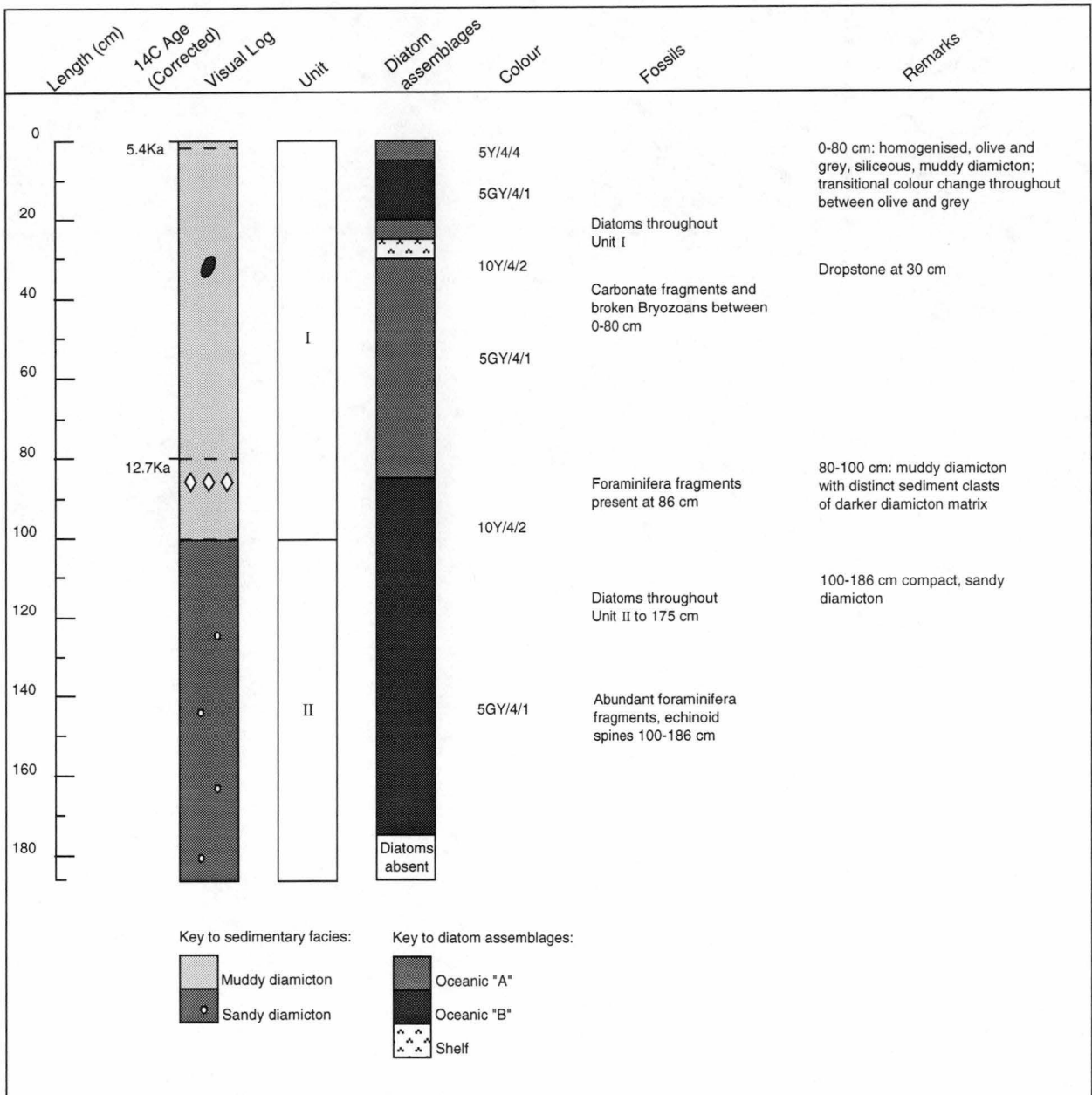


Fig. 18.1. AA186 core log, radiocarbon dates and diatom assemblages compared to surface sediment.

18.4 AA186 – Results

18.4.1 Radiocarbon Dates

Two AMS radiocarbon dates, based on bulk organic carbon, were obtained from AA186 (Table 18.1). The core has an uncorrected surface age of 7 175 (± 70)yBP. Even after applying an ocean reservoir-correction factor of 1800 radiocarbon years (after Domack *et al.*, 1989), to obtain a corrected surface ^{14}C date of 5 425 yBP, this is considerably older than other cores discussed herein (e.g. GC1, GC2 and GC29, which range from 900 yBP to 2 600 yBP). At 80-82 cm, a reservoir-corrected age of 12 702 yBP was obtained. At this interval the sediment grades from homogenised, siliceous, muddy diamicton to muddy diamicton. Although this date is tentative (discussed below), it does correlate approximately with the onset of open-marine conditions in Prydz Bay. A reservoir-corrected age from nearby ODP Site 740 suggests that open marine deposition commenced here $\sim 10\,700$ yBP (Domack *et al.*, 1991a).

*Table 18.1. Uncorrected and corrected AMS radiocarbon dates obtained from bulk organic carbon for core AA186. A correction factor of 1 750 radiocarbon years was applied (after Domack *et al.*, 1989).*

| Interval (cm) | ^{14}C Date (yBP) | | Deposition rate (cm yr $^{-1}$)† |
|------------------|----------------------------|-----------|--------------------------------------|
| | Uncorrected | Corrected | |
| 0.0 - 2.0 | 7175 \pm 70 | 5425 | |
| 80.0 - 82.0 | 14 452 \pm 89 | 12 702 | 0.01 |

† Deposition rates determined between 2-82 cm.

Several factors could account for, or contribute to, the anomalously old radiocarbon age at the surface of AA186. They are discussed in Chapter 17, where anomalously older ages were also observed in AA149. Based on the sedimentation rate of AA149, up to 54.25 cm may have been lost from the top of the core during the recovery process. Compared to the relatively “soupy” consistency of the biosiliceous ooze present in the Mac.Robertson Shelf cores (GC1 and GC2), from which only the upper 200 years of

sediment was lost, the sediment in AA186 is much more compact. There was also no evidence upon recovery of the core to indicate that large portions of the sediment had been lost. Reworking and / or input of reservoir organic carbon material are therefore the most likely factors for the old age.

To compensate for the anomolous ^{14}C ages in AA149, a correction factor of 7 175 yBP has been applied, based on the date obtained from the core top. This assumes that mixing throughout the core has evenly distributed old carbon. The surface of AA186 is therefore recalculated to be 0 Ka, and ~7 000 yBP at 80-82 cm. A similar method was used to compensate for the anomolously old radiocarbon age obtained from the core top of AA149.

18.4.2 Diatom Assemblages

Diatoms are abundant and generally well preserved, except for normal mechanical damage, to a depth of 175 cm. The assemblage is comprised typically of Holocene taxa, with members of the genus *Fragilariopsis* most abundant. *Fragilariopsis curta*, *F. kerguelensis* and *T. antarctica* resting spores dominate.

Extinct taxa are present at all core intervals and are indicative of sediment reworking. They are most abundant below 85 cm, where there is a transitional sediment boundary that changes from biosiliceous, muddy diamicton to sandy diamicton. *Thalassiosira torokina* is the most abundant, reworked species, forming up to 7.7% of the total frustules observed at 130 cm. Other extinct taxa are not present at >2.0%.

18.4.3 Statistical analyses

AA186

A dendrogram illustrating core sample affinities is illustrated in Fig. 18.2. Eighteen species with an abundance >2% are observed in 31 samples (Appendix 9). Sample 160 cm is identified as an outlier in the preliminary cluster analysis (Appendix 10) and was removed from further analysis. Subsequent analysis identified three cluster groups at 26.9% dissimilarity, with a cophenetic correlation of 0.67. Indicator species, based on

\log_{10} values, in each cluster group are listed in Table 18.2. All values in the following discussion are based on arithmetic mean abundance, unless otherwise stated.

Cluster group 1 is the largest cluster group identified, containing 14 samples. It occurs at 0 cm, and from 20-80 cm. The diatom assemblage is dominated by *F. curta* (41.4%), which forms >50% of the total number of frustules observed at 30 cm. *Thalassiosira antarctica* resting spores are subdominant (10.9%). The less abundant taxa, but common (>2%), are *Chaetoceros* resting spores, *E. antarctica*, *F. angulata*, *F. cylindrus*, *F. kerguelensis*, *F. obliquecostata*, *T. gracilis*, and the Chrysophyte *P. corona*. No indicator species are present. The diatom assemblage in cluster group 1 can be distinguished from cluster groups 2 and 3, however, by a significantly greater abundance of several taxa the are outlined in Table 17.2.

Cluster group 2 is present from 5-15 cm, 85-90 cm, 100 cm, 145 cm, and 170-175 cm; it is the smallest cluster group in the core. *Thalassiosira antarctica* resting spores are the most abundant taxa (25.7%); *F. curta* (20.7%) and *F. kerguelensis* (18.1%) are subdominate. Also common (>2%) are *Chaetoceros* resting spores, *E. antarctica*, *F. cylindrus*, *F. obliquecostata*, *T. gracilis*, and *T. lentiginosa*. The assemblage is most similar to that observed in cluster group 1, but *T. antarctica* resting spores are unique indicators. The abundance of *E. antarctica* and *F. kerguelensis* is also significantly greater in cluster group 2 compared to cluster group 1.

Cluster group 3 contains samples 95 cm, 105 cm, 115 cm, 120-140 cm, and 150-165 cm. The diatom assemblage is dominated by *F. kerguelensis* (28.0%) in significantly greater abundance compared to that observed in cluster groups 1 and 2. *Eucampia antarctica* (17.4%) and *T. antarctica* resting spores (12.7%) are subdominants. Less abundant are *Chaetoceros* resting spores, *F. curta*, *F. separanda*, *T. gracilis*, *T. lentiginosa*, and the extinct species *T. torokina*. The latter, in association with *T. lentiginosa* and *Stellarima microtrias*, is a unique indicator of the cluster group 3.

AA186 and Surface Samples

A dendrogram illustrating AA186 and surface sample affinities is illustrated in Fig. 18.3. Outliers in the core and surface samples, identified previously, are not included. Twenty-six diatom species with an abundance >2% are observed in the 136 samples. Five cluster groups are identified at 37.60% dissimilarity, with a cophenetic correlation of 0.66. Significantly abundant and indicator species for each cluster group are listed in Table 18.3.

Cluster groups 1, 2 and 4 contain all surface sediment samples identified as the coastal, shelf and cape diatom assemblages, respectively. The shelf assemblage contains one sample from AA186: 25 cm. There are no other samples from AA186 containing analogous assemblages and they will not be further discussed here.

Cluster group 3 contains all but two surface samples identified as the oceanic assemblage, and AA186 samples 0 cm, 20 cm, 30-80 cm. In this chapter, the assemblage shall be referred to as the oceanic "A" assemblage, to avoid confusion. *Fragilariopsis curta* (32.7%) dominates the assemblage, but is statistically less abundant compared to that in cluster groups 1, 2 and 4. Three taxa are subdominant: *F. kerguelensis* (11.5%), *F. cylindrus* (11.4%) and *Chaetoceros* resting spores (10.0%). Abundant (>2%) are *F. angulata*, *F. obliquecostata*, *T. antarctica* resting spores, *T. gracilis*, *T. lentiginosa*, and *P. corona*. Although many of these species are most abundant in the oceanic assemblage, and significantly more abundant compared to one or more cluster groups (see Table 17.3), only two, numerically rare, diatoms were identified as unique indicators: *T. gracilis* var. *expecta* and *Trichotoxin reinboldii*. Neither is present at >3.0%, and both have a mean abundance <1.0%.

Cluster group 5 contains surface samples BANG22 and BANG24, and AA186 samples 5- 15 cm and 85-175 cm. As discussed in the previous chapter, BANG22 and BANG24 are amongst the group of surface samples recovered from furthest offshore of the continental shelf. In AA186 (and AA149) this, apparently, more open water assemblage

is referred to as the oceanic “B” assemblage, to avoid confusion with the oceanic “A” assemblage, and that originally described in the surface sediment. In the present analysis, *F. kerguelensis* dominates the “B” assemblage (23.3%) and is significantly more abundant compared to that in “A” assemblage (cluster group 3, above). The subdominant taxa are *T. antarctica* resting spores (18.9%), *F. curta* (14.6%) and *E. antarctica* (12.4%). Less abundant taxa are *Chaetoceros* resting spores, *F. obliquecostata*, *F. separanda*, *T. gracilis*, *T. lentiginosa*, and the extinct *T. torokina*. *Thalassiosira torokina* has a first appearance datum in Antarctic marine sediment 8.2-8.6 Ma, and a last appearance datum of 1.8 Ma (Harwood and Maruyama, 1992).

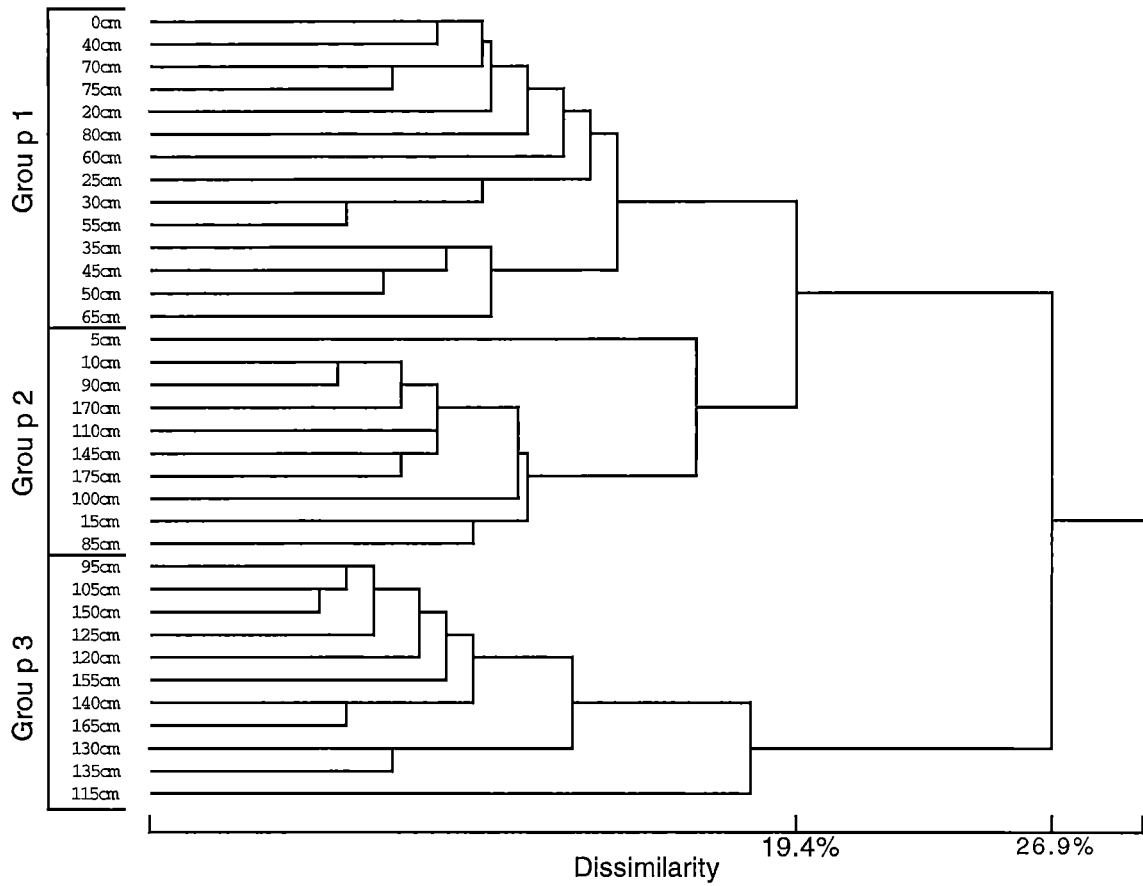


Fig. 18.2. Dendrogram of cluster analysis comparing AA186 samples. Analysis based on species abundance (>2% log10).

Table 18.2. Arithmetic mean abundance (%), analysis of variance (F) and SNK multiple range test of species in cluster groups of AA186.

| Species | Cluster Group | | | F | P |
|------------------------------------|---------------|-------------|-------------|--------|------|
| | 1 | 2 | 3 | | |
| <i>Chaetoceros</i> spores | 3.9 | 5.8 | 7.7 | 2.04 | n.s. |
| <i>C. criophilum</i> | 0.1 | 0.1 | 1.0 | 0.52 | n.s. |
| <i>D. antarcticus</i> | 1.2 | 1.2 | 1.2 | 0.02 | n.s. |
| <i>D. speculum</i> | 1.9 | 1.8 | 1.1 | 3.21 | n.s. |
| <i>E. antarctica</i> | <u>2.4</u> | <u>6.9</u> | <u>17.4</u> | 111.19 | n.s. |
| <i>F. angulata</i> | <u>3.3</u> | <u>1.1</u> | <u>0.6</u> | 61.69 | *** |
| <i>F. curta</i> | <u>41.4</u> | <u>20.7</u> | <u>9.0</u> | 130.88 | *** |
| <i>F. cylindrus</i> | <u>6.5</u> | <u>2.3</u> | <u>0.5</u> | 64.53 | *** |
| <i>F. kerguelensis</i> | <u>7.9</u> | <u>18.1</u> | <u>28.0</u> | 72.25 | *** |
| <i>F. lineata</i> | <u>1.3</u> | <u>0.6</u> | <u>0.2</u> | 24.65 | *** |
| <i>F. obliquecostata</i> | <u>5.4</u> | <u>2.9</u> | <u>1.3</u> | 53.58 | *** |
| <i>F. separanda</i> | 1.9 | 1.7 | 2.5 | 1.99 | n.s. |
| <i>P. corona</i> | <u>2.3</u> | <u>1.3</u> | <u>0.1</u> | 29.38 | *** |
| <i>S. microtrias</i> | 0.6 | 0.8 | <u>1.5</u> | 8.81 | *** |
| <i>T. antarctica</i> spores | 10.9 | <u>25.7</u> | 12.7 | 27.81 | *** |
| <i>T. gracilis</i> | 2.6 | 2.0 | 2.1 | 1.72 | n.s. |
| <i>T. lentiginosa</i> | 1.6 | <u>2.1</u> | <u>4.1</u> | 20.21 | *** |
| <i>T. torokina</i> | <u>0.2</u> | <u>1.3</u> | <u>4.3</u> | 81.45 | *** |

Analyses were carried out on $\log_{10}(x+1)$ transformed abundance. Degrees of freedom 2, 32. ANOVA P values: * <0.05, ** <0.005, *** <0.0005, – not significant. Bold type: species with significant differences in mean abundance. Underlined type: species with significantly different abundance in a cluster group.

Table 18.3. Arithmetic mean abundance (%), analysis of variance (F) and SNK multiple range test of species in cluster groups of AA186 and surface sediment samples.

| Species | Cluster Group | | | | | F | P |
|-----------------------------|---------------|-------------|-------------|-------------|-------------|--------|-----|
| | 1 | 2 | 3 | 4 | 5 | | |
| <i>A. actinochilus</i> | 0.1 | 0.2 | <u>0.7</u> | <u>0.5</u> | <u>0.7</u> | 24.83 | *** |
| <i>Chaetoceros</i> spp. | <u>0.4</u> | <u>0.2</u> | 0.1 | 0.0 | 0.0 | 5.72 | *** |
| <i>Chaetoceros</i> spores | <u>5.3</u> | <u>8.0</u> | <u>10.0</u> | 1.1 | <u>6.8</u> | 11.62 | *** |
| <i>C. criophilum</i> | 0.1 | 0.1 | 0.1 | 0.0 | 0.6 | 0.64 | – |
| <i>D. antarcticus</i> | 0.2 | 0.4 | <u>0.9</u> | <u>0.9</u> | <u>1.2</u> | 18.50 | *** |
| <i>D. speculum</i> | 0.3 | 0.5 | <u>1.1</u> | 0.6 | 1.4 | 12.38 | *** |
| <i>E. antarctica</i> | 0.1 | 0.4 | <u>1.5</u> | <u>2.3</u> | <u>12.4</u> | 87.03 | *** |
| <i>F. angulata</i> | <u>4.2</u> | <u>3.9</u> | <u>2.5</u> | <u>5.6</u> | 0.8 | 50.15 | *** |
| <i>F. curta</i> | <u>54.7</u> | <u>48.3</u> | <u>32.7</u> | <u>62.8</u> | 14.6 | 84.83 | *** |
| <i>F. cylindrus</i> | <u>22.3</u> | <u>16.1</u> | <u>11.5</u> | 2.6 | 1.3 | 68.12 | *** |
| <i>F. kerguelensis</i> | 0.5 | 1.0 | <u>10.9</u> | 2.0 | <u>23.3</u> | 153.54 | *** |
| <i>F. lineata</i> | <u>0.7</u> | <u>0.9</u> | <u>1.2</u> | <u>1.1</u> | 0.4 | 11.72 | *** |
| <i>F. obliquecostata</i> | 1.8 | 2.5 | 2.8 | 2.7 | 2.0 | 2.38 | – |
| <i>F. separanda</i> | 0.2 | <u>0.7</u> | <u>1.8</u> | <u>1.7</u> | <u>2.1</u> | 37.55 | *** |
| <i>F. sublineata</i> | <u>0.4</u> | <u>0.7</u> | <u>0.5</u> | <u>0.6</u> | 0.0 | 10.99 | *** |
| <i>P. corona</i> | <u>1.6</u> | <u>3.9</u> | <u>2.9</u> | 1.1 | 0.7 | 36.92 | *** |
| <i>P. glacialis</i> | 0.2 | <u>0.9</u> | 0.2 | 0.6 | 0.5 | 18.94 | *** |
| <i>P. turgiduloides</i> | <u>0.4</u> | 0.1 | 0.1 | 0.1 | 0.0 | 8.48 | *** |
| <i>S. microtrias</i> | 0.2 | 0.3 | <u>0.6</u> | <u>0.9</u> | <u>1.2</u> | 13.03 | *** |
| <i>T. antarctica</i> spores | 1.3 | <u>6.5</u> | <u>7.8</u> | <u>8.5</u> | <u>18.9</u> | 29.17 | *** |
| <i>T. antarctica</i> (veg) | <u>0.2</u> | 0.0 | 0.0 | 0.0 | 0.0 | 2.53 | * |
| <i>T. gracilis</i> | 0.8 | 1.3 | <u>3.4</u> | <u>2.1</u> | <u>2.1</u> | 31.50 | *** |
| <i>T. gracilis</i> var. | 0.2 | 0.2 | <u>0.6</u> | 0.0 | 0.1 | 12.51 | *** |
| <i>T. lentiginosa</i> | 0.2 | 0.4 | <u>2.0</u> | 0.8 | <u>3.2</u> | 65.22 | *** |
| <i>T. torokina</i> | 0.0 | 0.0 | 0.1 | 0.0 | <u>2.9</u> | 83.33 | *** |
| <i>T. reinboldii</i> | 0.1 | 0.3 | <u>0.8</u> | 0.2 | 0.2 | 13.90 | *** |

Analyses were carried out on $\log_{10}(x+1)$ transformed abundance. Degrees of freedom 4, 131. ANOVA P values: * <0.05, ** <0.005, *** <0.0005, – not significant. Bold type: species with significant differences in mean abundance. Underlined type: species with significantly different abundance in a cluster group. Cluster group (diatom assemblage) names: 1 = Coastal; 2 = Shelf; 3 = Oceanic “A”; 4 = Cape; 5 = Oceanic “B”.

18.5 Diatom Assemblages in AA186

18.5.1 Oceanic Assemblage “A”

The upper 80 cm of AA186 is dominated by a diatom assemblage that is analogous to the oceanic assemblage in the surface sediments of Prydz Bay and Mac.Robertson Shelf. Two surface samples that were included in this assemblage, as originally described in Chapter 9, however, form a subgroup when compared to AA149. To avoid confusion, they will be discussed below as oceanic assemblage “B”, and the larger assemblage, discussed here, will be referred to as oceanic assemblage “A”.

In Prydz Bay today, oceanic assemblage “A” is located primarily offshore of the continental shelf break, but extends as a “tongue” southwards into the bay, across Four Ladies Bank. Although dominated by the sea ice diatom *F. curta*, the assemblage is characterised by an abundance of open water taxa. These include *F. kerguelensis*, *F. cylindrus* and *Chaetoceros* resting spores. Less abundant, but statistically significant, are *T. gracilis* var. *expect* and *Trichotoxin reinboldii*. It is speculated that assemblage has been transported onshore via the cyclonic Prydz Bay gyre.

Fragilariopsis kerguelensis is a major indicator of open water. It is negatively correlated with sea ice concentration (Burckle *et al.*, 1987), increases in abundance with distance from the Antarctic continental shelf in both sedimentary and planktonic diatom assemblages (Kozlova, 1966; Leventer, 1992), and dominates summer surface waters (Burckle and Cirilli, 1987; Burckle *et al.*, 1987; Krebs *et al.*, 1987). Similarly, *F. cylindrus* is associated with open water conditions, but may also occur in both sub-sea ice and ice edge environments (Burckle *et al.*, 1987; Kang and Fryxell, 1992; Leventer *et al.*, 1993). *Chaetoceros* resting spores do not occur in sea ice communities but are higher in abundance at the sea ice edge (Garrison *et al.*, 1987). Leventer (1992) and Leventer *et al.* (1996) suggest that the resting spores may be associated with stratified, low salinity and poorly mixed water columns that occur along a stationary ice edge following its maximum summer retreat.

18.5.2 Oceanic Assemblage “B”

Oceanic assemblage “B” consists of core samples most similar to the surface samples BANG22 and BANG24. In the analysis of the surface samples alone, both formed part of the oceanic assemblage. When compared to the core, however, they form a subgroup, which is based on the high abundance of *F. kerguelensis*. The abundance of

F. kerguelensis, and other open water indicator taxa in BANG22 and BANG24 is attributed to their geographic location. This was discussed in detail in Chapter 17, where both samples also formed part of an oceanic assemblage “B” when compared to AA149. In summary, they were recovered furthest offshore from the continental shelf, and probably less influenced by coastal oceanographic processes.

In AA186, oceanic assemblage “B” has been deposited from 5-15 cm, and as a continuous sequence in the lower half of the core, below 85 cm. It is characterised by a significantly higher abundance of *F. kerguelensis*, and a significantly lower abundance of *F. curta* (Fig. 18.4). Simple linear regression indicates that they have a negative correlation ($R^2 = 0.786$). Below 95 cm, the abundance of *F. kerguelensis* is greater than *F. curta*. In the surface samples, this was observed only in BANG22 and BANG24 and further suggests that deposition has occurred under a more open water regime.

An important component of the oceanic assemblage “B” is the presence of reworked, extinct taxa (Table 18.4, Fig. 18.5). Most are present in rare abundance (<2%), but *T. torokina* has a maximum abundance of 7.7% at 135 cm, and, in AA186, has a positive correlation with *F. kerguelensis* ($R^2 = 0.679$). A similar diversity of extinct taxa were noted in the reworked assemblage described in AA149, and both may be correlatable with the SMO-2 and SMO-3 beds described by Domack *et al.* (1998). The reworked assemblage in AA149, however, formed a cluster group distinct from the oceanic assemblage “B” described in that core. Based on the biostratigraphic marker *T. complicata*, the bed from which the assemblage in AA186 has been reworked was deposited 4.3 Ma to 3.1 Ma (Harwood and Maruyama, 1992).

Table 18.4. Extinct diatom taxa identified in AA186. Datums based on Harwood and Maruyama (1992). FAD: first appearance datum; LAD: last appearance datum.

| Species | FAD (My) | LAD (My) |
|---------------------------------|----------|----------|
| <i>Denticula</i> sp. A | ? | ? |
| <i>Hemidiscus ovalis</i> | 7.9 | 5.7 |
| <i>Nitzschia praecurta</i> | 10.5 | 3.6 |
| <i>Rouxia</i> spp. | ~20.0 | ~1.5 |
| <i>Thalassiosira complicata</i> | 4.3 | 3.1 |
| <i>T. inura</i> | 4.5-4.8 | 1.8 |
| <i>T. torokina</i> | 8.2-8.6 | 1.8 |

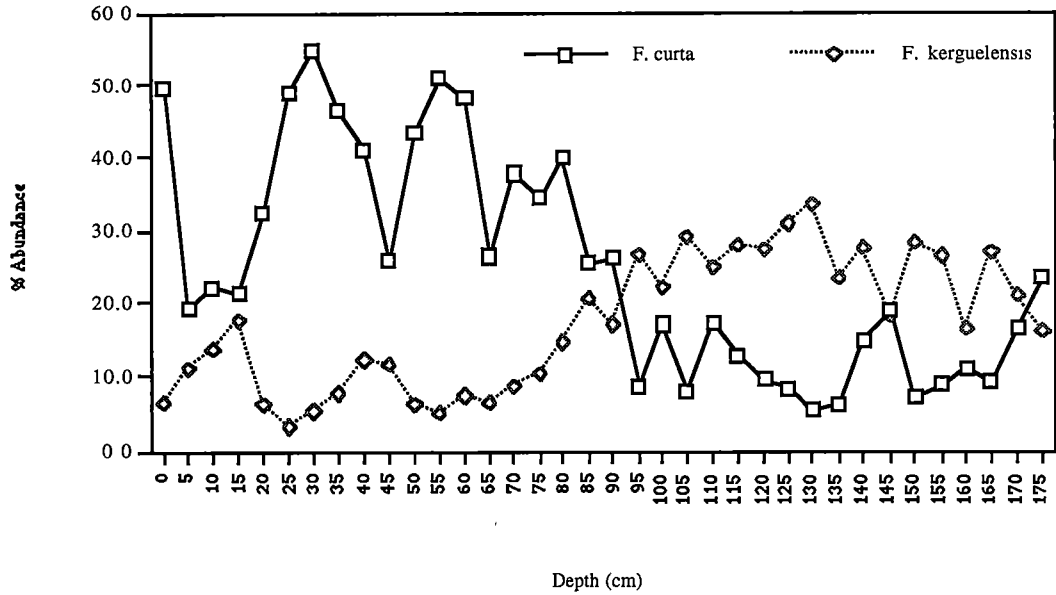


Fig. 18.4. Distribution of *F. curta* and *F. kerguelensis* in AA186. Note the relatively high abundance of *F. kerguelensis* in oceanic assemblage "B" (5-15 cm, 85-175 cm) compared to *F. curta*. (The sample from 160 cm was identified as an outlier in the initial cluster analysis and removed from subsequent analyses).

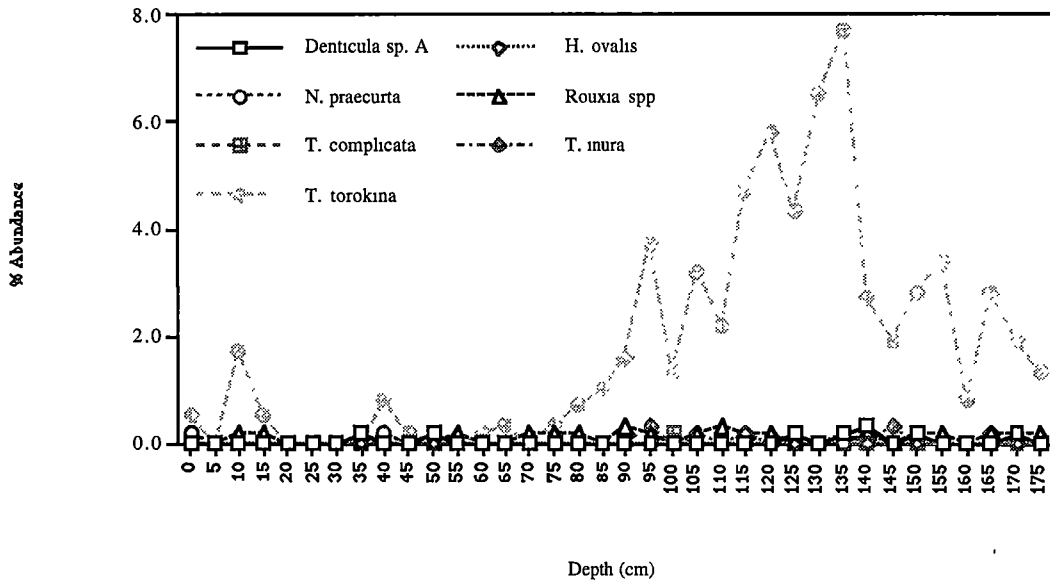


Fig. 18.5. Distribution of extinct taxa in AA186. Only *T. torokina* (8.2-8.6 Ma to 1.8 Ma) has an abundance >2% and is significant in the oceanic assemblage "B". (The sample from 160 cm was identified as an outlier in the initial cluster analysis and removed from subsequent analyses).

18.5.3 Shelf Assemblage

Deposition of the oceanic assemblage “A” in the upper core is interrupted by deposition of the shelf assemblage. In AA186, it is present at 25 cm. Like the oceanic assemblage “A”, it is dominated by *F. curta*, but in significantly less abundance. More abundant are *F. angulata*, *F. cylindrus*, *F. sublineata*, *Porosira glacialis*, and the Chrysophyte *P. corona*. Today, the shelf assemblage represents Antarctic inshore areas and ice edge waters where summer sea ice is absent. Centric species, such as *P. glacialis*, are present in significantly greater abundance. *Porosira glacialis* is indicative of nearby sea ice and often occurs in ice edge blooms (Krebs *et al.*, 1987), but does not form part of within sea ice algal communities (Watanabe, 1988; Garrison and Buck, 1989; Scott *et al.*, 1994). Relatively little is known of the ecology of *P. corona*, but interpretation of the surface sediment samples also suggests that it is indicative of cold water and / or ice edge conditions, but does not occur within-ice communities.

18.6 Upper Pleistocene / Holocene Palaeoecology of Prydz Bay (Four Ladies Bank)

Contamination by old carbon has limited the value of the radiocarbon dates from AA186. In an attempt to correct for this, contamination is assumed to be evenly mixed throughout the core, and an age of zero is calculated for the core top, using a correction factor of 7.2 Ka (the AMS date obtained from the 0-2 cm sample). At 80-82 cm the core is estimated to be 7.3 Ka. With only two AMS obtained from AA186, a linear sedimentation rate must be assumed. This is most likely incorrect. One would expect the sedimentation rate in lithological unit 2 (sandy diamicton) to be lower than in the muddy unit above (Kellogg and Kellogg, 1988; Hambrey, 1994). Unit 2 was probably deposited beneath a floating ice shelf; unit 1 deposited in an open marine setting.

18.6.1 Upper Pleistocene to Early Holocene (~17.0 Ka to ~7.7 Ka)

The bottom of AA186 is Upper Pleistocene in age, ~17.0 Ka, based on the above assumptions. Diatom frustules are rare in the lower-most samples (185 cm and 180 cm) and were not observed in quantifiable abundance. Above 175 cm, they become increasing abundant and better preserved, but not as concentrated as one would observe in biosiliceous ooze. Small and fragile species are relatively uncommon. Foraminifera fragments and sponge spicules are abundant throughout, from the bottom of the core to 100 cm, coinciding with lithological unit 2.

Lithological unit 2 extends from the bottom of the core to 100 cm. This unit is composed of compact, sandy diamicton, and is typical of relict, glacial-marine sediment deposited beneath, or within close proximity to, an ice shelf and / or having been winnowed by strong water currents (Dunbar *et al.*, 1985). The abundance of open water diatom taxa in the diatom assemblage infers open water. Based on the similarity of this assemblage with that in the surface samples BANG22 and BANG24, the immediate assumption may be that, at the time of deposition, the palaeoenvironment was characterised by open water, less sea ice and, probably, warmer sea surface temperatures.

It is important to note the features of the diatom assemblage within unit 2, however, before such an assumption can be made. The frustules are poorly concentrated, have undergone extensive damage and are characterised by robust, heavily silicified taxa. Combined with the core's lithology, this implies deposition beneath, or near, an ice shelf, where biotic activity, diversity and abundance are lower than in open water conditions (Kellogg and Kellogg, 1988). Dissolution is also greater beneath an ice shelf as sediment accumulation rates are slower (Kellogg and Kellogg, 1988; Hambrey, 1994), during which time many of the smaller and more fragile diatom frustules, often sea-ice associated (McMinn, 1995), are lost. The resulting fossil assemblage contains a disproportionate number of heavily silicified and robust frustules – such as the open water taxa *F. kerguelensis*, *S. microtrias* and *T. lentiginosa*. The heavily silicified frustules of *E. antarctica* are also significantly more abundant in this assemblage. *Eucampia antarctica* is typically found in sea ice communities (Jousé *et al.*, 1962; Burckle, 1984a), and in fossil assemblages is often related to glacial events (Jousé *et al.*, 1962).

The abundance of *E. antarctica* in AA186 may be comparable to that observed by Truesdale and Kellogg (1979). They noted *E. antarctica* to dominate a sedimentary transition zone of well sorted sand in a core recovered from the Ross Sea. The zone overlies a till unit characterised by a reworked diatom flora with widely differing biostratigraphic ranges. The till unit is interpreted to have been deposited beneath the grounded ice from the West Antarctic Ice Sheet during the LGM. The transition zone was probably deposited following the retreat of the grounding line and under a regime of strong bottom currents (Truesdale and Kellogg, 1979). Whilst *E. antarctica* is not dominant in AA186, it occurs in maximum abundance in the sandy, lithological unit 2 (forming up to 25% of the total frustules counted) and may be indicative of a similar environment to that described by Truesdale and Kellogg (1979).

It is hypothesised that AA186 unit 2, and the associated diatom assemblage, were deposited on Four Ladies Bank beneath, or near, a floating ice shelf during the LGM. There may have also been a synchronous increase in strength of bottom water currents. As outlined in Chapter 17, there is a general lack of data for the LGM in East Antarctica (Stuiver *et al.*, 1981). In West Antarctica, it is widely accepted to have commenced 24 Ka to 22.5 Ka, reaching a maximum 21.0 Ka to 17.0 Ka, and retreating after 12.5 Ka (Stuiver *et al.*, 1981; Denton *et al.*, 1989). In East Antarctica, $\delta^{18}\text{O}$ values from a Vostok ice core suggest that warming commenced ~ 18.0 Ka (Lorius *et al.*, 1985). Data from New Zealand and South America suggest that it ended in the Southern Hemisphere ~ 14.0 Ka (Burrow, 1979 in Pickard *et al.* 1984) and was followed by a transitional period between to fully interglacial conditions of the present (Pickard *et al.*, 1984).

In Prydz Bay, sedimentological evidence supports the hypothesis that ice advanced across the bay during the LGM, via drainage of the Lambert Glacier / Amery Ice Shelf, and grounded along the periphery of the Prydz Channel (Domack *et al.*, 1998). Deposition below an ice shelf in Prydz Bay during the earliest Holocene also supports the findings of O'Brien (1992) and Franklin (1997). Could the hypothesised ice shelf on Four Ladies Bank therefore represent the terminus of an advanced Lambert Glacier, or could it be sourced from elsewhere? The most likely alternative would be the Sørtdal Glacier, which today borders the south of the Vestfold Hills and is the closest glacial outlet to Four Ladies Bank. For the Sørtdal Glacier to have advanced that far, an extensive, north-trending advance of ice across the Vestfold Hills would be required. This has not been documented. At most, the Sørtdal Glacier appears to have undergone a minor, northerly readvance ~ 3.0 - 1.5 Ka (Adamson and Pickard, 1986), based on glacial striae near Chelnok Lake in the Vestfold Hills. However, even this advance is questioned by Bronge (1996), who argues that the ice would neither have been thick enough, nor warm enough, to melt underneath and create the extensive striae upon which Adamson and Pickard's (1986) theory is based.

18.6.2 Mid to Late Holocene (~ 7.7 Ka to ~ 2.7 Ka)

Open marine conditions are estimated to have commenced on Four Ladies Bank ~ 7.7 Ka. There is a distinct sediment boundary at 100 cm, changing from compact, sandy diamicton (unit 2) to muddy diamicton (unit 1). Above 80 cm, this grades into homogenous, siliceous, muddy ooze. At 85 cm, the oceanic assemblage "B" is replaced by assemblage "A". Assemblage "A" is analogous the surface sediment oceanic assemblage being

deposited on the continental shelf of Prydz Bay, and adjacent offshore zone. Although reworked, extinct taxa are present in the core samples, their abundance is statistically insignificant compared to that in the assemblage “B”.

The data from AA186 supports the findings of Domack *et al.* (1991a and 1991b) and Pushina *et al.* (1997), who suggest that open marine conditions and siliceous, muddy ooze deposition commenced in Prydz Bay sometime in the Early Holocene. Domack *et al.* (1991a) estimate this as having commenced 10.7 Ka. Whilst the date estimated in AA186 is 3 000 years later than Domack’s *et al.* (1991a) estimation, the discrepancy may be due to the tentative radiocarbon dating assigned to AA186. Alternatively, an isolated, small ice shelf may have remained “trapped” on Four Ladies Bank. Regardless of the mechanism, the transition to open marine conditions in this area ~7.7 Ka is correlatable to the mid-Holocene warming observed elsewhere in Antarctic records (e.g. Burckle, 1972; Truesdale and Kellogg, 1979, Domack *et al.*, 1991a and 1991b; Shevenell *et al.*, 1996; Pushina *et al.*, 1997; Kirby *et al.*, 1998).

18.6.3 Late Holocene (2.7 Ka to 0.5 Ka)

A brief, cool period is interpreted to have taken place for deposition of the shelf diatom assemblage to occur in AA186 ~2.3 Ka. In the modern environment, this assemblage differs from the oceanic assemblage by having a greater abundance of ice-associated and ice edge indicator species. It is distributed in the surfaced sediments on the continental shelf and does not extend beyond this. This is replaced by assemblage “A” ~2.3 Ka, suggesting that warming recommenced.

A shelf assemblage has also been deposited in GC29, inner Prydz Bay, 2.8 Ka (Chapter 16). This is interpreted to be a response to the onset of Late Holocene cooling and an increase in temporal ice cover. There is extensive evidence for cooling, or a Neoglacial, in Antarctica during the Late Holocene, commencing ~ 2.8 Ka (e.g. Leventer *et al.*, 1993; Ciais *et al.*, 1994; Domack *et al.*, 1994; Kreutz *et al.*, 1997; Domack and Mayewski, in press). In GC29, the shelf assemblage is replaced by one suggestive of more open water conditions 2.3 Ka – similar to the transition from the shelf to oceanic assemblage “A” in AA186 over the same time period. In GC29, it is hypothesised that climate and oceanographic conditions during the transition period, from a warm mid Holocene to cool Late Holocene, on the East Antarctic continental shelf were unstable. Alternatively, it could represent a previously brief, undocumented, warm interval in what was otherwise a period of general cooling. Cooling is estimated to have re-commenced in GC29 2.0 Ka

and remained unaltered to the present.

In AA186, the oceanic assemblage “A” is also replaced after only a period of brief deposition, similar to the shelf assemblage, with the oceanic assemblage “B” present from ~1.8 Ka to 0.5 Ka. Unlike the presence of this assemblage in the lower half of the core, however, there is no corresponding sandy diamict facies to suggest glacial marine deposition. Rather, it is interpreted here to have been deposited as a result of increase water current strength

An increase in bottom water current strength could account for the relatively low abundance of small and fragile frustules in this assemblage, such as *F. cylindrus* and *P. corona*, and disproportionate abundance of heavily silicified, mostly open water, indicator species. Alternatively, the Prydz Bay cyclonic gyre could have intensified and increased in extent over Prydz Bay. The gyre is a large, cyclonic system located on the continental shelf in the vicinity of 63° - 80°E (Hosie, 1994) and centered inside the bay at about 73°E (Wong, 1994). An intensified current speed, and / or increased geographic size of the gyre, during the Late Holocene could have extended its range into Prydz Bay and increased its potential to transport a greater number of open water diatoms across the continental shelf. Increased current speed could also account for the lower abundance of small and fragile diatom species in the assemblage. The absence of these species in the surface sediments of the cape assemblage has been interpreted as removal by current winnowing. Gyre intensification is also suggested as the agent being responsible for the formation of a similar diatom assemblage observed in AA149, from the Prydz Bay Trough Mouth Fan.

18.6.4 Late Holocene to Present (<0.5 Ka)

Deposition of the oceanic assemblage “A” recommenced in AA186 ~0.5 Ka. From this it is inferred that the hypothesised increase in strength of bottom water currents and / or gyre intensification, from 1.8-0.5 Ka, decreased. From 0.5 Ka, the depositional environment on Four Ladies Bank has been analogous to the present, with an open water diatom assemblage being transported onto the shelf, via water circulation. The cyclonic Prydz Bay gyre is the mechanism attributed as the transport mechanism. From this, the oceanic diatom assemblage extends as a “tongue” across the continental shelf before being mixed and dispersed amongst the shelf and coastal diatom assemblages.

18.7 Conclusion

The palaeoecological interpretation of AA186 is summarised in Table 18.5. Sediment reworking and contamination by older carbon (from extinct diatom taxa, upwelled deep water and / or ice release) are the most likely sources of anomalously old radiocarbon dates obtained from the core. The surface has an uncorrected age of 7.2 Ka, which is up to almost six times greater than that observed elsewhere in Prydz Bay or Mac.Robertson Shelf. To correct for this, it was assumed that contamination was distributed evenly throughout, and an age of zero assigned to the core top, based on a correction factor of 7.2 Ka.

Assuming a constant sedimentation rate, the base of the core is assigned a corrected radiocarbon age of ~17.0 Ka. The core lithology and diatom assemblages suggest that it was deposited under, or in close proximity to, a floating ice shelf that advanced across Prydz Bay during the LGM. Light penetration beneath the ice shelf was probably insufficient for photosynthesis to occur, and frustules were advected under the ice shelf by water currents. The currents may have been strong enough for sediment winnowing to take place, removing a significant proportion of the smaller and more fragile diatom frustules, and reworking the sediment.

Open marine conditions are estimated to have commenced ~7.7 Ka, with the deposition of biosiliceous, muddy ooze and the oceanic diatom assemblage "A". This was followed by a relatively rapid series of climate and oceanographic changes during the Late Holocene. Cooling is thought to have occurred ~2.7–2.3 Ka, with deposition of a shelf diatom assemblage, followed by a brief period of warmer and more open water conditions ~2.3–1.8 Ka. The diatom assemblage is analogous to that deposited on Four Ladies Bank today.

Between ~1.8–0.5 Ka, the reworked oceanic assemblage "B" was redeposited. Unlike that at the bottom of the core, however, the assemblage near the top does not coincide

with compact, sandy diamicton. Deposition is assumed to have occurred in a seasonally ice free, open marine environment, but water currents during this time may have intensified. Whether this was in the form of stronger bottom currents and / or intensification of the Prydz Bay gyre, and whether atmospheric or water temperatures varied, cannot be determined. Deposition of the modern oceanic assemblage on Four Ladies Bank recommenced ~0.5 Ka. It has been deposited continuously since then and with relatively minor disturbance except for, perhaps, infrequent iceberg grounding.

Table 18.5. Summary of Holocene palaeoclimate in inner Prydz Bay (Four Ladies Bank) inferred from AA186.

| Corrected ¹⁴ C Age (Ka) | Core Lithology | Diatom Assemblage | Major Species | Climate Interpretation |
|------------------------------------|--------------------------|-------------------|--|--|
| <0.5 | Biosiliceous, muddy ooze | Oceanic "A" | <i>F. curta</i> <i>F. cylindrus</i> <i>Chaetoceros</i> spores <i>T. antarctica</i> spores | Modern conditions; seasonal sea ice & open water in summer; gyre-influenced |
| 0.5 – 1.8 | Biosiliceous, muddy ooze | Oceanic "B" | As for above | Increase water current strength & / or gyre intensification; cooling? |
| 1.8 – 2.3 | Biosiliceous, muddy ooze | Oceanic "A" | As for above | Brief Late Holocene warming |
| 2.3 – 2.7 | Biosiliceous, muddy ooze | Shelf | As for above | Late Holocene cooling; seasonally open water with nearby ice edge |
| 2.7 – 7.7 | Biosiliceous, muddy ooze | Oceanic "A" | <i>F. curta</i> <i>F. cylindrus</i> <i>F. kerguelensis</i> <i>Chaetoceros</i> spores | Onset of open marine deposition, followed by mid Holocene warming; seasonally open water |
| 7.7 – 17.0 | Compact, sandy diamicton | Oceanic "B" | <i>F. kerguelensis</i> <i>T. antarctica</i> spores <i>F. curta</i> <i>E. antarctica</i> | Deposition beneath, or in close proximity, to an ice shelf; LGM |

– Chapter 19 –

KROCK GC33

19.1 Site Description

Core KROCK/163/GC33 (GC33, hereafter) was recovered from Fram Bank (67° 10.88'S, 68° 32.30'E; Fig. 13.1) during ANARE's 1993 Krill and Rock (KROCK) Survey aboard the RSV *Aurora Australis*. Fram Bank borders the north west of the Amery Depression and, together with Four Ladies Bank to the northeast, its shallow banks form a partial barrier to water exchange with the deep ocean (Smith and Tréguer, 1994). The shallow banks also ground icebergs, which suspend and rework sediment, before they break up, calve and drift across the relatively deeper depressions without further disturbing the seafloor. In an attempt to minimise the effect of iceberg reworking, the coring site for GC33 was located in a bathymetric low on the western half of Fram Bank, in a water depth of 376 m. Here a layer of Late Holocene, carbonate-rich sand covers the bank.

19.2 Core Description

The core is 195 cm long. Two lithological units can be recognised, separated by a transitional boundary (Fig. 19.1). Unit 1 consists of moderate, olive brown (5Y 4/4), siliceous mud and ooze from 0-80 cm. Laminations are present below 28 cm; there is no evidence of bioturbation. Between 80 cm and 95 cm the colour grades into olive grey (5Y 3/2). Unit 2 occurs from 80-195 cm. It consists of olive black (5Y 2/1), well sorted, muddy sand or sandy mud. Iceberg rafted debris (IRD) is present in unit 2 as minor clasts, with pebble-sized dropstones observed at 100 cm and 170 cm.

19.3 Fossil Assemblages

Diatoms are present to a depth of 80 cm. The frustules are abundant and generally well preserved. They have undergone normal mechanical breakage. At 80 cm, frustules are present in quantifiable abundance, but are noticeably less concentrated than from samples higher in the core. Diatoms are not observed in quantifiable abundance below 80 cm, becoming increasingly rare to absent over the transitional sedimentary boundary between units 1 and 2.

Foraminifera are present in low abundance. No other fossils are observed in the core.

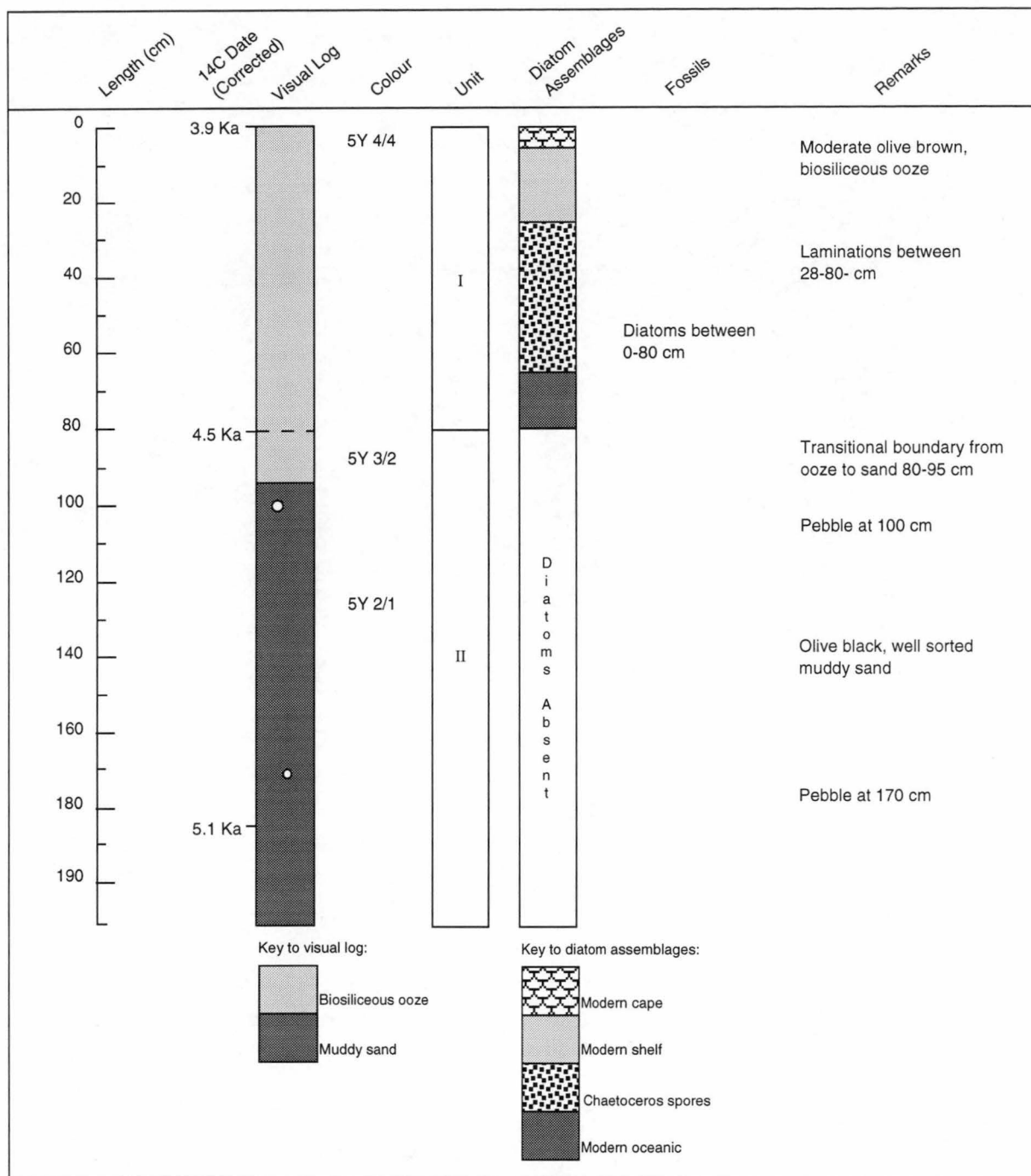


Fig. 19.1. GC33 core log, radiocarbon dates and diatom assemblages compared to surface sediment.

19.4 GC33 – Results

19.4.1 Radiocarbon Dates

Three reliable radiocarbon dates, based on bulk organic carbon, were obtained from GC33 (Rathburn *et al.*, 1997; Table 19.1). The core has a corrected surface age of 2.1 Ka, after applying a reservoir correction factor of 1.3 Ka (after Rathburn *et al.*, 1997), and extends into the mid Holocene, with a reservoir-corrected age of 3.8 Ka obtained at 185 cm. The corrected surface age is considerably older than that of undisturbed and uncontaminated modern sediments in eastern Prydz Bay, which range from 1.3-1.8 Ka (Adamson and Pickard, 1986; Domack *et al.*, 1989), and Mac.Robertson Shelf, discussed herein (0.3-0.9 Ka). The likely reasons for this are discussed below, and Rathburn *et al.* (1997) stress that the chronology must be regarded as tentative until further studies are undertaken.

Simple linear regression indicates a good age v depth correlation ($R^2 = 0.995$; Fig.19.2). A sedimentation rate of 0.137 cm yr^{-1} is calculated from 0-82 cm, and a slightly higher rate of 0.176 cm yr^{-1} from 82-185 cm. This is similar to the average Holocene sedimentation rate of 0.166 cm yr^{-1} , determined from ODP Site 740 in eastern Prydz Bay (Domack *et al.*, 1991a). Assuming constant deposition rate, Rathburn *et al.* (1997) consider it unlikely that the upper 350 cm of the core could have been lost during the recovery process or by erosion. The old surface date from the core has therefore most likely been affected by contamination of older carbon.

Table 19.1. Uncorrected and corrected AMS radiocarbon dates obtained from bulk organic carbon for core GC33 (Rathburn *et al.*, 1997). A correction factor of 1 300 radiocarbon years was applied (after Rathburn *et al.*, 1997).

| Interval (cm) | ¹⁴ C Date | | Deposition Rate (cm yr ⁻¹)† |
|------------------|----------------------|-----------|--|
| | Uncorrected | Corrected | |
| 0 - 1 | 3 860 +/- 100 | 2 560 | |
| 82 - 83 | 4 460 +/- 60 | 3 160 | 0.137 |
| 185 - 186 | 5 050 +/- 70 | 3 750 | 0.176 |

† Deposition rates determined between 0-82 cm, and 82-186 cm.

Sediment reworking could have contributed to carbon contamination in the core. The depth at which the core was recovered (376 m) is well within the range that iceberg gouging can rework sediment, which is 690 m in Prydz Bay (O'Brien, 1994). The core site is located within a bathymetric low on Fram Bank, however, and although some icebergs may ground, it is reasonable to expect that most would ground on the shallower banks to either side, calve and break up before drifting over the core site. Strong bottom currents are more likely to have an affect on sediment reworking at this location. As discussed in Chapters 9 and 10, diatom assemblages in the vicinity of Cape Darnley and on Fram Bank contain fewer small and fragile frustules compared to assemblages elsewhere on the continental shelf between Prydz Bay and Mac.Robertson Shelf. An assemblage composed of large, robust frustules suggests that the assemblage has been reworked by water currents, with many of the smaller species having been winnowed away. Grain size analysis carried out on surface sediment supports this hypothesis. Reworking by episodic, but probably infrequent, iceberg grounding and strong bottom currents may redeposit material and transport older material (Domack *et al.*, 1989).

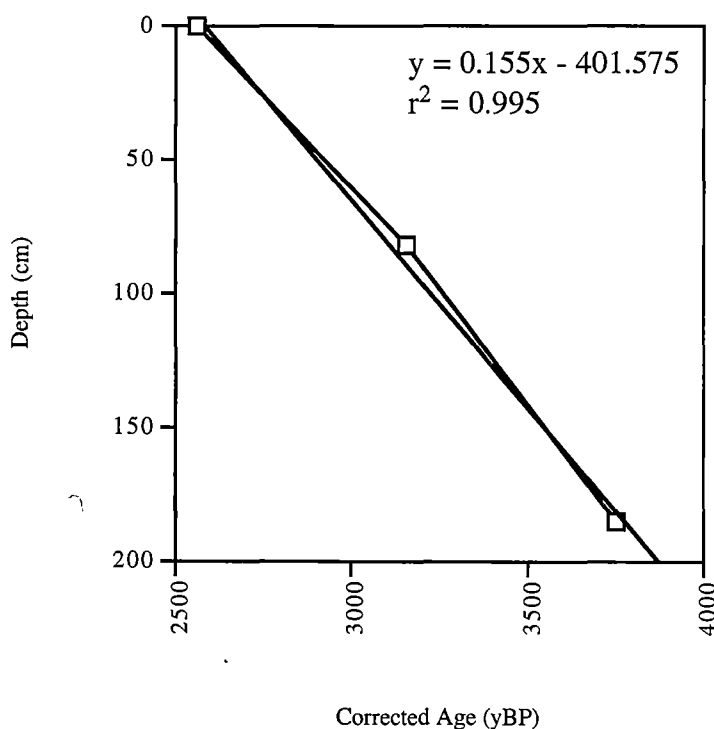


Fig. 19.2. Linear regression of corrected radiocarbon dates versus depth.

Upwelling along the edge of the continental shelf can also provide a source of older carbon. This has been estimated to affect ages by only ~400 years, however (Stuiver and Ostlund, 1983). The presence of sea ice can limit the mixing and dilution of older CO₂ in upwelled water with modern, atmospheric CO₂. Limited mixing and retention of old carbon upwelled from along the continental shelf edge could certainly account for the older radiocarbon age observed in GC33. Anomolously old radiocarbon ages have also been observed in cores AA149 and AA186. Both are located near the edge of the continental shelf in Prydz Bay and may have been contaminated by upwelled water. They also contain reworked, fossil diatom taxa, although the contribution of this to the total carbon is likely to have been minimal (Domack *et al.*, 1989).

19.4.2 Diatom Assemblages

Diatoms are abundant and well preserved in the upper 70 cm. Below this, frustules become increasingly rare and are not observed in quantifiable abundance below 80 cm. This coincides with the sedimentary transition in the core, from biosiliceous ooze to muddy sand. Below 100 cm, diatom frustules are rare to absent.

Fragilariopsis curta is the most abundant species, between 0-20 cm. From 25-30 cm and 60-80 cm, the assemblage is dominated by *Chaetoceros* resting spores and subdominated by *F. curta* and *T. antarctica* resting spores. An almost monospecific assemblage of *Chaetoceros* resting spores is present between 35-55 cm. The spores form up to 90% of the frustules observed.

19.4.3 Statistical Analyses

GC33

A dendrogram illustrating core sample affinities illustrated in Fig. 19.3. Sixteen diatom species with an abundance >2% are observed in 17 core samples (Appendix 11). Three cluster groups are identified at 38.2% dissimilarity, with a cophenetic correlation of 0.58. Indicator species for each cluster group are identified by a one-way ANOVA (Table 19.2). The SNK test could not be carried out in this instance due to a low dispersion matrix. Statistical analyses are carried out on log₁₀ species abundance; the following discussion is based on arithmetic mean percent abundance, unless otherwise stated.

Cluster group 1 occurs in the upper 20 cm of GC33. The diatom assemblage is dominated by *F. curta* (62.5%). There are no obvious subdominant species, with the second most abundant, *F. cylindrus*, having an average abundance of only 7.0%. Also common

(>2%) are *F. angulata*, *Chaetoceros* resting spores, *F. obliquecostata*, *T. antarctica* resting spores, and the Chrysophyte *P. corona*. Three species are abundance indicators: *F. obliquecostata*, *F. separanda* and *P. corona*. *Fragilariopsis curta* and *T. gracilis* are significantly more abundant in cluster group 1 compared to cluster groups 2 and 3, but are not indicator species of the assemblage.

Cluster group 2 contains samples from 25 cm, 30 cm and 60-80 cm. *Chaetoceros* resting spores dominate (40.4%), and are significantly more abundant compared to that in cluster group 1. *Fragilariopsis curta* (17.4%) and *T. antarctica* resting spores (14.4%) co-subdominate. Common (>2%) are *F. cylindrus* and *F. kerguelensis*. *Thalassiosira antarctica* resting spores are unique indicators of the diatom assemblage, along with the numerically rare *T. lentiginosa*. The cluster group can be further distinguished from cluster group 1 by a significantly greater abundance of *E. antarctica* and *F. kerguelensis*.

Cluster group 3 forms a distinct layer in GC33 from 35-55 cm. The assemblage is dominated by *Chaetoceros* resting spores (76.4%). The spores have a maximum abundance of 90.5%, forming an almost monospecific assemblage. Their abundance is significantly greater compared to that in both cluster groups 1 and 2. Although not obviously subordinate, *F. curta* (6.7%) and *F. cylindrus* (6.6%) are the only other species whose average abundance is > 5%: *Thalassiosira antarctica* resting spores are relatively common. No species were identified by the one-way ANOVA as unique abundance indicators in the assemblage.

GC33 and Surface Samples

A dendrogram illustrating GC33 and surface sediment sample affinities is illustrated in Fig. 19.4. Twenty four diatom species are present in >2% abundance, from 117 samples. Five cluster groups are identified at 42.1% dissimilarity, with a cophenetic correlation of 0.72. The SNK test is used to identify indicator species present in each cluster group (Table 19.3). Statistical analyses were carried out using \log_{10} abundance values. The following discussion is based on arithmetic mean percent abundance, unless otherwise indicated.

Cluster group 1 contains all surface sediment samples identified as the cape assemblage. This includes the surface (0 cm) of GC33. *Fragilariopsis curta* dominates the assemblage (62.8%), but does not significantly differ from its abundance observed in cluster groups 2 or 3, based on \log_{10} values. There are no obvious subdominant species, with all others

having an average abundance <8.5%. These are *E. antarctica*, *F. angulata*, *F. cylindrus*, *F. kerguelensis*, *F. obliquecostata*, *T. antarctica* resting spores, and *T. gracilis*. There are no unique abundance indicators in the cape assemblage, but there are several species significantly more abundant compared to at least one other cluster group (see Table 19.3). A notable feature of the cape assemblage is the low abundance of small diatom species, including *F. cylindrus* which forms the subordinate member of the other diatom assemblages present on the continental shelf, and increased abundance of species more typically associated with open water, oceanic environments. This feature, along with grain-size analysis, supports the hypothesis that the cape assemblage has undergone current reworking and preferential dissolution of small, fragile species, leaving a lag deposit on the continental shelf that is characterised by large, robust species – many of which are associated with the open marine environment.

Cluster group 2 contains all surface sediment samples identified as the shelf assemblage, and GC33 samples 5-20 cm. The assemblage is dominated by *F. curta* (49.2%) and subdominated by *F. cylindrus* (15.3%). Based on \log_{10} values, neither has a significantly different abundance from that of cluster groups 1 or 3. Common (>2%) are *Chaetoceros* resting spores, *F. angulata*, *F. obliquecostata*, *T. gracilis* var. *expecta*, and *P. corona*. There are no indicators in the assemblage, but several species are significantly more abundant in cluster group 2 compared to at least one other cluster group (see Table 19.3).

Cluster group 3 contains all surface sediment sample identified as the coastal assemblage. There are no intervals from GC33 that are analogous to this assemblage. The assemblage is described in detail in Chapters 9 and 10, and will not be discussed further here.

Cluster group 4 contains all surface sediment samples identified as the oceanic assemblage, and GC33 samples 65-80 cm. The assemblage is dominated by *F. curta* (27.7%), but it is significantly less abundant compared to that in cluster groups 1, 2 and 3. Three taxa are subdominant: *Chaetoceros* resting spores (14.1%), *F. kerguelensis* (13.1%) and *F. cylindrus* (12.6%). Present at >2% are *F. angulata*, *T. antarctica* resting spores, *T. gracilis*, *T. lentiginosa*, and *P. corona*. The cluster group is characterised four unique abundance indicator species: *F. kerguelensis*, *T. lentiginosa*, and the numerically rare *T. gracilis* var. *expecta* and *Trichotoxin reinboldii*. There are several other species significantly more abundant in the cluster group compared to one or more other cluster groups, but not present as unique indicators. These are listed in Table 19.3.

Cluster group 5 contains GC33 samples 25-60 cm. There are no surface sediments in Prydz Bay or Mac.Robertson Shelf that contain an analogous diatom assemblage.

Chaetoceros resting spores are dominant (69.0%). *Fragilariopsis curta* is subdominant, but has a maximum abundance of only 18.5% and, on average, forms <10%. Less abundant, but relatively common (>2%), are *F. curta*, *F. cylindrus*, *F. kerguelensis*, and *T. antarctica* resting spores. There are no unique indicator species present, although the *Chaetoceros* resting spores are significantly more abundant compared to all their abundance in all other cluster groups.

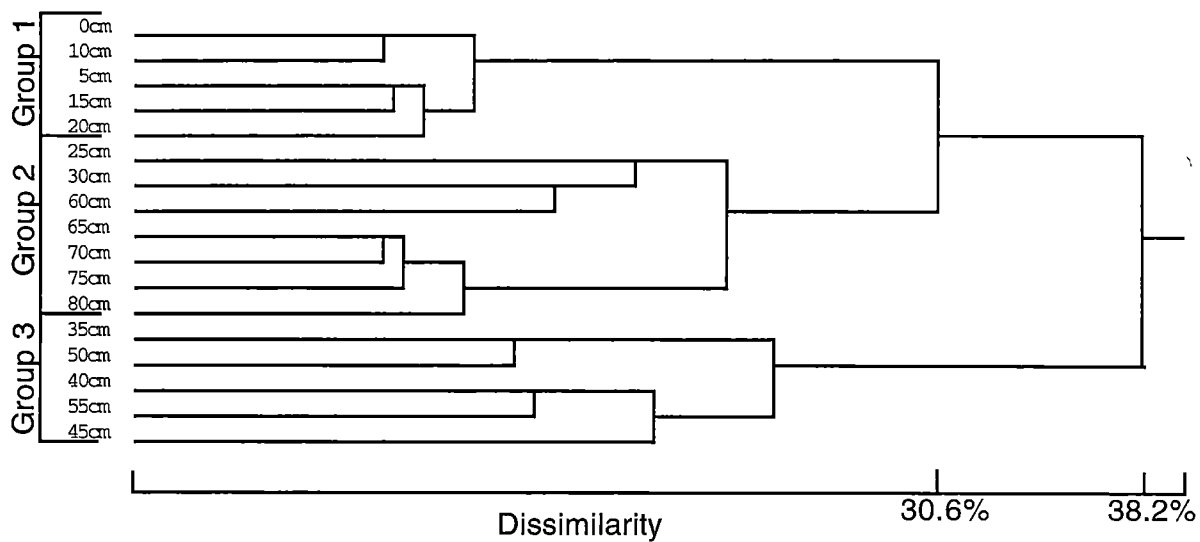


Fig. 19.3. Dendrogram of cluster analysis comparing GC33 samples. Analysis based on species abundance (>2% log10).

Table 19.2. Arithmetic mean abundance (%), analysis of variance (F) and one way ANOVA of species in cluster groups from GC33.

| Species | Cluster Group | | | F | P |
|------------------------------------|---------------|-------------|-------------|--------|-----|
| | 1 | 2 | 3 | | |
| <i>Chaetoceros</i> spores | 3.8 | <u>40.4</u> | <u>76.5</u> | 75.345 | *** |
| <i>C. criophilum</i> | 0.2 | 0.1 | 1.5 | 0.813 | – |
| <i>D. speculum</i> | 0.5 | 1.1 | 0.5 | 2.577 | – |
| <i>E. antarctica</i> | 1.1 | <u>1.7</u> | 0.3 | 6.036 | * |
| <i>F. angulata</i> | <u>5.7</u> | <u>1.7</u> | 0.1 | 38.792 | *** |
| <i>F. curta</i> | <u>65.2</u> | <u>17.4</u> | 6.7 | 43.746 | *** |
| <i>F. cylindrus</i> | 7.0 | 7.0 | 6.6 | 0.672 | – |
| <i>F. kerguelensis</i> | 0.8 | <u>5.5</u> | 1.7 | 8.785 | ** |
| <i>F. obliquecostata</i> | <u>3.3</u> | 1.2 | 0.9 | 15.835 | *** |
| <i>F. separanda</i> | <u>1.3</u> | 0.3 | 0.0 | 28.456 | *** |
| <i>P. corona</i> | <u>1.3</u> | 0.3 | 0.0 | 8.727 | ** |
| <i>P. glacialis</i> | 1.4 | 1.3 | 0.1 | 4.541 | * |
| <i>P. turgiduloides</i> | 0.1 | 0.6 | 0.8 | 2.083 | – |
| <i>T. antarctica</i> spores | 4.1 | <u>14.5</u> | 4.3 | 24.462 | *** |
| <i>T. gracilis</i> | <u>1.7</u> | <u>1.1</u> | 0.3 | 25.746 | *** |
| <i>T. lentiginosa</i> | 0.5 | <u>1.3</u> | 0.1 | 3.866 | * |

Analyses were carried out on $\log_{10}(x+1)$ transformed abundance. Degrees of freedom 2, 14. ANOVA P values: * <0.05, ** <0.005, *** <0.0005, – not significant. Bold type: species with significant differences in mean abundance. Underlined type: species with significantly higher abundance in a cluster group.

Table 19.3. Arithmetic mean abundance (%), analysis of variance (F) and SNK multiple range test of species in cluster groups from GC33 and surface sediment samples.

| Species | Cluster Group | | | | | F | P |
|---|---------------|-------------|-------------|-------------|-------------|-------|-----|
| | 1 | 2 | 3 | 4 | 5 | | |
| <i>A. actinochilus</i> | <u>0.5</u> | <u>0.2</u> | 0.1 | <u>0.7</u> | 0.0 | 24.98 | *** |
| <i>Chaetoceros</i> spp. | 0.0 | 0.2 | 0.4 | 0.1 | 0.2 | 2.63 | * |
| <i>Chaetoceros</i> spores | 1.1 | <u>7.8</u> | <u>5.3</u> | <u>14.1</u> | <u>69.0</u> | 64.25 | *** |
| <i>D. antarcticus</i> | <u>0.9</u> | 0.5 | 0.2 | <u>0.8</u> | 0.2 | 6.83 | *** |
| <i>D. speculum</i> | 0.6 | 0.5 | 0.3 | <u>0.8</u> | 0.5 | 4.32 | ** |
| <i>E. antarctica</i> | <u>2.3</u> | 0.4 | 0.1 | <u>1.2</u> | 0.9 | 12.11 | *** |
| <i>F. angulata</i> | <u>5.6</u> | <u>4.0</u> | <u>4.2</u> | <u>2.1</u> | 0.3 | 43.01 | *** |
| <i>F. curta</i> | <u>62.8</u> | <u>49.2</u> | <u>54.7</u> | <u>27.7</u> | 9.6 | 67.00 | *** |
| <i>F. cylindrus</i> | 2.6 | <u>15.2</u> | <u>22.3</u> | <u>12.6</u> | 6.3 | 14.80 | *** |
| <i>F. kerguelensis</i> | 2.0 | 1.0 | 0.5 | <u>13.1</u> | <u>2.1</u> | 66.95 | *** |
| <i>F. lineata</i> | <u>1.1</u> | <u>0.9</u> | <u>0.7</u> | <u>1.0</u> | 0.0 | 8.04 | *** |
| <i>F. obliquocostata</i> | <u>2.7</u> | <u>2.5</u> | <u>1.8</u> | <u>1.8</u> | 0.9 | 9.79 | *** |
| <i>F. separanda</i> | <u>1.7</u> | <u>0.8</u> | 0.2 | <u>1.6</u> | 0.1 | 21.36 | *** |
| <i>F. sublineata</i> | 0.6 | 0.7 | 0.4 | 0.4 | 0.1 | 4.49 | ** |
| <i>P. corona</i> | <u>1.1</u> | <u>3.7</u> | <u>1.6</u> | <u>2.8</u> | 0.3 | 17.72 | *** |
| <i>P. glacialis</i> | 0.6 | <u>1.0</u> | 0.2 | 0.4 | 0.2 | 12.41 | *** |
| <i>P. turgiduloides</i> | 0.1 | 0.1 | 0.4 | 0.1 | 0.6 | 5.22 | ** |
| <i>S. microtrias</i> | <u>0.9</u> | <u>0.4</u> | 0.2 | <u>0.6</u> | 0.1 | 8.51 | *** |
| <i>T. antarctica</i> spores | <u>8.5</u> | <u>6.5</u> | 1.3 | <u>7.2</u> | <u>5.9</u> | 11.70 | *** |
| <i>T. antarctica</i> (veg.) | <u>0.0</u> | <u>0.0</u> | 0.2 | 0.0 | 0.0 | 2.10 | – |
| <i>T. gracilis</i> | <u>2.1</u> | <u>1.3</u> | 0.8 | <u>3.5</u> | 0.5 | 31.24 | *** |
| <i>T. gracilis</i> var. <i>expecta</i> | 0.0 | 0.2 | 0.2 | <u>0.6</u> | 0.0 | 10.31 | *** |
| <i>T. lentiginosa</i> | 0.8 | 0.4 | 0.2 | 2.2 | 0.2 | 47.92 | *** |
| <i>T. reinboldii</i> | 0.2 | 0.3 | 0.1 | 0.8 | 0.1 | 14.07 | *** |

Analyses were carried out on $\log_{10}(x+1)$ transformed abundance. Degrees of freedom 4, 114. ANOVA P values: * <0.05, ** <0.005, *** <0.0005, – not significant. Bold type: species with significant differences in mean abundance. Underlined type: species with significantly higher abundance in a cluster group. Cluster group (diatom assemblage) names: 1 = Cape; 2 = Shelf; 3 = Coastal; 4 = Oceanic; 5 = *Chaetoceros*.

19.5 Diatom Assemblages in GC33

19.5.1 Cape Assemblage

The cape diatom assemblage, deposited at the surface of GC33, is described in detail in the surface assemblages of Prydz Bay (Chapters 9 and 10). To summarise, it is characterised by an abundance of large, robust and heavily silicified diatom frustules (such as *E. antarctica* and *F. kerguelensis*) that are indicative of either sea ice or open water. In the surface sediments of Prydz Bay today, the assemblage is restricted to an area just north of Cape Darnley, on Fram Bank (Fig. 9.2). The assemblage is dominated by *F. curta*, which forms up to 72%. Although relatively small (minimum dimensions of 10 μm x 3.5 μm are recorded by Medlin and Priddle, 1990), *F. curta* is also noted for its resistance to dissolution (Kozlova, 1966) and is well preserved in sediment. Many of the fragile and lightly silicified species that are abundant elsewhere on the continental shelf or adjacent offshore, such as *F. cylindrus*, are conspicuously low in abundance in the cape assemblage.

The modern cape assemblage is likened to that described in surface sediment of the Ross Sea by Truesdale and Kellogg (1979). They observed an assemblage dominated by *E. antarctica*, which they consider to indicate a lag deposit from which more fragile diatom frustules have been selectively winnowed by strong bottom currents. In Prydz Bay, the cape assemblage occurs in the vicinity of a strong (8 cm sec^{-1}), westward flowing coastal current, associated with the East Wind Drift, exiting the bay. Here, water converges with the narrow, westward flowing slope current (Wong, 1994). The currents are strong enough to decouple primary production in the surface waters from the underlying sediments and transport material falling through the water column before it settles (O'Brien *et al.*, 1995a). It is the strength of the currents exiting Prydz Bay here that are attributed to the winnowed nature of the cape diatom assemblage.

19.5.2 Shelf Assemblage

Below 5 cm in GC33, the cape assemblage is replaced by one analogous to the shelf assemblage, which is being deposited today in the surface sediments of Prydz Bay and Mac.Robertson Shelf. In GC33, the shelf assemblage has been deposited to a depth of 20 cm. It is dominated by *F. curta* (49%), similar to the cape assemblage, but it is significantly less abundant. *Fragilariopsis cylindrus* is subdominant, forming up to 34%. This is significantly greater compared to the cape assemblage, where *F. cylindrus* does not exceed 5%.

In the modern depositional setting of Prydz Bay, the shelf assemblage represents a planktonic diatom community influenced by sea ice. The sea ice seasonally breaks out during the summer months, but the assemblage remains in close proximity to the receding ice-edge. In shallower and near-coastal areas, the ice-edge may persist over many years. This is indicated by the abundance of species that regularly form in ice-edge blooms but do not live within the sea ice habitat, such as *T. antarctica* resting spores and *P. glacialis*. The species composition, geographic distribution, and ecology of the shelf assemblage are discussed in full detail in Chapters 9 and 10.

19.5.3 *Chaetoceros* Assemblage

There is a significant change in the diatom assemblage deposited in GC33 below 25 cm. The shelf assemblage is replaced by one where *Chaetoceros* resting spores are present in near-monospecific abundance (up to 90%) (Fig. 19.5). The subdominant taxa, *F. curta*, *F. cylindrus* and *T. antarctica* resting spores, each do not exceed an average abundance of 10%. The *Chaetoceros*-dominated assemblage is the largest assemblage identified in the core, and has been deposited to a depth of 60 cm.

There is no analogue to the *Chaetoceros* assemblage in the surface sediments of Prydz Bay and Mac.Robertson Shelf. Documentation of similar assemblages elsewhere in modern Antarctic sediments is also rare. *Chaetoceros* resting spores have been observed in abundance, however, in several Holocene cores recovered from the Antarctic continental shelf, including the Ross Sea (Leventer *et al.*, 1993), the Palmer Deep (Leventer *et al.*, 1996), Vincennes Bay (Harris *et al.*, 1997a), and Iceberg Alley (GC1, herein; O'Brien *et al.*, 1995a; Harris *et al.*, 1997a). Their high concentration in sediment is generally considered indicative of very high primary production and melt-water stratification in the upper water column (Donegan and Schrader, 1982; Leventer, 1992; Leventer *et al.*, 1993, 1996), such as that which occurs during the Antarctic spring diatom bloom. During this time nutrients may become so depleted that diatom growth becomes limited and resting spore formation is triggered (Nelson and Smith, 1986; McMinn *et al.*, 1995). Sediment dominated by *Chaetoceros* resting spores have also been considered indicative of increase seasonal sea ice or a stationary summer ice-edge (Leventer, 1992). Here, vegetative cells that are advected under the ice during summer could be induced to form resting spores (Leventer, 1992). Both hypotheses and the significance of resting spore formation are discussed in detail in Chapter 14.



Fig. 19.5. Distribution of *Chaetoceros* resting spores in GC33. The spores form a distinct assemblage in the core from 25 cm to 65 cm.

19.5.3 Oceanic Assemblage

Below 65 cm, the *Chaetoceros*-dominated assemblage is replaced by one analogous to the modern oceanic assemblage. The oceanic assemblage has been deposited in GC33 to a depth of 80 cm, after which frustules become increasing rare to absent and were not quantified. The assemblage is dominated by *F. curta*, as is characteristic of the Prydz Bay and Mac.Robertson Shelf continental shelf and adjacent offshore zone, and subdominated by *Chaetoceros* resting spores, *F. cylindrus* and *F. kerguelensis*.

Fragilariopsis kerguelensis is a statistical indicator species of the oceanic assemblage. This species is indicative of open water. It is negatively correlated with sea ice (Burckle *et al.*, 1987), increases in abundance with distance from the Antarctic continental shelf (Kozlova, 1966; Leventer, 1992), and dominates summer surface waters between 52°S and 63° S where temperatures are $>0^{\circ}\text{C}$ (Burckle and Cirilli, 1987; Burckle *et al.*, 1987; Krebs *et al.*, 1987). Similarly, *F. cylindrus* is associated with open water conditions, but may also occur in both sub-sea ice and ice edge environments (Burckle *et al.*, 1987; Kang and Fryxell, 1992; Leventer *et al.*, 1993). *Chaetoceros* resting spores do not occur in sea ice communities but are high in abundance at the sea ice edge (Garrison *et al.*, 1987).

Leventer (1992) and Leventer *et al.* (1996) suggest that the resting spores may be associated with stratified, low salinity and poorly mixed water columns that occur along a stationary ice edge following its maximum summer retreat. The abundance of open water associated taxa in the oceanic assemblage is used as a proxy for a less extensive sea ice distribution and warmer surface waters.

19.6 Holocene Palaeoecology of Mac.Robertson Shelf (Fram Bank)

The mid to Late Holocene palaeoecology of Fram Bank is recorded by diatom assemblages in GC33. Prior to 3.1 Ka, diatom frustules are rare to absent and, combined with the core's lithology, an ice shelf is interpreted to have been grounded over the site. Open water deposition commenced 3.1 Ka. It has been followed by deposition of three different diatom assemblages, culminating in the modern cape assemblage that is present in the surface sediments of Fram Bank today. Deposition of the cape assemblage commenced 2.6 Ka.

19.6.1 Mid Holocene (3.8 Ka to 3.1 Ka)

Diatom frustules are not observed in quantifiable abundance from the base of the core to 85 cm. This is synchronous with lithological unit 2, which consists of black, sticky, sandy mud and muddy sand with IRD. It is typical of basal tills that have been deposited beneath grounded ice (Anderson *et al.*, 1980; Anderson, 1989). Based on the reservoir-corrected radiocarbon chronology, it is estimated that unit 2 was deposited between 3.8 Ka and 3.1 Ka.

For an ice shelf to have grounded over Fram Bank during the mid-Holocene, the most likely climatic event to which it could be correlated is the Antarctic hypsithermal. The hypsithermal is a warm period widely recognised in Northern Hemisphere sedimentary records, between 7.0 Ka and 4.0 Ka (Pielou, 1990). Evidence is less extensive in the Southern Hemisphere, although sedimentological records from ODP Site 740 prompt Domack *et al.* (1991b) to suggest that an ice shelf grounded over Prydz Bay between 7.0 Ka and 3.8 Ka. Ice retreated and open marine deposition commenced after the collapse of the hypsithermal and the onset of Late Holocene cooling. This differs from the sedimentological record and radiocarbon chronology from GC33, which suggests that the ice shelf continued to be ground over Fram Bank for at least 7,000 years after it had

retreated across Prydz Bay and Amery Depression. Whether ice did indeed remain grounded on Fram Bank for this extended period of time, after it had already commenced to retreat across eastern Prydz Bay, or whether the apparent discrepancy between the two sites is due to the poor age constraint used to date GC33 cannot yet be determined.

19.6.2 Mid Holocene (3.1 Ka to 3.0 Ka)

Diatom frustules in GC33 first appear in quantifiable abundance at 80 cm. The assemblage is analogous to the oceanic diatom assemblage, which today is distributed primarily in surface sediments offshore of the continental shelf zone (Fig. 9.2). The assemblage is dominated by the sea ice diatom *F. curta*, and subdominated by *Chaetoceros* resting spores, *F. cylindrus*, and the open water species *F. kerguelensis*. The latter is a unique abundance indicator of the assemblage. The ecological significance of the oceanic assemblage is fully discussed in Chapter 10. In GC33, it has been deposited from 3.1 Ka to 3.0 Ka.

Whilst diatom frustules are present in quantifiable abundance in GC33's oceanic assemblage, it is important to note that their concentration is relatively poor compared to that in modern, biosiliceous ooze. Frustule concentration does increase up-core, however. This corresponds with the transitional sediment boundary from the sandy facies of lithological unit 2, to the siliceous, muddy ooze of unit 1. The transition zone is interpreted to have been deposited beneath, or in close proximity to, a floating ice shelf following the retreat of a grounded ice. The relatively low abundance of frustules in this zone may be due to one of two alternatives:

1. Biotic activity, diversity and abundance are typically lower beneath ice shelves (Kellogg and Kellogg, 1988), as light penetration under the ice is often insufficient to support primary production. Where diatom frustules are present in the sediment, they are more likely to have been advected under the ice by water currents and settled out of suspension here.
2. Frustules are deposited in front of the ice shelf where bottom currents are sufficiently strong to sort and rework the assemblage.

Hypothesis 2 is suggested by Truesdale and Kellogg (1979) as responsible for the formation of an *E. antarctica*-dominated assemblage in Holocene, sandy sediment from the Ross Sea. They suggest that strong bottom currents have winnowed the more fragile frustules out of the assemblage. Whilst this may explain the abundance of *F. kerguelensis* and *Chaetoceros* resting spores in GC33, one would not expect to find

the small, fragile frustule of *F. cylindrus* subdominant in a current-reworked assemblage. Hypothesis 1 is therefore favoured, as abundance beneath an ice shelf is typically lower than in an open water setting (Kellogg and Kellogg, 1988).

Retreat of a grounded ice shelf across Fram Bank about 3.1 Ka is correlatable to mid-Holocene climatic warming. This has been observed elsewhere in Antarctic marine sediments (e.g. Burckle, 1972; Truesdale and Kellogg, 1979; Domack *et al.*, 1989, 1991a, 1991b; Shevenell *et al.*, 1996; Pushina *et al.*, 1997; Kirby *et al.*, 1998; Cunningham *et al.*, in press). Evidence for mid-Holocene warming has also been noted herein, from GC1 and GC2 (Mac.Robertson Shelf), GC29 (inner Prydz Bay), and AA186 (outer Prydz Bay). Based on the chronology used in GC33, it is questionable whether this retreat is related to the end of the Antarctic hypsithermal, which Domack *et al.* (1991b) place at 3.8 Ka. The onset of open marine deposition in GC33 3.1 Ka may instead be related to other glacial events in East Antarctica.

There is evidence from glacial striae in the southern Vestfold Hills that the Sørødal Glacier underwent a restricted, northerly-flowing ice advance 3.0-1.5 Ka (the “Chelnok Glaciation”) (Adamson and Pickard, 1986). The extent of this advance has been questioned, however, by Bronge (1996). A core recovered from Long Fjord in the Vestfold Hills also indicates that a localised ice sheet grounded prior to 3.1 Ka (McMinn, *pers. comm.*). From the sedimentological and diatom record, ice is interpreted to have retreated from Long Fjord 3.1-2.5 Ka, readvanced 2.5-1.8 Ka, and then subsequently retreated again (McMinn, *pers. comm.*). Although the events recorded in Sørødal Glacier and Long Fjord are apparently localised, a widespread advance and retreat of ice over Prydz Bay and Mac.Robertson Shelf, including Fram Bank, during, or just after, the hypsithermal maximum could have occurred as the ice adjusted to the transition in palaeoclimate and palaeoceanography. If the retreat of grounded ice across Fram Bank cannot be directly correlatable with the end of the hypsithermal, it may be associated with one of these more localised events.

19.6.3 Late Holocene (3.0 Ka to 2.7 Ka)

Based on reservoir-corrected radiocarbon dates, the *Chaetoceros* assemblage of GC33 was deposited 3.0-2.7 Ka. Diatom assemblages dominated by *Chaetoceros* resting spores are inferred to be associated with extremely high primary production and unusual, early-season warmth (Leventer *et al.*, 1993, 1996). For such as assemblage to form on Fram Bank, portions of Mac.Robertson Shelf may have experienced long intervals of open

water with a shallow, stratified surface layer and less extensive pack ice than now (Rathburn *et al.*, 1997). Stability of the water column implies an influx of fresh water (Rathburn *et al.*, 1997). The most likely source of fresh water would be ice melt from a retreating ice shelf. In Prydz Bay today, sea ice breakout commences in early summer and open water (<10% sea ice) dominates for one or two months of the year (usually January and February). On Fram Bank, however, ice concentrations <10% usually occur for only one month of the year, based on 1978 - 1991 satellite passive microwave data. This is due to the presence of grounded icebergs on the bank that trap the ice and prevent its breakup and dispersal earlier in the season. During deposition of the *Chaetoceros* assemblage on Fram Bank, sea ice breakout may have commenced earlier in the season. Coupled with the influx of fresh water from ice shelf retreat, a stable layer of relatively warm, open water would have existed for a greater period of time over summer, as also suggested by Rathburn *et al.* (1997), creating conditions conducive to diatom blooms and extremely high productivity. It was also suggested in Section 14.6, that the *Chaetoceros* layer at the base of GC1 (Iceberg Alley) was deposited during the transition from the LGM to Holocene interglacial, during which water column conditions may have been similar.

The abundance of *Chaetoceros* resting spores in GC33 may be indicative of increased sea ice, however, based on the hypothesis of Leventer (1992). Analysis of the less abundant, or “background”, diatom taxa in the *Chaetoceros* assemblage from GC33 assist in answering this hypothesis. If sea ice was more extensive it could account for the increased abundance of the sea ice indicator *Pseudonitzschia turgiduloides* in the *Chaetoceros* assemblage, compared to its abundance in the modern coastal assemblage. Alternatively, less extensive sea ice could account for the increased abundance of the open water indicator *F. kerguelensis*, compared to its abundance in either the modern coastal or shelf assemblages. In this instance, it can be argued that development of a more stable water column with the release of relatively warm, fresh water from ice melt could have aided the preferential preservation *P. turgiduloides*' fragile frustules. Weaker water currents during this period would also prevent further mechanical damage to the frustules prior to their burial at the sediment water interface. Based on this evidence, it seems more likely that the *Chaetoceros* assemblage deposited in GC33 from 3.0-2.7 Ka was associated with less extensive sea ice and a well stratified, warm surface water layer, following the retreat of a mid-Holocene ice shelf.

19.6.4 Late Holocene to Present (<2.7 Ka)

Late Holocene cooling commenced 2.7 Ka, as indicated by the onset of deposition of the shelf diatom assemblage and was followed by deposition of the cape assemblage from 2.6 Ka. This assemblage continues to be deposited in the vicinity of Cape Darnley and Fram Bank today. The findings agree with those of Rathburn *et al.* (1997) who, based on an analysis of microfaunal, microfloral and stable-isotope data, also indicate the deposition of an *F. curta* dominated diatom assemblage, similar to modern deposition in Prydz Bay, commenced some time around 2.0-2.7 Ka. In their study, however, the smaller-scale differences between the shelf and cape diatom assemblage, described herein, are not noted.

It is important to comment on the change from the shelf to cape diatom assemblage 2.6 Ka. As observed in this study, even such a subtle change as this is sufficient to indicate that current strength and the depositional regime over Fram Bank was altered in the late Holocene, during the transition from the shelf to cape assemblage. This may have been caused by an increase in the strength and / or extent in the Prydz Bay gyre. Today waters associated with the gyre exit via Cape Darnley / Fram Bank; some continues as a westward flow along Mac.Robertson Shelf, and a portion is recirculated back into the bay by the clockwise motion of the gyre. The westward flowing coastal current is a strong current flowing up to 8.0 sec cm^{-1} (Wong, 1994). There is no evidence to suggest that there was a simultaneous change in sea ice concentration associated with the transition from a cape to shelf diatom assemblage.

There is an increasing amount of evidence to support Late Holocene cooling in Antarctica following a mid- to Late Holocene climatic optimum. This comes from both glacial marine records (Burckle, 1972; Shevenell *et al.*, 1996), lake records (Birnie, 1991; Björk *et al.*, 1991, 1996) and ice core records (Ciais *et al.*, 1992, 1994; Mosley-Thompson, 1996), and infers a strong atmospheric-oceanic interaction. Down core diatom assemblages from the South Atlantic reveal a strong warming during the mid Holocene, followed by a cooling trend in the Late Holocene (Burckle, 1972). This is similarly noted in ice cores from both the Antarctic coast and plateau, which indicate cooling has occurred between 2.0-1.0 Ka (Ciais *et al.*, 1994). More recently, continuously-dated ^{14}C sedimentary records and from the Palmer Deep (Antarctic Peninsula) indicate that cooling commenced 2.4 Ka (Domack and Mayewski, in press). Of significant value is the correlation this record has with the onset of the Northern Hemisphere Neoglacial, which peaks in the Greenland GISP-2 ice core 3.1 Ka and 2.5 Ka, and suggests a linkage between the North Atlantic and Pacific Antarctic (Domack and Mayewski, in press).

19.7 Conclusion

The mid to Late Holocene, depositional environment on Fram Bank is summarised in Table 19.5. The radiocarbon chronology from this core is tentative, due to an anomalously old radiocarbon age from the surface, but the record can be at least closely correlated to other Antarctic climatic events. Prior to 3.8 Ka, an ice shelf is hypothesised to have grounded over Fram Bank. The core lithology consists of sticky, black sandy muds and muddy sands, and is typical of that deposited beneath a basal ice shelf. Diatom frustules are rare to absent in this unit. Open marine deposition commenced 3.1 Ka. There is a transitional lithological boundary in the core, from sand to muddy biosiliceous ooze, and a corresponding increase in concentration of diatom frustules.

From 3.1 Ka to 3.0 Ka, the diatom assemblage in GC33 is analogous to the oceanic assemblage that is today deposited primarily offshore of the continental shelf zone. In GC33, this assemblage is suggested to have been deposited beneath a floating ice shelf as it retreated across Fram Bank. Ice retreat may have been in association with the collapse of the Antarctic hypsithermal, or during the retreat of a more localised glacial event. Uncertainty is due to the tentative age chronology used to date the core.

An assemblage dominated by *Chaetoceros* resting spores was deposited between 3.0 Ka and 2.7 Ka. The assemblage has no modern analogue in Prydz Bay or Mac.Robertson Shelf, but is inferred to represent a period mid-Holocene warming. During this time, unusually early seasonal warmth and an influx of relatively warm, fresh water, from early and complete sea ice breakout runoff from a retreating ice shelf, would lead to the development of a stabilised surface water column. In these favourable conditions, diatom blooms develop and deplete the water column of nutrients, triggering *Chaetoceros* resting spore formation.

Mid- to Late Holocene cooling is represented by the onset of deposition of a shelf diatom assemblage. The shelf assemblage was deposited 2.7-2.6 Ka. Development of

this assemblage in the sediment is dependent on seasonally open water with a nearby sea ice edge, or a recently retreated ice edge. After 2.6 Ka, deposition of the cape assemblage, present in the surface sediments of Fram Bank today, commenced. This current-reworked assemblage implies that during the latest Holocene, bottom water currents become sufficiently strong to be capable of decoupling primary production in the surface waters from the underlying sediment before it settles and is buried. The periodic grounding of icebergs may also cause reworking as they drift across the bank.

Table 19.4. Summary of Holocene palaeoclimate in inner Prydz Bay inferred from GC33.

| Corrected ¹⁴ C Age (Ka) | Core Lithology | Diatom Assemblage | Major Species | Climate Interpretation |
|------------------------------------|---|--------------------|---|--|
| <2.6 | Biosiliceous ooze | Cape | <i>F. curta</i> <i>T. antarctica</i> spores <i>E. antarctica</i> | Modern conditions; increased water current strength & / or gyre intensification compared to Mid / Late Holocene |
| 2.6 – 2.7 | Biosiliceous ooze | Shelf | <i>F. curta</i> <i>F. cylindrus</i> | Mid to Late Holocene climatic cooling; seasonally open water in close proximity to a stable ice shelf |
| 2.7 – 3.0 | Biosiliceous ooze | <i>Chaetoceros</i> | <i>Chaetoceros</i> spores | Mid Holocene climatic warming; open water with stabilised water column (melt-water stratification?); high primary production |
| 3.0 – 3.1 | Transitional boundary from sandy mud to biosiliceous ooze | Oceanic | <i>F. curta</i> <i>F. kerguelensis</i> <i>Chaetoceros</i> spores <i>F. cylindrus</i> | Advance of a floating ice shelf; diatoms advected underneath |
| 3.1 – 3.8 | Sandy mud and muddy sand with IRD | Absent | | Grounded ice shelf; hypsothermal? |

– Chapter 20 –

General Discussion

*Pleistocene / Holocene Climate History of Prydz Bay and
Mac.Robertson Shelf*

The Holocene is widely regarded by some as a period of climatic stability in both the Northern and Southern Hemispheres (Petit *et al.*, 1990; Johnsen *et al.*, 1992; Broecker, 1994; Ciais *et al.*, 1994; Alley *et al.*, 1997). This is despite early hypotheses that the apparent, synchronous advance of alpine glaciers in North America and Europe was due to a far more variable Holocene climate than that implied by the overall trends identified in pollen and marine records (Denton and Karlén, 1973). More recently, however, data is supporting the idea that, although the Holocene is relatively stable compared to, for example, the major climate fluctuations recorded during the Late Pleistocene, it has been subject to rapid climate changes (Stager and Mayewski, 1997; Ice Core Working Group, 1998).

Measurements of soluble impurities from the Greenland Ice Sheet Project (GISP2) ice core indicate that the Holocene has been characterised by a series of millennial-scale climatic shifts (O'Brien *et al.*, 1995b). Similar millennial- and century-scale shifts have also been observed in East Antarctic ice cores (O'Brien *et al.*, 1995b; Mosley-Thompson, 1996; Mayewski *et al.*, 1996) and deep sea sediment cores from the Antarctic Peninsula (Leventer *et al.*, 1996; Shevenell *et al.*, 1996; Brachfeld, 1997; Kirby *et al.*, 1998; Mayewski and Domack, in press), and North Atlantic (Kennett and Ingram, 1995; Bond *et al.*, 1997). The results from the present study, of marine sediments from Prydz Bay and Mac.Robertson Shelf, supplement these findings, providing further evidence to the growing hypothesis that, globally, the Holocene has been a period of rapid, and significant, climate change.

The Pleistocene – Holocene palaeoecology of Prydz Bay and Mac.Robertson Shelf is summarised in Table 20.1, based on the statistical diatom analyses presented herein. The three cores recovered from Prydz Bay (GC29, AA149 and AA186) extend in age from the Late Pleistocene to the present. In the case of AA149 and AA186, the radiocarbon dates are tentative, however, and it is stressed that they be regarded with caution. The Mac.Robertson Shelf cores (GC1, GC2 and GC33) provide a more detailed record for Holocene. The records from GC1 and GC2 are the most intact, and provide the highest resolution data. Both were recovered from quiet, depositional environments on the shelf, and show no evidence of reworking or disturbance. This is supported by the geochemical analyses of Sedwick *et al* (in press).

20.1 Upper Pleistocene (>30.0 Ka to 12.4 Ka)

A tentative, reservoir-corrected radiocarbon age >30.0 Ka is assigned to the base of AA149, from outer Prydz Bay. At this time, open marine deposition was occurring, and the open water indicator *F. kerguelensis* dominated the sedimentary diatom assemblage. The abundance of this species, and other open water taxa, compared to that on the outer shelf today, suggest that seasonal sea ice was less extensive and that warmer surface waters (associated with the ACC?) were probably penetrating across the shelf. Sea ice must have been present for at least some months of the year, as taxa indicative of ice are present in the assemblage. The assemblage is interpreted to have been deposited during an interstadial, intermediate between full glacial and full interglacial conditions, that preceded the LGM.

Evidence for interstadials preceding the LGM, in East Antarctica, have been noted in the Vostok ice core (Lorius *et al.*, 1985; 1992) (Fig. 20.1). The core indicates that an ~100 Ka glacial-interglacial oscillation has occurred over the last 160 Ka, with two well-marked interstadials 103.0-73.0 Ka, and 58.0-30.0 Ka (Lorius *et al.*, 1985; 1992). During these events, air temperatures were significantly warmer than during the Holocene, and up to 3° to 4°C warmer than during the LGM (Lorius *et al.*, 1992). The latter event is tentatively correlated to the warm period inferred by the diatom assemblage at the base of AA149. AA149 is the only core analysed in the present study

to extend back to this age, and the widespread affect that such a warm event could have had over the rest of the bay and Mac.Robertson Shelf is not speculated upon here. On the outer shelf, however, it is at least assumed that seasonal sea ice was less extensive, and warmer surface waters were probably penetrating onto the shelf.

A cold period is indicated in the Vostok ice core from 30.0 Ka to 13.0 Ka (Lorius *et al.*, 1985). Cooling, associated with the onset of LGM conditions, commenced in Prydz Bay, too, ~30.0 Ka, based on the AA149 record. During this time, a floating ice shelf is thought to have formed, extending at least as far as the edge of the continental shelf, and remained in place until 22.5 Ka. The sedimentary diatom assemblage contains poorly preserved frustules in relatively low abundance, evidence for current winnowing and reworking. Light penetration beneath an ice shelf could have been insufficient to support primary production, so diatoms would have been advected under the shelf and then settled at a slower rate compared to open marine deposition. Between 22.5 Ka and 16.5 Ka, the ice shelf became unstable. Changes in the diatom assemblage indicate a transition to open water primary production, and decreased reworking, between 21.4 Ka and 18.0 Ka, followed by ice readvance, until 16.5 Ka.

The diatom and lithology records from inner Prydz Bay (GC29) and Four Ladies Bank (AA186) support the hypothesis that an ice shelf advanced across the continental shelf during the LGM. Ice probably grounded over the inner bay from at least 23.0 Ka, to 12.4 Ka, but formed as a floating ice shelf over Four Ladies Bank from at least 17.0 Ka, to 7.7 Ka. The advancing ice was most likely sourced from an extension of the Lambert Glacier / Amery Ice Shelf, rather than a widespread advance of the East Antarctic ice sheet (Domack *et al.*, 1998) (Fig. 20.2).

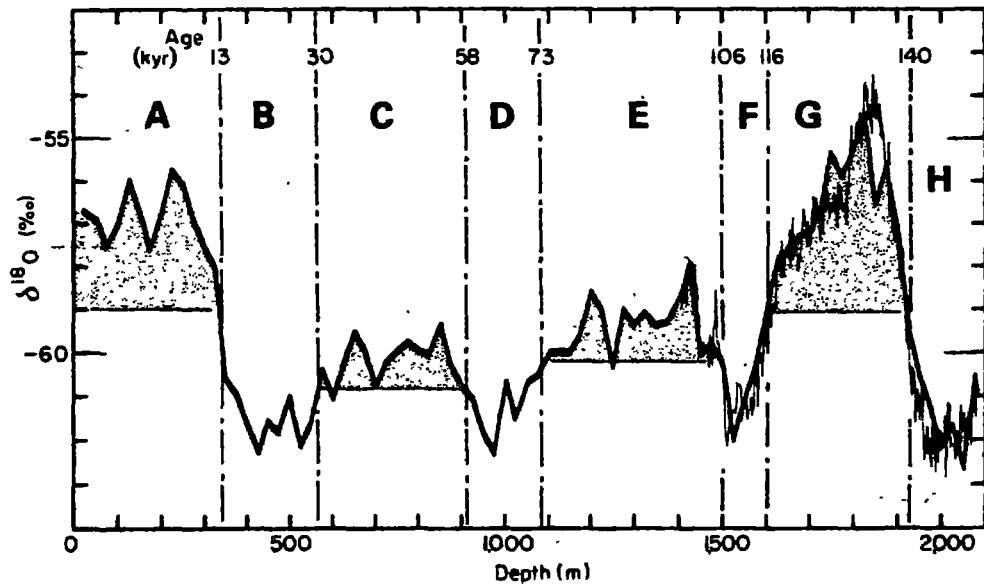


Fig. 20.1. ^{18}O versus depth in the Vostok ice core, defining successive stages and the ages corresponding to the limits between those stages. Warm periods (shaded) are designated A, C, E, and G. Cold periods are designated B, D, F, and H. (From Lorius et al, 1985).

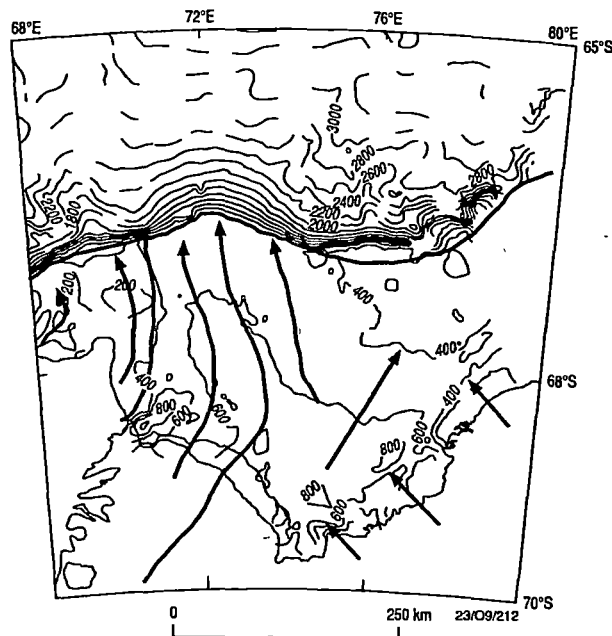


Fig. 20.2. Interpreted ice-flow paths for periods of maximum ice extent in Prydz Bay. (From O'Brien and Harris, 1996).

Vostok $\delta^{18}\text{O}$ records indicate that warming in East Antarctica commenced ~ 18.0 Ka, and was followed by a gradual increase in surface temperature by $\sim 8^\circ\text{C}$, until the Holocene interglacial (Lorius *et al.*, 1985). By 16.5 Ka, the AA149 record indicates that ice had retreated from the edge of the continental shelf, and a diatom assemblage characterised by *F. kerguelensis* was being deposited. This was followed by the retreat of grounded ice from the inner bay, 12.4 Ka, and subsequent deposition of a *F. curta* / *T. antarctica* diatom assemblage. The assemblage is interpreted to indicate the presence of seasonally open water, but perhaps with some loose sea ice present.

20.2 Early to Mid Holocene (<10.0 Ka to 5.0 Ka)

The termination of the LGM, and onset of the Holocene interglacial is a globally recognised event dated at 10.0 Ka (Lorius *et al.*, 1985; Saari *et al.*, 1987). The base of GC1 (Iceberg Alley) has an age of at least ~ 11.5 Ka. If an ice shelf had advanced across Mac.Robertson Shelf during the LGM, by 11.5 Ka it had retreated and a diatom assemblage characterised by the near-monospecific abundance of *Chaetoceros* resting spores was being deposited. The abundance of *Chaetoceros* resting spores is used as a proxy to delineate the maximum summer sea ice retreat at this time. Alternatively, the spores may be indicative of water column stabilisation as a result of fresh water influx from, for example, a retreating ice shelf and / or winter sea ice melt in a warming climate.

A Holocene climatic optimum 11.0-8.0 Ka (Lorius *et al.*, 1979; Ciais *et al.* 1992), at the end of the LGM transition, is suggested based on ice core records from Dome C (East Antarctica). During this time, atmospheric temperatures are estimated to have been 1° to 2°C warmer than today (Ciais *et al.*, 1992). Significant cooling followed (8.0-4.0 Ka) (Ciais *et al.*, 1994), and a prominent climatic event recorded in GISP2 proxies indicate a period of brief cooling ~ 8.2 Ka (Alley *et al.*, 1997). The cause of this event is unknown, but synchronous events in climate proxy records worldwide suggest that it was a global in extent (Alley *et al.*, 1997). Data show it to have been a cold, dry, windy period in, and around, the North Atlantic basin, with at least half the amplitude of the Younger Dryas. The Younger Dryas was the most dramatic climate event to have

occurred since the LGM, during which a rapid change to near glacial conditions 12.9-11.6 Ka occurred (Mayewski *et al.*, 1996). The event is well documented in the Northern Hemisphere, but less well understood in the Southern Hemisphere. Stable isotope records from Antarctic ice cores suggest that its most likely analogue in Antarctica was a slight cooling (an Antarctic cold reversal) that interrupted a two-step deglaciation comprising two warming trends (Jouzel *et al.*, 1995).

In comparison, glacial marine records suggest a mid Holocene climatic optimum 8.0-2.7 Ka (review in Kirby *et al.*, 1998). The mid Holocene diatom record from Prydz Bay and Mac.Robertson Shelf is generally characterised by more open water assemblages, suggesting climatic warming and less extensive sea ice. In Iceberg Alley, however, sea ice was probably not breaking out fully during the summer months between the termination of the LGM and ~7.0. Rather, summer ice conditions similar to that in shallow, coastal areas of Prydz Bay today were present. The GC1 record suggests a climatic optimum between 6.9 Ka and 6.5 Ka, during which *Corethron*-rich layers formed in the sediment. The layers are interpreted to represent periods during which unusual episodes of warmth occurred, resulting in intense water stratification and enhanced spring *Corethron* blooms. The unusual conditions may have triggered mass sexual reproduction and, for the frustules to preserve in sediment, concentration in the water column by an oceanographic eddy. On Four Ladies Bank, open water deposition, characterised by an oceanic, sedimentary diatom assemblage, commenced 7.7 Ka, and continued throughout the mid Holocene until 2.7 Ka.

Around the same time, open marine conditions were becoming established in Nielsen Basin, between 5.7 Ka and 5.5 Ka. Prior to this, the diatom record from GC2 implies that a floating ice shelf persisted here. The assemblage is characteristic of one that has undergone dissolution, probably due to slower sedimentation rates beneath, for example, floating ice. Without a longer record from this site, the duration over which such an ice shelf existed can only be speculated upon. It may have been a remnant of the LGM, although this seems unlikely given that open water deposition was occurring elsewhere on Mac.Robertson Shelf and in Prydz Bay from at least 10.0 Ka. GC2 may record the

presence of an ice shelf over or near Nielsen Basin during the last stages of a Younger Dryas (or similar) cold episode. Evidence for the Younger Dryas indicate that it was an event mainly concentrated in the Northern Hemisphere (Broecker *et al.*, 1985), but eustatic sea level variation would have affected marine-based ice around Antarctica (Denton *et al.*, 1989). Larter and Vanneste (1995) suggest that a subglacial deltas on the west Antarctic Peninsula were produced by a late-stage readvance of grounding lines during the Younger Dryas. Alternatively, an ice shelf over Nielsen Basin may have reformed during the ice advance associated with the Antarctic hypsithermal.

20.3 Mid Holocene to Present (<5.0 Ka)

The Late Holocene is characterised by a stable average temperature with short-lived fluctuations (Ciais *et al.*, 1994). A noticeably warmer climatic episode occurred around 4.0 Ka, and an important cooling occurred between 2.0 Ka and 1.0 Ka (Ciais *et al.*, 1994). The present study suggests that climatic cooling has generally occurred in coastal East Antarctica since the mid Holocene, interrupted by brief warm intervals before the development of modern conditions. The transition in diatom assemblages, from shelf to coastal, in Nielsen Basin 5.5 Ka suggests that the persistence of summer sea ice became more frequent. A similar transition in inner Prydz Bay occurred between 3.2 Ka and 2.8 Ka. Over Fram Bank, an ice shelf may have readvanced and grounded 3.8-3.1 Ka, then retreated with climatic warming to become a floating ice shelf 3.1-3.0 Ka, before retreating completely. The diatom assemblage deposited following the, hypothesised, final retreat is characterised by *Chaetoceros* resting spores, perhaps formed in response to the localised influx of fresh water, stabilised water column. Between 2.7 Ka and 2.6 Ka, the diatom assemblage on Fram Bank suggests that water was seasonally ice free (<10% cover), but a stationary ice edge remained nearby. Conditions have since seen the deposition of the modern, reworked cape assemblage – interpreted as forming in response to increasing water current strength.

On Four Ladies Bank, there has been a general change in the diatom assemblages deposited since 2.7 Ka, from one indicative of seasonally open water with a nearby, stationary ice shelf, to one indicative of more open water conditions between 2.3 Ka and

1.8 Ka. Evidence for a brief, late Holocene warm interval also comes from inner Prydz Bay, between 2.8 Ka and 2.0 Ka, and the *Corethron* layer in Iceberg Alley, deposited between 1.9 Ka and 1.8 Ka. This event is not recorded in Nielsen Basin, less than 90 km away. The apparently stable conditions implied by the deposition of the coastal assemblage in GC2, since 5.5 Ka, supports the findings of Sedwick *et al.* (in press), however, based on geochemical analyses. They suggest that GC1, on the outer shelf (Iceberg Alley) records three episodes of intense export production during the Holocene, separated by periods of ~1500 years, and the less pronounced “bloom” (*Corethron*) episodes. In the present study, these episodes are calculated to occur on average every ~250 years as peaks in *Corethron* abundance. In contrast, GC2, on the inner shelf (Nielsen Basin), suggests that there has been a roughly constant proportion of biogenic and lithogenic material accumulating at this site since the mid to Late Holocene (Sedwick *et al.*, in press).

Table 20.1. Pleistocene / Holocene palaeoenvironments in Prydz Bay and Mac.Robertson Shelf – summary of results

| Corrected radiocarbon years (Ka) | Core | Palaeoenvironment |
|----------------------------------|-------|---|
| <30.0 Ka | AA149 | Interstadial; warmer (by ~2°C?). Open marine deposition on Fram Bank (outer shelf), dominated by <i>F. kerguelensis</i> . |
| 30.0 – 22.5 | AA149 | Ice shelf advance over outer shelf (pre LGM glacial maximum). Diatom assemblage reworked and winnowed due to increased currents and/or iceberg calving. |
| 23.0 - 12.4 | GC29 | Ice grounded over inner bay and persists till 12.4 Ka. |
| 22.5 – 16.5 | AA149 | Alternating open water – reworked diatom assemblages. Ice shelf retreats from Trough Mouth Fan (= interstadial or brief warming event pre-LGM). Ice shelf advances and reaches maximum 22.5-21.4 Ka (LGM), retreats 21.4-18.0 Ka, and advances again 18.0-16.5 Ka. Remains grounded over inner bay. |
| 17.0 – 7.7 | AA186 | Ice shelf present Four Ladies Bank. |
| ? – 10.0 Ka | GC1 | <i>Chaetoceros</i> resting spores may delineate max. summer ice retreat on Mac.Robertson Shelf during LGM. OR, influx of fresh water during decline of LGM and ice retreat. |
| 16.5 – 2.5 | AA149 | Ice shelf retreats from Fram Bank; deposition dominated by <i>F. kerguelensis</i> . |
| 12.4 – 3.2 | GC29 | Grounded ice shelf retreats from inner bay, onset of open water deposition. Seasonally open water with loose sea ice (<i>F. curta</i> / <i>T. antarctica</i>). |
| ? – 5.7 | GC2 | Ice shelf present over Nielsen Basin. |

Table 20.1 Cont.

| Corrected radiocarbon years (Ka) | Core | Palaeoenvironment |
|----------------------------------|---------|--|
| 10.0 - 6.9 | GC1 | Seasonal sea ice that does not fully break out over the shelf. Preferential preservation in the deep basin of Iceberg Alley. |
| 7.7 - 2.7 | AA186 - | Onset of open marine deposition over Four Ladies Bank; seasonally open water with oceanic assemblage. |
| 6.9 - 6.5 | GC1 | Climatic optimums recorded by <i>Corethron</i> . |
| 5.7 - 5.5 | GC2 | Onset of open marine deposition over Nielsen Basin. |
| <5.5 | GC2 | Cooling; shelf to coastal deposition; increased persistence of summer ice. |
| 3.8 - 3.1 | GC33 | Ice grounded over Fram Bank. |
| 3.2 - 2.8 | GC29 | Cooling; transition from open shelf to shelf; seasonally open water with nearby stationary ice edge. |
| 3.1 - 3.0 | GC33 | Floating ice shelf. |
| 3.0 - 2.7 | GC33 | Influx of fresh water; <i>Chaetoceros</i> deposition. |
| 2.8 - 2.0 | GC29 | Brief warming in inner bay and/or increased wind? <i>F. curta</i> / <i>T. antarctica</i> . |
| 2.7 - 2.6 | GC33 | Cooling; seasonally open water by nearby stationary ice edge. |
| <2.6 | GC33 | Increased current strength and / or gyre intensification around Cape Darnley as water exits bay. Associated with cooling? |

Table 20.1 Cont.

| Corrected radiocarbon years (Ka) | Core | Palaeoenvironment |
|----------------------------------|-------|---|
| 2.7 - 2.3 | AA186 | Cooling; change from oceanic to shelf deposition. |
| <2.5 | AA149 | Cooling; transition from oceanic B (most open) to oceanic A (less <i>F. kerguelensis</i>). |
| 2.3 - 1.8 | AA186 | Warming; transition from shelf to oceanic A. |
| <2.0 | GC29 | Cooling; transition from open shelf to shelf; modern assemblage. |
| 1.9 - 1.8 | GC1 | Climatic optimum; <i>Corethron</i> deposition. |
| 1.8 - 0.5 | AA186 | Increased current strength and / or gyre intensification over Four Ladies Bank. Associated with cooling? |
| <0.5 | AA186 | Modern oceanic assemblage. |

– Chapter 21 –

Summary and Future Recommendations

21.1 Summary

The objectives of this project have been achieved successfully. Diatom abundance and distribution in surface sediment from Prydz Bay and Mac.Robertson Shelf were determined from over 100 samples. Using statistical methods (cluster analysis, NMDS, SNK, ANOVA, and multiple regression) to objectively analyse the data, four diatom assemblages were identified, and their relationship to oceanographic variables determined. The assemblages identified were:

1. Coastal – characterised by sea ice taxa. Distributed in near-shore and shallow water areas where sea ice may not seasonally break out.
2. Shelf – characterised by sea ice and ice edge taxa. Distributed on the continental shelf where seasonally open water is present.
3. Oceanic – characterised by open water taxa. Distributed offshore of the continental shelf break, and where the Prydz Bay gyre transports water from offshore into Prydz Bay.
4. Cape – a current winnowed assemblage characterised by robust and heavily silicified taxa. Distributed on Mac.Robertson Shelf, adjacent to Cape Darnley.

Six gravity cores were analysed using the same methods as above, and the down core diatom assemblages compared to those in the surface sediment. Deposition of analogous assemblages was inferred to have occurred during ecologically similar conditions to those forming the assemblages today. Assemblages with no modern analogue were compared to similar assemblages described elsewhere in Antarctic marine sediment, and their known ecology considered. The results, summarised in Table 20.1, suggest that, in East Antarctica, the Holocene has been subject to rapid climate changes. These findings agree with other marine and ice core studies, both Antarctic and global (e.g. Kennett and Ingram, 1995; O'Brien *et al.*, 1995b; Leventer *et al.*, in press; Mayewski *et al.*, 1996; Mosley-Thompson, 1996; Bond *et al.*, 1997; Mayewski and Domack, in press).

21.2 Future Recommendations

To enhance the contributions of this study, several recommendations are suggested that could be carried out as future research:

1. Due to time and equipment restraints, magnetic susceptibility and organic carbon analyses were not conducted. Both are now relatively routine procedures and can be used as measures of palaeoproductivity.
2. The production of quantitative (rather than qualitative) diatom slides to determine absolute diatom abundance is recommended. This is a relatively important, but efficient and economical, procedure that can be used to improve palaeocological interpretations (Scherer, 1995). It also has the advantage of producing permanent slides in which the diatom frustules are evenly distributed, without the “clumping” effect of qualitative slides that can make counting difficult and less accurate.
3. A more detailed analysis of cores from Nielsen Basin and Iceberg Alley. The sedimentary and diatom data obtained from these sites provided the most intact and detailed records. The quiet, sedimentary environments of both are ideal for recording long- and short-term depositional / climatic events.

A more extensive coring program from Nielsen Basin, in particular, could yield comparable, ultra-high resolution records similar to those obtained, for example, from the Antarctic Peninsula's Palmer Deep (Leventer *et al.*, 1996; Kirby *et al.*, 1998; Domack and Mayewski, in press). Burton Basin, adjacent to Nielsen Basin on Mac.Robertson, and the Nanok and Lambert Deeps (if sea ice conditions were favourable) should also be regarded as future coring sites.

A comparison of these with other marine records from West Antarctica will contribute to our understanding the response of the Antarctic Ice Sheet to past, and future, climate change.

– Chapter 22 –

References

- Adamson, D.A. and Pickard, J., 1986. Cainozoic history of the Vestfold Hills. In: J. Pickard (Editor), *Antarctic Oasis. Terrestrial Environments and History of the Vestfold Hills*. Academic Press, Sydney, pp. 63-93.
- Alldrege, A.L. and Silver, M.W., 1982. Abundance and production rates of floating diatom mats (*Rhizosolenia castracanei* and *R. imbricata* var. *shrubsolei*) in the eastern Pacific Ocean. *Marine Biology*, 66: 83-88.
- Alley, R.B., Mayewski, P.A., Sowers, T., Stuiver, M. and Clark, P.U., 1997. Holocene climatic instability: a prominent, widespread event 8200 yr ago. *Geology*, 25(6): 483-486.
- Allison, I., Tivendale, C., Akerman, G., Tann, J. and Willis, R.H., 1982. Seasonal variations in the surface energy exchanges over Antarctic sea ice and coastal waters. *Annals of Glaciology*, 3: 12-16.
- Allison, I., 1989. The East Antarctic sea ice zone: ice characteristics and drift. *GeoJournal*, 18(1): 103-115.
- Allison, I., Brandt, R. and Warren, S., 1993. East Antarctic sea ice: albedo, thickness distribution, and snow cover. *Journal of Geophysical Research*, 98(C7): 12417-12429.
- Anderson, J., Kurtz, D., Domack, E. and Balshaw, K., 1980. Glacial and glacial marine sediments of the Antarctic continental shelf. *Journal of Geology*, 88: 399-414.
- Anderson, J., 1989. Antarctica's glacial setting. In: J. Anderson and B. Molnia (Editors), *Short Course in Geology. Glacial Marine Sedimentation*. American Geophysical Union, Washington DC, pp. 11-58.
- Andreas, E.L. and Ackley, S.F., 1982. On the differences in ablation seasons of Arctic and Antarctic sea ice. *Journal of Atmospheric Science*, 39: 440-447.
- Arrigo, K.R., Robinson, D.H. and Sullivan, C.W., 1993. A high resolution study of the platelet ice ecosystem in McMurdo Sound, Antarctica: photosynthetic and bio-optical characteristics of a dense microalgal bloom. *Marine Ecology Progress Series*, 98: 173-185.

- Baldauf, J. and Barron, J., 1990. Evolution of biosiliceous sedimentation patterns - Eocene through Quaternary: paleoceanographic response to polar cooling. In: U. Bleil and J. Thiede (Editors), *Geological History of the Polar Oceans: Arctic Versus Antarctic. NATO ASI Series*. Kluwer Academic Publishers, Dordrecht, pp. 575 - 609.
- Baldauf, J. and Barron, J., 1991. Diatom biostratigraphy: Kerguelen Plateau and Prydz Bay regions of the Southern Ocean. *Proceedings of the Ocean Drilling Program, Scientific Results*, 119: 547-598.
- Barker, P., Fontes, J., Gasse, F. and Druart, J., 1994. Experimental dissolution of diatom silica in concentrated salt solutions and implications for paleoenvironmental reconstruction. *Limnology and Oceanography*, 39(1): 99-110.
- Barron, J., 1985. Miocene to Holocene plankton diatoms. In: H. Bolli, J. Saunders and K. Perch-Nielsen (Editors), *Plankton Stratigraphy*. Cambridge University Press, Cambridge, pp. 763-809.
- Barron, J., 1993. Diatoms. In: J. Lipps (Editor), *Fossil Prokaryotes and Protists*. Blackwell Scientific Publications, Boston, pp. 155-167.
- Battarbee, R., 1986. Diatom Analysis. In: B. Berglund (Editor), *Handbook of Holocene Palaeoecology and Palaeohydrology*. John Wiley and Sons, New York, pp. 527-569.
- Beals, E., 1984. Bray-Curtis ordination: an effective strategy for analysis of multivariate ecological data. *Advances in Ecological Research*, 14: 1-55.
- Birnie, J., 1990. Holocene environmental change in South Georgia: evidence from lake sediments. *Journal of Quaternary Science*, 5(3): 171-187.
- Björck, S., Hjort, C., Ingolsson, O. and Skog, G., 1991. Radiocarbon dates from the Antarctic Peninsula region: problems and potential. *Quaternary Proceedings*, 1: 55-65.
- Björck, S., Olsson, S., Ellis-Evans, C., Håkansson, H., Humlum, O. and de Lirio J.M., 1996. Late Holocene palaeoclimatic records from lake sediments on James Ross Island, Antarctica. *Palaeogeography, Palaeoclimatology, Palaeoecology*, 121: 195-220.

- Boden, B.P. and Reid, F.M.H., 1989. Marine plankton diatoms between Cape Town and Prince Edward Islands (SW Indian Ocean). *South African Journal of Antarctic Research*, 19(2): 2-45.
- Bond, G., Showers, W., Cheseby, M., Lotti, R., Almasi, P., deMenocal, P., Priore, P., Cullen, H., Haidas, I., and Bonani, G., 1997. A pervasive millennial-scale cycle in North Atlantic Holocene and glacial climates. *Science*, 278: 1257-1266.
- Boulton, G.S., 1990. Sedimentary and sea level changes during glacial cycles and their control on glacial marine facies architecture. *Glacial Marine Environments: Processes and Sediments*, 53 (Geological Society Special Publication): 15-52.
- Brachfeld, S., 1997. Research on Holocene climate variability using magnetic methods. In: I. Goodwin (Editor), *Late Quaternary Sedimentary Record of the Antarctic Ice Margin Evolution (ANTIME) Workshop Abstracts*, Hobart, Tasmania, p.15.
- Brady, H.T., 1977. *Thalassiosira torokina* n. sp. (diatom) and its significance in Late Cenozoic biostratigraphy. *Antarctic Journal of the United States*, 122-123.
- Broecker, W.S., Peteet, D.M. and Rind, D., 1985. Does the ocean-atmosphere system have more than one stable mode of operation? *Nature*, 315: 21-26.
- Broecker, W.S., 1994. Massive iceberg discharges as triggers for global climate change. *Nature*, 372: 421-424.
- Bronge, C., 1996. Hydrographic and climatic changes in influencing the proglacial Druzhby drainage system, Vestfold Hills, Antarctica. *Antarctic Science*, 8(4): 379-388.
- Buck, K., Bolt, P. and Garrison, D., 1990. Phagotrophy and fecal pellet production by an athecate dinoflagellate in Antarctic sea ice. *Marine Ecology Progress Series*, 66: 75-84.
- Budd, W.F., Corry, M.J. and Jacka, T.H., 1982. Results from the Amery Ice Shelf Project. *Annals of Glaciology*, 3: 36-41.
- Burckle, L., 1972. Diatom evidence bearing on the Holocene in the South Atlantic. *Quaternary Research*, 2: 323-326.
- Burckle, L., 1984a. Diatom distribution and paleoceanographic reconstruction in the Southern Ocean - present and last glacial maximum. *Marine Micropaleontology*, 9: 241-261.

- Burckle, L., 1984b. Ecology and paleoecology of the marine diatom *Eucampia antarctica* (Castr.) Manguin. *Marine Micropaleontology*, 9: 77-86
- Burckle, L. and Cirilli, J., 1987. Origin of diatom ooze belt in the Southern Ocean: Implications for late Quaternary paleoceanography. *Micropaleontology*, 33(1): 82-86.
- Burckle, L., Jacobs, S. and McLaughlin, R., 1987. Late austral spring diatom distribution between New Zealand and the Ross Ice Shelf, Antarctica: hydrographic and sediment correlations. *Micropaleontology*, 33(1): 74-81.
- Calvert, S.E., 1968. Silica balance in the oceans and diagenesis. *Nature*, 2: 919-920.
- Ciais, P., Petit, J.R., Jouzel, J., Lorius, C., Barkov, N.I., Lipenkov, V. and Nicolaïev, V., 1992. Evidence for an early Holocene climatic optimum in the Antarctic deep ice-core record. *Climate Dynamics*, 6: 169-177.
- Ciais, P., Jouzel, J., Petit, J.R., Lipenkov, V. and White, J.W.C., 1994. Holocene temperature variations inferred from six Antarctic ice cores. *Annals of Glaciology*, 20: 427-436.
- Ciesielski, P. and Weaver, F., 1974. Early Pliocene temperature changes in the Antarctic seas. *Geology*, 2: 511-515.
- Clemons, M.J. and Miller, C.B., 1984. Blooms of large diatoms in the oceanic, subarctic Pacific. *Deep-Sea Research*, 31: 85-99.
- Colhoun, E., 1991. Geological evidence for changes in the East Antarctic ice sheet (60° - 120°E) during the last glaciation. *Polar Record*, 27(163): 345 - 355.
- Cook, E.T., Bird, T., Peterson, M., Barbetti, M., Buckley, B., D'Arrigo, R., and Francey, R., 1992. Climatic change over the last millennium in Tasmania reconstructed from tree-rings. *The Holocene*, 2(3): 205-217.
- Crawford, R. and Round, F., 1989. *Corethron* and *Mallomonas* - some striking morphological similarities. In: J.C. Green, B.S.C. Leadbeater and W.C. Diver (Editors), *The Chromophyte Algae: Problems and Perspectives*. Clarendon Press, Oxford.
- Crawford, R., 1995. The role of sex in the sedimentation of a marine diatom bloom. *Limnology and Oceanography*, 40(1): 200-204.

- Cunningham, W., 1997. *The Use of Modern and Fossil Diatom Assemblages as Climate Proxies in the Central and Western Ross Sea, Antarctica*. Masters Thesis, University of Colorado, 233 pp.
- Cunningham, W.L., Leventer, A., Andrews, J.T., Jennings, A.E. and Licht, K.J., in press. Late Pleistocene - Holocene marine conditions in the Ross Sea, Antarctica: evidence from the diatom record. *The Holocene*.
- Davis, C.O., Hollibaugh, J.T., Seibert, D.L.R., Thomas, W.H., and Harrison, P.J., 1980. Formation of resting spores by *Leptocylindrus danicus* (Bacillariophyceae) in a controlled experimental ecosystem. *Journal of Phycology*, 16: 296-302.
- DeFelice, D. and Wise, S., 1981. Surface lithofacies, biofacies, and diatom diversity patterns as models for delineation of climatic change in the southeast Atlantic Ocean. *Marine Micropaleontology*, 6: 29-70.
- DeMaster, D.J., 1981. The supply and accumulation of silica in the marine environment. *Geochimie et Cosmochimie Acta*, 45: 1715-1732.
- DeMaster, D.J., Dunbar, R.B., Gordon, L.I., Leventer, A., Nittrouer, C.A., and Walker, O.S., 1992. Cycling and accumulation of biogenic silica and organic matter in high latitude environments: the Ross Sea. *Oceanography*, 5(3): 146-153.
- Denton, G.H. and Karlén, W., 1973. Holocene climatic variations - their pattern and possible cause. *Quaternary Research*, 3: 155-205.
- Denton, G.H., Blockheim, J.G., Wilson, J.G. and Stuiver, M., 1989. Late Wisconsin and Early Holocene glacial history, inner Ross Embayment, Antarctica. *Quaternary Research*, 31: 151-182.
- Domack, E., 1988. Biogenic facies in the Antarctic glacimarine environment: Basis for a polar glacimarine summary. *Palaeogeography, Palaeoclimatology, Palaeoecology*, 63: 357-372.
- Domack, E., Jull, A., Anderson, J., Linick, T. and Williams, C., 1989. Application of tandem accelerator mass-spectrometer dating to Late-Pleistocene-Holocene sediments of the East Antarctic continental shelf. *Quaternary Research*, 31: 277-287.

- Domack, E., Jull, A. and Donahue, D., 1991a. Holocene chronology for the unconsolidated sediments at Hole 740A: Prydz Bay, East Antarctica. *Proceedings of the Ocean Drilling Program, Scientific Results*, 119: 727-750.
- Domack, E., Jull, A. and Nakao, S., 1991b. Advance of East Antarctic outlet glaciers during the hypsithermal: Implications for the volume state of the Antarctic ice sheet under global warming. *Geology*, 19(11): 1059-1062.
- Domack, E.W., Mashiotta, T.A., Ishman, S.E. and Burkley, L.A., 1993. 300-year productivity cyclicity in organic matter preservation in Antarctic fjord sediments. In: J. Kennett and D. Warnke (Editors), *The Antarctic Paleoenvironment: A Perspective on Global Change*. American Geophysical Union, Washington DC, pp. 262-272.
- Domack, E., McClennen, C., Manley, P. and Ishman, S., 1994. Very high resolution stratigraphy of Late Quaternary glacial marine sediments in fjords and offshore basins, Antarctic Peninsula. *Terra Antarctica*, 1(2): 269-270.
- Domack, E., O'Brien, P., Harris, P., Taylor, F., Quilty, P., DeSantis, L., Raker, B., 1998. Late Quaternary sediment facies in Prydz Bay, East Antarctica and their relationship to glacial advance onto the continental shelf. *Antarctic Science*, 10(3): 234-244.
- Domack, E.W. and Mayewski, P.A., in press. Bi-polar ocean linkages: evidence from Late Holocene Antarctic marine and Greenland ice core records. *The Holocene*.
- Donegan, D. and Schrader, H., 1982. Biogenic and abiogenic components of laminated hemipelagic sediments in the central Gulf of California. *Marine Geology*, 48: 215-237.
- Dunbar, R., Dehn, M. and Leventer, A., 1984. Distribution of biogenic components in surface sediments from the Antarctic continental shelf. *Antarctic Journal of the United States*: 126-128.
- Dunbar, R., Anderson, J. and Domack, E., 1985. Oceanographic influences on sedimentation along the Antarctic continental shelf. In: S. Jacobs (Editor), *Oceanology of the Antarctic Shelf*. *Antarctic Research Series*, 43. American Geophysical Union, Washington DC, pp. 291-312.

- Dunbar, R., Leventer, A. and Stockton, W., 1989. Biogenic sedimentation in McMurdo Sound, Antarctica. *Marine Geology*, 85: 155-179.
- Eglinton, T., Benitez-Nelson, B.C., Pearson, A., McNichol, A.P., Bauer, J., and Druffel, E.R.M., 1997. Variability in radiocarbon ages of individual organic compounds from marine sediments. *Science*, 227: 796-799.
- El Sayed, S.Z., Biggs, D.C. and Holm-Hansen, O., 1983. Phytoplankton standing crop, primary productivity, and near-surface nitrogenous nutrient fields in the Ross Sea, Antarctica. *Deep-Sea Research*, 30: 871-886.
- Everitt, D.A. and Thomas, D.P., 1986. Observations of seasonal changes in diatoms at inshore localities near Davis Station, East Antarctica. *Hydrobiologia*, 139: 3-12.
- Feldman, D., Gagnon, J., Hofmann, R. and Simpson, J., 1988. *StatView*. Abacus Concepts Inc., Berkeley, California.
- Fenner, J., Schrader, H. and Wienigk, H., 1976. Diatom phytoplankton studies in the Southern Pacific Ocean, composition and correlation to the Antarctic Convergence and its paleoecological significance. *Initial Reports of the Deep Sea Drilling Project*, 35: 757-813.
- Field, J., Clarke, K. and Warwick, R., 1982. A practical strategy for analysing multispecies distribution patterns. *Marine Ecology Progress Series*, 8: 37-52.
- Franklin, D., 1993. Recent diatom and foraminiferal assemblages in surficial sediments of Prydz Bay, Antarctica. *ANARE Research Notes*, 90, Antarctic Division, Kingston, Tasmania, 28 pp.
- Franklin, D. and Marchant, H., 1995. Parmales in sediments of Prydz Bay, East Antarctica: a new biofacies and paleoenvironmental indicator of cold water description? *Micropaleontology*, 41(1): 89-94.
- Franklin, D.C., 1997. *The Sedimentology of Holocene Prydz Bay: Sedimentary Patterns and Processes*. PhD Thesis, Institute of Antarctic and Southern Ocean Studies, University of Tasmania, Hobart, 204 pp.
- Fryxell, G. and Hasle, R., 1971. *Corethron criophilum* Castracane: its distribution and structure. In: G.A. Llano and I.E. Wallen (Editors), *Biology of the Southern Seas (IV)*. *Antarctic Research Series*, 17(4). American Geophysical Union, Washington DC, pp. 335-346.

- Fryxell, G., 1977. *Thalassiosira australis* Peragallo and *T. lentiginosa* (Janish) G. Fryxell, comb. nov.: two Antarctic diatoms (Bacillariophyceae). *Phycologia*, 16(1): 95-104.
- Fryxell, G. and Hasle, G.R., 1979a. The genus *Thalassiosira*: *T. trifulta* sp. nova and other species with tricolunar supports on strutted processes. *Nova Hedwigia*, 64: 13-32.
- Fryxell, G.A. and Hasle, G.R., 1979b. The genus *Thalassiosira*: species with internal extensions of the strutted processes. *Nova Hedwigia, Beih*, 54: 67-98.
- Fryxell, G. and Hasle, G.R., 1980. The marine diatom *Thalassiosira oestrupii*: structure, taxonomy and distribution. *American Journal of Botany*, 67(5): 804-814.
- Fryxell, G., Doucette, G. and Hubbard, G., 1981. The genus *Thalassiosira*: the bipolar diatom *T. antarctica* Comber. *Botanica Marina*, 24: 321-335.
- Fryxell, G. and Hasle, G.R., 1983. The Antarctic diatoms *Thalassiosira dichotomica* (Kozlova) comb. Nov. and *T. ambigua* Kozlova. *Polar Biology*, 2: 53-62.
- Fryxell, G., Kang, S. and Reap, M., 1987. AMERIEZ 1986: phytoplankton at the Weddell Sea ice edge. *Antarctic Journal of the United States*, 22: 173-175.
- Fryxell, G., Reap, M. and Kang, S., 1988. Antarctic phytoplankton - dominants, life stages, and indicators. *Antarctic Journal of the United States*, 23: 129-133.
- Fryxell, G.A. and Kendrick, G.A., 1988. Austral spring microalgae across the Weddell Sea ice edge: spatial relationships found along a northward transect during AMERIEZ 83. *Deep-Sea Research*, 35(A): 1-20.
- Fryxell, G., 1994. Planktonic marine diatom winter stages: Antarctic alternatives to resting spores. *Proceedings of the 11th International Diatom Symposium*. California Academy of Sciences, pp. 437-448.
- Fukai, F., Omoto, K. and Okabe, S., 1986. Nutrient depression in the blooming area of Prydz Bay, Antarctica. *Memoirs of the National Institute of Polar Research*, 44: 43-54.
- Garrison, D. and Buck, K., 1985. Sea-ice algal communities in the Weddell Sea: species composition in the ice and plankton assemblages. In: J. Gray and M. Christiansen (Editors), *Marine Biology of Polar Regions and Effects of Stress on Marine Organisms*. John Wiley and Sons Ltd., pp. 103-121.

- Garrison, D.L., Buck, K.R. and Fryxell, G.A., 1987. Algal assemblages in Antarctic pack ice and ice-edge plankton. *Journal of Phycology*, 23: 564-572.
- Garrison, D.L. and Buck, K.R., 1989. The biota of Antarctic pack ice in the Weddell Sea and Antarctic Peninsula regions. *Polar Biology*, 10: 211-219.
- Garrison, D. and Close, A., 1993. Winter ecology of the sea ice biota in Weddell Sea pack ice. *Marine Ecology Progress Series*, 96: 17-31.
- Gauch, H.G.J., 1982. *Multivariate Analysis in Community Ecology*. Cambridge University Press, Cambridge, 289 pp.
- Gersonde, R., 1984. Siliceous microorganisms in sea ice and their record in sediments in the southern Weddell Sea (Antarctica). In: M. Ricard (Editor), *Proceedings of the Eight International Diatom Symposium*. Koeltz Scientific Books, Koenigstein, pp. 549-566.
- Gersonde, R. and Wefer, G., 1987. Sedimentation of biogenic siliceous particles in Antarctic waters from the Atlantic sector. *Marine Micropaleontology*, 11: 311-332.
- Gloersen, P., Campbell, W.J., Cavalieri, D.J., Comiso, J.C., Parkinson, C.L., and Zwally, H.J., 1992. *Arctic and Antarctic sea ice, 1978-1987: Satellite Passive-Microwave Observations and Analysis*. NASA Special Publication (511), Washington DC, 290 pp.
- Gordon, A., 1971. Oceanography of Antarctic waters. In: J. Reid (Editor), *Antarctic Oceanology 1. Antarctic Research Series*, 15. American Geophysical Union, Washington DC, pp. 169-203.
- Gordon, A. and Molinelli, E.M., 1982. *Southern Ocean Atlas. Thermohaline Chemical Distributions and the Atlas Data Set*. Columbia University Press, New York, 111 pp.
- Grigor'yev, Y.A., 1970. Hydrological investigations in Prydz Bay. *Trudy Sovetskoi Antarkticheskoi Ekspeditsii*, 54: 180-199.
- Grove, J.H., 1988. *The Little Ice Age*. Methuen, New York, 498 pp.
- Hallegraeff, G.M. (1986) Taxonomy and morphology of the marine plankton diatoms *Thalassionema* and *Thalassiothrix*. *Diatom Research*, 1(1): 57-80.
- Hambrey, M.J., 1994. *Glacial Environments*. UCL Press, London, 292 pp.

- Harden, S.L., DeMaster, D.J. and Nittrouer, C.A., 1992. Developing sediment geochronologies for high-latitude continental shelf deposits. *Marine Geology*, 103: 69-97.
- Harris, P., O'Brien, P., Sedwick, P. and Truswell, E., 1996. Late Quaternary history of sedimentation on the Mac.Robertson Shelf, East Antarctica: problems with ¹⁴C-dating of marine sediment cores. *Papers and Proceedings of the Royal Society of Tasmania*, 130(2): 47-53.
- Harris, P. and O'Brien, P., 1996. Geomorphology and sedimentology of the continental shelf adjacent to Mac.Robertson Land, East Antarctica: a scalped shelf. *Geo-Marine Letters*, 16: 287-296.
- Harris, P., O'Brien, P.E., Quilty, P.G., Taylor, F., Domack, E., DeSantis, L., and Raker, B., 1997a. *Post Cruise Report, Antarctic CRC Marine Geoscience: Vincennes Bay, Prydz Bay and Mac.Robertson Shelf: AGSO Cruise 186, ANARE Voyage 5, 1996/97 (BRAD)*, Antarctic CRC, Hobart (Australia).
- Harris, P., Taylor, F., Domack, E., DeSantis, L., Goodwin, I., Quilty, P.G., and O'Brien, P.E., 1997b. Glacimarine siliclastic muds from Vincennes Bay, East Antarctica: preliminary results of an exploratory cruise in 1997. *Terra Antarctica*, 4(1): 11-20.
- Harris, P.T. and O'Brien, P.E., in press. Bottom currents, sedimentation and ice-sheet retreat facies successions on the Mac.Robertson Shelf, East Antarctica. *Marine Geology*.
- Harris, P.T., Taylor, F., Leitchenkov, G., Pushina, Z., O'Brien, P.E. and Masotov, VN, in press. Lithofacies distribution in relation to the geomorphic provinces of Prydz Bay, East Antarctica. ANTIME issue of *Antarctic Science*.
- Hart, T.J., 1934. On the phytoplankton of the southwest Atlantic and the Bellingshausen Sea, 1929-1931. *"Discovery" Report*, 8: 1-268.
- Hart, T., 1942. Phytoplankton periodicity in Antarctic surface waters. *"Discovery" Report*, 21: 261-356.
- Harwood, D. and Maruyama, T., 1992. Middle Eocene to Pleistocene diatom biostratigraphy of Southern Ocean sediments from the Kerguelen Plateau, Leg 120. *Proceedings of the Ocean Drilling Program, Scientific Results*, 120: 683-733.

- Hasle, G. and Heimdal, B., 1968. Morphology and distribution of the marine centric diatom *Thalassiosira antarctica* Comber. *Journal of the Royal Microscopy Society*, 88(3): 357-369.
- Hasle, G., 1969. An analysis of the phytoplankton of the Pacific Southern Ocean: abundance, composition, and distribution during the Bratigg Expedition, 1947-1948. *Hvalradets Skrifter*, 52: 1-168.
- Hasle, G. and Semina, H.J., 1987. The marine planktonic diatoms *Thalassiothrix longissima* and *Thalassiothrix antarctica* with comments on *Thalassionema* spp. and *Synedra reinboldii*. *Diatom Research*, 2(2): 175-192.
- Hasle, G., Sims, P.A., and Syvertsen, E.E.. 1988. Two recent *Stellarima* species: *S. microtrias* and *S. stellaris* (Bacillariophyceae). *Botanica Marina*, 31: 195-206.
- Heath, G. (Editor), 1974. Dissolved silica and deep-sea sediments. *Studies in paleo-oceanography, Special Publication No. 20. Society of Economic Paleontologists and Mineralogists*, pp. 77-93.
- Hellmer, H. and Jacobs, S., 1992. Ocean interactions with the base of Amery Ice Shelf, Antarctica. *Journal of Geophysical Research*, 97(12): 20305-20317.
- Hendey, N.I., 1937. The plankton diatoms of the southern seas. "*Discovery*" Report, 16: 151-364.
- Hollin, J.T., 1962. On the glacial history of Antarctica. *Journal of Glaciology*, 4(32): 173-196.
- Holm-Hansen, O., El Sayed, S.A., Franceschini, B.A. and Cuhel, R., 1977. Primary production and the factors controlling phytoplankton growth in the Antarctic seas. In: G.A. Llano (Editor), *Adaptations within Antarctic Ecosystems: Proceedings of Third SCAR Symposium on Antarctic Biology*, pp. 11-50.
- Honjo, S., Manganini, S. and Poppe, L., 1982. Sedimentation of lithogenic particles in the deep ocean. *Marine Geology*, 50: 199-220.
- Horner, R.A., 1985. Ecology of sea ice microalgae. In: R.A. Horner (Editor), *Sea-ice Biota*. CRC Press, Boca-Raton, pp. 83-103.
- Horner, R., 1990. Ice-associated ecosystems. In: L.K. Medlin and J. Priddle (Editors), *Polar Marine Diatoms*. Cambridge University Press, Cambridge, pp. 9-18.

- Hosie, G.W., 1994. Multivariate analyses of the macrozooplankton community and euphausiid larval ecology in the Prydz Bay region, Antarctica. *ANARE Reports*, 137, Antarctic Division, Kingston, Tasmania, 209 pp.
- Hughes, T.J., Denton, G.H., Anderson, B.G., Schilling, D.H., Fastook, and J.L., Lingle, C.S., 1981. The last great ice sheets: a global view. In: G.H. Denton and T.J. Hughes (Editors), *The Last Great Ice Sheets*. Wiley-Interscience, New York, pp. 263-317.
- Hurd, D., 1972. Factors affecting solution rate of biogenic opal in seawater. *Earth and Planetary Science Letters*, 15: 411 - 417.
- Huybrechts, P. and Oerlemans, J., 1990. Response of the Antarctic ice sheet to future greenhouse warming. *Climate Dynamics*, 5: 93-102.
- Ice Core Working Group, 1998. *Ice Core Contributions to Global Change Research: Past Successes and Future Directions*. National Ice Core Laboratory - Science Management Office, Climate Research Center, Institute for the Study of Earth, Oceans and Space, University of New Hampshire, Durham, 48 pp.
- Imbrie, J. and Kipp, N., 1971. A new micropaleontological method for quantitative paleoclimatology: application to a Late Pleistocene Caribbean core. In: K. Turekian (Editor), *The Late Cenozoic Glacial Ages*. Yale University Press, pp. 71-181.
- Imbrie, J. and Imbrie, K.P., 1986. *Ice Ages: Solving the Mystery*. Harvard University Press, Cambridge, Massachusetts, 224 pp.
- Jacka, T.H., 1983. A computer database for Antarctic sea ice extent. *ANARE Research Series*, 13, Antarctic Division, Kingston, Tasmania, 54 pp.
- Jacka, T., Allison, I., Thwaites, R. and Wilson, J., 1987. Characteristics of the seasonal sea ice of East Antarctica and comparisons with satellite observations. *Annals of Glaciology*, 9: 85-91.
- Jacobs, S.S. and Georgi, D.T., 1977. Observations on the southwest Indian/Antarctic Ocean. In: M. Angel (Editor), *A Voyage of Discovery. G.E. Deacon 70th Anniversary Supplement to Deep-Sea Research*, pp. 43-48.

- Jacobs, S.S., Hellmer, H.H., Doake, C.S.M., Jenkins, A., and Frolich, R., 1992. Melting of iceshelves and the mass balance of Antarctica. *Journal of Glaciology*, 33: 373-387.
- Johansen, J. and Fryxell, G., 1985. The genus *Thalassiosira* (Bacillariophyceae): studies on species occurring south of the Antarctic Convergence Zone. *Phycologia*, 24(2): 155-179.
- Johnsen, S.J., Clausen, H.B., Dansgaard, W., Fuhrer, K., Gundestrup, N., Hammer, C.U., Iversen, P., Jouzel, J., Stauffer, B., and Steffensen, J.P. 1992. Irregular glacial interstadials recorded in a Greenland ice core. *Nature*, 359: 311-313.
- Jongman, R., ter Braak, C. and van Tongeren, O., 1987. *Data Analysis in Community and Ecology Landscape*. Pudoc Wageningen, 299 pp.
- Jordan, R., Priddle, J., Pudsey, C., Barker, P. and Whitehouse, M., 1991. Unusual diatom layers in Upper Pleistocene sediments from the northern Weddell Sea. *Deep-Sea Research*, 38(7): 829-843.
- José, A., Koroleva, G. and Nagaeva, G., 1962. Diatoms in the surface layer of sediment in the Indian Sector of the Antarctic. *Akademiya Nauk SSSR. Institut Okeanologii. Trudy*, 61: 19-93.
- José, A.P., Koroleva, G.S. and Nagaeva, G.A., 1963. Stratigraphical and paleogeographical investigations in the Indian sector of the Southern Ocean (in Russian). *Okeanology*, 8: 137-161.
- José, A., Kozlova, O. and Muhina, V., 1971. Distribution of diatoms in the surface layer of sediment from the Pacific Ocean. In: B.M. Funnell and W.R. Riedel (Editors), *The Micropalaeontology of Oceans*. Cambridge University Press, Cambridge, 263-269 pp.
- Jouzel, J., Vaikmae, R., Petit, J. R., Martin, M., Duclos, Y., Stievenard, M., Lorius, C., Toots, M., Melieres, M. A., Burckle, L. H., Barkov, N. I., Kotlyakov, V. M., 1995. The two-step shape and timing of the last deglaciation in Antarctica. *Climate Dynamics*, 11(3): 151-161.
- Kamatani, A. and Riley, J., 1979. Rate of dissolution of diatom silica walls in seawater. *Marine Biology*, 55: 29 - 53.

- Kang, S. and Fryxell, G., 1992. *Fragilariopsis cylindrus* (Grunow) Krieger: The most abundant diatom in water column assemblages of Antarctic marginal ice-edge zones. *Polar Biology*, 12: 609-627.
- Kato, K., 1993. Deletion of less-abundant species from ecological data. *Diatom*, 8: 1-5.
- Kellogg, T. and Truesdale, R., 1979. Late Quaternary paleoecology and paleoclimatology of the Ross Sea: the diatom record. *Marine Micropaleontology*, 4: 137-158.
- Kellogg, D. and Kellogg, T., 1987. Microfossil distributions in modern Amundsen Sea sediments. *Marine Micropaleontology*, 12: 203-222.
- Kellogg, T. and Kellogg, D., 1988. Antarctic cryogenic sediments: biotic and inorganic facies of ice shelf and marine-based ice sheet environments. *Paleoceanography, Paleoclimatology, Paleoecology*, 67: 51-74.
- Kennett, J.P. and Ingram, B.L., 1995. A 20,000 year record of ocean circulation and climate change from the Santa Barbara Basin. *Nature*, 377: 510-514.
- Kerry, K. and Woehler, E., 1987. Oceanographic data: Prydz Bay region - Antarctic Division BIOMASS Experiment 1, MV *Nella Dan*, November-December 1982. *ANARE Research Notes*, 52, Antarctic Division Kingston, Tasmania, 166 pp.
- Kerry, K.R., Woehler, E.J., Wright, S. and Dong, Z., 1987a. Oceanographic data: Prydz Bay region - FIBEX, MV *Nella Dan*, January-March 1981. *ANARE Research Notes*, 49, Antarctic Division, Kingston, Tasmania, 114 pp.
- Kerry, K., Woehler, E. and Robb, M., 1987b. Oceanographic data: Prydz Bay region - SIBEX II, MV *Nella Dan*, January 1985. *ANARE Research Notes*, 53, Antarctic Division, Kingston, Tasmania, 122 pp.
- Kirby, M.E., Domack, E.W. and McClennen, C.E., 1998. Magnetic stratigraphy and sedimentology of Holocene glacial marine deposits in the Palmer Deep, Bellingshausen Sea, Antarctica: implications for climate change? *Marine Geology*, 152(4): 247-259.
- Kopczynska, E., Goeyens, L., Semeneh, M. and Dehairs, F., 1995. Phytoplankton composition and cell carbon distribution in Prydz Bay, Antarctica; relation to organic particulate matter and its $\delta^{13}\text{C}$ values. *Journal of Plankton Research*, 17(4): 685-707.

- Kozlova, A.P., 1966. *Diatom algae of Indian and Pacific Sectors of Antarctica*. Academy of Sciences of the USSR Institute of Oceanology, Moscow, 191 pp.
- Kozlova, O. and Mukhina, V., 1967. Diatoms and silicoflagellates in suspension and floor sediments of the Pacific Ocean. *International Geology*, 9(10): 1322-1342.
- Krebs, W., Lipps, J. and Burckle, L., 1987. Ice diatom flora, Arthur Harbor, Antarctica. *Polar Biology*, 7: 163-171.
- Kreutz, K.J., Mayewski, P.A., Meeker, L.D., Twickler, M.S., Whitlow, S.I., and Pittalwala, I.I. 1997. Bipolar changes in atmospheric circulation during the Little Ice Age. *Science*, 277: 1294-1296.
- Kruskal, J. and Wish, M., 1978. Multidimensional Scaling. *Quantitative Applications in the Social Sciences*, 11. Sage Publications Inc., Newbury Park, 93 pp.
- Lamb, H.H., 1965. The early mediaeval warm epoch and its sequel. *Palaeogeography, Palaeoclimatology, Palaeoecology*, 1: 13-37.
- Larter, R.D. and Vanneste, L.E., 1995. Relict subglacial deltas on the Antarctic Peninsula outer shelf. *Geology*, 23(1): 33-36.
- Leventer, A. and Dunbar, R., 1986. Dissolution and transport of particulate silica McMurdo Sound, Antarctica. *Antarctic Journal of the United States*, 21: 134-137.
- Leventer, A. and Dunbar, R., 1987a. Surface sediment diatom assemblages, McMurdo Sound, Antarctica. *Antarctic Journal of the United States*, 22: 194-196.
- Leventer, A. and Dunbar, R., 1987b. Diatom flux in McMurdo Sound, Antarctica. *Marine Micropaleontology*, 12: 46-64.
- Leventer, A. and Dunbar, R., 1988. Recent diatom record of McMurdo Sound, Antarctica: implications for history of sea ice extent. *Paleoceanography*, 3(3): 259-274.
- Leventer, A., 1992. Modern distribution of diatoms in sediments from the George V Coast, Antarctica. *Marine Micropaleontology*, 19: 315-332.
- Leventer, A., Dunbar, R. and DeMaster, D.J., 1993. Diatom evidence for Late Holocene climatic events in Granite Harbor, Antarctica. *Palaeoceanography*, 8(3): 373-386.
- Leventer, A. and Harwood, D., 1993. *The geological use of polar marine diatoms. Workshop on Antarctic Glacial Marine and Biogenic Sedimentation. Notes for a Short Course. Part 2. Biogenic Sedimentation.* pp. 134-253.

- Leventer, A. Domack, E.W., Ishman, S.E., Brachfeld, S., McClennen, C.E., and Manley, P., 1996. Productivity cycles of 200-300 years in the Antarctic Peninsula region: understanding linkages among the sun, atmosphere, oceans, sea ice, and biota. *GSA Bulletin*, 108(12): 1626-1644.
- Leventer, A. and Dunbar, R., 1996. Factors influencing the distribution of diatoms and other algae in the Ross Sea. *Journal of Geophysical Research*, 101(C8): 18489-18500.
- Lewis, M.R., Horne, E.P.W., Cullen, J.J., Oakey, N.S., and Platt, T., 1984. Turbulent motions may control phytoplankton photosynthesis in the upper ocean. *Nature*, 311: 49-50.
- Ligowski, E., 1983. Phytoplankton of the Olaf Prydz Bay (Indian Ocean, East Antarctica) in February 1969. *Polish Polar Research*, 4(1-4): 21-32.
- Lisitzin, A., 1971. Distribution of siliceous microfossils in suspension and in bottom sediments. In: B. Funnell and W. Riedel (Editors), *The Micropalaeontology of Oceans*. Cambridge University Press, Cambridge, pp. 173-195.
- Lisitzin, A., 1985. The silica cycle during the last ice age. *Palaeogeography, Palaeoclimatology, Palaeoclimatology*, 50: 241-270.
- Lizotte, M.P. and Sullivan, C.W., 1991. Rates of photoadaptation in sea ice diatoms from McMurdo Sound, Antarctica. *Journal of Phycology*, 27: 367-373.
- Lorius, C., Merlivat, L., Jouzel, J., and Pourchet, M., 1979. A 30,000-yr climatic record from Antarctic ice. *Nature*, 280: 644-648.
- Lorius, C., Jouzel, J., Ritz, C., Merlivat, L., Barkov, N.I., Korotkevich, Y.S., and Kotlyakov, V.M., 1985. A 150,000-year climatic record from Antarctic ice. *Nature*, 316: 591-596.
- Lorius, C., Jouzel, J. and Raynaud, D., 1992. The ice core record: past archive of the climate and signpost of the future. *Philosophical Transactions of the Royal Society of London*, 38: 227-234.
- Mantyla, A.W. and Reid, J.R., 1983. Abyssal characteristics of the world ocean. *Deep-Sea Research*, 30: 805-833.
- Marchant, H., 1993. Antarctic marine nanoplankton. *Current Topics in Botanical Research*, 1: 189-201.

- Marra, J. and Boardman, D., 1984. Late winter chlorophyll a distributions in the Weddell Sea. *Marine Ecology Progress Series*, 19: 197-205.
- Mashiotta, T.A., 1992. *Biogenic Sedimentation in Andvord Bay, Antarctica: A 3000 Year Record of Paleoproductivity*. B.Sc. Thesis, Hamilton College, Clinton, 86 pp.
- Mayewski, P.A., Twickler, M.S., Whitlow, S.I., Meeker, L.D., Yang, Q., Thomas, J., Kreutz, K., Grootes, P.M., Morse, D.L., Steig, E.J., Waddington, E.D., Saltzman, E.S., Whung, P.Y., and Taylor, K.C., 1996. Climate change during the last deglaciation in Antarctica. *Science*, 272: 1636-1638.
- McMinn, A., Gibson, J., Hodgson, D. and Aschman, J., 1995. Nutrient limitation in Ellis Fjord, eastern Antarctica. *Polar Biology*, 15: 269-276.
- McMinn, A., 1995. Comparison of diatom preservation between oxic and anoxic basins. *Diatom Research*, 10(1): 145-151.
- McMinn, A., 1996. Preliminary investigation of the contribution of fast-ice algae to the spring phytoplankton bloom in Ellis Fjord, eastern Antarctica. *Polar Biology*, 16: 301-307.
- McMinn, A., in press. Species succession in fast ice algal communities; a response to UV-B radiation? *Korean Journal of Polar Research*, 8: 47-52.
- McMinn, A., Ashworth C., and Ryan, K., in press a. Growth and productivity of Antarctic sea ice algae under PAR and UV irradiances. *Botanica Marina*.
- McMinn, A., Skerratt, J., Trull, T., Ashworth, C., and Lizotte, M., in press b. Nutrient stress gradient in the bottom 5 cm of fast ice, McMurdo Sound, Antarctica. *Polar Biology*.
- Medlin, L. and Hasle, G.R., 1990. Some *Nitzschia* and related diatom species from fast ice samples in the Arctic and Antarctic. *Polar Biology*, 10: 451-479.
- Medlin, L. and Priddle, J., 1990. *Polar Marine Diatoms*. British Antarctic Survey, Cambridge, 214 pp.
- Mercer, J.H., 1978. Glacial development and temperature trends in the Antarctic and in South America. In: J. Van Zinderen Bakker (Editor), *Antarctic Glacial History and World Paleoenvironments*. AA Balkema, Rotterdam, pp. 73-93.
- Middleton, J. and Humphries, S., 1989. Thermohaline structure and mixing in the region of Prydz Bay, Antarctica. *Deep-Sea Research*, 38(8): 1255-1266.

- Mikkelsen, N., 1990. Experimental dissolution of Pliocene diatoms. *Nova Hedwigia*, 33: 489-907.
- Mitchell, B.G., Brady, E.A., Holm-Hansen, O., McClain, C. and Bishop, J., 1991. Light limitation of phytoplankton biomass and macronutrient utilisation in the Southern Ocean. *Limnology and Oceanography*, 36(8): 1662-1667.
- Mitchell, B.G. and Holm-Hansen, O., 1991. Observations and modeling of the Antarctic phytoplankton crop in relation to mixing depth. *Deep-Sea Research*, 38: 981-1007.
- Mosley-Thompson, E. and Thompson, L.G., 1982. Nine centuries of microparticle deposition in the South Pole. *Quaternary Research*, 17(1): 1-13.
- Mosley-Thompson, E., 1992. Paleoenvironmental conditions in Antarctica since AD 1500. In: R.S. Bradley and P.D. Jones (Editors), *Climate Since AD 1500*. Routledge, London, pp. 572-591.
- Mosley-Thompson, E., 1996. Holocene climate changes recorded in an East Antarctic ice core. In: P.D. Jones, R.S. Bradley and J. Jouzel (Editors), *Climatic Variations and Forcing Mechanisms of the Last 2000 Years*. Springer-Verlag, Berlin, pp. 243-262.
- Nelson, D.M. and Smith, W.O., 1986. Phytoplankton bloom dynamics of the western Ross Sea ice edge - II. Mesoscale cycling of nitrogen and silicon. *Deep-Sea Research*, 33: 1389-1412.
- Nelson, S.M., Smith, W.O., Gordon, L.I. and Huber, B.A., 1987. Spring distributions of density, nutrients and phytoplankton biomass in the ice edge zone of the Weddell-Scotia Sea. *Journal of Geophysical Research*, 92: 7181-7190.
- Nelson, D.M. and Smith, W.O., 1991. Sverdrup revisited: critical depths, maximum chlorophyll levels, and the control of Southern Ocean productivity by the irradiance-mixing regime. *Limnology and Oceanography*, 36(8): 1650-1661.
- Nelson, D.M. and Tréguer, P., 1992. Role of silicon as a limiting nutrient to Antarctic diatoms: evidence from kinetic studies in the Ross Sea ice-edge zone. *Marine Ecology Progress Series*, 80: 255-264.
- Nunes Vaz, R. and Lennon, G., 1996. Physical oceanography of the Prydz Bay region of Antarctic waters. *Deep-Sea Research*, 43: 603-641.

- O'Brien, P.E., 1992. *Cruise Preview Report, Prydz Bay and Mac.Robertson Shelf, Antarctica, January - March 1993*. AGSO Report 1992/78, Canberra (Australia).
- O'Brien, P., 1994. Morphology and late glacial history of Prydz Bay, Antarctica, based on echo sounder data. *Terra Antarctica*, 1(2): 403-405.
- O'Brien, P., Truswell, E. and Burton, T., 1994. Morphology, seismic stratigraphy and sedimentation history of the Mac.Robertson Shelf, East Antarctica. *Terra Antarctica*, 1(2): 407-408.
- O'Brien, P. and Harris, P., 1995. Prydz Trough Mouth Fan - a major record of Antarctic glacial history. *VII International Symposium on Antarctic Earth Sciences*, Siena (Italy), p. 283.
- O'Brien, P.E., Harris, P.T., Quilty, P.G., Taylor, F. and Wells, P., 1995a. *Post Cruise Report, Antarctic CRC Marine Geoscience: Prydz Bay, Mac.Robertson Shelf and Kerguelen Plateau. ANARE Voyage 6, 1995/29 (BANGSS)*, Australian Geological Survey Organisation, Canberra (Australia).
- O'Brien, P.E. and Harris, P.T., 1996. Deposits of the Lambert Glacier in Prydz Bay - a record of Cenozoic climate change in Antarctica. *13th Australian Geological Convention*, Canberra (Australia), pp. 320.
- O'Brien, P.E. and Harris, P.T., 1996a. Patterns of glacial erosion and deposition in Prydz Bay and the past behavior of the Lambert Glacier. *Papers and Proceedings of the Royal Society of Tasmania*, 130(2): 79-85.
- O'Brien, P.E., Leitchenkov, G. and Harris, P.T., 1997. Iceberg plough marks, subglacial bedforms and grounding zones moraines in Prydz Bay, Antarctica. In: T.A. Davies, T. Bell, A.K. Cooper, H. Josenhans, L. Polyak, A. Solheim, A. Stoker, and J.A. Stravers (Editors), *Glaciated Continental Margins: An Atlas of Acoustic Images*. Chapman and Hall, London, pp. 228-231.
- O'Brien, S.R., Mayewski, P.A., Meeker, L.D., Meese, D.A., Twickler, M.S., and Whitlow, S.I., 1995b. Complexity of Holocene climate as reconstructed from a Greenland ice core. *Nature*, 270: 1962-1964.
- Omoto, K., 1983. The problem and significance of radiocarbon geochronology in Antarctica. In: R.L. Oliver, P.R. James and J.B. Jago (Editors), *Antarctic Earth Science*. Australian Academy of Science, Canberra, pp. 450-452.

- Parkinson, C.L., Comiso, J.C., Zwally, H.J., Cavalieri, D.J., Gloersen, P., and Campbell, W.J., 1987. *Arctic sea ice 1973-1976: satellite passive-microwave observations*. NASA Special Publication (489), Washington DC, 296 pp.
- Perch-Nielsen, K., 1985. Silicoflagellates. In: H. Bolli, J. Saunders and K. Perch-Nielsen (Editors), *Plankton Stratigraphy*. Cambridge University Press, Cambridge, pp. 811-846.
- Petit, J.R., Barkov, N.I., Benoist, J.P., Jouzel, J., Korotkevich, Y.S., Kotlyakov, V.M. and Lorius, C., 1990. Holocene climatic records from Antarctic ice. *Annals of Glaciology*, 14.
- Pichon, J., Labracherie, M., Labeyrie, L. and Duprat, J., 1987. Transfer functions between diatom assemblages and surface hydrology in the Southern Ocean. *Palaeogeography, Palaeoclimatology, Palaeoecology*, 61: 79-95.
- Pichon, J.J., Labeyrie, L.D., Bareille, G., Labracherie, M., Duprat, J., and Jouzel, J., 1992. Surface water temperature changes in the high latitudes of the Southern Hemisphere over the last glacial-interglacial cycle. *Paleoceanography*, 7(3): 289-318.
- Pickard, J., 1982. Holocene winds of the Vestfold Hills, Antarctica. *New Zealand Journal of Geology and Geophysics*, 25:353-358.
- Pickard, J., Selkirk, P. and Selkirk, D., 1984. Holocene climates of the Vestfold Hills, Antarctica, and Macquarie Island. In: J. Vogel (Editor), *Late Cenozoic Palaeoclimates of the Southern Hemisphere*. AA Balkema, Rotterdam, pp. 173-182.
- Pielou, E., 1991. *After the Ice Age*. University of Chicago Press, Chicago, 399 pp.
- Pimental, R. and Smith, J., 1985. *BioStat*. Sigma Soft, Placentia, California.
- Priddle, J. and Fryxell, G., 1985. *Handbook of Common Plankton Diatoms of the Southern Ocean: Centrales except the Genus Thalassiosira*. British Antarctic Survey, Cambridge.
- Priddle, J., Hawes, I. and Ellis-Evans, C., 1986. Antarctic aquatic ecosystems as habitats for phytoplankton. *Biological Reviews*, 61: 199-238.

- Pudsey, C., 1990. Grain size and diatom content of hemipelagic sediments at Site 697, ODL Leg 113; a record of Pliocene-Pleistocene climate. *Proceedings of the Ocean Drilling Program, Scientific Results*, 113: 111-120.
- Pushina, Z., Kolobov, D. and Druzhinina, N., 1997. Biostratigraphy and paleoecology of the bottom sediments in Prydz Bay. In: C. Ricci (Editor), *The Antarctic Region: Geological Evolution and Processes*. Terra Antarctica Publications, Siena, pp. 869-874.
- Quilty, P., 1985. Distribution of foraminiferids in sediments of Prydz Bay, Antarctica. *Special Publication, South Australian Department of Mines and Energy*, 5: 329-340.
- Rathburn, A., Pichon, J., Ayress, M. and De Deckker, P., 1997. Microfossil and stable-isotope evidence for changes in Late Holocene palaeoproductivity and palaeoceanographic conditions in the Prydz Bay region of Antarctica. *Palaeogeography, Palaeoclimatology, Palaeoecology*, 131: 485-510.
- Rivera, P.R., 1981. Beitrage zur Taxonomie und Verbreitung der Gattung *Thalassiosira* Cleve (Bacillariophyceae) in den Kustengewassen Chiles. *Biolitheca Phycologia*, 56: 1-220.
- Roberts, D. and McMinn, A., 1996. Relationships between surface sediment diatom assemblages and water chemistry gradients in saline lakes of the Vestfold Hills, Antarctica. *Antarctic Science*, 8: 331-341.
- Roberts, D. and McMinn, A., 1998. A weight-average regression and calibration model for inferring lakewater salinity from fossil diatom assemblages in saline lakes of the Vestfold Hills: implications for interpreting Holocene lake histories in Antarctica. *Journal of Paleolimnology*, 19: 99-210.
- Robinson, D.H., Arrigo, K.R., Iturriaga, R. and Sullivan, C.W., 1995. Microalgal light-harvesting in extreme low-light environments in McMurdo Sound, Antarctica. *Journal of Phycology*, 31: 508-520.
- Saari, M.R., Yuen, D.A. and Schubert, G., 1987. Climatic warming and basal melting of large ice sheets: possible implications for East Antarctica. *Geophysical Research Letters*, 14(1): 33-36.

- Sancetta, C., Villareal, T. and Falkowski, P., 1991. Massive fluxes of rhizosolenoid diatoms: a common occurrence? *Limnology and Oceanography*, 36: 1452-1457.
- Scherer, R., 1995. A new method for the determination of absolute abundance of diatoms and other silt-sized sedimentary particles. *Journal of Paleolimnology*, 12: 171-179.
- Schmaljohann, R., Röttger, R., 1978. The ultrastructure and taxonomic identity of the symbiotic algae of *Heterostegina depressa* (Foraminifera: Nummulitidae). *Journal of the Marine Biology Association of the United Kingdom*, 58: 227-237.
- Schrader, H., 1971. Fecal pellets: role in sedimentation of pelagic diatoms. *Science*, 174: 55-57.
- Schroeder, L.D., Sjoquist, D.L. and Stephan, P.E., 1986. *Understanding Regression Analysis*. Sage Publications, Beverley Hills, 95 pp.
- Scott, P., McMinn, A. and Hosie, G., 1994. Physical parameters influencing diatom community structure in eastern Antarctic sea ice. *Polar Biology*, 14: 507-517.
- Sedwick, P.N., Harris, P.T., Robertson, L.G., McMurtry, G.M., Cremer, M.D., and Robinson, P., in press. A geochemical study of marine sediments from the Mac.Robertson Shelf, East Antarctica: initial results and paleoenvironmental implications. *Annals of Glaciology*, 27.
- Shanks, A. and Trent, J., 1980. Marine snow: sinking rates and potential role in vertical flux. *Deep-Sea Research*, 27(A): 137-143.
- Shemesh, A., Burckle, L. and Froelich, P., 1989. Dissolution and preservation of Antarctic diatoms and the effect on sediment thanatocoenoses. *Quaternary Research*, 31: 288-308.
- Shevenell, A., Domack, E. and Kernan, G., 1996. Record of Holocene palaeoclimate change along the Antarctic Peninsula: evidence from glacial marine sediments, Lallemand Fjord. *Papers and Proceedings of the Royal Society of Tasmania*, 130(2): 55-64.
- Shi, G., 1993. Multivariate data analysis in paleoecology and palaeobiogeography - a review. *Palaeogeography, Palaeoclimatology, Palaeoceanography*, 105: 199-234.
- Shi, G., 1995. Spatial aspects of palaeobiogeographical data and multivariate analysis. *Memoirs of the Association of Australian Palaeontologists*, 18: 179-188.

- Singer, J. and Anderson, J., 1984. Use of total grain-size distributions to define bed erosion and transport for poorly sorted sediment undergoing simulated bioturbation. *Marine Geology*, 57: 335-359.
- Smetacek, V., 1985. Role of sinking in diatom life-history cycles: ecological, evolutionary and geological significance. *Marine Biology*, 84: 239-251.
- Smetacek, V., Scharek, R., Gordon, L.I., Eicken, H., Fahrback, E., Rohardt, G., and Moore, S., 1992. Early spring phytoplankton blooms in ice platelet layers of the southern Weddell Sea, Antarctica. *Deep-Sea Research*, 39: 153-168.
- Smith, N., Zhaoqian, D., Kerry, K. and Wright, S., 1984. Water masses and circulation in the region of Prydz Bay, Antarctica. *Deep-Sea Research*, 31: 1121-1147.
- Smith, N. and Tréguer, P. (Editors), 1994. *Physical and Chemical Oceanography in the Vicinity of Prydz Bay, Antarctica. Southern Ocean Ecology: The BIOMASS Perspective*. Cambridge University Press, Cambridge, 25-45 pp.
- Smith, W.O. and Nelson, D.M., 1985. Phytoplankton bloom produced by a receding ice edge in the Ross Sea: coherence with the density field. *Science*, 227: 163-166.
- Smith, W.O. and Nelson, D.M., 1986. Importance of ice edge phytoplankton production in the Southern Ocean. *Bioscience*, 36: 564-572.
- Stager, J.C. and Mayewski, P.A., 1997. Abrupt mid-Holocene climatic transitions registered at the equator and the poles. *Science*, 276: 1834-1836.
- Stagg, H., 1985. The structure and origin of Prydz Bay and Mac.Robertson Shelf, East Antarctica. *Tectonophysics*, 114: 315-340.
- Stockwell, D., Kang, S. and Fryxell, G., 1991. Comparisons of diatom biocoenoses with Holocene sediments assemblages in Prydz Bay, Antarctica. *Proceedings of the Ocean Drilling Program, Scientific Results*, 119: 667-673.
- Stradner, H. and Allram, F., 1982. Notes on an enigmatic siliceous cyst, Middle America Trench, Deep Sea Drilling Project Hole 490. *Initial Reports of the Deep Sea Drilling Project*, 66: 641-642.
- Streten, N.A. and Pike, D.J., 1984. Some observations of the sea-ice in the southwest Indian Ocean. *Australian Meteorological Magazine*, 32: 195-206.
- Stuiver, M., Denton, G.H., Hughes, T.J. and Fastook, J.L., 1981. History of the marine ice sheet in West Antarctica during the last glaciation: a working hypothesis. In:

- G. Denton and T. Hughes (Editors), *The Last Great Ice Sheets*. Wiley-Interscience, New York, pp. 319-436.
- Stuiver, M. and Ostlund, H.G., 1983. GEOSECS Indian Ocean and Mediterranean radiocarbon. *Radiocarbon*, 25: 1-28.
- Syvetsen, E.E. and Hasle, G.R., 1983. The diatom genus *Eucampia*: morphology and taxonomy. *Bacillaria*, 6: 169-210.
- Tanimura, Y., Fukuchi, M., Watanabe, K. and Moriwaki, K., 1990. Diatoms in water column and sea-ice in Lützow-Holm Bay, Antarctica, and their preservation in the underlying sediments. *Bulletin of the National Science Museum*, 16(1): 15-39.
- Taylor, F., McMinn, A., and Franklin, D., 1997. Distribution of diatoms in surface sediments of Prydz Bay, Antarctica. *Marine Micropaleontology*, 32: 209-229.
- Tingey, R.J., 1982. The development and fluctuation of Antarctica's Cainozoic glaciation - the terrestrial record. *Australian Meteorological Magazine*, 30: 181-189.
- Tréguer, P., Kamatani, A., Gueneley, S. and Queguiner, B., 1989. Kinetics of dissolution of Antarctic diatom frustules and the biogeochemical cycle of silicon in the Southern Ocean. *Polar Biology*, 9: 397-403.
- Truesdale, R. and Kellogg, T., 1979. Ross Sea diatoms: modern assemblage distributions and their relationship to ecologic, oceanographic and sedimentary conditions. *Marine Micropaleontology*, 4: 13-31.
- Vargo, G., Fanning, K., Heil, C. and Bell, L., 1986. Growth rates and the salinity response of an Antarctic ice microflora community. *Polar Biology*, 5: 241-247.
- Villalba, R., 1990. Climatic fluctuations in northern Patagonia during the last 1000 years as inferred from tree-ring records. *Quaternary Research*, 34: 346-360.
- Villareal, T.A. and Fryxell, G.A., 1983a. Temperature effects on the valve structure of the bipolar diatoms *Thalassiosira antarctica* and *Porosira glacialis*. *Polar Biology*, 2: 163-169.
- Villareal, T.A. and Fryxell, G.A., 1983b. The genus *Actinocyclus* (Bacillariophyceae): Frustule morphology of *A. sagittulus* sp. nov. and two related species. *Journal of Phycology* (19) 452-466.

- Watanabe, K., 1988. Sub-ice microalgal strands in the Antarctic coastal fast ice area near Syowa Station. *Japanese Journal of Phycology*, 36: 221-229.
- Webb, T. and Bryson, R., 1972. Late- and postglacial climate change in the Northern Midwest, USA: quantitative estimates derived from fossil pollen spectra by multivariate statistical analysis. *Quaternary Research*, 2: 70-115.
- Williams, D.M., 1986. Comparative morphology of some species of *Synedra* Ehrenb. with a new definition of the genus. *Diatom Research*, 1(1): 131-152.
- Woehler, E., Shearer, J. and Kerry, K., 1987. Oceanographic data: Prydz Bay region - geoscience cruise, MV *Nella Dan*, January - March 1982. *ANARE Research Notes*, 51. Antarctic Division, Kingston, Tasmania, 22 pp.
- Woehler, E.J. and Williams, R., 1988. Oceanographic data: Prydz Bay region: Australian Antarctic Marine Biological Ecosystem Research 86/87, MV *Nella Dan*, February-April 1987. *ANARE Research Notes*, 63, Antarctic Division, Kingston, Tasmania, 136 pp.
- Wong, A., 1994. *Structure and Dynamics of Prydz Bay, Antarctica, as Inferred From a Summer Hydrographic Data Set*. MPOSc Thesis, Institute of Antarctic and Southern Ocean Studies, University of Tasmania, pp. 104.
- Zar, J.H., 1984. *Biostatistical Analysis*. Prentice-Hall Inc., New Jersey, 718 pp.
- Zhang, Q. and Peterson, J.A., 1984. A geomorphology and late Quaternary geology of the Vestfold Hills. *ANARE Report*, 133, Antarctic Division, Kingston, Tasmania.
- Zielinski, U., 1997. Parmales species (siliceous marine nanoplankton) in surface sediments of the Weddell Sea, Southern Ocean; indicators for sea ice environment? *Marine Micropaleontology*, 32(3/4): 387-395.
- Zielinski, U. and Gersonde, R., 1997. Diatom distribution in Southern Ocean surface sediments (Atlantic Sector): implications for paleoenvironmental reconstructions. *Palaeogeography, Palaeoclimatology, Palaeogeography*, 129: 213-250.

– *Appendix 1* –

Abundance (%) and distribution of species in surface samples

| Species | Site | DCF93019 | DCF93032 | DCF93047 | KRGR1 | KR2A | KRGR4 | KRGR5 | KRGR6 | KRGR7 | KRGR8 | KRGR9 | KRGR10 | KRGR11 | KRGR12 | KRGR13 | KRGR14 | KRGR15 | KRGR16 |
|---|------|----------|----------|----------|-------|-------|-------|-------|-------|-------|-------|-------|--------|--------|--------|--------|--------|--------|--------|
| <i>Actinocyclus actinochilus</i> | | 0 00 | 0 00 | 0 52 | 1 03 | 0 68 | 0 34 | 0 00 | 0 51 | 0 00 | 0 17 | 0 34 | 0 00 | 0 17 | 0 34 | 0 68 | 0 00 | 0 00 | 0 17 |
| <i>Chaetoceros spp</i> | | 0 18 | 0 36 | 0 00 | 1 03 | 1 02 | 0 17 | 0 00 | 0 00 | 0 00 | 0 17 | 0 34 | 0 34 | 0 00 | 0 17 | 0 17 | 0 51 | 0 00 | 0 00 |
| <i>Chaetoceros spores</i> | | 3 36 | 2 70 | 0 87 | 3 28 | 1 54 | 4 25 | 6 42 | 4 90 | 7 45 | 6 84 | 3 37 | 4 07 | 5 56 | 9 68 | 5 41 | 2 03 | 3 36 | 5 75 |
| <i>Dactylosolen antarcticus</i> | | 0 35 | 0 54 | 0 00 | 1 03 | 0 00 | 0 51 | 0 00 | 0 68 | 0 00 | 0 17 | 0 00 | 0 34 | 0 34 | 0 17 | 0 00 | 0 17 | 0 50 | 0 17 |
| <i>Diastephanus speculum</i> | | 0 35 | 0 54 | 0 35 | 0 52 | 0 85 | 1 36 | 0 17 | 0 00 | 0 00 | 0 17 | 0 34 | 0 68 | 0 84 | 0 51 | 0 68 | 1 19 | 0 17 | 0 17 |
| <i>Eucampia antarctica</i> | | 0 00 | 0 36 | 0 00 | 0 86 | 0 51 | 0 00 | 0 17 | 0 34 | 0 00 | 0 00 | 0 17 | 0 00 | 0 17 | 0 17 | 0 00 | 0 00 | 0 00 | 0 17 |
| <i>Fragilaropsis angulata</i> | | 7 07 | 7 01 | 4 36 | 2 07 | 6 31 | 2 89 | 5 07 | 3 55 | 3 05 | 2 22 | 2 19 | 2 89 | 4 04 | 1 87 | 2 37 | 4 41 | 2 18 | 5 58 |
| <i>Fragilaropsis curta</i> | | 66 61 | 76 08 | 59 34 | 34 48 | 56 14 | 54 59 | 53 38 | 50 00 | 45 85 | 47 69 | 42 09 | 54 16 | 54 21 | 38 03 | 37 39 | 49 15 | 62 75 | 43 49 |
| <i>Fragilaropsis cylindrus</i> | | 13 07 | 5 40 | 29 14 | 27 76 | 16 21 | 16 16 | 6 76 | 28 04 | 28 26 | 24 10 | 34 85 | 21 90 | 10 61 | 29 20 | 28 93 | 17 63 | 16 28 | 22 00 |
| <i>Fragilaropsis kerguelensis</i> | | 0 88 | 0 54 | 0 17 | 12 76 | 0 17 | 0 17 | 1 18 | 0 17 | 0 51 | 0 17 | 0 34 | 0 51 | 2 53 | 4 07 | 7 11 | 0 17 | 0 50 | 0 00 |
| <i>Fragilaropsis lineata</i> | | 1 24 | 0 54 | 0 87 | 0 86 | 1 54 | 0 51 | 0 51 | 0 34 | 0 17 | 0 85 | 0 51 | 0 34 | 1 85 | 0 85 | 1 02 | 1 69 | 0 34 | 0 68 |
| <i>Nitzschia obliquecostata</i> | | 1 24 | 2 70 | 1 22 | 1 72 | 3 75 | 3 23 | 1 18 | 1 35 | 1 69 | 0 85 | 2 36 | 2 04 | 3 20 | 3 06 | 2 03 | 3 39 | 1 51 | 2 20 |
| <i>Nitzschia separanda</i> | | 0 18 | 0 00 | 0 17 | 1 21 | 0 68 | 0 00 | 0 17 | 0 00 | 0 34 | 1 03 | 0 67 | 0 68 | 0 84 | 1 36 | 1 86 | 0 51 | 1 01 | 0 85 |
| <i>Nitzschia sublineata</i> | | 0 18 | 0 36 | 0 17 | 0 86 | 2 56 | 0 68 | 1 69 | 1 01 | 1 52 | 0 68 | 1 01 | 1 02 | 2 36 | 0 34 | 1 35 | 1 02 | 0 84 | 1 52 |
| <i>Pentalamina corona</i> | | 1 59 | 0 54 | 0 17 | 1 55 | 1 88 | 4 25 | 3 04 | 3 72 | 4 57 | 8 72 | 3 70 | 3 06 | 3 87 | 4 41 | 3 55 | 4 75 | 1 34 | 5 58 |
| <i>Porosira glacialis</i> | | 0 18 | 0 18 | 0 00 | 0 00 | 0 34 | 2 38 | 1 86 | 0 51 | 0 85 | 0 51 | 0 84 | 0 68 | 1 18 | 0 00 | 0 00 | 2 54 | 1 34 | 0 68 |
| <i>Pseudonitzschia turgiduloides</i> | | 0 53 | 0 00 | 0 17 | 0 00 | 0 00 | 0 00 | 0 00 | 0 17 | 0 00 | 0 17 | 0 51 | 0 00 | 0 00 | 0 00 | 0 00 | 0 51 | 0 00 | 0 34 |
| <i>Stellatnma microtrias</i> | | 0 00 | 0 18 | 0 00 | 0 86 | 0 17 | 0 17 | 0 17 | 0 17 | 0 00 | 0 00 | 0 00 | 0 00 | 0 51 | 0 00 | 0 17 | 0 17 | 0 17 | 0 17 |
| <i>Thalassiosira antarctica (spores)</i> | | 2 30 | 0 72 | 0 52 | 1 55 | 2 56 | 7 14 | 16 39 | 3 38 | 4 91 | 4 96 | 5 56 | 5 94 | 5 05 | 2 55 | 2 20 | 9 32 | 5 87 | 9 48 |
| <i>Thalassiosira antarctica (veg)</i> | | 0 00 | 0 00 | 0 00 | 0 00 | 0 00 | 0 17 | 0 17 | 0 00 | 0 00 | 0 00 | 0 00 | 0 00 | 0 00 | 0 00 | 0 00 | 0 00 | 0 00 | 0 00 |
| <i>Thalassiosira gracilis</i> | | 0 18 | 0 00 | 1 57 | 3 97 | 2 22 | 0 34 | 0 84 | 0 68 | 0 68 | 0 34 | 0 67 | 0 85 | 1 68 | 2 21 | 2 71 | 0 51 | 1 68 | 0 85 |
| <i>Thalassiosira gracilis var expecta</i> | | 0 00 | 0 00 | 0 17 | 0 00 | 0 00 | 0 00 | 0 00 | 0 00 | 0 00 | 0 00 | 0 00 | 0 00 | 0 00 | 0 00 | 0 00 | 0 00 | 0 00 | 0 00 |
| <i>Thalassiosira lentiginosa</i> | | 0 35 | 0 36 | 0 17 | 0 86 | 0 51 | 0 34 | 0 84 | 0 34 | 0 17 | 0 17 | 0 00 | 0 51 | 0 67 | 0 68 | 1 35 | 0 00 | 0 17 | 0 00 |
| <i>Trichotoxin reinboldi</i> | | 0 18 | 0 00 | 0 00 | 1 72 | 0 34 | 0 34 | 0 00 | 0 17 | 0 00 | 0 00 | 0 17 | 0 00 | 0 34 | 0 34 | 0 85 | 0 34 | 0 00 | 0 17 |

| Species | Site | KRGR17 | KRGR18 | KRGR19 | KRGR23 | KRGR24 | KRGR25 | KRGR26 | KRGR27 | KRGR28 | KRGR29 | KRGR30 | KRGR31 | KRGR32 | KRGR34 | KRGR35 | KRGC1 | KRGC2 | KRGC8 |
|---|------|--------|--------|--------|--------|--------|--------|--------|--------|--------|--------|--------|--------|--------|--------|--------|-------|-------|-------|
| <i>Actinocyclus actinochilus</i> | | 0 34 | 0 00 | 0 00 | 0 00 | 0 17 | 1 02 | 0 68 | 0 34 | 0 51 | 0 34 | 0 17 | 1 42 | 0 00 | 1 23 | 0 00 | 0 00 | 0 35 | 0 67 |
| <i>Chaetoceros spp</i> | | 0 00 | 1 36 | 0 17 | 0 00 | 0 00 | 0 34 | 0 00 | 0 00 | 0 00 | 0 00 | 0 00 | 0 00 | 11 84 | 0 18 | 0 00 | 0 87 | 0 88 | 0 00 |
| <i>Chaetoceros cysts</i> | | 5 56 | 2 90 | 2 39 | 2 88 | 3 72 | 9 81 | 8 52 | 10 71 | 2 89 | 3 24 | 10 46 | 18 66 | 5 30 | 15 29 | 22 55 | 13 37 | 6 88 | 0 67 |
| <i>Dactylosolen antarcticus</i> | | 0 17 | 0 00 | 0 00 | 0 68 | 0 17 | 2 03 | 1 70 | 0 68 | 0 17 | 1 36 | 0 17 | 1 01 | 0 00 | 1 23 | 1 72 | 0 52 | 0 53 | 1 50 |
| <i>Diastephanus speculum</i> | | 0 34 | 0 17 | 0 51 | 0 34 | 0 17 | 0 85 | 0 68 | 0 17 | 0 17 | 0 85 | 0 34 | 0 00 | 0 18 | 0 35 | 0 17 | 0 00 | 0 71 | 1 00 |
| <i>Eucampia antarctica</i> | | 0 00 | 0 00 | 0 17 | 0 00 | 0 17 | 0 51 | 0 17 | 1 36 | 0 51 | 0 00 | 0 69 | 7 91 | 0 88 | 0 70 | 0 00 | 0 00 | 0 35 | 1 00 |
| <i>Fragilaropsis angulata</i> | | 2 53 | 3 24 | 2 39 | 3 72 | 4 40 | 2 54 | 3 24 | 4 59 | 4 08 | 4 43 | 4 80 | 4 87 | 1 94 | 3 87 | 5 34 | 2 95 | 5 64 | 6 84 |
| <i>Fragilaropsis curta</i> | | 59 43 | 45 14 | 60 48 | 61 59 | 58 04 | 37 73 | 33 39 | 37 59 | 40 82 | 53 49 | 41 34 | 34 28 | 35 69 | 32 16 | 36 83 | 35 42 | 57 14 | 68 28 |
| <i>Fragilaropsis cylindrus</i> | | 17 17 | 38 16 | 26 06 | 9 14 | 17 26 | 9 14 | 23 00 | 3 91 | 34 18 | 21 47 | 23 67 | 8 32 | 34 63 | 19 33 | 17 21 | 37 50 | 19 58 | 1 50 |
| <i>Fragilaropsis kerguelensis</i> | | 0 34 | 0 34 | 0 17 | 0 85 | 0 51 | 4 06 | 6 64 | 11 22 | 2 04 | 1 02 | 0 51 | 2 23 | 0 35 | 7 91 | 1 38 | 0 87 | 0 18 | 2 67 |
| <i>Fragilaropsis lineata</i> | | 0 17 | 0 68 | 0 68 | 0 51 | 1 02 | 1 86 | 1 36 | 0 68 | 1 36 | 0 85 | 0 51 | 1 01 | 0 35 | 1 23 | 0 34 | 0 35 | 1 06 | 0 83 |
| <i>Nitzschia obliquecostata</i> | | 1 68 | 2 04 | 1 70 | 2 71 | 1 02 | 2 03 | 2 73 | 0 85 | 1 36 | 0 51 | 2 40 | 1 62 | 1 77 | 2 11 | 3 44 | 2 78 | 1 23 | 3 01 |
| <i>Nitzschia separanda</i> | | 0 34 | 0 17 | 0 34 | 1 69 | 0 34 | 2 20 | 2 21 | 2 38 | 0 68 | 0 85 | 0 86 | 1 42 | 0 18 | 2 28 | 1 20 | 0 35 | 0 53 | 1 00 |
| <i>Nitzschia sublineata</i> | | 0 34 | 1 19 | 1 36 | 1 02 | 1 18 | 1 18 | 0 17 | 1 53 | 1 19 | 1 19 | 1 37 | 1 62 | 1 41 | 1 23 | 1 72 | 0 17 | 0 18 | 0 67 |
| <i>Pentalamina corona</i> | | 4 38 | 1 19 | 1 36 | 2 88 | 3 21 | 4 06 | 4 94 | 3 91 | 4 25 | 2 56 | 2 06 | 0 81 | 0 00 | 3 34 | 4 13 | 1 56 | 0 88 | 1 00 |
| <i>Porosira glacialis</i> | | 1 35 | 0 00 | 0 00 | 2 03 | 0 34 | 1 02 | 0 17 | 1 02 | 0 17 | 0 17 | 3 26 | 0 20 | 0 18 | 0 53 | 0 00 | 0 00 | 0 71 | 0 50 |
| <i>Pseudonitzschia turgiduloides</i> | | 0 00 | 0 34 | 0 68 | 0 00 | 0 00 | 0 00 | 0 00 | 0 00 | 0 34 | 0 00 | 0 00 | 0 00 | 4 24 | 0 18 | 0 17 | 0 87 | 1 23 | 0 33 |
| <i>Stellatnma microtrias</i> | | 0 17 | 0 17 | 0 00 | 0 68 | 0 00 | 0 00 | 0 68 | 0 51 | 0 34 | 0 34 | 0 00 | 1 01 | 0 00 | 0 18 | 0 17 | 0 00 | 0 35 | 0 50 |
| <i>Thalassiosira antarctica (spores)</i> | | 5 22 | 1 53 | 1 19 | 8 12 | 7 45 | 16 07 | 4 77 | 13 27 | 1 87 | 2 56 | 5 15 | 6 29 | 0 71 | 2 11 | 1 72 | 1 74 | 0 71 | 4 67 |
| <i>Thalassiosira antarctica (veg)</i> | | 0 00 | 0 00 | 0 00 | 0 00 | 0 00 | 0 00 | 0 00 | 0 00 | 0 00 | 0 00 | 0 00 | 0 00 | 0 00 | 0 00 | 0 00 | 0 00 | 0 00 | 0 00 |
| <i>Thalassiosira gracilis</i> | | 0 17 | 1 19 | 0 34 | 1 02 | 0 85 | 2 54 | 2 56 | 2 72 | 1 19 | 3 24 | 1 37 | 2 43 | 0 00 | 2 46 | 1 20 | 0 17 | 0 53 | 2 17 |
| <i>Thalassiosira gracilis var expecta</i> | | 0 00 | 0 00 | 0 00 | 0 00 | 0 00 | 0 00 | 0 00 | 0 17 | 0 34 | 0 00 | 0 00 | 0 00 | 0 18 | 0 00 | 0 00 | 0 17 | 0 00 | 0 00 |
| <i>Thalassiosira lentiginosa</i> | | 0 00 | 0 00 | 0 00 | 0 00 | 0 00 | 0 68 | 1 70 | 1 53 | 0 51 | 0 51 | 0 17 | 3 45 | 0 00 | 1 41 | 0 69 | 0 17 | 0 35 | 0 83 |
| <i>Trichotoxin reinboldi</i> | | 0 34 | 0 17 | 0 00 | 0 17 | 0 00 | 0 34 | 0 68 | 0 85 | 1 02 | 1 02 | 0 69 | 1 42 | 0 18 | 0 70 | 0 00 | 0 17 | 0 00 | 0 33 |

| Species | Site | KRGC9 | KRGC14 | KRGC15 | KRGC16 | KRGC20 | KRGC24 | KRGC28 | KRGC32 | KRGC33 | GEO2 | GEO5 | GEO15 | GEO16 | GEO19 | GEO22 | GEO25 | RC3116 | RC3305 |
|---|------|-------|--------|--------|--------|--------|--------|--------|--------|--------|-------|-------|-------|-------|-------|-------|-------|--------|--------|
| <i>Actinocyclus actinochilus</i> | | 0.36 | 0.67 | 0.51 | 0.34 | 0.34 | 0.52 | 0.00 | 0.34 | 0.34 | 0.53 | 0.17 | 0.69 | 1.17 | 0.34 | 0.17 | 0.51 | 0.17 | 0.17 |
| <i>Chaetoceros spp</i> | | 0.00 | 0.00 | 0.00 | 0.00 | 0.00 | 0.00 | 0.34 | 0.00 | 0.17 | 0.00 | 0.51 | 0.00 | 0.00 | 0.00 | 0.17 | 0.00 | 0.17 | 0.34 |
| <i>Chaetoceros spores</i> | | 7.33 | 1.01 | 2.03 | 0.84 | 14.73 | 4.65 | 4.06 | 0.84 | 1.02 | 13.91 | 10.46 | 18.51 | 21.98 | 5.89 | 10.20 | 13.75 | 23.01 | 6.95 |
| <i>Dactylosolen antarcticus</i> | | 0.72 | 1.01 | 0.34 | 0.34 | 0.34 | 0.34 | 0.34 | 1.35 | 1.19 | 1.06 | 0.51 | 1.73 | 1.01 | 0.17 | 0.33 | 0.85 | 0.34 | 0.00 |
| <i>Distephanus speculum</i> | | 1.25 | 0.84 | 0.68 | 0.51 | 0.86 | 1.38 | 0.85 | 0.00 | 0.68 | 0.88 | 0.34 | 0.17 | 0.17 | 0.51 | 0.33 | 1.19 | 0.68 | 1.02 |
| <i>Eucampia antarctica</i> | | 3.94 | 3.69 | 5.58 | 1.18 | 1.03 | 1.38 | 0.17 | 1.35 | 1.19 | 1.06 | 1.03 | 0.87 | 1.34 | 0.51 | 0.39 | 1.36 | 0.68 | 0.17 |
| <i>Fragilaropsis angulata</i> | | 0.72 | 5.86 | 3.72 | 4.89 | 0.51 | 4.48 | 4.57 | 6.08 | 6.62 | 2.64 | 3.26 | 2.08 | 2.18 | 5.89 | 3.51 | 2.55 | 1.18 | 2.88 |
| <i>Fragilaropsis curta</i> | | 9.84 | 44.56 | 56.01 | 71.50 | 44.52 | 54.22 | 59.90 | 71.79 | 68.59 | 25.88 | 39.62 | 17.99 | 17.28 | 60.77 | 57.69 | 30.56 | 12.01 | 57.97 |
| <i>Fragilaropsis cylindrus</i> | | 2.68 | 1.01 | 3.05 | 2.02 | 12.50 | 12.74 | 11.68 | 3.89 | 4.58 | 22.01 | 9.78 | 3.98 | 4.70 | 5.89 | 11.87 | 8.66 | 8.46 | 11.02 |
| <i>Fragilaropsis kerguelensis</i> | | 45.80 | 5.70 | 1.35 | 0.67 | 5.14 | 0.69 | 1.02 | 1.35 | 0.51 | 12.50 | 1.54 | 25.95 | 16.11 | 1.01 | 1.34 | 11.38 | 1.18 | 0.68 |
| <i>Fragilaropsis lineata</i> | | 0.54 | 0.84 | 2.37 | 1.01 | 1.37 | 1.72 | 0.17 | 0.84 | 0.85 | 1.23 | 0.86 | 0.52 | 0.34 | 0.34 | 0.33 | 0.68 | 0.17 | 1.36 |
| <i>Nitzschia obliquecostata</i> | | 1.07 | 2.18 | 4.74 | 1.18 | 3.08 | 4.30 | 1.86 | 2.36 | 2.89 | 1.06 | 2.74 | 0.69 | 1.51 | 1.68 | 1.34 | 0.34 | 3.55 | 3.39 |
| <i>Nitzschia separanda</i> | | 2.50 | 4.36 | 0.51 | 0.84 | 1.03 | 0.52 | 0.68 | 2.36 | 1.19 | 2.11 | 0.69 | 2.77 | 2.85 | 0.67 | 1.84 | 3.74 | 0.51 | 0.17 |
| <i>Nitzschia sublineata</i> | | 0.18 | 0.67 | 0.68 | 1.01 | 0.51 | 0.00 | 0.00 | 0.17 | 0.68 | 0.00 | 0.69 | 0.17 | 0.50 | 0.51 | 0.17 | 0.34 | 0.68 | 0.34 |
| <i>Pentalamina corona</i> | | 0.72 | 0.17 | 1.35 | 2.87 | 1.20 | 1.72 | 4.06 | 0.68 | 0.85 | 2.99 | 8.06 | 3.98 | 5.87 | 6.90 | 3.68 | 6.28 | 4.57 | 4.07 |
| <i>Porosira glacialis</i> | | 0.00 | 0.84 | 0.85 | 0.84 | 0.00 | 1.55 | 0.68 | 0.00 | 0.85 | 0.00 | 2.06 | 0.17 | 0.34 | 0.51 | 0.67 | 0.51 | 0.51 | 1.36 |
| <i>Pseudonitzschia turgiduloides</i> | | 0.00 | 0.00 | 0.00 | 0.17 | 0.00 | 0.00 | 0.00 | 0.00 | 0.00 | 0.00 | 0.00 | 0.00 | 0.00 | 0.00 | 0.00 | 0.00 | 0.00 | 0.00 |
| <i>Stellanma microtrias</i> | | 0.72 | 2.51 | 0.85 | 0.51 | 0.34 | 0.86 | 0.00 | 0.68 | 0.51 | 0.88 | 1.72 | 0.52 | 0.00 | 0.51 | 0.33 | 0.34 | 0.34 | 0.00 |
| <i>Thalassiosira antarctica (spores)</i> | | 6.08 | 21.11 | 11.51 | 5.73 | 7.88 | 8.09 | 9.14 | 3.72 | 4.75 | 1.41 | 13.04 | 9.86 | 17.11 | 7.07 | 4.18 | 11.88 | 40.10 | 6.61 |
| <i>Thalassiosira antarctica (veg)</i> | | 0.00 | 0.00 | 0.00 | 0.00 | 0.00 | 0.00 | 0.00 | 0.00 | 0.00 | 0.00 | 0.00 | 0.00 | 0.00 | 0.00 | 0.00 | 0.00 | 0.00 | 0.00 |
| <i>Thalassiosira gracilis</i> | | 5.01 | 1.51 | 2.71 | 3.04 | 2.57 | 0.52 | 0.34 | 1.35 | 1.87 | 3.52 | 1.37 | 4.67 | 2.52 | 0.34 | 0.50 | 2.21 | 1.52 | 0.85 |
| <i>Thalassiosira gracilis var expecta</i> | | 0.36 | 0.00 | 0.00 | 0.00 | 0.86 | 0.17 | 0.17 | 0.00 | 0.00 | 0.70 | 0.34 | 1.04 | 0.50 | 0.17 | 0.33 | 0.00 | 0.17 | 0.00 |
| <i>Thalassiosira lentiginosa</i> | | 8.59 | 1.51 | 1.02 | 0.17 | 1.20 | 0.17 | 0.00 | 0.68 | 0.68 | 3.52 | 0.86 | 2.60 | 1.51 | 0.00 | 0.00 | 1.53 | 0.00 | 0.51 |
| <i>Trichotoxin reinboldi</i> | | 1.61 | 0.00 | 0.17 | 0.34 | 0.00 | 0.00 | 0.00 | 0.17 | 0.00 | 2.11 | 0.34 | 1.04 | 1.01 | 0.34 | 0.67 | 1.36 | 0.00 | 0.17 |

| Species | Site | RC3606 | RC3607 | RC3616 | RG3109 | RG3111 | RG3117 | RG3119 | RG3121 | RG3203 | RG3205 | RG3207 | RG3218 | RG3219 | RG3222 | RG3314 | RG3315 | RG3318 | RG3321 |
|---|------|--------|--------|--------|--------|--------|--------|--------|--------|--------|--------|--------|--------|--------|--------|--------|--------|--------|--------|
| <i>Actinocyclus actinochilus</i> | | 1.24 | 0.86 | 0.17 | 0.51 | 0.17 | 0.17 | 0.34 | 0.34 | 0.17 | 0.17 | 0.00 | 0.52 | 0.69 | 0.17 | 0.69 | 0.52 | 0.68 | 0.34 |
| <i>Chaetoceros spp</i> | | 0.00 | 0.34 | 0.17 | 0.51 | 0.17 | 0.00 | 0.17 | 0.00 | 0.17 | 0.00 | 0.00 | 0.69 | 0.51 | 0.17 | 0.00 | 0.00 | 0.34 | 0.00 |
| <i>Chaetoceros spores</i> | | 17.41 | 14.38 | 7.60 | 12.69 | 9.17 | 6.91 | 8.46 | 9.60 | 12.78 | 5.08 | 5.91 | 11.34 | 9.78 | 19.38 | 22.81 | 7.79 | 19.80 | 5.94 |
| <i>Dactylosolen antarcticus</i> | | 0.36 | 0.00 | 1.01 | 0.34 | 0.17 | 0.17 | 0.34 | 0.67 | 0.00 | 0.00 | 0.00 | 0.17 | 0.69 | 0.17 | 2.06 | 0.00 | 0.34 | 0.17 |
| <i>Distephanus speculum</i> | | 1.89 | 0.51 | 0.51 | 0.17 | 0.51 | 0.34 | 0.85 | 0.51 | 0.34 | 0.51 | 0.17 | 0.86 | 0.86 | 0.17 | 2.06 | 0.69 | 0.85 | 0.51 |
| <i>Eucampia antarctica</i> | | 1.24 | 0.86 | 0.84 | 0.17 | 0.85 | 1.18 | 0.34 | 0.17 | 0.51 | 0.17 | 0.17 | 0.86 | 0.17 | 1.20 | 0.86 | 0.17 | 1.02 | 0.00 |
| <i>Fragilaropsis angulata</i> | | 1.07 | 2.05 | 4.05 | 4.23 | 3.40 | 3.88 | 2.03 | 2.19 | 2.56 | 6.09 | 2.20 | 3.09 | 2.40 | 1.89 | 0.86 | 1.04 | 3.92 | 2.21 |
| <i>Fragilaropsis curta</i> | | 21.85 | 30.48 | 54.73 | 51.27 | 51.27 | 50.93 | 46.53 | 47.14 | 58.77 | 70.90 | 51.86 | 39.35 | 37.05 | 28.13 | 19.55 | 43.77 | 36.52 | 37.35 |
| <i>Fragilaropsis cylindrus</i> | | 11.19 | 15.58 | 7.94 | 9.48 | 10.87 | 9.61 | 16.92 | 9.26 | 6.98 | 10.15 | 31.93 | 15.98 | 27.27 | 24.36 | 7.89 | 30.97 | 18.60 | 21.05 |
| <i>Fragilaropsis kerguelensis</i> | | 12.79 | 3.25 | 1.01 | 0.34 | 1.70 | 1.35 | 0.17 | 1.35 | 0.51 | 0.00 | 0.51 | 3.09 | 3.60 | 5.49 | 10.46 | 0.87 | 4.10 | 11.04 |
| <i>Fragilaropsis lineata</i> | | 0.89 | 1.03 | 0.51 | 0.68 | 1.70 | 1.35 | 1.02 | 1.35 | 0.17 | 0.51 | 0.17 | 2.06 | 0.69 | 0.34 | 2.74 | 2.25 | 0.85 | 1.70 |
| <i>Nitzschia obliquecostata</i> | | 1.07 | 0.86 | 2.70 | 1.86 | 1.36 | 3.71 | 1.18 | 2.36 | 1.36 | 1.18 | 1.18 | 4.47 | 2.74 | 1.89 | 1.54 | 1.21 | 1.37 | 1.87 |
| <i>Nitzschia separanda</i> | | 2.49 | 1.03 | 0.34 | 1.52 | 0.51 | 1.35 | 0.68 | 0.51 | 1.36 | 0.00 | 0.00 | 0.34 | 0.51 | 1.20 | 2.23 | 0.52 | 0.68 | 2.04 |
| <i>Nitzschia sublineata</i> | | 0.00 | 0.86 | 0.00 | 0.34 | 0.51 | 0.00 | 0.85 | 0.17 | 0.34 | 0.34 | 0.17 | 0.00 | 0.69 | 0.17 | 0.00 | 0.35 | 0.51 | 0.51 |
| <i>Pentalamina corona</i> | | 5.51 | 7.19 | 5.41 | 4.06 | 4.41 | 6.07 | 4.40 | 3.87 | 2.21 | 1.86 | 2.20 | 3.26 | 3.60 | 3.09 | 4.46 | 3.63 | 3.58 | 1.19 |
| <i>Porosira glacialis</i> | | 0.18 | 0.17 | 0.84 | 1.02 | 1.02 | 1.18 | 1.02 | 1.35 | 0.51 | 0.00 | 0.00 | 0.52 | 0.17 | 0.17 | 0.17 | 0.17 | 0.34 | 0.00 |
| <i>Pseudonitzschia turgiduloides</i> | | 0.00 | 0.00 | 0.00 | 0.00 | 0.34 | 0.00 | 0.00 | 0.00 | 0.00 | 0.00 | 0.17 | 0.00 | 0.17 | 0.00 | 0.00 | 0.00 | 0.00 | 0.00 |
| <i>Stellanma microtrias</i> | | 0.89 | 0.86 | 0.68 | 0.85 | 0.68 | 1.01 | 0.85 | 0.67 | 0.17 | 0.00 | 0.68 | 0.69 | 0.17 | 0.69 | 1.37 | 0.52 | 0.17 | 1.19 |
| <i>Thalassiosira antarctica (spores)</i> | | 9.06 | 13.87 | 8.45 | 8.12 | 8.83 | 8.77 | 11.84 | 13.97 | 8.52 | 1.69 | 1.52 | 8.76 | 3.60 | 4.97 | 10.12 | 1.56 | 2.05 | 1.87 |
| <i>Thalassiosira antarctica (veg)</i> | | 0.00 | 0.00 | 0.00 | 0.00 | 0.00 | 0.00 | 0.00 | 0.00 | 0.00 | 0.00 | 0.00 | 0.00 | 0.00 | 0.00 | 0.00 | 0.00 | 0.00 | 0.00 |
| <i>Thalassiosira gracilis</i> | | 7.64 | 3.08 | 1.69 | 0.34 | 1.53 | 0.51 | 1.02 | 2.19 | 0.17 | 0.68 | 0.34 | 1.55 | 1.54 | 2.40 | 2.74 | 2.08 | 1.71 | 7.30 |
| <i>Thalassiosira gracilis var expecta</i> | | 1.07 | 0.68 | 0.84 | 0.51 | 0.17 | 1.01 | 0.17 | 0.34 | 0.51 | 0.17 | 0.34 | 0.17 | 1.54 | 1.54 | 2.40 | 1.21 | 0.68 | 1.36 |
| <i>Thalassiosira lentiginosa</i> | | 2.13 | 1.71 | 0.51 | 0.34 | 0.17 | 0.34 | 0.85 | 1.35 | 0.68 | 0.34 | 0.34 | 1.72 | 0.51 | 1.03 | 2.74 | 0.52 | 1.19 | 1.53 |
| <i>Trichotoxin reinboldi</i> | | 1.07 | 0.34 | 0.00 | 0.68 | 0.51 | 0.17 | 0.00 | 0.67 | 1.19 | 0.17 | 0.17 | 0.52 | 1.03 | 1.37 | 2.23 | 0.17 | 0.68 | 0.85 |

| Species | Site | RG3324 | RG3326 | RG3328 | RG3329 | RG3331 | RG3333 | RG3335 | RG3346 | BANG7 | BANG8 | BANG10 | BANG11 | BANG12 | BANG13 | BANG14 | BANG15 | BANG16 | BANG17 |
|---|------|--------|--------|--------|--------|--------|--------|--------|--------|-------|-------|--------|--------|--------|--------|--------|--------|--------|--------|
| <i>Actinocyclus actinochilus</i> | | 0 68 | 1 04 | 2 74 | 0 51 | 1 20 | 0 68 | 0 00 | 0 00 | 0 00 | 0 00 | 0 36 | 0 00 | 0 17 | 0 18 | 0 17 | 0 53 | 0 87 | 1 57 |
| <i>Chaetoceros spp</i> | | 0 00 | 0 00 | 0 00 | 0 00 | 0 00 | 0 17 | 0 17 | 0 00 | 0 00 | 0 53 | 0 36 | 0 69 | 0 85 | 0 00 | 0 52 | 0 18 | 0 00 | 0 00 |
| <i>Chaetoceros spores</i> | | 13 36 | 15 03 | 14 87 | 15 38 | 14 70 | 8 46 | 14 29 | 4 05 | 18 18 | 13 27 | 12 79 | 21 38 | 10 09 | 12 54 | 12 94 | 12 28 | 10 63 | 9 23 |
| <i>Dactylosolen antarcticus</i> | | 0 86 | 0 35 | 0 34 | 0 68 | 0 85 | 0 34 | 0 00 | 0 17 | 0 34 | 0 35 | 0 36 | 0 52 | 0 85 | 1 24 | 0 87 | 0 70 | 2 09 | 1 05 |
| <i>Distephanus speculum</i> | | 1 54 | 0 69 | 1 54 | 0 68 | 2 74 | 0 85 | 1 87 | 0 34 | 0 17 | 0 00 | 0 36 | 0 52 | 0 00 | 0 88 | 0 00 | 0 18 | 1 57 | 1 22 |
| <i>Eucampia antarctica</i> | | 0 34 | 0 35 | 2 22 | 1 37 | 0 68 | 0 34 | 0 17 | 0 00 | 0 00 | 0 35 | 0 89 | 0 52 | 0 34 | 0 88 | 0 35 | 1 05 | 5 57 | 2 44 |
| <i>Fragilaropsis angulata</i> | | 0 34 | 2 76 | 1 88 | 2 74 | 2 22 | 2 03 | 2 72 | 5 23 | 4 80 | 7 43 | 5 68 | 3 45 | 4 62 | 5 12 | 1 75 | 0 70 | 2 44 | 2 26 |
| <i>Fragilaropsis curta</i> | | 28 94 | 35 23 | 22 05 | 31 45 | 37 95 | 41 29 | 38 10 | 60 20 | 44 77 | 44 78 | 44 58 | 36 38 | 54 36 | 48 06 | 37 06 | 17 19 | 18 47 | 27 87 |
| <i>Fragilaropsis cylindrus</i> | | 27 23 | 8 46 | 5 30 | 8 72 | 11 62 | 24 20 | 18 71 | 19 06 | 10 81 | 16 81 | 15 45 | 18 97 | 15 56 | 9 89 | 23 25 | 4 21 | 5 57 | 6 97 |
| <i>Fragilaropsis kerguelensis</i> | | 8 22 | 8 12 | 11 28 | 7 35 | 3 59 | 1 35 | 1 19 | 1 18 | 0 69 | 1 59 | 0 36 | 0 34 | 0 68 | 2 47 | 3 85 | 40 18 | 30 66 | 23 69 |
| <i>Fragilaropsis lineata</i> | | 1 71 | 1 73 | 2 39 | 2 39 | 2 05 | 0 68 | 1 87 | 0 17 | 1 20 | 1 59 | 1 24 | 1 03 | 0 17 | 1 06 | 0 70 | 0 70 | 0 52 | 1 57 |
| <i>Nitzschia obliquecostata</i> | | 1 03 | 2 76 | 2 39 | 2 91 | 2 91 | 2 88 | 3 40 | 2 53 | 3 43 | 3 36 | 3 20 | 4 48 | 2 91 | 2 65 | 4 02 | 1 40 | 3 48 | 1 74 |
| <i>Nitzschia separanda</i> | | 0 86 | 1 73 | 2 05 | 2 39 | 0 68 | 1 35 | 0 00 | 0 17 | 0 69 | 0 53 | 0 71 | 0 34 | 0 17 | 1 59 | 0 35 | 1 93 | 1 92 | 2 79 |
| <i>Nitzschia sublineata</i> | | 0 34 | 0 35 | 0 85 | 0 00 | 0 85 | 0 68 | 0 85 | 0 17 | 0 51 | 0 35 | 0 71 | 0 00 | 0 68 | 0 53 | 0 17 | 0 00 | 0 00 | 0 35 |
| <i>Pentalamina corona</i> | | 2 23 | 2 07 | 2 39 | 3 76 | 3 93 | 5 25 | 3 74 | 3 04 | 5 15 | 2 65 | 3 37 | 2 76 | 2 05 | 3 89 | 4 72 | 1 40 | 1 05 | 0 87 |
| <i>Porosira glacialis</i> | | 0 00 | 0 17 | 0 51 | 0 34 | 0 51 | 0 34 | 0 85 | 0 17 | 0 86 | 0 35 | 0 18 | 1 03 | 1 03 | 1 06 | 0 35 | 0 00 | 0 00 | 0 00 |
| <i>Pseudonitzschia turgiduloides</i> | | 0 17 | 0 17 | 0 00 | 0 00 | 0 17 | 0 00 | 0 00 | 0 00 | 0 00 | 0 18 | 0 89 | 0 34 | 1 54 | 0 00 | 0 70 | 0 00 | 0 00 | 0 00 |
| <i>Stellanma microtrias</i> | | 0 86 | 0 86 | 1 88 | 0 68 | 1 54 | 0 51 | 0 51 | 0 00 | 0 69 | 0 00 | 0 00 | 0 17 | 0 17 | 0 18 | 0 17 | 0 70 | 0 70 | 0 70 |
| <i>Thalassiosira antarctica (spores)</i> | | 3 94 | 7 77 | 15 21 | 10 77 | 7 35 | 5 41 | 9 35 | 2 02 | 3 60 | 3 19 | 4 44 | 5 00 | 0 00 | 4 42 | 4 72 | 5 44 | 4 53 | 2 26 |
| <i>Thalassiosira antarctica (veg)</i> | | 0 00 | 0 00 | 0 00 | 0 00 | 0 00 | 0 00 | 0 00 | 0 00 | 0 00 | 0 00 | 0 00 | 0 00 | 2 56 | 0 00 | 0 00 | 0 00 | 0 00 | 0 00 |
| <i>Thalassiosira gracilis</i> | | 5 14 | 5 70 | 5 47 | 5 13 | 2 22 | 1 52 | 1 19 | 1 01 | 3 26 | 1 95 | 3 55 | 1 21 | 0 85 | 2 12 | 2 62 | 5 79 | 4 01 | 5 92 |
| <i>Thalassiosira gracilis var expecta</i> | | 1 03 | 1 55 | 0 51 | 1 20 | 1 37 | 0 68 | 0 51 | 0 00 | 0 34 | 0 35 | 0 36 | 0 69 | 0 34 | 0 53 | 0 00 | 0 70 | 0 87 | 1 22 |
| <i>Thalassiosira lentiginosa</i> | | 1 20 | 2 59 | 3 42 | 1 54 | 0 85 | 0 68 | 0 51 | 0 17 | 0 17 | 0 18 | 0 18 | 0 00 | 0 00 | 0 18 | 0 70 | 3 68 | 3 83 | 4 88 |
| <i>Trichotoxin reinboldii</i> | | 0 00 | 0 52 | 0 68 | 0 00 | 0 00 | 0 34 | 0 00 | 0 34 | 0 34 | 0 18 | 0 00 | 0 17 | 0 00 | 0 53 | 0 00 | 1 05 | 1 22 | 1 39 |

| Species | Site | BANG18 | BANG20 | BANG21 | BANG22 | BANG23 | BANG24 | BANG25 | BANG28 | BANG31 | BANG32 | BANG37 | BANG38 | BANG42 | BANG44 |
|---|------|--------|--------|--------|--------|--------|--------|--------|--------|--------|--------|--------|--------|--------|--------|
| <i>Actinocyclus actinochilus</i> | | 1 05 | 0 00 | 0 86 | 1 03 | 1 22 | 1 04 | 1 04 | 0 00 | 0 34 | 0 34 | 0 00 | 0 17 | 0 00 | 0 18 |
| <i>Chaetoceros spp</i> | | 0 00 | 0 00 | 0 00 | 0 00 | 0 00 | 0 00 | 0 00 | 0 00 | 0 00 | 0 00 | 0 00 | 0 52 | 0 00 | 0 18 |
| <i>Chaetoceros spores</i> | | 6 67 | 9 09 | 11 02 | 25 99 | 14 24 | 11 13 | 6 60 | 7 12 | 5 94 | 7 13 | 9 64 | 11 38 | 10 95 | 13 27 |
| <i>Dactylosolen antarcticus</i> | | 0 88 | 0 69 | 0 52 | 1 20 | 1 91 | 2 09 | 0 00 | 1 19 | 0 85 | 1 19 | 0 17 | 1 21 | 0 18 | 0 71 |
| <i>Distephanus speculum</i> | | 0 70 | 0 51 | 0 34 | 0 52 | 1 22 | 1 22 | 0 17 | 1 02 | 0 34 | 0 17 | 0 00 | 0 00 | 0 00 | 0 18 |
| <i>Eucampia antarctica</i> | | 1 05 | 0 34 | 1 55 | 0 86 | 0 17 | 2 26 | 2 26 | 0 00 | 1 02 | 0 34 | 0 34 | 0 86 | 0 00 | 0 35 |
| <i>Fragilaropsis angulata</i> | | 2 63 | 1 89 | 2 07 | 0 17 | 0 87 | 1 04 | 1 22 | 3 39 | 4 24 | 2 72 | 5 51 | 6 55 | 4 42 | 3 89 |
| <i>Fragilaropsis curta</i> | | 29 82 | 38 77 | 28 06 | 10 67 | 20 66 | 7 48 | 4 17 | 43 73 | 51 61 | 46 01 | 42 34 | 39 14 | 42 05 | 45 66 |
| <i>Fragilaropsis cylindrus</i> | | 9 82 | 12 18 | 12 74 | 5 34 | 6 42 | 0 17 | 0 17 | 11 36 | 9 68 | 16 64 | 28 74 | 18 28 | 27 39 | 11 50 |
| <i>Fragilaropsis kerguelensis</i> | | 21 23 | 9 95 | 15 49 | 39 76 | 34 03 | 54 96 | 71 18 | 6 44 | 2 38 | 1 87 | 0 17 | 1 55 | 0 71 | 4 07 |
| <i>Fragilaropsis lineata</i> | | 1 40 | 0 51 | 1 38 | 0 34 | 1 04 | 0 00 | 0 52 | 1 69 | 1 36 | 1 19 | 0 69 | 1 38 | 0 18 | 2 30 |
| <i>Nitzschia obliquecostata</i> | | 1 75 | 1 03 | 2 41 | 0 17 | 1 39 | 0 52 | 1 04 | 1 02 | 2 38 | 3 74 | 3 10 | 3 45 | 3 71 | 2 65 |
| <i>Nitzschia separanda</i> | | 1 75 | 1 72 | 0 52 | 1 72 | 2 43 | 3 13 | 3 13 | 1 36 | 1 19 | 1 87 | 0 86 | 1 21 | 0 35 | 1 24 |
| <i>Nitzschia sublineata</i> | | 0 53 | 0 00 | 0 17 | 0 17 | 0 35 | 0 35 | 0 87 | 0 17 | 0 17 | 0 17 | 0 17 | 1 03 | 0 53 | 0 53 |
| <i>Pentalamina corona</i> | | 1 93 | 4 46 | 1 89 | 0 86 | 1 22 | 0 35 | 0 00 | 4 75 | 3 23 | 5 26 | 2 58 | 4 48 | 3 53 | 4 78 |
| <i>Porosira glacialis</i> | | 0 18 | 0 00 | 0 17 | 0 17 | 0 17 | 0 00 | 0 00 | 0 34 | 0 17 | 0 68 | 0 34 | 1 38 | 0 18 | 0 18 |
| <i>Pseudonitzschia turgiduloides</i> | | 0 00 | 0 00 | 0 00 | 0 17 | 0 00 | 0 00 | 0 00 | 0 00 | 0 00 | 0 17 | 0 17 | 0 52 | 0 71 | 0 00 |
| <i>Stellanma microtrias</i> | | 0 88 | 0 34 | 0 69 | 0 00 | 0 00 | 0 35 | 0 87 | 0 85 | 0 51 | 0 17 | 0 69 | 0 17 | 0 18 | 0 18 |
| <i>Thalassiosira antarctica (spores)</i> | | 3 68 | 8 58 | 8 95 | 3 27 | 1 74 | 3 83 | 0 87 | 9 15 | 10 19 | 6 96 | 1 89 | 3 45 | 3 00 | 1 77 |
| <i>Thalassiosira antarctica (veg)</i> | | 0 00 | 0 00 | 0 00 | 0 00 | 0 00 | 0 00 | 0 00 | 0 00 | 0 00 | 0 00 | 0 00 | 0 00 | 0 00 | 0 00 |
| <i>Thalassiosira gracilis</i> | | 6 84 | 5 83 | 5 85 | 4 13 | 3 82 | 3 65 | 0 17 | 4 68 | 3 06 | 1 87 | 1 72 | 1 90 | 1 77 | 4 25 |
| <i>Thalassiosira gracilis var expecta</i> | | 0 70 | 0 34 | 0 86 | 0 17 | 0 87 | 0 35 | 0 00 | 0 17 | 0 68 | 0 85 | 0 34 | 0 52 | 0 00 | 1 24 |
| <i>Thalassiosira lentiginosa</i> | | 3 33 | 2 57 | 3 10 | 3 10 | 4 51 | 5 04 | 5 03 | 1 36 | 0 17 | 0 51 | 0 52 | 0 69 | 0 18 | 0 88 |
| <i>Trichotoxin reinboldii</i> | | 3 16 | 1 20 | 1 38 | 0 17 | 1 74 | 1 04 | 0 69 | 0 34 | 0 51 | 0 17 | 0 00 | 0 17 | 0 00 | 0 00 |

| Site | BANG18 | BANG20 | BANG21 | BANG22 | BANG23 | BANG24 | BANG25 | BANG28 | BANG31 | BANG32 | BANG37 | BANG38 | BANG42 | BANG44 |
|---|--------|--------|--------|--------|--------|--------|--------|--------|--------|--------|--------|--------|--------|--------|
| Species | | | | | | | | | | | | | | |
| <i>Actinocyclus actinochilus</i> | 1 05 | 0 00 | 0 86 | 1 03 | 1 22 | 1 04 | 1 04 | 0 00 | 0 34 | 0 34 | 0 00 | 0 17 | 0 00 | 0 18 |
| <i>Chaetoceros spp</i> | 0 00 | 0 00 | 0 00 | 0 00 | 0 00 | 0 00 | 0 00 | 0 00 | 0 00 | 0 00 | 0 00 | 0 52 | 0 00 | 0 18 |
| <i>Chaetoceros spores</i> | 6 67 | 9 09 | 11 02 | 1 25 | 99 | 14 24 | 11 13 | 6 60 | 7 12 | 5 94 | 7 13 | 9 64 | 11 38 | 10 95 |
| <i>Dactylosolen antarcticus</i> | 0 88 | 0 69 | 0 52 | 1 20 | 1 91 | 2 09 | 0 00 | 1 19 | 0 85 | 1 19 | 0 17 | 1 21 | 0 18 | 0 71 |
| <i>Distophanus speculum</i> | 0 70 | 0 51 | 0 34 | 0 52 | 1 22 | 1 22 | 0 17 | 1 02 | 0 34 | 0 17 | 0 00 | 0 00 | 0 00 | 0 18 |
| <i>Eucampia antarctica</i> | 1 05 | 0 34 | 1 55 | 0 86 | 0 17 | 2 26 | 2 26 | 0 00 | 1 02 | 0 34 | 0 34 | 0 86 | 0 00 | 0 35 |
| <i>Fragilaropsis angulata</i> | 2 63 | 1 89 | 2 07 | 0 17 | 0 87 | 1 04 | 1 22 | 3 39 | 4 24 | 2 72 | 5 51 | 6 55 | 4 42 | 3 89 |
| <i>Fragilaropsis curta</i> | 29 82 | 38 77 | 28 06 | 10 67 | 20 66 | 7 48 | 4 17 | 43 73 | 51 61 | 46 01 | 42 34 | 39 14 | 42 05 | 45 66 |
| <i>Fragilaropsis cylindrus</i> | 9 82 | 12 18 | 12 74 | 5 34 | 6 42 | 0 17 | 0 17 | 11 36 | 9 68 | 16 64 | 28 74 | 18 28 | 27 39 | 11 50 |
| <i>Fragilaropsis kerguelensis</i> | 21 23 | 9 95 | 15 49 | 39 76 | 34 03 | 54 96 | 71 18 | 6 44 | 2 38 | 1 87 | 0 17 | 1 55 | 0 71 | 4 07 |
| <i>Fragilaropsis lineata</i> | 1 40 | 0 51 | 1 38 | 0 34 | 1 04 | 0 00 | 0 52 | 1 69 | 1 36 | 1 19 | 0 69 | 1 38 | 0 18 | 2 30 |
| <i>Nitzschia obliquecostata</i> | 1 75 | 1 03 | 2 41 | 0 17 | 1 39 | 0 52 | 1 04 | 1 02 | 2 38 | 3 74 | 3 10 | 3 45 | 3 71 | 2 65 |
| <i>Nitzschia separanda</i> | 1 75 | 1 72 | 0 52 | 1 72 | 2 43 | 3 13 | 3 13 | 1 36 | 1 19 | 1 87 | 0 86 | 1 21 | 0 35 | 1 24 |
| <i>Nitzschia sublineata</i> | 0 53 | 0 00 | 0 17 | 0 17 | 0 35 | 0 35 | 0 87 | 0 17 | 0 17 | 0 17 | 0 17 | 1 03 | 0 53 | 0 53 |
| <i>Pentalamina corona</i> | 1 93 | 4 46 | 1 89 | 0 86 | 1 22 | 0 35 | 0 00 | 4 75 | 3 23 | 5 26 | 2 58 | 4 48 | 3 53 | 4 78 |
| <i>Porosira glacialis</i> | 0 18 | 0 00 | 0 17 | 0 17 | 0 17 | 0 00 | 0 00 | 0 34 | 0 17 | 0 68 | 0 34 | 1 38 | 0 18 | 0 18 |
| <i>Pseudonitzschia turgiduloides</i> | 0 00 | 0 00 | 0 00 | 0 17 | 0 00 | 0 00 | 0 00 | 0 00 | 0 00 | 0 17 | 0 17 | 0 52 | 0 71 | 0 00 |
| <i>Stellanma microtrias</i> | 0 88 | 0 34 | 0 69 | 0 00 | 0 00 | 0 35 | 0 87 | 0 85 | 0 51 | 0 17 | 0 69 | 0 17 | 0 18 | 0 18 |
| <i>Thalassiosira antarctica (spores)</i> | 3 68 | 8 58 | 8 95 | 3 27 | 1 74 | 3 83 | 0 87 | 9 15 | 10 19 | 6 96 | 1 89 | 3 45 | 3 00 | 1 77 |
| <i>Thalassiosira antarctica (veg)</i> | 0 00 | 0 00 | 0 00 | 0 00 | 0 00 | 0 00 | 0 00 | 0 00 | 0 00 | 0 00 | 0 00 | 0 00 | 0 00 | 0 00 |
| <i>Thalassiosira gracilis</i> | 6 84 | 5 83 | 5 85 | 4 13 | 3 82 | 3 65 | 0 17 | 4 58 | 3 06 | 1 87 | 1 72 | 1 90 | 1 77 | 4 25 |
| <i>Thalassiosira gracilis var expecta</i> | 0 70 | 0 34 | 0 86 | 0 17 | 0 87 | 0 35 | 0 00 | 0 17 | 0 68 | 0 85 | 0 34 | 0 52 | 0 00 | 1 24 |
| <i>Thalassiosira lentiginosa</i> | 3 33 | 2 57 | 3 10 | 3 10 | 4 51 | 5 04 | 5 03 | 1 36 | 0 17 | 0 51 | 0 52 | 0 69 | 0 18 | 0 88 |
| <i>Trichotoxon reinboldii</i> | 3 16 | 1 20 | 1 38 | 0 17 | 1 74 | 1 04 | 0 69 | 0 34 | 0 51 | 0 17 | 0 00 | 0 17 | 0 00 | 0 00 |

– *Appendix 2* –

Preliminary cluster analyses of surface sediment samples

SIMEX PROVIDED THE ASSOCIATION MATRIX FROM DATA IN FILE surface dek
ASSOCIATION MATRIX IS A DISSIMILARITY MATRIX FROM BRAY-CURTIS

NUMBER OF INDIVIDUALS = 104
NUMBER OF VARIABLES = 24

ASSOCIATION MATRIX IS FROM SIMEX

METHOD GROUP AVERAGE (UNWEIGHTED PAIR GROUP METHOD USING ARITHMETIC AVERAGES)

| LABELS | DCF93019 | DCF93032 | DCF93047 | KGR1 | KGR2A | KGR4 | KGR5 | KGR6 | KGR7 | KGR8 |
|--------|----------|----------|----------|--------|--------|--------|--------|--------|--------|--------|
| KGR9 | KGR10 | KGR11 | KGR12 | KGR13 | KGR14 | KGR15 | KGR16 | KGR17 | KGR18 | KGR19 |
| KGR22 | KGR24 | KGR25 | KGR26 | KGR27 | KGR28 | KGR29 | KGR30 | KGR31 | KGR32 | KGR33 |
| KGR34 | KGR35 | KGR36 | KGR37 | KGR38 | KGR39 | KGR40 | KGR41 | KGR42 | KGR43 | KGR44 |
| GEO22 | GEO25 | RC3116 | RC3205 | RC3603 | RC3607 | RC3616 | RC3109 | RC3111 | RC3117 | RC3119 |
| RC3119 | RC3121 | RC3203 | RC3205 | RC3207 | RC3218 | RC3219 | RC3222 | RC3314 | RC3317 | RC3318 |
| RC3318 | RC3321 | RC3324 | RC3326 | RC3328 | RC3329 | RC3331 | RC3333 | RC3335 | RC3346 | RC3347 |
| BAN7 | BAN8 | BAN10 | BAN11 | BAN12 | BAN13 | BAN14 | BAN15 | BAN16 | BAN17 | BAN18 |
| BAN18 | BAN20 | BAN21 | BAN22 | BAN23 | BAN24 | BAN25 | BAN28 | BAN31 | BAN32 | BAN33 |
| BAN37 | BAN38 | BAN42 | BAN44 | | | | | | | |

FORMAT (SE14 7)

ALGORITHM FOR ASSOCIATION MATRIX USED = BRAY-CURTIS

| PAIRING ITEM | SEQUENCE JOINS ITEM | AT DISTANCE | AT DISTANCE X INDIVIDUALS |
|-----------------|------------------------|-------------|------------------------------|
| 74 | 76 | 079 | 1 902 |
| 91 | 93 | 089 | 2 139 |
| 14 | 15 | 091 | 2 180 |
| 86 | 99 | 092 | 2 212 |
| 67 | 78 | 093 | 2 221 |
| 82 | 102 | 094 | 2 265 |
| 36 | 45 | 095 | 2 309 |
| 57 | 60 | 097 | 2 324 |
| 9 | 12 | 097 | 2 339 |
| 48 | 49 | 099 | 2 364 |
| 25 | 32 | 100 | 2 403 |
| 92 | 98 | 101 | 2 431 |
| 59 | 62 | 102 | 2 437 |
| 101 | 103 | 102 | 2 455 |
| 89 | 90 | 102 | 2 458 |
| 26 | 52 | 104 | 2 499 |
| 51 | 58 | 104 | 2 501 |
| 18 | 23 | 105 | 2 513 |
| 9 | 11 | 105 | 2 518 |
| 6 | 19 | 105 | 2 527 |
| 47 | 59 | 106 | 2 550 |
| 82 | 83 | 106 | 2 552 |
| 55 | 74 | 111 | 2 654 |
| 86 | 100 | 111 | 2 668 |
| 43 | 50 | 112 | 2 692 |
| 13 | 54 | 113 | 2 707 |
| 51 | 63 | 114 | 2 728 |
| 17 | 22 | 114 | 2 744 |
| 46 | 91 | 115 | 2 765 |
| 67 | 71 | 116 | 2 777 |
| 14 | 25 | 116 | 2 782 |
| 36 | 44 | 116 | 2 790 |
| 89 | 95 | 116 | 2 791 |
| 20 | 21 | 116 | 2 794 |
| 57 | 86 | 117 | 2 812 |
| 9 | 18 | 118 | 2 826 |
| 37 | 88 | 119 | 2 851 |
| 47 | 61 | 119 | 2 855 |
| 1 | 80 | 121 | 2 902 |
| 81 | 82 | 122 | 2 935 |
| 8 | 9 | 125 | 2 993 |

| | | | |
|----|-----|-----|--------|
| 55 | 75 | 125 | 2 994 |
| 66 | 79 | 127 | 3 042 |
| 8 | 10 | 127 | 3 050 |
| 26 | 48 | 127 | 3 059 |
| 41 | 77 | 129 | 3 096 |
| 14 | 67 | 131 | 3 150 |
| 46 | 55 | 132 | 3 175 |
| 47 | 57 | 134 | 3 214 |
| 6 | 16 | 134 | 3 218 |
| 27 | 28 | 134 | 3 227 |
| 81 | 101 | 135 | 3 231 |
| 1 | 64 | 136 | 3 261 |
| 13 | 66 | 140 | 3 354 |
| 87 | 104 | 140 | 3 361 |
| 37 | 89 | 141 | 3 381 |
| 4 | 72 | 141 | 3 385 |
| 43 | 51 | 143 | 3 427 |
| 46 | 69 | 143 | 3 441 |
| 41 | 56 | 143 | 3 442 |
| 13 | 47 | 144 | 3 445 |
| 14 | 68 | 145 | 3 472 |
| 36 | 40 | 147 | 3 531 |
| 8 | 29 | 147 | 3 535 |
| 81 | 84 | 147 | 3 537 |
| 14 | 87 | 148 | 3 543 |
| 46 | 92 | 151 | 3 617 |
| 6 | 8 | 151 | 3 626 |
| 41 | 73 | 153 | 3 681 |
| 6 | 17 | 155 | 3 730 |
| 13 | 42 | 156 | 3 747 |
| 65 | 70 | 157 | 3 759 |
| 33 | 81 | 158 | 3 796 |
| 26 | 46 | 158 | 3 799 |
| 13 | 24 | 162 | 3 883 |
| 14 | 41 | 166 | 3 974 |
| 13 | 43 | 167 | 4 010 |
| 1 | 2 | 170 | 4 089 |
| 37 | 96 | 172 | 4 131 |
| 5 | 27 | 176 | 4 233 |
| 20 | 34 | 177 | 4 245 |
| 36 | 39 | 178 | 4 264 |
| 37 | 94 | 179 | 4 301 |
| 6 | 7 | 179 | 4 302 |
| 35 | 85 | 180 | 4 319 |
| 4 | 14 | 183 | 4 391 |
| 13 | 33 | 185 | 4 432 |
| 6 | 13 | 189 | 4 525 |
| 4 | 26 | 190 | 4 566 |
| 20 | 65 | 201 | 4 835 |
| 1 | 20 | 208 | 4 991 |
| 36 | 38 | 208 | 4 993 |
| 5 | 6 | 209 | 5 005 |
| 4 | 30 | 218 | 5 242 |
| 1 | 3 | 221 | 5 301 |
| 1 | 35 | 230 | 5 532 |
| 1 | 5 | 237 | 5 691 |
| 4 | 37 | 240 | 5 760 |
| 1 | 53 | 252 | 6 294 |
| 1 | 36 | 277 | 6 651 |
| 1 | 4 | 283 | 6 790 |
| 1 | 31 | 389 | 9 336 |
| 1 | 97 | 475 | 11 394 |

COHEN'S CORRELATION COEFFICIENT = 629366

BIOSTAT II HIERARCHICAL CLUSTER ANALYSIS (VER 3 5)

SIMK PROVIDED THE ASSOCIATION MATRIX FROM DATA IN FILE surface del2
 ASSOCIATION MATRIX IS A DISSIMILARITY MATRIX FROM BRAY-CURTIS

NUMBER OF INDIVIDUALS = 102
 NUMBER OF VARIABLES = 24

ASSOCIATION MATRIX IS FROM SIMK

| METHOD | GROUP AVERAGE | (UNWEIGHTED PAIR GROUP METHOD USING ARITHMETIC AVERAGES) | | | | | | | | | | | | | | | | | | | | | | | | | | | | | | | | | | | | | | | | | | | | | | | | | | | | | | | | | | | | | | | | | | | | | | | | | | | | | | | | | | | | | | | | | | | | | | | | | | | | | | | | | | | | | | | | | | | | | | | | | | | | | | | | | | | | | | | | | | | | | | | | | | | | | | | | | | | | | | | | | | | | | | | | | | | | | | | | | | | | | | | | | | | | | | | | | | | | | | | | | | | | | | | | | | | | | | | | | | | | | | | | | | | | | | | | | | | | | | | | | | | | | | | | | | | | | | | | | | | | | | | | | | | | | | | | | | | | | | | | | | | | | | | | | | | | | | | | | | | | | | | | | | | | | | | | | | | | | | | | | | | | | | | | | | | | | | | | | | | | | | | | | | | | | | | | | | | | | | | | | | | | | | | | | | | | | | | | | | | | | | | | | | | | | | | | | | | | | | | | | | | | | | | | | | | | | | | | | | | | | | | | | | | | | | | | | | | | | | | | | | | | | | | | | | | | | | | | | | | | | | | | | | | | | | | | | | | | | | | | | | | | | | | | | | | | | | | | | | | | | | | | | | | | | | | | | | | | | | | | | | | | | | | | | | | | | | | | | | | | | | | | | | | | | | | | | | | | | | | | | | | | | | | | | | | | | | | | | | | | | | | | | | | | | | | | | | | | | | | | | | | | | | | | | | | | | | | | | | | | | | | | | | | | | | | | | | | | | | | | | | | | | | | | | | | | | | | | | | | | | | | | | | | | | | | | | | | | | | | | | | | | | | | | | | | | | | | | | | | | | | | | | | | | | | | | | | | | | | | | | | | | | | | | | | | | | | | | | | | | | | | | | | | | | | | | | | | | | | | | | | | | | | | | | | | | | | | | | | | | | | | | | | | | | | | | | | | | | | | | | | | | | | | | | | | | | | | | | | | | | | | | | | | | | | | | | | | | | | | | | | | | | | | | | | | | | | | | | | | | | | | | | | | | | | | | | | | | | | | | | | | | | | | | | | | | | | | | | | | | | | | | | | | | | | | | | | | | | | | | | | | | | | | | | | | | | | | | | | | | | | | | | | | | | | | | | | | | | | | | | | | | | | | | | | | | | | | | | | | | | | | | | | | | | | | | | | | | | | | | |
|--------|---------------|--|----------|------|-------|------|------|------|------|------|------|-------|-------|-------|-------|-------|-------|-------|-------|-------|-------|-------|-------|-------|-------|-------|-------|-------|-------|-------|-------|-------|-------|-------|-------|-------|-------|-------|-------|-------|-------|-------|-------|-------|-------|-------|-------|-------|-------|-------|-------|-------|-------|-------|-------|-------|-------|-------|-------|-------|-------|-------|-------|-------|-------|-------|-------|-------|-------|-------|-------|-------|-------|-------|-------|-------|-------|-------|-------|-------|-------|-------|-------|-------|-------|-------|-------|-------|-------|-------|-------|-------|-------|-------|-------|-------|-------|-------|-------|-------|-------|--------|--------|--------|--------|--------|--------|--------|--------|--------|--------|--------|--------|--------|--------|--------|--------|--------|--------|--------|--------|--------|--------|--------|--------|--------|--------|--------|--------|--------|--------|--------|--------|--------|--------|--------|--------|--------|--------|--------|--------|--------|--------|--------|--------|--------|--------|--------|--------|--------|--------|--------|--------|--------|--------|--------|--------|--------|--------|--------|--------|--------|--------|--------|--------|--------|--------|--------|--------|--------|--------|--------|--------|--------|--------|--------|--------|--------|--------|--------|--------|--------|--------|--------|--------|--------|--------|--------|--------|--------|--------|--------|--------|--------|--------|--------|--------|--------|--------|--------|--------|--------|--------|--------|--------|--------|--------|--------|--------|--------|--------|--------|--------|--------|--------|--------|--------|--------|--------|--------|--------|--------|--------|--------|--------|--------|--------|--------|--------|--------|--------|--------|--------|--------|--------|--------|--------|--------|--------|--------|--------|--------|--------|--------|--------|--------|--------|--------|--------|--------|--------|--------|--------|--------|--------|--------|--------|--------|--------|--------|--------|--------|--------|--------|--------|--------|--------|--------|--------|--------|--------|--------|--------|--------|--------|--------|--------|--------|--------|--------|--------|--------|--------|--------|--------|--------|--------|--------|--------|--------|--------|--------|--------|--------|--------|--------|--------|--------|--------|--------|--------|--------|--------|--------|--------|--------|--------|--------|--------|--------|--------|--------|--------|--------|--------|--------|--------|--------|--------|--------|--------|--------|--------|--------|--------|--------|--------|--------|--------|--------|--------|--------|--------|--------|--------|--------|--------|--------|--------|--------|--------|--------|--------|--------|--------|--------|--------|--------|--------|--------|--------|--------|--------|--------|--------|--------|--------|--------|--------|--------|--------|--------|--------|--------|--------|--------|--------|--------|--------|--------|--------|--------|--------|--------|--------|--------|--------|--------|--------|--------|--------|--------|--------|--------|--------|--------|--------|--------|--------|--------|--------|--------|--------|--------|--------|--------|--------|--------|--------|--------|--------|--------|--------|--------|--------|--------|--------|--------|--------|--------|--------|--------|--------|--------|--------|--------|--------|--------|--------|--------|--------|--------|--------|--------|--------|--------|--------|--------|--------|--------|--------|--------|--------|--------|--------|--------|--------|--------|--------|--------|--------|--------|--------|--------|--------|--------|--------|--------|--------|--------|--------|--------|--------|--------|--------|--------|--------|--------|--------|--------|--------|--------|--------|--------|--------|--------|--------|--------|--------|--------|--------|--------|--------|--------|--------|--------|--------|--------|--------|--------|--------|--------|--------|--------|--------|--------|--------|--------|--------|--------|--------|--------|--------|--------|--------|--------|--------|--------|--------|--------|--------|--------|--------|--------|--------|--------|--------|--------|--------|--------|--------|--------|--------|--------|--------|--------|--------|--------|--------|--------|--------|--------|--------|--------|--------|--------|--------|--------|--------|--------|--------|--------|--------|--------|--------|--------|--------|--------|--------|--------|--------|--------|--------|--------|--------|--------|--------|--------|--------|--------|--------|--------|--------|--------|--------|--------|--------|--------|--------|--------|--------|--------|--------|--------|--------|--------|--------|--------|--------|--------|--------|--------|--------|--------|--------|--------|--------|--------|--------|--------|--------|--------|--------|--------|--------|--------|--------|--------|--------|--------|--------|--------|--------|--------|--------|--------|--------|--------|--------|--------|--------|--------|--------|--------|--------|--------|--------|--------|--------|--------|--------|--------|--------|--------|--------|--------|--------|--------|--------|--------|--------|--------|--------|--------|--------|--------|--------|--------|--------|--------|--------|--------|--------|--------|--------|--------|--------|--------|--------|--------|--------|--------|--------|--------|--------|--------|--------|--------|--------|--------|--------|--------|--------|--------|--------|--------|--------|--------|--------|--------|--------|--------|--------|--------|--------|--------|--------|--------|--------|--------|--------|--------|--------|--------|--------|--------|--------|--------|--------|--------|--------|--------|--------|--------|--------|--------|--------|--------|--------|--------|--------|--------|--------|--------|--------|--------|--------|--------|--------|--------|--------|--------|--------|--------|--------|--------|--------|--------|--------|--------|--------|--------|--------|--------|--------|--------|--------|--------|--------|--------|--------|--------|--------|--------|--------|--------|--------|--------|--------|--------|--------|--------|--------|--------|--------|--------|--------|--------|--------|--------|--------|--------|--------|--------|--------|--------|--------|--------|--------|--------|--------|--------|--------|--------|--------|--------|--------|--------|--------|--------|--------|--------|--------|--------|--------|--------|--------|--------|--------|--------|--------|--------|--------|--------|--------|--------|--------|--------|--------|--------|--------|--------|--------|--------|--------|--------|--------|--------|--------|--------|--------|--------|--------|--------|--------|--------|--------|--------|--------|--------|--------|--------|--------|--------|--------|--------|--------|--------|--------|--------|--------|--------|--------|--------|--------|--------|--------|--------|--------|--------|--------|--------|--------|--------|--------|--------|--------|--------|--------|--------|--------|--------|--------|--------|--------|--------|--------|--------|--------|--------|--------|--------|--------|--------|--------|--------|--------|--------|--------|--------|--------|--------|--------|--------|--------|--------|--------|--------|--------|--------|--------|--------|--------|--------|--------|--------|--------|--------|--------|--------|--------|--------|--------|--------|--------|--------|--------|--------|--------|--------|--------|--------|--------|--------|--------|--------|--------|--------|--------|--------|--------|--------|--------|--------|--------|--------|--------|--------|--------|--------|--------|--------|--------|--------|--------|--------|--------|--------|--------|--------|--------|--------|--------|--------|--------|--------|--------|--------|--------|--------|--------|--------|--------|--------|--------|--------|--------|--------|--------|--------|--------|--------|--------|--------|--------|--------|--------|--------|--------|--------|--------|--------|--------|--------|--------|--------|--------|--------|--------|--------|--------|--------|--------|--------|--------|--------|--------|--------|--------|--------|--------|--------|--------|--------|--------|--------|--------|--------|--------|--------|--------|--------|--------|--------|--------|--------|--------|--------|--------|--------|--------|--------|--------|--------|--------|--------|--------|--------|--------|--------|--------|--------|--------|--------|--------|--------|--------|--------|--------|--------|--------|---------|
| LABELS | DCP93019 | DCP93032 | DCP93047 | KRC1 | KRC2A | KRC4 | KRC5 | KRC6 | KRC7 | KRC8 | KRC9 | KRC10 | KRC11 | KRC12 | KRC13 | KRC14 | KRC15 | KRC16 | KRC17 | KRC18 | KRC19 | KRC20 | KRC21 | KRC22 | KRC23 | KRC24 | KRC25 | KRC26 | KRC27 | KRC28 | KRC29 | KRC30 | KRC31 | KRC32 | KRC33 | KRC34 | KRC35 | KRC36 | KRC37 | KRC38 | KRC39 | KRC40 | KRC41 | KRC42 | KRC43 | KRC44 | KRC45 | KRC46 | KRC47 | KRC48 | KRC49 | KRC50 | KRC51 | KRC52 | KRC53 | KRC54 | KRC55 | KRC56 | KRC57 | KRC58 | KRC59 | KRC60 | KRC61 | KRC62 | KRC63 | KRC64 | KRC65 | KRC66 | KRC67 | KRC68 | KRC69 | KRC70 | KRC71 | KRC72 | KRC73 | KRC74 | KRC75 | KRC76 | KRC77 | KRC78 | KRC79 | KRC80 | KRC81 | KRC82 | KRC83 | KRC84 | KRC85 | KRC86 | KRC87 | KRC88 | KRC89 | KRC90 | KRC91 | KRC92 | KRC93 | KRC94 | KRC95 | KRC96 | KRC97 | KRC98 | KRC99 | KRC100 | KRC101 | KRC102 | KRC103 | KRC104 | KRC105 | KRC106 | KRC107 | KRC108 | KRC109 | KRC110 | KRC111 | KRC112 | KRC113 | KRC114 | KRC115 | KRC116 | KRC117 | KRC118 | KRC119 | KRC120 | KRC121 | KRC122 | KRC123 | KRC124 | KRC125 | KRC126 | KRC127 | KRC128 | KRC129 | KRC130 | KRC131 | KRC132 | KRC133 | KRC134 | KRC135 | KRC136 | KRC137 | KRC138 | KRC139 | KRC140 | KRC141 | KRC142 | KRC143 | KRC144 | KRC145 | KRC146 | KRC147 | KRC148 | KRC149 | KRC150 | KRC151 | KRC152 | KRC153 | KRC154 | KRC155 | KRC156 | KRC157 | KRC158 | KRC159 | KRC160 | KRC161 | KRC162 | KRC163 | KRC164 | KRC165 | KRC166 | KRC167 | KRC168 | KRC169 | KRC170 | KRC171 | KRC172 | KRC173 | KRC174 | KRC175 | KRC176 | KRC177 | KRC178 | KRC179 | KRC180 | KRC181 | KRC182 | KRC183 | KRC184 | KRC185 | KRC186 | KRC187 | KRC188 | KRC189 | KRC190 | KRC191 | KRC192 | KRC193 | KRC194 | KRC195 | KRC196 | KRC197 | KRC198 | KRC199 | KRC200 | KRC201 | KRC202 | KRC203 | KRC204 | KRC205 | KRC206 | KRC207 | KRC208 | KRC209 | KRC210 | KRC211 | KRC212 | KRC213 | KRC214 | KRC215 | KRC216 | KRC217 | KRC218 | KRC219 | KRC220 | KRC221 | KRC222 | KRC223 | KRC224 | KRC225 | KRC226 | KRC227 | KRC228 | KRC229 | KRC230 | KRC231 | KRC232 | KRC233 | KRC234 | KRC235 | KRC236 | KRC237 | KRC238 | KRC239 | KRC240 | KRC241 | KRC242 | KRC243 | KRC244 | KRC245 | KRC246 | KRC247 | KRC248 | KRC249 | KRC250 | KRC251 | KRC252 | KRC253 | KRC254 | KRC255 | KRC256 | KRC257 | KRC258 | KRC259 | KRC260 | KRC261 | KRC262 | KRC263 | KRC264 | KRC265 | KRC266 | KRC267 | KRC268 | KRC269 | KRC270 | KRC271 | KRC272 | KRC273 | KRC274 | KRC275 | KRC276 | KRC277 | KRC278 | KRC279 | KRC280 | KRC281 | KRC282 | KRC283 | KRC284 | KRC285 | KRC286 | KRC287 | KRC288 | KRC289 | KRC290 | KRC291 | KRC292 | KRC293 | KRC294 | KRC295 | KRC296 | KRC297 | KRC298 | KRC299 | KRC300 | KRC301 | KRC302 | KRC303 | KRC304 | KRC305 | KRC306 | KRC307 | KRC308 | KRC309 | KRC310 | KRC311 | KRC312 | KRC313 | KRC314 | KRC315 | KRC316 | KRC317 | KRC318 | KRC319 | KRC320 | KRC321 | KRC322 | KRC323 | KRC324 | KRC325 | KRC326 | KRC327 | KRC328 | KRC329 | KRC330 | KRC331 | KRC332 | KRC333 | KRC334 | KRC335 | KRC336 | KRC337 | KRC338 | KRC339 | KRC340 | KRC341 | KRC342 | KRC343 | KRC344 | KRC345 | KRC346 | KRC347 | KRC348 | KRC349 | KRC350 | KRC351 | KRC352 | KRC353 | KRC354 | KRC355 | KRC356 | KRC357 | KRC358 | KRC359 | KRC360 | KRC361 | KRC362 | KRC363 | KRC364 | KRC365 | KRC366 | KRC367 | KRC368 | KRC369 | KRC370 | KRC371 | KRC372 | KRC373 | KRC374 | KRC375 | KRC376 | KRC377 | KRC378 | KRC379 | KRC380 | KRC381 | KRC382 | KRC383 | KRC384 | KRC385 | KRC386 | KRC387 | KRC388 | KRC389 | KRC390 | KRC391 | KRC392 | KRC393 | KRC394 | KRC395 | KRC396 | KRC397 | KRC398 | KRC399 | KRC400 | KRC401 | KRC402 | KRC403 | KRC404 | KRC405 | KRC406 | KRC407 | KRC408 | KRC409 | KRC410 | KRC411 | KRC412 | KRC413 | KRC414 | KRC415 | KRC416 | KRC417 | KRC418 | KRC419 | KRC420 | KRC421 | KRC422 | KRC423 | KRC424 | KRC425 | KRC426 | KRC427 | KRC428 | KRC429 | KRC430 | KRC431 | KRC432 | KRC433 | KRC434 | KRC435 | KRC436 | KRC437 | KRC438 | KRC439 | KRC440 | KRC441 | KRC442 | KRC443 | KRC444 | KRC445 | KRC446 | KRC447 | KRC448 | KRC449 | KRC450 | KRC451 | KRC452 | KRC453 | KRC454 | KRC455 | KRC456 | KRC457 | KRC458 | KRC459 | KRC460 | KRC461 | KRC462 | KRC463 | KRC464 | KRC465 | KRC466 | KRC467 | KRC468 | KRC469 | KRC470 | KRC471 | KRC472 | KRC473 | KRC474 | KRC475 | KRC476 | KRC477 | KRC478 | KRC479 | KRC480 | KRC481 | KRC482 | KRC483 | KRC484 | KRC485 | KRC486 | KRC487 | KRC488 | KRC489 | KRC490 | KRC491 | KRC492 | KRC493 | KRC494 | KRC495 | KRC496 | KRC497 | KRC498 | KRC499 | KRC500 | KRC501 | KRC502 | KRC503 | KRC504 | KRC505 | KRC506 | KRC507 | KRC508 | KRC509 | KRC510 | KRC511 | KRC512 | KRC513 | KRC514 | KRC515 | KRC516 | KRC517 | KRC518 | KRC519 | KRC520 | KRC521 | KRC522 | KRC523 | KRC524 | KRC525 | KRC526 | KRC527 | KRC528 | KRC529 | KRC530 | KRC531 | KRC532 | KRC533 | KRC534 | KRC535 | KRC536 | KRC537 | KRC538 | KRC539 | KRC540 | KRC541 | KRC542 | KRC543 | KRC544 | KRC545 | KRC546 | KRC547 | KRC548 | KRC549 | KRC550 | KRC551 | KRC552 | KRC553 | KRC554 | KRC555 | KRC556 | KRC557 | KRC558 | KRC559 | KRC560 | KRC561 | KRC562 | KRC563 | KRC564 | KRC565 | KRC566 | KRC567 | KRC568 | KRC569 | KRC570 | KRC571 | KRC572 | KRC573 | KRC574 | KRC575 | KRC576 | KRC577 | KRC578 | KRC579 | KRC580 | KRC581 | KRC582 | KRC583 | KRC584 | KRC585 | KRC586 | KRC587 | KRC588 | KRC589 | KRC590 | KRC591 | KRC592 | KRC593 | KRC594 | KRC595 | KRC596 | KRC597 | KRC598 | KRC599 | KRC600 | KRC601 | KRC602 | KRC603 | KRC604 | KRC605 | KRC606 | KRC607 | KRC608 | KRC609 | KRC610 | KRC611 | KRC612 | KRC613 | KRC614 | KRC615 | KRC616 | KRC617 | KRC618 | KRC619 | KRC620 | KRC621 | KRC622 | KRC623 | KRC624 | KRC625 | KRC626 | KRC627 | KRC628 | KRC629 | KRC630 | KRC631 | KRC632 | KRC633 | KRC634 | KRC635 | KRC636 | KRC637 | KRC638 | KRC639 | KRC640 | KRC641 | KRC642 | KRC643 | KRC644 | KRC645 | KRC646 | KRC647 | KRC648 | KRC649 | KRC650 | KRC651 | KRC652 | KRC653 | KRC654 | KRC655 | KRC656 | KRC657 | KRC658 | KRC659 | KRC660 | KRC661 | KRC662 | KRC663 | KRC664 | KRC665 | KRC666 | KRC667 | KRC668 | KRC669 | KRC670 | KRC671 | KRC672 | KRC673 | KRC674 | KRC675 | KRC676 | KRC677 | KRC678 | KRC679 | KRC680 | KRC681 | KRC682 | KRC683 | KRC684 | KRC685 | KRC686 | KRC687 | KRC688 | KRC689 | KRC690 | KRC691 | KRC692 | KRC693 | KRC694 | KRC695 | KRC696 | KRC697 | KRC698 | KRC699 | KRC700 | KRC701 | KRC702 | KRC703 | KRC704 | KRC705 | KRC706 | KRC707 | KRC708 | KRC709 | KRC710 | KRC711 | KRC712 | KRC713 | KRC714 | KRC715 | KRC716 | KRC717 | KRC718 | KRC719 | KRC720 | KRC721 | KRC722 | KRC723 | KRC724 | KRC725 | KRC726 | KRC727 | KRC728 | KRC729 | KRC730 | KRC731 | KRC732 | KRC733 | KRC734 | KRC735 | KRC736 | KRC737 | KRC738 | KRC739 | KRC740 | KRC741 | KRC742 | KRC743 | KRC744 | KRC745 | KRC746 | KRC747 | KRC748 | KRC749 | KRC750 | KRC751 | KRC752 | KRC753 | KRC754 | KRC755 | KRC756 | KRC757 | KRC758 | KRC759 | KRC760 | KRC761 | KRC762 | KRC763 | KRC764 | KRC765 | KRC766 | KRC767 | KRC768 | KRC769 | KRC770 | KRC771 | KRC772 | KRC773 | KRC774 | KRC775 | KRC776 | KRC777 | KRC778 | KRC779 | KRC780 | KRC781 | KRC782 | KRC783 | KRC784 | KRC785 | KRC786 | KRC787 | KRC788 | KRC789 | KRC790 | KRC791 | KRC792 | KRC793 | KRC794 | KRC795 | KRC796 | KRC797 | KRC798 | KRC799 | KRC800 | KRC801 | KRC802 | KRC803 | KRC804 | KRC805 | KRC806 | KRC807 | KRC808 | KRC809 | KRC810 | KRC811 | KRC812 | KRC813 | KRC814 | KRC815 | KRC816 | KRC817 | KRC818 | KRC819 | KRC820 | KRC821 | KRC822 | KRC823 | KRC824 | KRC825 | KRC826 | KRC827 | KRC828 | KRC829 | KRC830 | KRC831 | KRC832 | KRC833 | KRC834 | KRC835 | KRC836 | KRC837 | KRC838 | KRC839 | KRC840 | KRC841 | KRC842 | KRC843 | KRC844 | KRC845 | KRC846 | KRC847 | KRC848 | KRC849 | KRC850 | KRC851 | KRC852 | KRC853 | KRC854 | KRC855 | KRC856 | KRC857 | KRC858 | KRC859 | KRC860 | KRC861 | KRC862 | KRC863 | KRC864 | KRC865 | KRC866 | KRC867 | KRC868 | KRC869 | KRC870 | KRC871 | KRC872 | KRC873 | KRC874 | KRC875 | KRC876 | KRC877 | KRC878 | KRC879 | KRC880 | KRC881 | KRC882 | KRC883 | KRC884 | KRC885 | KRC886 | KRC887 | KRC888 | KRC889 | KRC890 | KRC891 | KRC892 | KRC893 | KRC894 | KRC895 | KRC896 | KRC897 | KRC898 | KRC899 | KRC900 | KRC901 | KRC902 | KRC903 | KRC904 | KRC905 | KRC906 | KRC907 | KRC908 | KRC909 | KRC910 | KRC911 | KRC912 | KRC913 | KRC914 | KRC915 | KRC916 | KRC917 | KRC918 | KRC919 | KRC920 | KRC921 | KRC922 | KRC923 | KRC924 | KRC925 | KRC926 | KRC927 | KRC928 | KRC929 | KRC930 | KRC931 | KRC932 | KRC933 | KRC934 | KRC935 | KRC936 | KRC937 | KRC938 | KRC939 | KRC940 | KRC941 | KRC942 | KRC943 | KRC944 | KRC945 | KRC946 | KRC947 | KRC948 | KRC949 | KRC950 | KRC951 | KRC952 | KRC953 | KRC954 | KRC955 | KRC956 | KRC957 | KRC958 | KRC959 | KRC960 | KRC961 | KRC962 | KRC963 | KRC964 | KRC965 | KRC966 | KRC967 | KRC968 | KRC969 | KRC970 | KRC971 | KRC972 | KRC973 | KRC974 | KRC975 | KRC976 | KRC977 | KRC978 | KRC979 | KRC980 | KRC981 | KRC982 | KRC983 | KRC984 | KRC985 | KRC986 | KRC987 | KRC988 | KRC989 | KRC990 | KRC991 | KRC992 | KRC993 | KRC994 | KRC995 | KRC996 | KRC997 | KRC998 | KRC999 | KRC1000 |

FORMAT (SE14 7)

ACRONYM FOR ASSOCIATION MATRIX USED = BRAY-CURTIS

| PAIRING ITEM | SEQUENCE JOINS ITEM | AT DISTANCE | X INDIVIDUALS |
|--------------|---------------------|-------------|---------------|
| 73 | 75 | 079 | 1 902 |
| 90 | 92 | 089 | 2 139 |
| 14 | 15 | 091 | 2 180 |
| 85 | 97 | 092 | 2 212 |
| 66 | 77 | 093 | 2 221 |
| 81 | 100 | 094 | 2 266 |
| 36 | 45 | 096 | 2 309 |
| 56 | 59 | 097 | 2 324 |
| 9 | 12 | 097 | 2 339 |
| 48 | 49 | 099 | 2 364 |
| 25 | 32 | 100 | 2 403 |
| 91 | 96 | 101 | 2 431 |
| 58 | 61 | 102 | 2 437 |
| 98 | 101 | 102 | 2 455 |
| 88 | 89 | 102 | 2 458 |
| 26 | 52 | 104 | 2 499 |
| 51 | 57 | 104 | 2 501 |
| 18 | 23 | 105 | 2 513 |
| 9 | 11 | 105 | 2 518 |
| 6 | 19 | 105 | 2 527 |
| 47 | 58 | 106 | 2 550 |
| 81 | 82 | 106 | 2 552 |
| 54 | 73 | 111 | 2 654 |
| 85 | 98 | 111 | 2 668 |
| 43 | 50 | 112 | 2 692 |
| 13 | 53 | 113 | 2 707 |
| 51 | 62 | 114 | 2 728 |
| 17 | 22 | 114 | 2 744 |
| 46 | 90 | 115 | 2 765 |
| 66 | 70 | 116 | 2 777 |
| 14 | 25 | 116 | 2 782 |
| 36 | 44 | 116 | 2 790 |
| 88 | 94 | 116 | 2 791 |
| 20 | 21 | 116 | 2 794 |
| 56 | 85 | 117 | 2 812 |
| 9 | 18 | 118 | 2 826 |
| 37 | 87 | 119 | 2 851 |
| 47 | 60 | 119 | 2 855 |
| 1 | 79 | 121 | 2 902 |
| 80 | 81 | 122 | 2 935 |

| | | | |
|----|-----|-----|-------|
| 8 | 9 | 125 | 2 993 |
| 54 | 74 | 125 | 2 994 |
| 65 | 78 | 127 | 3 042 |
| 8 | 10 | 127 | 3 050 |
| 26 | 48 | 127 | 3 059 |
| 41 | 76 | 129 | 3 096 |
| 14 | 66 | 131 | 3 150 |
| 46 | 54 | 132 | 3 175 |
| 47 | 56 | 134 | 3 214 |
| 6 | 16 | 134 | 3 218 |
| 27 | 28 | 134 | 3 227 |
| 80 | 99 | 135 | 3 231 |
| 1 | 63 | 136 | 3 261 |
| 13 | 65 | 140 | 3 354 |
| 86 | 102 | 140 | 3 361 |
| 37 | 88 | 141 | 3 381 |
| 4 | 71 | 141 | 3 385 |
| 43 | 51 | 143 | 3 427 |
| 46 | 68 | 143 | 3 441 |
| 41 | 55 | 143 | 3 442 |
| 13 | 47 | 144 | 3 445 |
| 14 | 67 | 145 | 3 472 |
| 36 | 40 | 147 | 3 531 |
| 8 | 29 | 147 | 3 535 |
| 80 | 83 | 147 | 3 537 |
| 14 | 86 | 148 | 3 543 |
| 46 | 91 | 151 | 3 577 |
| 6 | 8 | 151 | 3 626 |
| 41 | 72 | 153 | 3 681 |
| 6 | 17 | 155 | 3 730 |
| 13 | 42 | 156 | 3 747 |
| 64 | 69 | 157 | 3 759 |
| 33 | 80 | 158 | 3 796 |
| 26 | 46 | 158 | 3 799 |
| 13 | 24 | 162 | 3 883 |
| 14 | 41 | 166 | 3 974 |
| 13 | 43 | 167 | 4 010 |
| 1 | 2 | 170 | 4 089 |
| 37 | 95 | 172 | 4 131 |
| 5 | 27 | 176 | 4 233 |
| 20 | 34 | 177 | 4 245 |
| 36 | 39 | 178 | 4 264 |
| 37 | 93 | 179 | 4 301 |
| 6 | 7 | 179 | 4 302 |
| 35 | 84 | 180 | 4 319 |
| 4 | 14 | 183 | 4 391 |
| 13 | 33 | 185 | 4 432 |
| 6 | 13 | 189 | 4 525 |
| 4 | 26 | 190 | 4 565 |
| 20 | 64 | 201 | 4 835 |
| 1 | 20 | 208 | 4 991 |
| 36 | 38 | 208 | 4 993 |
| 5 | 6 | 209 | 5 005 |
| 4 | 30 | 218 | 5 242 |
| 1 | 3 | 221 | 5 301 |
| 1 | 35 | 230 | 5 532 |
| 1 | 5 | 237 | 5 691 |
| 4 | 37 | 240 | 5 760 |
| 1 | 36 | 276 | 6 628 |
| 1 | 4 | 283 | 6 790 |
| 1 | 31 | 389 | 9 326 |

COHENETIC CORRELATION COEFFICIENT = 577295

– *Appendix 3* –

Abundance (%) and distribution of species in GC1

| Species | Sample | 0cm | 10cm | 15cm | 20cm | 25cm | 30cm | 35cm | 40cm | 45cm | 55cm | 60cm | 65cm | 70cm | 75cm | 80cm | 85cm | 90cm | 100cm |
|---|--------|-------|-------|-------|-------|-------|-------|-------|-------|-------|-------|-------|-------|-------|-------|-------|-------|-------|-------|
| <i>Chaetoceros spp</i> | | 0 83 | 1 00 | 0 67 | 0 00 | 0 17 | 1 67 | 0 83 | 0 17 | 4 50 | 2 50 | 1 33 | 1 33 | 0 33 | 0 33 | 0 67 | 3 17 | 0 33 | 0 67 |
| <i>Chaetoceros spores</i> | | 12 83 | 6 50 | 5 67 | 6 83 | 4 17 | 7 00 | 5 00 | 5 17 | 7 17 | 4 17 | 1 17 | 2 17 | 2 17 | 8 00 | 2 00 | 4 00 | 5 50 | 3 17 |
| <i>Corethron criophilum</i> | | 0 67 | 0 67 | 1 17 | 1 50 | 0 17 | 5 33 | 1 83 | 0 83 | 2 00 | 1 00 | 3 17 | 6 50 | 7 33 | 0 83 | 5 67 | 10 00 | 1 17 | 0 83 |
| <i>Dactyliosolen antarcticus</i> | | 0 50 | 0 33 | 1 00 | 0 33 | 1 17 | 0 33 | 0 17 | 0 67 | 0 83 | 0 67 | 0 00 | 0 33 | 0 00 | 0 50 | 0 33 | 0 83 | 0 83 | 1 17 |
| <i>Distephanus speculum</i> | | 0 00 | 0 50 | 1 17 | 0 00 | 0 00 | 1 00 | 1 00 | 1 00 | 0 83 | 0 50 | 0 00 | 0 17 | 0 33 | 0 83 | 0 33 | 1 83 | 0 50 | 0 67 |
| <i>Eucampia antarctica</i> | | 0 00 | 0 33 | 0 33 | 0 00 | 0 00 | 0 33 | 0 33 | 0 17 | 0 83 | 0 00 | 0 00 | 0 00 | 1 00 | 0 00 | 0 33 | 0 17 | 0 17 | 0 00 |
| <i>Fragilaropsis angulata</i> | | 2 83 | 2 83 | 3 17 | 3 83 | 5 50 | 5 33 | 3 50 | 4 50 | 4 67 | 3 17 | 4 00 | 1 50 | 2 67 | 2 83 | 4 17 | 6 17 | 3 33 | 5 00 |
| <i>Fragilaropsis curta</i> | | 34 00 | 50 17 | 37 50 | 41 83 | 35 33 | 28 50 | 34 00 | 43 67 | 29 00 | 32 50 | 55 83 | 15 67 | 23 67 | 30 17 | 30 50 | 25 17 | 41 50 | 27 00 |
| <i>Fragilaropsis cylindrus</i> | | 36 00 | 22 50 | 30 67 | 30 17 | 37 50 | 30 33 | 41 00 | 26 83 | 33 17 | 42 33 | 23 50 | 61 00 | 42 33 | 38 50 | 39 50 | 31 83 | 33 33 | 51 17 |
| <i>Fragilaropsis kergulensis</i> | | 0 83 | 0 17 | 1 17 | 1 00 | 1 00 | 0 50 | 0 33 | 1 00 | 1 00 | 1 00 | 0 17 | 0 00 | 0 50 | 1 00 | 0 00 | 0 00 | 0 83 | 0 17 |
| <i>Fragilaropsis obliquecostata</i> | | 2 67 | 1 17 | 4 00 | 2 17 | 1 67 | 3 17 | 2 17 | 2 17 | 2 00 | 1 33 | 0 83 | 1 17 | 2 17 | 1 00 | 2 83 | 2 00 | 1 50 | 0 33 |
| <i>Fragilaropsis pseudonana</i> | | 1 50 | 1 67 | 2 00 | 1 17 | 2 50 | 5 17 | 2 50 | 0 67 | 1 33 | 1 67 | 2 50 | 5 33 | 4 17 | 0 83 | 1 17 | 3 83 | 1 50 | 2 17 |
| <i>Fragilaropsis ntschen</i> | | 0 17 | 0 17 | 0 67 | 0 17 | 0 33 | 0 00 | 0 17 | 0 83 | 0 83 | 0 50 | 1 33 | 0 50 | 0 83 | 1 33 | 2 33 | 1 33 | 0 50 | 0 17 |
| <i>Fragilaropsis separanda</i> | | 0 33 | 0 17 | 0 67 | 0 83 | 0 33 | 0 50 | 0 33 | 0 33 | 0 17 | 0 83 | 0 00 | 0 33 | 0 17 | 0 33 | 0 33 | 1 00 | 0 17 | 0 17 |
| <i>Pentalamina corona</i> | | 1 50 | 3 50 | 1 33 | 2 33 | 2 33 | 2 17 | 2 33 | 1 50 | 0 83 | 1 17 | 0 67 | 0 17 | 0 67 | 1 83 | 1 00 | 0 67 | 0 33 | 1 50 |
| <i>Pseudonitzschia turgiduloides</i> | | 0 83 | 1 17 | 0 50 | 0 33 | 0 33 | 0 67 | 0 50 | 0 00 | 0 33 | 0 83 | 0 00 | 0 17 | 0 50 | 0 83 | 0 50 | 1 67 | 0 33 | 1 00 |
| <i>Rhizosolenia hebetata fo Semispina</i> | | 0 00 | 0 00 | 0 00 | 0 00 | 0 00 | 0 00 | 0 00 | 0 00 | 0 33 | 0 00 | 0 17 | 0 00 | 0 00 | 0 00 | 0 00 | 0 00 | 0 00 | 0 17 |
| <i>Thalassiosira margantae</i> | | 1 67 | 0 83 | 1 33 | 0 83 | 0 50 | 0 50 | 0 33 | 0 17 | 0 83 | 0 17 | 0 17 | 0 33 | 0 33 | 0 33 | 0 50 | 0 50 | 0 83 | 0 17 |
| <i>Thalassiosira gracilis</i> | | 0 17 | 0 67 | 1 00 | 2 00 | 1 17 | 0 67 | 0 33 | 1 33 | 2 00 | 0 67 | 0 67 | 0 00 | 1 00 | 3 00 | 1 50 | 0 17 | 0 17 | 1 17 |
| <i>Thalassiosira gracilis var expecta</i> | | 0 17 | 0 50 | 0 50 | 0 00 | 0 83 | 0 00 | 0 00 | 0 17 | 0 67 | 0 33 | 0 33 | 0 17 | 0 83 | 0 67 | 0 50 | 0 33 | 0 17 | 0 00 |
| <i>Thalassiosira lentiginosa</i> | | 0 17 | 0 00 | 1 33 | 0 00 | 0 17 | 0 17 | 0 17 | 1 00 | 0 33 | 0 50 | 0 33 | 0 00 | 0 67 | 0 33 | 0 17 | 0 50 | 0 00 | 0 00 |
| <i>Unknown Genus A</i> | | 0 00 | 0 83 | 0 83 | 0 67 | 0 33 | 0 33 | 1 17 | 0 00 | 0 17 | 0 00 | 0 67 | 1 67 | 2 17 | 0 67 | 0 83 | 1 33 | 1 67 | 0 50 |

| Species | Sample | 105cm | 110cm | 115cm | 120cm | 125cm | 130cm | 135cm | 140cm | 145cm | 150cm | 155cm | 160cm | 165cm | 170cm | 180cm | 185cm | 195cm | 200cm |
|---|--------|-------|-------|-------|-------|-------|-------|-------|-------|-------|-------|-------|-------|-------|-------|-------|-------|-------|-------|
| <i>Chaetoceros spp</i> | | 0 00 | 2 17 | 0 33 | 1 33 | 1 33 | 0 17 | 0 50 | 3 67 | 1 17 | 1 00 | 2 33 | 0 67 | 0 00 | 0 33 | 1 00 | 0 33 | 1 17 | 0 33 |
| <i>Chaetoceros spores</i> | | 5 17 | 11 83 | 4 83 | 3 17 | 4 50 | 4 67 | 5 83 | 6 50 | 7 00 | 4 50 | 2 67 | 4 50 | 4 00 | 10 50 | 7 00 | 8 33 | 4 17 | 16 31 |
| <i>Corethron criophilum</i> | | 0 17 | 2 67 | 2 00 | 1 83 | 3 33 | 0 33 | 0 50 | 3 50 | 1 00 | 2 67 | 4 00 | 0 50 | 18 33 | 0 50 | 0 83 | 1 67 | 9 00 | 1 00 |
| <i>Dactyliosolen antarcticus</i> | | 0 17 | 0 17 | 1 33 | 0 83 | 0 33 | 1 83 | 1 17 | 0 50 | 1 17 | 1 17 | 1 00 | 1 67 | 0 17 | 1 00 | 2 50 | 1 83 | 1 17 | 1 66 |
| <i>Distephanus speculum</i> | | 0 17 | 0 33 | 0 67 | 0 83 | 0 33 | 0 50 | 0 17 | 0 67 | 0 17 | 1 00 | 0 17 | 0 00 | 1 17 | 0 67 | 0 50 | 0 50 | 1 00 | 0 83 |
| <i>Eucampia antarctica</i> | | 0 17 | 0 67 | 0 83 | 0 00 | 0 33 | 0 83 | 0 67 | 0 67 | 0 50 | 1 00 | 1 00 | 1 17 | 2 50 | 0 00 | 0 67 | 1 67 | 0 33 | 0 50 |
| <i>Fragilaropsis angulata</i> | | 3 00 | 2 00 | 2 33 | 1 83 | 2 00 | 6 83 | 6 00 | 1 83 | 5 00 | 6 50 | 4 50 | 5 67 | 3 83 | 5 67 | 8 33 | 7 17 | 5 00 | 4 99 |
| <i>Fragilaropsis curta</i> | | 36 50 | 21 50 | 38 33 | 36 33 | 33 50 | 41 83 | 36 00 | 22 33 | 43 00 | 35 67 | 37 00 | 26 83 | 44 67 | 39 00 | 49 50 | 41 67 | 31 00 | 27 95 |
| <i>Fragilaropsis cylindrus</i> | | 37 67 | 43 50 | 36 33 | 39 50 | 41 83 | 21 83 | 27 33 | 46 33 | 25 50 | 27 50 | 34 83 | 36 00 | 10 00 | 21 33 | 10 00 | 17 00 | 31 83 | 27 79 |
| <i>Fragilaropsis kergulensis</i> | | 0 50 | 0 33 | 0 67 | 0 17 | 0 33 | 0 83 | 1 83 | 0 67 | 0 67 | 0 33 | 0 17 | 2 50 | 0 67 | 2 17 | 1 67 | 1 83 | 0 17 | 1 33 |
| <i>Fragilaropsis obliquecostata</i> | | 2 17 | 1 00 | 1 33 | 0 67 | 1 17 | 2 33 | 3 67 | 2 17 | 2 17 | 2 83 | 1 00 | 3 83 | 2 83 | 2 83 | 4 00 | 4 67 | 4 00 | 3 00 |
| <i>Fragilaropsis pseudonana</i> | | 1 17 | 3 00 | 1 17 | 5 33 | 2 17 | 1 00 | 1 00 | 1 50 | 0 67 | 1 83 | 1 17 | 0 50 | 0 83 | 0 00 | 0 00 | 0 00 | 1 83 | 0 50 |
| <i>Fragilaropsis ntschen</i> | | 0 00 | 0 00 | 0 33 | 0 00 | 0 17 | 1 17 | 0 83 | 0 33 | 0 50 | 0 00 | 0 33 | 0 17 | 0 00 | 0 00 | 0 17 | 0 50 | 0 00 | 0 00 |
| <i>Fragilaropsis separanda</i> | | 0 33 | 0 50 | 0 67 | 0 17 | 0 67 | 2 17 | 2 00 | 0 00 | 0 67 | 0 33 | 0 17 | 1 17 | 0 33 | 1 17 | 1 33 | 1 00 | 0 17 | 1 00 |
| <i>Pentalamina corona</i> | | 4 83 | 1 67 | 1 17 | 1 00 | 1 33 | 1 83 | 0 67 | 2 33 | 0 83 | 2 00 | 1 33 | 0 33 | 2 83 | 2 00 | 3 17 | 0 67 | 3 99 | |
| <i>Pseudonitzschia turgiduloides</i> | | 0 33 | 0 33 | 0 33 | 0 50 | 1 33 | 0 50 | 0 33 | 0 67 | 0 50 | 1 17 | 1 00 | 0 67 | 0 17 | 0 50 | 0 33 | 0 17 | 0 83 | 0 17 |
| <i>Rhizosolenia hebetata fo Semispina</i> | | 0 17 | 0 00 | 0 00 | 0 17 | 0 00 | 0 00 | 0 00 | 0 00 | 0 00 | 0 17 | 0 50 | 0 00 | 0 33 | 0 00 | 0 00 | 0 00 | 0 00 | 0 00 |
| <i>Thalassiosira margantae</i> | | 0 33 | 0 00 | 0 50 | 0 50 | 0 17 | 0 17 | 1 17 | 0 17 | 0 50 | 1 00 | 0 17 | 1 00 | 0 17 | 1 17 | 1 33 | 1 00 | 0 67 | 1 00 |
| <i>Thalassiosira gracilis</i> | | 1 00 | 0 67 | 1 33 | 1 50 | 0 67 | 2 00 | 2 00 | 0 33 | 0 67 | 0 67 | 1 00 | 1 67 | 1 00 | 3 33 | 2 17 | 2 00 | 1 00 | 1 66 |
| <i>Thalassiosira gracilis var expecta</i> | | 1 67 | 0 00 | 0 33 | 0 50 | 0 67 | 1 00 | 0 83 | 0 00 | 0 17 | 0 50 | 0 33 | 1 00 | 0 00 | 0 17 | 0 67 | 0 00 | 0 50 | 0 33 |
| <i>Thalassiosira lentiginosa</i> | | 0 33 | 0 67 | 0 00 | 0 00 | 0 33 | 0 17 | 0 83 | 0 00 | 0 17 | 0 83 | 0 33 | 0 83 | 1 00 | 0 17 | 0 33 | 0 17 | 0 00 | 0 67 |
| <i>Unknown Genus A</i> | | 0 17 | 0 17 | 0 17 | 0 33 | 0 50 | 0 00 | 0 33 | 1 67 | 0 17 | 0 50 | 0 83 | 0 67 | 3 17 | 0 33 | 0 00 | 0 17 | 2 00 | 0 00 |

- *Appendix 4* -

Preliminary cluster analysis of GCI

GC1.01

 BIOSSTAT II: HIERARCHICAL CLUSTER ANALYSIS (VER. 3.5)

SIMDK PROVIDED THE ASSOCIATION MATRIX FROM DATA IN FILE gc1.dak
 ASSOCIATION MATRIX IS A DISSIMILARITY MATRIX FROM BRAY-CURTIS

NUMBER OF INDIVIDUALS = 68
 NUMBER OF VARIABLES = 22

ASSOCIATION MATRIX IS FROM SIMDK

METHOD: GROUP AVERAGE (UNWEIGHTED PAIR GROUP METHOD USING ARITHMETIC AVERAGES)

| LABELS: | 0cm | 10cm | 15cm | 20cm | 25cm | 30cm | 35cm | 40cm | 45cm | 55cm |
|---------|-------|-------|-------|-------|-------|-------|-------|-------|-------|-------|
| | 60cm | 65cm | 70cm | 75cm | 80cm | 85cm | 90cm | 100cm | 105cm | 110cm |
| | 115cm | 120cm | 125cm | 130cm | 135cm | 140cm | 145cm | 150cm | 155cm | 160cm |
| | 165cm | 170cm | 180cm | 185cm | 195cm | 200cm | 205cm | 210cm | 215cm | 220cm |
| | 225cm | 230cm | 235cm | 240cm | 245cm | 250cm | 255cm | 260cm | 265cm | 270cm |
| | 275cm | 280cm | 285cm | 290cm | 295cm | 300cm | 305cm | 310cm | 315cm | 320cm |
| | 325cm | 330cm | 335cm | 340cm | 345cm | 350cm | 355cm | 360cm | | |

FORMAT: (5E14.7)

ACRONYM FOR ASSOCIATION MATRIX USED = BRAY-CURTIS

PAIRING SEQUENCE:

| ITEM | JOINS ITEM | AT DISTANCE | AT DISTANCE X INDIVIDUALS |
|------|------------|-------------|------------------------------|
| 65 | 66 | .000 | .000 |
| 25 | 30 | .084 | 1.859 |
| 33 | 44 | .085 | 1.859 |
| 36 | 43 | .092 | 2.014 |
| 39 | 40 | .103 | 2.269 |
| 28 | 35 | .107 | 2.352 |
| 27 | 48 | .109 | 2.406 |
| 55 | 56 | .110 | 2.411 |
| 32 | 36 | .110 | 2.414 |
| 64 | 65 | .111 | 2.444 |
| 45 | 47 | .111 | 2.452 |
| 10 | 23 | .112 | 2.465 |
| 6 | 7 | .113 | 2.480 |
| 58 | 59 | .116 | 2.542 |
| 1 | 37 | .120 | 2.635 |
| 33 | 34 | .120 | 2.646 |
| 24 | 25 | .122 | 2.679 |
| 5 | 19 | .122 | 2.682 |
| 32 | 33 | .125 | 2.741 |
| 17 | 21 | .126 | 2.774 |
| 3 | 8 | .130 | 2.849 |
| 18 | 22 | .133 | 2.919 |
| 55 | 58 | .134 | 2.945 |
| 9 | 27 | .136 | 2.995 |
| 42 | 45 | .137 | 3.008 |
| 13 | 15 | .137 | 3.023 |
| 1 | 38 | .139 | 3.057 |
| 4 | 17 | .140 | 3.077 |
| 6 | 28 | .141 | 3.101 |
| 10 | 20 | .141 | 3.104 |
| 3 | 14 | .145 | 3.180 |
| 24 | 32 | .149 | 3.272 |
| 55 | 60 | .149 | 3.276 |
| 3 | 4 | .150 | 3.295 |
| 1 | 39 | .151 | 3.332 |
| 41 | 42 | .154 | 3.385 |
| 10 | 29 | .157 | 3.447 |
| 16 | 49 | .158 | 3.468 |
| 3 | 9 | .158 | 3.478 |
| 63 | 64 | .160 | 3.514 |
| 24 | 41 | .160 | 3.523 |
| 2 | 6 | .160 | 3.530 |

| | | | |
|----|----|------|--------|
| 10 | 26 | .161 | 3.549 |
| 2 | 10 | .167 | 3.666 |
| 24 | 51 | .168 | 3.704 |
| 3 | 5 | .172 | 3.786 |
| 2 | 18 | .174 | 3.820 |
| 61 | 62 | .174 | 3.827 |
| 1 | 3 | .177 | 3.885 |
| 13 | 52 | .178 | 3.913 |
| 24 | 55 | .186 | 4.092 |
| 50 | 54 | .186 | 4.099 |
| 1 | 2 | .189 | 4.157 |
| 1 | 46 | .202 | 4.446 |
| 13 | 16 | .203 | 4.473 |
| 50 | 53 | .205 | 4.505 |
| 1 | 13 | .213 | 4.679 |
| 1 | 24 | .226 | 4.976 |
| 11 | 12 | .233 | 5.133 |
| 63 | 67 | .240 | 5.284 |
| 63 | 68 | .259 | 5.688 |
| 11 | 50 | .259 | 5.704 |
| 1 | 57 | .284 | 6.257 |
| 1 | 61 | .288 | 6.329 |
| 1 | 31 | .292 | 6.420 |
| 1 | 11 | .302 | 6.648 |
| 1 | 63 | .502 | 11.046 |

 COPHENETIC CORRELATION COEFFICIENT = .839741

– *Appendix 5* –

Abundance (%) and distribution of species in GC2

| | Samples | 7cm | 10cm | 15cm | 20cm | 25cm | 30cm | 35cm | 40cm | 45cm | 50cm | 55cm | 60cm | 65cm | 70cm | 75cm | 80cm | 85cm | 90cm |
|--|---------|-------|-------|-------|-------|-------|-------|-------|-------|-------|-------|-------|-------|-------|-------|-------|-------|-------|-------|
| Species | | | | | | | | | | | | | | | | | | | |
| <i>Chaetoceros spp</i> | | 0 50 | 2 50 | 2 70 | 0 30 | 3 50 | 1 50 | 2 50 | 1 20 | 2 80 | 0 70 | 0 50 | 3 30 | 0 20 | 1 00 | 1 00 | 1 30 | 0 20 | 1 30 |
| <i>Chaetoceros spores</i> | | 14 20 | 8 00 | 7 70 | 6 50 | 4 20 | 6 60 | 10 60 | 10 30 | 7 70 | 12 60 | 30 30 | 4 50 | 7 10 | 1 80 | 2 30 | 4 30 | 5 30 | 2 30 |
| <i>Corethron cnophilum</i> | | 0 20 | 0 50 | 1 20 | 0 20 | 0 50 | 1 30 | 0 50 | 0 80 | 3 30 | 0 50 | 0 00 | 0 50 | 0 20 | 0 20 | 0 50 | 0 70 | 0 30 | 0 50 |
| <i>Dactylosolen antarcticus</i> | | 0 70 | 0 20 | 0 50 | 0 30 | 1 30 | 0 80 | 0 50 | 0 30 | 1 50 | 0 80 | 0 80 | 1 30 | 0 50 | 1 00 | 0 50 | 0 30 | 0 30 | 0 80 |
| <i>Distephanus speculum</i> | | 0 20 | 0 20 | 1 30 | 0 30 | 1 20 | 1 30 | 1 00 | 0 50 | 1 00 | 0 30 | 1 00 | 0 20 | 1 00 | 0 20 | 0 70 | 0 80 | 0 70 | 0 20 |
| <i>Eucampia antarctica</i> | | 1 30 | 0 00 | 1 70 | 0 70 | 0 50 | 0 70 | 0 80 | 1 00 | 0 30 | 0 30 | 0 00 | 1 30 | 0 30 | 0 20 | 0 80 | 0 50 | 0 50 | 0 30 |
| <i>Fragilaropsis angulata</i> | | 3 50 | 4 80 | 2 70 | 5 30 | 3 70 | 5 50 | 3 30 | 6 00 | 2 00 | 3 10 | 2 00 | 2 80 | 2 00 | 4 50 | 4 60 | 2 30 | 1 70 | 5 30 |
| <i>Fragilaropsis curta</i> | | 54 00 | 57 30 | 56 10 | 60 80 | 59 50 | 50 20 | 57 90 | 55 20 | 65 80 | 48 10 | 42 30 | 63 70 | 64 10 | 60 20 | 74 80 | 66 40 | 72 30 | 64 10 |
| <i>Fragilaropsis cylindrus</i> | | 13 20 | 15 40 | 13 10 | 11 80 | 8 00 | 12 20 | 7 20 | 10 90 | 6 20 | 20 50 | 12 40 | 7 60 | 7 10 | 11 80 | 7 10 | 12 50 | 8 80 | 11 30 |
| <i>Fragilaropsis kerguelensis</i> | | 0 00 | 0 20 | 0 70 | 0 30 | 0 30 | 0 50 | 0 20 | 0 00 | 0 00 | 0 00 | 0 50 | 0 20 | 0 20 | 1 20 | 0 20 | 0 20 | 0 30 | 0 70 |
| <i>Fragilaropsis obliquecostata</i> | | 3 50 | 2 50 | 4 50 | 2 20 | 7 30 | 5 80 | 5 00 | 4 00 | 3 50 | 2 80 | 3 10 | 4 30 | 4 80 | 3 20 | 3 00 | 2 70 | 4 00 | 4 90 |
| <i>Fragilaropsis separanda</i> | | 0 20 | 0 00 | 0 00 | 1 00 | 0 20 | 0 70 | 0 00 | 0 30 | 0 20 | 0 30 | 0 00 | 0 00 | 1 00 | 0 30 | 0 50 | 0 20 | 0 20 | 0 00 |
| <i>Pentalamina corona</i> | | 0 00 | 0 20 | 0 20 | 0 00 | 0 50 | 0 50 | 0 00 | 0 20 | 0 00 | 0 20 | 0 00 | 0 20 | 0 50 | 0 50 | 0 20 | 0 30 | 0 00 | 0 30 |
| <i>Porosira glacialis</i> | | 0 50 | 0 50 | 0 30 | 2 30 | 0 80 | 2 00 | 0 80 | 1 50 | 0 80 | 1 20 | 2 40 | 1 00 | 1 80 | 3 20 | 1 00 | 0 80 | 1 00 | 1 60 |
| <i>Pseudonitzschia turgiduloides</i> | | 1 70 | 1 20 | 1 80 | 1 50 | 2 20 | 1 20 | 2 20 | 1 70 | 1 00 | 2 00 | 1 00 | 3 60 | 1 50 | 1 70 | 0 30 | 1 20 | 1 00 | 1 60 |
| <i>Thalassiosira antarctica spores</i> | | 2 70 | 1 70 | 1 50 | 1 80 | 2 50 | 4 30 | 3 80 | 1 00 | 1 20 | 1 30 | 1 30 | 1 70 | 2 10 | 3 00 | 0 50 | 1 50 | 1 70 | 1 20 |
| <i>Thalassiosira gracilis</i> | | 0 50 | 0 30 | 0 80 | 0 70 | 0 80 | 1 30 | 0 80 | 0 80 | 0 30 | 0 70 | 0 30 | 0 80 | 0 70 | 1 70 | 0 00 | 0 80 | 0 30 | 0 20 |
| <i>Thalassiosira lentiginosa</i> | | 0 20 | 0 20 | 0 20 | 0 00 | 0 00 | 0 20 | 0 00 | 0 50 | 0 00 | 0 50 | 0 20 | 0 20 | 0 30 | 0 00 | 0 00 | 0 00 | 0 00 | 0 00 |

| | Samples | 95cm | 100cm | 105cm | 110cm | 115cm | 120cm | 125cm | 130cm | 135cm | 140cm | 145cm | 150cm | 155cm | 160cm | 165cm | 170cm | 175cm | 180cm |
|--|---------|-------|-------|-------|-------|-------|-------|-------|-------|-------|-------|-------|-------|-------|-------|-------|-------|-------|-------|
| Species | | | | | | | | | | | | | | | | | | | |
| <i>Chaetoceros spp</i> | | 0 80 | 0 20 | 0 20 | 0 90 | 1 00 | 1 00 | 0 80 | 0 00 | 0 90 | 0 70 | 0 30 | 0 80 | 0 30 | 0 30 | 0 20 | 0 70 | 0 20 | 0 30 |
| <i>Chaetoceros spores</i> | | 9 30 | 2 00 | 3 80 | 2 20 | 3 60 | 4 60 | 3 00 | 4 80 | 5 50 | 5 00 | 3 70 | 2 00 | 2 00 | 2 80 | 2 70 | 3 60 | 8 60 | 3 00 |
| <i>Corethron cnophilum</i> | | 0 20 | 0 30 | 0 20 | 0 00 | 0 30 | 1 00 | 0 20 | 0 30 | 0 00 | 0 00 | 0 30 | 0 30 | 0 80 | 0 70 | 0 20 | 1 10 | 0 70 | 0 50 |
| <i>Dactylosolen antarcticus</i> | | 0 50 | 0 20 | 1 20 | 1 30 | 0 00 | 0 70 | 1 50 | 1 20 | 0 30 | 1 30 | 0 30 | 1 20 | 0 20 | 1 80 | 2 00 | 1 50 | 1 20 | 0 70 |
| <i>Distephanus speculum</i> | | 1 20 | 1 20 | 0 70 | 0 90 | 0 50 | 0 50 | 0 70 | 1 80 | 0 60 | 0 30 | 0 30 | 0 30 | 0 80 | 0 30 | 0 80 | 0 50 | 0 20 | 0 70 |
| <i>Eucampia antarctica</i> | | 1 00 | 0 50 | 1 20 | 0 60 | 0 00 | 0 80 | 0 30 | 1 00 | 0 30 | 0 30 | 1 00 | 0 30 | 0 80 | 0 80 | 0 20 | 1 10 | 0 50 | 1 20 |
| <i>Fragilaropsis angulata</i> | | 4 20 | 5 80 | 3 70 | 2 10 | 5 30 | 2 50 | 2 80 | 3 00 | 4 80 | 7 80 | 5 50 | 4 80 | 6 30 | 4 40 | 5 50 | 4 10 | 6 80 | 6 10 |
| <i>Fragilaropsis curta</i> | | 65 00 | 62 90 | 64 70 | 55 00 | 68 50 | 70 50 | 65 70 | 62 70 | 68 30 | 56 30 | 69 20 | 59 00 | 66 00 | 61 20 | 65 20 | 60 20 | 51 10 | 55 60 |
| <i>Fragilaropsis cylindrus</i> | | 5 30 | 14 90 | 9 20 | 21 00 | 10 60 | 9 30 | 12 20 | 10 70 | 6 60 | 13 20 | 6 50 | 14 80 | 8 80 | 9 20 | 5 20 | 8 80 | 10 00 | 16 10 |
| <i>Fragilaropsis kerguelensis</i> | | 0 30 | 0 70 | 0 20 | 0 50 | 0 20 | 0 30 | 0 20 | 0 70 | 0 30 | 0 20 | 0 70 | 0 20 | 0 30 | 0 80 | 1 20 | 0 50 | 0 50 | 0 30 |
| <i>Fragilaropsis obliquecostata</i> | | 4 80 | 3 30 | 4 50 | 4 90 | 5 10 | 2 80 | 5 30 | 4 80 | 3 20 | 4 50 | 6 20 | 3 60 | 4 80 | 7 10 | 3 80 | 4 90 | 11 80 | 4 70 |
| <i>Fragilaropsis separanda</i> | | 0 20 | 0 00 | 0 50 | 0 50 | 0 20 | 0 00 | 0 00 | 0 20 | 0 60 | 0 70 | 0 00 | 0 00 | 0 00 | 1 50 | 0 30 | 0 50 | 0 50 | 0 30 |
| <i>Pentalamina corona</i> | | 0 50 | 0 30 | 0 50 | 0 50 | 0 50 | 0 20 | 0 80 | 0 80 | 0 80 | 1 70 | 0 30 | 0 70 | 0 20 | 0 50 | 2 50 | 0 20 | 0 20 | 1 00 |
| <i>Porosira glacialis</i> | | 1 20 | 1 80 | 1 80 | 1 70 | 1 00 | 1 20 | 2 00 | 1 50 | 1 40 | 1 30 | 1 50 | 2 20 | 2 50 | 0 80 | 2 20 | 2 40 | 1 80 | 2 00 |
| <i>Pseudonitzschia turgiduloides</i> | | 0 50 | 2 00 | 1 30 | 1 10 | 0 30 | 1 70 | 1 30 | 1 20 | 0 30 | 1 70 | 0 00 | 1 00 | 1 00 | 1 30 | 0 80 | 1 30 | 1 00 | 0 80 |
| <i>Thalassiosira antarctica spores</i> | | 2 70 | 0 70 | 1 80 | 0 60 | 0 30 | 0 20 | 0 50 | 1 20 | 0 80 | 1 30 | 1 00 | 1 00 | 1 70 | 1 10 | 1 50 | 1 80 | 1 30 | 0 80 |
| <i>Thalassiosira gracilis</i> | | 0 20 | 0 70 | 1 00 | 0 60 | 0 20 | 0 20 | 0 20 | 0 80 | 1 40 | 0 80 | 1 20 | 1 70 | 0 50 | 0 80 | 0 70 | 1 50 | 1 20 | 1 20 |
| <i>Thalassiosira lentiginosa</i> | | 0 20 | 0 00 | 0 20 | 0 30 | 0 00 | 0 20 | 0 00 | 0 00 | 0 20 | 0 30 | 0 30 | 0 50 | 0 30 | 0 00 | 0 00 | 0 00 | 0 20 | 0 50 |

| Species | Samples | 185cm | 190cm | 195cm | 200cm | 205cm | 210cm | 215cm | 220cm | 225cm | 230cm | 235cm | 240cm | 245cm | 250cm | 255cm | 260cm | 265cm | 270cm |
|--|---------|-------|-------|-------|-------|-------|-------|-------|-------|-------|-------|-------|-------|-------|-------|-------|-------|-------|-------|
| <i>Chaetoceros spp</i> | | 0 20 | 0 50 | 0 60 | 0 30 | 0 20 | 0 20 | 0 20 | 0 30 | 1 00 | 0 50 | 0 30 | 1 60 | 0 50 | 1 70 | 0 80 | 0 70 | 1 20 | 1 00 |
| <i>Chaetoceros spores</i> | | 4 30 | 1 60 | 3 60 | 5 20 | 3 50 | 6 40 | 5 80 | 7 90 | 7 60 | 9 40 | 2 00 | 11 10 | 8 20 | 10 10 | 9 50 | 7 60 | 10 80 | 3 50 |
| <i>Corethron cnophilum</i> | | 0 30 | 0 20 | 1 60 | 0 70 | 0 00 | 0 00 | 0 00 | 0 00 | 0 00 | 0 30 | 0 20 | 0 70 | 0 20 | 0 30 | 0 30 | 0 50 | 0 20 | 0 20 |
| <i>Dactylosolen antarcticus</i> | | 0 70 | 1 00 | 0 50 | 1 30 | 0 70 | 0 80 | 1 70 | 1 10 | 0 50 | 1 50 | 0 30 | 0 70 | 1 00 | 1 00 | 0 30 | 1 00 | 0 00 | 1 70 |
| <i>Distephanus speculum</i> | | 0 70 | 0 80 | 0 80 | 0 80 | 0 80 | 0 20 | 1 80 | 0 20 | 0 80 | 1 50 | 0 50 | 1 30 | 2 80 | 1 50 | 0 80 | 0 80 | 0 70 | 0 50 |
| <i>Eucampia antarctica</i> | | 0 30 | 0 60 | 1 70 | 1 20 | 0 70 | 0 80 | 0 80 | 0 80 | 0 30 | 1 80 | 0 50 | 1 00 | 1 00 | 0 70 | 1 20 | 0 30 | 1 00 | 0 70 |
| <i>Fragilaropsis angulata</i> | | 4 30 | 4 40 | 3 60 | 4 80 | 5 10 | 6 00 | 6 30 | 7 10 | 10 50 | 7 00 | 10 00 | 8 00 | 7 20 | 4 50 | 5 20 | 4 50 | 4 20 | 5 20 |
| <i>Fragilaropsis curta</i> | | 61 70 | 57 30 | 60 30 | 50 10 | 60 90 | 58 60 | 45 60 | 57 90 | 56 10 | 47 50 | 64 50 | 49 40 | 50 70 | 48 70 | 40 30 | 46 00 | 38 30 | 51 70 |
| <i>Fragilaropsis cylindrus</i> | | 9 50 | 18 00 | 12 20 | 17 10 | 9 40 | 11 80 | 18 50 | 13 10 | 10 60 | 13 10 | 4 70 | 11 90 | 14 30 | 13 50 | 27 10 | 23 40 | 32 80 | 23 60 |
| <i>Fragilaropsis kerguelensis</i> | | 0 30 | 0 00 | 0 20 | 1 00 | 0 20 | 1 40 | 0 80 | 0 20 | 0 70 | 0 00 | 0 50 | 0 20 | 0 00 | 0 70 | 0 50 | 0 70 | 0 70 | 0 50 |
| <i>Fragilaropsis obliquecostata</i> | | 5 30 | 4 50 | 6 20 | 5 50 | 5 50 | 4 40 | 7 80 | 4 00 | 7 10 | 8 40 | 6 70 | 4 60 | 4 30 | 5 50 | 4 30 | 5 50 | 4 30 | 4 30 |
| <i>Fragilaropsis separanda</i> | | 0 20 | 0 00 | 0 30 | 0 30 | 1 00 | 0 60 | 0 50 | 0 20 | 0 20 | 0 20 | 0 30 | 0 20 | 0 50 | 0 50 | 0 30 | 1 00 | 0 20 | 0 30 |
| <i>Pentalamina corona</i> | | 1 30 | 0 60 | 0 60 | 0 70 | 0 80 | 0 50 | 0 50 | 0 00 | 0 00 | 0 00 | 0 00 | 0 30 | 0 30 | 0 30 | 0 20 | 0 30 | 0 30 | 0 00 |
| <i>Porosira glacialis</i> | | 1 10 | 1 60 | 1 90 | 0 70 | 2 60 | 1 90 | 3 50 | 0 00 | 0 70 | 1 30 | 4 30 | 1 60 | 1 20 | 1 50 | 1 80 | 1 30 | 0 80 | 0 50 |
| <i>Pseudonitzschia turgiduloides</i> | | 1 50 | 1 00 | 0 90 | 0 30 | 0 50 | 1 30 | 0 30 | 0 60 | 0 50 | 0 80 | 0 20 | 0 30 | 0 30 | 0 80 | 0 80 | 0 80 | 0 00 | 2 20 |
| <i>Thalassiosira antarctica spores</i> | | 1 60 | 2 30 | 0 80 | 3 20 | 2 00 | 0 80 | 0 80 | 1 60 | 0 70 | 1 50 | 2 30 | 1 30 | 4 30 | 5 50 | 1 50 | 1 50 | 1 70 | 1 00 |
| <i>Thalassiosira gracilis</i> | | 1 30 | 0 60 | 0 80 | 0 70 | 1 20 | 0 60 | 0 30 | 1 60 | 0 50 | 1 30 | 0 70 | 1 80 | 0 70 | 1 20 | 1 30 | 0 80 | 1 30 | 0 30 |
| <i>Thalassiosira lentiginosa</i> | | 0 30 | 1 00 | 0 00 | 0 50 | 0 00 | 0 00 | 0 20 | 0 30 | 0 20 | 0 00 | 0 00 | 0 70 | 0 30 | 0 50 | 0 20 | 0 80 | 0 00 | 0 00 |

| Species | Samples | 275cm | 280cm | 285cm | 290cm | 295cm | 300cm |
|--|---------|-------|-------|-------|-------|-------|-------|
| <i>Chaetoceros spp</i> | | 2 80 | 1 00 | 0 70 | 0 20 | 0 00 | 1 30 |
| <i>Chaetoceros spores</i> | | 4 30 | 2 80 | 11 80 | 27 60 | 6 50 | 3 30 |
| <i>Corethron cnophilum</i> | | 0 80 | 0 50 | 0 80 | 0 00 | 0 00 | 0 30 |
| <i>Dactylosolen antarcticus</i> | | 0 00 | 0 50 | 0 50 | 1 70 | 2 00 | 3 20 |
| <i>Distephanus speculum</i> | | 1 20 | 0 50 | 1 30 | 0 50 | 1 70 | 1 20 |
| <i>Eucampia antarctica</i> | | 1 70 | 0 30 | 2 50 | 1 00 | 3 50 | 1 70 |
| <i>Fragilaropsis angulata</i> | | 9 30 | 13 30 | 9 50 | 4 60 | 14 10 | 10 30 |
| <i>Fragilaropsis curta</i> | | 37 60 | 38 00 | 42 60 | 28 50 | 34 50 | 32 80 |
| <i>Fragilaropsis cylindrus</i> | | 27 50 | 28 00 | 15 40 | 12 60 | 6 60 | 9 50 |
| <i>Fragilaropsis kerguelensis</i> | | 0 70 | 0 30 | 1 00 | 1 50 | 3 80 | 5 30 |
| <i>Fragilaropsis obliquecostata</i> | | 6 80 | 6 50 | 4 80 | 6 10 | 7 10 | 8 70 |
| <i>Fragilaropsis separanda</i> | | 0 00 | 0 20 | 0 70 | 1 00 | 3 00 | 2 80 |
| <i>Pentalamina corona</i> | | 0 00 | 0 00 | 0 00 | 0 20 | 0 70 | 0 20 |
| <i>Porosira glacialis</i> | | 0 50 | 1 00 | 1 50 | 1 70 | 1 00 | 1 20 |
| <i>Pseudonitzschia turgiduloides</i> | | 2 20 | 0 70 | 0 30 | 0 20 | 0 20 | 0 00 |
| <i>Thalassiosira antarctica spores</i> | | 1 00 | 0 50 | 1 20 | 3 80 | 5 30 | 5 00 |
| <i>Thalassiosira gracilis</i> | | 0 70 | 0 70 | 1 00 | 3 80 | 3 20 | 3 80 |
| <i>Thalassiosira lentiginosa</i> | | 0 20 | 0 70 | 0 70 | 1 00 | 1 00 | 2 30 |

- Appendix 6 -

Preliminary cluster analysis of GC2

GC2.01

 BIOSTAT II: HIERARCHICAL CLUSTER ANALYSIS (VER. 3.5)

SIMDK PROVIDED THE ASSOCIATION MATRIX FROM DATA IN FILE gc2.dak
 ASSOCIATION MATRIX IS A DISSIMILARITY MATRIX FROM BRAY-CURTIS

NUMBER OF INDIVIDUALS = 60
 NUMBER OF VARIABLES = 18

ASSOCIATION MATRIX IS FROM SIMDK

METHOD: GROUP AVERAGE (UNWEIGHTED PAIR GROUP METHOD USING ARITHMETIC AVERAGES)
 LABELS: 7cm 10cm 15cm 20cm 25cm 30cm 35cm 40cm 45cm
 50cm
 100cm 55cm 60cm 65cm 70cm 75cm 80cm 85cm 90cm 95cm
 150cm 105cm 110cm 115cm 120cm 125cm 130cm 135cm 140cm 145cm
 200cm 155cm 160cm 165cm 170cm 175cm 180cm 185cm 190cm 195cm
 250cm 205cm 210cm 215cm 220cm 225cm 230cm 235cm 240cm 245cm
 300cm 255cm 260cm 265cm 270cm 275cm 280cm 285cm 290cm 295cm

FORMAT: (5E14.7)

ACRONYM FOR ASSOCIATION MATRIX USED = BRAY-CURTIS

| PAIRING SEQUENCE: | | AT DISTANCE X | |
|-------------------|------------|---------------|-------------|
| ITEM | JOINS ITEM | AT DISTANCE | INDIVIDUALS |
| 6 | 50 | .062 | 1.113 |
| 21 | 34 | .068 | 1.230 |
| 51 | 53 | .076 | 1.361 |
| 30 | 36 | .079 | 1.427 |
| 48 | 57 | .084 | 1.508 |
| 5 | 7 | .084 | 1.518 |
| 37 | 41 | .091 | 1.632 |
| 21 | 37 | .091 | 1.645 |
| 16 | 17 | .094 | 1.689 |
| 18 | 25 | .094 | 1.698 |
| 8 | 10 | .095 | 1.706 |
| 4 | 42 | .095 | 1.707 |
| 30 | 38 | .095 | 1.710 |
| 5 | 12 | .097 | 1.738 |
| 6 | 49 | .099 | 1.783 |
| 21 | 26 | .100 | 1.800 |
| 40 | 52 | .101 | 1.824 |
| 20 | 31 | .103 | 1.848 |
| 59 | 60 | .104 | 1.875 |
| 35 | 46 | .105 | 1.891 |
| 1 | 8 | .106 | 1.900 |
| 21 | 39 | .108 | 1.939 |
| 22 | 30 | .109 | 1.971 |
| 15 | 23 | .110 | 1.973 |
| 3 | 55 | .110 | 1.977 |
| 27 | 29 | .110 | 1.981 |
| 6 | 40 | .110 | 1.984 |
| 45 | 56 | .112 | 2.015 |
| 13 | 19 | .112 | 2.023 |
| 16 | 24 | .114 | 2.046 |
| 4 | 28 | .115 | 2.063 |
| 21 | 32 | .116 | 2.090 |
| 6 | 48 | .119 | 2.139 |
| 35 | 44 | .119 | 2.140 |
| 21 | 22 | .123 | 2.205 |

| | | | |
|----|----|------|-------|
| 18 | 54 | .123 | 2.222 |
| 6 | 51 | .129 | 2.317 |
| 4 | 21 | .130 | 2.346 |
| 1 | 2 | .132 | 2.381 |
| 15 | 27 | .132 | 2.385 |
| 4 | 18 | .135 | 2.424 |
| 3 | 5 | .136 | 2.440 |
| 6 | 35 | .136 | 2.452 |
| 4 | 20 | .136 | 2.453 |
| 14 | 33 | .139 | 2.495 |
| 13 | 16 | .141 | 2.542 |
| 4 | 14 | .146 | 2.637 |
| 6 | 43 | .149 | 2.674 |
| 1 | 13 | .149 | 2.686 |
| 1 | 3 | .155 | 2.788 |
| 4 | 15 | .157 | 2.826 |
| 6 | 45 | .158 | 2.852 |
| 1 | 9 | .162 | 2.911 |
| 58 | 59 | .164 | 2.954 |
| 4 | 6 | .164 | 2.955 |
| 1 | 4 | .170 | 3.058 |
| 1 | 47 | .195 | 3.501 |
| 1 | 11 | .198 | 3.558 |
| 1 | 58 | .254 | 4.565 |

 COPHENETIC CORRELATION COEFFICIENT = .616978

***** DENDROGRAM *****
 DERIVED FROM BRAY-CURTIS

| CASE | LABEL |
|------|-------|
| 1 | 7cm |
| 8 | 40cm |
| 10 | 50cm |
| 2 | 10cm |
| 13 | 65cm |
| 19 | 95cm |
| 16 | 80cm |
| 17 | 85cm |
| 24 | 120cm |
| 3 | 15cm |
| 55 | 275cm |
| 5 | 25cm |
| 7 | 35cm |
| 12 | 60cm |
| 9 | 45cm |
| 4 | 20cm |
| 42 | 210cm |
| 28 | 140cm |
| 21 | 105cm |
| 34 | 170cm |
| 37 | 185cm |
| 41 | 205cm |
| 26 | 130cm |
| 39 | 195cm |
| 32 | 160cm |
| 22 | 110cm |
| 30 | 150cm |
| 36 | 180cm |
| 38 | 190cm |
| 18 | 90cm |
| 25 | 125cm |
| 54 | 270cm |
| 20 | 100cm |
| 31 | 155cm |
| 14 | 70cm |
| 33 | 165cm |
| 15 | 75cm |
| 23 | 115cm |
| 27 | 135cm |
| 29 | 145cm |
| 6 | 30cm |
| 50 | 250cm |
| 49 | 245cm |
| 40 | 200cm |
| 52 | 260cm |
| 48 | 240cm |
| 57 | 285cm |
| 51 | 255cm |
| 53 | 265cm |
| 35 | 175cm |
| 46 | 230cm |
| 44 | 220cm |
| 43 | 215cm |
| 45 | 225cm |
| 56 | 280cm |
| 47 | 235cm |
| 11 | 55cm |
| 58 | 290cm |
| 59 | 295cm |
| 60 | 300cm |

NORMAL PROGRAM TERMINATION.

– *Appendix 7* –

Abundance (%) and distribution of species in GC29

| Species | Sample | 0cm | 5cm | 10cm | 15cm | 20cm | 25cm | 30cm | 35cm | 40cm | 45cm | 50cm | 55cm | 60cm | 65cm | 70cm | 75cm | 80cm | 85cm |
|--|--------|-------|-------|-------|-------|-------|-------|-------|-------|-------|-------|-------|-------|-------|-------|-------|-------|-------|-------|
| <i>Chaetoceros spores</i> | | 3 48 | 2 00 | 3 50 | 5 66 | 5 67 | 7 67 | 11 50 | 12 17 | 13 67 | 9 17 | 9 00 | 12 81 | 9 95 | 12 83 | 11 90 | 19 50 | 19 17 | 12 83 |
| <i>Dactyliosolen antarcticus</i> | | 0 50 | 0 00 | 0 17 | 0 00 | 0 33 | 0 17 | 0 83 | 1 67 | 0 50 | 0 67 | 0 33 | 0 82 | 0 50 | 0 50 | 0 83 | 0 33 | 0 50 | 1 17 |
| <i>Distephanus speculum</i> | | 1 82 | 1 33 | 0 67 | 1 00 | 1 17 | 1 50 | 2 83 | 1 17 | 1 67 | 1 33 | 0 33 | 0 33 | 1 16 | 2 17 | 1 49 | 2 67 | 1 67 | 2 67 |
| <i>Euampia antarctica</i> | | 0 00 | 0 33 | 0 50 | 0 17 | 0 50 | 0 67 | 1 33 | 0 00 | 0 67 | 0 67 | 0 67 | 0 99 | 1 00 | 0 33 | 0 99 | 0 50 | 1 00 | 0 67 |
| <i>Fragilaropsis angulata</i> | | 3 48 | 3 50 | 3 00 | 5 16 | 3 00 | 3 83 | 5 00 | 2 00 | 4 50 | 3 83 | 6 17 | 3 45 | 3 32 | 3 17 | 2 98 | 0 50 | 1 00 | 0 67 |
| <i>Fragilaropsis curta</i> | | 56 79 | 65 17 | 54 33 | 44 43 | 41 33 | 36 83 | 29 50 | 27 33 | 26 83 | 23 00 | 29 67 | 22 82 | 24 54 | 29 33 | 24 63 | 17 17 | 25 50 | 26 00 |
| <i>Fragilaropsis cylindrus</i> | | 4 80 | 4 50 | 8 00 | 7 15 | 7 00 | 12 67 | 7 33 | 10 83 | 7 50 | 14 67 | 9 50 | 6 57 | 7 30 | 10 50 | 12 07 | 8 83 | 4 17 | 6 50 |
| <i>Fragilaropsis kerguelensis</i> | | 0 83 | 1 67 | 1 17 | 0 67 | 1 33 | 0 17 | 1 33 | 1 00 | 1 50 | 1 83 | 1 83 | 1 31 | 1 33 | 2 17 | 1 65 | 2 33 | 2 00 | 2 17 |
| <i>Fragilaropsis obliquecostata</i> | | 5 46 | 2 50 | 3 50 | 3 99 | 4 50 | 2 50 | 2 00 | 2 83 | 3 17 | 5 00 | 4 17 | 4 27 | 5 14 | 6 33 | 4 63 | 5 33 | 5 33 | 2 50 |
| <i>Fragilaropsis separanda</i> | | 0 66 | 0 50 | 0 33 | 0 50 | 0 83 | 0 50 | 2 00 | 2 17 | 1 33 | 1 67 | 0 50 | 1 15 | 0 33 | 0 17 | 0 66 | 0 33 | 0 00 | 0 17 |
| <i>Pentalamina corona</i> | | 1 32 | 5 33 | 5 17 | 4 99 | 4 67 | 6 33 | 3 67 | 5 00 | 8 67 | 2 00 | 2 33 | 4 76 | 1 49 | 2 83 | 2 64 | 1 50 | 4 17 | 4 50 |
| <i>Porosira glacialis</i> | | 2 15 | 1 83 | 3 00 | 2 16 | 1 33 | 1 17 | 1 17 | 1 00 | 1 33 | 2 33 | 1 00 | 1 31 | 0 83 | 0 33 | 0 50 | 1 00 | 0 67 | 0 67 |
| <i>Thalassiosira antarctica spores</i> | | 12 42 | 7 50 | 11 83 | 18 97 | 23 67 | 20 00 | 26 67 | 27 83 | 24 50 | 27 00 | 28 33 | 33 99 | 36 98 | 25 33 | 31 57 | 34 50 | 31 00 | 32 50 |
| <i>Thalassiosira gracilis</i> | | 0 66 | 0 67 | 1 00 | 0 83 | 0 67 | 0 67 | 1 50 | 1 17 | 0 50 | 0 83 | 1 50 | 0 49 | 1 99 | 0 50 | 1 32 | 1 17 | 1 00 | 1 50 |
| <i>Thalassiosira lentiginosa</i> | | 0 50 | 0 17 | 0 33 | 0 50 | 0 67 | 0 83 | 0 83 | 0 33 | 0 83 | 1 67 | 1 17 | 0 99 | 0 66 | 0 33 | 0 00 | 0 00 | 0 17 | 0 17 |

| Species | Sample | 90cm | 95cm | 100cm | 105cm | 110cm | 115cm | 120cm | 125cm | 130cm | 135cm |
|--|--------|-------|-------|-------|-------|-------|-------|-------|-------|-------|-------|
| <i>Chaetoceros spores</i> | | 11 17 | 9 17 | 9 15 | 4 33 | 6 83 | 3 50 | 4 33 | 13 16 | 9 15 | 22 55 |
| <i>Dactyliosolen antarcticus</i> | | 0 67 | 1 00 | 0 50 | 1 00 | 1 33 | 0 67 | 1 00 | 0 82 | 0 67 | 0 66 |
| <i>Distephanus speculum</i> | | 1 50 | 5 00 | 1 83 | 2 67 | 1 67 | 1 67 | 0 67 | 1 15 | 1 16 | 0 83 |
| <i>Euampia antarctica</i> | | 0 83 | 0 83 | 0 67 | 0 67 | 1 33 | 1 50 | 0 33 | 0 82 | 0 67 | 1 00 |
| <i>Fragilaropsis angulata</i> | | 2 50 | 0 67 | 0 67 | 0 50 | 1 00 | 1 67 | 1 50 | 1 32 | 0 83 | 1 16 |
| <i>Fragilaropsis curta</i> | | 30 83 | 32 00 | 35 27 | 26 83 | 28 00 | 32 50 | 29 95 | 29 11 | 25 12 | 29 02 |
| <i>Fragilaropsis cylindrus</i> | | 11 83 | 4 50 | 5 99 | 1 50 | 5 00 | 3 17 | 5 66 | 1 64 | 2 16 | 0 66 |
| <i>Fragilaropsis kerguelensis</i> | | 2 00 | 2 17 | 3 83 | 7 33 | 5 00 | 4 67 | 6 32 | 4 93 | 6 82 | 6 97 |
| <i>Fragilaropsis obliquecostata</i> | | 5 00 | 4 83 | 4 49 | 3 67 | 5 17 | 4 50 | 7 65 | 3 13 | 3 33 | 5 31 |
| <i>Fragilaropsis separanda</i> | | 0 17 | 0 00 | 0 17 | 0 33 | 0 17 | 0 83 | 0 83 | 0 49 | 0 33 | 0 66 |
| <i>Pentalamina corona</i> | | 5 50 | 4 67 | 2 83 | 0 50 | 1 50 | 0 67 | 1 50 | 0 66 | 0 50 | 0 33 |
| <i>Porosira glacialis</i> | | 0 50 | 0 67 | 0 33 | 0 83 | 0 17 | 0 33 | 0 00 | 0 16 | 0 17 | 0 00 |
| <i>Thalassiosira antarctica spores</i> | | 20 00 | 28 50 | 27 12 | 42 00 | 35 67 | 36 67 | 34 78 | 36 18 | 43 76 | 25 37 |
| <i>Thalassiosira gracilis</i> | | 1 00 | 1 67 | 1 50 | 0 67 | 1 67 | 0 67 | 1 00 | 0 33 | 0 83 | 1 16 |
| <i>Thalassiosira lentiginosa</i> | | 0 17 | 0 17 | 0 50 | 0 33 | 0 83 | 0 50 | 0 33 | 0 33 | 0 33 | 0 33 |

– *Appendix 8* –

Abundance (%) and distribution of species in AA149

| Species | Sample | 0cm | 5cm | 10cm | 15cm | 20cm | 25cm | 30cm | 35cm | 40cm | 45cm | 50cm | 55cm | 60cm | 65cm | 70cm* | 75cm | 80cm | 85cm* |
|--|--------|-------|-------|-------|-------|-------|-------|-------|-------|-------|-------|-------|-------|-------|-------|-------|-------|-------|-------|
| <i>Chaetoceros</i> spores | | 6 98 | 4 67 | 33 89 | 22 20 | 16 00 | 8 83 | 12 50 | 16 33 | 14 67 | 20 17 | 22 50 | 10 17 | 7 33 | 11 17 | 20 33 | 11 83 | 29 17 | 22 00 |
| <i>Dactyliosolen antarcticus</i> | | 1 17 | 1 33 | 0 67 | 2 34 | 2 33 | 4 00 | 3 50 | 1 50 | 1 67 | 0 50 | 3 50 | 1 67 | 2 00 | 1 83 | 1 67 | 1 67 | 0 67 | 0 67 |
| <i>Eucampia antarctica</i> | | 0 00 | 2 67 | 0 50 | 1 84 | 1 83 | 1 17 | 0 67 | 0 83 | 1 00 | 1 83 | 1 50 | 1 33 | 1 33 | 0 50 | 4 00 | 1 00 | 0 83 | 5 00 |
| <i>Fragilanopsis angulata</i> | | 3 32 | 3 83 | 0 83 | 1 67 | 2 50 | 1 83 | 2 33 | 1 50 | 2 17 | 0 67 | 2 00 | 2 67 | 2 17 | 1 33 | 2 33 | 1 33 | 0 33 | 0 83 |
| <i>Fragilanopsis curta</i> | | 42 86 | 25 67 | 22 04 | 22 04 | 26 00 | 25 33 | 28 17 | 34 00 | 20 67 | 14 83 | 21 83 | 24 67 | 26 00 | 18 17 | 11 00 | 31 00 | 19 00 | 11 17 |
| <i>Fragilanopsis cylindrus</i> | | 11 13 | 6 83 | 1 67 | 4 84 | 4 33 | 1 33 | 0 67 | 3 33 | 1 67 | 0 33 | 2 00 | 0 83 | 0 83 | 1 33 | 1 33 | 3 33 | 4 67 | 2 50 |
| <i>Fragilanopsis kerguelensis</i> | | 6 31 | 7 50 | 24 37 | 26 88 | 21 83 | 29 67 | 34 33 | 20 83 | 28 33 | 38 00 | 23 00 | 32 50 | 32 17 | 37 33 | 32 33 | 29 00 | 26 50 | 33 83 |
| <i>Fragilanopsis obliquecostata</i> | | 1 00 | 2 50 | 1 00 | 1 00 | 2 00 | 3 33 | 1 50 | 2 50 | 2 83 | 2 00 | 1 67 | 2 50 | 2 67 | 2 33 | 0 00 | 0 67 | 0 83 | 0 50 |
| <i>Fragilanopsis separanda</i> | | 1 33 | 2 33 | 1 00 | 1 00 | 2 00 | 2 50 | 1 67 | 0 67 | 1 00 | 0 83 | 2 67 | 1 67 | 2 50 | 1 50 | 5 33 | 0 17 | 0 17 | 6 00 |
| <i>Pentalamina corona</i> | | 4 65 | 2 83 | 0 00 | 0 17 | 0 33 | 0 50 | 0 00 | 0 50 | 0 17 | 0 00 | 0 00 | 0 17 | 0 17 | 0 33 | 0 00 | 0 33 | 0 00 | 0 17 |
| <i>Stellarima microtrias</i> | | 0 83 | 0 50 | 0 17 | 0 00 | 0 50 | 0 33 | 0 00 | 0 00 | 0 67 | 0 00 | 0 00 | 0 00 | 0 50 | 0 00 | 1 00 | 0 17 | 0 33 | 2 00 |
| <i>Thalassiosira antarctica</i> spores | | 8 97 | 23 50 | 5 18 | 6 34 | 8 00 | 10 83 | 6 00 | 8 33 | 10 67 | 8 17 | 8 50 | 8 50 | 8 50 | 12 00 | 6 67 | 9 33 | 8 33 | 3 00 |
| <i>Thalassiosira gracilis</i> | | 4 49 | 3 17 | 1 50 | 1 67 | 2 33 | 1 50 | 1 33 | 1 67 | 2 50 | 2 33 | 1 17 | 2 50 | 2 33 | 2 67 | 2 00 | 1 83 | 2 50 | 2 33 |
| <i>Thalassiosira lentiginosa</i> | | 1 33 | 3 33 | 1 17 | 1 34 | 1 67 | 2 67 | 2 17 | 1 67 | 2 00 | 2 67 | 1 50 | 3 17 | 1 83 | 1 17 | 1 00 | 2 17 | 1 67 | 3 33 |
| <i>Thalassiosira torokina</i> | | 0 00 | 0 00 | 0 00 | 0 00 | 0 00 | 0 00 | 0 00 | 0 00 | 0 00 | 0 00 | 0 00 | 0 00 | 0 33 | 0 17 | 2 67 | 0 00 | 0 00 | 2 17 |
| <i>Thalassiothrix antarctica</i> | | 0 50 | 0 50 | 0 17 | 0 50 | 1 00 | 0 67 | 0 50 | 0 33 | 0 50 | 0 50 | 0 17 | 0 17 | 0 33 | 1 00 | 2 00 | 0 17 | 0 00 | 0 67 |

| Species | Sample | 90cm | 95cm* | 100cm* | 105cm* | 110cm* | 115cm* | 120cm | 125cm* | 130cm* | 135cm | 140cm | 145cm | 150cm |
|--|--------|-------|-------|--------|--------|--------|--------|-------|--------|--------|-------|-------|-------|-------|
| <i>Chaetoceros</i> spores | | 9 17 | 46 00 | 32 47 | 11 00 | 17 67 | 22 33 | 21 59 | 13 62 | 13 67 | 8 33 | 14 00 | 8 33 | 12 00 |
| <i>Dactyliosolen antarcticus</i> | | 1 17 | 0 33 | 0 65 | 1 17 | 2 67 | 0 33 | 2 33 | 2 66 | 2 50 | 2 50 | 0 83 | 1 17 | 2 83 |
| <i>Eucampia antarctica</i> | | 1 17 | 6 33 | 5 52 | 6 67 | 5 67 | 7 00 | 5 98 | 2 99 | 0 33 | 2 17 | 0 67 | 2 17 | 2 00 |
| <i>Fragilanopsis angulata</i> | | 0 50 | 0 67 | 2 60 | 1 33 | 0 67 | 0 67 | 1 33 | 2 66 | 1 17 | 1 50 | 1 17 | 1 50 | 2 17 |
| <i>Fragilanopsis curta</i> | | 22 83 | 7 67 | 11 36 | 20 17 | 12 67 | 9 00 | 17 61 | 8 31 | 28 67 | 21 17 | 20 83 | 32 33 | 30 83 |
| <i>Fragilanopsis cylindrus</i> | | 1 50 | 0 33 | 1 62 | 1 67 | 2 00 | 2 00 | 1 33 | 0 66 | 2 33 | 0 33 | 3 00 | 1 83 | 0 83 |
| <i>Fragilanopsis kerguelensis</i> | | 36 33 | 22 00 | 28 25 | 35 33 | 27 67 | 33 67 | 28 90 | 47 84 | 28 00 | 38 67 | 35 50 | 25 33 | 25 83 |
| <i>Fragilanopsis obliquecostata</i> | | 1 83 | 0 00 | 0 00 | 0 33 | 0 67 | 0 00 | 0 33 | 0 00 | 1 00 | 2 00 | 2 00 | 2 50 | 2 83 |
| <i>Fragilanopsis separanda</i> | | 2 17 | 3 67 | 5 19 | 4 17 | 4 67 | 5 33 | 4 32 | 5 98 | 0 50 | 2 17 | 1 00 | 0 17 | 1 83 |
| <i>Pentalamina corona</i> | | 0 00 | 0 00 | 0 00 | 0 00 | 0 33 | 0 67 | 1 00 | 0 00 | 0 00 | 0 00 | 0 17 | 0 00 | 0 17 |
| <i>Stellarima microtrias</i> | | 0 17 | 0 00 | 0 65 | 1 33 | 2 00 | 0 67 | 0 00 | 0 33 | 0 00 | 0 17 | 0 33 | 0 00 | 1 00 |
| <i>Thalassiosira antarctica</i> spores | | 10 50 | 3 00 | 2 92 | 3 17 | 7 33 | 4 33 | 0 00 | 6 31 | 9 17 | 10 50 | 9 67 | 11 17 | 8 00 |
| <i>Thalassiosira gracilis</i> | | 2 83 | 1 67 | 0 97 | 1 67 | 3 33 | 1 00 | 3 99 | 1 33 | 2 83 | 1 50 | 1 33 | 1 50 | 0 67 |
| <i>Thalassiosira lentiginosa</i> | | 1 33 | 2 00 | 2 60 | 3 33 | 2 33 | 3 67 | 1 66 | 1 99 | 0 67 | 3 17 | 2 33 | 3 50 | 2 33 |
| <i>Thalassiosira torokina</i> | | 0 00 | 1 00 | 0 00 | 3 33 | 4 33 | 2 67 | 4 98 | 0 66 | 0 00 | 0 00 | 0 00 | 0 00 | 0 00 |
| <i>Thalassiothrix antarctica</i> | | 1 00 | 1 67 | 0 97 | 1 00 | 2 00 | 0 67 | 0 33 | 0 33 | 0 33 | 0 50 | 0 50 | 0 50 | 0 33 |

* denotes samples from which only 300 valves were counted

- Appendix 9 -

Abundance (%) and distribution of species in AA186

| Species | Sample | 0cm | 5cm | 10cm | 15cm | 20cm | 25cm | 30cm | 35cm | 40cm | 45cm | 50cm | 55cm | 60cm | 65cm | 70cm | 75cm | 80cm | 85cm |
|--|--------|-------|-------|-------|-------|-------|-------|-------|-------|-------|-------|-------|-------|-------|-------|-------|-------|-------|-------|
| <i>Chaetoceros spores</i> | | 3.96 | 4.71 | 5.33 | 2.67 | 7.83 | 3.91 | 2.14 | 2.00 | 3.44 | 5.30 | 4.30 | 2.17 | 2.62 | 7.08 | 2.99 | 2.66 | 3.63 | 5.16 |
| <i>Corethron cnophilum</i> | | 0.17 | 0.49 | 0.00 | 0.00 | 0.00 | 0.00 | 0.00 | 0.00 | 0.16 | 0.00 | 0.00 | 0.17 | 0.00 | 0.00 | 0.17 | 0.33 | 0.00 | 0.00 |
| <i>Dactylosolen antarcticus</i> | | 1.65 | 1.30 | 0.67 | 1.67 | 1.67 | 0.65 | 0.82 | 0.67 | 0.49 | 0.96 | 1.32 | 1.50 | 1.96 | 1.15 | 0.66 | 1.66 | 1.32 | 0.67 |
| <i>Distephanus speculum</i> | | 0.99 | 3.57 | 1.50 | 1.17 | 2.50 | 1.14 | 1.15 | 2.00 | 0.98 | 2.89 | 2.81 | 2.00 | 0.98 | 4.45 | 2.16 | 1.83 | 0.66 | 2.16 |
| <i>Eucampia antarctica</i> | | 2.64 | 3.90 | 8.50 | 3.33 | 2.33 | 1.14 | 0.99 | 3.16 | 2.46 | 2.89 | 2.15 | 1.67 | 1.80 | 4.12 | 2.82 | 1.83 | 3.80 | 5.49 |
| <i>Fragilaropsis angulata</i> | | 2.48 | 1.95 | 0.50 | 1.50 | 2.67 | 3.42 | 3.79 | 3.33 | 1.80 | 4.01 | 4.30 | 3.67 | 5.89 | 3.62 | 2.49 | 2.83 | 1.98 | 1.16 |
| <i>Fragilaropsis curta</i> | | 49.83 | 19.16 | 22.17 | 21.33 | 32.33 | 48.86 | 54.70 | 46.42 | 41.15 | 25.68 | 43.31 | 50.83 | 48.28 | 26.36 | 37.65 | 34.44 | 39.93 | 25.46 |
| <i>Fragilaropsis cylindrus</i> | | 7.76 | 3.57 | 2.67 | 1.67 | 11.83 | 16.29 | 7.25 | 2.66 | 6.39 | 3.69 | 3.80 | 6.50 | 3.44 | 4.28 | 5.64 | 7.82 | 2.97 | 1.83 |
| <i>Fragilaropsis kerguelensis</i> | | 6.60 | 10.88 | 13.67 | 17.50 | 6.17 | 3.09 | 5.27 | 7.65 | 12.13 | 11.56 | 6.12 | 5.00 | 7.36 | 6.59 | 8.46 | 10.32 | 14.52 | 20.63 |
| <i>Fragilaropsis lineata</i> | | 1.16 | 0.65 | 0.50 | 0.67 | 1.00 | 0.81 | 0.66 | 2.16 | 0.82 | 2.25 | 1.49 | 1.17 | 1.15 | 0.82 | 1.16 | 2.66 | 0.33 | 0.33 |
| <i>Fragilaropsis obliquecostata</i> | | 5.28 | 6.66 | 2.67 | 2.67 | 5.83 | 3.09 | 4.78 | 4.16 | 5.25 | 4.82 | 3.97 | 5.00 | 5.89 | 7.74 | 6.97 | 7.32 | 5.94 | 3.33 |
| <i>Fragilaropsis separanda</i> | | 1.16 | 1.62 | 2.17 | 1.17 | 2.00 | 0.65 | 1.32 | 2.50 | 1.64 | 3.69 | 3.14 | 2.00 | 3.60 | 1.98 | 1.16 | 1.16 | 0.99 | 1.00 |
| <i>Pentalamna corona</i> | | 1.32 | 0.00 | 1.33 | 1.17 | 0.67 | 3.26 | 2.97 | 0.83 | 0.49 | 2.25 | 2.15 | 2.83 | 1.64 | 3.46 | 2.82 | 3.49 | 3.30 | 0.33 |
| <i>Stellamma microtrnas</i> | | 0.33 | 0.65 | 1.83 | 0.17 | 0.33 | 0.33 | 0.49 | 1.83 | 0.33 | 0.80 | 0.66 | 0.67 | 0.60 | 1.32 | 0.33 | 0.50 | 0.33 | 0.33 |
| <i>Thalassiosira antarctica spores</i> | | 5.78 | 35.39 | 25.50 | 35.33 | 14.33 | 4.40 | 5.27 | 9.65 | 12.79 | 14.61 | 9.92 | 7.83 | 9.33 | 15.98 | 15.92 | 13.81 | 12.71 | 24.63 |
| <i>Thalassiosira gracilis</i> | | 2.31 | 1.95 | 2.67 | 2.67 | 2.17 | 3.26 | 2.64 | 3.49 | 2.30 | 5.78 | 2.81 | 2.17 | 1.47 | 2.97 | 2.32 | 1.66 | 1.49 | 1.66 |
| <i>Thalassiosira lentiginosa</i> | | 0.99 | 0.65 | 2.67 | 1.67 | 1.50 | 0.65 | 0.82 | 2.83 | 1.64 | 3.21 | 2.81 | 1.00 | 0.98 | 2.47 | 0.83 | 1.33 | 1.49 | 1.83 |
| <i>Thalassiosira torokina</i> | | 0.50 | 0.00 | 1.67 | 0.50 | 0.00 | 0.00 | 0.00 | 0.00 | 0.82 | 0.16 | 0.00 | 0.00 | 0.16 | 0.33 | 0.00 | 0.33 | 0.66 | 1.00 |

| Species | Sample | 90cm | 95cm | 100cm | 105cm | 110cm | 115cm | 120cm | 125cm | 130cm | 135cm | 140cm | 145cm | 150cm | 155cm | 160cm | 165cm | 170cm | 175cm |
|--|--------|-------|-------|-------|-------|-------|-------|-------|-------|-------|-------|-------|-------|-------|-------|-------|-------|-------|-------|
| <i>Chaetoceros spores</i> | | 5.74 | 7.99 | 2.53 | 7.73 | 6.85 | 0.00 | 9.11 | 6.48 | 2.32 | 2.87 | 14.22 | 7.06 | 6.61 | 10.74 | 54.73 | 17.03 | 10.63 | 6.89 |
| <i>Corethron cnophilum</i> | | 0.00 | 0.00 | 0.00 | 0.00 | 0.00 | 10.81 | 0.00 | 0.00 | 0.00 | 0.00 | 0.00 | 0.00 | 0.00 | 0.00 | 0.00 | 0.00 | 0.00 | 0.31 |
| <i>Dactylosolen antarcticus</i> | | 1.15 | 1.84 | 1.26 | 0.93 | 0.62 | 1.05 | 1.57 | 0.83 | 0.77 | 0.91 | 0.97 | 2.25 | 1.26 | 2.56 | 0.33 | 0.79 | 1.77 | 0.94 |
| <i>Distephanus speculum</i> | | 1.31 | 0.61 | 0.79 | 0.62 | 1.40 | 1.05 | 0.31 | 1.42 | 1.24 | 1.51 | 1.13 | 2.73 | 1.92 | 0.66 | 1.26 | 1.29 | 1.56 | 1.56 |
| <i>Eucampia antarctica</i> | | 6.23 | 19.05 | 7.27 | 19.01 | 10.28 | 13.36 | 13.34 | 20.38 | 21.67 | 25.08 | 10.99 | 10.59 | 20.47 | 15.87 | 2.92 | 12.46 | 5.84 | 7.51 |
| <i>Fragilaropsis angulata</i> | | 0.82 | 0.77 | 0.63 | 0.46 | 0.47 | 0.60 | 0.78 | 0.47 | 0.62 | 0.30 | 1.13 | 1.77 | 0.47 | 0.16 | 0.00 | 0.79 | 0.84 | 1.56 |
| <i>Fragilaropsis curta</i> | | 26.07 | 8.60 | 17.06 | 7.88 | 17.45 | 12.76 | 9.58 | 8.37 | 5.26 | 6.34 | 14.86 | 18.94 | 7.09 | 8.97 | 11.11 | 9.15 | 16.43 | 23.16 |
| <i>Fragilaropsis cylindrus</i> | | 3.44 | 0.77 | 2.21 | 0.77 | 1.40 | 0.30 | 0.31 | 0.63 | 0.15 | 0.15 | 0.32 | 1.28 | 0.63 | 0.48 | 0.33 | 0.95 | 2.90 | 1.88 |
| <i>Fragilaropsis kerguelensis</i> | | 16.89 | 26.73 | 21.96 | 28.90 | 24.77 | 27.93 | 27.15 | 30.81 | 33.44 | 23.41 | 27.63 | 18.30 | 28.19 | 26.28 | 16.42 | 26.97 | 20.77 | 15.96 |
| <i>Fragilaropsis lineata</i> | | 0.66 | 0.31 | 0.47 | 0.31 | 0.31 | 0.00 | 0.16 | 0.00 | 0.46 | 0.30 | 0.00 | 0.64 | 0.31 | 0.48 | 0.17 | 0.00 | 0.64 | 1.10 |
| <i>Fragilaropsis obliquecostata</i> | | 2.30 | 2.00 | 2.37 | 1.08 | 3.27 | 1.80 | 1.10 | 0.79 | 2.01 | 0.91 | 0.97 | 2.09 | 1.42 | 1.12 | 0.66 | 1.10 | 0.97 | 2.35 |
| <i>Fragilaropsis separanda</i> | | 2.46 | 3.23 | 1.58 | 2.63 | 1.25 | 2.25 | 2.98 | 1.58 | 1.86 | 0.76 | 4.20 | 1.61 | 2.68 | 1.60 | 0.17 | 3.79 | 2.58 | 1.72 |
| <i>Pentalamna corona</i> | | 2.30 | 0.31 | 2.53 | 0.46 | 1.25 | 0.00 | 0.00 | 0.00 | 0.00 | 0.00 | 0.16 | 1.28 | 0.00 | 0.00 | 0.17 | 0.16 | 2.09 | 0.78 |
| <i>Stellamma microtrnas</i> | | 1.15 | 1.38 | 0.32 | 1.24 | 1.40 | 0.45 | 1.73 | 1.90 | 1.70 | 2.42 | 1.13 | 0.96 | 2.20 | 1.12 | 0.33 | 0.79 | 0.81 | 0.78 |
| <i>Thalassiosira antarctica spores</i> | | 17.70 | 12.29 | 30.33 | 13.76 | 19.78 | 12.91 | 14.13 | 13.11 | 9.75 | 12.69 | 10.34 | 20.87 | 12.44 | 16.19 | 4.31 | 11.51 | 23.35 | 24.41 |
| <i>Thalassiosira gracilis</i> | | 2.79 | 1.08 | 0.63 | 3.09 | 2.02 | 1.95 | 3.92 | 1.58 | 1.70 | 1.96 | 1.45 | 1.77 | 2.05 | 1.60 | 1.33 | 2.68 | 1.93 | 2.35 |
| <i>Thalassiosira lentiginosa</i> | | 2.46 | 3.53 | 2.69 | 4.33 | 1.56 | 3.45 | 4.71 | 3.95 | 5.57 | 6.95 | 2.42 | 3.21 | 4.88 | 2.56 | 2.32 | 3.79 | 2.58 | 2.03 |
| <i>Thalassiosira torokina</i> | | 1.64 | 3.69 | 1.26 | 3.25 | 2.18 | 4.65 | 5.81 | 4.27 | 6.50 | 7.70 | 2.75 | 1.93 | 2.83 | 3.37 | 0.83 | 2.84 | 1.93 | 1.25 |

- Appendix 10 -

Preliminary cluster analysis of AA186

AA186.01

 BIOPSTAT II: HIERARCHICAL CLUSTER ANALYSIS (VER. 3.5)

SIMDK PROVIDED THE ASSOCIATION MATRIX FROM DATA IN FILE aa186.dek
 ASSOCIATION MATRIX IS A DISSIMILARITY MATRIX FROM BRAY-CURTIS

NUMBER OF INDIVIDUALS = 36
 NUMBER OF VARIABLES = 18

ASSOCIATION MATRIX IS FROM SIMDK

MEIHOD: GROUP AVERAGE (UNWEIGHTED PAIR GROUP MEIHOD USING ARITHMETIC AVERAGES)

| LABELS: | 0cm | 5cm | 10cm | 15cm | 20cm | 25cm | 30cm | 35cm | 40cm | 45cm |
|---------|-------|-------|-------|-------|-------|-------|-------|-------|-------|-------|
| | 50cm | 55cm | 60cm | 65cm | 70cm | 75cm | 80cm | 85cm | 90cm | 95cm |
| | 100cm | 105cm | 110cm | 115cm | 120cm | 125cm | 130cm | 135cm | 140cm | 145cm |
| | 150cm | 155cm | 160cm | 165cm | 170cm | 175cm | | | | |

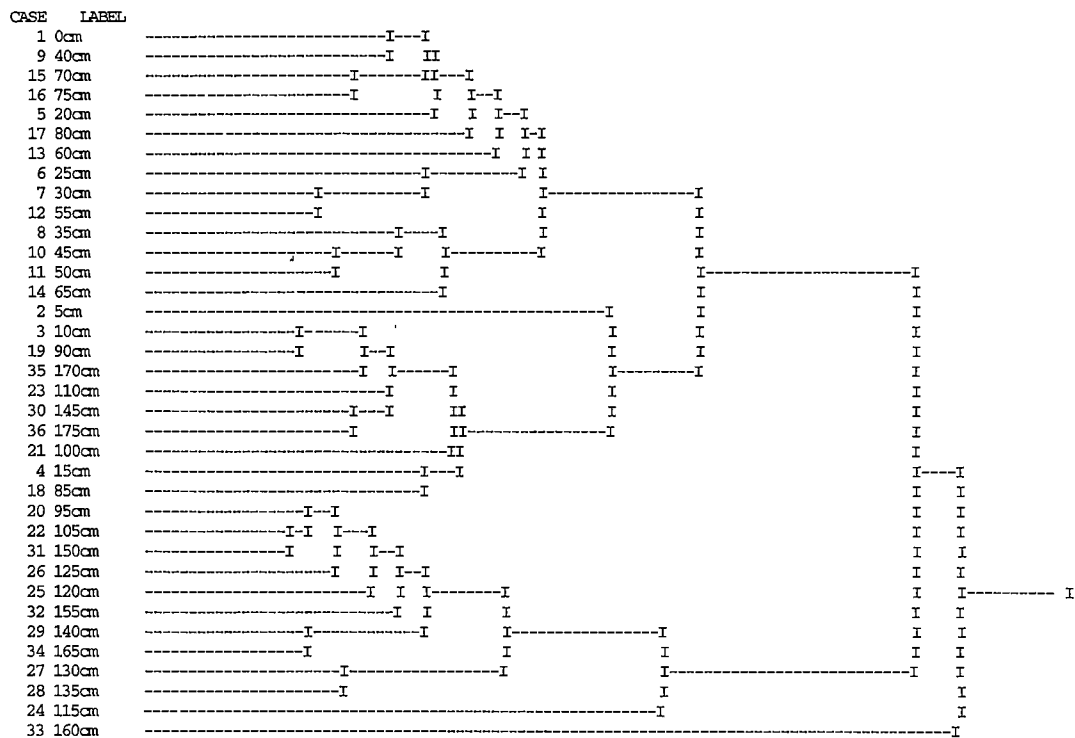
FORMAT: (5E14.7)

ACRONYM FOR ASSOCIATION MATRIX USED = BRAY-CURTIS

| PAIRING SEQUENCE: | | AT DISTANCE X | |
|-------------------|------------|---------------|-------------|
| ITEM | JOINS ITEM | AT DISTANCE | INDIVIDUALS |
| 22 | 31 | .051 | .924 |
| 3 | 19 | .056 | 1.008 |
| 29 | 34 | .059 | 1.062 |
| 20 | 22 | .059 | 1.064 |
| 7 | 12 | .060 | 1.088 |
| 20 | 26 | .069 | 1.233 |
| 10 | 11 | .069 | 1.236 |
| 27 | 28 | .072 | 1.291 |
| 15 | 16 | .073 | 1.308 |
| 30 | 36 | .074 | 1.332 |
| 3 | 35 | .076 | 1.373 |
| 20 | 25 | .079 | 1.428 |
| 23 | 30 | .085 | 1.526 |
| 1 | 9 | .085 | 1.537 |
| 3 | 23 | .087 | 1.570 |
| 8 | 10 | .089 | 1.609 |
| 20 | 32 | .090 | 1.617 |
| 4 | 18 | .098 | 1.759 |
| 20 | 29 | .098 | 1.761 |
| 1 | 15 | .098 | 1.769 |
| 6 | 7 | .100 | 1.800 |
| 1 | 5 | .102 | 1.839 |
| 8 | 14 | .104 | 1.863 |
| 3 | 21 | .109 | 1.967 |
| 3 | 4 | .112 | 2.011 |
| 1 | 17 | .113 | 2.033 |
| 1 | 13 | .124 | 2.225 |
| 20 | 27 | .126 | 2.263 |
| 1 | 6 | .132 | 2.367 |
| 1 | 8 | .139 | 2.502 |
| 2 | 3 | .164 | 2.953 |
| 20 | 24 | .181 | 3.256 |
| 1 | 2 | .194 | 3.495 |
| 1 | 20 | .269 | 4.839 |
| 1 | 33 | .308 | 5.550 |

 COPHENETIC CORRELATION COEFFICIENT = .676325

***** DENDROGRAM *****
 DERIVED FROM BRAY-CURTIS



NORMAL PROGRAM TERMINATION

– *Appendix 11* –

Abundance (%) and distribution of species in GC33

| Species | Sample | 0cm | 5cm | 10cm | 15cm | 20cm | 25cm | 30cm | 35cm | 40cm | 45cm | 50cm | 55cm | 60cm | 65cm | 70cm | 75cm | 80cm |
|--|--------|-------|-------|-------|-------|-------|-------|-------|-------|-------|-------|-------|-------|-------|-------|-------|-------|-------|
| <i>Chaetoceros spores</i> | | 1 00 | 6 50 | 3 32 | 3 80 | 4 16 | 40 76 | 63 67 | 90 50 | 63 80 | 63 50 | 84 83 | 79 83 | 64 83 | 36 93 | 21 13 | 25 12 | 30 00 |
| <i>Corethron criophilum</i> | | 0 00 | 0 33 | 0 17 | 0 00 | 0 33 | 0 00 | 0 17 | 0 00 | 0 33 | 7 17 | 0 00 | 0 00 | 0 17 | 0 16 | 0 33 | 0 17 | 0 00 |
| <i>Distephanus speculum</i> | | 0 67 | 0 33 | 0 66 | 0 66 | 0 33 | 0 66 | 0 17 | 0 17 | 0 83 | 0 50 | 0 83 | 0 33 | 0 83 | 1 14 | 1 00 | 2 64 | 1 50 |
| <i>Eucampia antarctica</i> | | 1 17 | 0 67 | 1 83 | 0 50 | 1 16 | 4 62 | 0 67 | 0 00 | 0 17 | 0 67 | 0 33 | 0 33 | 0 50 | 1 47 | 1 33 | 1 32 | 2 17 |
| <i>Fragilaropsis angulata</i> | | 6 50 | 5 67 | 7 14 | 4 95 | 4 33 | 0 66 | 0 67 | 0 00 | 0 33 | 0 00 | 0 33 | 0 00 | 0 50 | 1 63 | 1 83 | 4 30 | 2 33 |
| <i>Fragilaropsis curta</i> | | 67 17 | 65 33 | 59 30 | 65 51 | 55 24 | 18 48 | 16 67 | 3 17 | 7 93 | 14 17 | 2 50 | 5 50 | 8 50 | 18 30 | 24 13 | 13 88 | 21 67 |
| <i>Fragilaropsis cylindrus</i> | | 4 50 | 6 83 | 5 65 | 7 43 | 10 65 | 4 62 | 8 00 | 0 83 | 18 02 | 5 83 | 1 17 | 7 17 | 4 67 | 8 33 | 10 82 | 9 09 | 3 50 |
| <i>Fragilaropsis kerguelensis</i> | | 0 50 | 1 33 | 0 66 | 0 33 | 1 33 | 1 32 | 1 00 | 2 17 | 1 82 | 1 00 | 2 17 | 1 17 | 6 50 | 4 74 | 8 99 | 9 59 | 6 17 |
| <i>Fragilaropsis obliquecostata</i> | | 2 83 | 3 17 | 4 15 | 2 64 | 3 49 | 0 99 | 0 83 | 0 50 | 1 32 | 1 67 | 0 50 | 0 67 | 0 33 | 1 63 | 1 33 | 2 15 | 1 33 |
| <i>Fragilaropsis separanda</i> | | 1 17 | 0 67 | 1 83 | 1 49 | 1 16 | 0 66 | 0 00 | 0 00 | 0 00 | 0 17 | 0 00 | 0 00 | 0 17 | 0 00 | 0 33 | 0 33 | 0 50 |
| <i>Pentalamina corona</i> | | 1 00 | 1 00 | 0 33 | 1 82 | 2 50 | 1 65 | 0 50 | 0 00 | 0 00 | 0 00 | 0 00 | 0 00 | 0 00 | 0 00 | 0 00 | 0 17 | 0 00 |
| <i>Porosira glacialis</i> | | 0 83 | 0 67 | 1 16 | 1 16 | 3 00 | 0 33 | 0 33 | 0 17 | 0 00 | 0 00 | 0 33 | 0 17 | 0 17 | 2 45 | 0 67 | 2 15 | 3 17 |
| <i>Pseudonitzschia turgiduloides</i> | | 0 00 | 0 00 | 0 17 | 0 17 | 0 00 | 0 17 | 0 17 | 0 00 | 1 82 | 1 33 | 0 67 | 0 33 | 0 00 | 0 49 | 2 50 | 0 83 | 0 00 |
| <i>Thalassiosira antarctica spores</i> | | 4 67 | 3 17 | 6 48 | 2 64 | 3 33 | 21 62 | 4 83 | 1 33 | 2 31 | 1 33 | 4 33 | 2 33 | 8 83 | 16 18 | 16 81 | 18 35 | 17 33 |
| <i>Thalassiosira gracilis</i> | | 1 83 | 1 00 | 2 33 | 0 99 | 2 16 | 1 49 | 1 00 | 0 33 | 0 00 | 0 17 | 0 00 | 0 00 | 0 67 | 1 14 | 1 16 | 1 65 | 0 50 |
| <i>Thalassiosira lentiginosa</i> | | 0 67 | 0 33 | 0 83 | 0 17 | 0 50 | 0 17 | 0 33 | 0 17 | 0 17 | 0 17 | 0 17 | 0 00 | 0 33 | 1 14 | 1 00 | 2 48 | 3 67 |

– *Appendix 12* –

Taxonomy and species plates

Only those species with an abundance >2% are described and illustrated below. All taxonomic characters are based on published accounts, unless where stated “herein”, and selected synonyms (cited).

Actinocyclus actinochilus (Ehrenberg) Simonsen

Plate 1, Fig. 1.

Basionym: *Coscinodiscus actinochilus* Ehrenberg 1844

Synonym: *Anisodiscus apollinis* Brown 1920, *Charcotia actinochilus* (Ehrenberg)

Peragallo 1921

Jousé *et al.* 1962: Plate 5, Figs. 8-11

Kozlova 1966: Plate 2, Fig. 7

Priddle and Fryxell 1985: p. 102, 103

Villareal and Fryxell 1983b: Figs. 20-21

Everitt and Thomas 1986: Fig. 2B

Kim *et al.* 1991: Plate 1, Figs. 14-15

Kozlova 1966, Pichon *et al.* 1987, Medlin and Priddle 1990

Description: Cell solitary and disc-shaped; diameter 20-112 μm (30-73 μm , herein). Areolae pattern radial; areolae 5-11 in 10 μm (4-10, herein). Complete radial rows extend from near each marginal labiate process to the valve centre, dividing valve into fascicles. Areolae rows generally parallel to the central row within each fascicle. Mantle striae 13-21 in 10 μm (4-11, herein); separated from radial areolae by hyaline band. Single row of large, laterally expanded labiate processes evident around margin, 9.5-15 μm apart. (Description based on Villareal and Fryxell, 1983b; Medlin and Priddle, 1990).

Distribution: Antarctic, limited to the vicinity of the ice edge (Villareal and Fryxell, 1983b).

***Chaetoceros* (vegetative cells and resting spores)**

Plate 1, Figs. 2-5 (vegetative cells)

Plate 2, Figs. 1-4 (resting spores)

Leventer *et al.* 1993: Fig. 8C

Priddle and Fryxell 1985: pp. 15-53

Description: cells bear long setae at the ends of both valves. Solitary or chain forming, linked by setae arising from the valves. Both heterovalvate and isovalvate species are present. Terminal cells in chains may differ from the others. Resting spores are known from several species and associated valves usually have modified setae. (Description from Priddle and Fryxell, 1985.).

Distribution: Widespread and abundant in Antarctic phytoplankton.

***Corethron criophilum* Castracane**

Plate 2, Figs. 5-6

Jousé *et al.* 1962: Plate 2, Fig. 16

Kozlova 1966: Plate 5, Fig. 1

Priddle and Fryxell 1985: p. 54-55

Leventer *et al.* 1993: Fig. 8B

Description: Valves heteropolar and cylindrical, diameter 11-47 μm herein; cingulum of numerous elements joining upper and lower domed valves. Cells solitary and robust. Two types of spines on upper valves: one type long and barbed, the other short and terminating with a heavily silicified hook (visible by LM) fitting into chambers along the valve margin. Hook has a thickened, finger-like projection at the distal extreme of the spine and at 90° to the spine, and a second parallel to the first. (Description based on Medlin and Priddle, 1990).

Distribution: Marine planktonic, with greatest abundance south of the Antarctic Polar Front.

Dactyliosolen antarcticus Castracane

Plate 3, Fig. 1

Kozlova 1966: Plate 5, Fig. 2

Priddle and Fryxell 1985: p. 58-59

Description: Valve diameter 16-72 μm (15-50 μm , herein). Girdle band costae prominent in more heavily silicified specimens. Junctions of individual bands arranged spirally on the guide. Valve with branching or reticulate irregular ornamentation. Single labiate process at or near margin. (Description based on Priddle and Fryxell, 1985).

Distephanus speculum (Ehrenberg) Haeckel

Plate 3, Fig. 2

Synonyms: *D. rotundus* Stöhn 1880

Jousé *et al.* 1962: Plate 6, Fig. 19

Perch-Nielsen 1985: Figs. 18-20

Description: Diameter 15-25 μm (herein). System of long crests with ridge-like knots approximately 90° to the axis of the long crest. 6-sided basal and apical ring, covered by net-like ornamentation of short crests and depressions. Crests are almost of equal length on the basal ring. (Description based on Perch-Nielsen, 1985).

Eucampia antarctica (Castracane) Manguin

Plate 3, Figs. 3-4

Synonyms: *Hemiaulus antarcticus* Ehrenberg 1844; *Moelleria antarctica* Castracane 1886; *Eucampia balaustium* Castracane 1886; *E. balaustium* var. *minor* Castracane 1886; *E. balaustium* f. *hiberna* Heiden in Heiden and Koble 1928; *E. balaustium* f. *aestiva* Heiden in Heiden and Koble 1928.

Jousé *et al.* 1962: Plate 5, Figs. 14-17

Kozlova 1966: Plate 2, Figs. 8-10

Syvertsen and Hasle 1983: Fig. 4, Plates 10-14.

Burckle 1984b: Plate 1, Figs. 1-7

Priddle and Fryxell 1985: p. 66-67

Description: Girdle of numerous very thin open bands, numbering 10-20 per epitheca. Bands perforated by transverse row of elongate pores, approximately 10 pores per row, and separated by a narrow rib 2-4 pores from the advalvar edge of the band. 28-32 pores in 10 μm . Valve outline elliptical, with 2 horns 0.5-0.75x the length of the apical axis. Valve mantle curved smoothly downwards in broad girdle view and rounded upwards towards the apices. Apical axis 18-92 μm ; transapical axis 15-20 μm . Valve consists of very large areolae decreasing in size on the horns and valve margins. Single marginal labiate process. Striae start at the labiate process and consist of 3-10 poroid areolae in 10 μm . Horn top plates do not occupy the whole top area of the horn. (Description based on Syvertsen and Hasle, 1983).

Distribution: Antarctic to subantarctic (Syvertsen and Hasle, 1983). Although widely distributed throughout the Southern Ocean, it forms only a minor part of the oceanic plankton. In the vicinity of sea ice, icebergs and the Antarctic coastline, however, this species becomes a more abundant, but not dominant, component of the plankton. Burckle (1984b) considers *E. antarctica* a neritic

species.

Fragilariopsis angulata Hustedt

Plate 3, Figs. 5-7

Synonym: *Nitzschia angulata*, *N. rhombica*, *F. rhombica*

Jousé *et al.* 1962: Plate 6, Figs. 7, 8

Kozlova 1966: Plate 3, Fig. 9

Medlin and Priddle 1990: Plate 24.1, Fig. 6; Plate 24.2, Fig. 19, Plate 24.4, Figs. 1-6

Kim *et al.* 1991: Plate 1, Figs. 6-8

Description: Valves broadly lanceolate, larger specimens with straight middle part. Apical axis 8-53 μm (6 - 43 μm , herein); transapical axis 7-13 μm (4-12 μm , herein). Central nodule absent. Striae with 2 rows of areolae, clearly visible by SEM but may not be discernable by LM; 8-16 striae in 10 μm (7-13 striae, herein); 8-16 fibulae in 10 μm . (Description based on Medlin and Priddle, 1990).

Distribution: Antarctic plankton (Medlin and Priddle, 1990).

Fragilariopsis curta (Van Heurck) Hasle

Plate 4, Figs. 1,3, 6

Plate 5, Fig. 6

Basionym: *Fragilaria curta* Van Heurck 1909

Synonym: *Nitzschia curta* (Van Heurck 1909) Hasle 1972

Jousé *et al.* 1962: Plate 6, Figs. 4, 5

Kozlova 1966: Plate 3, Figs. 13-15

Everitt and Thomas 1986: Fig. 2E

Medlin and Priddle 1990: Plate 24.6, Figs. 2-5

Kim *et al.* 1991: Plate 1, Figs. 2-3

Burckle *et al.* 1987, Leventer and Dunbar 1988, Ligowski *et al.* 1988

Description: Valves linear, apices heteropolar. Apical axis 14-52 μm (10-42 μm , Medlin and Priddle, 1990); transapical axis 5-6 μm (3.5-6 μm , Medlin and Priddle, 1990). Central nodule absent. Striae with 2 rows of areolae (clearly visible by SEM), 9-13 striae in 10 μm ; 9-12 fibulae in 10 μm (Medlin and Priddle, 1990).

Distribution: Antarctic plankton and ice (Medlin and Priddle, 1990). A dominant member of pack ice and fast ice assemblages (Stockwell *et al.*, 1985; Scott *et al.*, 1994).

Fragilariopsis cylindrus (Grunow?) Hasle

Plate 4, Fig. 2

Basionym: *Fragilaria cylindrus* Grunow

Synonym: *Nitzschia cylindrus*

Jousé *et al.* 1962: Plate 6, Fig. 4

Kozlova 1966: Plate 3, Figs. 18-19

Medlin and Priddle 1990: Plate 24.6, Figs. 6-12

Kim *et al.* 1991: Plate 1, Fig. 1 (= *N. cylindra*)

Kang and Fryxell 1992: Figs. 5-12

Burckle *et al.* 1987, Leventer *et al.* 1992, Leventer 1993, Scott *et al.* 1994

Description: Valves linear isopolar, with rounded apices. Apical axis 3-48 μm (5-23 μm , herein); transapical axis 2-4 μm (2-3 μm , herein). Central nodule absent. Striae with 2-4 rows of areolae (clearly visible by SEM); 13-17 striae in 10 μm (10-17, herein); 13-17 fibulae in 10 μm . (Description based on Medlin and Priddle, 1990).

Distribution: Bipolar, plankton and ice (Medlin and Priddle, 1990). A dominant member of pack ice and fast ice assemblages (Stockwell *et al.*, 1985; Scott *et al.*, 1994).

Fragilariopsis kerguelensis (O'Meara) Hasle

Plate 4, Fig. 3

Basionym: *Terebraria kerguelensis* O'Meara 1877

Synonym: *Nitzschia kerguelensis*, *Fragilariopsis antarctica* (Castracane) Hustedt

Jousé *et al.* 1962: Plate 3, Figs. 4-7

Kozlova 1966: Plate 5, Figs. 9-11

Medlin and Priddle 1990: Plate 24.2, Figs. 11-18, Plate 24.3, Fig. 9

Kim *et al.* 1991: Plate 1, Figs. 4-5

Hendley 1937, Fenner *et al.* 1976, Burckle and Cirilli 1987, Burckle *et al.* 1987

Description: Valves lanceolate, with rounded apices. Larger specimens may be heteropolar. Apical axis 10-76 μm (14-50 μm , herein); transapical axis 5-11 μm (6-10 μm , herein). Central nodule absent. Valve structure coarse. Striae with 2 rows of areolae clearly visible by LM. 4-7 striae in 10 μm (4-8 striae, herein); 4-7 fibulae in 10 μm (Description based on Medlin and Priddle, 1990).

Distribution: Antarctic plankton (Medlin and Priddle, 1990). Typically dominating summer surface waters between 52-63°S (Burckle and Cirilli, 1987; Burckle *et al.* 1987) where water temperatures >0°C (Krebs *et al.* 1987).

Fragilariopsis lineata (Castracane) Hasle

Plate 4, Fig. 4

Synonym: *F. linearis*, *Nitzschia lineata*

Medlin and Priddle 1990: Plate 24.6, Fig. 17; Plate 24.7, Figs. 9-11

Description: Valves linear, isopolar and with rounded apices. Apical axis 40-72 μm (36-54 μm , herein); transapical axis 7-9 μm (4-5 μm , herein); 7.5-9 striae in 10 μm (7-12 striae in 10 μm , herein), striae with 2 rows of areolae clearly visible by SEM. Central nodule absent. (Description based on Medlin and Priddle, 1990).

Distribution: ice, Antarctic (Medlin and Priddle, 1990)

Fragilariopsis obliquecostata Heiden

Plate 4, Figs. 5-6

Basionym: *Fragilariopsis obliquecostata* Van Heurck 1909

Synonym: *Nitzschia obliquecostata* (Van Heurck) Hasle 1972

Jousé *et al.* 1962: Plate 6, Figs. 10-16 (*Fragilariopsis sublinearis*)

Kozlova 1966: Plate 6, Fig. 16

Medlin and Priddle 1990: Plate 24.3, Figs. 2-7

Description: Valves narrowly elliptical and often slightly heteropolar. Apical axis 57-110 μm (36-101 μm , herein); transapical axis 8-10 μm (5-8 μm , herein). Central nodule absent. Interstriae oblique and often most evident towards one apex. Striae with 2 rows of areolae (often visible by LM in larger specimens). 6-8 striae in 10 μm (5-10 striae in 10 μm , herein); 6.5-8 fibulae in 10 μm . (Description based on Medlin and Priddle, 1990).

Distribution: Antarctic, plankton (Medlin and Priddle, 1990).

Fragilariopsis pseudonana Hasle

Not illustrated

Medlin and Priddle 1990: Plate 24.1, Figs. 7-14, Plate 24.2, Figs. 20-21

Description: Valves lanceolate to narrowly linear. Apical axis 4-20 μm ; transapical axis 3.5-5 μm . Central nodule absent. Valve structure fine; 18-22 striae in 10 μm ; 18-22 fibulae in 10 μm . 2 rows of areolae (visible by SEM). (Description based on Medlin and Priddle, 1990).

Distribution: Antarctic, plankton (Medlin and Priddle, 1990).

Fragilariopsis ritscheri (Hustedt) Hasle

Plate 4, Fig. 7

Synonym: *Nitzschia ritscheri* Castracane

Jousé *et al.* 1962: Plate 6, Fig. 9

Kozlova 1966: Plate 3, Fig. 20

Medlin and Priddle 1990: Plate 24.1, Fig. 20; Plate 24.2, Figs. 1-10; Plate 24.3, Fig. 8

Description: Valves broadly elliptical, middle part almost straight, tapering part short. Larger specimens often slightly heteropolar. Apical axis 22-57 μm (32-59 μm , herein); transapical axis 8-9 μm (6-10 μm , herein). Central nodule absent. Striae with 2-3 rows of areolae, often clearly visibly by LM. 6-11 striae in 10 μm (5-11 striae in 10 μm , herein) ; 6-11 fibulae in 10 μm . (Description based on Medlin and Priddle, 1990).

Distribution: Antarctic, plankton (Medlin and Priddle, 1990).

Fragilariopsis separanda (Hustedt) Halse

Plate 5, Fig. 1

Synonym: *Nitzschia separanda* Hustedt 1901

Jousé *et al.* 1962: Plate 3, Fig. 8

Kozlova 1966: Plate 5, Fig. 8

Medlin and Priddle 1990: Plate 24.4, Figs. 7-10

Kim *et al.* 1991: Plate 1, Fig. 9

Description: Valves broadly lanceolate, larger specimens with straight middle part. Apical axis 10-33 μm (10-30 μm , herein); transapical axis 8-13 μm (7-11 μm , herein). Central nodule absent. Valve structure coarse. Striae with single row of clearly visible areolae. 10-14 striae in 10 μm ; 10-14 fibulae in 10 μm . (Description based, Medlin and Priddle, 1990).

Distribution: Antarctic, plankton (Medlin and Priddle, 1990).

Fragilariopsis sublineata Hasle

Plate 5, Fig. 2

Basionym: *Fragilaria sublinearis* Van Heurck 1901

Synonym: *Fragilariopsis sublinearis* (Van Heurck) Heiden, *Nitzschia sublineata* Hasle 1971

Medlin and Priddle 1990: Plate 24.3, Fig. 1, Plate 24.5, Figs. 1-10, Plate 24.6, Fig. 1

Description: Valves sunlinear, tapering towards narrowly rounded apices. Central nodule absent. Apical axis 30-92 μm (35-45 μm , herein); transapical axis 5.5-6.5 μm (6-8 μm , herein). Striae with 2 rows of areolae, clearly visible by

SEM. 7.5-9 striae in 10 μm (6-9, herein); 7.5-9 fibulae in 10 μm . (Description based on Medlin and Priddle, 1990).

Distribution: Antarctic, ice (Medlin and Priddle, 1990).

Pentalamina corona Marchant

Plate 5, Figs. 3-4

Silver *et al.* 1980: Figs. 1, 2

Marchant and McEldowney 1986: Plate 1, Figs. 2, 4

Booth and Marchant 1987: Figs. 6-7

Franklin and Marchant 1995: Plate 1, Fig. a; Plate 2, Figs. a, c, e

Zielinski 1997: Plate 1, Figs. 1-16, Plate 2, Figs. 1-9, 11.

Description: Planktonic, solitary spheroid cell, diameter 5-5.8 μm . Cell wall composed of 5 round and triradiate plates, with or without oblong girdle plates, all fitting edge to edge. Central area of round plates slightly raised; processes may or may not arise from the rim of this area. Processes may be rounded, spatula-shaped or branched (Description based on Booth and Marchant, 1987).

Distribution: occurs widely in Antarctic waters, and has been reported from the Weddell Sea, Kita-no-seto Strait, and Prydz Bay (Booth and Marchant, 1987)

Porosira glacialis (Grunow) Jørgensen

Plate 5, Fig. 5

Priddle and Fryxell 1985: p. 142-143

Medlin and Priddle 1990: Plate 11.1, Fig. 9

Description: Valve diameter 23-70 μm (20-52 μm , herein). Weakly silicified. Wavy striae of mainly rectangular areolae (25-25 in 10 μm) and an irregular

annulus. Single labiate process near valve margin. Strutted processes distributed unevenly over valve face, visible as small spots and more densely concentrated at the margin. (Description based on Priddle and Fryxell, 1985; Medlin and Priddle, 1990).

Distribution: Antarctic, ice-edge (Medlin and Priddle, 1990).

Pseudonitzschia turgiduloides (Hasle) Hasle

Plate 5, Figs. 6-7

Synonym: *Nitzschia turgiduloides* Hasle

Medlin and Priddle 1990: Plate 22.3, Figs. 9-14

Watanabe 1988, Scott *et al.* 1994

Description: Apical axis 63-126 μm (70-110 μm , herein); transapical axis 1.2-2.7 μm (1-4 μm , herein). Central nodule present. 10-13 fibulae in 10 μm (9-14, herein); 17-21 striae in 10 μm . Apices rounded. (Description by Johansen and Fryxell, 1985; Medlin and Priddle 1990).

Distribution: Antarctic, in association with pack and fast ice (Scott *et al.* 1994).

Notes: It is very difficult to distinguish this species from *Nitzschia lineola* (*barkleyi*) Cleve, based on the above description. The size range of both species overlap, with the exception of striae per 10 μm (22-28 in *N. lineola*), which are difficult to quantify under the light microscope. The rounded apices (*P. turgiduloides*) and pointed apices (*N. lineola*) are not always taxonomically separable. Whole cells are rarely preserved intact. End pieces are frequently observed.

Rhizosolenia hebetata* fo. *semispina (Hensen) Gran

Plate 6, Fig. 1

Kozlova 1966: Plate 5, Fig. 5

Priddle and Fryxell 1985: p. 86-87

Medlin and Priddle (1990) describe *R. hebetata* fo. *semispina* as an Arctic species, and *R. antennata* fo. *semispina* as Antarctic. Priddle and Fryxell (1985) describe *Rhizosolenia hebetata* fo. *semispina* as an Antarctic species. The latter name is used herein.

Description: Valve acutely conoidal and bilaterally symmetrical, with ventral margin prolonged; diameter 4.2-25 μm . Marginal ridge of contiguous area and claspers visible in permanent mounts. Process long, but usually broken in permanent mounts; wide at the base and tapering into a long, narrow tube. Otaria small and pointed. (Description based on *Rhizosolenia hebetata* fo. *semispina*, Medlin and Priddle, 1990).

Stellarima microtrias (Ehrenberg) Hasle & Sims

Plate 6, Fig. 2

Basionym: *Coscinodiscus stellaris* Roper 1858z

Synonyms: *Coscinodiscus furcatus* Karsten; *Symbolophora microtrias* Ehrenberg 1844; *S.?* *tetras* Ehrenberg 1844; *S.?* *pentas* Ehrenberg; *S.?* *hexas* Ehrenberg 1844; *Coscinodiscus symbolophorus* Grunow 1884; *C. adumbratus* Østrup 1895; *C. furcatus* Karsten 1905; *C. pentas* (Ehren.) Mann 1907; *Coscosira stellaris* (Roper) Heiden var. *symbolophora* (Grun.) Heiden in Heiden and Koble 1928; *Coscinodiscus* (*symbolophorus* var.?) *signatus* Mann 1937; *Podosira liotadii* Manguin 1960; *Symbolphora furcata* (Karsten) Nikolaev 1983.

Jousé *et al.* 1962: Plate 4, Fig. 11

Hasle and Sims 1986: Figs. 18-27

Hasle *et al.* 1988: Figs. 1-25

Description: Vegetative cell diameter 35-105 μm . Areolae pattern furcate; 11-16 areolae in 10 μm . 2-8 conspicuous central labiate processes. No marginal processes. Resting spore diameter 40-199 μm (35-60 μm , herein). Areolae pattern fasciculate; 9-12 areolae in 10 μm (10-14 areolae in 10 μm , herein). 3-5 conspicuous central labiate processes (2-4 labiate processes, herein). No marginal processes. (Description based on Medlin and Priddle, 1990).

Distribution: Resting spores frequently present in ice-samples and net-samples collected in the vicinity of ice (Medlin and Priddle, 1990).

Thalassiosira antarctica Comber (vegetative cells)

Not illustrated

Fryxell *et al.* 1981: Figs. 1-5, 11, 12

Johansen and Fryxell 1985: Figs. 37 & 38.

Description: Valve diameter 16-56 μm . Areolae pattern bifurcating, or occasionally fasciculated. 15-24 areolae in 10 μm . 4-14 central strutted processes. Marginal strutted processes arranged in ≥ 2 rings. Labiate process inside inner ring. 0-4 occluded processes in 10 μm . (Description based on Johansen and Fryxell, 1985).

Distribution: Antarctic, near ice (Medlin and Priddle, 1990).

Thalassiosira antarctica (resting spores)

Plate 6, Fig. 3

Fryxell *et al.* 1981: Figs. 12, 17-20

Johansen and Fryxell 1985: Fig. 39

Kim *et al.* 1991: Plate 1, Fig. 10

Description: Valve diameter 13-44 μm (8-32 μm , herein). Areolae pattern radial. 8-12 areolae in 10 μm at centre of valve. 3-6 strutted processes in 10 μm at mantle; central cluster of 2-6 strutted processes (1-4 strutted processes, herein). 1 marginal labiate process in occluded process ring. 2-5 occluded processes in 10 μm . (Description based on Johansen and Fryxell, 1985; Medlin and Priddle 1990).

Distribution: Antarctic, near ice (Medlin and Priddle, 1990).

Notes: The marginal labiate process is not always visible with the light microscope; the strutted processes around the mantle are rarely observed with the light microscope. This species is also referred to as *T. margaritae* by Kozlova (1966).

Thalassiosira gracilis (Karsten) Hustedt

Plate 6, Figs. 4-5

Basionym: *Coscinodiscus gracilis* Karsten 1905

Synonyms: *Coscinodiscus minimus* Karsten 1905; *Thalassiosira gracilis* var. *gracilis* (Karsten) Hustedt 1958; *Coscinodiscus anomalus* Van Landingham 1968.

José *et al.* 1962: Plate 4, Figs. 4-10

Kozlova 1966: Plate 6, Figs. 2-5

Fryxell and Hasle 1979b: Figs. 12-22

Rivera 1981: Figs. 415-420

Johansen and Fryxell 1985: Figs. 8, 58, 59

Kim *et al.* 1991: Plate 1, Figs. 11-12

Hustedt 1958, Kozlova 1966, Johansen and Fryxell 1985, Burckle 1987, Medlin and Priddle 1990

Description: Valve diameter 5-28 μm (7-20 μm , herein). Areolae distinctly coarse in centre, 8-12 in 10 μm (7-14 μm , herein), becoming finer towards margin (16-20 in 10 μm). 1 central strutted process. Marginal strutted processes 3-4 in 10 μm . 1 labiate process located away from margin. (Description based on Johansen and Fryxell, 1985).

Distribution: Antarctic, subantarctic (Medlin and Priddle, 1990), characteristically south of 58°S (Fryxell and Hasle, 1979b).

Thalassiosira gracilis var. *expecta* (Van Landingham) Fryxell & Hasle

Not illustrated

Basionym: *Thalassiosira expecta* Van Landingham 1978

Synonym: *Thalassiosira delicatula* Hustedt 1958

Fryxell and Hasle 1979b: Figs. 23-28

Johansen and Fryxell 1985: Figs. 8, 60-63

Description: Valve diameter 7-26 μm (7-12 μm , herein). Areolae pattern radial, 14-14 in 10 μm (12-16 in 10 μm , herein), becoming finer towards margin (16-20 in 10 μm). 1 central strutted process. Marginal strutted processes 3-4 in 10 μm (4-5 in 10 μm , herein). 1 labiate process located away from margin. (Description based on Johansen and Fryxell, 1985).

Distribution: Antarctic, subantarctic (Medlin and Priddle, 1990), usually in association with, but less abundant than, *T. gracilis* (Fryxell and Hasle, 1979b; Johansen and Fryxell, 1985).

Notes: This species may be easily confused with *T. gracilis*, although it is most often smaller in diameter.

Thalassiosira gravida Cleve

Plate 6, Fig. 6

Synonym: *Thalassiosira tcherniai* Manguin 1957

Johansen and Fryxell 1985: Figs. 27, 43

Fryxell and Kendrick 1988, Medlin and Priddle 1990

Description: Valve diameter 13-63 μm . Areolae pattern radial, often fasciculated; 20 in 10 μm . Small cluster of strutted processes located in centre. Strutted processes with external extensions scattered evenly over valve face; denser towards margin. Approximately 6 strutted processes in 10 μm in marginal ring. 1 marginal labiate process. (Description based on Johansen and Fryxell, 1985).

Distribution: Antarctic, subantarctic (Medlin and Priddle, 1990).

Thalassiosira lentiginosa (Janisch) Fryxell

Plate 6, Fig. 7

Basionym: *Cosconidiscus lentiginosus* Janisch 1878

Jousé *et al.* 1962: Plate 1, Figs. 13-18

Kozlova 1966: Plate 4, Fig. 6, 7

Fryxell 1977: Figs. 13, 14

Fenner *et al.* 1976, Burckle 1987

Description: Valve diameter 29-120 μm (25-60 μm , herein). Areolae pattern fasciculated, 7-9 in 10 μm (7-10, herein). Strutted processes scattered evenly across valve face, resembling small areolae. Marginal strutted processes arranged in a single ring, 3-4 in 10 μm . 1 distinct marginal labiate process, radially aligned.

(Description based on Johansen and Fryxell, 1985).

Distribution: Antarctic plankton (Medlin and Priddle, 1990). Widespread south of the Antarctic Convergence Zone (Johansen and Fryxell, 1985).

Thalassiosira torokina Brady

Plate 7, Fig. 1

Synonyms: *Coscinodiscus denarius* Schmidt var. Van Heurck 1909,
T. cf. burckliana Gombos

Brady 1977: Figs. 1-4

Baldauf and Barron 1991: Plate 6, Fig. 1

McMinn and Harwood 1995: Figs. 1e-g, 1j

Description: Valve diameter 50-60 μm . Valves surface varies from slightly convex to convex-concave. Areolae hexagonal in shape and evenly sized over valve face; 3-4 in 10 μm . A variable number of pores (12-30) characterise the central area. Margin very distinct and of 2-3 rows of smaller areolae. (Description based on Brady, 1977).

Distribution: An extinct species from Antarctic marine sediment. First appearance datum 8.2-8.6 Ma; last appearance datum 1.8 Ma (Harwood and Maruyama, 1992).

Thalassiothrix antarctica Fryxell

Plate 7, Fig. 2

Synonyms: *Thalassiothrix longissima* Cleve & Grunow var. *antarctica* Grunow ex Van Heurck, *Thalassiothrix antarctica* Schimper ex Karsten, *Thalassiothrix antarctica* var. *echinata* Karsten

Jousé *et al.* 1962: Plate 3, Fig. 10

Hallegraeff 1986: Figs. 15-22

Hasle and Semina 1987: Figs. 26-59

Medlin and Priddle 1990: Plate 17.1, Figs. 4-6

Hart 1934, Kozlova 1966, Gombos 1977, Ligowski 1983

Description: Valve length 420-5680 μm , width 1.5-6 μm . Cells mostly solitary, but may be united in bundles or tangled masses. Narrow, linear valves usually slightly heteropolar. Foot-pole rounded and smooth; head-pole with 2 winged spines. Delicate marginal spines turned towards head-apex; 2-3 in 10 μm near the middle, fewer towards the poles, arising from the central part of the areolae. Quadrangular areolae in one row along each edge of the valve (10-16 in 10 μm). Externally, areolae alternate with narrow marginal ribs. Striae 12-17 in 10 μm . Labiate process present internally on each valve pole. (Description based on Hallegraeff, 1986; Medlin and Priddle, 1990).

Distribution: Antarctic, planktonic (Medlin and Priddle, 1990).

Notes: *Thalassiothrix* frustules are rarely preserved intact in sediment. End pieces are frequently observed.

Trichotoxin reinboldii (Van Heurck) Reid & Round

Plate 7, Fig. 3

Basionym: *Synedra reinboldii* Van Heurck

Synonym: *Synedra spathula*

Medlin and Priddle 1990: Plate 17.1, Figs. 7-9

Boden and Reid (1989)

Description: Valves curved. Apical axis 904-3600 μm ; transapical axis 3-10 μm . Marginal spines absent. Spineless rounded cell apices. Striae 8-10 in 10 μm . Labiate process close to each apex and low mantle. (Description based on Medlin and Priddle, 1990).

Distribution: Antarctic, plankton (Medlin and Priddle, 1990).

Notes: *Trichotoxin* frustules are rarely preserved intact in sediment. End pieces are frequently observed.

Unknown Genus A

Plate 7, Fig. 4

Description: Centric frustule, diameter 3-5 μm . 9-15 distinct areolae in centre of valve. Valve face otherwise smooth. No visible marginal striae or processes.

Plate 1

Fig. 1 *Actinocyclus actinochilus* (Ehrenberg) Simonsen

Figs. 2 - 5 *Chaetoceros* vegetative cells

Fig. 2 *C. bulbosum* (Ehrenberg), broad girdle view of cells in “atlanticum” phase

Fig. 3 *C. dichchaeta* Ehrenberg, broad girdle view of cells

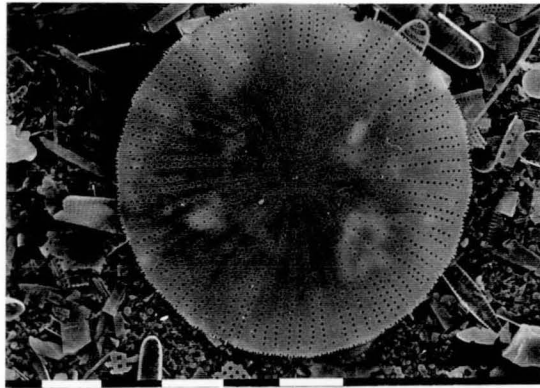
Fig. 4 *C. dichchaeta* Ehrenberg, broad girdle view of terminal valve

Fig. 5 *C. bulbosum* (Ehrenberg) Heiden, solitary cell in “bulbosum” phase

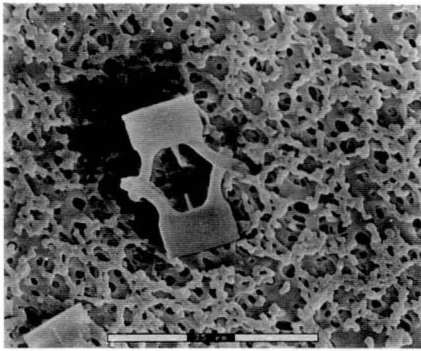
Fig. 1 scale bars = 10 μm

Fig. 2,3,5 scale bars = 35 μm

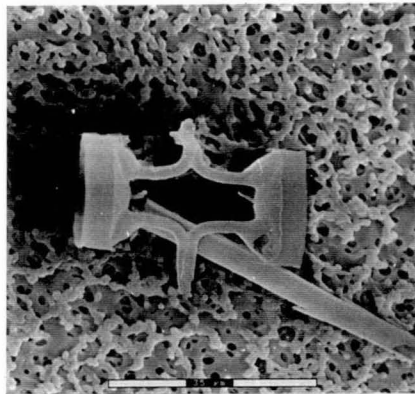
Fig. 4 scale bar = 50 μm



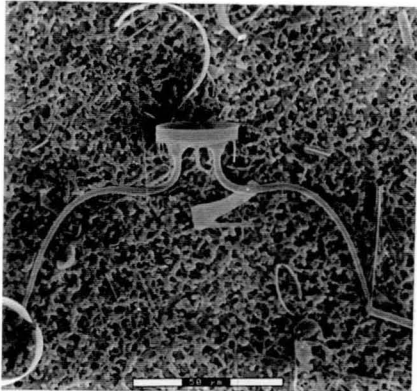
1



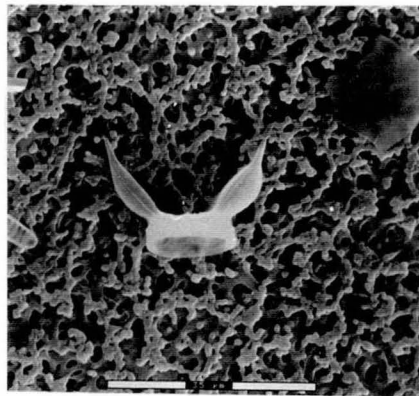
2



3



4



5

Plate 2

Figs. 1-4 *Chaetoceros* resting spores

Fig. 5 *Corethron criophilum* Castracane, girdle view

Fig. 6 *C. criophilum*, interval view of valve

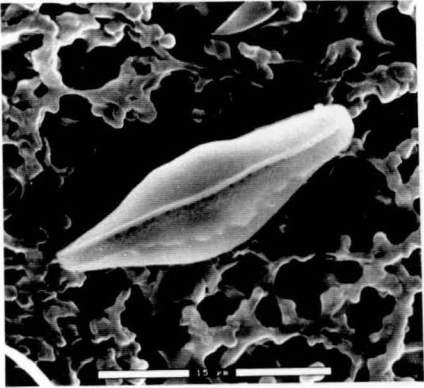
Figs. 1-2 scale bar = 15 μm

Fig. 3 scale bar = 4 μm

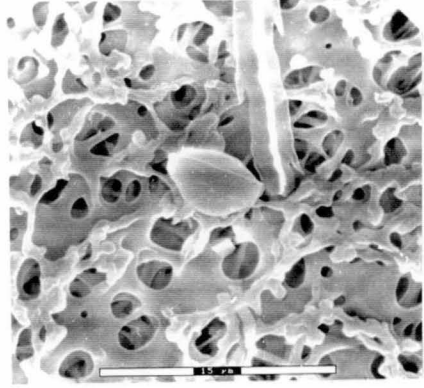
Fig. 4 scale bar = 5 μm

Fig. 5 scale bar = 100 μm

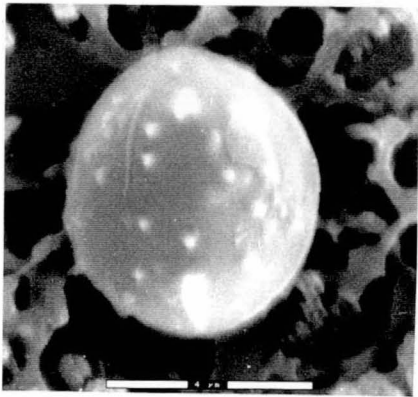
Fig. 6 scale bar = 30 μm



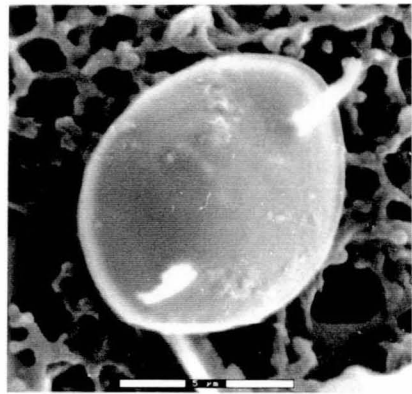
1



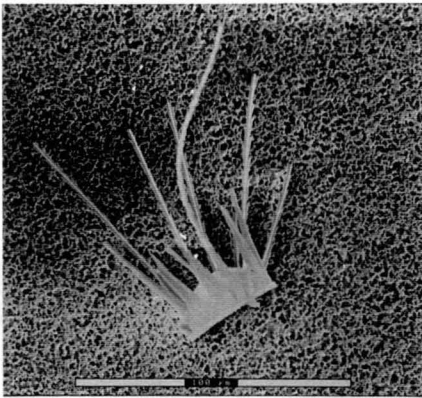
2



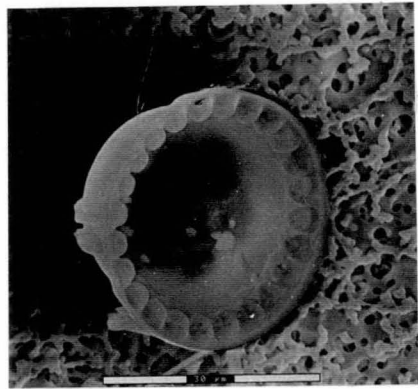
3



4



5



6

Plate 3

Fig. 1 *Dactyliosolen antarcticus* Castracane, girdle band

Fig. 2 *Distephanus speculum* (Ehrenberg) Haeckel

Figs. 3-4 *Eucampia antarctica* (Castracane) Manguin, broad girdle view of “winter stage”

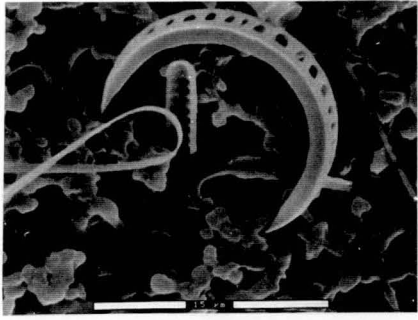
Fig. 5-7 *Fragilariopsis angulata* Hustedt

Figs. 1, 7 scale bar = 15 μm

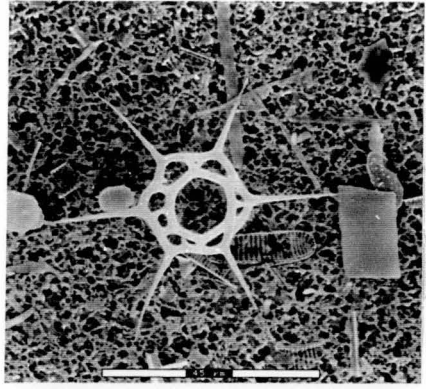
Figs. 2, 4 scale bar = 45 μm

Fig. 3 scale bar = 50 mm

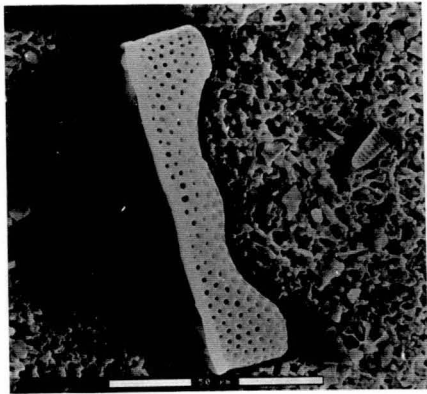
Figs. 5, 6 scale bars = 10 μm



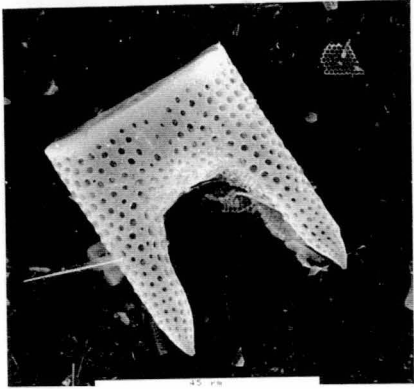
1



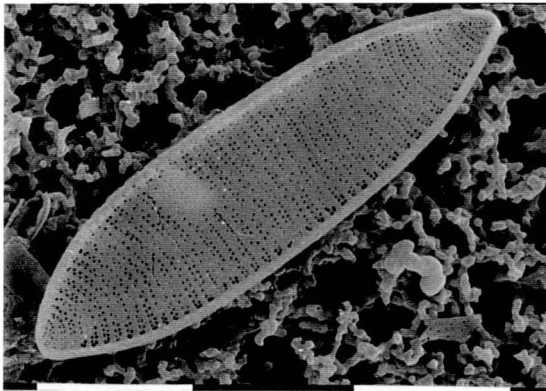
2



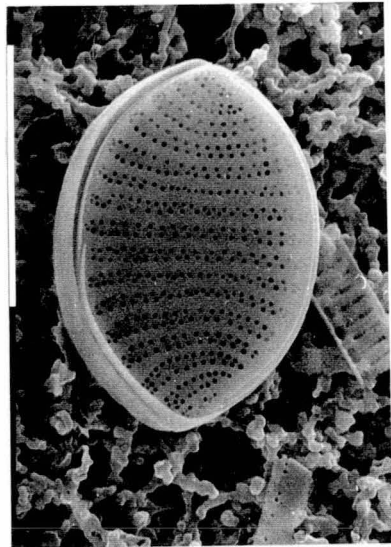
3



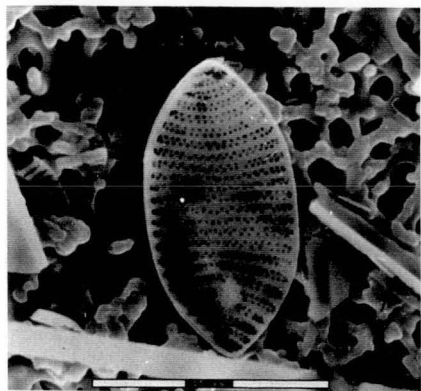
4



5



6



7

Plate 4

Figs. 1, 3, 6 *Fragilariopsis curta* (Van Heurck) Hasle

Fig. 3 (with *F. kerguelensis*)

Fig. 6 (with *F. obliquecostata*)

Fig. 2 *F. cylindrus* (Grunow?) Hasle

Fig. 3 *F. kerguelensis* (O'Meara) Hasle

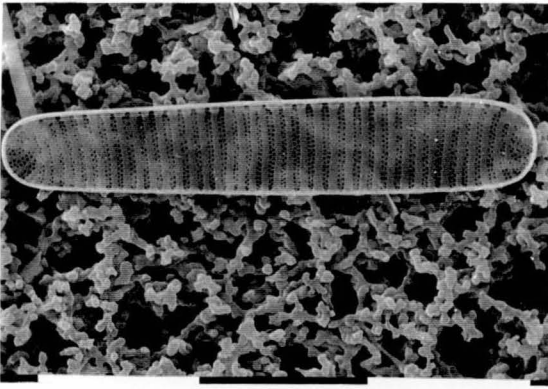
Fig. 4 *F. lineata* (Castracane) Hasle

Figs. 5-6 *F. obliquecostata* Heiden

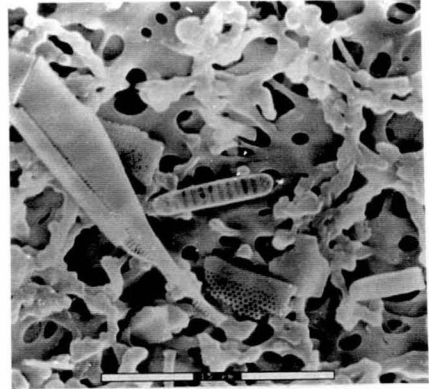
Fig. 7 *F. ritscheri* (Hustedt) Hasle

Figs. 1, 3-7 scale bars = 10 μm

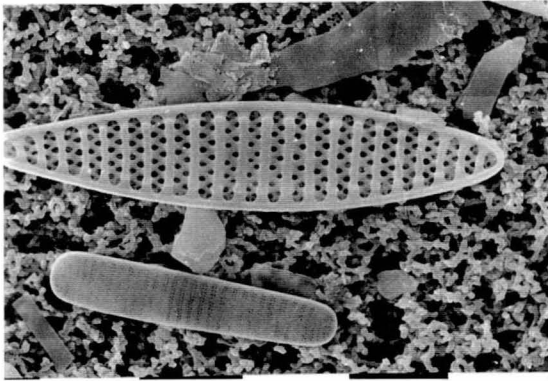
Fig. 2 scale bar = 15 μm



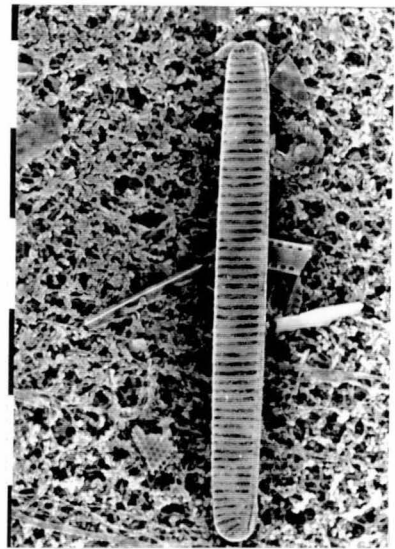
1



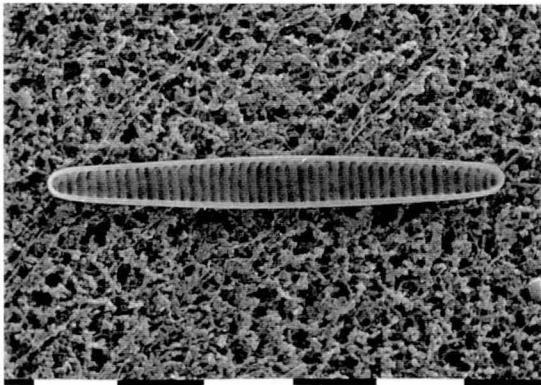
2



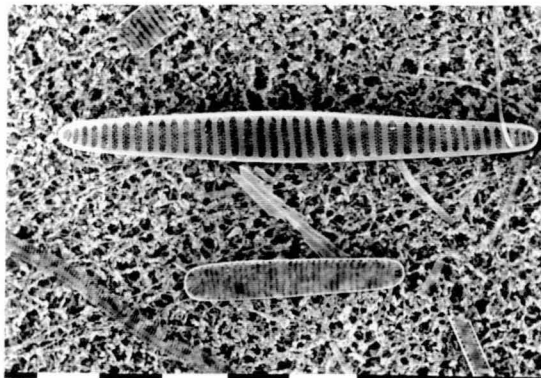
3



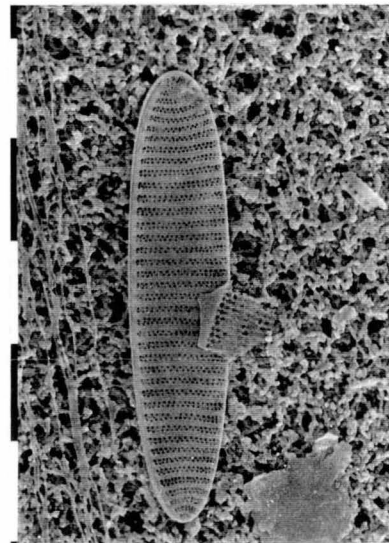
4



5



6



7

Plate 5

Fig. 1 *Fragilariopsis separanda* (Hustedt) Hasle

Fig. 2 *F. sublineata* Hasle

Figs. 3-4 *Pentalamina corona* Marchant

Fig. 3 Light micrograph, illustrating size compared to *F. curta*

Fig. 4 Scanning electron micrograph of shield plate

Fig. 5 *Porosira glacialis* (Grunow) Jørgensen

Figs. 6-7 *Pseudonitzschia turgiduloides* (Hasle) Hasle

Fig. 6 Complete frustule, with *F. curta*

Fig. 7 Close-up illustrating central nodule

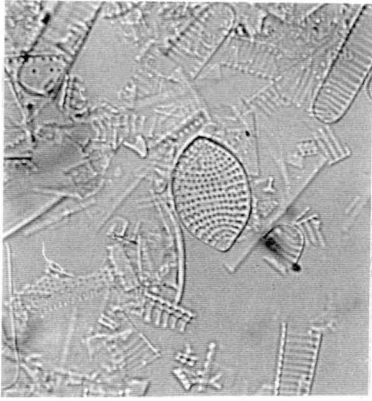
Figs. 1, 3 x1400

Fig. 2 scale bar = 30 μm

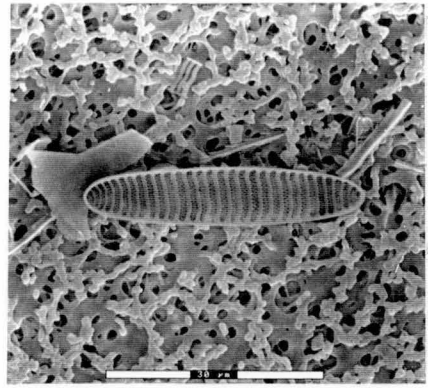
Figs. 4, 7 scale bar = 4 μm

Fig. 5 scale bars = 10 μm

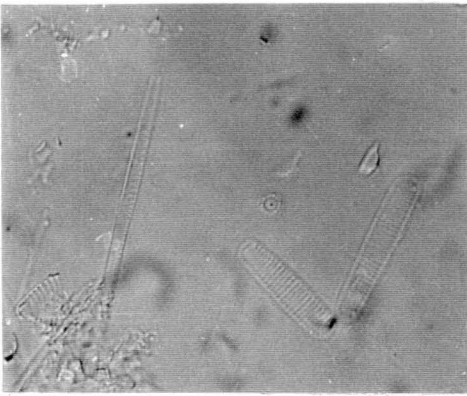
Fig. 6 scale bar = 40 μm



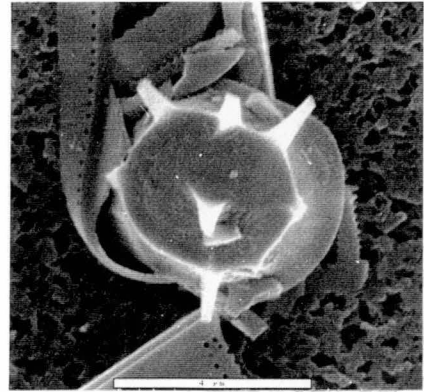
1



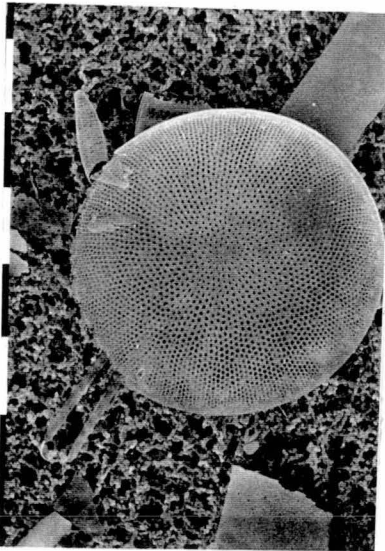
2



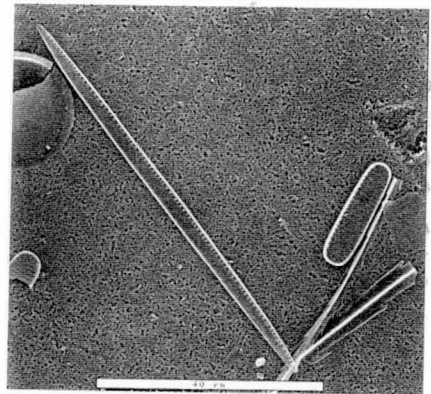
3



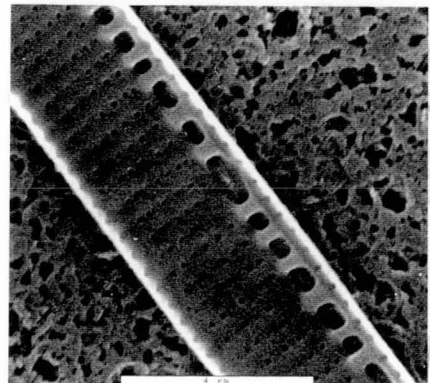
4



5



6



7

Plate 6

Fig. 1 *Rhizosolenia hebetata* fo. *semispina* (Hensen) Gran

Fig. 2 *Stellarima microtrias* (Ehrenberg) Hasle & Sims

Fig. 3 *Thalassiosira antarctica* Comber (resting spore)

Figs. 4-5 *T. gracilis* (Karsten) Hustedt

Fig. 6 *T. gravida* Cleve

Fig. 7 *T. lentiginosa* (Janisch) Fryxell

Fig. 1 x1400

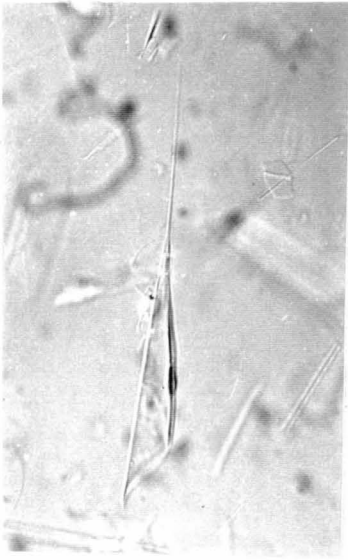
Fig. 2 scale bar = 30 μm

Fig. 3 scale bar = 20 μm

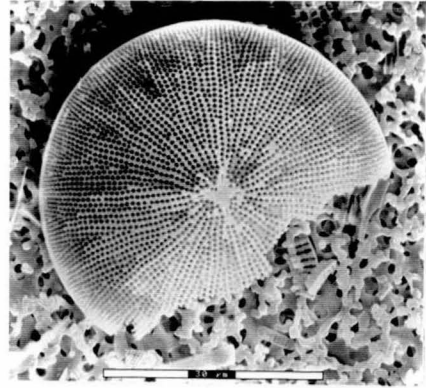
Figs. 4-5 scale bar = 10 μm

Fig. 6 scale bar = 25 μm

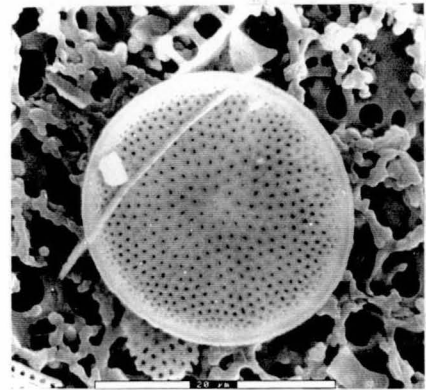
Fig. 7 scale bar = 40 μm



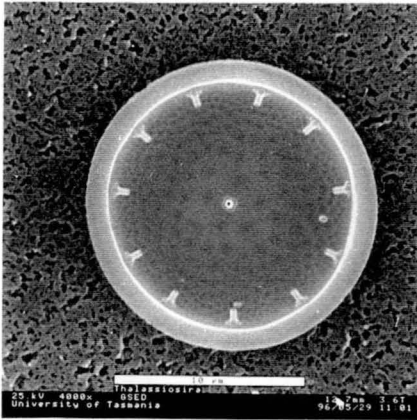
1



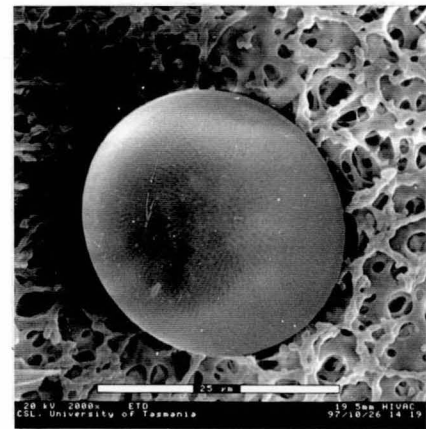
2



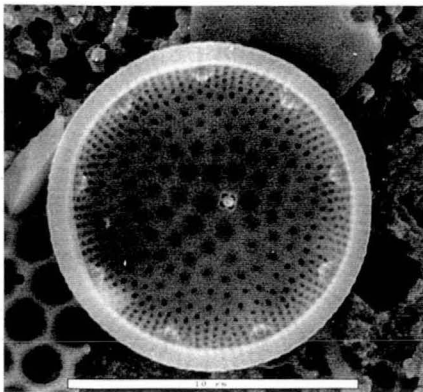
3



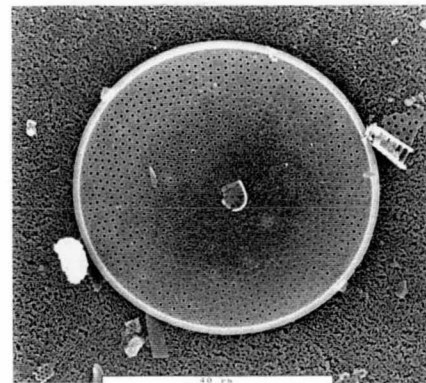
4



6



5



7

Plate 7

Fig. 1 *Thalassiosira torokina* Brady

Fig. 2 *Thalassiothrix antarctica* Fryxell

Fig. 3 *Trichotoxin reinboldii* (Van Heurck) Reid & Round

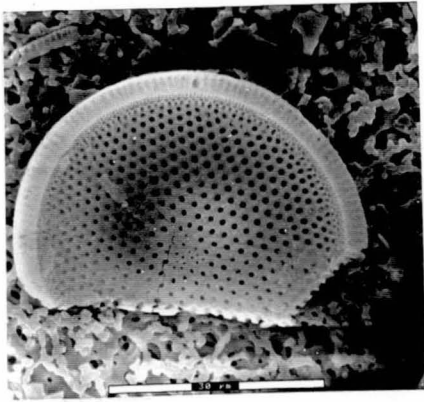
Fig. 4 Unknown Genus A

Fig. 1 scale bar = 30 μm

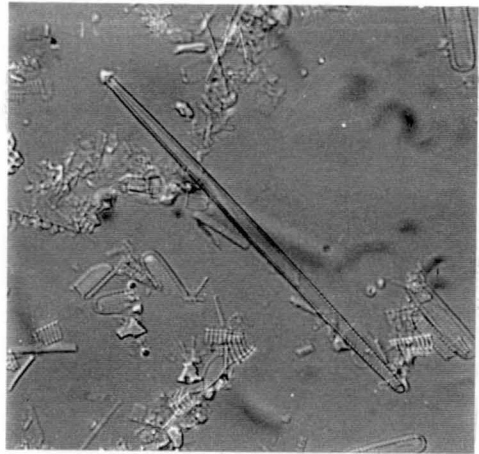
Fig. 2 x1400

Fig. 3 x630

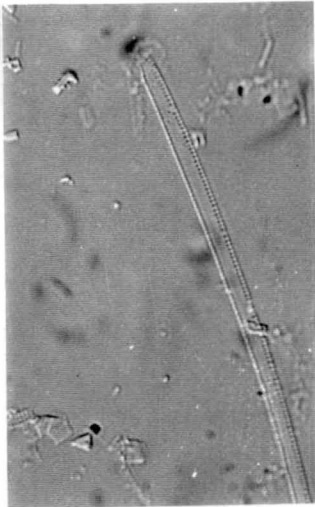
Fig. 4 x630



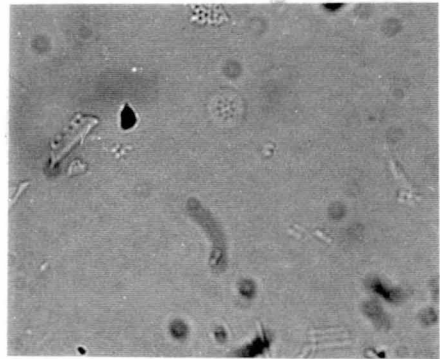
1



2



3



4

Reprinted from

MARINE MICROPALAEONTOLOGY

Marine Micropaleontology 32 (1997) 209–229

Distribution of diatoms in surface sediments of Prydz Bay, Antarctica

Fiona Taylor*, Andrew McMinn, Dennis Franklin

Antarctic CRC and Institute of Antarctic and Southern Ocean Studies, GPO Box 252-80, Hobart, Tasmania 7001, Australia

Received 14 October 1996; revised version received 22 January 1997; accepted 22 January 1997

This article has been removed
for copyright or proprietary
reasons.

